EDITORIAL

ROLE OF TH17 IN THE PATHOGENESIS OF CUTANEOUS INFLAMMATORY DISEASES

A. CHIRICOZZI[1,2], S. ZHANG[2,3], A. DATTOLA[1], M. GABELLINI[1], S. CHIMENTI[1] and S.P. NISTICÒ[1]

[1]Department of Dermatology, University of Rome Tor Vergata, Rome, Italy; [2]Laboratory for Investigative Dermatology, The Rockefeller University, New York, USA; [3]Ronald O. Perelman Department of Dermatology, New York University Langone Medical Center, New York, USA

Received January 31, 2012 – Accepted June 6, 2012

Th17 cells are a new T-cell subtype characterized by the capability of producing IL-17. They are reported to be involved in a wide range of cutaneous immune-mediated conditions and, particularly in this review, we sought to elucidate the Th17 role in the pathogenesis of some common inflammatory diseases including psoriasis, allergic contact dermatitis and atopic dermatitis.

Th17: a novel T helper cell subpopulation

The adaptive immune response was originally thought to be regulated by two types of helper T cells, Th1 and Th2, which express different kinds of cytokines. The Th1 cell subtype is responsible for cell-mediated effects and for T-cytotoxic lymphocyte activation, while Th2 cell subtype is key-mediator for humoral immunity (1).

However, the paradigm Th1/Th2 has been recently challenged with the discovery of Th17 cells, a novel T helper cell subpopulation. Th17 cells were first characterized in 2005 as a distinct T cell lineage that differed from Th1 and Th2 cells in function and pathological role (2).

The main cytokine distinguishing Th17 from the other T helper cell subpopulations is IL-17A, also known as IL-17. This proinflammatory cytokine was initially described as CTLA-8, a rodent T cell-derived cDNA transcript, similar to a viral homolog of IL-17A encoded in the T cell–tropic gamma herpes virus, *Herpesvirussaimiri* (3). In addition to IL-17A, Th17 cells also produce other cytokines including IL-17F, IL-22, and to a lesser extent, TNF-α and IFN-γ.

The differentiation, proliferation, and survival of Th17 are dependent on IL-6, TGF-β, IL-1β, IL-23 and IL-21 (4, 5). In particular, IL-23 is crucial for Th17 maintenance, and to drive expansion and pathogenicity at later stages of Th17 development (6). Structurally, IL-23 is similar to IL-12 because they share a common p40 subunit that is covalently linked either to a p35 or p19 subunit to form IL-12 or IL-23, respectively. Activated myeloid dendritic cells secrete IL-23, driving T cell differentiation towards Th17 subset, and also release IL-12, inducing Th1 differentiation (7). The differentiation of naïve T cells into Th17 cells is also influenced by cytokines produced by the other T helper lineages, Th1, Th2 (2).

We review the pathogenesis of some common inflammatory cutaneous diseases with an emphasis on the pathogenesis function of Th17 from data

Key words: Th17, IL-17, psoriasis, atopic dermatitis, allergic contact dermatitis

Mailing Address: Dr. Andrea Chiricozzi,
Department of Dermatology,
University of Rome Tor Vergata
Viale Oxford 81,
00133 Rome. Italy
Tel.: +39 06 20902743 Fax: +39 06 20902742
e-mail: chiricozziandrea@gmail.com

0393-974X (2012)

DISCLOSURE: ALL AUTHORS REPORT NO CONFLICTS OF INTEREST RELEVANT TO THIS ARTICLE.

recently published in the literature.

Allergic contact dermatitis

Allergic contact dermatitis (ACD) is caused by repeated exposure to a hapten or allergen that provokes a T-cell-mediated, delayed-type hypersensitivity reaction. Clinical manifestations vary from erythema and intense pruritus in the acute Phase, to lichenification, chronically. Microscopic examination is nonspecific but shows spongiotic vesciculation, dermal inflammatory monocyte infiltrate and, hyperkeratosis in the chronic Phase. New understanding of ACD reveals a potential shared role among Th1 and Th17 cells and CD8+ T cells. Th1 and Th17 cytokines such as IFNγ, TNFα, IL-17 were shown to mediate the inflammation seen in this condition.

Experiments by Albanesi et al. demonstrated that contact sensitized, nickel-specific CD4+ T-cell clones are able to secrete IL-17 and they also found elevated levels of IL-17 messenger RNA (mRNA) in the skin where nickel patch testing was performed (8).

Models of nickel-induced ACD strongly suggest that IL-17 is capable of regulating the inflammatory cascade underlying this disorder. Exposure of IL-17-deficient and wild-type mice to [1-fluoro-2,4-dinitrobenzene (DNFB) or tri-nitro-chloro-benzene(TNCB)] hapten induced typical contact hypersensitivity reaction in healthy controls, but not inIL-17-knockout mice, which exhibited an impressive reduction in epidermal spongiosis and inflammatory cell infiltration. When T cells isolated from this IL-17-deficient mice model were transferred to naïve recipients, they induced remarkably weaker ACD reactions as compared to the cutaneous manifestations caused by sensitized T cells of wild-type mice (9). A CD4+ T cell-deprived murine model presenting an ACD reaction exclusively boosted by CD8+ T cells, demonstrated that the crucial role played by CD8+ T cells was mediated by IL-17, not by IFNγ (10).

Overall, these studies strongly underscore the importance of Th17 cells in ACD pathogenesis.

Psoriasis

Psoriasis is a common, chronic, inflammatory cutaneous disorder characterized by marked epidermal hyperplasia, neoangiogenesis and dense dermal and epidermal immune cell infiltrate. Emerging insights into its pathogenesis suggest that psoriasis, previously considered a pure Th1–driven disease, is likely mediated by Th17 and Th1 with a more relevant role played by Th17 cell subpopulation. This new concept is supported by genetic, clinical and experimental evidence.

Some of the Th17 pathway-related genes, including IL-23R, IL-12/IL-23 p40 subunit, IL-23p19 subunit, have been identified as psoriasis susceptibility genes. Moreover, in psoriatic lesional skin, CD8+ and CD4+ T cell mostly express IL-17, which is highly upregulated in lesional psoriatic skin similar to IL-23, IL-22 and IL-21 (11-14). Additionally, serum expression levels of IL-22 and IL-17 correlate with psoriasis severity (15, 16).

Th17-related cytokines contribute to psoriatic plaque phenotype by inducing epidermal hyperplasia, recruiting memory T cells and neutrophils, and stimulating keratinocyte production of AMPs, proinflammatory chemokines and cytokines. IL-17, in synergy with TNFα, mediates key inflammatory circuits in psoriasis and induces *in vitro* expression of CCL20, S100A7 (psoriasin), IL-8, defensin beta 4 (DEFB4), IL-23A, IL-19, IL-6. These genes represent some of the highest upregulated gene transcripts in lesional psoriatic skin (17).

The relevance of IL-23/Th17 axis is underscored by the hyper-expression of IL-23, but not IL-12, in lesional psoriatic skin, mirroring the discrepancy between IL-23 and IL-12 levels observed in mice psoriatic skin (14-18). Indeed, murine models injected with IL-23, but not with IL-12, developed psoriasiform lesions showing epidermal acanthosis, neutrophil recruitment, dermal infiltration of CD4+ and CD8+ T cells that produced IL-17 and IL-22 (18). Therefore, the neutralization of IL-23 alone may represent the optimal treatment for psoriasis.

Therapeutic approaches suppressing the Th17 pathway were highly effective in resolving psoriasis, demonstrating the key-role played by the IL-23/Th17 axis (19). The use of neutralizing monoclonal antibodies against IL-23, IL-22 and IL-17 to treat psoriasis is currently undergoing Phase I, Phase II and Phase III clinical trials.

New emerging drugs targeting IL-17 or its receptor have recently tested in clinical studies for

the treatment of psoriasis and psoriatic arthritis. Overall, one humanized antibody blocking the IL-17 receptor and three humanized antibodies neutralizing IL-17 have been designed.

Brodalumab (AMG827), an anti-IL-17-receptor monoclonal antibody, has been proven safe and effective in the treatment of moderate-to-severe plaque psoriasis in a Phase II, randomized, double-blind, placebo-controlled, dose-ranging study (20). This study, including 198 patients, showed a satisfactory safety profile and good clinical efficacy across the 5 groups of patients treated with Brodalumab at different concentrations (70 mg, 140 mg, 210 mg, or 280 mg). After 12 weeks of treatment, an improvement of at least 75% in the Psoriasis Area and Severity Index (PASI) was observed in 77% and 82% of the patients in the 140-mg and 210-mg Brodalumab groups, respectively (20). The most common adverse events were nasopharyngitis (8%), upper respiratory tract infection (8%), and injection-site erythema (6%). Three serious adverse events were reported: 2 cases of grade 3 neutropenia in the 210-mg brodalumab group and renal colic in one patient in the 70-mg brodalumab group (20). Phase III studies are currently underway but clinical outcomes have not been yet published.

A Phase II, randomized, double-blind, placebo-controlled dose-ranging trial tested safety and efficacy of Ixekizumab (LY2439821), a humanized anti–interleukin-17 monoclonal antibody, in 142 patients with chronic moderate-to-severe plaque psoriasis. Study population was divided into 4 groups, each treated with Ixekizumab at different concentrations (10, 25, 75, or 150 mg) and a placebo group (21).

At 12 weeks, 82.1% and 82.8% of patients treated with 150 mg and 75 mg, respectively, showed a reduction in the PASI score by at least 75% without reporting any serious adverse event or major cardiovascular accident (21). Among the drug-groups: nasopharyngitis (11%), upper respiratory tract infection (10%), and injection-site erythema (7%) were the most common adverse events. After the successful completion of Phase I and Phase II studies, Ixekizumab is currently under evaluation at the dosage of 80 mg in a Phase III trial for the treatment of psoriasis.

Unlike Brodalumab and Ixekizumab, which are both administered subcutaneously, Secukinumab (AIN648), a fully human monoclonal anti-IL-17 antibody, may be injected subcutaneously or intravenously. A proof-of-concept, placebo-controlled study including 36 patients affected by psoriasis has been recently published. After a single intravenous administration of Secukinumab at the dosage of 3 mg Kg^{-1}, patients showed a satisfactory clinical improvement that was maintained throughout 12 weeks of follow-up, although one serious adverse event (worsening of preexisting congestive cardiac disease) occurred in the drug group (22).

Further Phase II trials with a larger number of patients have been performed: one of these showed 81% of patients, receiving 150 mg Secukinumab subcutaneously once a month, experienced at least a 75% improvement of PASI after 12 weeks of treatment (23). In another study, 83% of patients showed an improvement of PASI $\geq$75% if treated with an intravenous injection of Secukinumab (24). Secukinumab is currently being tested in Phase III studies.

A newer therapeutic agent neutralizing IL-17 is represented by a humanized monoclonal antibody, RG4934, has been investigated in terms of safety and efficacy for the treatment of psoriatic arthritis through Phase I clinical trials but data have not yet been published.

Atopic dermatitis

Atopic Dermatitis (AD) is a chronic cutaneous disorder characterized by immune dysregulation and altered skin barrier function. It represents the cutaneous manifestation of a broad spectrum of diseases including asthma, food allergy, allergic rhinitis and conjunctivitis, belonging to the so-called "atopic march". Some studies distinguish an acute Phase (clinically characterized by erythematous papules, intense itching, excoriation, serous exudation) as associated with Th2/T22 immune polarization and marked eosinophilia, from a chronic stage characterized by lichenification that likely involves the Th1 cell subtype.

The pathogenic mechanism of AD is two-pronged: (i) impaired skin barrier, resulting in an increased susceptibility to bacterial infections and permeability to allergens, and (ii) a pathologic Th2/T22 immune response (25). High expression levels

of IL-4, IL-13, IL-31 in AD patients suggest that AD, as well as asthma, is predominantly associated with Th2 pathway (26).

T22, a heterogeneous subset of IL-22-producing T cells consisting of both CD8+ and CD4+ T cells, is thought to greatly contribute to the pathogenesis of AD as suggested by the correlation between the increased number of IL-22-producing CD8+ T cells and the AD disease severity index. Moreover, the hyper-expression of IL-22 may explain the epidermal hyperplasia and the defective terminal differentiation pattern observed in this disease (27).

A potential role of Th17 in the pathogenic mechanism underlying AD and, more generally, atopy, has been suggested. Tesmer et al. showed increased levels of IL-17A in the peripheral blood, sputum, and airways of asthmatic patients (28). These upregulated levels were found to positively correlate with the degree of bronchial hyper-reactivity (29, 30). Furthermore, mouse models of asthma showed a crucial role of IL-17–producing T cells in mediating inflammation and destruction of lung epithelium, and in neutrophil recruitment and activation (31). However, these observations contradict findings from other mouse models of asthma, in which IL-17 seemed to assume a protective role, reducing eosinophilia and bronchial hyper-reactivity in the chronic Phase (32).

High expression level of IL-17, IL-6 and TGF-β were found in both acute skin lesions and serum of AD patients (33,34). As seen with CD8+T22, the percentage of circulating Th17 T-cells appeared to correlate with increased severity of the disease (34).

Additionally, CCR4, a receptor expressed on the cell surface of both Th2 and Th17, is highly expressed in T cells detected in lesional AD skin (35). Moreover, 70-80% of AD patients have increased serum IgE. Intriguingly, a recent study showed that Th17 cells are capable of inducing IgE production *in vitro* (36).

However, other studies only reported a modest upregulation of IL-17, IL-23 and IL-23R genes in lesional AD skin compared to healthy skin. Particularly compared to lesional psoriatic skin, in which a marked hyperexpression of Th17 pathway genes occurs, the expression of IL-23/Th17 axis is weak (37). Importantly, Guttman-Yassky et al. found a significantly decreased number of CD4+ Th17 cells in lesional AD skin compared to psoriatic skin. Interestingly, lesional AD skin also lacked a peculiar dendritic cell subpopulation that specifically drives Th17 differentiation (37). The dominating Th2 microenvironment and the relatively deficient Th17/IL-23 axis activation may potentially account for the poor IL-17-related AMPs production in chronic AD, resulting in the reduced innate immune defense and the increased propensity to skin infections observed in this disease (38). Moreover, in AD lesional skin, the expression of CCR6, and its ligand, CCL20, are reduced in T cell clones isolated from the skin of AD patients as compared to those from psoriatic patients (39, 40).

While a marked hyperexpression of Th17 pathway genes occurs in psoriasis, Th17 expression levels are likely modest in AD. Since Th17 cells represent a skin resident T cell population that bridges the innate and adaptive immunity arms, its presence in lesional AD skin may be an epiphenomenon of a persistent inflammatory state. Further studies will be necessary in order to clarify Th17 role in the pathogenesis of atopic dermatitis.

CONCLUSION

Emerging evidence indicates the importance of the Th17 cell subset in the human immune system, and thus challenging the previously held Th1/Th2 paradigm. Th17 cells are known to be involved in the protective response against fungus and bacteria infections and now studies suggest they may also be master regulators of a broad spectrum of inflammatory skin disorders and autoimmune diseases.

Currently, Th17 have demonstrated a clear, pivotal role in certain dermatoses such as psoriasis and CAD, however, further investigations are needed to clarify their role in other disorders.

Elucidating the pathogenic relevance of Th17 in diseases such as AD will contribute to the development of therapeutics targeting this pathway.

REFERENCES

1. Romagnani S. The Th1/Th2 paradigm. Immunol Today 1997; 18(6):263-6.
2. Harrington LE, Hatton RD, Mangan PR, Turner H,

Murphy TL, Murphy KM, Weaver CT. Interleukin 17-producing CD4+ effector T cells develop via a lineage distinct from the T helper type 1 and 2 lineages. Nat Immunol 2005; 6(11):1123-32.

3. Rouvier E, Luciani MF, Mattei MG, Denizot F, Golstein P. CTLA□8, cloned from an activated T cell, bearing AU□rich messenger RNA instability sequences, and homologous to a Herpes virus Saimiri gene. J Immunol 1993; 150:5445–5456.
4. Yang L, Anderson DE, Baecher-Allan C, Hastings WD, Bettelli E, Oukka M, Kuchroo VK, Hafler DA. IL-21 and TGF-beta are required for differentiation of human T(H)17 cells. Nature 2008; 454(7202):350-2.
5. Sutton C, Brereton C, Keogh B, Mills KH, Lavelle EC. A crucialrole for interleukin (IL)-1 in the induction of IL-17-producing T cells that mediate autoimmune encephalomyelitis. J Exp Med 2006; 203(7):1685-91.
6. Aggarwal S, Ghilardi N, Xie MH, de Sauvage FJ, Gurney AL. Interleukin-23 promotes a distinct CD4 T cell activation state characterized by the production of interleukin-17. J Biol Chem 2003; 278:1910-14.
7. Oppmann B, Lesley R, Blom B, et al. Novel p19 proteinen gages IL-12p40 to form a cytokine, IL-23, with biological activities similar as well as distinct from IL-12. Immunity 2000; 13(5):715-25.
8. Albanesi C, Cavani A, Girolomoni G. IL-17 is produced by nickel-specific T lymphocytes and regulates ICAM-1 expression and chemokine production in human keratinocytes: synergistic or antagonist effects with IFN-gamma and TNF-alpha. J Immunol 1999; 162:494-502.
9. 9.Nakae S, Komiyama Y, Nambu A, Sudo K, Iwase M, Homma I, Sekikawa K, Asano M, Iwakura Y. Antigen-specific T cell sensitization is impaired in IL-17-deficient mice, causing suppression of allergic cellular and humoral responses. Immunity 2002; 17(3):375-87.
10. He D, Wu L, Kim HK, Li H, Elmets CA, Xu H.CD8+ IL-17-producing T cells are important in effector functions for the elicitation of contact hypersensitivity responses. J Immunol 2006; 177(10):6852-8.
11. Lowes MA, Kikuchi T, Fuentes-Duculan J, Cardinale I, Zaba LC, Haider AS, Bowman EP, Krueger JG. Psoriasis vulgaris lesions contain discrete populations of Th1 and Th17 T cells. J Invest Dermatol 2008; 128(5):1207-11.
12. Ortega C, Fernández-A S, Carrillo JM, Romero P, Molina IJ, Moreno JC, Santamaría M. IL-17-producing CD8+ T lymphocytes from psoriasis skin plaques are cytotoxic effector cells that secrete Th17-related cytokines. J Leukoc Biol 2009; 86(2):435-43.
13. Caruso R, Botti E, Sarra M, et al. Involvement of interleukin-21 in the epidermal hyperplasia of psoriasis. Nat Med 2009; 15(9):1013-5.
14. Lee E, Trepicchio WL, Oestreicher JL, Pittman D, Wang F, Chamian F, Dhodapkar M, Krueger JG. Increased expression of interleukin 23 p19 and p40 in lesional skin of patients with psoriasis vulgaris. J Exp Med 2004; 199(1):125-30.
15. Wolk K, Witte E, Wallace E, et al. IL-22 regulates the expression of genes responsible for antimicrobial defense, cellular differentiation, and mobility in keratinocytes: a potential role in psoriasis. Eur J Immunol 2006; 36(5):1309-23.
16. Arican O, Aral M, Sasmaz S, Ciragil P. Serum levels of TNF-alpha, IFN-gamma, IL-6, IL-8, IL-12, IL-17, and IL-18 in patients with active psoriasis and correlation with disease severity. Mediators Inflamm 2005; 2005(5):273-9.
17. Chiricozzi A, Guttman-Yassky E, Suárez-Fariñas M, Nograles KE, Tian S, Cardinale I, Chimenti S, Krueger JG. Integrative responses to IL-17 and TNF-α in human keratinocytes account for key inflammatory pathogenic circuits in psoriasis. J Invest Dermatol 2011; 131(3):677-87.
18. Chan JR, Blumenschein W, Murphy E, et al. IL-23 stimulates epidermal hyperplasia via TNF and IL-20R2-dependent mechanisms with implications for psoriasis pathogenesis. J Exp Med 2006; 203(12):2577-87.
19. Leonardi CL, Kimball AB, Papp KA, et al. Efficacy and safety of ustekinumab, a human interleukin-12/23 monoclonal antibody, in patients with psoriasis: 76-week results from a randomised, double blind, placebo-controlled trial (PHOENIX 1). Lancet 2008; 371:1665-74.
20. Papp KA, Leonardi C, Menter A, et al. Brodalumab, an anti-interleukin-17-receptor antibody for psoriasis. N Engl J Med 2012; 366(13):1181-9.
21. Leonardi C, Matheson R, Zachariae C, Cameron G,

Li L, Edson-Heredia E, Braun D, Banerjee S. Anti-interleukin-17 monoclonal antibody ixekizumab in chronic plaque psoriasis. N Engl J Med 2012; 366(13):1190-9.
22. Hueber W, Patel DD, Dryja T, et al. Effects of AIN457, a fully human antibody to interleukin-17A, on psoriasis, rheumatoid arthritis, and uveitis. Sci Transl Med 2010; 2(52):52ra72.
23. Papp KA, et al. 'Secukinumab efficacy and safety preliminary results from a phase II subcutaneous dose-ranging study in the treatment of moderate-to-severe plaque psoriasis.' Presented at: 20th Congress of the European Academy of Dermatology and Venereology; 20-24 October, 2011; Lisbon, Portugal. Oral presentation FC01.5.
24. Papp KA, et al. 'Secukinumab, a novel fully human antibody to interleukin-17A, in the treatment of moderate-to-severe plaque psoriasis: Efficacy and safety interim results from a phase II intravenous induction dose-ranging study.' Presented at: 20th Congress of the European Academy of Dermatology and Venereology; 20-24 October, 2011; Lisbon, Portugal. Oral presentation FC01.7.
25. Guttman-Yassky E, Suárez-Fariñas M, Chiricozzi A, et al. Broad defects in epidermal cornification in atopic dermatitis identified through genomic analysis. J Allergy Clin Immunol 2009; 124(6):1235-1244.
26. Leung DY, Boguniewicz M, Howell MD, Nomura I, Hamid QA. New insights into atopic dermatitis. J Clin Invest 2004; 113(5):651-7.
27. Nograles KE, Zaba LC, Shemer A, et al. IL-22-producing "T22" T cells account for upregulated IL-22 in atopic dermatitis despite reduced IL-17-producing TH17 T cells. J Allergy Clin Immunol 2009; 123(6):1244-52.
28. Tesmer LA, Lundy SK, Sarkar S, Fox DA. Th17 cells in human disease. Immunol Rev 2008; 223:87-113.
29. Al-Ramli W, Préfontaine D, Chouiali F, Martin JG, Olivenstein R, Lemière C, Hamid Q. T(H)17-associated cytokines (IL-17A and IL-17F) in severe asthma. J Allergy Clin Immunol 2009; 123(5):1185-7.
30. Molet S, Hamid Q, Davoine F, et al. IL-17 is increased in asthmatic airways and induces human bronchial fibroblasts to produce cytokines. J Allergy Clin Immunol 2001; 108(3):430-8.
31. Laan M, Cui ZH, Hoshino H, Lötvall J, Sjöstrand M, Gruenert DC, Skoogh BE, Lindén A. Neutrophil recruitment by human IL-17 via C-X-C chemokine release in the airways. J Immunol 1999; 162(4):2347-52.
32. Schnyder-Candrian S, Togbe D, Couillin I, et al. Interleukin-17 is a negative regulator of established allergic asthma. J Exp Med 2006; 203(12):2715-25.
33. Toda M, Leung DY, Molet S, et al. Polarized in vivo expression of IL-11 and IL-17 between acute and chronic skin lesions. J Allergy Clin Immunol 2003; 111(4):875-81.
34. Koga C, Kabashima K, Shiraishi N, Kobayashi M, Tokura Y. Possible pathogenic role of Th17 cells for atopic dermatitis. J Invest Dermatol 2008; 128(11):2625-30.
35. Nakatani T, Kaburagi Y, Shimada Y, Inaoki M, Takehara K, Mukaida N, Sato S. CCR4 memory CD4+ T lymphocytes are increased in peripheral blood and lesional skin from patients with atopic dermatitis. J Allergy Clin Immunol 2001; 107(2):353-8.
36. Milovanovic M, Drozdenko G, Weise C, Babina M, Worm M. Interleukin-17A promotes IgE production in human B cells. J Invest Dermatol 2010; 130(11):2621-8.
37. Guttman-Yassky E, Lowes MA, Fuentes-Duculan J, et al. Low expression of the IL-23/Th17 pathway in atopic dermatitis compared to psoriasis. J Immunol 2008; 181(10):7420-7.
38. Nograles KE, Suárez-Fariñas M, Shemer A, et al. Atopic dermatitis keratinocytes exhibit normal T(H)17 cytokine responses. J Allergy Clin Immunol 2010; 125(3):744-6, 746.e1-746.e2.
39. Ong PY, Leung DY. The chemokine receptor CCR6 identifies interferon-gamma expressing T cells and is decreased in atopic dermatitis as compared with psoriasis. J Invest Dermatol 2002; 119(6):1463-4.
40. Schmuth M, Neyer S, Rainer C, Grassegger A, Fritsch P, Romani N, Heufler C. Expression of the C-C chemokine MIP-3 alpha/CCL20 in human epidermis with impaired permeability barrier function. Exp Dermatol 2002; 11(2):135-42.

EDITORIAL

INTERLEUKIN-9 AND MAST CELLS

S. TETÈ[1], A.SAGGINI[2], G. MACCAURO[3], M. ROSATI[4], F. CONTI[4], E. CIANCHETTI[5], D. TRIPODI[1], E. TONIATO[6], M. FULCHERI[7], V. SALINI[8], A. CARAFFA[9], P. ANTINOLFI[9], S. FRYDAS[10], F. PANDOLFI[11], P. CONTI[6] and T.C. THEOHARIDES[12]

[1]Dental School, University of Chieti-Pescara, Italy; [2]Department of Dermatology, University of Rome Tor Vergata, Rome, Italy; [3]Department of Orthopedics, Catholic University of Rome, Rome, Italy; [4]Gynecology Division, Pescara Hospital, Pescara, Italy; [5]Ortona Hospital, University of Chieti-Pescara, Italy; [6]Immunology Division, Medical School, University of Chieti-Pescara, Italy; [7]Psychology Department, University of Chieti; [8]Orthopeadics Division, University of Chieti-Pescara, Italy; [9]Orthopeadics Division, University of Perugia, Perugia Italy; [10]Parasitology Department, Veterinary School, Thessaloniki, Greece; [11]Department of Internal Medicine, Catholic University of the Sacred Heart, Rome, Italy; [12]Department of Pharmacology and Experimental Therapeutics, Biochemistry and Internal Medicine Tufts University School of Medicine, Tufts-New England Medical Center, Boston, MA, USA.

Received January 15, 2012 – Accepted July 16, 2012

Mast cells are granulated hematopoietic cells derived from stem cells that reside in nearly all tissues and are involved in protection of a host from bacterial infection with a protective and pathogenic activity. Mast cells are important for both innate and adaptive immunity in tissues which are in close contact with the environment. These cells express proinflammatory cytokines such as IL-1, IL-6, IL-8 and tumor necrosis factor which are necessary for innate immunity. Mast cells also produce interleukin-9 and enhance mast cell expression of several cytokines including IL-1beta, IL-5, IL-6, IL-9 and IL-13. In addition, IL-9 can induce mast cell production of TGF-beta which can have proinflammatory downstream effects. IL-9 can function as either a positive or a negative regulator of immune responses and can have a detrimental role in allergy and autoimmunity. Furthermore, IL-9 contributes to disease by promoting mast cell expansion and production of IL-13 which in turn contributes to airway hyperresponsiveness. Here, in this editorial we review the interrelationship between IL-9 and mast cells.

Mast cells were first described in 1879, but their origin remained controversial for almost a century. At least two easily identifiable types of human mast cells have been reported: connective tissue mast cells that contain tryptase and chymase (TC mast cells), and mucosal mast cells that contain only tryptase (T mast cells) (1-3). These two cell types differ in the number and type of secretory granules they contain, as well as their responsiveness to stimuli (4-9). For instance, TC mast cells contain more heparin, whereas T mast cells contain more chondroitin sulphate; in addition, TC mast cells respond to neuropeptides, whereas T mast cells do not (10-14). Mast cells express primarily pro-inflammatory

Key words: IL-9, mast cells, inflammation, cytokine

Mailing address: Prof. S. Tetè,
Dipartimento di Scienze Orali,
Università "G. d'Annunzio" Chieti- Pescara",
Via dei Vestini, 31
Chieti, Italy
Tel./Fax: +39 0871 3554095
e-mail: tete@unich.it

0393-974X (2012)

DISCLOSURE: ALL AUTHORS REPORT NO CONFLICTS OF INTEREST RELEVANT TO THIS ARTICLE.

Table I. *Biological effects of IL-9 on multiple cell types.*

- **Growth factor (T cells)**
- **IgE production (B cells)**
- **Enhances Treg function**
- **Promotes Th17 differentiation**
- **Mast cell growth and survival**
- **Induces expression of Fc RI alpha**
- **Increases expression of IL-6, mast cell proteases**
- **Involved in cell metaplasia**
- **Enhances chemokine production in several cell types**
- **Supports erythroid colony formation**
- **Promotes maturation of hematopoietic stem/hematopoietic progenitors**
- **Activates production of IL-8, IL-13, and eotaxin**

cytokines such as IL-1, IL-6, IL-8 and tumor necrosis factor-α (TNF-α), which are necessary for innate immunity (15-18). Both the expression and the synthesis of these cytokines, however, depend on: 1) the state of maturation of the mast cells; 2) the location of mast cells within compartments of the same or different tissues (19); and 3) the type of cytokine(s) present during mast cell activation (20-23). However, mast cells can also produce cytokines that are released from T helper 2 (Th2) cells (so-called Th2 cytokines), such as IL-4 and IL-13, which are present in increased levels in several diseases (24-28). Th9 phenotype cells develop *in vitro* in the presence of IL-4 and TGF-β and secrete high levels of IL-9 as well as IL-10, CCL17 and CCL22 (29-34).

Mast cells have also been reported to produce IL-9 (35-40). One of the main targets of IL-9 is the mast cell and, as mentioned earlier, initial studies described a role for IL-9 in promoting the expansion of mast cell populations (41-44). Subsequent research on mice that were deficient for both IL-9 and IL-9Rα showed that IL-9 is not required for the generation of mast cell precursors, as the basal numbers of mast cells in these mice were normal. However, mice that were deficient for IL-9 or IL-9Rα showed defective expansion and recruitment of mast cell populations in response to intestinal nematode infection or following the induction of experimental autoimmune encephalomyelitis (EAE) (45-50). IL-9 can induce mast cell production of TGFβ, which can have pro-inflammatory downstream effects on neurons in a murine stroke model and on epithelial cells during intestinal inflammation (51-54). Following antigen-specific crosslinking of surface IgE molecules on mast cells, IL-9 can enhance mast cell expression of several cytokines, including IL-1β, IL-5, IL-6, IL-9, IL-10 and IL-13 (55-59). Of these cytokines, IL-5 and IL-13 are of particular interest, as the previously described direct effects of IL-9 in promoting eosinophilia and mucus production in the lung and the gut instead seem to be indirect effects mediated through the induction of these cytokines by IL-9 (60-63).

IL-9 can function as both a positive and negative regulator of immune responses (Table I). In general, it seems that IL-9 has detrimental roles during allergy and autoimmunity (64-67). However, during parasitic infections, IL-9 can help to clear the pathogen, and during skin transplantation, IL-9 can promote the maintenance of a tolerant environment (68-69). During some allergic responses in the lung, which are traditionally thought of as being T_H2 cell-mediated, IL-9 contributes to disease by promoting mast cell expansion and production of IL-13, which in turn promotes the release of mucus that contributes to airway hyperresponsiveness (70-72). The initial influx of mast cells in this model is likely to be driven by IL-9 that is derived from NKT cells (73-75). In addition, T_H9 cells also seem to contribute to disease in this model, as mice with PU.1-deficient T cells and a global IL-25 deficiency are protected from allergic airway inflammation (76-78).

Interleukin-9 (IL-9)

IL-9 cloned more than 20 years ago was originally identified as a T-cell growth factor and is a member of the common γ-chain-receptor cytokine family, with other members including IL-2, IL-4, IL-7, IL-15 and IL-21. (79). Moreover, IL-9 has been reported to be expressed by T helper 2 (T_h2), T_h9, and regulatory T (T_{Reg}) cell subsets and appears to increase the suppressive effect of Treg cells as well as enhance the proliferation and/or accumulation of Th17 cells (80-81). The Th17 cells have been also reported as a T-cell subset that has the ability to produce IL-9 both *in vitro* and *in vivo* (82). There is much evidencs to suggest that IL-9 production in Th17 cells is pathogenic in several immunological diseases. It is now clear that IL-9, along with IL-17 play a role in modulating immune responses in some types of infections.

IL-9 was first purified and characterized as a T cell and mast cell growth factor respectively termed P40, based on m.w., or mast cell growth-enhancing activity and has pleiotropic functions in the immune system (83). The major source of IL-9 is T lymphocytes; however, mast cells involved in the pathogenesis of inflammatory diseases are also a source of IL-9 in response to LPS, IL-1, histamine, and antigen-specific immunoglobulin E antigen. However, IL9 itself can help to facilitate mast cell growth and expansion.

In certain conditions regulatory T cells (Tregs) may also produce IL-9. It has been found that TGF-β and IL-4 enhance IL-9 production from activated T cells. IL-9 has biological effects on a number of distinct cell types such as: lymphocytes, mast cells, smooth muscle cells, epithelial cells and demonstrates proinflammatory activity in several models of inflammation. Therefore, IL-9 affects immune cells, as well as resident tissue cells that contribute to the development of inflammation.

Results from other reports demonstrated that IL-9 is involved in autoimmune inflammation. Interleukin (IL)-9 regulates the development of airway inflammation, mucus production, airway hyperresponsiveness, and airway fibrosis largely by increasing mast cell numbers and activity in the airways. Thus, targeting the IL-9 pathway may provide a new therapeutic modality for asthma, and allergic and inflammatory diseases.

Interleukin-9 (IL-9) has attracted renewed interest owing to the identification of its expression by multiple T helper (T(H)) cell subsets, including T(H)2 cells, T(H)9 cells, T(H)17 cells and regulatory T (T(Reg)) cells.

Interleukin-9 (IL-9) activates a heterodimeric receptor that consists of the IL-9 receptor α-chain (IL-9Rα) and the γ-chain and promotes the cross-phosphorylation of Janus kinase 1 (JAK1) and JAK3. This leads to the activation of signal transducer and activator of transcription 1 (STAT1), STAT3 and STAT5 and the upregulation of IL-9-inducible gene transcription (79). IL-9 was first linked to T helper 2 (T_H2) cells, which express IL-4, IL-5 and IL-13 during parasitic infections and provides a protective role in immunity to intestinal parasites (68). This is good evidence that IL-9 plays a role in regulating immunity to infectious diseases. Production of IL-9 occurs in an autocrine manner in response to IL-9-induced signals and as a consequence of the cross-linking of IgE molecules on the surface of mast cells. Histamine and IL-1β, can promote further IL-9 production. As IL-9 is a growth factor for mast cells, it is thought that these pathways promote the survival and expansion of mast cells during an active immune response. Results from other reports demonstrated that IL-9 is involved in autoimmune inflammation.

The purpose of this editorial is to summarize the interrelationship between IL-9 and mast cells in the pathogenesis of inflammatory diseases. Cytokine receptor antagonists, combined with natural substances that inhibit mast cells, such as plant-derived flavonoids (84, 85), provide new therapeutic options for diseases where inflammatory mast cells are involved.

REFERENCES

1. Mekori YA Metcalfe DD. Mast cells in innate immunity. Immunol Rev 2000; 173:131-40.
2. Di Muzio G, Perricone C, Ballanti E, et al. Complement system and rheumatoid arthritis: relationships with autoantibodies, serological, clinical features, and anti-TNF treatment. Int J Immunopathol Pharmacol 2011; 24:357-66.
3. Colombo C, Faelli N, Tirelli AS, et al. Analysis of inflammatory and immune response biomarkers in

sputum and exhaled breath condensate by a multi-parametric biochip array in cystic fibrosis. Int J Immunopathol Pharmacol 2011; 24:423-32.
4. Wedemeyer J, Tsai M, Galli SJ. Roles of mast cells and basophils in innate and acquired immunity. Curr Opin Immunol 2000; 12:624-31.
5. Marzano AV, Cugno M, Trevisan V, Lazzari R, Fanoni D, Berti E, Crosti C. Inflammatory cells, cytokines and matrix metalloproteinases in amicrobial pustulosis of the folds and other neutrophilic dermatoses. Int J Immunopathol Pharmacol 2011; 24:451-60.
6. Nisticò R, Mehdawy B, Piccirilli S, Mercuri N. Paraquat- and rotenone-induced models of Parkinson's disease. Int J Immunopathol Pharmacol 2011; 24:313-22.
7. Belloli L, Carlo-Stella N, Ughi N, Marasini B. Cancer in Italian patients with systemic sclerosis. Eur J Inflamm 2011; 9:151-6.
8. Mirzaei K, Hossein-Nezhad A, Mokhtari F, Najmafshar A, Khoshniat Nikoo M. VISFATIN/NAMPT/PBCEF and cytokine concentration in multiple sclerosis patients compared to healthy subjects. Eur J Inflamm 2011; 9:31-37.
9. Cantarini L, Iacoponi F, Lucherini OM, et al. Validation of a diagnostic score for the diagnosis of autoinflammatory diseases in adults. Int J Immunopathol Pharmacol 2011; 24:695-702.
10. Bryce PJ, Miller ML, Miyajima I, Tsai M, Galli SJ, Oettgen HC. Immune sensitization in the skin is enhanced by antigen-independent effects of IgE. Immunity 2004; 20:381-92
11. 11.Scaparrotta A, Verrotti A, Consilvio NP, Cingolani A, Di Pillo S, Di Gioacchino M, Verini M, Chiarelli F. Pathogenesis and clinical approaches to anticonvulsant hypersensitivity syndrome: current state of knowledge. Int J Immunopathol Pharmacol 2011; 24:277-84.
12. Rivetti S, Lauriola M, Voltattorni M, et al. Gene expression profile of human colon cancer cells treated with cross-reacting material 197, a diphtheria toxin non-toxic mutant. Int J Immunopathol Pharmacol 2011; 24:639-49.
13. Saggini A, Tripodi D, Maccauro G, et al. Tumor necrosis factor-alpha and mast cells: revisited study. Eur J Inflamm 2011; 9:17-22.
14. Aslani S, Hossein-Nezhad A, Mirzaei K, Maghbooli Z, Asgarabad SN, Karimi F. Tandem repeats of the CATT element of macrophage migration inhibitory factor gene may predict gestational diabetes mellitus severity. Eur J Inflamm 2011; 9:193-7.
15. Gagari E, Tsai M, Lantz CS, Fox LG, Galli SJ. Differential release of mast cell interleukin-6 via c-kit. Blood 1997; 89:2654-63.
16. Wu KG, Li TH, Chen CJ, Cheng HI, Wang TY. Correlations of serum Interleukin-16, total IgE, eosinophil cationic protein and total eosinophil counts with disease activity in children with atopic dermatitis. Int J Immunopathol Pharmacol 2011; 24:15-23.
17. Wu KG, Li TH, Chen CJ, Cheng HI, Wang TY. A pilot study evaluating the clinical and immunomodulatory effects of an orally administered extract of Dendrobium huoshanense in children with moderate to severe recalcitrant atopic dermatitis. Int J Immunopathol Pharmacol 2011; 24:367-75.
18. Sancilio S, Di Giacomo V, Quaglietta AM, et al. TRAIL promotes a pro-survival signal in erythropoietin-deprived human erythroblasts through the activation of an NF-κB/IκBα pathway. J Biol Regul Homeost Agents 2011; 25:375-386.
19. Theoharides TC, Donelan JM, Papadopoulou N, Cao J, Kempuraj D, Conti P. Mast cells as targets of corticotropin-releasing factor and related peptides. Trends in Pharmacol Sci 2004; 25: 563-8
20. Nenna R, Papoff P, Moretti C, et al. Detection of respiratory viruses in the 2009 winter season in Rome: 2009 influenza A (H1N1) complications in children and concomitant type 1 diabetes onset. Int J Immunopathol Pharmacol 2011; 24:651-9.
21. Drago L, Vassena C, Dozio E, Corsi MM, De Vecchi E, Mattina R, Romanò C. Procalcitonin, C-reactive protein, interleukin-6, and soluble intercellular adhesion molecule-1 as markers of postoperative orthopaedic joint prosthesis infections. Int J Immunopathol Pharmacol 2011; 24:433-40.
22. Nakanishi K. Basophils are potent antigen-presenting cells that selectively induce Th2 cells. Eur J Immunol 2010; 40:1836-42.
23. Pollice R, Bianchini V, Marola V, et al. Post-traumatic and psychiatric symptoms among young earthquake survivors in primary care camp hospital. Eur J Inflamm 2011; 9:39-44.

24. Obara W, Kawa Y Ra C, Nishioka K, Soma Y, Mizoguchi M. T cells and mast cells as a major source of interleukin-13 in atopic dermatitis. Dermatology 2002; 205:11-17.
25. Artini M, Scoarughi GL, Papa R, et al. A new anti-infective strategy to reduce adhesion-mediated virulence in Staphylococcus aureus affecting surface proteins. Int J Immunopathol Pharmacol 2011; 24:661-72.
26. Sakellaropoulou AV, Hatzistilianou MN, Emporiadou MN, Aivazis VT, Rousso I, Athanasiadou-Piperopoulou F. Evaluation of thyroid gland function in children with obstructive apnea hypopnea syndrome. Int J Immunopathol Pharmacol 2011; 24:377-86.
27. Di Paola R, Mazzon E, Paterniti I, Impellizzeri D, Bramanti P, Cuzzocrea S. Apocynin, a plant-derived drug, might be useful in the treatment of myocardial ischemia reperfusion injury in rat hearts. Eur J Inflamm 2011; 9:169-74.
28. Zhu J-S, Xu Z-P, Song M-Q, Zhang Q. Effect of oxymatrine combined with low dose 5-FU on lymphatic vessel and microvascular endothelial cell growth of gastric cancer in a severe combined immunodeficient mouse orthotopic implantation model. Eur J Inflamm 2011; 9:45-51.
29. Schmitt E, Germann T, Goedert S, et al. IL-9 production of naive CD4+ T cells depends on IL-2, is synergistically enhanced by a combination of TGF-beta and IL-4, and is inhibited by IFN-gamma. J Immunol 1994; 153:3989-96.
30. Losi M, Bocchino M, Matarese A, et al. Role of the quantiferon-TB test in ruling out pleural tuberculosis: a multi-centre study. Int J Immunopathol Pharmacol 2011; 24:159-65.
31. Iezzi M, Quaglino E, Cappello P, et al. HCG hastens both the development of mammary carcinoma and the metastatization of HCG/LH and ERBB-2 receptor-positive cells in mice. Int J Immunopathol Pharmacol 2011; 24:621-30.
32. Carlesimo M, Narcisi A, Cortesi G, Mari E, Fidanza L, De Marco G, Rossi A, Camplone G. An 18-year follow-up of a case of D-penicillamine-induced Elastosis perforans serpiginosa. Int J Immunopathol Pharmacol 2011;24(1):257-9.
33. Saggini A, Anogeianaki A, Maccauro G, Teté S, Salini V, Caraffa A, Conti P, Shaik-Dasthagirisaheb YB. What you should know about *Escherichia coli* infection. Eur J Inflamm 2011; 9:103-6.
34. Maghbooli Z, Hossein-Nezhad A, Shirzad M, Behzadi H. The role of osteoprotegrin/ nuclear factor kb ligand in coronary collateral development Eur J Inflamm 2011; 9:57-64.
35. Merz H, Kaehler C, Hoefig KP, et al. Interleukin-9 (IL-9) and NPM-ALK each generate mast cell hyperplasia as single 'hit' and cooperate in producing a mastocytosis-like disease in mice. Oncotarget 2010; 1:104-19.
36. Racciatti D, Gorgoretti V, Sepede G, Gambi F, Pizzigallo E. An Italian study on health-related quality of life and fatigue in patients with chronic fatigue syndrome and patients with chronic HCV virus infection: similarities and differences. Int J Immunopathol Pharmacol 2011; 24:673-81.
37. Palumbo P, Cinque B, Miconi G, et al. Biological effects of low frequency high intensity ultrasound application on ex vivo human adipose tissue. Int J Immunopathol Pharmacol 2011; 24:411-22.
38. Pierangeli A, Degener AM, Ferreri ML, et al. Interferon-induced gene expression in cervical mucosa during human papillomavirus infection. Int J Immunopathol Pharmacol 2011; 24:217-23.
39. Tsoucalas G, Karamanou M, Androutsos G. Travelling through time with aspirin, a healing companion. Eur J Inflamm 2011; 9:13-16.
40. Ciprandi G, De Amici M, Quaglini S, et al. Prediction of allergy by total serum IgE measurements in infancy: a 10-year follow-up. Eur J Inflamm 2011; 9:199-203.
41. Noelle RJ, Nowak EC. Cellular sources and immune functions of interleukin-9. Nat Rev Immunol 2010; 10:683-7.
42. Sharma JN, Kesavarao U. The effects of captopril on cardiac regression, blood pressure and bradykinin components in diabetic Wistar Kyoto rats. Int J Immunopathol Pharmacol 2011; 24:337-43.
43. Almerigogna F, Fassio F, Giudizi MG, et al. Natural killer cell deficiencies in a consecutive series of children with herpetic encephalitis. Int J Immunopathol Pharmacol 2011; 24:231-8.
44. Mazzoccoli G, Carughi S, Sperandeo M, Pazienza V, Giuliani F, Tarquini R. Neuro-endocrine correlations

of hypothalamic-pituitary-thyroid axis in healthy humans. J Biol Regul Homeost Agents 2011; 25:249-57.

45. Migueres M, Fontaine JF, Haddad T, Grosclaude M, Saint-Martin F, Bem David D, Crestani B. Characteristics of patients with respiratory allergy in France and factors influencing immunotherapy prescription: a prospective observational study (REALIS). Int J Immunopathol Pharmacol 2011; 24:387-400.
46. Stephens GL, Swerdlow B, Benjamin E, Coyle AJ, Humbles A, Kolbeck R, Fung M. IL-9 is a Th17-derived cytokine that limits pathogenic activity in organ-specific autoimmune disease. Eur J Immunol 2011; 4:952-62.
47. Shi Q, Gao ZY, Xie F, et al. A novel monoclonal antibody against human CD80 and its immune protection in a mouse lupus-like disease. Int J Immunopathol Pharmacol 2011; 24:583-93.
48. Marchisio P, Bianchini S, Galeone C, et al. Use of complementary and alternative medicine in children with recurrent acute otitis media in Italy. Int J Immunopathol Pharmacol 2011; 24:441-9.
49. Ciprandi G, De Amici M, Berardi L, Vignini M, Marseglia G. Serum IgE for Bet v 1 in patients affected by atopic dermatitis. Eur J Inflamm 2011; 9:205-7.
50. Failli A, Legitimo A, Mazzoni A, Urbani L, Scatena F, Mosca F, Consolini R. The combination of immunosuppressive drugs with 8-methoxypsoralen and ultraviolet a light modulates the myeloid-derived dendritic cell function. Int J Immunopathol Pharmacol 2011; 24:89-99.
51. Binici DN, Güneş N, Kayataş K, Pişkinpaşa N. The effects of interferon-α2b on intestinal flora in peritoneal fibrosis. Eur J Inflamm 2011; 9:135-139.
52. Jones TG, Hallgren J, Humbles A, Burwell T, Finkelman FD, Alcaide P, Austen KF, Gurish MF. Antigen-induced increases in pulmonary mast cell progenitor numbers depend on IL-9 and CD1d-restricted NKT cells. J Immunol 2009; 183:5251-60.
53. Tsoupras AB, Chini M, Tsogas N, Mangafas N, Demopoulos CA, Lazanas MC. *In vivo* effects of a *Ginkgo biloba* extract on platelet activating factor metabolism in two asymptomatic HIV-infected patients. Eur J Inflamm 2011; 9:107-16.
54. Bellisai F, Morozzi G, Scaccia F, Chellini F, Simpatico A, Pecetti G, Galeazzi M. Evaluation of the effect of Bosentan treatment on proinflammatory cytokine serum levels in patients affected by Systemic Sclerosis. Int J Immunopathol Pharmacol 2011; 24(1):261-4.
55. Tammaro A, Narcisi A, Persechino S, De Marco G, Camplone G. Contact allergy to disperse blue dye in goggles for swimming-bath. Eur J Inflamm 2011; 9:83-84.
56. Steenwinckel V, Louahed J, Lemaire MM, et al. IL-9 promotes IL-13-dependent paneth cell hyperplasia and up-regulation of innate immunity mediators in intestinal mucosa. J Immunol 2009; 182:4737-43.
57. Veda P. Why are neutrophils polymorphonuclear? Eur J Inflamm 2011; 9:85-93.
58. Li XF, Guo YJ, Wang ML,et al. Inducing-apoptotic activity of the ethanol extract of Duchesnea indica Focke on treatment of herpes simplex encephalitis. Int J Immunopathol Pharmacol 2011; 24:631-8.
59. Salini V, Conti P. Inflammatory markers: serum amyloid A, fibrinogen and C-reactive protein – a revisited study. Eur J Inflamm 2011; 9:95-102.
60. Giganti MG, Minella D, Testa B, et al. A pilot study on the transcriptional response of androgen- and insulin-related genes in peripheral blood mononuclear cells induced by testosterone administration in hypogonadal men. J Biol Regul Homeost Agents 2011; 25:291-4.
61. Nouri-Aria KT, Pilette C, Jacobson MR, Watanabe H, Durham SR. IL-9 and c-Kit+ mast cells in allergic rhinitis during seasonal allergen exposure: effect of immunotherapy. J Allergy Clin Immunol 2005; 116:73-9.
62. Tremolada S, Delbue S, Ferraresso M, Carloni C, Elia F, Larocca S, Bortolani E, Ferrante P. Search for genomic sequences of microbial agents in atherosclerotic plaques. Int J Immunopathol Pharmacol 2011;24(1):243-6.
63. Symeonidou I, Hatzistilianou M, Papadopoulos E, et al . Susceptibility and resistance to canine leishmaniosis is associated to polymorphisms of the canine TNF-α gene. Eur J Inflamm 2011; 9:23-29.
64. Gallenga PE, Del Boccio M, Rapinese M, Di Iorio A, Toniato E, Martinotti S. Molecular approach by PCR is the best method to detect the presence of

Chlamydia trachomatis and to define the true agent of ocular bacterial inflammation. Int J Immunopathol Pharmacol 2011; 24:285-96.

65. Demoulin JB, Louahed J, Dumoutier L, Stevens M, Renauld JC. MAP kinase activation by interleukin-9 in lymphoid and mast cell lines. Oncogene 2003; 22:1763-70.
66. Rossi A, Iorio A, Scali E, Fortuna MC, Mari E, Palese E, Greco P, Carlesimo M. Monilethrix treated with minoxidil. Int J Immunopathol Pharmacol 2011; 24(1):239-42.
67. Hossein-Nezhad A, Mirzaei K, Aslani S, Tootee A, Karimi F. MIF expression in induced peripheral blood mononuclear cells by vitamin D3 and its potential correlation with resting metabolic rate in obesity. Eur J Inflamm 2011; 9:125-34.
68. Rigante D, Zampetti A, Bersani G, Candelli M, Piras A, Rendeli C, Antuzzi D, Feliciani C, Stabile A. Serum interleukin-18 in children with Henoch-Schönlein purpura: a promising marker of disease activity. Eur J Inflamm 2011; 9:157-168.
69. McDermott JR, Bartram RE, Knight PA, Miller HR, Garrod DR, Grencis RK. Mast cells disrupt epithelial barrier function during enteric nematode infection. Proc Natl Acad Sci USA 2003; 100:7761-6.
70. Silambarasan G, Ramanathan T, Nabeel MA, Kalaichelvan VK, Kathiresan K, Balasubramanian T. Anti-inflammatory activity of the marine cyanobacterium *trichodesmium erythraeum* against carrageenan-induced paw oedema in wistar albino rats. Eur J Inflamm 2011; 9:53-56.
71. Soussi-Gounni A, Kontolemos M, Hamid Q. Role of IL-9 in the pathophysiology of allergic diseases. J Allergy Clin Immunol 2001; 107:575-82.
72. Benucci M, Saviola G, Baiardi P, Manfredi M, Sarzi-Puttini P, Atzeni F. Efficacy and safety of leflunomide or methotrexate plus subcutaneous tumour necrosis factor-alpha blocking agents in rheumatoid arthritis. Int J Immunopathol Pharmacol. 2011; 24(1):269-74.
73. De Amici M, Villani MA, Milanesi E, Rossini B, Barco S, Gerletti M, Ciprandi G. Adverse reactions to anaesthetics prevented by the use of specific laboratory tests Eur J Inflamm 2011; 9:79-81
74. Jones TG, Hallgren J, Humbles A, Burwell T, Finkelman FD, Alcaide P, Austen KF, Gurish MF. Antigen-induced increases in pulmonary mast cell progenitor numbers depend on IL-9 and CD1d-restricted NKT cells. J Immunol 2009; 183:5251-60.
75. Re M, Magliulo G, Tarchini P, Mallardi V, Rubini C, Santarelli A, Lo Muzio L. p53 and BCL-2 over-expression inversely correlates with histological differentiation in occupational ethmoidal intestinal-type sinonasal adenocarcinoma. Int J Immunopathol Pharmacol 2011; 24:603-9.
76. Tripodi D, D'Ercole S, Pasini M, Nastasio S, Bonini S, Giuca MR. Inflammatory and immunitary modifications in saliva of subjects with labial and tongue piercing. Eur J Inflamm 2011; 9:185-191.
77. Neill DR, McKenzie AN. TH9 cell generation. TH9: the latest addition to the expanding repertoire of IL-25 targets. Immunol Cell Biol 2010; 88:502-4.
78. Bruzzese V. Therapeutic effectiveness of minimal doses of rituximab in a patient with rheumatoid arthritis. Int J Immunopathol Pharmacol.2011; 24(1):265-7.
79. Guillén D, Millán O, Brunet M. *In vitro* studies of the immunomodulatory effects of statins alone and in combination with immunosuppressive drugs. Eur J Inflamm 2011; 9:117-124.
80. Noelle RJ, Nowak EC. Cellular sources and immune functions of interleukin-9. Nat Rev Immunol 2010; 10:683-7.
81. Arendse B, Van Snick J, Brombacher F. IL-9 is a susceptibility factor in Leishmania major infection by promoting detrimental Th2/type 2 responses. J Immunol 2005; 174:2205-11.
82. Altorjay I, Veréb Z, Serfozo Z, et al. Anti-TNF-alpha antibody (infliximab) therapy supports the recovery of eNOS and VEGFR2 protein expression in endothelial cells. Int J Immunopathol Pharmacol 2011; 24:323-35.
83. Fallon PG, Jolin HE, Smith P, Emson CL, Townsend MJ, Fallon R, Smith P, McKenzie AN. IL-4 induces characteristic Th2 responses even in the combined absence of IL-5, IL-9, and IL-13. Immunity 2002; 17:7-17.
84. Goswami R, Kaplan MH. A brief history of IL-9. J Immunol 2011; 186:3283-8.
85. Middleton Jr E, Kandaswami C, Theoharides TC.The effects of plant flavonoids on mammalian cells: implications for inflammation, heart disease and cancer. Pharmacol Rev 2000; 52:673-751.

EFFECTIVE PROPERTIES OF A STURGEON-BASED BIOACTIVE COMPOUND ON STRESS-INDUCED HIPPOCAMPAL DEGENERATION AND ON *IN VITRO* NEUROGENESIS

F. MAROTTA[1], D.H. CHUI[2], H. YADAV[3], A. LORENZETTI[1], G. CELEP[4], S. JAIN[3], A. BOMBA[5], A. POLIMENI[1], K. ZHONG[2] and F. ALLEGRI[5]

[1]ReGenera Research Group for Aging-Intervention, Milano, Italy; [2]Neuroscience Research Institute, Peking University, Beijing, China; [3]NIDDK, National Institute of Health, Bethesda, USA; [4]Gazi University, Nutrition and Food Technology Division, Ankara, Turkey; [5]Institute of Experimental Medicine, Pavol Josef Safarik University of Kosice, Slovakia; [6]Internal Medicine Dept, FBF Hospital, Milano, Italy

Received April 4, 2012 – Accepted July 13, 2012

The aim of this study is to test the activity of a marine bioactive compound containing high-purity caviar-derived DNA, collagen elastin and protein extracts from sturgeon (LD-1227, Caviarlieri, Laboratoires Dom, Switzerland) to exert neuroprotective properties in an experimental setting while also being potential triggers of neurogenesis in a separate *in vitro* study. Supplementation with high-DHA mixture of LD-1227 was applied for 30 days to stress model rats. Both supplementations significantly mitigated the histological brain damage when analyzing hippocampal subregions and corticosterone level. However, LD-1227 was most significantly efficient in preventing SOD, Catalase and ascorbic acid decrease in brain tissue. Both supplementations stimulated neurogenesis *in vitro* and neuron markers in particular but og olygodendrocyte markers and glia increased only in LD-1227-enriched medium. Taken together, these data suggest that LD-1227 is able to significantly protect the brain structure redox system to higher degree than DHA. Moreover, from *in vitro* study it appears that marine bioactive compound, through it wide array of small unsaturated fatty acids, phospholipids and neurotransmitter precursors, is likely to influence neuronal and glial lineage to act differently from a DHA-rich mixture.

While low levels of reactive oxygen species (ROS) and reactive nitrogen species (RNS) have a physiological effect on cellular functions including neuronal plasticity (1) when in excess, they bring about oxidation/nitrosylation of lipids, proteins, and nucleic acids finally ensuing in neuronal cell death. Thus, the delicate balance between pro- and antioxidant reactions is critical for maintaining normal neuronal function. In this regard, antioxidants have been proposed for treating the neurodegenerative disorders of normal aging.

As a matter of fact, the nervous system is extremely enriched with a huge array of complex lipids which are not fully known but among which polyunsaturated fatty acids (PUFAs) prevail (2). The docosahexaenoic acid [22:6(n-3)] (DHA) content of brain is much more elevated than the EPA content, and DHA is a major component of neuronal membrane phospholipids. Since the membrane phospholipid fatty acid composition is essential for the configuration and function of neurotransmitter receptors, DHA has been suggested to be the most

Key words: LD-1227, neuroprotection, stress-induced neurodegeneration, neurogenesis

Mailing address:
Prof. Francesco Marotta, MD, PhD
Piazza Firenze, 12
20154 Milano, Italy
Tel/fax +39 02 4077243
e-mail: fmarchimede@libero.it

0393-974X (2012)

important n-3 fatty acid for brain function (3, 4). Indeed, DHA is the most abundant (n-3) fatty acid in the mammalian brain, and its levels in brain membrane lipids are altered by the type and amount of fatty acids in the diet increasing with development and decreasing with aging (5). Despite their abundance in the mammalian brain, *de novo* synthesis of PUFAs such as arachidonic acid (AA) and docosahexanoic acid (DHA) does not occur. Thus, the diet is the sole source of these fatty acids or their precursors and, fatty acid preparations with high DHA content have shown a favourable effect on brain function (6). The antioxidant (7) as well as anti-inflammatory properties (8) of PUFA have been documented. Interestingly, it has been suggested that PUFA is an important modulator for unfolded protein-aggregation in relation to disease pathogenesis (9). Moreover, also marine collagen has antioxidant properties that have been used to prevent or tentatively repair the damage caused by environmental factors (10), as well as damage associated with the aging process although basic-science evidence is still limited. Very recently it has also been shown that PUFA increase cortisol transport in the blood-brain-barrier models thanks to membrane fluidification and some effect on tight junction integrity (11). Indeed, imbalances in the level of circulating glucocorticoids during both development and adulthood have been shown to alter the physiology as well as main functional properties of the hippocampus related to learning and memory processes. Under stress and exogenous administration, glucocorticoids induce several catabolic responses and damage to the hippocampus. Quite recently, using the C17.2 cell line as a model to study developmental neurotoxicity *in vitro*, it was shown that glucocorticosteroids can increase cellular sensitivity to oxidative stress and also alter the phenotype of neural stem cells (NSCs) (12). NSCs are defined as undifferentiated cells that can both self-renew and generate the three major cell types that constitute the CNS, i.e. neurons, astrocytes and oligodendrocytes (13, 14) which are distinctly identifiable through specific molecular probes. The quiescent neural progenitors are regarded as being the multipotent stem cells residing on the hippocampus (15) and adult hippocampal neurogenesis represents an important and, until recently, underestimated form of neuroplasticity, specifically in the hippocampal development, a brain structure involved in several neuropsychiatric disorders (16). Thus, NSCs exist as radial glia or as matrix cells in the ventricular zone (VZ) of the neural tube and recent evidence has shown that NSCs continue to undergo neurogenesis in adult mammalian brain (17) including human brain (18).

The aim of the present study is to test the activity of LD-1227 (containing high-purity caviar-derived DNA, collagen elastin and protein extracts from sturgeon, LD-1227, Caviarlieri, all extracted and processed under strict quality-controlled procedures, Laboratoires Dom, Switzerland) to exert neuroprotective properties in an experimental setting while also being potential triggers of neurogenesis in a separate *in vitro* study.

MATERIALS AND METHODS

Sprague-Dawley rats weighing 120±7 gm were housed in laboratory and water was available ad-libitum. They were housed in separate cages in a 12-hour light/dark cycle. Rat weights were measured weekly throughout the study. Rats were randomly divided into four groups and fed regular rat chow pellets (control) while the remaining three received a diet enriched as below indicated.

Stress protocol: Rats were kept in ventilated small tightly fit plastic box for 4 hours a day, where they were unable to move, for 30 days. Colonic/Rectal temperature were measured immediately before and after the stress and other hyperactivity signs such as prostration, salivation, etc., were also recorded. Gastric ulcerations or erosions were observed in all the animals to confirm the stress. Rats were subjected to immobilization stress and given:

A. regular chow food (n. 20)

B: a natural fish oil rich in DHA (10 mg, 7.7% EPA and 28.0% DHA) in their regular diet (n 20)

C: LD-1227 orally (10 mg) in their regular diet (n 20).

All the groups received drug treatment between 10.00 a.m. and 12.00 noon. Treatment was continued up to 30 days and on the 31st day the rats were sacrificed. Healthy animals, fed regular chow food served as unstressed-control.

Tissue preparation

The animals were sacrificed by decapitation and blood was collected in a sterilized vial, the brain was quickly removed and placed in ice cold phosphate buffer saline (PBS). Tissue was maintained at 4°C throughout the preparation. Brain was rinsed in PBS (3 X 3 changes) to remove the blood. After cooling down for at least 5

minutes, the brain was dissected on the ice to obtain the cerebral hemispheres. The tissue was weighed, then diluted ten times in cold 100 mM phosphate buffer at pH 7.2. Tissue was then grounded in a Teflon mechanical homogenizer, the homogenate was spun at 10,000 x g for 15 min and the supernatant was used for enzymatic assay. Serum obtained from the blood was used for the glucocorticoid estimation.

Histological study

Animals were fixed by transcardial perfusion using phosphate buffer saline (pH 7.2) followed by 4% paraformaldehyde prepared in phosphate buffer pH 7.4. After perfusion the brain tissue was dissected and was kept in 4% paraformaldehyde solution at 4°C for 8 h. Brains were then processed for paraffin embedding. Paraffin embedded serial sagittal sections of 10 mm thickness passing through the hippocampal subregion (bregma:2.3 mm to 4.3 mm) were stained for degenerating neurons using the silver impregnation method. Separate series of sections were also stained by cresyl violet to stain the neuron cell bodies. Further, neuronal cell count was performed using an ocular micrometer, and the crude count was subjected to the Abercombie's formula to get the absolute neuronal count.

Biochemical assays

Superoxide dismutase activity (SOD) was measured at 560 nm as the rate of suppression of reduction of nitrotetrazolium blue and for 1 unit of activity, the amount of protein was taken which provided 50% inhibition of nitrotetrazolium blue reduction under standard conditions. Catalase (CAT) activity was calculated at 240 nm by measuring the rate of H_2O_2 utilization with the molar extinction coefficient for H_2O_2 being 43.6 M^{-1} cm^{-1}. The amount of the enzyme utilizing 1 µmol H_2O_2 per min was taken as 1 activity unit.

Malondyaldehyde (MDA) determination: tissue MDA was assayed by the spectrophotometric method and the concentration of thiobarbituric acid was calculated by the absorbance coefficient of MDA-TBA complex 1.56 x 10^5 cm^{-1} M^{-1} and expressed in nmol/ml. The amount of phosphorus released by the enzymes was calculated as a quantitative measure of the activities of total ATPase.

Ascorbic acid measurements were made by high-pressure liquid chromatography with ultraviolet detection. Plasma MDA concentrations were also determined by high-performance liquid chromatography with ultraviolet detection. Blood was collected in EDTA-coated tubes kept in ice and centrifuged at 1000 x g for 20 min. at 4°C. Plasma was separated and aliquots were stored at –70°C for corticosterone estimation. A High Performance Liquid Chromatography (HPLC)/Ultraviolet (UV) system was used for quantification of plasma corticosterone using dexamethasone as an internal standard. Briefly, 500 µL of plasma containing a known quantity of dexamethasone was extracted with 5 mL of dichloromethane (DCM). The DCM extract was evaporated to dryness and dissolved in 100 µL of the mobile phase. Twenty microliters of the extract was injected into an HPLC system for quantification. The mobile phase consisted of methanol:water (70:30) at a flow rate of 1.2mL/min and corticosterone was detected at 250 nm using a UV detector. A gradient HPLC with a LC-10AT pump, UV detector and RP-C18 column (250 mm x 4.6 mm ID; Gemini 5 µm 110A) was used.

In vitro neurogenesis: effect of LD-1227

In a separate set of experiment DHA or LD-1227 were mixed with PBS (25% w/v) and shaken slowly ovemight at 4°C. The mixture was centrifuged at 12,000 r g for 10 min at 4°C, and the supernatant was further diluted with culture medium and used in the experiments.

Primary cultures. NSCs were obtained from the telencephalon of 20-day-old rat embryos, and cultured in proliferation medium containing equal volumes of Dulbecco's modified Eagle's minimum essential medium and F12 medium supplemented with insulin (25pg/mL), apotransferrin (100pg/mL), progesterone (20 nM), putrescine (100 µM), selenium (30 nM), and basic flbroblast growth factor (FGF-2; 10ng/ml). Cultures were replenished with fresh proliferation medium every day and passaged 5 days after seeding. For the differentiation experiments, the cells were plated on coverslips coated with poly-L-ornithine, and cultured in FGF-2-free differentiation medium. This is because NSCs proliferate vigorously as neurospheres in the presence of FGF-2, but stop proliferation and differentiate when FGF-2 is withdrawn from the culture medium.

Immunocytochemical assay

For fluorescence immunostaining, cells were fixed for 3 min by adding an equal volume of 4% (w/v) paraformaldehide solution in 0.1 M phosphate buffer (pH7.4) to the culture medium, and post-fixed for 10 min with the same fixative solution. After washings with PBS, the cells were treated with PBS containing 2% w/v skim milk for 30 min to reduce non-specific antibody binding. They were then reacted with primary antibody at 4°C overnight. The primary antibodies included anti-neuron-specific class III B-tubulin (Tuj1) mouse antibody (R & D Systems, Minneapolis, MN, USA), anti-2',3'-cyclic nucleotide 3'-phosphodiesterase (CNPase) mouse antibody (Sigma, St. Louis, MO, USA) and anti-glial fibrillary acidic protein (GFAP) rabbit antibody and anti-nestin mouse antibody (BD Biosciences Pharmingen, San Diego, CA, USA). After washing for 5 min with PBS, the

cells were incubated with Alexa Fluor 4S8-conjugated anti-mouse antibodies (1.0µg/mL. Nakalai Tesque, Inc. Japan for 2 h at room temperature, washed with PBS and mounted in Permafluor (Thermo Fisher; Waltham, MA, USA).

Statistical analyses

The SPSS 10.1 software package (SPSS, Inc., Chicago, Illinois, USA) was used for the statistical analyses. Multiple comparisons were made by one-way ANOVA followed by the post hoc least square test. *p*-values <0.05 were adopted as significant. Data are presented as mean ± SD.

RESULTS

Stress-induced neuronal cell death in hippocampus: effect of LD-1227 supplementation

Light microscopic studies: Hippocampal sublayers were identified using stereotaxic coordinates as described by Paxinos and Watson (19). Silver stained sections from the control rats passing through the hippocampal subregion demonstrated normal neuronal morphology. Cells in Ammon's horn were arranged compactly in tiers (3-5 cells thick), no silver impregnated cells were observed. Cells in dentate gyrus exhibited specific morphological characteristics of granule cells and were stacked approximately 4-10 cells deep. These cells were comparatively smaller than the pyramidal cells. Polymorphic, fusiform and modified pyramidal cells in the hilus of Dg demonstrated their normal neuronal characteristics. No degenerating cells were observed in any of the six layers of hippocampus (Oriens, Radiatum, L Moleculare and Molecular cell layer. Group A: Animals subjected to stress for 4 hours demonstrated neuron cell degeneration in the CAl, CA2, CA4 and also in Dg of hippocampus. Nerve cell degeneration was observed in almost all the six layers of hippocampus. Cell bodies of the oriens cell layer (Or) demonstrated approximately l5% degeneration where most of the cell bodies were stained dark. Pyramidal cells (Py) in CAl, CA2, CA4 demonstrated degenerating characteristics, although the cellular processes was not stained clearly. Quantitative data for cell count are reported in Table I. No degeneration was found in the radiatum (Rad) layer, Lacunosum moleculare layer (L Mol) or the Molecular (Mol) layer.

In group B and C the number of degenerating cell bodies were significantly reduced and to a comparable extent. Cell bodies of all the six layers of the hippocampus demonstrated normal neuronal morphology. Cells in the Ammon's horn were found to be stacked 3-5 layers deep and the granule cells

Table I. *Cell count in hippocampal subregion: effect of LD-1227.*

Hippocampal sublayers	Experimental Groups			
	Control	**A**	**B**	**C**
CA1	299 ± 16	184 ± 9*	278 ± 12**	273 ± 3**
CA2	63 ± 11	32 ± 4 *	53 ± 7**	50 ± 3**
CA3	193 ± 13	130 ± 8 *	189 ± 13**	184 ± 17**
CA4	62 ± 6	44 ± 3 *	56 ± 9**	51 ± 4**
Dg	628 ± 16	386 ± 19 *	465 ± 15**	503 ± 22**

** p<0.01 vs control; ** p<0.05 vs group A.*

Table II. *Effect of LD-1227 on redox balance during stress.*

	Experimental Groups			
	Control	**A**	**B**	**C**
Protein (mg/ml)	0.3 ± 0.09	0.3 ± 0.08	0.3 ± 0.1	0.2 ± 0.07
Corticosterone (µg/100ml)	81 ± 1.5	158 ± 8.5 *	122 ± 2.4 **	129 ± 9.3 **
Ascorbic acid (mg/100ml)	2.4 ± 0.5	1.4 ± 0.6 *	1.9 ± 0.8	2.5 ± 0.7 ***
SOD	77 ± 9.8	51 ± 12.2 *	63 ± 11.4	75 ± 11.7 ***
Catalase (µmol H_20_2/min/ mg protein)	20 ± 6.2	12 ± 2.1 *	14.8 ± 2.3	17 ± 1.7 ***
MDA (nmol/ml)	1.9 ± 0.9	2.9 ± 0.6 *	1.8 ± 0.6 **	1.6 ± 0.3**

** p<0.01 vs control; ** p<0.05 vs group A and ***p<0.05 vs group A and B.*

of Dentate gyrus were 4-10 deep and arranged in the form of tire. The small cell layer (Or, Rad, L Mol and Mol) of the hippocampus also demonstrated normal neuronal morphology (data not shown).

Biochemical studies

Results showed that corticosterone activity was significantly increased (156.6µg/100ml) in rats after applying the stress regimen. Corticosterone level almost doubled in stressed animals and both treatments brought about a comparable partial improvement ($p<0.01$ *vs* stressed animals). Ascorbic acid content in the brain tissue, which can be a preliminary marker of stress, decreased in stress treated animals (1.4mg/100ml) as compared to healthy controls (2.4mg/100 ml of tissue; $p < 0.01$). After treatment with both supplements, an increase in the ascorbic acid content was observed but this reached a statistic significance only in LD-1227-treated animals ($p < 0.01$). Accordingly, the SOD activity was significantly decreased by more than 33% in stressed animals compared to the controls ($p < 0.005$), and it was restored only in C group ($p<0.05$ *vs* B group, $p<0.001$ *vs* A group). Catalase level in the experimental groups demonstrated a significant change as compared to control with a decrease in the A group by 40% and was restored only in C group ($p<0.05$ *vs* B group, $p<0.01$ *vs* A group). The spontaneous MDA activity was the highest in the stress group (2.9nmoles/ml) when compared to respective concentration of MDA in rats treated with either supplement in which the content normalized (A group *vs* healthy control: $p <0.001$) (Table II).

In vitro effect of LD-1227 on differentiation of NSCs

Both DHA and LD-1227 significantly increased the percentage of Tujl-positive cells (neurons) and decreased that of nestin-positive undifferentiated cells ($p<0.01$). However, only LD-1227 also determined a significant increase of CNPase-positive cells (oligodendrocytes) and GFAP-positive cells (astrocytes) in the total cell population ($p<0.01$, Fig. 1). We also examined the ratio of nestin-positive cells to total cells after treatment with either DHA

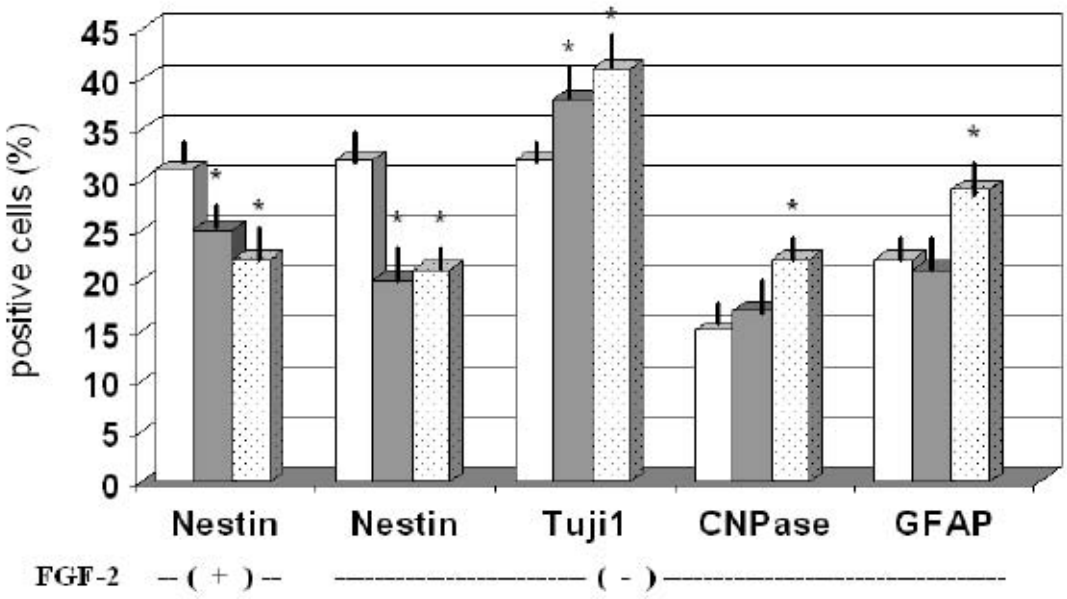

Fig. 1. *Effect of LD-1227 on NCSc. White bars: unsupplemented control; Grey bars: supplemented with DHA; Dotted bars: supplemented with LD-1227. Panel **A**) ratio of nestin-positive cells over total cell population. * p<0.01; Panel **B**) effect of DHA and LD-1227 in a FGF-2-deprived medium, * p<0.01*

or LD-1227 in the proliferation or differentiation medium. The ratio was essentially the same in both circumstances (Fig. 1), suggesting that both supplements facilitated cell differentiation rather than maintaining cell survival. Exposure of the cells to LD-1227 after the removal of FGF-2 increased the percentage of Tujl-positive cells and simultaneously decreased that of CNPase-positive or GFAP- positive cells.

DISCUSSION

Stress is an unavoidable phenomenon that affects the body system at various levels and chronic stressful events lead to consistent hyperactivity of the HPA axis which in turn leads to increased secretion of adrenocorticotrophic hormone (ACTH) from adenohypophysis (19). These phenomena are known to adversely influence the regular psychosomatic homeostasis responsible for the pathogensis of several psychiatric disorders. Various biological amines such as catecholamines, histamine and 5-HT have been implicated in the regulation of the HPA-axis (20). Their effects on ACTH are largely indirect, exerted via activation of hypothalamic corticotrophin releasing hormone (CRH) neurons (21). In this context, plasma corticosterone level, being a direct quick-acting stress effector, is regarded as an important marker to evaluate stress response. The elevated plasma corticosterone under stressful conditions is necessary to maintain the energy balance.

However, exposure to elevated glucocorticoid concentrations increases the toxicity of free radicals and both of these factors go hand in hand in damaging the hippocampal neurons during stress. Results demonstrated that exposure to specific stress produces degenerative changes in neuron cell bodies of hippocampal subregions CAI-CA4 and Dg. These changes are correlated with disruption of antioxidant defence mechanism, i.e., decrease in antioxidant enzymes, viz., SOD and CAT and increase in MDA level which indicate high lipid peroxidation, indicative of cellular damage. Study also shows

that treatment with LD-1227 significantly reduces the degenerating cell bodies in selective areas of hippocampal subregions of female rats. Although cell bodies with degenerative characteristics were present in all the subregions, significant effect of the treatment was observed in Cal and CA4 only. Decrease in the antioxidant profile after stress exposure and the restoration of the same after the treatment also provides necessary evidence in favor of not only the antioxidant but also the neuroprotective properties of LD-1227. Thus, it appears that the glucocorticoid-modulating and free radical scavenging activity of LD-1227 work concomitantly in preventing the stress-induced neuronal loss. These data are somewhat in accordance with the observation that patients consuming 25-g ordinary Scandinavian caviar paste daily for 3 weeks improved the beneficial fatty acids profile and lipid peroxidation markers (22). In particular, caviar has an extremely rich array of triglycerides and phospholipids containing more n-3 fatty acids, especially eicosapentaenoic and docosahexaenoic acid, than n-6 fatty acids together with good amounts of copper and zinc (23). Interestingly, these effects cannot be ascribed only to DHA content since the overall beneficial effect of LD-1227 was significantly more considerable than DHA even when used at high concentration.

The results of the present study demonstrate that the antioxidant capacity of nerve cell bodies is decreased after stress. Concomitant decrease in the SOD activity indicates that superoxide radicals damage the cells during the elevated levels of glucocorticoids and the same can also be presumed for the peroxide ions, as a decrease in catalase activity and an increase in the MDA content were also observed. Such abnormalities were improved by both supplementations but the data obtained by using LD-1227 were significantly more consistent ($p<0.05$ *vs* B group).

Elevated levels of endogenous glucocorticoids during aging and chronic stress have been reported to induce nerve cell degeneration in hippocampus and in certain other areas (24). Glucocorticoid-induced neuroendangerment consistently correlates with the disruption of the energy pathways and cellular antioxidant status is closely related to cellular energy state and energy deficits increase the basal level of ROS. Glucocorticoids have indeed been implicated as a regulatory factor for the antioxidant enzymes. It is therefore possible that the levels of protective antioxidant enzymes in neuronal tissue may be affected by presence of glucocorticoids. Indeed, McIntosh et al. (25) demonstrated that exogenous elevation of glucocorticoids in adrenalectomized rats lowers the antioxidant capacity of the brain tissue in a region-specific manner.

It has also been recently shown that oxidative stress of neurons and neuronal progenitor cells is improved by omega-3 and omega 6 (26). Moreover, recent work has demonstrated that PUFA supplementation stimulates the expression of neuronal hemeoxygenase-1, a stress-sensitive protein inducible by oxidative stress (27).

Thus, it is of interest to note from our *in vitro* study an interesting property of LD-1227, i.e. that it facilitates the differentiation of whole sets of brain cells (neurons, astrocytes and oligodendrocytes). The observed reciprocal response between neuronal and glial populations suggests that LD-1227 affected a neuronal lineage of the neural progenitor cells having the ability to generate both neuronal and glial cells. Thus, LD-1227 hypothetically committed neural progenitors to the fate of neuronal lineage similarly to BDNF. Kawakita et al. (28) recently reported that DHA promotes neuronal differentiation of NSCs in culture, and directly stimulates the neurogenesis in the dentate gyrus of the hippocampus. As suggested by this present study, LD-1227 may be able to stimulate neurogenesis in the mature brain and play a role even more significant than DHA even when administered at higher dosage. Although it is now indisputably accepted that neurogenesis occurs in the adult brain, its functional relevance still remains to be fully established. While it is clear that this phenomenon is confined to very discrete brain regions, the generation of new neurons in the post-natal period constitutes a new dimension of plasticity, with both direct and indirect impact on neuronal remodelling and repair. Notably, abnormal alterations in the hippocampal neurogenesis process have been implicated in several neuropsychiatric disorders (29). We suggest that LD-1227 contains multiple active components that differently influences neuronal and glial lineage although the nature of its likely multiple intracellular signals that regulate the fate of NSCs will be a matter of future

studies, as it has been recently outlined for DHA (30). One cannot rule out that LD-1227 may contain other smaller unsaturated fatty acids, structural phospholipids and neurotransmitter precursors, which may pass through blood-brain barrier and which remain to be defined by further ongoing studies. A further limitation in this study is the lack of a more detailed neurosteroid and hormonal status assessment as well as an immunohistochemistry analysis of neurodegeneration findings and Western blots for redox maker proteins.

REFERENCES

1. Kishida KT, Klann E. Sources and targets of reactive oxygen species in synaptic plasticity and memory. Antioxidants and Redox Signaling. 2007; 9:233-44.
2. Salem N Jr, Litman B, Kim HY, Gawrisch K. Mechanisms of action of docosahexanoic acid in the nervous system. Lipids 2001; 36:945-59.
3. Stevens LJ, Zentall SS, Abate ML. Omega-3 fatty acids in boys with behavior, learning and health problems. Physiol Behav 1996; 59:915-20.
4. Willats P, Forsyth JS, DiModugno MK. Effect of long-chain polyunsaturated fatty acids in infant formula on problem solving at 10 months of age. Lancet 1998; 352:688-91.
5. Guisto NM, Salvador GA, Castagnet PI. PAsquare SJ, Ilincheta de Bschero MG. Age-associated changes in central nervous system glycerophospholipids composition and metabolism. Neurochem Res 2002; 27:1513-23.
6. Birch EE, Hoffman DR, Uauy R, Birch DG, Prestidge C. Visual acuity and the essentiality of docosahexaenoic acid and arachidonic acid in the diet of term infants. Pediatr Res 1998; 44:201-9.
7. Saw CL, Huang Y, Kong AN. Synergistic anti-inflammatory effects of low doses of curcumin in combination with polyunsaturated fatty acids: docosahexanoic acid or eicosapentanoic acid. Biochem Pharmacol 2010; 79:421-30.
8. Kim YJ, Takahashi R. Role of polyunsaturated fatty acids for misfolding protein aggregations: implication for neurodegenerative diseases. Ann NY Acad Sci 2006; 1086:11-20.
9. Richter-Landsberg C, Goldbaum O. Stress proteins in neural cells: functional roles in health and disease. Cell. Mol. Life Sci 2003; 60:337-49.
10. Zhao M, Zhang Z, Liang J, Li Y. Protective effect of marine collagen peptide on liver and renal injuries in diabetic rats induced by alloxan. Wei Sheng Yan Jiu 2010; 39:147-9.
11. Navarro C, González-Álvarez I, González-Álvarez M, Manku M, Merino V, Casabó VG, Bermejo M. Influence of polyunsaturated fatty acids on Cortisol transport through MDCK and MDCK-MDR1 cells as blood-brain barrier in vitro model. Eur J Pharm Sci 2011; 42:290-99.
12. Mutsaers HA, Tofighi R. Dexamethasone enhances oxidative stress-induced cell death in murine neural stem cells. Neurotox Res 2012; 22(2):127-37.
13. Okano H. Neural stem cells: progression of basic research and perspective for clinical application. Keio J Med 2002; 51:115-28.
14. Okano H. Stem cell biology of the central nervous system. J Neurosci Res 2002; 69:698-707.
15. Seri B, Garcia-Verdugo JM, Collado-Morente L, McEwen BS, Alvarez-Buylla A. Cell types, lineage, and architecture of the germinal zone in the adult dentate gyrus. The J Comp Neurol 2004; 478:359-78.
16. Hsieh J, Eisch AJ. Epigenetics, hippocampal neurogenesis, and neuropsychiatric disorders: unraveling the genome to understand the mind. Neurobiol Dis 2010; 39:73-84.
17. Temple S, Alvarez-Buylla A. Stem cells in the adult mammalian central nervous system. Curr Opin Neurobiol 1999; 9:135-41.
18. Eriksson PS, Per_lieva E, Bjork-Eriksson T, Alborn AM, Nordborg C, Peterson DA, Gage FH. Neurogenesis in the adult human hippocampus. Nat Med 1998; 4:1313-17.
19. Paxinos G, Watson CR, Emson PC. AChE-stained horizontal sections of the rat brain in stereotaxic coordinates. J Neurosci Methods 1980; 3:129-49.
20. Naka H, Nakamura, Shimazaki, T, Okano, H. Requirement for COUP-TFI and II in the temporal specification of neural stem cells in central nervous system development. Nat Neurosci 2008; 11:1014-23.
21. Tanaka, EM, Ferretti P. Considering the evolution of regeneration in the central nervous system. Nat Rev Neurosci 2009; 10:713-23.

22. Engström K, Wallin R, Saldeen T. Effects of Scandinavian caviar paste enriched with a stable fish oil on plasma phospholipid fatty acids and lipid peroxidation. Eur J Clin Nutr 2003; 57:1052-59.
23. Wirth M, Kirschbaum F, Gessner J, Krüger A, Patriche N, Billard R. Chemical and biochemical composition of caviar from different sturgeon species and origins. Nahrung 2000; 44:233-37.
24. Marchetti B, Serra PA, L'Episcopo F, et al. Hormones are key actors in gene x environment interactions programming the vulnerability to Parkinson's disease: glia as a common final pathway. Ann NY Acad Sci 2005;1 057:296-318.
25. McIntosh LJ, Hong KE, Sapolsky RM. Glucocorticoids may alter antioxidant enzyme capacity in the brain: baseline studies. Brain Res 1998; 791:209-14.
26. Kim SJ, Zhang Z, Saha A, Sarkar C, Zhao Z, Xu Y, Mukherjee AB. Omega-3 and omega-6 fatty acids suppress ER- and oxidative stress in cultured neurons and neuronal progenitor cells from mice lacking PPT1. Neurosci Lett 2010; 479:292-96.
27. Brand A, Bauer NG, Hallott A, Goldbaum O, Ghebremeskel K, Reifen R, Richter-Landsberg C. Membrane lipid modification by polyunsaturated fatty acids sensitizes oligodendroglial OLN-93 cells against oxidative stress and promotes up-regulation of heme oxygenase-1 (HSP32) J Neurochem 2010; 113:465-76.
28. Kawakita E, Hashimoto M, Shido O. Docosahexaenoic acid promotes neurogenesis *in vitro* and *in vivo*. Neuroscience 2006; 139:991-97
29. Eisch AJ, Cameron Ha, Encinas JM, Meltzer La, Ming G-L, Overstreet-Wadiche LS. Adult neurogenesis, mental health, and mental illness: hope or hype? J Neurosci 2008; 28:11785-91.
30. Ma D, Zhang M, Larsen CP, Xu F, Hua W, Yamashima T. DHA promotes the neuronal differentiation of rat neural stem cells transfected with GPR40 gene. Brain Res 2010; 1330:1-8.

BENEFICIAL EFFECT OF A STURGEON-BASED BIOACTIVE COMPOUND ON GENE EXPRESSION OF TUMOR NECROSIS FACTOR-α, MATRIX METALLOPROTEINASES AND TYPE-10 COLLAGEN IN HUMAN CHONDROCYTES

R. CATANZARO[1], F. MAROTTA[2], S. JAIN[3], R. RASTMANESH[4], F. ALLEGRI[5], G. CELEP[6], A. LORENZETTI[2], A. POLIMENI[2] and H. YADAV[3]

[1]Dept of Internal Medicine, University of Catania, Catania, Italy; [2]ReGenera Research Group for Aging-Intervention, Milano, Italy; [3]NIDDK, National Institute of Health, Bethesda, USA; [4]Shahid Beheshti University of Medical Sciences, National Nutrition and Food Technology Research Institute, Tehran, Iran; [5]Internal Medicine Dept, FBF Hospital, Milano, Italy; [6]Gazi University, Family and Consumer Sciences Department, Nutrition and Food Technology Division, Turkey

Received April 4, 2012 – Accepted July 24, 2012

In the present study, we examined the effect of a marine bioactive compound containing high-purity caviar-derived DNA, collagen elastin and protein extracts from sturgeon (LD-1227, Caviarlieri, Laboratoires Dom, Switzerland) on ILβ -induced activation and production of TNFα and MMP-13 in human osteo-arthritis (OA) chondrocytes and intracellular signaling factors. Human chondrocytes were derived from OA cartilage and stimulated with ILβ. Gene expression of TNFα, MMP-13, MMP-1 and Col10A1 was measured by quantitative RT-PCR. TNFα protein in culture medium was determined using cytokine-specific ELISA. Western immunoblotting was used to analyze the MMP-13 production in the culture medium and the activation of NF-κB. DNA binding activity of NF-κB p65 was determined using a highly sensitive and specific ELISA. MMP-13 activity in the culture medium was assayed by gelatine zymography. LD-1227 significantly decreased ILβ-stimulated gene expression and production of TNFα, MMP-1, MMP-13 and Col10A1 in human chondrocytes. The inhibitory effect of LD-1227 on the ILβ-induced expression of these genes was mediated at least in part via suppression of NF-κB p65. These data show that LD-1227 can inhibit IL-1β-induced proliferation and inflammatory reactions via inhibited activation of the transcription factor NF-κB pathway in human chondrocytes derived from OA patients. These novel pharmacological actions of LD-1227 on ILβ-stimulated human OA chondrocytes provide suggestions that this marine biology compound may inhibit cartilage degradation by suppressing ILβ-mediated activation and the catabolic response in human chondrocytes.

Osteoarthritis (OA) of the knee is very common in middle-aged and elderly people, and knee pain and dysfunction can critically affect the patient's quality of life. About 10% of men over 60 years of age are liable to eventually develop osteoarthritis (1, 2). Indeed, a prospective study of 1000 arthroscopies of the knee joint found cartilage defects in 61% of cases, 44% of these due to osteoarthritis, 28% due to focal cartilage defects, and 2% due to osteochondral defect (3). Osteoarthritis tends to evolve from local inflammatory disease of articular cartilage to progressive degenerative joint disease

Key words: osteoarthritis, chondhrocyte, LD-1227, ILβ-stimulation, marine biology compound

Mailing address:
Prof. Francesco Marotta, MD, PhD
Piazza Firenze, 12
20154 Milano, Italy
Tel./fax: +39 024077243
e-mail: fmarchimede@libero.it

0393-974X (2012)

with inflammation and degeneration that ultimately results in exposure of underlying bone, pain and disability (4). Current medical practice typically uses non-steroidal anti-inflammatory drugs (NSAIDs) to control the pain associated with OA of the knee. However, NSAIDs have some adverse effects on gastrointestinal tract and often cannot be tolerated (5). Therefore, it is advisable to develop alternative methods to reduce the pain associated with OA. Many risk factors that contribute to disease onset have been identified, including systemic factors such as genetics, estrogen use, and bone density, and local biomechanical factors such as muscle weakness, obesity and joint laxity. The most important risk factor for OA besides female sex, obesity and joint trauma is aging (1). Moreover, experimental evidence in OA-prone mice show that exercise can accelerate the process of cartilage degeneration. Indeed, Wang et al. (6) has found that after treadmill training the incidence of OA was 66.7% for C57 black mice in the 12th week and 88.3% in the 20th week. Whatever the causative phenomena, the progressive degeneration of articular cartilage involves depletion of the aggregating cartilage proteoglycan, aggrecan (ACAN) which along with type II collagen (COL2A1) are crucial for the efficient mechanical properties to the cartilage and the regulation of matrix components, such as proteoglycan and collagen (7). In fact, enzymatic cleavage by matrix metalloproteinases (MMPs) is thought to be involved in the destruction of articular cartilage, so the high expression of MMP-13/ collagenase-3 detected in the pathologic synovium and cartilage samples is believed to contribute to OA pathogenesis (8). It is well established that IL-1β stimulates cartilage breakdown (9). Consequently, *in vitro* studies have used this cytokine in models of inflammatory OA (10). Such studies have highlighted the pro-catabolic effects of IL-1 by measuring the expression of inflammatory markers such as MMP levels and cyclooxygenase (COX) and the release of matrix degradation products (11).

IL-1β is implicated in the degeneration of articular cartilage due to its induction of proteoglycan loss and matrix degradation (12) and elevated levels of IL-1 occur in the synovial fluid and cartilage tissue of patients with OA (13), further supporting its role in cartilage breakdown and disease pathogenesis (14). Indeed, the pleoitropic effect of inflammatory cytokines demands a multifaceted regulation to minimize collateral damage to normal tissue. On one hand, inflammatory cytokines such as interleukin 1β (IL-1β) and IL-18 are present as inactive zymogens that need proteolytic cleavage mediated by the so-called "inflammasome" (15). This proteolytic maturation acts concomitantly with NF-κB–dependent transcriptional activation of genes encoding the zymogens to catalyze a considerable increase in the levels of secreted, bioactive proteins. Other inflammatory cytokines such as tumor necrosis factor (TNF) and IL-6 are induced primarily at the transcriptional level and, in the case of TNF, subject to posttranscriptional messenger RNA stabilization through the dissociation of the mRNA-binding protein tristetraprolin from its adenine- and uridine-rich region (16). In recent years it has been shown that polyunsaturated fatty acids may reduce the expression of key proteins in model systems for studying OA (17).

Thus, in the present study we addressed the question of a possible inhibitory effect of LD-1227 (containing high-purity caviar-derived DNA, collagen elastin and protein extracts from sturgeon, LD-1227, Caviarlieri, all extracted and processed under strict quality-controlled procedures, Laboratoires Dom, Switzerland) on IL1β-induced expression and production of TNFα, MMP-13, MMP-1 and COL10A1 in OA chondrocytes.

MATERIALS AND METHODS

Specimen selection

Human chondrocytes were prepared by enzymatic digestion of cartilage obtained from discarded and de-identified cartilage samples obtained from the knee joints of 13 OA patients aged 58 to 77 years (mean age, 66±5.2 years; 11 female and two male Caucasians) who underwent joint replacement surgery at local hospital. These studies were approved as "exempt" and that no informed consent was required. OA was diagnosed according to the American College of Rheumatology criteria (18). Specimens that included the full thickness cartilage and subchondral bone were washed with sterile PBS and the macroscopic cartilage degeneration was determined by staining of femoral head samples with India ink. Portions of the cartilage with smooth articular surface (unaffected cartilage) were used to prepare chondrocytes

Table I. *The modified Mankin scoring system.*

Structure	Score	Cellularity	Score	Matrix staining	Score	Tidemark integrity	Score
Smooth surface/normal	0	Normal arrangement	0	Normal staining	0	Normal and intact	0
Roughened surface/single crack or area of delamination	1	Clustering in superficial layer or loss of cells up to 10 %	1	Slight loss of stain	1	Disrupted	1
Multiple cracks/moderate delamination	2	Disorganisation or loss up to 25%	2	Moderate loss of stain	2		
Fragmentation in cartilage or severe delamination	3	Cell rows absent or loss up to 50%	3	Severe loss of stain	3		
Loss of fragments	4	Very few cells present	4	No stain present	4		
Complete erosion to tidemark	5						
Erosion beyond tidemark	6						

by the pronase and collagenase enzymatic digestion (OA chondrocytes). Primary OA chondrocytes were plated at the seeding density of 1×10^6 cell/35 mm dish and at 80% confluence were used for all the studies. Histological analysis of some of the unaffected cartilage samples was performed on 5-µm-thick sections stained with H & E and Safronin O and graded using the Mankin score (19). Grading of the histology slides (data not shown) revealed that all of the cartilage pieces taken from the unaffected area had a Mankin score <2 for structure and a Mankin score of 1 for cellularity.

Cell culture and chondrogenic phenotype control

Well-preserved cartilage from femoral condyles was used for chondrocyte isolation as described previously (20). The cartilage was minced and digested for 45 min with 9 $U \cdot mL^{-1}$ Pronase (Sigma-Aldrich, USA), and for 14 h with 80 $U \cdot mL^{-1}$ Collagenase type IV (Sigma-Aldrich). After being washed and filtered, the isolated cells were cultivated in complete medium consisting of 1:1 DMEM/Hams F12 supplemented with 10% fetal bovine serum, 0.5% penicillin/streptomycin, 0.5% l-glutamine and 10 $\mu g \cdot mL^{-1}$ 2-phospho-l-ascorbic acid trisodium salt (Sigma-Aldrich, USA). After 24 h incubation, adhered chondrocytes were treated with trypsin (trypsin/EDTA 0.05%/0.02% in PBS) and frozen in complete medium containing 5% dimethyl sulphoxide (DMSO, Roth, Karlsruhe, Germany). We determined whether isolated human OA chondrocytes used in these studies maintained their phenotype – by analyzing the expression of type-2 collagen, aggrecan and SOX-9 mRNA, which are considered to be signatures of the chondrogenic phenotype. Our results show that the employed human OA chondrocytes in monolayer culture maintained their phenotype, when they were plated (1×10^6/ml) in 35-mm culture dishes in complete Ham's F-12 medium with 10% FCS and were allowed to grow at 37°C and 5% CO^2 in a tissue culture incubator, as judged by the continued expression of COL2A1, aggrecan, and SOX-9 mRNAs, whereas COL10A1 mRNA was not expressed (in-house data not shown). Based on these data, OA chondrocytes were used within 72 hours after plating to avoid possible dedifferentiation.

Articular chondrocyte preparation: Cell viability analysis, stimulation with IL-1β and effect of LD-1227

Chondrocytes were treated with LD-1227 (100 µM) and after 24 h the cytotoxicity was examined using a cytotoxicity assay kit (CytoTox-Glo™, Promega, Madison, WI, USA) by evaluating by lactate dehydrogenase (LDH). Kit measures LDH activity present in the culture medium using a coupled two-step reaction. In the first step, LDH catalyzes the reduction of NAD^+ to NADH and H^+ by oxidation of lactate to pyruvate. In the second step of the reaction, diaphorase uses the newly-formed NADH

and H^+ to catalyze the reduction of a tetrazolium salt to highly-colored formazan which absorbs strongly at 490 nm using a microplate reader. The amount of the formazan dye generated by dehydrogenases in cells was directly proportional to the number of living cells. Primary chondrocytes were pretreated with LD-1227 100 μM for 2 h. Chondrocytes cultured without LD-1227 served as controls.

Stimulation of chondrocytes with IL-1β. Recombinant human IL-1β was purchased from R&D System (Minneapolis, Minnesota, USA). Monoclonal antibody (mAb) against NF-kB (p65) and β-actin were purchased from Cell Signaling (Beverly, MD, USA). Fetal bovine serum (FBS) was obtained from Gibco BRL (Life Technologies, Grand Island, NY, USA). Human OA chondrocytes (1×10^6/ml) were plated in 35-mm culture dishes (Becton-Dickinson, Franklin Lakes, NJ, USA) in complete Ham's F-12 medium and put in DMEM starving medium for 1 h then 2-16 h. They were pretreated with the HLM (1-10μg/ml) for 2 h and were then stimulated with IL-1β (5 ng/ml) for 8 h. We chose this dose because from prior in-house dose-depending study of TNFα and MMP-13 mRNA expression induction by IL-1β, we found that the maximum stimulation of chondrocytes occurred at 5.0ng/ml (data not shown). Based on these data, the concentration of 5.0ng/ml was employed for stimulation of chondrocytes in all of our experiments.

An inhibitor of nuclear factor-κB (NF-κB), MG132 (100 μM) was used as a positive control while OA chondrocytes cultured without IL-1β served as blank controls.

Quantitative real-time PCR

Real-time quantitative PCR was used to quantify the expression of mRNA for TNFα, matrix metalloproteinase 13 (MMP13), matrix metalloproteinase 1 (MMP1) and type-10 collagen (COL10A1), with expression of GAPDH as endogenous control. The total RNA of the cells was isolated by the acid guanidinium thiocyanate-phenol-chloroform extraction method using RNAiso plus (Takara Inc, Kyoto, Japan). RNA was then reverse transcribed to cDNA using reverse transcriptase (ReverTra Ace, Toyobo, Osaka, Japan) with Oligo dT primer. For all the genes analysed, the Power SYBR Green PCR Master Mix (Applied Biosystems, Darmstadt, Germany) was used according to the manufacturer's instructions. Primers used for PCR assisted amplification were: TNFα (NM_000595: forward, 5'-AGG ACG AAC ATC CAA CCT TCC CAA-3'; reverse, 5'-TTT GAG CCA GAA GAG GTT GAG GGT-3'), MMP-13 (NM_002427: forward, 5'-CGC CAG AAG AAT CTG TCT TTA AA-3'; reverse, 5'-CCA AAT TAT GGA GGA GAT GC-3'), and GAPDH (NM_002046.3: forward, 5'-TCG ACA GTC AGC CGC ATC TTC TTT-3'; reverse, 5'-ACC AAA TCC GTT GAC TCC GAC CTT-3'), MMP1 (NM_002421: forward, TACATGCGCACAAATCCCTTCTACC; reverse, GAAAAACCGGACTTCATCTCTGTCG) and COL10A1 (NM_000493: forward, 5'-TGA TCC TGG AGT TGG AGG AC-3'; reverse, 5'-GAG ATC GAT GAT GGC ACT CC-3'; expected size of the DNA fragment, 703 bp). The real-time PCR mixture consisted of 2.5 μl of SYBR Green Buffer, 2 mM MgCl2, 1 mM dNTP, 0.01U/ml AmpErase uracil N-glycosylase, 0.05Uμml AmpliTaq Gold (Applied Biosys-tems, part of Life Technologies Co., Carlsbad, CA, USA), forward and reverse primers (200 nM for IL-17A and glyceraldehyde-3-phosphate dehydrogenase, GAPDH), and 2 μl cDNA samples in a total volume of 25 μl. The PCR reactions were performed in a MicroAmp optical 96 well re-action plate for 40 cycles (95°C for 15 sec, 60°C for 1 min) in the ABI Prism 7500 Sequence Detector (Applied Biosystems). The fluorescent signals (δCt) detected during the threshold cycle were recorded by a software. To standardize the target gene level with respect to the variability in RNA and cDNA quality, GAPDH was amplified under the same conditions as an internal control.

Densitometric analysis

For standardization of the gene expression levels determined by TaqMan analysis, mRNA expression was normalized to 18SrRNA expression. PCR products were electrophoresed by using 1% agarose gels and visualized by staining with ethidium bromide. Densitometric analysis was performed on the relative intensity of each band using the Multi Gauge program, version 3.0 (Fuji flm, Tokyo, Japan). This consisted in subtracting threshold cycles (C_T) for ribosomal RNA from the C_T of the targeted gene (ΔC_T). Relative mRNA levels were then calculated as $2^{-\Delta\Delta CT}$, where $\Delta\Delta C_T$ refers to the ΔC_T of unstimulated minus treated cells. The values were obtained from at least three independent series of experiments, in which each treatment was performed in duplicate with each being analyzed twice in RT-PCR. Data were normalized to suitable loading controls and expressed as the mean ± standard deviation followed by appropriate statistical analysis.

Cytokine ELISA assay

TNFα present in the culture medium was quantified using the TNFα-specific ELISA according to the manufacturer's instructions (R&D Systems, Minneapolis, MN, USA). Plates were read at 450 nm using a Synergy HT microplate reader (Biotek Instrument, Winooski, VT, USA).

The assessment of tumor necrosis factor (TNF)*α* was carried out using commercially available ELISA kits (Bio-

Source, Invitrogen Life Sciences, CA). The sensitivity of the assays was <0.8 pg/mL for TNF-α. Each sample was run in duplicate. ELISA assay data (pg cytokine protein) were normalized to μg total protein, which was determined using a bicinchoninic acid (BCA) protein assay kit.

Western immunoblotting

Stimulated and control chondrocytes were washed with cold PBS and lysed using a cell lysis buffer (50 mM Tris-HCl, pH 7.4; 150 mM NaCl; 1% Triton X-100; 0.1% SDS; 0.5% sodium deoxycholate; 1 mM EDTA; 1 mM EGTA; Complete® protease and phosphatase inhibitors). Total lysate or nuclear/cytoplasmic fraction protein (45μg/lane) or concentrated cell culture supernatant was resolved by SDS-PAGE (10% resolving gel with 4% stacking) and was transferred to nitrocellulose membranes (Bio-Rad, Herkules, CA, USA). Membranes were blocked with blocking buffer containing non-fat dry milk powder in Tris-buffered saline and 0.1% Tween-20. Blots were probed with 1:200 to 1:1,000 diluted primary antibodies specific for the target protein. Immunoreactive proteins were visualized using 1:1,000 diluted horseradish peroxidase-linked secondary antibodies and enhanced chemiluminescence (ECL, Amersham Life Sciences, Arlington, IL, USA). Images were captured using AFP-Imaging System (Minimedical Series, Ems Ford, NY, USA). Anti-MMP-13 antibody was purchased from Calbiochem (La Jolla, CA), anti-NF-κB p65 antibody (IMG-150) from Imgenex (San Diego, CA, USA).

Gelatin zymography

Gelatin zymography was performed as follows. Briefly, an equal volume of cell culture supernatant was mixed with non-reducing sample buffer [4% SDS, 0.15 M Tris (pH 6.8), and 20% (volume/volume) glycerol containing 0.05% (weight/volume) bromophenol blue] and resolved on a 10% polyacrylamide gel containing copolymerized 0.2% gelatin (Bio-Rad). Commercially available MMP-13 (EMD Chemicals, Gibbstown, NJ, USA) was used as a positive control. The product used was supplied as concentrated conditioned medium, and 2.5 μl was used. After electrophoresis, gels were washed twice, for 15 mins each time, with 2.5% Triton X-100. Digestion was carried out by incubating the gel in the gelatinase buffer [50 mM Tris-HCl (pH 7.6), 10 mM CaCl2, 50 mM NaCl, and 0.05%. Brij-35] at 37°C for 16 h. The gel was stained with 0.1% Coomassie brilliant blue R350 and the locations of gelatinolytic activity were revealed as clear bands on a background of uniform light blue staining. Electrophoretic migration of MMP-13 in the supernatant was compared with known molecular weight standards and also with clear bands of MMP-13 activity produced by the positive control. The gels were photographed and the averages of the band intensity were measured as mentioned before.

Statistical analysis

All measurements were performed in duplicate and were repeated at least three times using different age-matched and sex-matched OA samples. SPSS 15.0 software was used for analysis of the data. The Mankin score for OA was used to measure the extent of cartilage degradation. Tests of normality showed the data are not normally distributed, and homogeneity test of variances showed heterogeneity of variances. Comparisons of data among groups were analyzed by Kruskal-Wallis test. Further comparisons between either two groups were analyzed by Nemenyi test. $P<0.05$ was considered significant.

RESULTS

Control of cell phenotype and viability

The OA cartilage used for the experiments, macroscopically, had a smooth surface and no severe osteoarthritic changes. As described elsewhere (20), analysis of collagen type II, aggrecan and cartilage oligomeric matrix protein expression confirmed a stable differentiation stage of the chondrocytes during the experimental period. Trypan blue staining showed comparable cell viability with and without IL-1β stimulation.

Effect of LD-1227 on production of TNFα in osteoarthritis chondrocytes

OA chondrocytes (80% confluent) were pretreated with LD-1227 (100 μM) for 2 h, and were then stimulated with IL-1β (5.0ng/ml) for 8 h. No cytotoxic effect of LD-1227 was noted at the dose used (data not shown). The level of TNFα mRNA was quantified by a highly sensitive and specific quantitative RT-PCR method, and values were compared with control. Our results showed that OA chondrocytes treated with IL-1β had a higher level of TNFα mRNA compared with unstimulated OA chondrocytes (Fig. 1). TNFα mRNA levels showed a marked decline, however, in the samples pretreated with LD-1227 and then stimulated with ILβ (Fig. 1). To determine whether inhibition of gene expression also affected the protein level, culture supernatants were assayed for TNFα protein using TNFα-specific ELISA. As shown in Fig. 2, pretreatment with 100 μM LD-1227 significantly decreased the IL-1β-

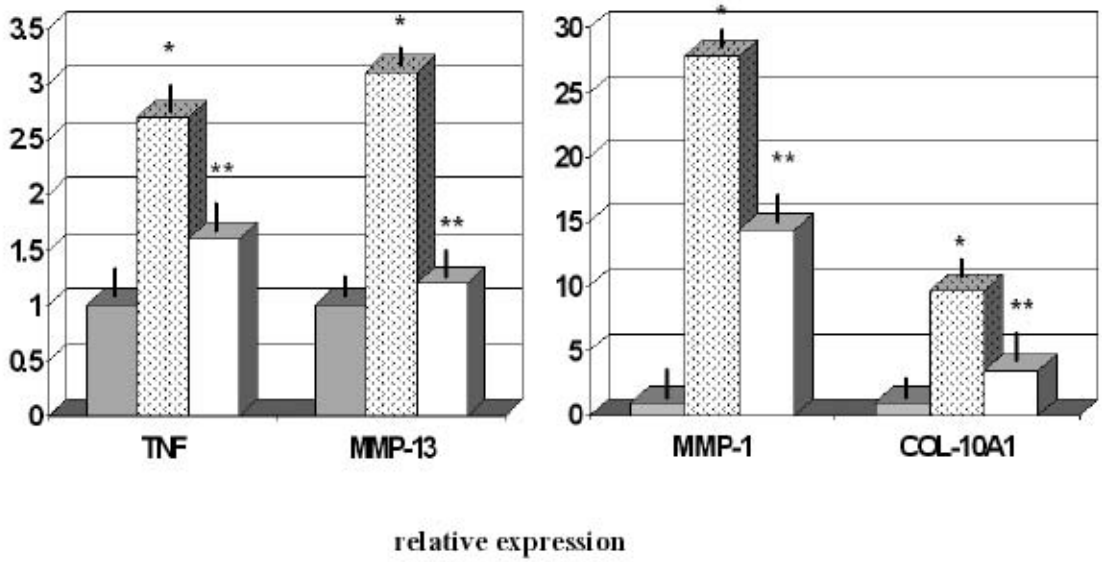

Fig. 1. *Effect of LD-1227 on TNF-alpha concentration in culture medium of stimulated chondrocytes. Grey bars: unstimulated OA chondrocytes; Dotted bars: OA chrondrocytes stimulated by IL1b and white bars: OA stimulated chondrocytes cultured with LD 1227. * p<0.001 vs unstimulated OA chrondrocytes, ** p<0.001 vs B group.*

induced TNFα production in the culture supernatant of ILβ-stimulated OA chondrocytes.

Expression and production of MMP-13, MMP1 and COL10A1 in IL-1β-stimulated osteoarthritis chondrocytes: effect of LD-1227

Pretreatment of OA chondrocytes with LD-1227 inhibited IL-1β-induced gene expression of MMP-13, MMP-1 and COL10A1 as determined by quantitative RT-PCR (Fig. 1). Again, the maximum inhibitory effect of LD-1227 had been found at 100 μM concentration in prior study. We also determined the effect of LD-1227 on the production of MMP-13 in the culture supernatant by Western immunoblotting using anti-MMP-13 antibody (Fig. 2). Analysis of the immunoblot revealed that the levels of MMP-13, MMP-1 and COL10A1 were high in the supernatant of chondrocytes treated with IL-1β when compared with the levels detected in untreated chondrocyte culture, where MMP-13 expression was nearly the same as that of the basal level (Fig. 2). These results were further verified using gelatin zymography. Zymographic analysis showed that OA chondrocytes stimulated with IL-1β had enhanced levels of all the above markers compared with the levels detected in control OA chondrocytes and pretreatment with LD-1227 exerted a significant decrease (data not shown).

Effect of LD-1227 on NF-κB activation in stimulated osteoarthritis chondrocytes

To investigate the mechanism responsible for the inhibitory effect of LD-1227 on proinflammatory cytokine gene expression, we examined its effect on NF-κB activation and translocation to the nucleus. NF-κB is an important transcriptional regulator of inflammatory cytokine gene expression and plays a crucial role in immune and inflammatory response. Exposure of OA chondrocytes to IL-1β significantly enhanced the DNA binding activity of NF-κB p65 compared with controls ($p < 0.0001$) whereas LD-1227 partly but significantly reduced the IL-1β-induced DNA binding activity of NF-κB p65 ($p < 0.05$) (Fig. 3).

DISCUSSION

Although arthritis is present in every population

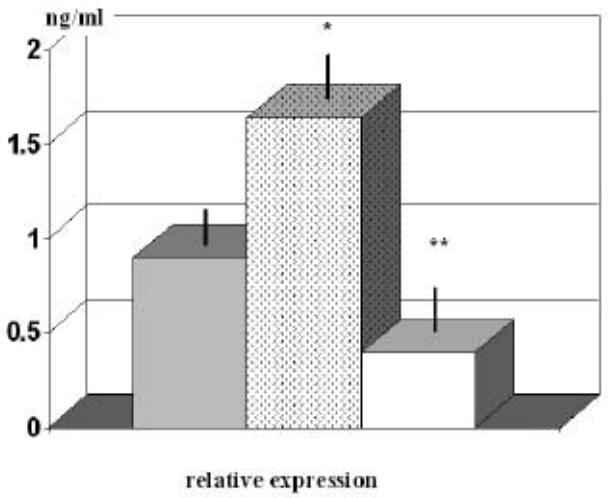

Fig. 2. *Effect of LD-1227 on gene expression of MMP-13, MMP1 and COL10A1 in IL-1β -stimulated osteoarthritis chondrocytes. Grey bars: unstimulated OA chondrocytes; Dotted bars: OA chrondrocytes stimulated by IL1b and white bars: OA stimulated chondrocytes cultured with LD 1227. * p<0.01 vs unstimulated OA chondrocytes, ** p<0.001 vs B group.*

and OA is the most common joint disorder, treatment is still limited to a few classes of drugs, primarily nonsteroidal anti-inflammatory drugs and corticosteroids. While providing relief from pain, however, none of these agents has been shown to inhibit cartilage breakdown or disease progress besides carrying a number of gastrointestinal toxicity side effects (5). Age is by far the most important risk factor for the development of OA (1). The mechanism by which aging is involved in the development of this debilitating disease remains largely unknown. With increasing age, the strength of the collagen matrix to withstand loading diminishes. Age-related changes in articular cartilage that influence the composition and strength of the cartilage matrix are therefore involved in the development of OA (8). Failure of the cartilage collagen network due to repetitive loading has long been recognized as one of the mechanisms involved in the development of OA (21). Chondrocytes are the only cellular components of cartilage and under normal physiologic conditions, chondrocytes maintain an equilibrium between anabolic and catabolic activities that is necessary for preservation of the structural and functional integrity of the tissue. Chondrocytes express inflammatory mediators such as TNFα and proteolytic enzymes – aggrecanases and MMPs – which under normal conditions, mediate a very low matrix turnover required for cartilage remodelling (15). However, an up-regulation of TNF protein has been described in IL-1β-treated chondrocytes (22), but also in OA cartilage and in the synovium of rheumatoid arthritis patients, and correlates with the course of the disease (23). Indeed, in pathologic conditions such as OA chondrocyte production of these inflammatory mediators and enzymes increases considerably, resulting in cartilage destruction (9). In particular, IL-1*β* is considered the most important cytokine in the pathogenic process of inflammation in general and may cause production of high levels of matrix metalloproteinase (24). From our data, it appeared that almost complete inhibition of both TNFα and MMP expression and production was observed at a concentration of 100 μM LD-1227 ($p < 0.01$). These finding are worthy of interest considering that recent studies have suggested a promising new approach for inhibition of cartilage degradation by acting on IL- β inhibition (25). However, further studies are required to define the exact mechanism underlying the inhibition of inflammatory reactions and to find active components in the LD-1227. It is known that the inactive NF-kB normally binds to IkB in the cytosol, and NF-kB can be activated by proinflammatory cytokines, IL-1β and TNF-α. Numerous studies have

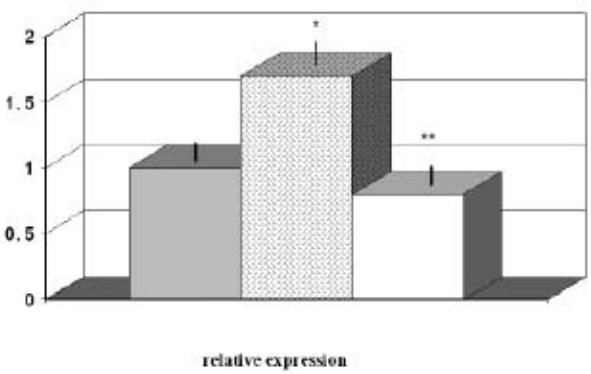

Fig. 3. *Effect of LD-1227 Gene Expression of NFkB 65 in IL-1β-stimulated osteoarthritis chondrocytes. Grey bars: unstimulated OA chondrocytes; Dotted bars: OA chrondrocytes stimulated by IL1b and white bars: OA stimulated chondrocytes cultured with LD 1227. * p<0.05 vs unstimulated OA chrondrocytes, ** p<0.05 vs B group.*

demonstrated that inhibitors of MAPKs or NF-kB decrease synovial inflammation, bone destruction and cartilage damage in animal models of arthritis, including adjuvant arthritis in rats (26). As TNFα and MMP genes are NF-kB-dependent, inhibition of NF-kB also inhibits their expression and production in IL-1*β*-stimulated chondrocytes. Based on our results, we can add that LD-1227 is a potent inhibitor of induction of TNFα and MMPs at a physiologically achievable concentration (100 μM). We therefore postulate that LD-1227 mediates its inhibitory effects on TNFα, MMP-1, Col10A and MMP-13 expressions, at least in part, through the suppression of NF-κB activity. In addition, DNA binding activity of nuclear NF-κB p65, as demonstrated by highly sensitive and specific ELISA, was also inhibited in OA chondrocytes. These data further confirm that LD-1227 attenuates the inflammatory stimuli-induced activation and DNA binding activity of NF-κB in human chondrocytes. Recent work from our group has shown that, at least some effects of the present sturgeon extract cannot be simply reconciled with its content of EPA/DHA (27, 28). Indeed, this compound contains collagen elastin, protein and a rich array of other smaller unsaturated fatty acids, and structural phospholipids still to be fully defined. Further investigation is also needed to discern how LD-1227 suppresses NF-kB activation, which components of NF-kB are suppressed, and what kind of intracellular signalling factors is specifically involved in the effect of LD-1227. Although the dosage of this compound employed in this *in vitro* study is regarded as being comparable to human use, a direct clinical inference needs a cautionary note and a clinical study is ongoing to confirm the above data.

REFERENCE

1. Zhang Y, Jordan JM. Epidemiology of osteoarthritis. Clin Geriatr Med 2010; 26:355-69.
2. Arden N, Nevitt MC. Osteoarthritis: epidemiology. Best Pract Res Clin Rheumatol 2006; 20:3-25.
3. Hjelle K, Solheim E, Strand T, Muri R, Brittberg M. Articular carti-lage defects in 1,000 knee arthroscopies. Arthroscopy 2002; 18:730-34.
4. Kemp JL, Collins NJ, Makdissi M, Schache AG, Machotka Z, Crossley K. Hip arthroscopy for intra-articular pathology: a systematic review of outcomes with and without femoral osteoplasty. Br J Sports Med 2011; [Epub ahead of print]
5. Filaretova LP, Bagaeva TR, Morozova OY, Zelena D. The healing of NSAID-induced gastric lesion may be followed by small intestinal and cardiovascular side effects. J Physiol Pharmacol 2011; 62:619-25.
6. Wang QC, Shi YY, Shen PZ, Xu Y. Effect of aging and sports-loading on articular cartilage of C57 black mice - a histopathological study[J]. Zhongguo Gu Shang 2000; 13:517-18. Chinese with abstract in English.
7. Flugge LA, Miller-Deist LA, Petillo PA. Towards a molecular understanding of arthritis. Chem Biol 1999; 6:R157-R166.
8. Takaishi H, Kimura T, Dalal S, Okada Y, D'Armiento J. Joint diseases and matrix metalloproteinases: a role for MMP-13. Curr Pharm Biotechnol 2008; 9:47-54.
9. Goldring MB, Otero M, Tsuchimochi K, Ijiri K, Li Y. Defining the roles of inflammatory and anabolic cytokines in cartilage metabolism. Ann Rheum Dis 2008; 67(S):iii75-iii82.
10. Little CB, Flannery CR, Hughes CE, Goodship A, Caterson B. Cytokine induced metalloproteinase expression and activity does not correlate with focal susceptibility of articular cartilage to degeneration. Osteoarthritis Cartilage 2005; 13:162-70.
11. Watanabe Y, Namba A, Honda K, Aida Y, Matsumura H, Shimizu O, Suzuki N, Tanabe N, Maeno M. IL-1β stimulates the expression of prostaglandin receptor EP4 in human chondrocytes by increasing production of prostaglandin E2. Connect Tissue Res 2009; 50:186-93.
12. Kobayashi M, Squires GR, Mousa A, Tanzer M, Zukor DJ, Antoniou J, Feige U, Poole AR. Role of interleukin-1 and tumor necrosis factor alpha in matrix degradation of human osteoarthritic cartilage. Arthritis Rheum 2005; 52:128-35.
13. Goldring SR, Goldring MB. The role of cytokines in cartilage matrix degeneration in osteoarthritis. Clin Orthop Relat Res 2004; 427:S27-36.
14. Pelletier JP, Caron JP, Evans C, Robbins PD, Georgescu HI, Jovanovic D. *In vivo* suppression of early experimental osteoarthritis by interleukin-1 receptor antagonist using gene therapy. Arthritis Rheum 1997; 40:1012-19.
15. Martinon F, Major A, Tschopp J. The inflammasomes: guardians of the body. Ann Rev Immunol 2008; 27:229-65.

16. Anderson P. Post-transcriptional regulation of tumour necrosis factor alpha production. Ann Rheum Dis 2000; 59:i3-i5.
17. Zainal Z, Longman AJ, Hurst S, Duggan K, Caterson B, Hughes CE, Harwood JL. Relative efficacies of omega-3 polyunsaturated fatty acids in reducing expression of key proteins in a model system for studying osteoarthritis. Osteoarthritis Cartilage 2009; 17:896-905.
18. Altman R, Alarcón G, Appelrouth D, Bloch D, Borenstein D, Brandt K. The American College of Rheumatology criteria for the classification and reporting of osteoarthritis of the hip. Arthritis Rheum 1991; 34:505-14.
19. van der Sluijs JA, Geesink RG, van der Linden AJ, Bulstra SK, Kuyer R, Drukker J. The reliability of the Mankin score for osteoarthritis. J Orthop Res 1992; 10:58-61.
20. Joos H, Albrecht W, Laufer S, Reichel H, Brenner RE. IL-1beta regulates FHL2 and other cytoskeleton-related genes in human chondrocytes. Mol Med 2008; 14:150-59.
21. L'Hermette MF, Tourny-Chollet C, Polle G, Dujardin FH. Articular cartilage, degenerative process and repair: current progress. Int J Sports Med 2006; 27:738-44.
22. Kwan Tat S, Amiable N, Pelletier JP, Boileau C, Lajeunesse D, Duval N. Modulation of OPG, RANK and RANKL by human chondrocytes and their implication during osteoarthritis. Rheumatology (Oxford) 2009; 48:1482-90.
23. Komuro H, Olee T, Kühn K, Quach J, Brinson DC, Shikhman A. The osteoprotegerin/receptor activator of nuclear factor kappaB/receptor activator of nuclear factor kappaB ligand system in cartilage. Arthritis Rheum 2001; 44:2768-76.
24. Clérigues V, Guillén MI, Castejón MA, Gomar F, Mirabet V, Alcaraz MJ. Heme oxygenase-1 mediates protective effects on inflammatory, catabolic and senescence responses induced by interleukin-1β in osteoarthritic osteoblasts. Biochem Pharmacol 2012; 83:395-405.
25. Kimura H, Yukitake H, Suzuki H, Tajima Y, Gomaibashi K, Morimoto S. The chondroprotective agent ITZ-1 inhibits interleukin-1beta-induced matrix metalloproteinase-13 production and suppresses nitric oxide-induced chondrocyte death. J Pharmacol Sci 2009; 110:201-11.
26. Mcintyre KW, Shuster DJ, Gillooly KM, et al. A highly selective inhibitor of I kappa B kinase, BMS-345541, blocks both joint inflammation and destruction in collagen-induced arthritis in mice. Arthritis Rheum 2003; 48:2652-59.
27. Marotta F, Polimeni A, Solimene U, Lorenzetti A, Minelli E, Jain S, Rastmanesh R, Sedriep S, Soresi V. Beneficial modulation from a high-purity caviar-derived homogenate on chronological skin aging. Rejuvenation Res 2012; 15:174-77.
28. Marotta F, Chui DH, Yadav H, et al. Effective properties of a sturgeon-based bioactive compound on stress-induced hippocampal degeneration and on *in vitro* neurogenesis. J Biol Regul Homeost Agents (in press).

EDITORIAL

NERVE GROWTH FACTOR AND BRAIN-DERIVED NEUROTROPHIC FACTOR CONCENTRATIONS IN SCHIZOPHRENIA: A REVIEW

G. MARTINOTTI, G. DI IORIO, S. MARINI, V. RICCI, D. DE BERARDIS and M. DI GIANNANTONIO

Department of Neuroscience and Imaging, University "G. d'Annunzio", Chieti-Pescara, Chieti, Italy

Received January 31, 2012 – Accepted July 30, 2012

There is growing interest in the role of neurotrophins in the pathophysiology of schizophrenia. Neurotrophins are a large family of dimeric polypeptides that promote the growth and the differentiation of developing neurons in the central and peripheral nervous systems as well as the survival of neuronal cells in response to stress. Nerve growth factor (NGF) and brain-derived neurotrophic factor (BDNF) concentrations are here reviewed in relation to medication-naive early psychotic patients and in medicated chronic schizophrenic patients. Most data point to decreased plasma and serum NGF and BDNF concentrations in naive drug and in medicated schizophrenic patients compared to healthy controls. Higher BDNF levels were observed in patients with the paranoid subtype of schizophrenia. Low serum BDNF levels were associated with reduction in hippocampal volume (HV) at the onset of schizophrenia. Evidence on the correlation between BDNF levels and positive and negative schizophrenic symptoms were ambiguous. There are contrasting results on a possible correlation between increase in BDNF concentrations and treatment with antipsychotics. Antipsychotic treatment can elevate NGF values, specifically atypical. Growth factors might be good candidates as prognostically and diagnostically useful markers in schizophrenia.

There is growing interest in the role of neurotrophins in the pathophysiology of several central nervous system (CNS) disorders, namely depression and schizophrenia (1, 2).

Neurotrophins are a large family of dimeric polypeptides, including nerve growth factor (NGF), brain-derived neurotrophic factor (BDNF), neurotrophin-3 (NT-3), NT-4, NT-5, that promote the growth and the differentiation of developing neurons in the central and peripheral nervous systems as well as the survival of neuronal cells in response to stress (3). In the CNS, NGF is found in greatest quantities within the cortex, including the hippocampus and the pituitary gland, though significant quantities are also produced in other areas of the CNS, such as the spinal cord. NGF promotes the survival of primary sensory neurons and of sympathetic and cholinergic neurons in the basal forebrain. It seems to play a role in the pathophysiology and the pharmacotherapy of neurodegenerative disorders, such as Alzheimer's dementia. In addition, it reduces neurodegeneration of cultured hippocampal neurons exposed to glutamate at toxic concentrations and preserves cell morphology (3).

NGF has neuroprotective effects (2). When cholinergic neurons are damaged in lesion experiments, NGF infusion rescues cholinergic neurons, stimulates axonal growth and improves

Key words: Nerve growth factor (NGF), brain-derived neurotrophic factor (BDNF), schizophrenia

Mailing address: Dr. G. Martinotti,
Clinica Villa Maria Pia,
Via del Forte Trionfale 36,
Rome 00135 Italy
Tel.: +39 3355627362
e-mail: giovanni.martinotti@gmail.com

0393-974X (2012)

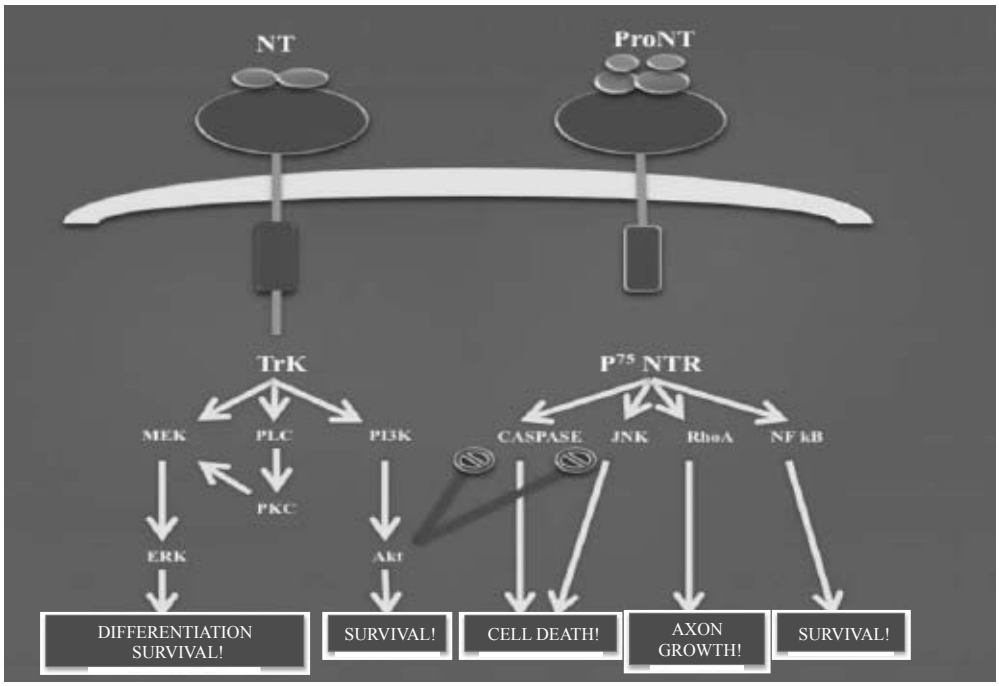

Fig. 1. *Trk and p75 NTR receptor-mediated signaling pathways. Trk and p75 NTR receptor-mediated signaling pathways. Binding of mature neurotrophins to Trk or pro-neurotrophins to P75NTR triggers the activation of different signaling pathways through different adaptors that result in diverse and at times opposite outcomes like survival, apoptosis, axonal growth, axonal collapse, and cell cycle arrest. Under normal circumstances, the biological responses of neurotrophins via their receptors include proliferation and survival; axonal and dendritic growth and remodeling; assembly and remodeling of the cytoskeleton; membrane trafficking and fusion; and synapse formation, function, and plasticity. But under pathological circumstances, the levels of pro-neurotrophins increase and, consequently, so do the levels of p75NTR receptor, thus resulting in increased neuronal, dendritic and synaptic apoptotic deterioration. Adapted from Buckley PF, Mahadik S, Pillai A, Terry A Jr. Neurotrophins and schizophrenia. Schizophr Res 2007; 94(1-3):1-11 [24].*

cholinergic function.

BDNF seems to be more widespread in the CNS than NGF (4). Like NGF, BDNF is abundant in the hippocampus, a brain region with a high degree of neural plasticity, that must be preserved throughout life in order to safeguard essential functions, such as learning and memory. It is noteworthy that the regulation of both NGF and BDNF within the hippocampus is at least partly controlled by the cholinergic and glutamatergic systems. Hippocampal damage upregulates BDNF levels in this region. In addition, BDNF, like NGF, also acts on primary sensory and cholinergic neurons in the basal forebrain. However, it does not affect sympathetic fibers. As opposed to NGF, BDNF has also been found to promote the survival of a wide range of neuronal cells, (2) such as the dopaminergic neurons of the substantia nigra, cerebellar granule neurons, motoneurons, neurons of the locus coeruleus and retinal ganglion cells. BDNF is known to modulate dopaminergic, GABAergic and serotonergic receptors. There is burgeoning literature on BDNF's role (and perhaps other neurotrophins) in the regulation of adult synaptic transmission and plasticity (5).

All neurotrophins have a similar basic structure, though they possess variable domains that account for specific receptor binding which, in turns, determines their biological effects (3). NGF mediates its biological effects by binding to TrkA, while BDNF and NT-4 bind to TrkB, and NT-3 binds to TrkC. In addition, all neurotrophins can interact with low affinity to another neurotrophin receptor, p75NTR, member of the tumor necrosis factor (TNF) receptor

superfamily. The Trk receptor signaling leads to survival pathways (Fig. 1).

Interactions of all pro-neurotrophins to p75NTR have been shown to initiate an apoptotic signal in neurons. Since Trk receptor signaling leads to survival and p75NTR receptor pro-neurotrophin signaling leads to apoptotic pathways, interactions of mature neurotrophin and pro-neurotrophins have opposite effects. During development, NTs regulate naturally occurring cell death, synaptic connectivity, fiber guidance and dendritic morphology. In addition, NTs contribute to brain plasticity, being involved in activity-dependent neuronal function (6). Several lines of evidence suggest that reduced NTs signaling in the adult brain may be implicated in the pathophysiology of psychiatric disorders (7). Brain plasticity refers to the brain's ability to change structure and function in response to a variety of stimuli. NTs are good candidates as "regulators" of synaptic plasticity, given that they are expressed in appropriate "plasticity loci", their expression is activity-dependent and they appear to affect synaptic function, membrane excitability as well as neuronal morphology and connectivity (6).

From latest gene research investigating correlations between BDNF levels and gene expressions, the role of Val66Met polymorphism in BDNF has been shown to play an important role in structural and functional plasticity in schizophrenia (8). NTs effects on synaptic plasticity have been described as ''very rapid local modes" since they do not require activation of gene transcription, being elicited within seconds from their application. There is evidence for short-term modulation of synaptic transmission by NTs as well as structural changes in axons and dendrites which underlie plastic rearrangements in the nervous system (4). Synthesis and release of BDNF is induced by neuronal activity and the subsequent TrkB activation leads to the stabilization of axonal and dendritic branches and strengthening of active synaptic connections (4).

Because of the fundamental role played by these neurotrophic factors in shaping brain function, a pathological alteration in NTs concentration or action early during postnatal life could exert long-term effects on synaptic plasticity, impairing the ability of the organism to cope with novel/stressful situations and leading to psychopathology. Many psychiatric disorders can be accounted for by a 'two hit model': genetic and/or environmental factors disrupt early CNS development leading to vulnerability to a ''second hit" which, in turn, leads to the onset of psychiatric symptoms (9). Numerous data suggest alterations in neurotrophin levels, as a result of exposure to stressful events in adulthood, could interact synergistically with epigenetic changes caused by early stress, leading to greater susceptibility for stress-related psychiatric disorders.

Approximately 1% of the general population is affected by schizophrenic psychoses. There is evidence that neurodevelopmental abnormalities, caused by genetic or other alterations, ultimately result in an increased predisposition to schizophrenia. Accordingly, the maldevelopment hypothesis postulates that abnormal structural development and maturation of specific brain areas (including disturbances of cell migration, disconnections and changes in neural plasticity) are important factors in the pathogenesis of schizophrenia (10).

Besides neural maldevelopment such as migrational deficits and disconnections, which are involved in the pathophysiology of schizophrenia and alteration in the expression and/or functioning of neurotrophic factors may, therefore, also cause altered neural plasticity and structural abnormalities. In adolescence, the brain of schizophrenic subjects will be unable to adapt to stress situations and to develop efficient coping strategies. These considerations led to the neurotrophic factor hypothesis of schizophrenia, which postulates that various pathomechanisms (e.g. genetic, infectious, traumatic) cause alterations in the expression of neurotrophic factors, and that these alterations are responsible for the morphological abnormalities occurring in the brains of schizophrenic patients, ultimately causing the characteristic psychopathological symptoms (11). A number of histopathological and neuroimaging findings support the maldevelopment and neurotrophic factor hypothesis of schizophrenic psychoses (12).

It is important to note that the neurotrophic factor hypothesis (Fig. 2) is not in contrast with models stressing the relevance of neurotransmitters in the pathophysiology of schizophrenia. Altered neurotransmitter activity of affected nerve cells can be regarded as the consequence of a neuronal maldevelopment caused by neurotrophic factor

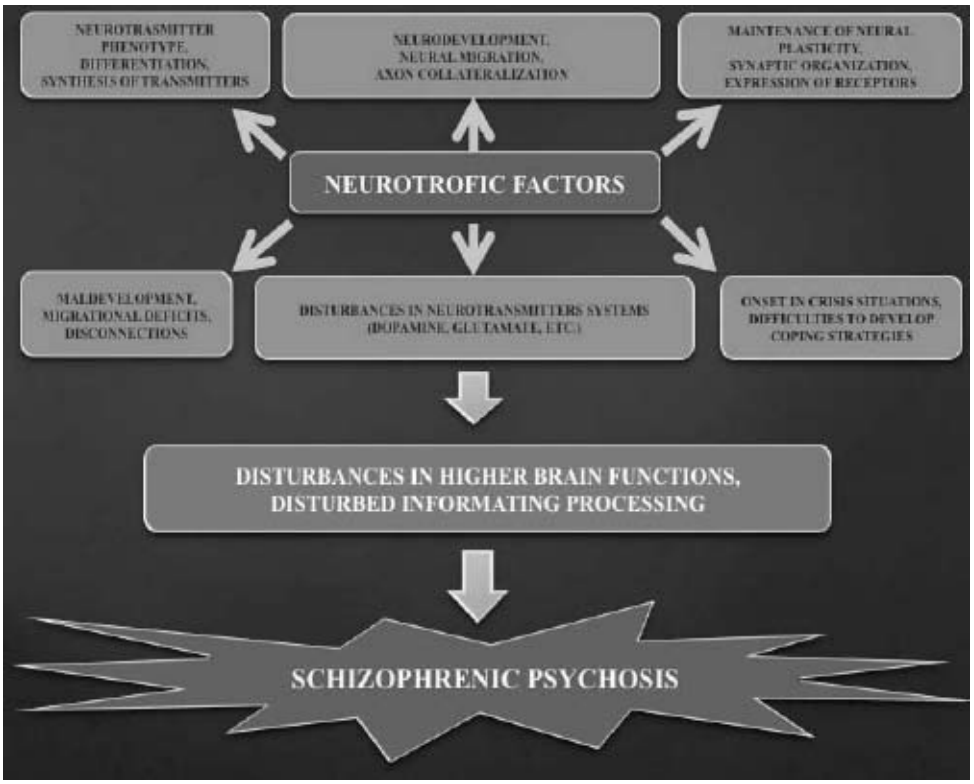

Fig. 2. *Neuromaldevelopment hypothesis of schizophrenia. Under physiological conditions, neurotrophic factors are involved in the regulation of neurodevelopment, neural migration and differentiation as well as in modulating neurotransmitter synthesis, synaptic organization and neural plasticity. Under pathological conditions, with impaired neurotrophic factor metabolism, neural maldevelopment, migrational deficits and disconnections arise. These neural alterations may cause disturbances in neurotransmitter systems and reduction of or changes in neural plasticity in adulthood, thereby impairing the individual's ability to develop coping strategies in crisis situations; this could explain the clinical observation that psychoses are often induced by challenging life events. Adapted from Durany N, Thome J. Neurotrophic factors and the pathophysiological of schizophrenic psychoses. Eur Psychiatry 2004; 19(6):326-37 [1].*

alterations. There is probably a sensitive balance of mutual regulation between neurotransmitter and neurotrophic factor metabolism. The neurotransmitter hypothesis of schizophrenia is mainly supported by the antidopaminergic effect of many antipsychotic drugs and the psychotropic properties of certain glutamatergic substances. Antipsychotic drugs probably modulate intracellular signal transduction and gene expression processes, which may be as important for their efficacy as their interaction with particular receptors.

NERVE GROWTH FACTOR LEVELS

There are very few studies reporting NGF levels in medication-naïve early psychotic patients and in medicated chronic schizophrenic patients. Aloe et al. (13) showed that haloperidol reduced basal NGF plasma levels in 8 neuroleptic-free schizophrenic patients. Jockers-Scherübl et al. (14) found that NGF serum concentrations could be influenced by cannabis abuse. In particular, long-term cannabis abuse may increase the risk of schizophrenia. Schizophrenic patients with regular cannabis intake (> 0.5 g on average per day for at least 2 years) had significantly raised NGF serum levels compared to controls and schizophrenic patients not consuming cannabis. In schizophrenic patients who abused of other substances in addition to cannabis, NGF concentrations were much higher. Polysubstance

Table I. *Antipsychotic drugs effects on NGF and BDNF concentrations.*

AUTHOR	PATIENTS	DRUG TREATMENTS	NGF-BDNF LEVELS	MAIN FINDINGS
Aloe L et al. 1997	schizophrenic patients pre and post treatment	Haloperidol	↓ NGF plasma levels	Haloperidol reduced the NGF plasma levels
Parikh V et al. 2003	medicated schizophrenic patients vs never-medicated first-episode psychotic patients	atypical antipsychotics vs typical antipsychotics	↑↑ NGF plasma levels	NGF levels were significantly higher in chronic schizophrenic patients treated with antipsychotics as compared to first-episode psychotic patients. NGF plasma levels were markedly higher in atypical antipsychotics treated patients compared to typical antipsychotics treated patients
Lee BH et al. 2009	schizophrenic patients re and post treatment vs healthy controls	Risperidone	←→ beta-NGF plasma levels ←→ BDNF plasma levels	Plasma BDNF and beta-NGF had no significant changes between pre and post treatment. Data suggest higher plasma BDNF levels might be associated with better response to risperidone treatment.
Toyooka K et al. 2002	schizophrenic patients vs healthy controls	Haloperidol, Chlorpromazine, Levomepromazine, Zotepin, Bromperidol, Risperidone, other	↓↓ BDNF serum levels (not in the whole blood)	The BDNF reduction in serum but not in whole blood suggests a potential deficit in neurotrophic factor release in schizophrenic patients
Shimizu E et al. 2003	antipsychotic-naive vs medicated schizophrenia patients vs healthy controls	not reported	= BDNF serum levels	No significant differences in BDNF serum levels among antipsychotic-naive and medicated patients and healthy controls
Huang TL et al. 2006	schizophrenic patients vs healthy controls	not reported	←→ BDNF serum levels	Patients with catatonic schizophrenia had lower BDNF serum levels than patients with paranoid or residual schizophrenia.
Hori H et al. 2007	schizophrenic patients vs healthy controls	Olanzapine	= BDNF plasma levels	olanzapine did not alter the plasma levels of brain-derived neurotrophic factor
Gama CS et al. 2007	schizophrenic patients vs healthy controls	Clozapine, typical and other atypical antipsychotics	↑↑ BDNF serum levels	Serum BDNF levels were significantly higher in schizophrenia patients when compared to controls
Grillo RW et al.2007	schizophrenic patients vs healthy controls	Clozapine vs typical antipsychotics (Chlorpromazine, Levopromazine, Haloperidol)	↑ BDNF serum levels	BDNF values from patients on clozapine were significantly higher than values from patients on typical antipsychotics. Serum BDNF was strongly and positively correlated with clozapine dose
Ikeda Y et al. 2008	schizophrenic patients vs healthy controls	not reported	↓ BDNF serum levels	Data suggest that pervasive, abnormal signaling of neurotrhophic factors underlies the pathophysiology of chronic schizophrenia
Reis HJ et al. 2008	schizophrenic patients vs healthy controls	Chlorpromazine, Haloperidol, Levopromazine, Trifluorperazine	↑ BDNF serum levels	BDNF serum levels correlated positively with the clinical scores at the negative subscale of the positive and negative syndrome scale
Xiu MH et al. 2009	schizophrenic patients vs healthy controls	Clozapine, Risperidone, Haloperidol, Chlorpromazine, Perphenazine, Sulpiride, other	↓↓ BDNF serum levels	Lower BDNF levels were observed in patients treated with risperidone. There was a sex difference in BDNF levels in patients with schizophrenia but not in normal controls. Decreased BDNF serum levels in chronic patients with schizophrenia may be related to gender, antipsychotic treatment and the severity of psychotic symptoms.
Rizos EN et al. 2010	schizophrenic patients vs healthy controls	Risperidone, Haloperidol, Olanzapine, Amisulpride	↓ BDNF serum levels (related to healthy controls) = BDNF serum levels (compared to levels at study entry)	BDNF serum levels were significantly increased in the subgroup receiving olanzapine compared to the other antipsychotics.
Chen CC et al. 2011	paranoid schizophrenia patients pre and post treatment	Risperidone, Clozapine	= BDNF serum levels relative to study entry. ↑ BDNF serum levels (in the subgroup receiving risperidone compared to that receiving clozapine only in male)	Gender might significantly influence the antipsychotic treatment of schizophrenia from the perspective of BDNF
Pedrini M et al. 2011	schizophrenic patients vs schizophrenic patients	Clozapine, typical antipsychotics	not reported	serum BDNF levels are correlated with clozapine daily dose but not with typical antipsychotic daily dose

dependent subjects are usually characterized by suicide attempts and self-mutilating or aggressive behaviors (15).

Antipsychotic treatment in schizophrenics with and without cannabis or additional substance abuse leads to recovery of neural integrity, as indicated by renormalized NGF values (16). Plasma NGF levels were significantly lower in both never-medicated first-episode psychotic (FEP) and medicated chronic patients as compared to normal subjects. NGF levels were significantly higher in chronic schizophrenic patients, which were treated with antipsychotics as compared to FEP (Table I). Moreover, NGF levels in chronic patients treated with atypical antipsychotics were markedly higher as compared to patients treated with typical antipsychotics. Parikh postulated that lower NGF levels in FEP patients at the onset of psychosis may have implications for neurodevelopmental abnormalities. Higher NGF levels in chronic patients treated with atypical antipsychotics may have implications for treatment outcome (16).

Shcherbakova et al. (17) found increased leukocyte elastase (LE) activity and elevated levels of autoantibodies to neurospecific protein - nerve growth factor (Aab to NGF) in acute stage schizophrenics' serum. Patients with predominantly positive symptoms showed significantly elevated Aab to NGF serum levels compared to patients with predominantly negative symptoms, who were more likely to exhibit high LE activity. Progression of positive symptoms was coupled with gradual increase of Aab to NGF level and reduction of LE activity. Based on these findings, Shcherbakova et al. concluded that high levels of Aab to NGF relate to a clinical picture characterized mainly by positive symptoms, whereas high LE activity relates to a clinical picture with predominant negative symptoms (17).

Bersani et al. found that the ultradian rhythmic NGF regulation is altered in schizophrenics as compared to controls, with higher levels in the morning and lower levels in the evening, supporting the hypothesis that NGF plays a relevant role in schizophrenia (18).

Kale et al. (19) conducted the first study comparing cerebrospinal fluid (CSF) and plasma NGF levels in patients and matched healthy controls. Significantly lower NGF levels in both CSF and plasma were observed in drug-naive first episode psychotic patients. In controls, CSF NGF levels correlated to plasma values (19).

Serum NGF and interleukin-2 (IL-2) were analyzed to examine the diagnostic efficiency and predictive capability of these two biomarkers in relation to a diagnosis of schizophrenia (20). Significantly lower serum IL-2 and NGF among schizophrenic patients compared to healthy controls were observed. The diagnostic efficiency of combined NGF and IL-2 was high in schizophrenic patients compared with healthy controls. Serum NGF and IL-2 appear to be promising as potential screening or diagnostic biomarkers for schizophrenia and may be a useful adjunct for clinical assessment. Morover, cytokine production can be influence by the psychopharmacological treatment, becoming a marker of treatment response (21).

Only one study simultaneously correlated BDNF and NGF plasma concentrations in medicated schizophrenic patients. Higher plasma BDNF levels might be associated with a better response to risperidone treatment, while plasma beta-NGF levels might have no effect on the clinical response in schizophrenia patients. At baseline, plasma BDNF did not significantly differ between schizophrenia patients and controls, but beta-NGF levels were significantly lower in schizophrenic patients than controls. Plasma BDNF and beta-NGF in all schizophrenic patients did not significantly change after treatment as compared to the pre-treatment phase. Baseline BDNF levels were significantly lower in non-responding patients than in the others. After treatment, highly improved patients had significantly greater plasma BDNF than non-responders. However, beta-NGF did not significantly differ between the two groups (22).

BRAIN DERIVED NEUROTROPHIC FACTOR LEVELS

Several evidences report decreased serum and plasma BDNF concentrations in schizophrenic patients compared to healthy controls.

In particular, in first episode psychotic or drug naive schizophrenic patients, many studies found significantly reduced BDNF levels (23-27). Morover,

in medicated (typical or atypical antipsychotics) or chronic schizophrenic patients, BDNF levels were decreased compared to normal controls (26, 28, 29). In contrast with these results other studies reported no significant differences (22, 30). Contrasting results have been reported regarding antipsychotics' capacity to increase BDNF concentrations. Depending on antipsychotic class, differential effects on BDNF levels were exerted (31-40). Clozapine might upregulate brain BDNF expression. In fact, serum BDNF strongly and positively correlates with clozapine dose and may account for cognitive enhancement.

Electroconvulsive therapy's (ECT) therapeutic effect is associated with an increase in BDNF serum levels (41). During the course of ECT, paranoid and hallucinatory symptoms gradually improved, whereas BDNF levels increased over time. In addition, there was a general improvement of positive and negative schizophrenic symptoms.

Low serum BDNF levels are associated with reduction in hippocampal volume (HV) at the onset of schizophrenia and might further support the theory of a neuroprogressive-neurotoxic reaction associated with the onset of psychosis. Corrected right HV of FEP patients were significantly smaller compared to corrected right HVs of healthy subjects. The serum BDNF levels in the sample of FEP patients was significantly reduced compared to healthy subjects. An interesting finding is that inferior frontal white matter alterations in fronto-temporo-limbic circuits might be associated with suicidality and self-aggression in schizophrenia (42).

The effects of socially relevant doses of cannabinoids on BDNF levels hint at the existence of a possible mechanism underlying the consequences of exposure to cannabis. This might be of particular importance for the developing brain and also in disorders believed to involve altered neurodevelopment such as schizophrenia. Cannabis is associated with elevated BDNF serum concentrations in chronic cannabis abusers or multiple substance abusers, prior to disease onset. Drug-naive schizophrenic patients without cannabis consumption showed similar results to normal controls and cannabis controls without schizophrenia (43).

BDNF levels were significantly higher in smokers than in nonsmokers. Higher BDNF levels correlated with fewer negative symptoms and with more cigarette smoking (44). The fewer positive symptoms in smokers and the fewer negative symptoms in heavy smokers may be associated with nicotine-induced BDNF upregulation. BDNF might play an important role in the occurrence of the different clinical subtypes of schizophrenia. In fact, patients with that paranoid or residual subtype of schizophrenia had higher BDNF levels compared to patients with catatonic schizophrenia (45).

Contrasting results were observed on the relationship between BDNF and weight gain, when gender was taken into account. BDNF levels negatively correlated with BMI gain in female but not in male patients (32). Likewise, conflicting data were reported with respect to the relationship between BDNF levels and dyskinetic movements associated with tardive dyskinesia (TD). Plasma BDNF levels in patients with TD were lower compared to those without TD and to controls. Plasma BDNF levels inversely correlated with Abnormal Involuntary Movement Scale (AIMS) total score. Decreased BDNF could play an important role in the pathophysiology of tardive dyskinesia (28).

Evidence on the correlation between BDNF levels and cognitive enhancement or decreased positive schizophrenic symptoms is also ambiguous. BDNF levels at the onset of schizophrenia may reflect associated pathophysiological processes as well as severity of positive and negative psychotic symptoms. There was no correlation between serum BDNF levels and PANSS scores in patients with schizophrenia (23). Plasma BDNF levels showed a significant negative correlation only with positive symptom scores at baseline (24, 25) and no significant correlations were found with any of the cognitive performance test battery or motor function test scores (24). Cognitive deficits have been correlated to language disturbance in schizophrenic patients (46).

CONCLUSIONS

Most data point to decreased plasma and serum NGF and BDNF concentrations in drug naive and in medicated schizophrenic patients compared to healthy controls. Antipsychotic treatment can elevate

NGF values. Atypical antipsychotics raise NGF levels more than typical antipsychotics. There are contrasting results on a possible correlation between increase in BDNF concentrations and treatment with antipsychotics. CSF NGF levels correlated with plasma values in controls.

Regular cannabis and additional substance intake significantly raised NGF and BDNF serum levels. BDNF levels were significantly higher in smokers than in nonsmokers. Higher BDNF levels were observed in patients with the paranoid subtype of schizophrenia. Low serum BDNF levels were associated with reduction in hippocampal volume at the onset of schizophrenia. ECT's therapeutic effects were associated with an increase in BDNF serum levels.

With respect to both the relationship between BDNF levels and dyskinetic movements associated with tardive dyskinesia and the correlation between BDNF levels and weight gain contrasting findings have been reported. Evidence on the correlation between BDNF levels and cognitive enhancement or decreased positive schizophrenic symptoms is also ambiguous.

Growth factors might be good candidates as prognostically and diagnostically useful markers in schizophrenia. Studies that assess alterations of peripheral growth factors in schizophrenics' first degree family members and explore the relationship between BDNF levels and other indices of developmental brain pathology, such as cortical gray matter loss, are needed. Physiological processes controlled by NTs may eventually yield innovative therapeutic tools such as new peptidergic drugs. Much remains to be understood about NGF's and BDNF's influence on CNS targets that regulate brain plasticity and behavioral coping. Studies that ascertain whether decreased BDNF is a state-related feature of acute symptomatology or is more of a trait and that examine alterations taking place during relapse are also warranted.

ACKNOWLEDGEMENTS

The authors would like to extend their sincere gratitude to Dr. Luisa De Risio for her helpful support in writing and revising the paper. This manuscript was entirely funded by the authors, and no pharmaceutical companies were informed of or were involved in the review. The authors have no potential conflicts of interest that are directly relevant to the contents of the manuscript. All authors have contributed to this review with equal efforts.

REFERENCES

1. Durany N, Thome J. Neurotrophic factors and the pathophysiological of schizophrenic psychoses. Eur Psychiatry 2004; 19(6):326-37.
2. Shoval G, Weizman A. The possible role of neurotrophins in the pathogenesis and therapy of schizophrenia. Eur Neuropsychopharmacol 2005; 15(3):319-29.
3. Sofroniew MV, Howe CL, Mobley WC. Nerve growth factor signaling, neuroprotection, and neural repair. Annu Rev Neurosci 2001; 24:1217-81.
4. Maness LM, Kastin AJ, Weber JT, Banks WA, Beckman BS, Zadina JE. The neurotrophins and their receptors: structure, function, and neuropathology. Neurosci Biobehav Rev 1994; 18(1):143-59.
5. Bramham CR, Messaoudi E. BDNF function in adult synaptic plasticity: the synaptic consolidation hypothesis. Prog Neurobiol 2005; 76(2):99-125.
6. Thoenen H. Neurotrophins and neuronal plasticity. Science 1995; 270(5236):593-8.
7. Castren E. Is mood chemistry? Nat Rev Neurosci 2005; 6(3):241-6.
8. Spalletta G, Morris DW, Angelucci F, et al. BDNF Val66Met polymorphism is associated with aggressive behavior in schizophrenia. Eur Psychiatry 2010; 25(6):311-3.
9. Ansorge MS, Hen R, Gingrich JA. Neurodevelopmental origins of depressive disorders. Curr Opin Pharmacol 2007; 7(1):8-17.
10. Takahashi M, Shirakawa O, Toyooka K, et al. Abnormal expression of brain-derived neurotrophic factor and its receptor in the corticolimbic system of schizophrenic patients. Mol Psychiatry 2000; 5(3):293-300.
11. Muglia P, Vicente AM, Verga M, King N, Macciardi F, Kennedy JL. Association between the BDNF gene and schizophrenia. Mol Psychiatry 2003; 8(2):146-7.
12. Spence SA, Hirsch SR, Brooks DJ, Grasby PM. Prefrontal cortex activity in people with schizophrenia

and control subjects. Evidence from positron emission tomography for remission of 'hypofrontality' with recovery from acute schizophrenia. Br J Psychiatry 1998; 172:316-23.

13. Aloe L, Iannitelli A, Bersani G, Alleva E, Angelucci F, Maselli P, Manni L. Haloperidol administration in humans lowers plasma nerve growth factor level: evidence that sedation induces opposite effects to arousal. Neuropsychobiology 1997; 36(2):65-8.
14. Jockers-Scherübl MC, Matthies U, Danker-Hopfe H, Lang UE, Mahlberg R, Hellweg R. Chronic cannabis abuse raises nerve growth factor serum concentrations in drug-naive schizophrenic patients. J Psychopharmacol 2003; 17(4):439-45.
15. Martinotti G, Carli V, Tedeschi D, Di Giannantonio M, Roy A, Janiri L, Sarchiapone M. Mono- and polysubstance dependent subjects differ on social factors, childhood trauma, personality, suicidal behaviour, and comorbid Axis I diagnoses. Addict Behav 2009; 34(9):790-3.
16. Parikh V, Evans DR, Khan MM, Mahadik SP. Nerve growth factor in never-medicated first-episode psychotic and medicated chronic schizophrenic patients: possible implications for treatment outcome. Schizophr Res 2003; 60(2-3):117-23.
17. Shcherbakova IV, Siryachenko TM, Mazaeva NA, Kaleda VG, Krasnolobova SA, Klyushnik TP. Leukocyte elastase and autoantibodies to nerve growth factor in the acute phase of schizophrenia and their relationship to symptomatology. World J Biol Psychiatry 2004; 5(3):143-8.
18. Bersani G, Iannitelli A, Massoni E, Garavini A, Grilli A, Di Giannantonio M, Conti CM, Pancheri P. Ultradian variation of nerve growth factor plasma levels in healthy and schizophrenic subjects. Int J Immunopathol Pharmacol 2004; 17(3):367-72.
19. Kale A, Joshi S, Pillai A, Naphade N, Raju M, Nasrallah H, Mahadik SP. Reduced cerebrospinal fluid and plasma nerve growth factor in drug-naïve psychotic patients. Schizophr Res 2009; 115(2-3):209-14.
20. Xiong P, Zeng Y, Wan J, Xiaohan DH, Tan D, Lu J, Xu F, Li HY, Zhu Z, Ma M. The role of NGF and IL-2 serum level in assisting the diagnosis in first episode schizophrenia. Psychiatry Res 2011; 189(1):72-6.
21. De Berardis D, Conti CM, Serroni N, Moschetta FS, Olivieri L, Carano A, Salerno RM, Cavuto M, Farina B, Alessandrini M, Janiri L, Pozzi G, Di Giannantonio M. The effect of newer serotonin-noradrenalin antidepressants on cytokine production: a review of the current literature. Int J Immunopathol Pharmacol 2010; 23(2):417-22.
22. Lee BH, Kim YK. Increased plasma brain-derived neurotropic factor, not nerve growth factor-Beta, in schizophrenia patients with better response to risperidone treatment. Neuropsychobiology 2009; 59(1):51-8.
23. Pirildar S, Gönül AS, Taneli F, Akdeniz F. Low serum levels of brain-derived neurotrophic factor in patients with schizophrenia do not elevate after antipsychotic treatment. Prog Neuropsychopharmacol Biol Psychiatry 2004; 28(4):709-13.
24. Buckley PF, Pillai A, Evans D, Stirewalt E, Mahadik S. Brain derived neurotropic factor in first-episode psychosis. Schizophr Res 2007; 91(1-3):1-5.
25. Pillai A, Kale A, Joshi S, Naphade N, Raju MS, Nasrallah H, Mahadik SP. Decreased BDNF levels in CSF of drug-naive first-episode psychotic subjects: correlation with plasma BDNF and psychopathology. Int J Neuropsychopharmacol 2010; 13(4):535-9.
26. Green MJ, Matheson SL, Shepherd A, Weickert CS, Carr VJ. Brain-derived neurotrophic factor levels in schizophrenia: a systematic review with meta-analysis. Mol Psychiatry 2010; 6(9):960-72.
27. Lee AH, Lange C, Ricken R, Hellweg R, Lang UE. Reduced brain-derived neurotrophic factor serum concentrations in acute schizophrenic patients increase during antipsychotic treatment. J Clin Psychopharmacol 2011; 31(3):334-6.
28. Tan YL, Zhou DF, Zhang XY. Decreased plasma brain-derived neurotrophic factor levels in schizophrenic patients with tardive dyskinesia: association with dyskinetic movements. Schizophr Res 2005; 74(2-3):263-70.
29. Xiu MH, Hui L, Dang YF, et al. Decreased serum BDNF levels in chronic institutionalized schizophrenia on long-term treatment with typical and atypical antipsychotics. Prog Neuropsychopharmacol Biol Psychiatry 2009; 33(8):1508-12.
30. Shimizu E, Hashimoto K, Watanabe H, et al. Serum brain-derived neurotrophic factor (BDNF) levels in schizophrenia are indistinguishable from controls.

Neurosci Lett 2003; 351(2):111-4.
31. Rizos EN, Michalopoulou PG, Siafakas N, et al. Association of serum brain-derived neurotrophic factor and duration of untreated psychosis in first-episode patients with schizophrenia. Neuropsychobiology 2010; 62(2):87-90.
32. Zhang XY, Tan YL, Zhou DF, et al. Serum BDNF levels and weight gain in schizophrenic patients on long-term treatment with antipsychotics. J Psychiatr Res 2007; 41(12):997-1004.
33. Toyooka K, Asama K, Watanabe Y, Muratake T, Takahashi M, Someya T, Nawa H. Decreased levels of brain-derived neurotrophic factor in serum of chronic schizophrenic patients. Psychiatry Res 2002; 110(3):249-57.
34. Grillo RW, Ottoni GL, Leke R, Souza DO, Portela LV, Lara DR. Reduced serum BDNF levels in schizophrenic patients on clozapine or typical antipsychotics. J Psychiatr Res 2007; 41(1-2):31-5.
35. Ikeda Y, Yahata N, Ito I, Nagano M, Toyota T, Yoshikawa T, Okubo Y, Suzuki H. Low serum levels of brain-derived neurotrophic factor and epidermal growth factor in patients with chronic schizophrenia. Schizophr Res 2008; 101(1-3):58-66.
36. Reis HJ, Nicolato R, Barbosa IG, Teixeira do Prado PH, Romano-Silva MA, Teixeira AL. Increased serum levels of brain-derived neurotrophic factor in chronic institutionalized patients with schizophrenia. Neurosci Lett 2008; 439(2):157-9.
37. Chen CC, Huang TL. Effects of antipsychotics on the serum BDNF levels in schizophrenia. Psychiatry Res 2011; 189(3):327-30.
38. Pedrini M, Chendo I, Grande I, et al. Serum brain-derived neurotrophic factor and clozapine daily dose in patients with schizophrenia: a positive correlation. Neurosci Lett 2011; 491(3):207-10.
39. Hori H, Yoshimura R, Yamada Y, Ikenouchi A, Mitoma M, Ida Y, Nakamura J. Effects of olanzapine on plasma levels of catecholamine metabolites, cytokines, and brain-derived neurotrophic factor in schizophrenic patients. Int Clin Psychopharmacol 2007; 22(1):21-7.
40. Gama CS, Andreazza AC, Kunz M, Berk M, Belmonte-de-Abreu PS, Kapczinski F. Serum levels of brain-derived neurotrophic factor in patients with schizophrenia and bipolar disorder. Neurosci Lett 2007; 420(1):45-8.
41. Martinotti G, Ricci V, Di Nicola M, Caltagirone C, Bria P, Angelucci F. Brain-derived neurotrophic factor and electroconvulsive therapy in a Schizophrenic patient with treatment-resistant paranoid-hallucinatory symptoms. J ECT 2011; 27(1):e44-6.
42. Rüsch N, Spoletini I, Wilke M, Martinotti G, Bria P, Trequattrini A, Bonaviri G, Caltagirone C, Spalletta G. Inferior frontal white matter volume and suicidality in schizophrenia. Psychiatry Res 2008; 164(3):206-14.
43. Jockers-Scherübl MC, Danker-Hopfe H, Mahlberg R, Selig F, Rentzsch J, Schürer F, Lang UE, Hellweg R. Brain-derived neurotrophic factor serum concentrations are increased in drug-naive schizophrenic patients with chronic cannabis abuse and multiple substance abuse. Neurosci Lett 2004; 371(1):79-83.
44. Zhang XY, Xiu MH, Chen da C, Yang FD, Wu GY, Lu L, Kosten TA, Kosten TR. Nicotine dependence and serum BDNF levels in male patients with schizophrenia. Psychopharmacology (Berl) 2010; 212(3):301-7.
45. Huang TL, Lee CT. Associations between serum brain-derived neurotrophic factor levels and clinical phenotypes in schizophrenia patients. J Psychiatr Res 2006; 40(7):664-8.
46. Marini A, Spoletini I, Rubino IA, et al. The language of schizophrenia: an analysis of micro and macrolinguistic abilities and their neuropsychological correlates. Schizophr Res 2008; 105(1-3):144-55.

TGF-β SIGNALING IN T CELLS IS NOT ESSENTIAL FOR TH17 CELL DEVELOPMENT IN THE MOUSE

J. SCHUMANN[1], U. MÜLLER[2] and M. BLESSING[2]

[1]Institute of Physiological Chemistry, Faculty of Veterinary Medicine, University of Leipzig, Leipzig, Germany; [2]Professorship for Molecular Pathogenesis, Center for Biotechnology and Biomedicine (BBZ), Faculty of Veterinary Medicine, University of Leipzig, Leipzig, Germany

Received May 28, 2010 – Accepted May 18, 2012

Th17 cells are potent pro-inflammatory effectors crucial for defense against extracellular bacteria. However, in this context and in the context of autoimmune disorders Th17 cells have been demonstrated to be key contributors to destructive pathological mechanism. A number of trials report TGF-β to be involved in Th17 cell development. Nevertheless, to date, the role that TGF-β plays in Th17 cell generation remains unclear. In this paper we highlight the role of TGF-β in Th17 cell development in the mouse. The effects of likewise T cell specific over-expression of TGF-β or inhibition of TGF-β signal transduction in these cells on Th17 cell development were investigated by means of transgenic mouse models. The T cell specific insensitivity to TGF-β does not prevent Th17 cell development *ex vivo* or *in vitro* in the murine system. In contrast, stimulation of T cells over-expressing TGF-β actually results in decreased Th17 cell numbers in comparison to the wild type. Thus, our data indicate that TGF-β signaling in T cells is dispensable or even inhibitory for generation of Th17 cells in the mouse. Moreover, we could show TGF-β to inhibit a LPS driven Th1 cell development suggesting the cytokine to act as an indirect effector in Th17 cell differentiation.

Transforming growth factor-beta (TGF-β) is of importance not only as a growth factor, but also as an immune modulating cytokine. Affected cell types include T cells, B cells, NK cells, dendritic cells, as well as macrophages (1). TGF-β acts both pro- and anti-inflammatory (1) representing a multifunctional cytokine playing a complex role in immune response. The effects provoked by TGF-β critically depend on the genetic background, cell type, state of cellular differentiation and activation, extracellular matrix, and likewise other regulatory factors (2).

Development of T helper cell subsets is due to mutual interactions of different immune regulating factors. Depending on cytokine milieu, T helper cell precursors differentiate in a variety of four known effector cell subsets: IFN-γ producing Th1 cells, IL-4 producing Th2 cells, TGF-β producing Treg cells and IL-17 producing Th17 cells. TGF-β interacts in this process in several ways. The cytokine inhibits the development of Th1 (3, 4) and Th2 cells (5-7). In addition, TGF-β induces the transcription factor FoxP3, thereby promoting Treg-cell development (8). For Th17 cell differentiation the situation is much less defined. In the murine system TGF-β in combination with IL-6 has been considered to be a precondition for the development of naïve T helper cells into Th17 cells (9-11). In contrast, differentiation of human naïve T helper cells into Th17 cells has been

Key words: cytokines, T cell differentiation, TGF-β, Th17 cells, transgenic mouse models

Mailing address: Dr. Julia Schumann,
Institute of Physiological Chemistry,
Faculty of Veterinary Medicine,
University of Leipzig,
An den Tierkliniken 1, 04103 Leipzig, Germany
Tel.: +49 341 9738107 Fax: +49 341 9738119
e-mail address: julia.schumann@vmf.uni-leipzig.de

0393-974X (2012)

reported not to depend on TGF-β (12-15). Moreover, TGF-β has been predicted to act as a suppressive on IL-17 production of human $CD4^+$ T cells (14, 15). In this context, cytokines such as IL-1b and IL-23 have been suggested to drive Th17 cell development in the human system (12-14). Due to the divergent observations made in murine and human systems to date, Th17 cell development in mice and humans has been assumed to be regulated differentially (16). However, actual data provide evidence that TGF-β is not directly required for the molecular orchestration of Th17 cell differentiation in the murine system (17, 18). In this paper we highlight the role of TGF-β in Th17 cell development in the mouse, investigating the effects of likewise T cell specific over-expression of TGF-β or inhibition of TGF-β signal transduction in these cells by means of transgenic mouse models.

MATERIALS AND METHODS

Mice

Generation and characterization of the transgenic mouse strains used, TgN(CD2Tb)1Mbl (TgTGF) and TgN(CD2DkTbRII)2Mbl (TgdnRII), is described elsewhere (19, 20). The mouse strain TgTGF constitutively expresses biologically active TGF-β1 in T cells under the control of the human CD2 promoter. The mouse strain TgdnRII is T cell specific insensitive for TGF-β signaling caused by a truncated TGF-β type II receptor (DkTbRII) that is under the control of the human CD2 promoter (total blocking of TGF-β pathway in T cells). Both transgenic mouse strains have similar levels of active TGF-β in the blood serum. All transgenic mouse strains were established and maintained hemizygous on an FVB/N background. For investigations, female mice between 8 and 10 weeks of age were used. Mice were bred and housed under specific pathogen-free conditions in accordance with the guidelines approved by the Animal Care and Use Committee of the institutional and governmental authorities.

Cultivation of Borrelia burgdorferi sensu stricto N40 and infection of mice

B. burgdorferi sensu stricto N40 were grown for ten days at 33°C in modified Barbour-Stoenner-Kelly (BSK) medium as previously described (21). Organisms were visualized by dark field microscopy and enumerated by using a Petroff-Hausser counting chamber. Anesthetized mice were infected using *B. burgdorferi* sensu stricto N40, passage 4 via injection of 100 ml BSK medium containing 1 x 10^7 viable spirochetes intradermally into the shaved back.

Generation of single-cell suspensions and cell purification

Single-cell suspensions were prepared from spleens and axillary lymph nodes of naïve and *B. burgdorferi*-infected mice (14, 21, 28 days post-infection) by pressing tissues through a fine wire mesh. For lysis of the erythrocytes, splenocytes were incubated for 5 min in a buffer containing 1.6 M ammonium chloride underlayed with heat inactivated fetal calf serum (FCS; PAA, Paschin, Austria) and subsequently rested in phosphate buffered saline (PBS) for 2 h at 4°C.

$CD4^+$ T cells were enriched from spleens of naïve mice by negative selection using the $CD4^+$ T cell isolation kit (Miltenyi Biotec, Bergisch-Gladbach, Germany) according to the manufacturer's instructions (90-96% purity controlled by flow cytometry).

Cell culture conditions

Lymphocytes (2 x 10^6cells/ml) were incubated at 37°C and 5% CO_2 in a humidified atmosphere in Iscoves modified Dulbecco's medium (IMDM, Sigma, Taufkirchen, Germany) supplemented with 2 x 10^{-3} M L-glutamine, 100U/ml penicillin, 100mg/ml streptomycin (all PAA, Paschin, Austria), 5 x 10^{-5} M 2-mercaptoethanol (Sigma, Taufkirchen, Germany) and heat inactivated fetal calf serum (FCS, PAA, Paschin, Austria) as indicated.

Cell culture conditions used for purified $CD4^+$ T cells from naïve mice

(i) To investigate the TGF-β signal transduction in T cells of the mouse strain TgdnRII in comparison to the wild type, cells were incubated for 30 min in medium containing 0.5% FCS in absence (TGF-β blocking antibody; 3mg/ml) or presence of TGF-β1 (0.5ng/ml) (all R & D Systems, Wiesbaden, Germany).

(ii) For Th17 cell generation, cells were cultured for 48 h in medium containing 10% FCS supplemented with TGF-β1 (0.5ng/ml), IL-6 (10ng/ml), IL-23 (20ng/ml), anti-IL-2-antibody (10mg/ml) (all R & D Systems, Wiesbaden, Germany) and in the last 5 h in the presence of GolgiPlug (5mg/ml) (BD Biosciences, Heidelberg, Germany). T cell stimulation was carried out by anti-mouse-CD3e-antibody (5mg/ml) (BD Biosciences, Heidelberg, Germany).

Cell culture conditions used for splenocytes from naïve mice

(i) To investigate the interaction of TGF-β and LPS in T helper cell differentiation, splenocytes were cultured according to the Th17 cell generation protocol in presence of IL-6, IL-23 and anti-IL-2-antibody. Supplements added to the cultivation medium were: I. TGF-β blocking

antibody (3mg/ml) + LPS (from Salmonella Minnesota R595, ultrapure TLR4 grade) (100ng/ml) (Alexis Biochemicals, Lausen, Switzerland); II. TGF-β1 (0.5ng/ml) + LPS (from Salmonella Minnesota R595, ultrapure TLR4 grade) (1001ng/ml) (Alexis Biochemicals, Lausen, Switzerland).

(ii) To specify the effects of activin A or its antagonist follistatin 288 on Th17 cell generation, splenocytes of the mouse strains FVB/N WT (WT) and TgdnRII were cultured according to the Th17 cell generation protocol in presence of IL-6, IL-23 and anti-IL-2-antibody. Supplements (all R & D Systems, Wiesbaden, Germany) added to the cultivation medium were: I. TGF-β1 (0.5ng/ml); II. TGF-β blocking antibody (3mg/ml); III. TGF-β blocking antibody (3mg/ml) + activin A (19ng/ml); IV. TGF-β blocking antibody (3mg/ml) + follistatin 288 (5ng/ml); V. TGF-β1 (0.5ng/ml) + follistatin 288 (5ng/ml).

Cell culture conditions used for lymphocytes from B. burgdorferi-infected mice

For re-stimulation, cells were incubated for 5 h in medium containing 10% FCS in presence of GolgiPlug (5mg/ml) (BD Biosciences, Heidelberg, Germany) and either Concanavalin A (ConA) (5mg/ml) (Biochrom, Berlin, Germany) or *B. burgdorferi* sensu stricto N40 (1 x 10^7 borrelia/ml).

Flow cytometry

Cells were stained for the surface marker (anti-CD4 PerCP-Cy5.5) (BD Biosciences, Heidelberg, Germany), fixed in 1% formaldehyde in PBS, permeabilized in 0.55% saponine, and subsequently labeled with specific antibodies [rabbit-anti-phospho-Smad2 (Chemicon, Hampshire, Great Britain); anti-rabbit-IgG FITC (Upstate, Hampshire, Great Britain); anti-IFN-γ APC and anti-IL-17 PE (all BD Biosciences, Heidelberg, Germany)]. In all cases, an Fc block (purified anti mouse CD16/CD32) (BD Biosciences, Heidelberg, Germany) was used. For comparison baseline data of cells without *in vitro* (re-) stimulation were determined. Specifity of staining was verified via isotope controls carried out for all antibodies used (complementary data). Cells were analyzed on a FacsCalibur using Cellquest Pro software (all Becton Dickinson, Heidelberg, Germany).

Statistical analysis

Data are shown as means ± standard deviation (SD). Two-way analysis of variance followed by unpaired Student's *t* test was used to identify significant differences between means. The statistical analysis was carried out by means of the program GraphPad Prism 4 (GaphPad Software, La Jolla, USA). In all cases, $p < 0.05$ was assumed to indicate significant differences.

RESULTS

Mouse strain TgdnRII is insensitive for TGF-β in T cells

To verify the inhibition of the TGF-β signal transduction in T cells of the mouse strain TgdnRII, we investigated the phosphorylation of the Smad2 protein, a component of the TGF-β signal transduction pathway.

Exposure of wild type (WT) T cells to TGF-β1 resulted in a significant increase of cells with phosphorylated Smad2 protein (Fig. 1 A, B). In comparison, T cells from the mouse strain TgdnRII expressing a truncated TGF-β type II receptor did not up-regulate Smad2 phosphorylation (Fig. 1 C, D). Binding specifity of the capture and detection antibody used was assessed via staining of cells with *(i)* rabbit-IgG-antibody + detection antibody (anti-rabbit-IgG FITC) or *(ii)* detection antibody alone. Both assays revealed no positive signals underlining the strictness of binding of the test system used (complementary data).

Hence, in accordance to functional analysis conducted earlier (20) our data evidence the mouse strain TgdnRII to be insensitive for TGF-β in T cells.

Despite T cell insensitivity to TGF-β the mouse strain TgdnRII develops Th17 cells

The effects of T cell specific alterations in TGF-β activity and sensitivity on Th17 cell development were assayed *ex vivo* using a *Borrelia burgdorferi*–based infection model.

Th17 cells were detectable in lymph nodes of both mouse strains, TgTGF as well as TgdnRII (Fig. 2). Significant differences in Th17 cell numbers could be seen. Naïve mice of the mouse strain TgTGF displayed more $CD4^+IL\text{-}17^+$ cells than naïve mice of the mouse strain TgdnRII (Fig. 2 A, C). Interestingly, after infection, numbers of Th17 cells detectable were inversed. At all time points investigated post-infection the mouse strain TgdnRII developed more Th17 cells than the mouse strain TgTGF, regardless of the kind of re-stimulation used (Fig. 2 B, C; complementary data). Of note, wild type mice showed intermediate Th17 cell numbers at all conditions tested (complementary data).

Summing up, inhibition of the TGF-β signal cascade in T cells does not prevent Th17 cell

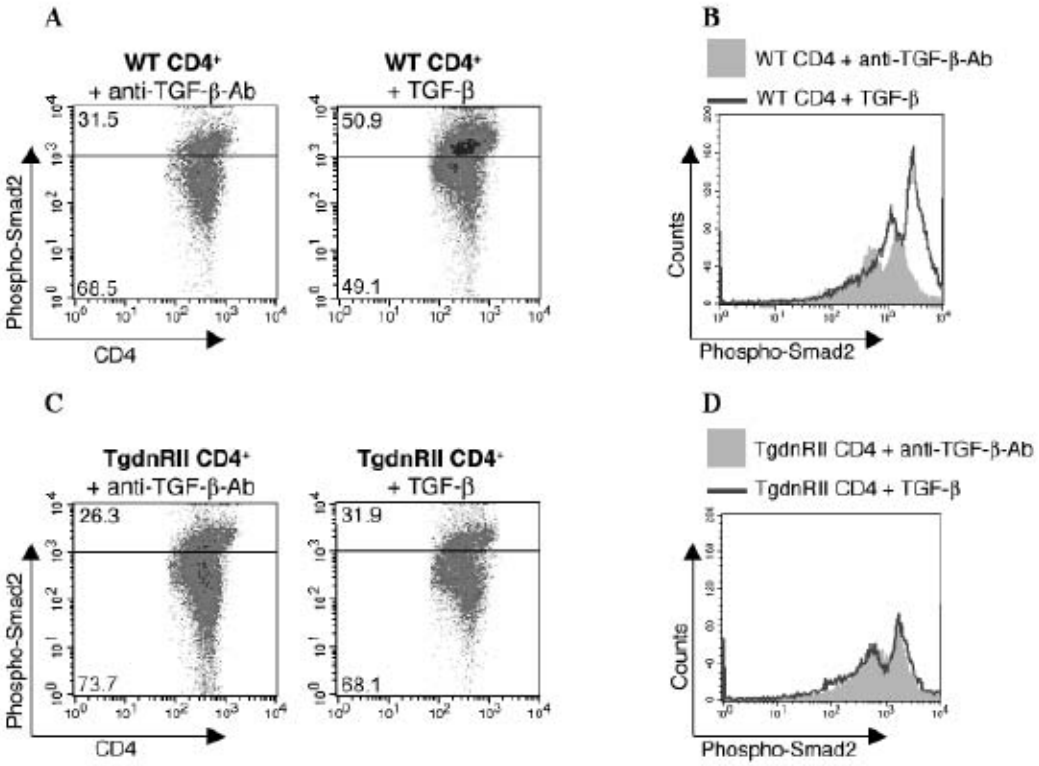

Fig. 1. *Mouse strain TgdnRII is insensitive for TGF-β in T cells. Purified CD4⁺ T lymphocytes from spleen were cultured for 30 min in absence (TGF-β blocking antibody) or presence of TGF-β1 (0.5ng/ml). Exposure of T cells from wild type mice to TGF-β1 increased the portion of CD4⁺Phospho-Smad2⁺ lymphocytes (**A**), thereby altering fluorescence intensity (**B**). No such effects were detectable in T cells from transgenic mice. Neither number of CD4⁺Phospho-Smad2⁺ cells (**C**) nor fluorescence intensity (**D**) was affected significantly by the presence of TGF-β1. Data shown are representative of three independent experiments with n = 6. Ab: antibody; WT: wild type.*

generation. Rather, our data indicate TGF-β signaling in T cells to be unnecessary for Th17 cell development *ex vivo* in the mouse.

TGF-β action on T cells is dispensable or even inhibitory for Th17 cell development

To further analyze the impact of the factor TGF-β on Th17 cell development, we performed an *in vitro* generation assay. The formation of Th17 cells *in vitro* confirmed the observations made in our *ex vivo* investigations. The TgdnRII genotype produced Th17 cells. Portions of detected $CD4^+IL\text{-}17^+$ lymphocytes thereby correspond to those observed in wild type animals (Fig. 3 A, B). The T cell specific TGF-β over-expressing mouse strain TgTGF displayed Th17 cells as well. However, the autocrine production of TGF-β appeared to be counterproductive on Th17 cell development. Compared to both the wild type and the mouse strain TgdnRII numbers of detectable Th17 cells were significantly decreased (Fig. 3 A, B).

Thus, induction by TGF-β is dispensable for Th17 cell generation *in vitro* in the murine system. Moreover, our data suggest even an inhibitory effect of TGF-β produced by T cells on the development of these pro-inflammatory effectors.

TGF-β inhibits LPS-induced Th1 cell development thereby promoting Th17 cell differentiation in an indirect positive way

To ascertain the interrelation between TGF-β and the Th1-Th17-cell balance, we investigated the effects of supplemental TGF-β in context of an LPS-induced Th1 cell generation.

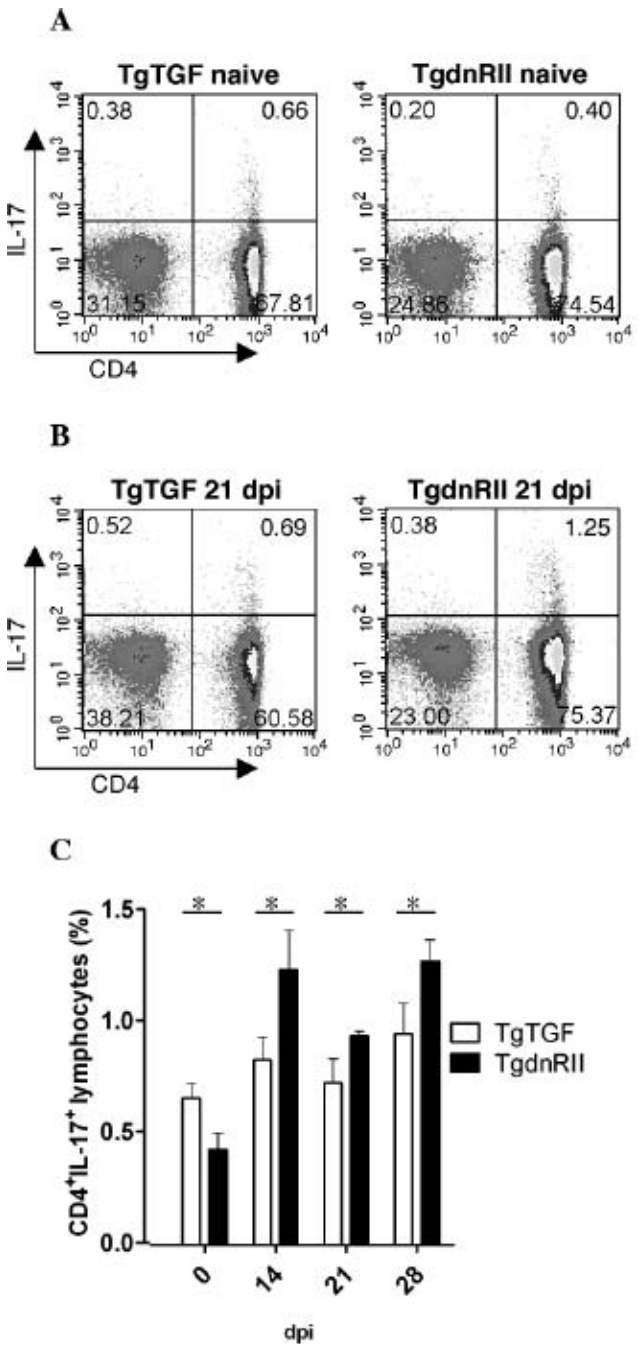

Fig. 2. *The mouse strain TgdnRII develops Th17 cells despite its T cell specific insensitivity to TGF-β. Stimulation of axillary lymph node cells from naïve (**A**) and B. burgdorferi-infected (**B**) mice for 5 h with borrelia organisms (1 x 10^7/ml). The histogram (**C**) shows portions of detectable $CD4^+IL\text{-}17^+$ lymphocytes on various days investigated. Note the presence of Th17 cells in the TgdnRII genotype. Data shown are as total cells and are representative of two independent experiments with n = 3. The differences are statistically significant for all days tested (*p < 0.05). Dpi: days post infection*

Development of Th1 cells driven by LPS was blocked by addition of TGF-β. Regarding the mouse strain tested following TGF-β supplementation, a drop in portion of $CD4^+IFN\text{-}\gamma^+$ cells and an increase in portion of $CD4^+IL\text{-}17^+$ could be seen (Fig. 4 A, B). Moreover, in absence of externally added TGF-β, the T cell specific TGF-β over-expressing mouse strain displayed less $CD4^+IFN\text{-}\gamma^+$ lymphocytes compared to both the wild type and the mouse strain TgdnRII (Fig. 4 A).

Thus, our data affirm TGF-β to be a potent suppressor of LPS-induced Th1 cell development.

Activin does not affect Th17 cell development

As a potential inducer of Th17 cells in the mouse, we tested activin, a TGF-β superfamily member, which like TGF-β itself uses the Smad2 signal transduction pathway.

The differentiation of splenocytes into Th17 cells succeeded with both the wild type and the mouse strain TgdnRII (Fig. 5). Addition of activin to the cultivation medium (in the absence of TGF-β1) did not affect the portion of detectable Th17 cells regardless of the mouse strain tested (Fig. 5). Likewise, the inhibition of activin via its antagonist follistatin neither in presence nor in absence of TGF-β brought about any changes in Th17 cell generation. Interestingly, inhibition of TGF-β via TGF-β blocking antibody resulted in a significant decrease in Th17 cell number for both mouse strains tested (Fig. 5). Since T cells of the mouse strain TgdnRII are insensitive to TGF-β this observation underlines indirect effects of TGF-β on Th17 cell differentiation via non-T cells in the splenocyte culture.

Taken together, our data show Th17 cell development to be independent from activin as well as from the activation of a Smad2 phosphorylation cascade.

DISCUSSION

Th17 cells are potent pro-inflammatory effectors crucial for the defense against extracellular bacteria (22). However, in this context and in the context of autoimmune disorders Th17 cells have been demonstrated to be key contributors to destructive pathological mechanism (22). Hence, there is an exigency to identify the mediators orchestrating

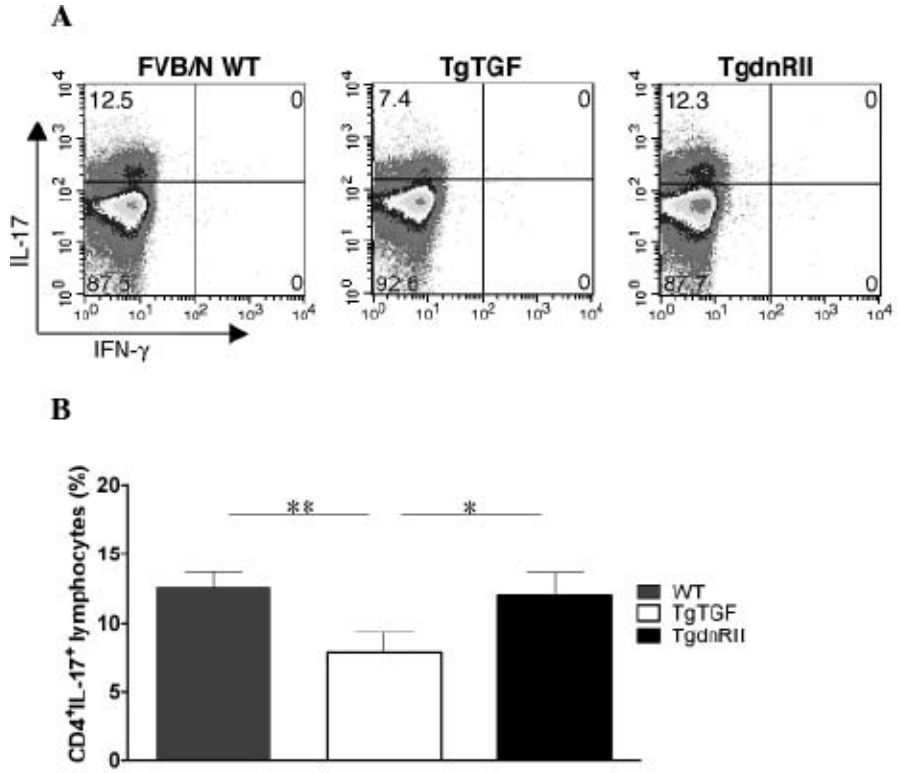

Fig. 3. *TGF-β action on T cells is not essential or even inhibitory for Th17 cell development. The stimulation of CD4⁺ lymphocytes of WT, TgTGF, TgdnRII for 48 h with anti-CD3e-antibody (5mg/ml) in the presence of TGF-β1 (0.5ng/ml), IL-6 (10ng/ml), IL-23 (20 ng/ml), anti-IL-2-antibody (10mg/ml) is shown in part (**A**). The histogram illustrates detectable numbers of developed CD4⁺IL-17⁺ cells (**B**). Note the presence of in vitro generated Th17 cells in the absence of TGF-β signaling (TgdnRII genotype). Data shown are representative of two independent experiments with n = 10. The differences are statistically significant (**p < 0.01; *p < 0.05). WT: wild type*

Th17 cell differentiation. A number of trials report TGF-β to be involved in Th17 cell development. Nevertheless, to date, the role TGF-β plays in Th17 cell generation remains unclear. In this study we investigate the interrelation between TGF-β and Th17 cell development in the murine system by means of transgenic mouse models.

The transgenic mouse strain TgdnRII expresses a truncated TGF-β type II receptor that is under the control of the human CD2 promotor. *In vitro* in a functional analysis it has been shown that IL-2 production of purified and specifically stimulated transgenic T cells could not be inhibited by adding TGF-β1 even at a concentration of 10 ng/ml (20). In addition, in our study cultivation of T cells from TgdnRII mice in presence of TGF-β did not up-regulate phosphorylation of the signal protein Smad2 as seen in T cells from wild type control animals. Smad2 is known to be sufficient for TGF-β signaling in T cells even in absence of Smad3 (23). Thus, our data clearly demonstrate the ability of the truncated receptor to compete with the endogenous TGF-β type II receptor resulting in a T cell specific insensitivity for TGF-β signaling.

Despite its T cell specific insensitivity to TGF-β, the mouse strain TgdnRII developed pro-inflammatory Th17 cells. Detection of Th17 cells succeeded both *ex vivo* after re-stimulation of lymph node cells of *B. burgdorferi*-infected mice and *in vitro* after T cell specific stimulation of splenocytes and purified CD4⁺ lymphocytes. Hence, our data affirm the dispensability of TGF-β signaling for Th17 cell development in the mouse. Moreover, over-expression of TGF-β by T cells of the mouse strain TgTGF has an inhibitory effect on Th17 cell development. Both after re-stimulation of lymph

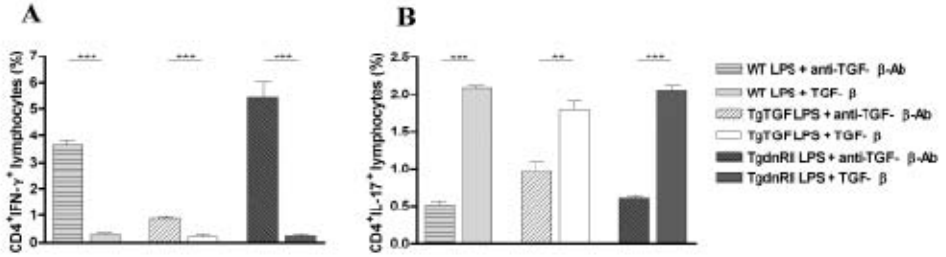

Fig. 4. *TGF-β inhibits LPS-induced Th1 cell development thereby promoting Th17 cell differentiation in an indirect positive way. Stimulation of splenocytes of WT, TgTGF, TgdnRII for 48 h with anti-CD3e-antibody (5mg/ml) plus LPS (100 ng/ml) in absence (TGF-β blocking antibody) or presence of TGF-β1 (0.5ng/ml). Addition of TGF-β effectively blocks development of CD4⁺IFN-γ⁺ cells (**A**) thereby promoting CD4⁺IL-17⁺ cell differentiation (**B**). Data shown are gated on CD4⁺ cells and are representative of two independent experiments with n = 5. The differences are statistically significant (**p < 0.01; *p < 0.05). Ab: antibody; WT: wild type*

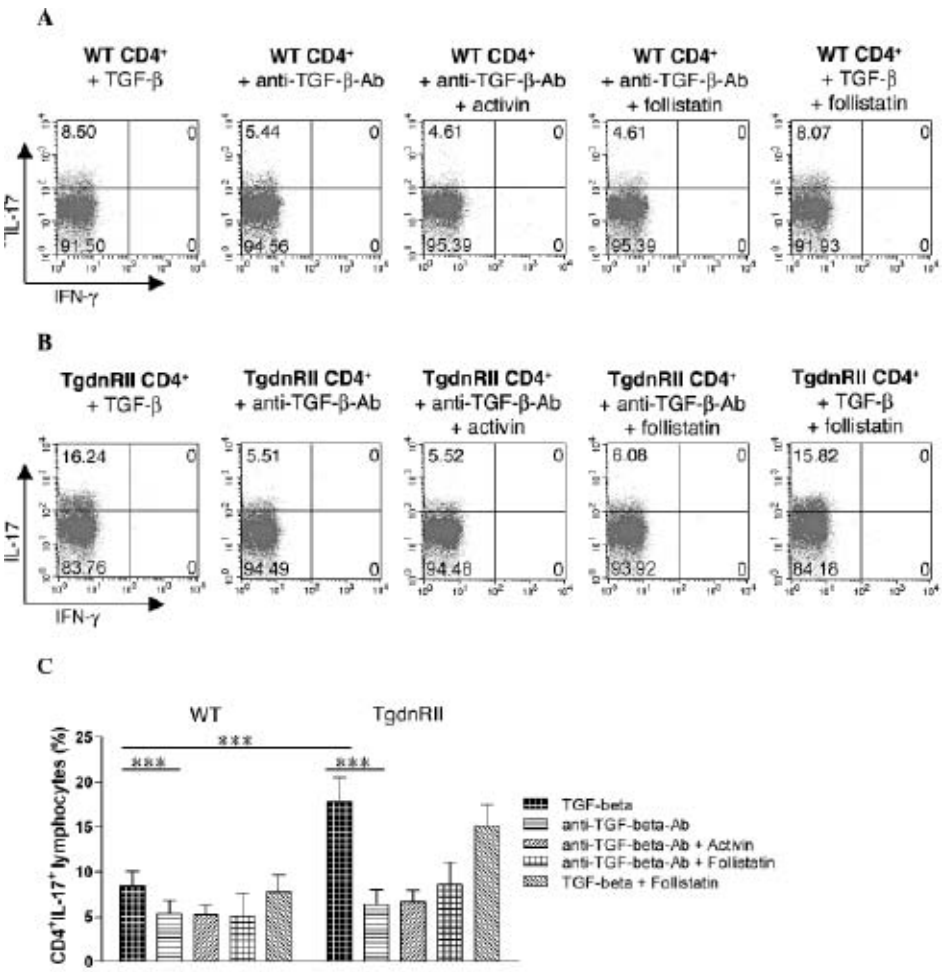

Fig. 5. *Activin does not affect Th17 cell development. Stimulation of splenocytes from either wild type (**A**) or TgdnRII genotype (**B**) for 48 h with anti-CD3e-antibody (5mg/ml) in the presence of IL-6 (10ng/ml), IL-23 (20ng/ml) and anti-IL-2-antibody (10mg/ml). TGF-β1 (0.5ng/ml), TGF-β blocking antibody (3mg/ml), activin (19ng/ml) and follistatin (5ng/ml) are added as indicated. **C**) The histogram shows detectable numbers of developed CD4⁺IL-17⁺ cells. Note the presence of in vitro generated Th17 cells in the absence of TGF-β (TGF-β blocking antibody). Supplementation of activin as well as follistatin does not alter Th17 cell number. Data shown are gated on CD4⁺ cells and are representative of two independent experiments with n = 8. The differences are statistically significant (***p < 0.001; (**p < 0.01). Ab: antibody; WT: wild type*

node cells from *B. burgdorferi*-infected mice and after generation of $CD4^+IL\text{-}17^+$ lymphocytes from naïve precursor T cells portion of detectable Th17 cells from TgTGF mice was decreased significantly in comparison to the wild type. TGF-β, therefore, is not only dispensable for Th17 cell generation but is even inhibitory if produced by T cells. This finding highly resembles the human situation (12-14).

In contrast to our results, Veldhoen reported that naïve $CD4^+$ T cells from a transgenic mouse strain expressing a dominant negative form of the TGF-β receptor II under the control of the CD4 promoter do not differentiate into Th17 cells (24). This discrepancy may be due to two crucial differences in experimental settings *(i)* genetic background and transgene promoter and *(ii)* conditions chosen for Th17 cell development. Regarding genetic background and transgene promoter, the mouse strain TgdnRII used in the present study was maintained on an FVB/N background. In contrast, the transgenic mouse strain used by Veldhoen was based on a C57BL/6 background (24). Besides, different promoters were used for gene expression. Veldhoen used mice expressing the transgene under the control of the CD4 promoter lacking the CD8 silencer (25). The mice used in our study expressed the transgene under the control of the CD2 promoter. Both mouse strains differ in their naïve phenotype, with the CD4 promoter transgenics developing spontaneous occurrence of T cell differentiation and autoimmunity (25) contrasted by a normal phenotype of the CD2 promoter transgenics. However, whether the differences seen in Th17 cell development between these two strains depend on genetic background or different promoter usage remains to be elucidated. Regarding the chosen conditions for Th17 cell development, possibly important differences between our study and the study by Veldhoen (9, 24) exist. In the latter study naïve $CD4^+$ T cells were co-cultivated with Treg cells and dendritic cells and were stimulated with anti-CD3-antibody and LPS in the presence of TGF-β blocking antibody (9, 24). Under these conditions $CD4^+$ T cells differentiated into IFN-γ producing Th1 cells. Presumably, the observations made by Veldhoen are effects resulting from the usage of LPS as a stimulant. LPS is known as strong inducer of Th1 reactions via a release of IL-12 by dendritic cells (26). As we show, TGF-β effectively inhibits this LPS-induced Th1 response. The effect of TGF-β in such a setting, therefore, is based rather on the prevention of Th1 cell development than on a true induction of Th17 cells. This interpretation is in accordance with recent findings both in the human as well as the murine system where TGF-β has been implicated to promote Th17 cell development indirectly by repressing Th1 and Th2 responses (17, 18, 27).

The inhibitory effects of TGF-β on Th1 and Th2 cells provide an optimal milieu for Treg and Th17 cell development. Since the cytokine represents an inducer for Treg cell generation, Th17 cell differentiation crucially depends on the presence of other so far unknown factors. As a potential candidate, activin was tested for its potency to influence Th17 cell development. Activin is part of the TGF-β family signaling via the same Smad-pathway as TGF-β (28). Furthermore, activin is up-regulated in a variety of autoimmune inflammatory diseases also linked with Th17 cells (29-34). Nevertheless, as shown in this study, activin does not affect detectable Th17 cell number. Thus, neither activin nor activation of a Smad2 pathway is necessary for Th17 cell development in the mouse.

Summing up, we could show TGF-β signaling in T cells to be dispensable or even inhibitory for generation of Th17 cells in the mouse. Furthermore, our data affirm TGF-β to inhibit an LPS-driven Th1 cell development, acting as an indirect effector in Th17 cell differentiation. Hence the impact of TGF-β in T helper cell specification is due to its inhibitory action on Th1 and Th2 cells in addition to its direct promotion of Treg cell amplification.

ACKNOWLEDGEMENTS

This work was supported by the Free State of Saxony, Germany.

REFERENCES

1. Li MO, Wan YY, Sanjabi S, Robertson AK, Flavell RA. Transforming growth factor-beta regulation of immune responses. Annu Rev Immunol 2006; 24:99-146.
2. Wahl SM. TGF-βeta in the evolution and resolution of inflammatory and immune processes. Microbes Infect 1999; 1:1247-9.
3. Gorelik L, Constant S, Flavell RA. Mechanism of

transforming growth factor beta-induced inhibition of T helper type 1 differentiation. J Exp Med 2002; 195:1499-505.
4. Lin JT, Martin SL, Xia L, Gorham JD. TGF-βeta 1 uses distinct mechanisms to inhibit IFN-γamma expression in CD4+ T cells at priming and at recall: differential involvement of Stat4 and T-bet. J Immunol 2005; 174:5950-8.
5. Chen CH, Seguin-Devaux C, Burke NA, Oriss TB, Watkins SC, Clipstone N, Ray A. Transforming growth factor beta blocks Tec kinase phosphorylation, Ca2+ influx, and NFATc translocation causing inhibition of T cell differentiation. J Exp Med 2003; 197:1689-99.
6. Gorelik L, Fields PE, Flavell RA. Cutting edge: TGF-βeta inhibits Th type 2 development through inhibition of GATA-3 expression. J Immunol 2000; 165:4773-7.
7. Heath VL, Murphy EE, Crain C, Tomlinson MG, O'Garra A. TGF-βeta1 down-regulates Th2 development and results in decreased IL-4-induced STAT6 activation and GATA-3 expression. Eur J Immunol 2000; 30:2639-49.
8. Chen W, Jin W, Hardegen N, Lei KJ, Li L, Marinos N, McGrady G, Wahl SM. Conversion of peripheral CD4+. J Exp Med 2003; 198:1875-86.
9. Veldhoen M, Hocking RJ, Atkins CJ, Locksley RM, Stockinger B. TGFbeta in the context of an inflammatory cytokine milieu supports de novo differentiation of IL-17-producing T cells. Immunity 2006; 24:179-89.
10. Mangan PR, Harrington LE, O'Quinn DB, et al. Transforming growth factor-beta induces development of the T(H)17 lineage. Nature 2006; 441:231-4.
11. Bettelli E, Carrier Y, Gao W, Korn T, Strom TB, Oukka M, Weiner HL, Kuchroo VK. Reciprocal developmental pathways for the generation of pathogenic effector TH17 and regulatory T cells. Nature 2006; 441:235-8.
12. Chen Z, Tato CM, Muul L, Laurence A, O'Shea JJ. Distinct regulation of interleukin-17 in human T helper lymphocytes. Arthritis Rheum 2007; 56:2936-46.
13. Wilson NJ, Boniface K, Chan JR, et al. Development, cytokine profile and function of human interleukin 17-producing helper T cells. Nat Immunol 2007; 8:950-7.
14. Acosta-Rodriguez EV, Napolitani G, Lanzavecchia A, Sallusto F. Interleukins 1beta and 6 but not transforming growth factor-beta are essential for the differentiation of interleukin 17-producing human T helper cells. Nat Immunol 2007; 8:942-9.
15. Manel N, Unutmaz D, Littman DR. The differentiation of human T(H)-17 cells requires transforming growth factor-beta and induction of the nuclear receptor RORgammat. Nat Immunol 2008; 9:641-9.
16. Annunziato F, Cosmi L, Liotta F, Maggi E, Romagnani S. Human Th17 cells: Are they different from murine Th17 cells? European Journal of Immunology 2009; 39:637-40.
17. Das J, Ren G, Zhang L, et al. Transforming growth factor beta is dispensable for the molecular orchestration of Th17 cell differentiation. J Exp Med 2009; 206:2407-16.
18. Ghoreschi K, Laurence A, Yang XP, et al. Generation of pathogenic T(H)17 cells in the absence of TGF-βeta signalling. Nature 2010; 467:967-71.
19. Schramm C, Huber S, Protschka M, et al. TGFbeta regulates the CD4+CD25+ T-cell pool and the expression of Foxp3 *in vivo*. Int Immunol 2004; 16:1241-9.
20. Schramm C, Protschka M, Kohler HH, et al. Impairment of TGF-βeta signaling in T cells increases susceptibility to experimental autoimmune hepatitis in mice. Am J Physiol Gastrointest Liver Physiol 2003; 284:G525-G535.
21. Knauer J, Siegemund S, Muller U, Al-Robaiy S, Kastelein RA, Alber G, Straubinger RK. *Borrelia burgdorferi* potently activates bone marrow-derived conventional dendritic cells for production of IL-23 required for IL-17 release by T cells. FEMS Immunol Med Microbiol 2007; 49:353-63.
22. Cua DJ, Kastelein RA. TGF-βeta, a 'double agent' in the immune pathology war. Nat Immunol 2006; 7:557-9.
23. Datto MB, Frederick JP, Pan L, Borton AJ, Zhuang Y, Wang XF. Targeted disruption of Smad3 reveals an essential role in transforming growth factor beta-mediated signal transduction. Mol Cell Biol 1999; 19:2495-504.
24. Veldhoen M, Hocking RJ, Flavell RA, Stockinger

B. Signals mediated by transforming growth factor-beta initiate autoimmune encephalomyelitis, but chronic inflammation is needed to sustain disease. Nat Immunol 2006; 7:1151-6.

25. Gorelik L, Flavell RA. Abrogation of TGFbeta signaling in T cells leads to spontaneous T cell differentiation and autoimmune disease. Immunity 2000; 12:171-81.
26. Pearce EJ, Kane CM, Sun J. Regulation of dendritic cell function by pathogen-derived molecules plays a key role in dictating the outcome of the adaptive immune response. Chem Immunol Allergy 2006; 90:82-90.
27. Volpe E, Servant N, Zollinger R, Bogiatzi SI, Hupe P, Barillot E, Soumelis V. A critical function for transforming growth factor-beta, interleukin 23 and proinflammatory cytokines in driving and modulating human T(H)-17 responses. Nat Immunol 2008; 9:650-7.
28. Phillips DJ. Activins, inhibins and follistatins in the large domestic species. Domest Anim Endocrinol 2005; 28:1-16.
29. Yu EW, Dolter KE, Shao LE, Yu J. Suppression of IL-6 biological activities by activin A and implications for inflammatory arthropathies. Clin Exp Immunol 1998; 112:126-32.
30. Ota F, Maeshima A, Yamashita S, et al. Activin A induces cell proliferation of fibroblast-like synoviocytes in rheumatoid arthritis. Arthritis Rheum 2003; 48:2442-9.
31. Hubner G, Brauchle M, Gregor M, Werner S. Activin A: a novel player and inflammatory marker in inflammatory bowel disease? Lab Invest 1997; 77:311-8.
32. Smith C, Yndestad A, Halvorsen B, et al. Potential anti-inflammatory role of activin A in acute coronary syndromes. J Am Coll Cardiol 2004; 44:369-75.
33. Cho SH, Yao Z, Wang SW, Alban RF, Barbers RG, French SW, Oh CK. Regulation of activin A expression in mast cells and asthma: its effect on the proliferation of human airway smooth muscle cells. J Immunol 2003; 170:4045-52.
34. Matsuse T, Ikegami A, Ohga E, et al. Expression of immunoreactive activin A protein in remodeling lesions associated with interstitial pulmonary fibrosis. Am J Pathol 1996; 148:707-13.

EFFECT OF CHRONIC FORCED RUNNING ON GENE EXPRESSION OF CATECHOLAMINE BIOSYNTHETIC ENZYMES IN STELLATE GANGLIA OF RATS

L. GAVRILOVIĆ[1], V. MANDUŠIĆ[2], V. STOJILJKOVIĆ[1], J. KASAPOVIĆ[1], S. STOJILJKOVIĆ[3], S.B. PAJOVIĆ[1] and S. DRONJAK[1]

[1]Institute of Nuclear Sciences "Vinča", Laboratory of Molecular Biology and Endocrinology, University of Belgrade, Belgrade, Serbia; [2]Institute of Nuclear Sciences "Vinča", Laboratory of Radiobiology and Molecular Genetics, University of Belgrade, Belgrade, Serbia, [3]University of Belgrade, Faculty of Sport and Physical Education, Belgrade, Serbia

Received August 19, 2011 – Accepted May 24, 2012

The sympathoneural system has a profound influence on the heart function. Sympathetic neurons are the major contributors to the huge rise of circulating noradrenaline (NA) level in response to stressful stimuli. Treadmill training in rats is forced exercise which has the propensity to induce both psychological and physical stress. The aim of this study is to examine how chronic forced running (CFR) affects the expression of catecholamine biosynthetic enzymes (tyrosine hydroxylase (TH), dopamine-ß-hydroxylase (DBH) and phenylethanolamine N-methyltransferase (PNMT)) and cAMP response element-binding (CREB) in stellate ganglia, as well as the concentrations of catecholamines, adrenocorticotropic hormone (ACTH) and corticosterone (CORT) in the plasma of rats. Also, we investigated how the additional acute immobilization stress changes the mentioned parameters. The rat training program consisted of 12 weeks running on a treadmill (20 m/min, 20 min/day). We found that CFR increases TH and DBH mRNA and protein levels in stellate ganglia, which is followed by increased NA concentration in the plasma. CFR reduces the level of PNMT mRNA, while the level of PNMT protein remains unchanged in stellate ganglia. The increased expression of TH and DBH genes positively correlates with the expression of CREB in stellate ganglia and with plasma ACTH level, while reduced level of PNMT mRNA in stellate ganglia correlates with reduced plasma CORT level. The additional acute immobilization stress increased gene expression of catecholamine biosynthetic enzymes in stellate ganglia, as well as catecholamines, ACTH and CORT levels in the plasma. The results presented here suggest that the continuous increase of the noradrenaline biosynthetic enzyme expression in stellate ganglia due to CFR may play a role in growing risk of cardiovascular diseases.

The sympathetic nervous system (SNS) plays an important role in regulating the function of the heart and has a central role in the cardiovascular response to stress. Sympathetic nerves innervating the heart originate from stellate ganglia and influence the catecholamine levels in the heart (1). Therefore, the expression of catecholamine biosynthetic enzymes in stellate ganglia and their modulation under stress conditions has a direct impact on the heart function. Treadmill training in rats is forced exercise which has the propensity to induce both psychological and physical stress (2). The effects of chronic treadmill

Key words: catecholamine, chronic forced running, immobilization stress, stellate ganglia, qRT-PCR

Mailing address:
Ljubica Gavrilović, Ph.D.
Institute of Nuclear Sciences "Vinča"
Laboratory of Molecular Biology and Endocrinology
P.O.B. 522-090 11000 Belgrade, Serbia
Tel/Fax: +381112455561
e-mail: gljubica@vinca.rs

0393-974X (2012)

training are likely to be associated with alterations in gene expression of catecholamine biosynthetic enzymes: tyrosine hydroxylase (TH) a "rate-limiting" of catecholamines biosynthesis, dopamine-β-hydroxylase (DBH) that converts dopamine (DA) into noradrenaline (NA) and phenyl ethanolamine N-methyltransferase (PNMT) catalyzing conversion NA to adrenaline (A). Although the response of the stellate ganglia is extremely important since it is the source of the major sympathetic innervations of the heart, the mechanism of regulation of catecholamine biosynthetic enzymes to chronic treadmill training is not sufficiently studied. Detecting regulatory physiological mechanism for catecholamine synthesis in stellate ganglia in stress conditions provoked by forced prolonged running is extremely important in the prevention of cardiovascular diseases in sports medicine and pathophysiology. One of the key questions in stress research is how the same stressor can elicit a variant or altered response depending on prior experience with the current or different stressor. Immobilization is frequently used as an additional acute stressor and is considered one of the most intensive stressors that significantly change gene expression (3). The response to novel additional acute immobilization stress might reveal the detailed mechanisms underlying the gene expression of catecholamine biosynthetic enzymes in stellate ganglia and the catecholamine impact on heart in conditions of chronic physical activity. In this study we investigated how chronic forced running (CFR), as well as the additional acute immobilization stress (CFR+IMM) affects the mRNA and protein levels of catecholamine biosynthetic enzymes in stellate ganglia, as well as on the concentrations of NA, A, ACTH and morning corticosterone (CORT) in the plasma of rats. We also investigated the level of cAMP response element-binding (CREB) mRNA in stellate ganglia of chronically stressed animals, since it was shown that CREB plays a major role in regulating the expression of TH and DBH genes during forced exercise (4, 5).

MATERIALS AND METHODS

Animals and treadmill running

In this study Wistar male rats (11-week-old) were used. Animals were under standard laboratory conditions with water and food ad libitum and kept three to four per cage. Care was taken to minimize the pain and discomfort of the animals according to the recommendations of the Ethics Committee of the "Vinča" Institute of Nuclear Sciences, Belgrade, Serbia, which are in accordance with the Guide for Care and Use of Laboratory Animals of the National Institute of Health, Bethesda, MD, U.S.A.

Animals were divided into four groups: i) The control group (n=10) was not exposed to any treatment; ii) CFR group (n=10) consisted of animals exposed to chronic forced running for a period of 12 weeks; iii) IMM group (n=40) consisted of animals exposed to acute immobilization stress, for a period of 2 h, and iv) CFR+IMM group (n=40) consisted of animals exposed to CFR stress for a period of 12 weeks, and after chronic stress, these animals were exposed to additional acute IMM stress for a period of 2 h.

Chronic forced running was achieved by the rats daily on the treadmill running. Animals assigned to an exercise training group were gradually introduced to treadmill running during a 7-day period. In our experience, about 15% of rats do not run well enough on the treadmill to achieve an exercise training effect. In order to judge rat trainability prior to the onset of the experiment, performance was rated by a scale from 1 to 5.5, the latter representing the best performance score (6). Animals with a mean rating of 3 or higher were considered to be performing well and assigned to the treadmill training groups. The treadmill speed required to approximate a relative workload throughout the training protocol was estimated from oxygen cost of running. Our training intensity was designed to elicit ~70-75% maximal oxygen uptake. Animals assigned to treadmill training ran on the treadmill 5 days a week for 12 weeks, during which period the exercise time was increased from 10 min to 20 min/day and treadmill speed gradually increased from 10 to 20 m/min by the end of the second week, maintaining the incline at 0º. The animals then ran according to this regimen for 10 additional weeks (20 min/day at a speed of 20 m/min, 5 days a week). In the present study, we exposed animals to a low-intensity treadmill training, since Erdem et al. (7), by using low-intensity training, suggested that exercise intensity is a pivotal factor in the effect of submaximal endurance training (12 weeks) on adrenomedullary catecholamine biosynthesis. Animals were monitored continuously during exercise.

Immobilization stress was provoked as described by Kvetnansky and Mikulaj (8). Groups IMM and IMM + CFR contained 40 animals. These groups were divided into four subgroups (n=10), because we examined changes in catecholamine biosynthetic enzymes in four different time periods after the cessation of immobilization. The animals were sacrificed after chronic stress, immediately after the

cessation of acute immobilization and 3 h, 6 h and 22 h after the acute immobilization. Literature data show that in these periods changes in gene expression of catecholamine biosynthetic enzymes in stellate ganglia are expected (3, 9). Samples of blood were collected and both stellate ganglia were isolated. Stellate ganglia were immediately frozen and stored in liquid nitrogen until analyzed. To determine whether CFR affects the diurnal rhythm of CORT in this experiment, we measured morning CORT.

RNA isolation and cDNA synthesis

Total RNAs were isolated using TRIZOL reagent (Invitrogen, USA). After the isolation of mRNA, DNA-ase treatment was applied with DNAse I (Fermentas, Lithuania). Concentration of total mRNA was measured in triplicate by a spectrophotometer. Quality of mRNA was checked on agarose gel. Reverse transcription was performed using Ready-To-Go You-Prime First-Strand Bead (Amersham Biosciences, UK) and pd (N)6 Random Hexamer (Amersham Biosciences, UK) primer according to the manufacturer's protocol.

Real-time RT-PCR

TaqMan PCR assays were carried out using Assay-on-Demand Gene Expression Products (Applied Biosystems, USA) for TH (Rn00562500_m1), DBH (Rn00565819_m1), PNMT (Rn01495589_g1) and CREB (Rn01441386_g1). The reference gene (endogenous control) was included in each analysis to correct for the differences in the inter-assay amplification efficiency and all transcripts were normalised to cyclophyline A (Rn00690933_m1) expression. Real-time RT-PCR assay was carried out exactly as previously described (10).

Western blot analysis

Western blot analysis was performed as previously described (10). Antibodies used for quantification of specific proteins were as follows: for TH the monoclonal primary antibody against mouse TH (monoclonal antibody against TH from mouse-mouse hybrid cells, clone 2/40/15, dilution 1:5000, Chemicon International, USA), for DBH the anti-dopamine-ß hydroxylase (N-terminal) antibody, sheep (dilution 1:5000, Sigma, USA), for PNMT the polyclonal ant-PNMT primary antibody, rabbit (dilution 1:1000, Protos Biotech Corporation, USA) and for β-actin the rabbit polyclonal anti-β-actin (ab8227, dilution 1:5000, Abcam, USA). Densitometry of protein bands on ECL film (Amersham Biosciences, UK) was performed by Image J analysis PC software. The result was expressed in arbitrary units normalized in relation to β actin.

Catecholamine, ACTH and CORT measurements

Plasma catecholamines were measured by a standard radioenzymatic assay described previously by Peuler and Johnson (11) and the values were expressed as pg/ml plasma. Catecholamines present in plasma aliquots were converted to their labeled O-methylated derivatives by S-(3H) adenosylmethionine (Lacomed, Czech Republic) and the lyophilized catechol-O-methyl transferase isolated from the rat liver. The O-methylated derivatives of the amines were then extracted along with unlabeled carrier compounds.

Plasma ACTH was determined by a chemiluminescent method using IMMULITE automatic analyzer (Diagnostic Products Corporation, Los Angeles, CA, USA) and the values were expressed as pg ACTH/ml plasma.

Plasma CORT was measured upon prior extraction directly, using RIA commercial kits (MP Biomedicals, Germany) and the values were expressed as ng CORT/ml plasma.

Data analysis

The data are presented as means ± S.E.M. Differences of gene expression (mRNA and protein levels) of catecholamine biosynthetic enzymes (TH, DBH and PNMT) and level of CREB mRNA in stellate ganglia and concentration of NA, A, ACTH and CORT in plasma were analyzed by One-way ANOVA. The effects of chronic forced running (CFR) and acute immobilization stress (IMM) compared to control animals, as well as the effects of additional acute immobilization stress after chronic forced running (CFR+IMM) compared to chronic forced running animals (CFR), were tested by Tukey post-hoc test.

Correlations of mRNA levels, protein levels and hormone levels were analyzed by the Spearman test, using the Sigma Plot v10.0 (with SigmaStat integration).

Statistical significance (p) was set to 0.05 statistical power (1-ß) exceeded 85%. Statistical power confirms that the number of animals (n=10) was sufficient for this experiment. Reliability test was designed so we did three repeated measurements of the level of gene expression of TH, DBH, PNMT and CREB. The calculated value of the ICCR test of >0.85 was considered to be satisfactory and it proves the reliability of the applied methods. Statistical analysis was carried out using the SPSS.

RESULTS

Changes in plasma concentrations of NA, A, ACTH and CORT

CFR treatment. CFR treatment increased plasma concentrations of NA by 20% ($p<0.05$, Tukey test, Fig. 1a), A by 25% ($p<0.05$, Tukey test, Fig. 1b) and ACTH by 100% ($p<0.01$, Tukey test, Fig. 1c) and

decreased CORT concentration by 15% ($p<0.05$, Tukey test, Fig. 1d), compared with control animals.

IMM and CFR+IMM treatment. The exposure of the animals to acute immobilization stress significantly increased concentration of NA by 48% ($p<0.05$, Tukey test, Fig. 1a) and A concentration by 60% ($p<0.05$, Tukey test, Fig. 1b), while the additional acute immobilization of CFR animals increased NA concentration by 60% ($p<0.01$, Tukey test, Fig. 1a) and A concentration by 71% ($p<0.01$, Tukey test, Fig. 1b) 3 h after the cessation of immobilization. Similar changes are found 22 h after the cessation of acute immobilization. Also, we found that acute IMM induced significant increase ACTH concentration by 900% ($p<0.01$, Tukey test, Fig. 1c) and CORT concentration by 66% ($p<0.01$, Tukey test, Fig. 1d), while the exposure of CFR animals to additional acute immobilization stress increased ACTH concentration by 1150% ($p<0.001$, Tukey test, Figure 1c) and CORT concentration by 96% ($p<0.001$, Tukey test, Fig. 1d) in the plasma immediately after the cessation of immobilization.

Changes of TH, DBH, PNMT and CREB mRNA levels in stellate ganglia

CFR treatment. The animals exposed to CFR showed increased levels of TH mRNA by 25% ($p<0.05$, Tukey test, Fig. 2a), DBH mRNA by 20% ($p<0.05$, Tukey test, Fig. 2b) and CREB mRNA by 40% ($p<0.05$, Tukey test, Fig. 2d), compared with

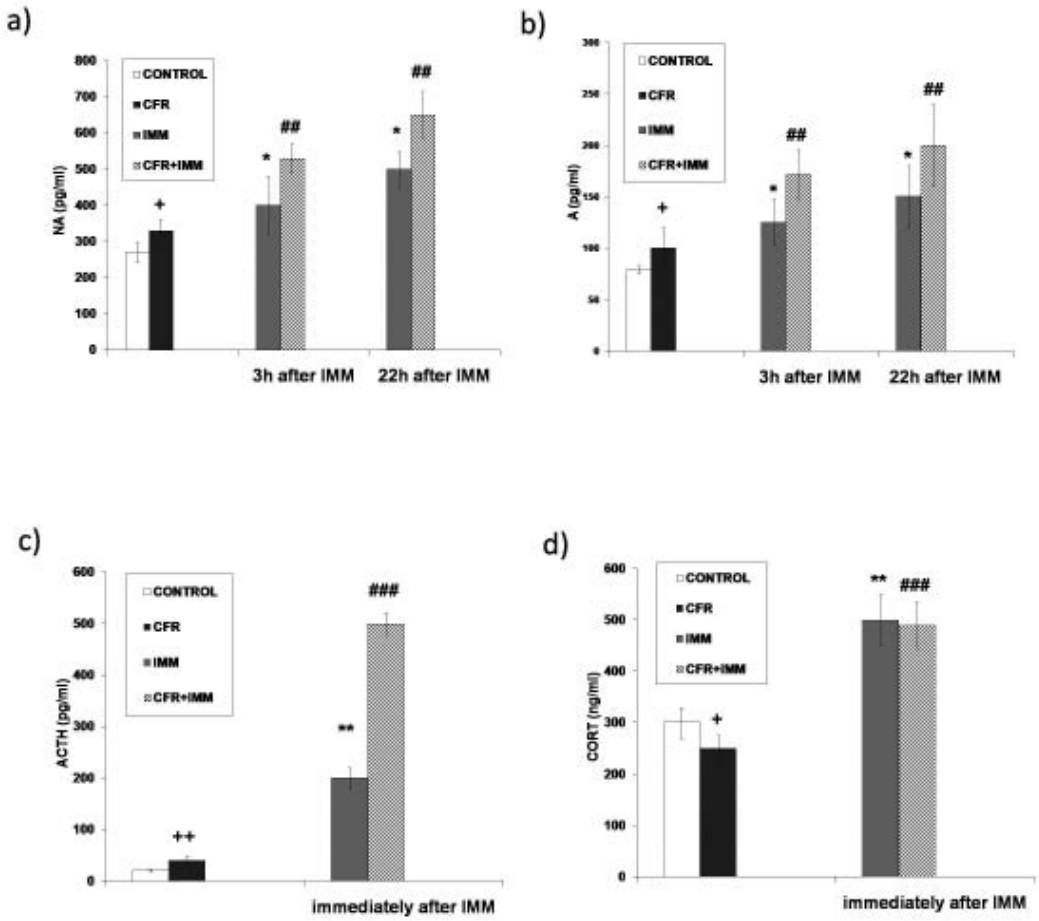

Fig. 1. *Effects of chronic forced running and additional acute immobilization stress on the concentration of noradrenaline (NA) [a], adrenaline (A) [b], adrenocorticotropic hormone (ACTH) [c] and corticosterone (CORT) [d] in the plasma. The values are means ± S.E.M. of 10 rats. Statistical significance: +p<0.05, ++p<0.01 animals exposed to chronic forced running vs control animals (Tukey test); *p<0.05, **p<0.01 animals exposed to acute 2-h immobilization vs control animals (Tukey test); ##p<0.01, ###p<0.001 animals exposed to additional acute 2-h immobilization stress after chronic forced running vs. animals exposed to chronic forced running (Tukey test).*

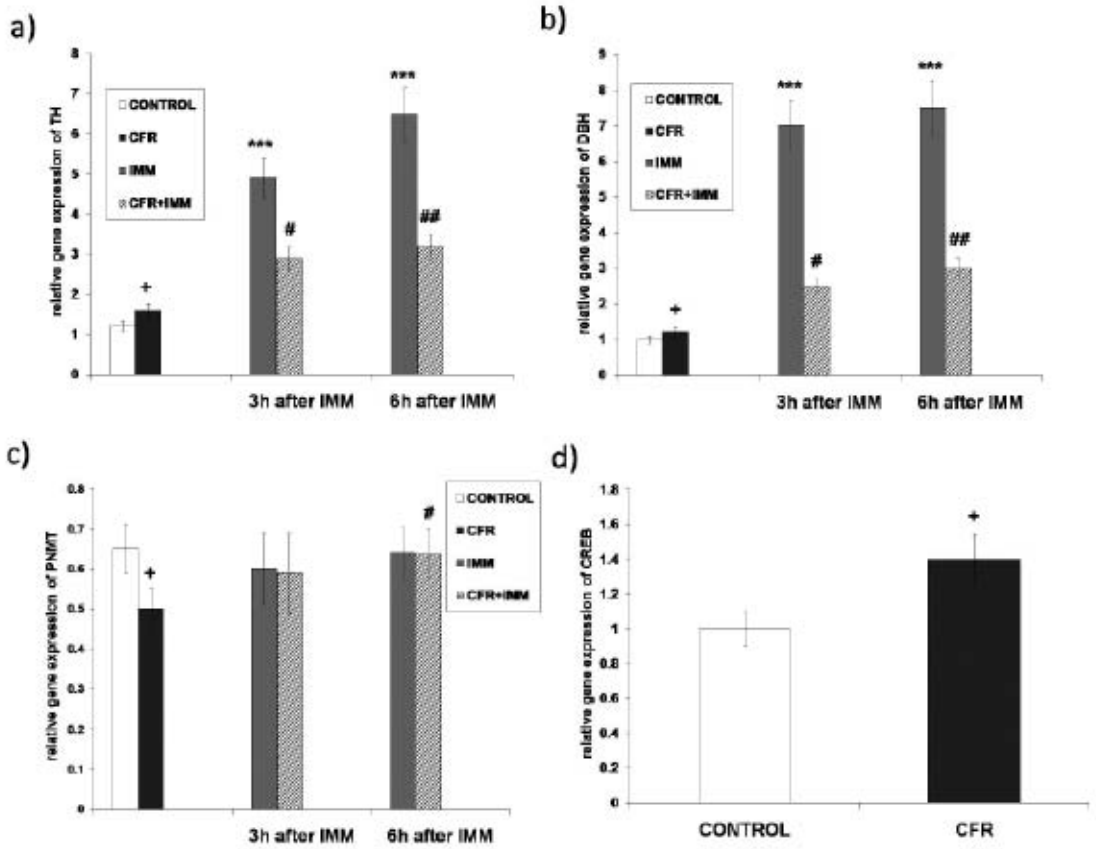

Fig. 2. *Effects of chronic forced running and additional acute immobilization stress on tyrosine hydroxylase (TH) [a], dopamine-ß-hydroxylase (DBH) [b], phenylethanolamine N-methyltransferase (PNMT) [c] and cAMP response element-binding (CREB) [d] mRNA levels in stellate ganglia. The values are means ± S.E.M. of 10 rats. Statistical significance: +p<0.05 animals exposed to chronic forced running vs. control animals (Tukey test); ***p<0.001 animals exposed to acute 2-h immobilization vs. control animals (Tukey test); #p<0.05, ##p<0.01 animals exposed to additional acute 2-h immobilization stress after chronic forced running vs animals exposed to chronic forced running (Tukey test). The final result was expressed as fold change relative to the calibrator and normalized to cyclophyline A.*

control animals. However, CFR decreased PNMT mRNA level by 20% ($p<0.05$, Tukey test, Fig. 2c), compared with control animals in the examined tissue.

In CFR animals we recorded significant positive correlation between the levels of:

- CREB mRNA and TH mRNA levels in stellate ganglia (Spearman, $\rho=0.738$, $P=0.0131$, Fig. 3a);
- CREB mRNA and DBH mRNA levels in stellate ganglia (Spearman, $\rho=0.705$, $P=0.0186$, Fig. 3b);
- ACTH level in the plasma and TH mRNA level in stellate ganglia (Spearman, $\rho=0.658$, $P=0.0332$, Fig. 3c);
- ACTH level in the plasma and DBH mRNA level in stellate ganglia (Spearman, $\rho=0.984$, $P<0.0005$, Fig. 3d);
- CORT level in the plasma and PNMT mRNA level in stellate ganglia (Spearman, $\rho=0.838$, $P<0.0005$, Fig. 3e).

IMM and CFR+IMM treatment

We found that IMM treatment significantly increased the levels of TH mRNA by 300% ($p<0.001$, Tukey test, Fig. 2a) and DBH mRNA by 620% ($p<0.001$, Tukey test, Fig. 2b) 3 h after the cessation of immobilization. Similar changes are found 6h after the cessation of acute immobilization. The exposure of CFR treated animals to additional acute immobilization stress led to increased mRNA levels of TH by 81% ($p<0.05$, Tukey test, Fig. 2a)

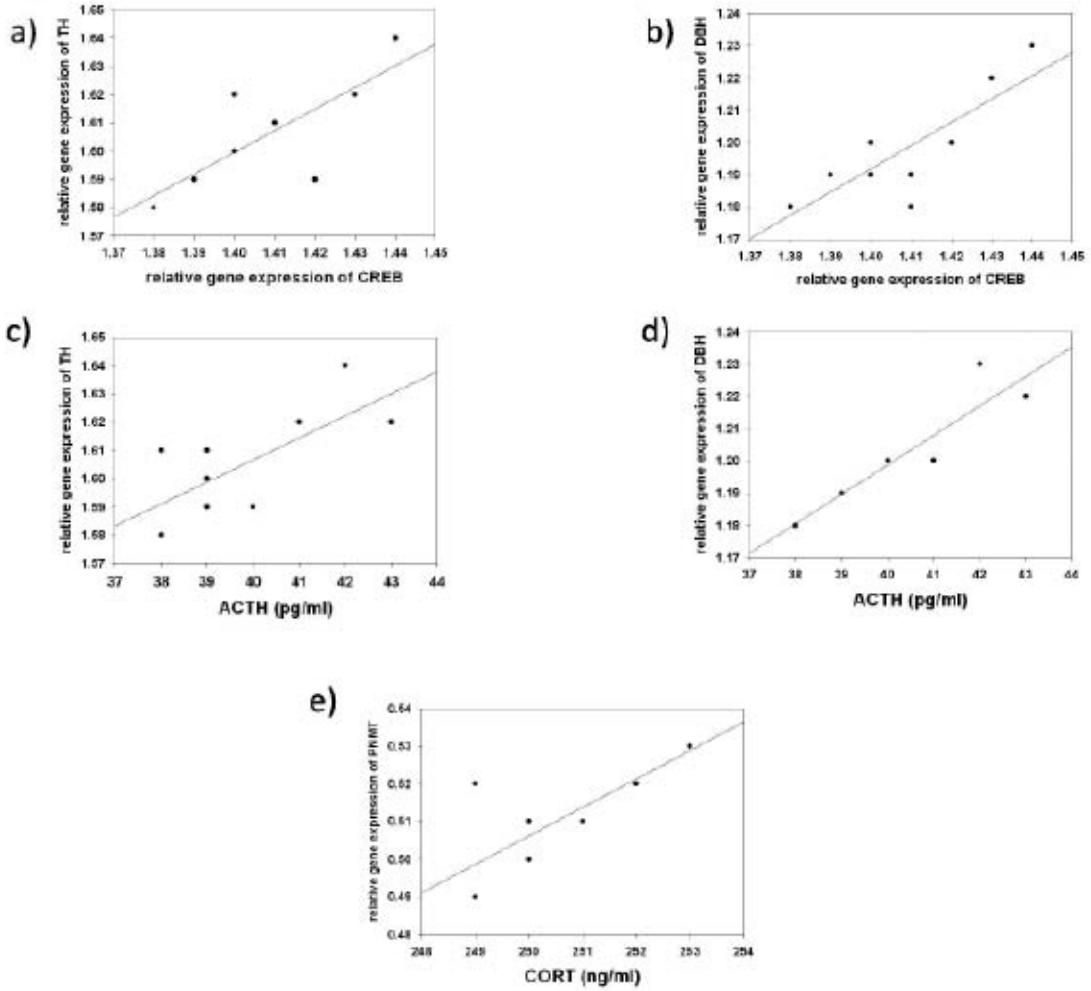

Fig. 3. *The correlations between TH and DBH mRNA levels with CREB mRNA level in stellate ganglia, as well as correlations between ACTH and CORT levels in the plasma with mRNA levels of catecholamine biosynthetic enzymes in stellate ganglia. a) The correlation in the levels of CREB mRNA and TH mRNA in stellate ganglia of animals exposed to CFR (Spearman). b) The correlation in the levels of CREB mRNA and DBH mRNA in stellate ganglia of animals exposed to CFR (Spearman). c) The correlation in the plasma concentrations of ACTH and level of TH mRNA in stellate ganglia of animals exposed to CFR (Spearman). d) The correlation in the plasma concentrations of ACTH and level of DBH mRNA in stellate ganglia of animals exposed to CFR (Spearman). e) The correlation in the plasma concentrations of CORT and level of PNMT mRNA in stellate ganglia of animals exposed to CFR (Spearman).*

and DBH by 100% ($p<0.05$, Tukey test, Fig. 2b) 3h after the cessation of immobilization, however, only 6h after the cessation of immobilization PNMT mRNA level was increased by 25% ($p<0.05$, Tukey test, Fig. 2c).

Changes of TH, DBH and PNMT protein levels in stellate ganglia

CFR treatment. CFR provoked the increased protein levels of TH by 20% ($p<0.05$, Tukey test, Fig. 4a) and DBH by 25% ($p<0.05$, Tukey test, Fig. 4b), compared with control animals. However, CFR did not affect the PNMT protein level (Fig. 4c).

In CFR animals we recorded significant positive correlation between the levels of:

- TH protein level in stellate ganglia and NA level in the plasma (Spearman, $\rho=0.823$, $P=0.0015$, Fig. 5a);

- DBH protein level in stellate ganglia and NA level in the plasma (Spearman, $\rho=0.853$, $P<0.0005$,

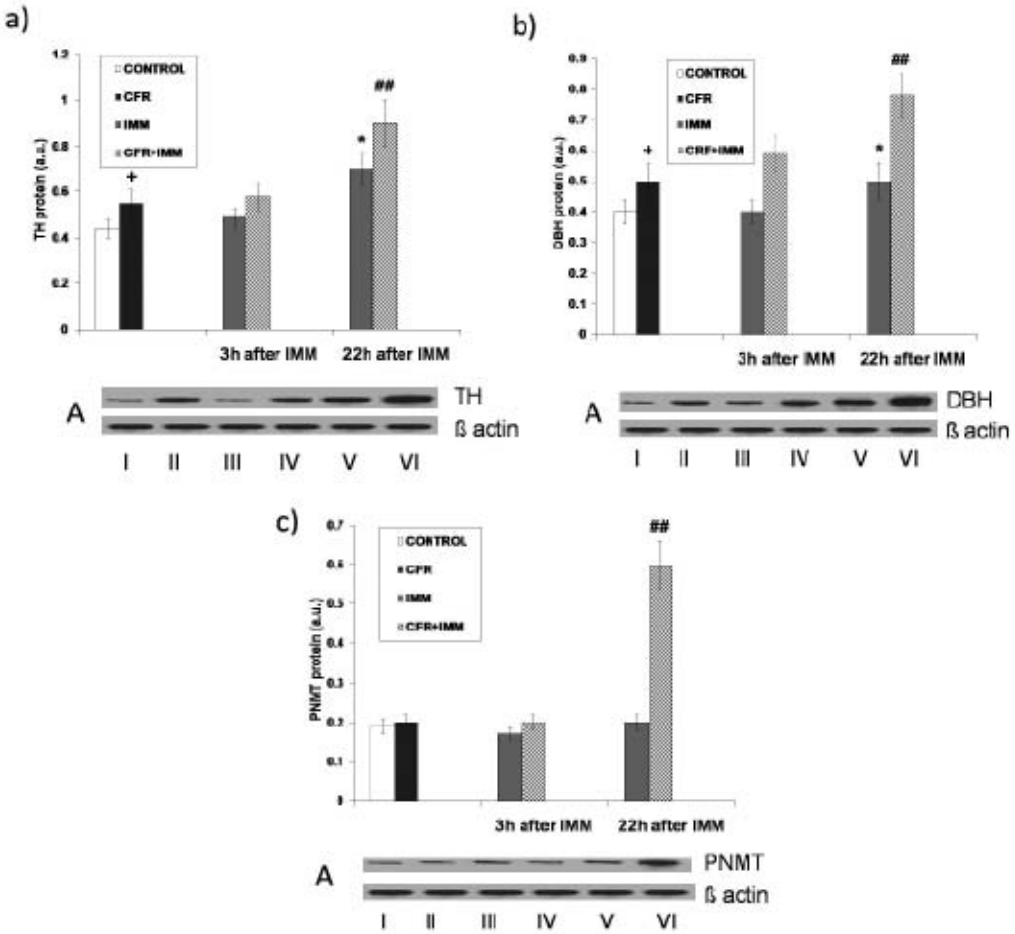

Fig. 4. *Effects of chronic forced running and additional acute immobilization stress on tyrosine hydroxylase (TH) [a], dopamine-ß-hydroxylase (DBH) [b] and phenylethanolamine N-methyltransferase (PNMT) [c] protein levels in stellate ganglia. The values are means ±S.E.M. of 10 rats. Statistical significance: +p<0.05 animals exposed to chronic forced running vs control animals; (Tukey test); *p<0.05 animals exposed to acute 2-h immobilization vs control animals (Tukey test); ##p<0.01 animals exposed to additional acute 2-h immobilization stress after chronic forced running vs animals exposed to chronic forced running (Tukey test). The result was expressed in arbitrary units normalized in relation to β actin. (A) Distribution of TH, DBH, PNMT and ß actin proteins in stellate ganglia of control animals [I], animals exposed to CFR [II], animals exposed to IMM (3 h after immobilization) [III], animals exposed to CFR+IMM (3 h after immobilization) [IV], animals exposed to IMM (22h after immobilization) [V] and animals exposed to CFR+IMM (22 h after immobilization) [VI].*

Fig. 5b).

IMM and CFR+IMM treatment. The exposure of the animals to acute immobilization stress increased the protein levels of TH by 59% ($p<0.05$, Tukey test, Fig. 4a) and DBH by 25% ($p<0.05$, Tukey test, Fig. 4b), while the additional exposure of CFR animals to acute immobilization stress led to increased protein levels of TH by 66% ($p<0.01$, Tukey test, Fig.4a), DBH by 52% ($p<0.01$, Tukey test, Fig. 4b) and PNMT by 200% ($p<0.01$, Tukey test, Fig.4c) 22 h after the cessation of immobilization.

In CFR animals we recorded significant positive correlation between the levels of:

-TH protein level in stellate ganglia and NA level in the plasma 22 h after immobilization of animals exposed to CFR (Spearman, $\rho=0.847$, $P<0.0005$, Fig. 5c);

-DBH protein level in stellate ganglia and NA level in the plasma 22 h after immobilization of

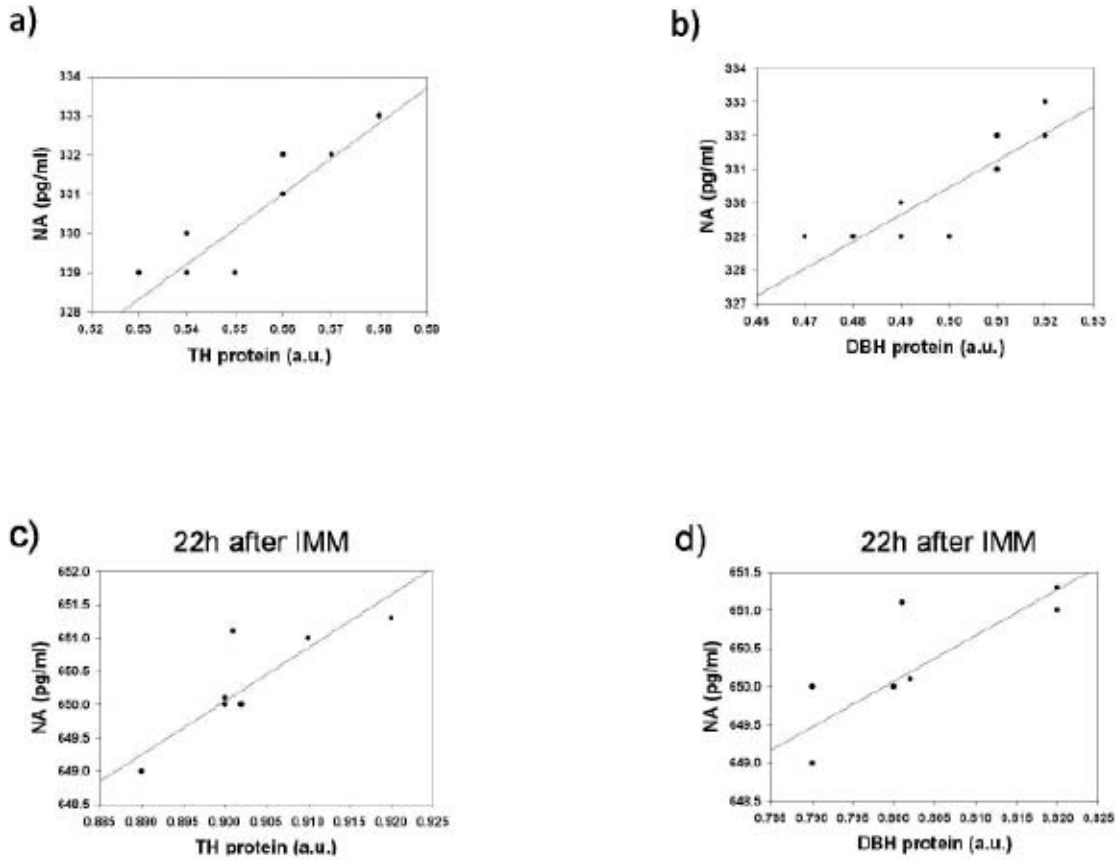

Fig. 5. *The correlations between TH and DBH protein levels in stellate ganglia with NA level in the plasma. a) The correlation in the levels of TH protein in stellate ganglia and NA concentrations in the plasma of animals exposed to CFR (Spearman). b) The correlation in the levels of DBH protein in stellate ganglia and NA concentrations in the plasma of animals exposed to CFR (Spearman). c) The correlation in the levels of TH protein in stellate ganglia and NA concentrations in the plasma 22 h after immobilization of animals exposed to CFR (Spearman). d) The correlation in the levels of DBH protein in stellate ganglia and NA concentrations in the plasma 22 h after immobilization of animals exposed to CFR (Spearman).*

animals exposed to CFR (Spearman, ρ=0.903, P<0.0005, Fig. 5d).

DISCUSSION

Changes in plasma concentrations of NA, A, ACTH and CORT

Chronic voluntary physical activity attenuates neural responses to stress in brain circuits responsible for regulating peripheral sympathetic activity, suggesting constraint on sympathetic responses to stress that could plausibly contribute to reductions in clinical disorders such as hypertension and heart failure (2). However, treadmill running (forced exercise) induced neuron hypertrophy in the stellate ganglia (12). The increased release of NA from stellate ganglia during chronic stress may play a role in growing risk for cardiovascular diseases. Also, it is known that chronic stress is associated with a transient suppression of the HPA axis, manifested by the lower morning cortisol and the reduced adrenal cortisol response to ACTH stimulation. This HPA response pattern is manifested by decreased morning plasma or urinary cortisol, especially in the subjects with post-traumatic stress disorder (13). The results of this work show that long-term treadmill running produced adaptive physiological changes which are indicative of chronic stress. The potentially negative

physiological adaptations after CFR were recorded as increased concentrations of catecholamine and ACTH, as well as decreased morning CORT concentration in the plasma. Also, we recorded that chronically stressed rats (CFR) exposed to novel additional acute stress have significantly increased concentrations of catecholamines, ACTH and CORT in the plasma. The heterotypic novel stressor (IMM) triggers an exaggerated elevation in plasma catecholamines in animals previously exposed to CFR, even 22 h after the exposure. This could mean that prior experience may condition physiological systems to "expect" a problem and therefore, be more ready to respond to a novel additional acute stressor. The readiness of the organism prolongedly exposed to homotypic stressor to respond to a heterotypic stressor by an exaggerated activation of catecholamines is considered to be an important adaptive phenomenon of the sympathetic-adrenomedullary system in rats (3).

Changes of the TH and DBH gene expression in stellate ganglia

CFR induces the increase of TH and DBH mRNA and protein levels in stellate ganglia. There is substantial evidence that CREB and ACTH induce TH and DBH gene expression in sympathetic ganglia (14, 15). We recorded that the increased expression of TH and DBH genes in stellate ganglia positively correlates with the expression of CREB in stellate ganglia and with plasma ACTH level. The continuous increase of the noradrenaline biosynthetic enzyme expression in stellate ganglia due to chronic physical stress, followed by increased NA concentration in the plasma, which is in accordance with the reports of Sabban et al. (14), may play a role in growing risk of cardiovascular diseases. In this work, we showed that IMM and CFR+IMM stressors induced the increase of TH and DBH mRNA levels in stellate ganglia three hours after immobilization. The expression of TH and DBH mRNA was even more intense six hours after the cessation of immobilization and was associated with the increased plasma concentrations of ACTH. Stellate ganglia show a surprisingly prolonged reaction (in the terms of mRNA levels), even upon a single immobilization (3). The slow transcriptional activation of these genes is the result of delayed expression of key transcription factors (16). Also, the increased level of mRNA six hours after immobilization could be due to the increased stability and prolonged half-life of mRNA. Our results showed that TH and DBH mRNAs in stellate ganglia of CFR rats were elevated compared with control rats and no exaggerated response was seen after acute exposure to novel stressor. This finding might be explained by the quality and especially intensity of the stressor used. Kvetnansky et al. (3) reported that novel stressors elicit exaggerated responses in pre-stressed animals when the novel stressor is of equal or greater intensity or duration and/or it is repeated. In this work, animals exposed to chronic stress (CFR) were already prepared to manage the new situation evoked by a novel stressor, and on the level of transcription the exaggerated response is not necessary. The increased levels of TH and DBH mRNAs were followed by increased synthesis of TH and DBH proteins 22 hours after the immobilization, in CFR+IMM, as well as in IMM animals. However, immobilization stress more significantly elevated TH and DBH protein levels in rats previously exposed to CFR. It is interesting to note that, although TH and DBH mRNAs are dramatically increased after IMM treatment, in CFR+IMM treatment regime this increase although lower still persists, and may lead to continuous accumulation of their proteins as an adaptation on applied stress regime. This adaptive response is necessary to maintain the catecholamine biosynthetic capacity in stellate ganglia during periods of sustained catecholamine secretion. It is known that long term stress induces appropriate translational mechanisms (17). Synthesis of TH and DBH proteins during CFR+IMM stress increases sustained catecholamine secretion. This is supported with significant positive correlation between the levels of TH and DBH in stellate ganglia and NA in the plasma 22 h after IMM of animals exposed to CFR. Our results confirm that the CFR shows adaptations that are indicative of chronic stress.

Changes of the PNMT expression in stellate ganglia

CFR provoked an increase of plasma A and a decrease of PNMT mRNA, while PNMT protein level remained unchanged. It is known that glucocorticoids are important regulators of PNMT gene expression on transcriptional and post-translation level (18). Our results also show that exposure to CFR leads to decreased plasma CORT

concentration witch correlates with the reduction of PNMT mRNA expression in stellate ganglia. In our previous work we showed the increased synthesis of PNMT enzyme after chronic stress in the adrenal medulla (10). These results demonstrate that the adrenal glands, but not stellate ganglia, are the main source of A in the circulation in response to chronic stress. IMM stress alone did not influence the PNMT expression, while CFR+IMM, six hours after the cessation of immobilization increased PNMT mRNA and 22 hours after the cessation of immobilization increased also PNMT protein level. The process of PNMT translation requires the continuous and longer exposure to stress (19). Therefore, only chronically stressed rats exposed to novel stressors exhibited exaggerated responses in gene expression of PNMT enzyme catalyzing conversion of NA to A. The increased release of A from stellate ganglia during the additional acute immobilization in rats previously exposed to CFR may be caused also by the increased synthesis of PNMT. Increased levels of PNMT enzyme in stellate ganglia may have pathophysiological impact, especially on the cardiovascular system, since A is a powerful β2 adrenergic receptor agonist.

In conclusion, our results showed that increase of the noradrenaline biosynthetic enzymes expression in stellate ganglia, which causes the increase of plasma NA levels, due to chronic forced running, may play a role in growing risk of cardiovascular diseases. Our results confirm that the CFR shows adaptations that are indicative of chronic stress.

ACKNOWLEDGEMENTS

This work was supported by the Ministry of Education and Science of the Republic of Serbia, Contract No. III 41027, III 41022 and ON 173044.

REFERENCES

1. Pardini BJ, Lund DD, Schmid PG. Innervation patterns of the middle cervical--stellate ganglion complex in the rat. Neurosci Lett 1990; 18;117(3):300-6.
2. Moraska A, Deak T, Spencer RL, Roth D, Fleshner M. Treadmill running produces both positive and negative physiological adaptations in Sprague-Dawley rats. Am J Physiol Regul Integr Comp Physiol 2000; 279:1321-9.
3. Kvetnansky R, Sabban EL, Palkovits M. Catecholaminergic Systems in stress: structural and molecular genetic. Approaches. Physiol Rev 2009; 89:535-606.
4. Erdös B, Broxson CS, Landa T, Scarpace PJ, Leeuwenburgh C, Zhang Y, Tümer N. Effects of life-long caloric restriction and voluntary exercise on age-related changes in levels of catecholamine biosynthetic enzymes and angiotensin II receptors in the rat adrenal medulla and hypothalamus. Exp Gerontol 2007; 42(8):745-52.
5. Tümer N, Demirel HA, Serova L, Sabban EL, Broxson CS, Powers SK. Gene expression of catecholamine biosynthetic enzymes following exercise: modulation by age. Neuroscience 2001; 103:703-11.
6. White-Welkley JE, Bunnell BN, Mougey EH, Meyerhoff JL, Dishman RK. Treadmill exercise training and estradiol differentially modulate hypothalamic-pituitary-adrenal cortical responses to acute running and immobilization. Physiol Behav 1995; 57(3):533-40.
7. Erdem SR, Demirel HA, Broxson CS, Nankova BB, Sabban EL, Tümer N. Effect of exercise on mRNA expression of select adrenal medullary catecholamine biosynthetic enzymes. J Appl Physiol 2002; 93(2):463-8.
8. Kvetnansky R, Mikulaj L. Adrenal and urinary catecholamines in rats during adaptation to repeated immobilization stress. Endocrinology 1970; 87:738-43.
9. Wong DL, Tank AW. Stress-induced catecholaminergic function: transcriptional and post-transcriptional control. Stress 2007; 10(2):121-30.
10. Gavrilovic L, Spasojevic N, Tanic N, Dronjak S. Chronic isolation of adult rats decreases gene expression of catecholamine biosynthetic enzymes in adrenal medulla. Neuro Endocrinol Lett 2008; 29(6):1015-20.
11. Peuler JD, Johnson GA. Simultaneous single isotope radioenzymatic assay of plasma norepinephrine, epinephrine and dopamine. Life Sci 1977; 21:625-36.
12. Cavalcanti RA, da Pureza DY, de Melo MP, de Souza RR, Bergamaschi CT, do Amaral SL, Tang H, Loesch A, Ribeiro AA. Low-intensity treadmill

exercise-related changes in the rat stellate ganglion neurons. J Neurosci Res 2009; 1;87(6):1334-42.

13. Yehuda R, Kahana B, Binder-Brynes K, Southwick SM, Mason JW, Giller EL. Low urinary cortisol excretion in Holocaust survivors with posttraumatic stress disorder Am J Psychiatry 1995; 152:982-6.
14. Sabban EL, Nankova BB, Serova LI, Kvetnansky R, Liu X. Molecular regulation of gene expression of catecholamine biosynthetic enzymes by stress: sympathetic ganglia versus adrenal medulla. Ann NY Acad Sci 2004; 1018:370-7.
15. Serova LI, Gueorguiev V, Cheng SY, Sabban EL. Adrenocorticotropic hormone elevates gene expression for catecholamine biosynthesis in rat superior cervical ganglia and locus coeruleus by an adrenal independent mechanism. Neuroscience 2008; 153:1380-89.
16. Sabban EL, Kvetnansky R. Stress-triggered activation of gene expression in catecholaminergic systems: dynamics of transcriptional events. Trends Neurosci 2001; 24:91-98.
17. Xu L, Chen X, Sun B, Sterling C, Tank AW. Evidence for regulation of tyrosine hydroxylase mRNA translation by stress in rat adrenal medulla. Brain Res 2007; 1158:1-10.
18. Wong DL, Lesage A, White S, Siddall B. Adrenergic expression in the rat adrenal gland: multiple developmental regulatory mechanisms. Brain Res Dev Brain Res 1992; 67(2):229-36.
19. Kvetnansky R, Sabban EL. Stress-induced changes in tyrosine hydroxylase and other catecholamine biosynthetic enzymes In: Tyrosine Hydroxylase: From Discovery to Cloning, (ed) Naoi M, Parvez SH. Utrecht, The Netherlands 1993; VSP.

INFLUENCE OF DIFFERENT OXYGEN SUPPLY ON METABOLIC MARKERS AND GENE RESPONSE IN MURINE ADIPOCYTES

P. QUINTERO, P. GONZÁLEZ-MUNIESA and J.A. MARTÍNEZ

Department of Nutrition, Food Science, Physiology and Toxicology, University of Navarra, Pamplona, Spain

Received April 18, 2012 – Accepted June 12, 2012

Obese subjects often present a low-grade chronic inflammation in the white adipose tissue, which seems to play an important role in the initiation and development of obesity-related diseases. It has been reported that this inflammatory process may be due to a hypoxic state occuring within this tissue. Oxygen is used in current medicine as a treatment for several conditions. The aim of this study is to analyze the effects of 95% O_2 on specific metabolic variables and on the expression of some genes on murine adipocytes. 3T3-L1 adipocytes were exposed during 48 h to different treatments: 95% O_2 hyperoxia (HPx group), $CoCl_2$ ($CoCl_2$ group), hyperoxia with $CoCl_2$ (HPx+$CoCl_2$ group) and 1% O_2 hypoxia (Hx group). Cell viability, intracellular ROS content, glucose utilization, lactate and glycerol concentrations were measured. Also, mRNA expression of HIF-1α, GLUT-1, ANGPTL4, PPAR-γ, adiponectin, IL-6 and MCP-1 genes was analyzed. Importantly, 95% O_2 decreased cell viability and increased intracellular ROS production. Also, glycerol and lactate release were significantly increased and decreased, respectively, in HPx treated cells. This treatment also provoked a down-regulation of GLUT-1 and ANGPTL-4, while IL-6 and MCP-1 were up-regulated. Exposure to a hyperoxia of 95% O_2 provoked an inflammatory response in adipocytes. The two hypoxia-inducing conditions ($CoCl_2$ and 1% O_2) produced different outcomes in metabolic measurements as well as in the expression of some genes (GLUT-1, ANPGTL4, PPAR-γ and adiponectin), while it remained similar in others (HIF-1α, IL-6 and MCP-1). Indeed, hyperoxia increased significantly the ROS levels and the lipolytic activity, while it reduced lactate production. In addition to the effects on inflammation, the changes in GLUT-1, ANGPTL4 and PPAR-γ genes lead to suppose that hyperoxia may be beneficial for the hypertrophied adipose tissues of obese subjects and for improving insulin sensitivity.

Obesity is a major metabolic disorder commonly accompanied by the onset and development of other important diseases such as type 2 diabetes, artheriosclerosis and several common cancers (1). These events are often associated with a chronic low-grade inflammation in white adipose tissue. Indeed, is now recognized that obesity can induce an aberrant production of several inflammatory markers such as IL-6, MCP-1 or TNF-α, which seem to play a causative role in the development of obesity-associated insulin resistance and cardiovascular disorders (2, 3).

In 2004 it was reported that hypoxia occurs in adipose tissue in obesity (4). Further investigations

Key words: adipocytes, cell culture, hyperoxia, hypoxia, inflammation, obesity

Mailing address: Professor J. A. Martinez
Department of Nutrition, Food Science, Physiology and Toxicology.
University of Navarra Irunlarrea 1,
31008, Pamplona. Spain
Fax: +34 948425740
e-mail: jalfmtz@unav.es

0393-974X (2012)

have corroborated this hypothesis, demonstrating a lower partial pressure of O_2 in adipose tissue in the state of obesity in rodents and humans (5, 6). Indeed, white adipose tissue expansion in obesity appears to impair the growth of adipocytes in size and number, resulting in an increased distance to the vasculature and a reduction of O_2 tension whithin this tissue. In the following years, this adipose tissue hypoxia was proposed as a possible factor that could play an important role in promoting inflammatory mechanisms in this tissue (7).

In this context, O_2 is used in current medicine as a treatment for several diseases (8, 9), as well as ozone (O_3) used under controlled conditions (10). Thus, normobaric and hyperbaric oxygen therapies (NBOT and HBOT, respectively) are important techniques under continuous investigation. Studies on animals have demonstrated that the treatment with hyperoxia might produce beneficial effects in different metabolic disorders, such as protecting the rat brain tissue against ischemia reperfusion injury (11), reducing severity of colitis (12) or ameliorating hemorrhagic shock-induced renal failure by decreasing intrarenal hypoxia and improving renal functions (13). Regarding inflammation, several studies have shown that hyperoxia can decrease the expression of some pro-inflammatory genes in different organs and cell types (14, 15). Some investigations have also demonstrated that HBOT attenuates pro-inflammatory cytokine production of systemic inflammation in animal models (16, 17). These findings are in agreement with HBOT studies carried out in *ex vivo* cell cultures (15, 18).

Taking all these studies into account, where high O_2 levels seem to produce beneficial effects on inflammatory markers, it was hypothesized that hyperoxia could be used as a specific therapeutic intervention for the improvement of obesity state (19). To our knowledge, there are no available data regarding the effects of a hyperoxic treatment on murine adipocytes. Therefore, in this study we investigated the effects of 95% of O_2, alone or in combination with cobalt chloride (as a hypoxia-generating agent), in the expression of some genes and in the regulation of specific metabolic variables in hypoxic adipocytes. This research was designed in order to understand the possible role and mechanisms of hyperoxia in combating low O_2 tension in the adipose tissue of obese patients.

MATERIALS AND METHODS

Cell culture

This research was carried out on 3T3-L1 mouse preadipocytes, that were cultured with Dulbecco's minimal essential media (DMEM) containing 4.5 g/L glucose and supplemented with 10% calf bovine serum. Two days after full confluence, cells were cultured in twelve-well plates. Their differentiation into adipocytes was induced by treating cells for 2 days with 0.5 mM isobutylmethylxanthine, 1 µM dexamethasone and 10 µg/ml insulin in DMEM supplemented with 10% fetal bovine serum (FBS), and then for 2 days with 10 µg/ml insulin in the same media. Thereafter, cells were maintained and re-fed every 2-3 days with FBS without any hormones until 14 days after differentiation induction, when between 80 and 90% of the cells exhibited the adipocyte phenotype. Also, 100 units/ml penicillin and 100 µg/ml streptomycin were added to all media. Cells were always maintained in a CytoGROW GLP incubator (Sanyo, San Diego, CA, USA) at 37ºC in a humidified atmosphere containing 5% CO_2.

Treatments

After 14 days post-differentiation, adipocytes were exposed to four different experimental treatments: environmental hyperoxia with 95% O_2/5% CO_2 (HPx group), $CoCl_2$ (a hypoxia mimetic which stabilizes HIF-1α (20)) at a concentration of 100 µM ($CoCl_2$ group), hyperoxia with $CoCl_2$ (HPx+$CoCl_2$ group), and ambient hypoxia with 1% O_2/94% N_2/5% CO_2 (Hx group) to compare whether $CoCl_2$ could mimic the effects produced by real hypoxia. Each of these treatments was generated in sealed chambers (Billups-Rosenberg, Del Mar, CA, USA) at 37ºC during 48 h. Non-treated cells placed in a standard incubator with 21% O_2/5% CO_2 were used as reference (Control group). After the experimental treatments, culture media were collected and stored at -80ºC for further measurements.

Cell viability assay and ROS determination

Cell viability was measured with the lactate dehydrogenase (LDH) Cytotoxicity Assay Kit at 48 h according to the manufacturer's instructions (Cayman Chemical Company, Ann Arbor, USA).

To determine intracellular ROS concentration, 2',7'-dichlorofluorescein (DCFH) was used following a protocol described elsewhere (21). This protocol, which measures H_2O_2 production, is commonly used as a surrogate of ROS generation (22). Briefly, cells were

incubated with 10 mM DCFH for 40 min at 37ºC in 5% CO_2, frozen for at least 1 h at -80ºC and then lysed with 1000 µl lysis buffer (150 mM NaCl, 0.1% Triton, and 10 mM Tris). Finally, 200 µl of each lysate were loaded on a 96-well black plate and fluorescence intensity was measured using a Fluoroskan Ascent FL (Thermo Fisher Scientific, Waltham, MA) at an excitation wavelength of 485 nm and at an emission of 530 nm.

Measurement of metabolic markers

The glucose (HK-CP kit; Horiba, Montpellier, France), lactate (ABX Diagnostic, Montpellier, France) and glycerol (GLY 105; Randox Laboratories, Antrim, UK) concentrations were measured from culture medium samples with a PENTRA C200 auto-analyzer (Horiba, Montpellier, France) after the 48 h treatment. The adipocyte glucose utilization was estimated by the difference between the content of glucose in the culture media at the beginning and at the end of the experiment, as previously described (21).

RT-PCR analyses

Total RNA was isolated from all samples using Trizol according to the manufacturer's instructions (Invitrogen, Paisley, UK). Purified total RNA from adipocytes was then treated with DNAse (DNAfree kit; Ambion Inc., Austin, USA) and used to generate cDNA with M-MLV reverse transcriptase (Invitrogen, Paisley, UK). Real-time PCR was performed in an ABI PRISM 7000 HT Sequence Detection System (Applied Biosystems, California, USA). Taqman probes for mouse HIF-1α, GLUT-1, ANGPTL4, PPAR-γ, adiponectin, IL-6 and MCP-1 were also supplied by Applied Biosystems (California, USA). Furthermore, it has been previously established that hypoxia can alter mRNA expression levels of some standard genes (23). Therefore, we considered necessary to characterize the suitability of various housekeeping genes to serve as internal RNA controls. Thus, the expression of 18s, cyclophilin, RNA polymerase II and 28s was determined, the latter being selected as the internal control because it demonstrated no significant expression changes after different treatments (data not shown). All procedures were performed according to a previously described protocol (24).

Statistical analysis

All data was evaluated using the Kruskal-Wallis test. When interaction was detected, the U Mann-Whitney test was used for group comparisons. All results are expressed as mean ± standard deviation (SD). Overall, 6 cell culture experiments were performed and the reported data come from a representative experiment with n = 6 as stated in all figures. Association analyses for selected biochemical markers and gene expression values were performed using the Spearman test. A probability of $p<0.05$ was set up for determining statistically significant differences. The statistical analyses were performed using SPSS 15 (Chicago, USA) and GraphPad Prism 5.0 (San Diego, USA) software.

RESULTS

Cell viability and ROS assessments

The activity of LDH was determined in the conditioned cell media in order to investigate the potential cytotoxicity of the applied treatments. As shown in Fig. 1, cell viability of 3T3-L1 adipocytes significantly decreased with both hyperoxia and hypoxia treatments. However, $CoCl_2$ did not show

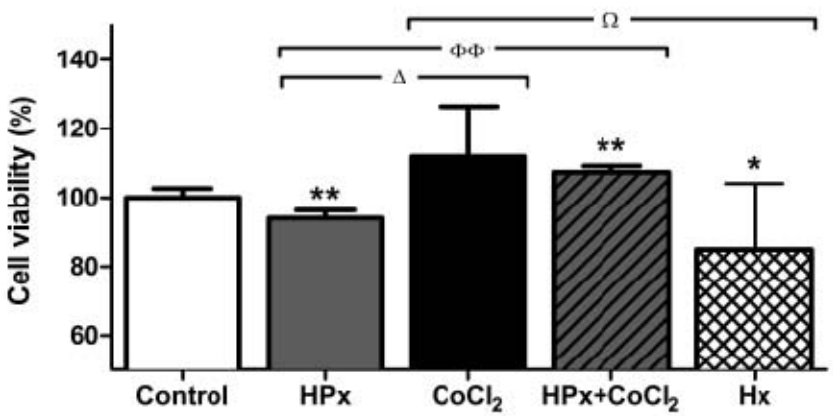

Fig. 1. *Cellular integrity in control and treated groups was measured at 48 h. One symbol means $p<0.05$, two symbols $p<0.01$. * Treatment groups vs Control; Δ HPx vs $CoCl_2$; φ HPx vs HPx+$CoCl_2$; Ω $CoCl_2$ vs Hx. Data (n=6) are expressed as mean ± SD.*

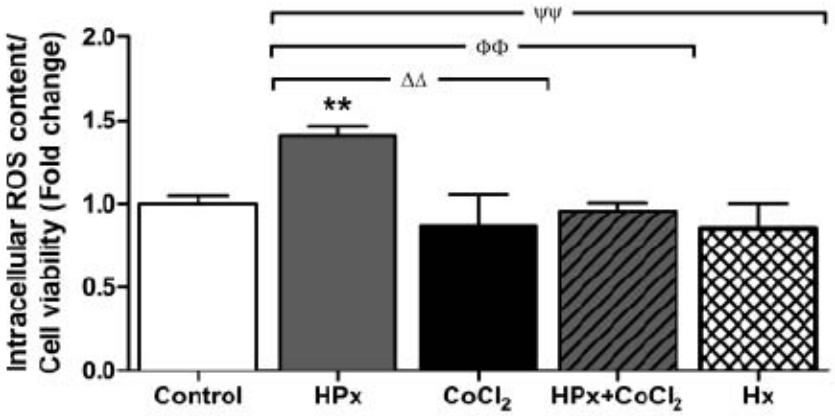

Fig. 2. *Intracellular ROS content at 48 h in 3T3-L1 adipocytes (14 days post-differentiation). Two symbols mean p<0.01. * Treatment groups vs Control; Δ HPx vs $CoCl_2$; φ HPx vs HPx+$CoCl_2$; ψ HPx vs Hx. Data (n=6) are expressed as mean ± SD.*

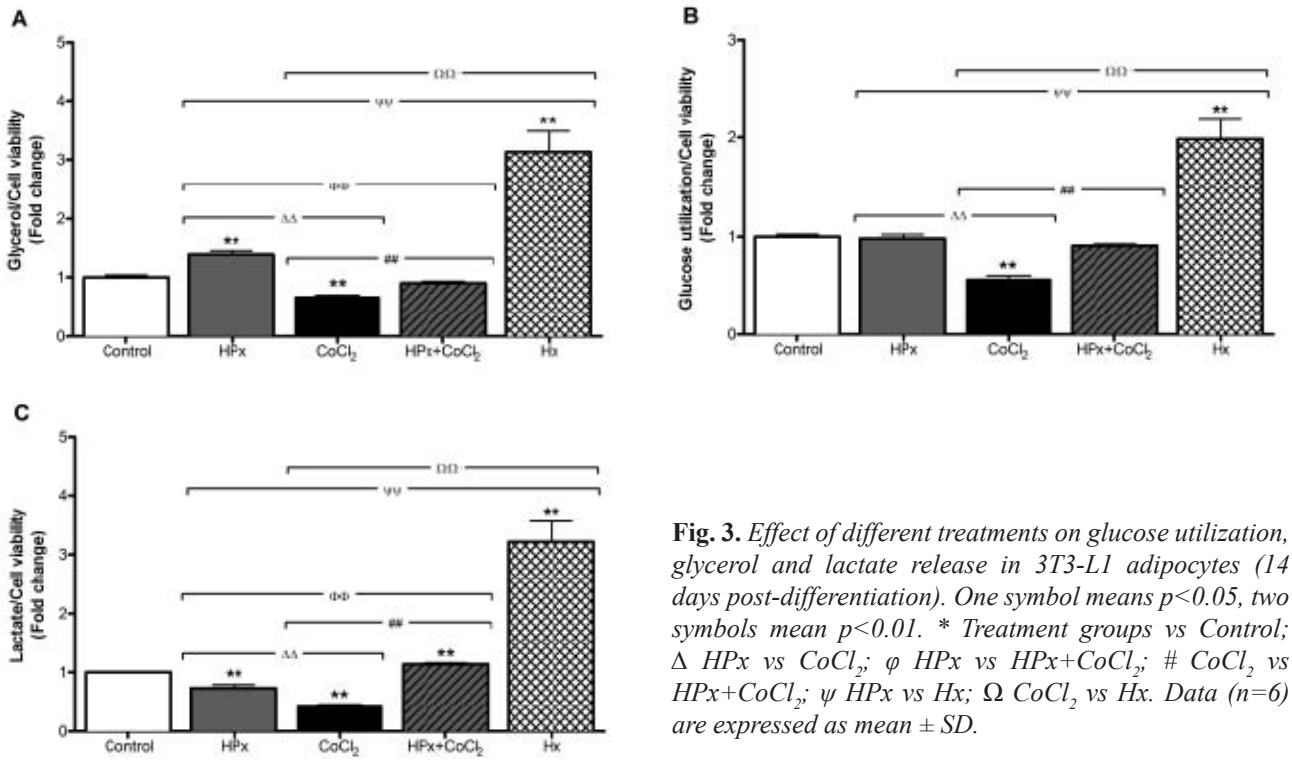

Fig. 3. *Effect of different treatments on glucose utilization, glycerol and lactate release in 3T3-L1 adipocytes (14 days post-differentiation). One symbol means p<0.05, two symbols mean p<0.01. * Treatment groups vs Control; Δ HPx vs $CoCl_2$; φ HPx vs HPx+$CoCl_2$; # $CoCl_2$ vs HPx+$CoCl_2$; ψ HPx vs Hx; Ω $CoCl_2$ vs Hx. Data (n=6) are expressed as mean ± SD.*

differences when compared to the control group and seemed to be protective against cell death when cells were treated with hyperoxia.

Furthermore, intracellular ROS production, corrected by cell viability, was significantly increased only by the hyperoxia exposure, while the other treatments did not show differences when compared to control (Fig. 2).

Culture media determinations

Glucose utilization, lactate production, and glycerol release of isolated adipocytes were determined after the 48 h treatment and were corrected by cell viability. Glycerol production was

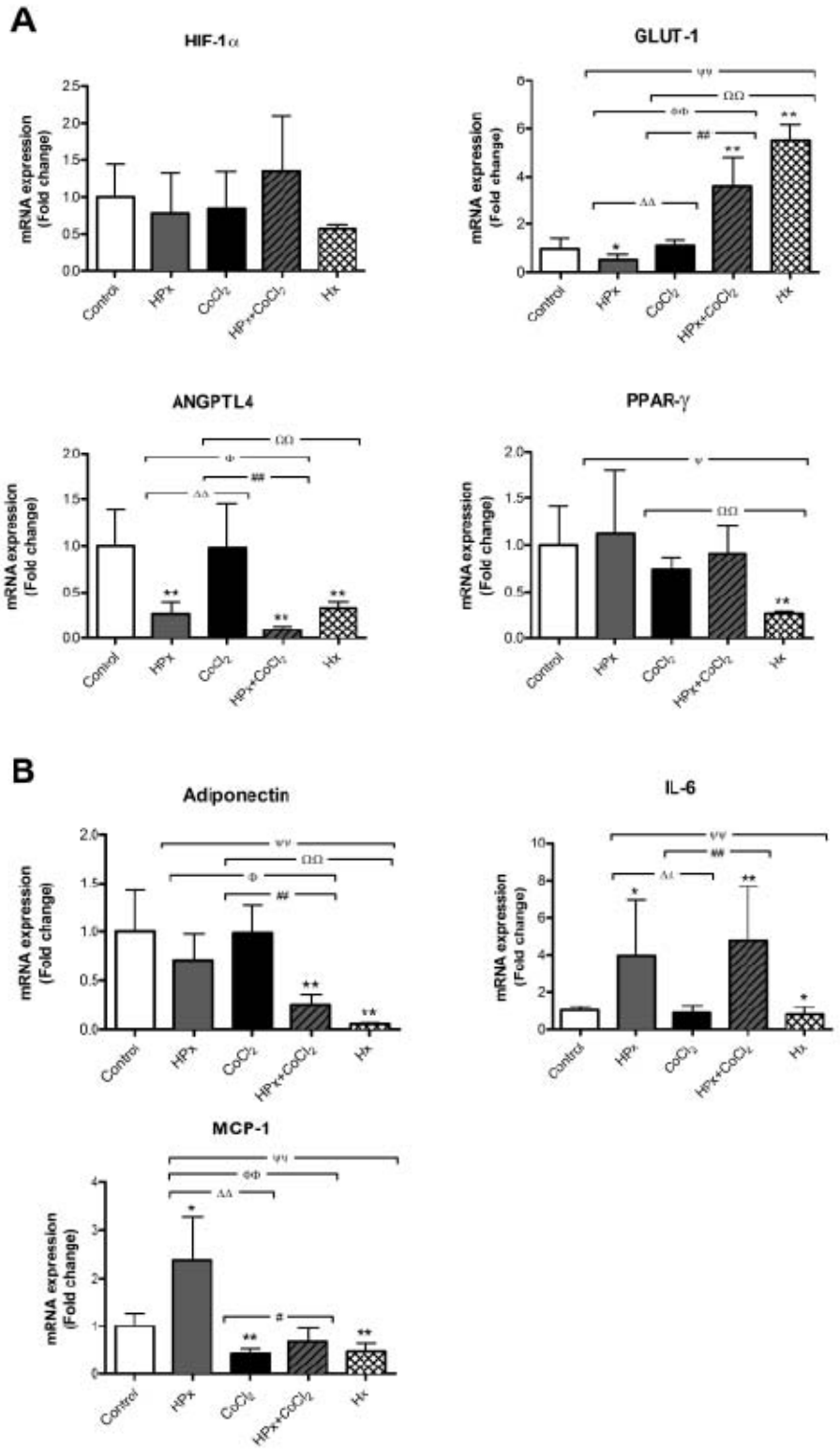

Fig. 4. *(**A**) Gene expression analysis of HIF-1α, GLUT-1, ANGPTL4 and PPAR-γ and (**B**) of inflammatory-related genes IL-6, MCP-1 and adiponectin at 48 h in 3T3-L1 adipocytes (14 days post-differentiation). One symbol means p<0.05, two symbols p<0.01. Treatment groups vs Control; Δ HPx vs $CoCl_2$; φ HPx vs HPx+$CoCl_2$; # $CoCl_2$ vs HPx+$CoCl_2$; ψ HPx vs Hx; Ω $CoCl_2$ vs Hx. Data (n=6) are expressed as mean ± SD.*

enhanced by both hyperoxia and hypoxia treatments, while it was significantly decreased by $CoCl_2$ (Fig. 3A). Glucose utilization was decreased by the $CoCl_2$ treatment and increased by hypoxia (Fig. 3B). Moreover, there was a significant elevation in lactate release in HPx+$CoCl_2$ and Hx groups, while HPx and $CoCl_2$ treatments significantly decreased it (Fig. 3C). In all three biochemical markers, hyperoxia counteracted the effect of $CoCl_2$. A high association between glucose utilization and lactate release was found ($r=0.607$; $p<0.01$). Moreover, these two biochemical parameters were also strongly correlated with GLUT-1 gene expression ($r=0.486$; $p<0.01$ and $r=0.639$; $p<0.001$, respectively).

Gene expression

Regarding gene expression, no changes were observed in HIF-1α mRNA levels in each of the four treatments when compared to control (Fig. 4A). A significant decrease in the expression of GLUT-1 was observed in HPx, while it was up-regulated in HPx+$CoCl_2$ and Hx groups. There was also a down-regulation of ANGPTL4 mRNA when treated with HPx, HPx+$CoCl_2$ and Hx, while no changes were observed with $CoCl_2$. PPAR-γ mRNA expression was down-regulated only by the hypoxia treatment (Fig. 4A). An association between GLUT-1 and glucose utilization ($r=0.9$; $p<0.03$) was found in the HPx group.

To determine whether these treatments induced changes in inflammatory adipokines, mRNA expression of adiponectin, MCP-1 and IL-6 was measured (Fig. 4B). Thus, adiponectin expression was down-regulated by Hx and HPx+$CoCl_2$, but no changes were observed with HPx and $CoCl_2$ treatments separately, showing that these two factors could provoke different situations if they act together. Finally, MCP-1 and IL-6 mRNA expression were both up-regulated by HPx. Unexpectedly, these two proinflammatory adipokines were down-regulated by the Hx group. $CoCl_2$ treatment decreased the expression of MCP-1, but did not change IL-6 expression. In these two proinflammatory adipokines, HPx seemed to reverse the effect of $CoCl_2$, as can be observed in the HPx+$CoCl_2$ group. Interestingly, a highly positive correlation between IL-6 and MCP-1 mRNA levels and glycerol release was found ($r=0.864$; $p<0.001$ and $r=0.845$; $p<0.001$, respectively) considering C and HPx groups. Furthermore, associations between the expression of PPAR-γ with HIF-1 ($r=0.597$; $p<0.001$) and IL-6 ($r=0.577$; $p<0.001$) were found.

DISCUSSION

The adipose tissue becomes poorly oxygenated leading to inflammatory processes and metabolic syndrome features in these subjects (7), although a decrease in adipose tissue O_2 tension may not always occur (25). In the current trial, the effects of hyperoxia in chemical-hypoxic adipocytes were investigated in an approach to counteract the hypoxic alterations that often occur in expanded adipose tissue.

The 48-h hyperoxia exposure produced a significant cell death in respect to control. In other experiment of our group, a 24-h exposure did not cause significant differences in cell death (26). Thus, cell damage caused by hyperoxia exposure could be related to the duration of the treatment. On the other hand, CoCl2 did not affect cell viability. Interestingly, CoCl2 has been observed to be protective to cell death in some conditions (27). In this experiment, CoCl2 also reverted the cell death of adipocytes induced by hyperoxia. Furthermore, 1% O_2 hypoxia significantly decreased this variable, as previously reported (28).

The enhanced generation of intracellular ROS by hyperoxia may lead to the cell death observed (29). Nevertheless, the HPx+CoCl2 group did not show significant differences on intracellular ROS release, being consistent with the cell viability result. Although it has been established that both environmental and chemical hypoxia increase ROS generation in adipocytes (30, 31), no differences in intracellular ROS release were found in Hx and CoCl2 treatments. Regarding CoCl2, this observation could be explained by the time and dose used (31).

The Hx group induced an increase on lipolysis, glucose utilization and lactate release, as has been previously described (28, 32). It is known that in anaerobic conditions the cell is not able to oxidize glucose fully through mitochondrial oxidation and in consequence, there is a lower adenosine-5'-triphosphate (ATP) production with respect to respiration. To compensate this lack of ATP, cells may increase their glucose uptake. This mechanism

could explain the response of glucose utilization observed with hyperoxia. Probably, a higher O_2 availability might induce the ATP production mainly through the aerobic metabolism and therefore, no compensatory pathways need to be activated. This outcome seems to be in accordance with the significant reduction observed in lactate production in hyperoxic conditions, and goes in the same direction as other investigations observed in other tissues (33). In obesity, it has been found that adipocyte-derived lactate by the hypoxic state may constitute another link between this disease and its associated pathologies (32). In this sense, since hyperoxia decreased lactate release in adipocytes, it might ameliorate some obesity-associated complications. Furthermore, a high association between glucose utilization and lactate release was found, confirming the relationship of these two metabolic pathways with O_2 tension. Contrary to expectations, the hypoxic mimetic CoCl2 did not follow the tendency observed with 1% O_2 on these biochemical parameters.

It is known that glucose uptake and GLUT-1 mRNA expression are increased in hypoxia (28, 34), as we observed in our experiment. Under hyperoxic conditions, GLUT-1 expression was significantly decreased by adipocytes. Interestingly, the expression of this glucose transporter did not change with the occurrence of CoCl2, although it was significantly increased when both conditions were placed together (HPx+CoCl2 group). An association of the expression of this gene with glucose utilization was also found, suggesting that a higher O_2 tension might also be able to participate on glucose metabolism in adipose tissue, as previously observed in muscle cells (35). Furthermore, ANGPTL4 is a gene involved in the regulation of plasma triacylglycerides metabolism (36). Thus, a down-regulation in ANGPTL4, as occurred with hyperoxia, may contribute to ameliorate some metabolic disorders. The analysis of Hx and CoCl2 groups revealed a decrease in the expression of this gene. Nevertheless, these results should be taken with caution, since they differ from experiments on human adipocytes (37).

Several trials have confirmed that the exposure to high O_2 concentrations seems to produce beneficial effects on inflammatory markers in both cell culture (15) and animal models (17). However, a significant increase in the expression of this type of cytokines has also been reported (38, 39). Nevertheless, these effects were not evident until the animals were treated for at least 48 h of hyperoxia, suggesting that inflammation is dependent on the duration of the O_2 exposure. Contrary to our initial expectations, mRNA levels of pro-inflammatory markers IL-6 and MCP-1 were up-regulated by hyperoxia. The induction of adipocyte death may be a mechanism by which hyperoxia could contribute to up-regulate the expression of these genes in 3T3-L1 adipocytes. Another possible explanation could be that free fatty acids released by lipolysis might contribute to this inflammatory response, as demonstrated in other cell types (40). This outcome is in accordance with a strong relationship observed in the current experiment between the expression of IL-6 and MCP-1 genes and glycerol release concerning C and HPx groups. Furthermore, the HPx+CoCl2 group increased MCP-1 and IL-6 gene expressions in respect to the CoCl2 group, suggesting that hyperoxia could exert a dominant effect in the expression of these genes in hypoxic conditions. Even though hyperoxia provoked the up-regulation of pro-inflammatory adipokines, this treatment did not modify the expression of adiponectin, known to be down-regulated by IL-6 (41). However, since the expression of this adipokine did not change with HPx and CoCl2 independently, it was significantly decreased in the HPx+CoCl2 group, probably due to cell stress produced by the combined effect of both conditions.

Adiponectin is also an important selective controlled modulator of insulin sensitivity whose expression is enhanced by PPAR-γ (42). In our experiment, PPAR-γ mRNA expression tended to increase in hyperoxia and this event may prevent the decrease of adiponectin expression by IL-6. Furthermore, it has been proposed that HBOT could increase insulin sensitivity in type 2 diabetes patients (43). On the other hand, Hx treatment produced a down-regulation of mRNA levels of PPAR-γ. This outcome is in agreement with the results from Kim et al., who suggested that hypoxic condition attenuates adipocyte differentiation inhibiting PPAR-γ expression by the activation of AMPK, which impairs clonal expansion phase (44).

Contradictory data has been found regarding the effects of CoCl2 and ambient hypoxia. Perhaps the

concentration of this hypoxia mimetic (100 μM) was not high enough to produce the same effects in 3T3-L1 mature adipocytes as 1% O_2 did. Since not always mRNA levels and protein secretion are related, data at the protein level could complement the value of this research, which was specifically focused on the transcriptomic effects of O_2 supply in adipocytes.

In summary, to the authors' knowledge this is the first study to combine the measurements of metabolic markers and the expression of genes involved in glucose and lipid metabolism as well as the inflammatory response in hypoxic 3T3-L1 adipocytes exposed to hyperoxia. Indeed, hyperoxia increased significantly the ROS levels and the lipolytic activity, while it reduced lactate production. The changes in genes not involved in inflammation, such as GLUT-1 and ANGPTL4 and PPAR-γ, led to hypothesize that hyperoxia is beneficial for the hypertrophied adipose tissues of obese subjects and for improving insulin sensitivity.

ACKNOWLEDGEMENTS

The authors wish to thank the EXPLORA-MICINN (Ministerio de Ciencia e Innovación), SAF2010-11630-E, the "Línea Especial" (LE/97) of the University of Navarra (Spain) and the "Asociación de Amigos de la Universidad de Navarra" for financial support. Also CIBERobn and RETICS Schemes are credited. Finally, the authors are grateful for the expert technical assistance of Verónica Ciaurriz and to Richard Marks (University of Surrey, Guilford) for technical support and for reviewing the English of the final version of the manuscript.

REFERENCES

1. Misra A, Khurana L. Obesity and the metabolic syndrome in developing countries. J Clin Endocrinol Metab 2008; 93:S9-30.
2. Hotamisligil GS. Inflammation and metabolic disorders. Nature 2006; 444:860-7.
3. Martinez JA. Mitochondrial oxidative stress and inflammation: a slalom to obesity and insulin resistance. J Physiol Biochem 2006; 62:303-6.
4. Trayhurn P, Wood IS. Adipokines: inflammation and the pleiotropic role of white adipose tissue. Br J Nutr 2004; 92:347-55.
5. Kabon B, Nagele A, Reddy D, et al. Obesity decreases perioperative tissue oxygenation. Anesthesiology 2004; 100:274-80.
6. Ye J, Gao Z, Yin J, He Q. Hypoxia is a potential risk factor for chronic inflammation and adiponectin reduction in adipose tissue of ob/ob and dietary obese mice. Am J Physiol Endocrinol Metab 2007; 293:E1118-28.
7. Hosogai N, Fukuhara A, Oshima K, et al. Adipose tissue hypoxia in obesity and its impact on adipocytokine dysregulation. Diabetes 2007; 56:901-11.
8. Bennett MH, French C, Schnabel A, Wasiak J, Kranke P. Normobaric and hyperbaric oxygen therapy for migraine and cluster headache. Cochrane Database Syst Rev 2008:CD005219.
9. Lin LC, Yau G, Lin TF, Lin TK, Tang YY, Wang KY. The efficacy of hyperbaric oxygen therapy in improving the quality of life in patients with problem wounds. J Nurs Res 2006; 14:219-27.
10. Bocci V, Aldinucci C. Rational bases for using oxygen-ozonetherapy as a biological response modifier in sickle cell anemia and beta-thalassemia: a therapeutic perspective. J Biol Regul Homeost Agents 2004; 18:38-44.
11. Bigdeli MR, Hajizadeh S, Froozandeh M, Rasulian B, Heidarianpour A, Khoshbaten A. Prolonged and intermittent normobaric hyperoxia induce different degrees of ischemic tolerance in rat brain tissue. Brain Res 2007; 1152:228-33.
12. Ercin CN, Yesilova Z, Korkmaz A, Ozcan A, Oktenli C, Uygun A. The effect of iNOS inhibitors and hyperbaric oxygen treatment in a rat model of experimental colitis. Dig Dis Sci 2009; 54:75-9.
13. Efrati S, Berman S, Ben Aharon G, Siman-Tov Y, Averbukh Z, Weissgarten J. Application of normobaric hyperoxia therapy for amelioration of haemorrhagic shock-induced acute renal failure. Nephrol Dial Transplant 2008; 23:2213-22.
14. Johnston CJ, Wright TW, Reed CK, Finkelstein JN. Comparison of adult and newborn pulmonary cytokine mRNA expression after hyperoxia. Exp Lung Res 1997; 23:537-52.
15. Weisz G, Lavy A, Adir Y, et al. Modification of in vivo and in vitro TNF-alpha, IL-1, and IL-6 secretion

by circulating monocytes during hyperbaric oxygen treatment in patients with perianal Crohn's disease. J Clin Immunol 1997; 17:154-9.
16. Yamashita M, Yamashita M. Hyperbaric oxygen treatment attenuates cytokine induction after massive hemorrhage. Am J Physiol Endocrinol Metab 2000; 278:811-6.
17. Yang ZJ, Bosco G, Montante A, Ou XI, Camporesi EM. Hyperbaric O_2 reduces intestinal ischemia-reperfusion-induced TNF-alpha production and lung neutrophil sequestration. Eur J Appl Physiol 2001; 85:96-103.
18. Benson RM, Minter LM, Osborne BA, Granowitz EV. Hyperbaric oxygen inhibits stimulus-induced proinflammatory cytokine synthesis by human blood-derived monocyte-macrophages. Clin Exp Immunol 2003; 134:57-62.
19. Quintero P, Milagro FI, Campion J, Martinez JA. Impact of oxygen availability on body weight management. Med Hypotheses 2010; 74:901-7.
20. Vengellur A, LaPres JJ. The role of hypoxia inducible factor 1alpha in cobalt chloride induced cell death in mouse embryonic fibroblasts. Toxicol Sci 2004; 82:638-46.
21. Garcia-Diaz DF, Arellano AV, Milagro FI, et al. Glucose and insulin modify thrombospondin 1 expression and secretion in primary adipocytes from diet-induced obese rats. J Physiol Biochem 2011; 67:453-61.
22. Cathcart R, Schwiers E, Ames BN. Detection of picomole levels of hydroperoxides using a fluorescent dichlorofluorescein assay. Analytical biochemistry 1983; 134:111-6.
23. Zhong H, Simons JW. Direct comparison of GAPDH, beta-actin, cyclophilin, and 28S rRNA as internal standards for quantifying RNA levels under hypoxia. Biochem Biophys Res Commun 1999; 259:523-6.
24. Garcia-Diaz DF, Campion J, Milagro FI, Boque N, Moreno-Aliaga MJ, Martinez JA. Vitamin C inhibits leptin secretion and some glucose/lipid metabolic pathways in primary rat adipocytes. J Mol Endocrinol 2010; 45:33-43.
25. Goossens GH, Bizzarri A, Venteclef N, et al. Increased adipose tissue oxygen tension in obese compared with lean men is accompanied by insulin resistance, impaired adipose tissue capillarization, and inflammation. Circulation 2011; 124:67-76.
26. Quintero P, Gonzalez-Muniesa P, Garcia-Diaz DF, Martinez JA. Effects of hyperoxia exposure on metabolic markers and gene expression in 3T3-L1 adipocytes. J Physiol Biochem 2012; E pub ahead of print.
27. Piret JP, Mottet D, Raes M, Michiels C. CoCl2, a chemical inducer of hypoxia-inducible factor-1, and hypoxia reduce apoptotic cell death in hepatoma cell line HepG2. Ann N Y Acad Sci 2002; 973:443-7.
28. Yin J, Gao Z, He Q, Zhou D, Guo Z, Ye J. Role of hypoxia in obesity-induced disorders of glucose and lipid metabolism in adipose tissue. Am J Physiol Endocrinol Metab 2009; 296:E333-42.
29. Conconi MT, Baiguera S, Guidolin D, et al. Effects of hyperbaric oxygen on proliferative and apoptotic activities and reactive oxygen species generation in mouse fibroblast 3T3/J2 cell line. J Investig Med 2003; 51:227-32.
30. Carriere A, Carmona MC, Fernandez Y, et al. Mitochondrial reactive oxygen species control the transcription factor CHOP-10/GADD153 and adipocyte differentiation: a mechanism for hypoxia-dependent effect. J Biol Chem 2004; 279:40462-9.
31. Kamiya T, Hara H, Inagaki N, Adachi T. The effect of hypoxia mimetic cobalt chloride on the expression of EC-SOD in 3T3-L1 adipocytes. Redox Rep 2010; 15:131-7.
32. Perez de Heredia F, Wood IS, Trayhurn P. Hypoxia stimulates lactate release and modulates monocarboxylate transporter (MCT1, MCT2, and MCT4) expression in human adipocytes. Pflugers Arch 2010; 459:509-18.
33. Graham TE, Pedersen PK, Saltin B. Muscle and blood ammonia and lactate responses to prolonged exercise with hyperoxia. J Appl Physiol 1987; 63:1457-62.
34. Wood IS, Wang B, Lorente-Cebrian S, Trayhurn P. Hypoxia increases expression of selective facilitative glucose transporters (GLUT) and 2-deoxy-D-glucose uptake in human adipocytes. Biochem Biophys Res Commun 2007; 361:468-73.
35. Bandali KS, Belanger MP, Wittnich C. Does hyperoxia affect glucose regulation and transport in the newborn? J Thorac Cardiovasc Surg 2003; 126:1730-5.
36. Yamada T, Ozaki N, Kato Y, Miura Y, Oiso Y. Insulin

downregulates angiopoietin-like protein 4 mRNA in 3T3-L1 adipocytes. Biochem Biophys Res Commun 2006; 347:1138-44.

37. Gonzalez-Muniesa P, de Oliveira C, Perez de Heredia F, Thompson MP, Trayhurn P. Fatty acids and hypoxia stimulate the expression and secretion of the adipokine ANGPTL4 (angiopoietin-like protein 4/ fasting-induced adipose factor) by human adipocytes. J Nutrigenet Nutrigenomics 2011; 4:146-53.
38. Barazzone C, Tacchini-Cottier F, Vesin C, Rochat AF, Piguet PF. Hyperoxia induces platelet activation and lung sequestration: an event dependent on tumor necrosis factor-alpha and CD11a. Am J Respir Cell Mol Biol 1996; 15:107-14.
39. Jensen JC, Pogrebniak HW, Pass HI, et al. Role of tumor necrosis factor in oxygen toxicity. J Appl Physiol 1992; 72:1902-7.
40. Wang L, Gill R, Pedersen TL, Higgins LJ, Newman JW, Rutledge JC. Triglyceride-rich lipoprotein lipolysis releases neutral and oxidized FFAs that induce endothelial cell inflammation. J Lipid Res 2009; 50:204-13.
41. Fasshauer M, Kralisch S, Klier M, et al. Adiponectin gene expression and secretion is inhibited by interleukin-6 in 3T3-L1 adipocytes. Biochem Biophys Res Commun 2003; 301:1045-50.
42. Spiegelman BM. PPAR-gamma: adipogenic regulator and thiazolidinedione receptor. Diabetes 1998; 47:507-14.
43. Wilkinson D, Chapman IM, Heilbronn LK. Hyperbaric oxygen therapy improves peripheral insulin sensitivity in humans. Diabet Med 2012:In press. doi: 10.1111/j.1464-5491.2012.03587.x
44. Kim KH, Song MJ, Chung J, Park H, Kim JB. Hypoxia inhibits adipocyte differentiation in a HDAC-independent manner. Biochemical and biophysical research communications 2005; 333:1178-84.

RAT MODEL OF BURN WOUND HEALING: EFFECT OF BOTOX

I. ABDALLAH HAJJ HUSSEIN[1], N. DALI BALTA[1], R.A. JURJUS[2], W. WATFA[3], A. GERGES[3], B. ATIYEH[4], C. PULLAR[5], A. LEONE[6] and A.R. JURJUS[1]

[1]Department of Anatomy, Cell Biology and Physiology, American University of Beirut, Beirut; [2]Department of Anatomy and Regenerative Biology, George Washington University, Washington DC, USA; [3]Lebanese Health Society; [4]Department of Surgery, American University of Beirut, Beirut; [5]Department of Cell Physiology and Pharmacology, University of Leicester, UK; [6]Section of Histology and Embryology, Department of Experimental Biomedicine and Clinical Neuroscience, University of Palermo, Italy

Received 2 March 17, 2012 - Accepted July 19, 2012

Animal models of burn play a crucial role in studying the mechanisms of burn wound progression and the factors that regulate various stages of healing. In this study, using a rat model, we assessed the effect of Botox in the healing process through parameters like transepidermal water loss (TEWL), histological alterations, transforming growth factor β (TGF-β_1) and tumor necrosis factor alpha (TNF-α). Fifty Sprague-Dawley rats were inflicted with 5 cm^2 second degree burn and divided into 2 groups; one group was injected intralesionally with Botox and the other with saline. Daily observation and transepidermal water loss measurement were performed. Biopsies were taken on days 0, 3, 8, 14, and 28 for histology and polymerase chain reaction, testing TGF-β and TNF-α. The results showed no significant difference in TEWL except for slightly better preservation of moisture with Botox. Histology revealed relatively better and faster regeneration with Botox, delayed lower grade inflammation, and increase in fibroblasts. TNF-α had an acute increase of 21-fold then tapered down while TGF-β levels increased on day 3 after TNF-α, peaked on day 8 and then started to decrease until complete healing. Botox improved the healing process and the cosmetic appearance of burn scar.

Burn wound models are essential for studying the mechanisms of burn wound progression and the factors that regulate re-epithelialization, fibroblast proliferation, extracellular matrix synthesis and scarring (1-4). In addition, they facilitate the testing of new therapeutic modalities that require investigation at the experimental level for preclinical evaluations of potential clinical use (5).

In addition to the well-known physical and environmental factors affecting the quality of wound closure such as an absence of infection, good blood supply, and minimal tension, the biochemical and immunological aspects of the wound healing process, as well as the severity of wound, have a profound effect on the final appearance of a wound (5-7).

Inflammation is the first stage of wound healing; it involves a vascular response, a cellular reaction, and a cascade of cytokines and growth factors. Each category is peaking at a particular time and contributing to wound healing probably through a different

Key words: botox, burn, animal models, TGF-β, TNF-α

Mailing address: Angelo Leone, DDS Sp.Ortho,
Department of Experimental Biomedicine
and Clinical Neuroscience, Section of Histology and Embryology,
University of Palermo Via Del Vespro, 127.
90129 Palermo Italy
Tel.: +39 091 6553581; Fax: +39 091 6553586
e-mail: angelo.leone@unipa.it

0393-974X (2012)

DISCLOSURE: ALL AUTHORS REPORT NO CONFLICTS OF INTEREST RELEVANT TO THIS ARTICLE.

mechanism (6, 7).

During inflammation, a panel of cytokines are produced and released by infiltrating platelets, macrophages, mast cells, fibroblasts, and other residential cells. Such cytokines include IL-1, PDGF, EGF, FGF, TGFβ1, TGFα, Hepatocyte Growth Factor (HGF) and TNF-α (7, 8). They facilitate cross-talk between cells at the injury site and promote physiological events including cell migration, proliferation, and extracellular matrix (ECM) protein synthesis and degradation leading to tissue remodeling, wound healing, or fibrosis formation (9). In addition, several studies have also revealed that modulation of inflammatory cytokines and growth factors in skin wounds can be performed by tropical application of different pharmaceutical agents (9).

TGFβ1 is a key cytokine with an array of activities in normal wound healing and fibrosis (10-12). It is important in inflammation, angiogenesis, re-epithelialization, connective tissue regeneration, and has an increased expression at the onset of injury (10). TGFβ1 plays a role in eliminating infection and debriding the wound, first by activating monocytes and leukocytes, then by promoting apoptosis of these cells and clearance by macrophages (12). In addition, TGFβ1 stimulates angiogenesis and increases deposition of ECM to reform the wound dermis. Finally, TGFβ1 also blocks the matrix degradation by decreasing production of proteases and increasing the level of protease inhibitors (13).

TNF-α is a potent pro-inflammatory cytokine expressed during the inflammatory phase of wound healing. In general, the concentrations of this cytokine seem to determine whether it exerts beneficial or harmful effects (14). Normally, it is absent during the re-epithelization and ECM re-organization phases (15). It has been shown to promote inflammation through the activation and induction of cytokines IL-1β, IL-6 and IL-8, and by the upregulation of adhesion molecules on endothelial cells, resulting in increased leukocyte extravasation (16, 17). Therefore, TNF-α is a central regulator of inflammatory cascades during both initiation and the amplification of inflammatory reactions (17).

Several cells involved in wound healing are affected by TNF-α during all phases of healing. Early data showed that the effects of TNF-α depend on its concentration and the duration of exposure, indicating its importance in balancing the pro-inflammatory signals which control wound healing. At low levels, TNF-α promotes wound healing by indirectly reducing inflammation and increasing macrophage produced growth factors, while at high levels, mainly during prolonged periods of time, it has a detrimental impact on healing by decreasing synthesis of ECM proteins and increasing synthesis of MMPs (15, 17).

Botulinum toxin (Botox) is an exotoxin of an anaerobic gram-positive rod-shaped bacterium, the *Clostridium botulinum*. *Clostridium botulinum* produces seven different neurotoxins or serotypes, designated according to the order of their discovery as types A to G (18).

Botulinum toxin type A is the most potent. It causes the majority of food-borne botulism cases in humans, has the longest synaptic blockade, and consequently the longest paralyzing effect 2-6 months (19).

We hypothesize that Botox would immobilize muscle groups underlying the cutaneous scar improving the final cosmetic result due to the decrease in tension in the wound resulting in less myofibroblast-mediated contraction and improved scaring (20, 21). In a study by Wilson in 2006, 40 patients with ugly facial scars were subjected to Botox A injections along the length of the scar to paralyze the muscles and minimize tension at the healing wound edges until the collagen could mature. This study yielded results superior to those of any other treatment modality (30). Moreover, in a blind, prospective, randomized clinical trial by Gassner et al. in 2006, 31 patients were randomized to Botox *vs* placebo injection into the musculature adjacent to the wound 24 hours after wound closure. The overall median visual analog scale score for Botox was 8.9, and for placebo 7.2, resulting in enhanced healing and improved cosmetic appearance of the experimentally immobilized scars (22, 23).

The aim of this study was to analyze the effect of intralesional botilinum toxin A (Botox) on the wound healing process using an experimental model of a second degree deep partial thickness skin burn wounds in rat skin. Histological alterations, transepidermal water loss and the temporal evolution of two cytokines TGFβ1 and TNF-α were assessed in the presence or absence of Botox at various time points up to 28 days post burn.

MATERIALS AND METHODS

Experimental animals and protocol

Fifty adult Sprague-Dawley rats (300-400g) were used in this study, according to the guidelines and recommendations of the Institutional Animal Care and Use Committee (IACUC) at the American University of Beirut. A day prior to the procedure, the backs of the animals were shaved with a standard electric shaver; then the area was also depilated with a commercial depilatory cream (Veet, Reckitt Benckiser, Slough, UK) to obtain smooth and hairless skin. The animals were kept under standard laboratory conditions and veterinary supervision with no restriction on water and food. Each animal was kept alone in a cage in order to avoid any negative effect to the wound by other rats. The animals were divided into two groups. The experimental group was injected with 0.5 ml (10 units) of Botox, and the control group with 0.5 ml of physiological sterile saline.

A modified protocol of the aluminum stamp described by Knabl et al. was used (3). The optimal temperature was achieved and controlled by an electronic temperature controller with a thermo-couple type feedback sensor and a dimmer. A round stamp of 2.5 cm diameter with an ordinary soldering iron of 20 W produced a burn area of 5 cm^2 on the back of the rat. The desired temperature of 70°C was applied for 25 seconds on the back of the rat in order to achieve a deep partial thickness burn. The burn was applied on rats under deep anesthesia by an intramuscular injection of ketamine at 75mg/kg (Ketaset, Fort Dodge, Ind., USA), and xylazine at 10 mg/kg (Rompun, Bayer, West Haven, Conn., USA). Only one deep partial thickness burn was made at the same position on the back of each rat.

Before giving the injections, the vial of Botox (Allergan Inc., Irvine, CA, USA), which contains 100 units, was diluted in 5 ml of 0.9% sterile saline. Each rat in the experimental group (total=25) received 0.5 ml or 10 units of Botox injected subcutaneously in the center of the wound immediately after creating the burn. Each rat in the control group (total=25) received 0.5 ml of 0.9% sterile saline injected subcutaneously in the center of the wound immediately after the burn.

Transepidermal water loss measurement

Wound healing by surface re-epithelization was assessed quantitatively by measuring the wound transepidermal water loss as an indicator of skin barrier function restoration. According to the literature, good hydration is the single most important external factor responsible for optimal wound healing. TEWL is a non-invasive technique aiming at evaluating the efficacy of epidermal integrity as a protective barrier and it is expressed in grams per hour per square meter. The measurement is made by using a DermaLab system (Cortex Technology, Hadsund, Denmark) equipped with a TEWL probe on the non-biopsied burn area and the surrounding skin, and is based on the vapor pressure gradient estimation method of Nilsson (24).

Daily observation

The animals were checked on a daily basis and each wound was irrigated with 10 ml of 0.9% sterile saline to clean the wound to decrease the bacterial load, remove necrotic tissues and foreign material, and probably reduce autolytic enzyme levels in the wound (9). The wound was kept uncovered during the whole procedure. Visual assessment of the wound healing process was made on a daily basis to observe the shape of the wound and its quality, color and texture.

Biopsies

Biopsies were taken on days 0, 3, 8, 14 and 28 post burn and at each time point, biopsies were taken from 5 experimental rats and 5 control rats. They were taken from the margin of the wound by using a 4mm Acu-Punch: Two biopsies were taken for Real-time PCR and one biopsy for histological study. The biopsies for Real-time PCR were frozen in liquid nitrogen and then stored at -80°C, while the biopsies for histology were fixed in 10% formaldehyde, processed for light microscopy, and stained with Hematoxylin and Eosin, according to standard procedures. In screening epidermal changes, the following histological scoring was used: 0 for well-shaped epithelium, 1 for partially disrupted epithelium, and 2 for completely disrupted epithelium.

Molecular testing

RNA was extracted for Real-time PCR, using Ribozol ™ RNA extraction reagent from Amresco (AMRESCO, Solon, OH), according to the manufacturer's instructions. Quantification of the extracted RNA was made using the Spectrophotometer Nanodrop (ND-1000) software iScript™ and a cDNA synthesis kit (Bio-rad Laboratories, Hercules, CA, USA) was used to convert RNA into cDNA. The procedure was followed according to the manufacturer's guidelines.

The primers used in Real-time PCR were for TNF-α, TGFβ1 and Glyceraldehyde 3-phosphate Dehydrogenase (GAPDH) as housekeeping gene. They were tested on positive controls in order to determine their annealing temperatures. TGFβ1 was tested on liver and TNF-α on inflamed brainstem by using two step RT-PCR and gel electrophoresis. GAPDH primer sequence was described by Sanders et al. in 2007 (25) and TGFβ1 by Miyazaki et al. in 2009 (26). TNF-α primer sequence was designed by using the NCBI (National Center for Biotechnology

Information) program. PCR Master Mix (2X) from Fermentas (Fermentas, Burlington, Canada) was used for the two-step RT-PCR. After testing the primers, Real-time PCR was performed using iQ™ SYBR Green Supermix from Biorad (Bio-rad Laboratories, Hercules, CA, USA). The data were analyzed using the ΔCT method and expressed as relative expression of the gene. DNA fragments were subjected to gel electrophoresis and photographed using a transilluminator (UV light box) and appeared as bands.

Statistical analysis

Significance for all data, except for TEWL and wound surface area, was calculated using the Two-way Measures of Analysis of Variance (ANOVA) test from SPSS for Windows version 17.0 (IBM Corporation, Armonk, NY). TEWL and wound surface area were analyzed using the Two-way Repeated (ANOVA) test from SPSS for Windows version 17.0 (IBM Corporation, Armonk, NY, USA). All data are presented as mean ± standard error of mean (SEM). Significance was ascribed if the P-value<0.05 (*).

RESULTS

Macroscopic findings

Wounds were assessed visually every day throughout the experimental time period. Immediately post-wounding, the burns were scored for shape, color, texture, and wound quality. On day 1 post-burn, inflammation started slightly on the edges with darkening of skin in the middle in both groups, however, the saline group had darker skin. On day 3 post-burn, inflammation was more prominent on the edges of the controls and a delay in necrosis was noticed in the Botox-treated wounds (Fig. 1-3A and 1-B). On day 7 post-burn, both Botox and saline treated wounds showed depressions within the wound, while the Botox-treated wounds had more crust which started to detach from the border. On day 9 post-burn, Botox-treated wounds revealed conspicuous redness on the wound border which is a sign of vascularization and re-epithelialization, while saline-treated wounds had an elevated crust leaving a depression behind (Fig. 1-9A and 9B). On day 11, saline showed an obvious redness on the border, a sign of vascularization and re-epithelization. On day 12, the crust pertaining to the saline-treated group denatured and in the Botox-treated group detached partially from the edge. On day 13, the Botox-treated group showed a more advanced crust detachment and a redness within the wound, while in saline

Table I. *Sequence of the primers and their band size.*

Gene	Sense primer	Anti-sense primer	Band size
GABDH	5'ATGCCGCCTGGAGAAACC3'	5'AGAATGGGAGTTGCTGTTGAAG3'	138
TGFβ1	5'CGCCTGCAGAGATTCAAGTCAA3'	5'GTCGGTTCATGTCATGGATGGT3'	300
TNF-α	5'AAATGGGCTCCCTCTCATCAGTTC3'	5'TCTGCTTGGTGGTTTGCTACGAC3'	111

Table II. *Comparison of morphological changes in Botox and saline groups.*

Parameter	Botox group	Saline group
Necrosis	Day 3	Day 1
Crust detachment	Day 7	Day 13
Re-epithelization	Day 9	Day 11

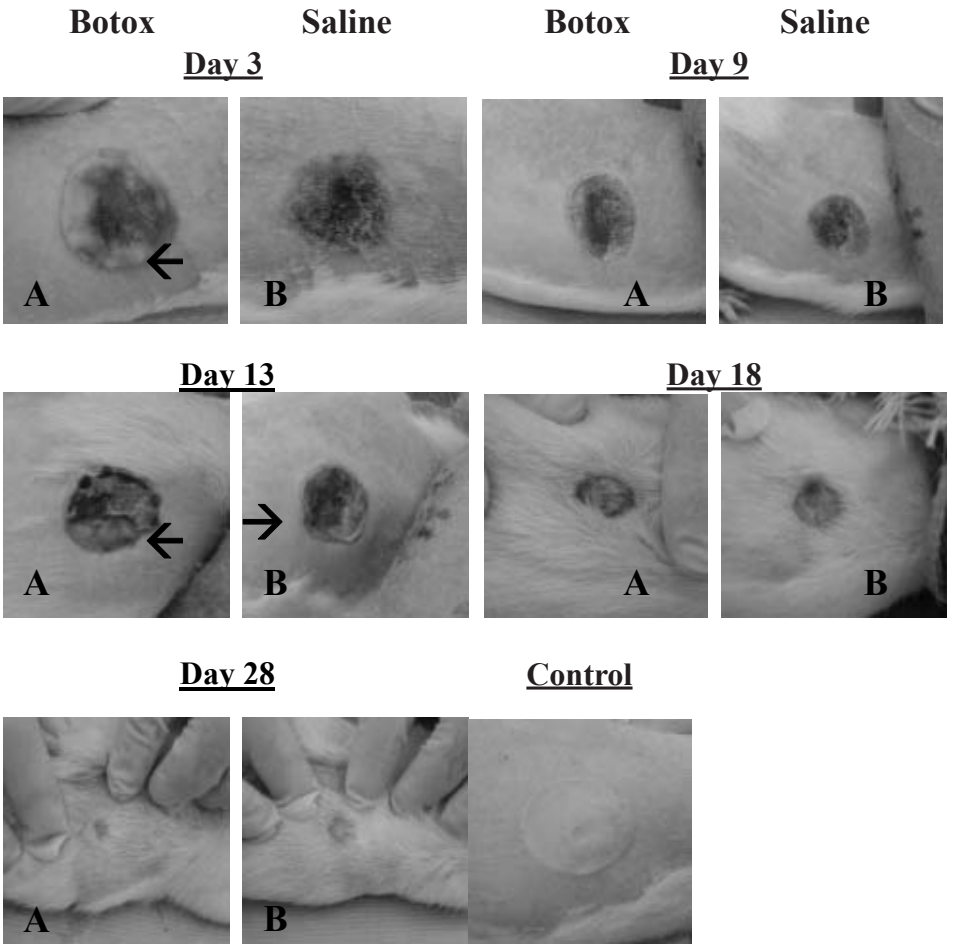

Fig. 1. *Representative images of the Botox and saline-treated wounds are shown at days 3, 9, 13, 18 and 28 post burn. Panorama of morphological changes over time in Botox and saline groups. Note in day 3: Inflammation on the border in both groups, delay in necrosis in Botox. Day 9: Prominent redness on the border suggesting vascularization in Botox. Day 13: Crust partially sloughed and inflammation in Botox, crust detached on the border in saline. Day 18: Crust completely sloughed in both groups. Day 28: Smaller surface area of the wound in Botox. Pictures were taken at the same magnification.*

the crust just started to detach from the border (Fig. 1-13A and 13B). On day 14 post burn, the Botox group showed an advanced crust detachment and a flat re-epithelization, while the saline group had a necrotic crust with vascularized and inflamed edges. On day 18, the crust was sloughed off completely in both groups (Fig.1-18A and 18B). On day 22, shaving was performed on all rats, since hair had grown extensively. On day 28, a smaller surface area of the wound was readily noticed in the Botox group ($0.19cm^2 \pm 0.03$ in Botox and $0.47cm^2 \pm 0.07$ in saline) (Fig. 1-28A and 28B). To summarize, saline-treated wounds had earlier and greater necrosis than Botox treated wounds. The crust started to detach from the border on day 7 in Botox treated wounds and on day 13 in saline-treated wounds resulting in a delay in crust detachment in the saline group. Re-epithelization was enhanced in the Botox-treated group and vascularization occurred 2 days earlier, on day 9, in Botox group, and on day 11 in saline group.

Microscopic findings

At each time point, six sections from each animal were examined under the light microscope by two

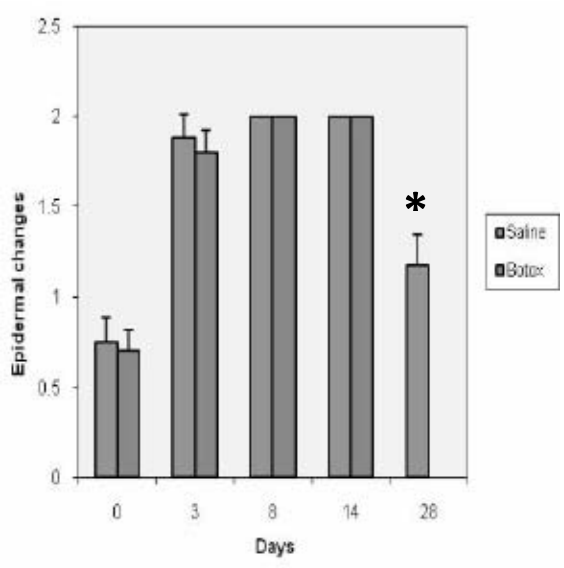

Fig. 2. *Visual assessment of re-epithelialization. Note the significant difference on day 28 (p-value<0.05).*

independent observers in a double-blind manner, according to a set of histological criteria, and scored. The following parameters were studied: overall architecture, the epidermal changes including a score of re-epithelialization and the number of epidermal layers, the number of inflammatory cells in the dermis infiltrate, the number of fibroblasts in the dermis and appearance of collagen fibers among others.

Epidermal changes

From day 0 to day 3, epidermal disruption was identical in both groups. However, the epidermal rim around the burn was redder in Botox-treated wounds, probably indicating delayed inflammation or earlier vascularization on day 8. On day 14, sloughing was observed in both groups. On day 28, the Botox group were re-epithelialized compared to the saline group which still showed a partial disrupted epithelium; the difference was statistically significant between the two groups on day 28 (p-value<0.05).

Newly generated epidermal layers

Generation of new epidermal layers started on day 8 with significantly more layers in Botox-treated wounds (p-value<0.005). The number of layers increased on day 14 and remained significantly higher in the Botox group. The same trend continued on day 28. The test revealed a high and sustained significant effect of the Botox compared to saline (p-value<0.05) (Fig. 3).

Inflammatory cells

Infiltration of inflammatory cells into the burned wound was examined according to the following histological gradient: 0 for no infiltration, 1 for minor infiltration (low prevalence of cells), 2 for moderate infiltration (intermediate prevalence of cells), and 3 for abundant infiltration (high prevalence of cells).

Many aggregates of necrotic and inflammatory cells were noted on day 3. Inflammation was significantly higher in the saline group (p-value<0.05) and decreased to moderate by day 8. In Botox-treated wounds, the infiltrate was low on day 3 but gradually increased later on days 8 and 14 to show moderate infiltration. On day 14, inflammation increased in the Botox-treated group, (p-value<0.05), however, on day 28 the inflammation decreased dramatically in both groups to reach very low levels. In brief, inflammation was induced strongly in the saline group and decreased with time, while in Botox it was delayed, increasing slowly until it became moderate to high on day 14. On day 3, inflammation was significantly reduced in Botox-treated wounds, while on day 14, it was significantly increased, suggesting a temporal delay in inflammatory cell recruitment to

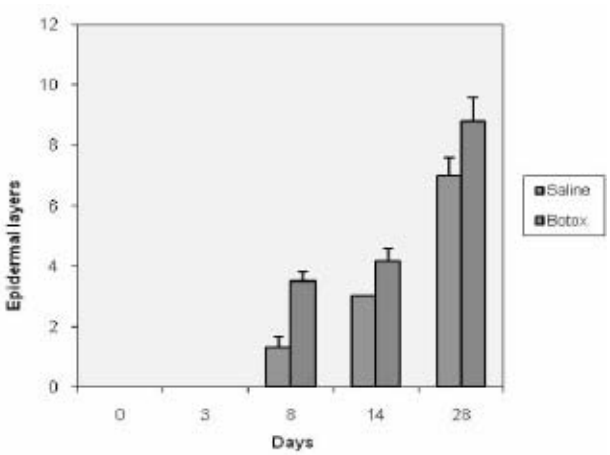

Fig. 3. *Newly generated epidermal layers in Botox and saline. Note the significant difference on days 8 and 14 (p-value<0.05).*

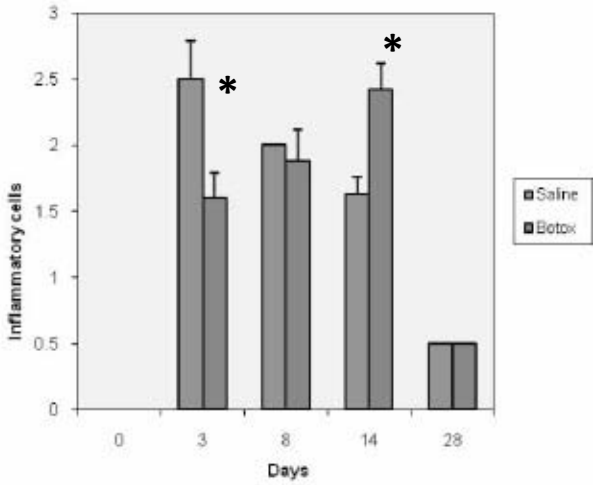

Fig. 4. *Rate of infiltration of inflammatory cells in Botox and saline. Note the significant difference on days 3 and 14.*

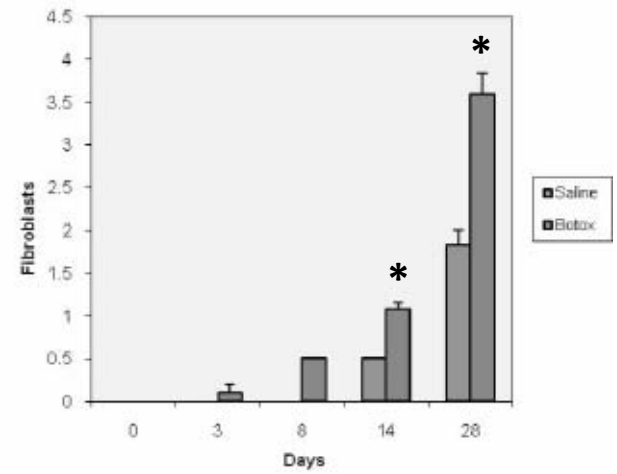

Fig. 5. *Rate of fibroblasts in Botox and saline. Note the significant difference on days 14 and 28.*

the burn wounds by Botox (Fig. 4).

Fibroblasts and collagen

To evaluate the number of fibroblasts in the burn wound dermis, the following histological gradient was used: 1 for low prevalence of cells, 2 for moderate prevalence of cells, and 3 for abundant prevalence of cells.

The number of fibroblasts started to increase on day 3 in Botox group while no fibroblast migration into the wound dermis was observed in the saline-treated wounds. On days 14 and 28, the number of fibroblasts was abundant, almost double in Botox-treated wounds, (p-value<0.005) (Fig. 5).

Collagen bundles started to disorganize since day 0, immediately after burn injury, but the disorganization was slightly higher in saline group. On day 3, it increased in both groups and was still slightly higher in saline. On day 8, collagen fibers started to reorganize in both groups. On days 14 and 28, the organization was better in Botox. The presence of fibroblasts correlated with the presence of collagen fibers since fibroblasts are the main source of collagen. Consequently, the amount of collagen produced was greater in Botox. The test revealed a p-value of the effect of Botox of 0.057 which is not statistically significant between the two groups and a p-value of the effect of Botox over the time of 0.920 that is not significant.

In summary, the normal skin shows a continuous epithelium (E), no eruptions and no infiltration of cells and debris in the dermis (D) (Fig. 6-Normal skin). On day 0 after burn, both groups had complete epithelial disruption with lack of dermal appendages. On day 3, aggregates of inflammatory cells (IC) and necrotic tissue (N) appeared in both groups but the infiltration was higher in saline-treated wounds (Fig. 6-3A and 3B). On day 8, epidermis was sloughed in both groups and dermal regeneration was obvious; this regeneration (R) was greater in Botox (Fig. 6-8A and 8B). On day 14, infiltration of inflammatory cells (IC) decreased in saline but increased greatly in Botox (Fig. 6-14A and 14B) and more fibroblasts appeared in Botox. On day 28, a multi layered epithelium was present in the Botox-treated group and also a higher number of active fibroblasts (F) in the dermis and increased vascularization compared with the saline-treated group (Fig. 6-28A and 28B).

Transepidermal water loss

The TEWL measurements for the Botox group were slightly less than those for the saline group except on day 0 when saline was injected into the wound, with only statistically significant difference at the level of p-value<0.05 on day 28 (Fig. 7).

The TEWL measurements revealed no significant differences between control and Botox-treated burn

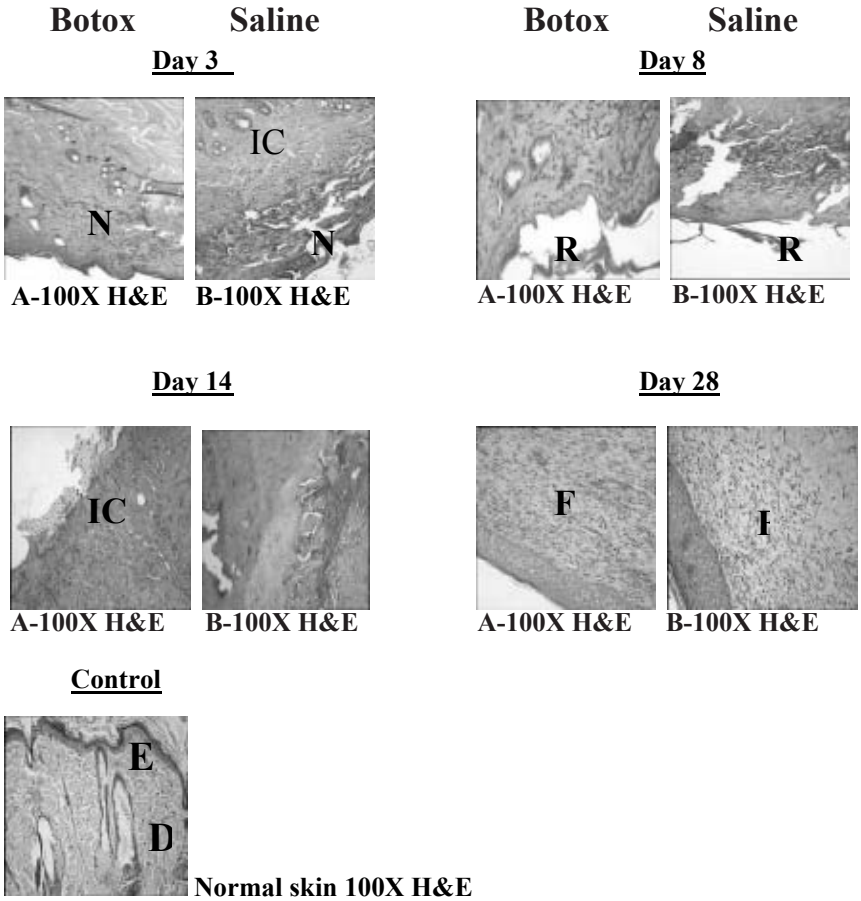

Fig. 6. *Representative panorama of histological changes over time in Botox and saline groups. (H and E stain, magnification 100x). Note the increase of inflammatory cells (IC) in the saline group by day 3 compared to Botox as well as disorganization in the upper layers of the skin. By day 6, the inflammation in the Botox group increased with more infiltration of cells. By day 14 epithelialization progressed in both groups but to a slightly better degree in the Botox group and more fibroblasts in the wound area. At the end of the experiment, day 28, the amount of fibroblasts was much higher in the Botox group.*

wounds at all time-points tested apart from on day 28 when a x% decrease was measured from the Botox-treated wounds related to the increase in the multi-layered epidermis in the Botox-treated wounds (tighter junctions).

Wound surface area

On day 0, the wound surface area was 5 cm^2 in both groups and it increased initially. Then it started to decrease with time as healing progressed without significant differences between both groups. However, at the end of the experiment, on day 28, this value reached 0.19 cm^2 in Botox and 0.47 cm^2 in saline (Fig. 8).

Wound area was measured throughout the experiment and was similar in all time points up to day 14 post burn. However, 28 days post-burn Botox –treated wounds were 60% smaller than control wounds (Figure 8).

Relative mRNA levels of TGFβ 1

Immediately after burn injury, the relative TGFβ1 expression was 2.63±0.29 folds higher in the Botox-treated group than saline, (p-value<0.05). This expression increased on days 3 and 8 to reach 4.36±2.06 and 4.62±3.11, respectively, but at days

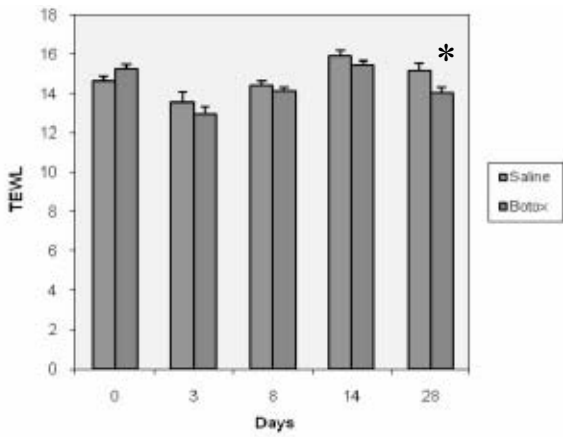

Fig. 7. *Rate of TEWL in Botox and saline. Note the significant difference on day 28 (p-value<0.05).*

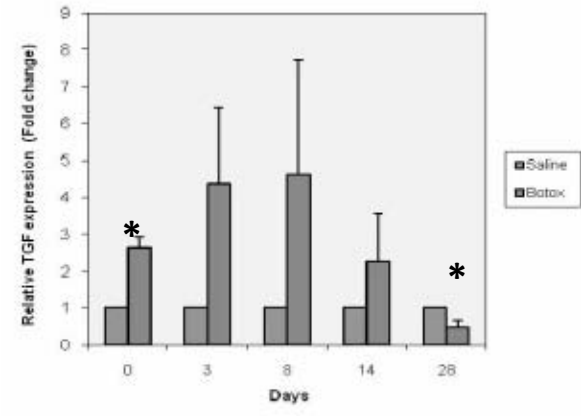

Fig. 9. *Relative mRNA levels of TGFβ1 in Botox and saline. Note the significant difference on days 0 and 28 (p-value<0.05).*

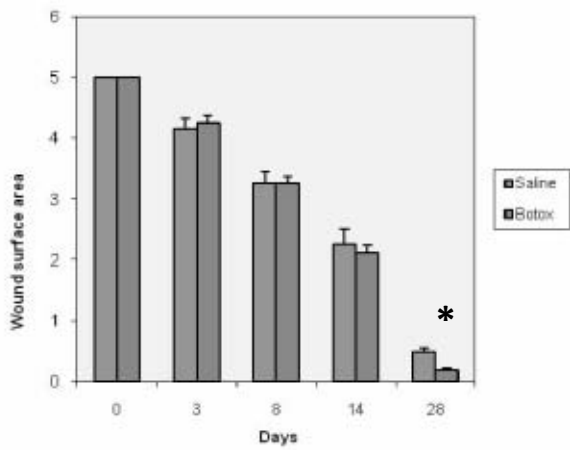

Fig. 8. *Rate of wound surface area in Botox and saline. Note the significant difference on day 28.*

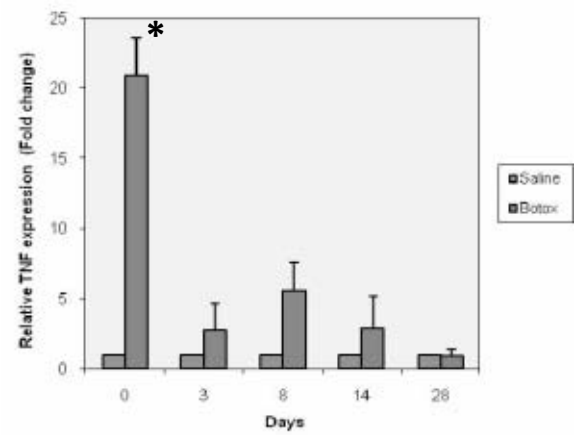

Fig. 10. *Relative mRNA levels of TNF-α in Botox and saline.*

14 and 28 to the levels of TGFβ1 were decreased compared to saline treated wounds (Fig. 9).

Relative mRNA levels of TNF-α

On day 0, the relative expression of TNF-α was higher in Botox-treated wounds compared to saline-treated wounds. This trend continued until day 14. However, on day 28, the level of TNFα decreased by 8% in the Botox-treated group (Fig. 10).

DISCUSSION

The main goal in wound healing is to achieve efficient healing with less complications and minimal scarring. Many new drugs, including Botox, have yielded effective results and some are still under investigation for the treatment of thermal injuries. This study, aimed at examining the effect of Botox on the wound healing process, using an experimental model of partial thickness burn wounds in rats, specifically assessing morphological changes by histology and evaluating the temporal profile of two cytokines TGFβ1 and TNF-α, throughout the healing process.

Following wounding, close inspection of the injury was performed on a daily basis in order to document parameters such as necrosis, crust detachment and re-epithelization. While the saline-treated group

showed a more blackish necrosis starting day 1, the Botox-treated group had a delay in necrosis till day 3. The crust started to detach earlier from the border on day 7 in the Botox-treated group compared to day 13 in the saline-treated group. Re-epithelization was enhanced upon Botox-treatment as vascularization was observed on day 9 in Botox, while on day 11 in the saline-treated group. On day 28, Botox wounds were 60% smaller than saline-treated wounds ($0.19cm^2 \pm 0.03$ in Botox and $0.47cm^2 \pm 0.07$ in saline) with p-value<0.05. Indeed, paralyzing subdermal muscles by Botox appears to have promoted wound healing (8, 9, 27). Gassner et al demonstrated significantly improved cosmetic appearance of forehead wounds that had been injected with Botulinum toxin as compared with those that were injected with saline (22).

Concerning the TEWL measurements, there was a trend but no significant difference between the Botox and saline groups throughout the procedure except on day 28 (p-value<0.05). The TEWL measurements were slightly less in the Botox group than in saline probably indicating a slightly better preservation of moisture in Botox (24). Indeed, the microscopic data revealed that the regeneration of new epidermis was greater in Botox. The new epidermis had a better shape in Botox than in saline on day 28 with a high proliferation of active fibroblasts in the dermis. In contrast to our results, Lee et al. in 2009 demonstrated that the Botox group had a smaller number of fibroblasts than saline at the 4th week; thereby this requires further investigation (23).

TGFβ1 is the most potent growth factor involved in wound healing (27). It has an increased expression with the onset of injury corresponding to TGFβ1 released by the alpha granules of platelets of a thrombus to mediate leukocyte recruitment by chemotaxis and stimulate pro-inflammatory cytokines (28). The results of this study revealed that TGFβ1 in the Botox group had a high relative expression, and this relative expression coincides with the proliferation of fibroblasts and appearance of myofibroblasts (9, 29). It could be assumed that the accelerated proliferative response of fibroblasts noticed in Botox on day 28 may be triggered by the ascending relative expression of TGFβ1. Xiao et al. in 2010 demonstrated that fibroblasts isolated from tissue specimens of hypertrophic scar and treated with Botox demonstrate slower growth than fibroblasts without Botox treatment. They also found that the TGFβ1 secreted per cell in fibroblasts without Botox was higher than that in fibroblasts with Botox by using the ELISA technique (28, 29). They suggested that Botox may lead to decrease of TGFβ1 protein and inhibit the growth of fibroblasts, however, these results cannot be considered since the study is incomplete with a short follow-up period of five days (28). On the other hand, a study published by Xiao et al. in 2009, whereby Botox was injected into hypertrophic scars in 19 patients, demonstrated that there was significant improvement in scar volume, appearance, erythema, pliability, and patient satisfaction. This study had a follow-up period of at least 6 months (30).

Our study is the first to test the effect of Botox on the relative expression of TNF-α. The results revealed that Botox-treatment increased (TNF-α) by almost 21-fold compared to wound controls on day 0 (p-value<0.05). This enormous increase in expression tapered down on day 3 to 2.72-fold with a slight increase on day 8 to 5.5-fold, and then decreased again on days 14 and 28. TNF-α is a central regulator of inflammatory cascades during both initiation and amplification of inflammatory reactions (15-17). Perhaps the increase in TNF-α expression played a role in the initial decrease in inflammation in the Botox-treated group. However, the inflammatory response does not rely on the expression of TNF-α alone. More pro-inflammatory markers should also be tested such as IL-1 β and IL-6.

The present data demonstrates moderate but important differences of the effect of Botox on burn wound healing. These results need to be consolidated. The Botox-treated wounds showed earlier reepithelization by two days, a delay in necrosis by two days, better regeneration of new epidermis, and an accelerated proliferative response of active fibroblasts compared to the saline-treated wounds. These factors may indicate an improvement of burn wound healing.

In addition to improving cosmetic appearance of scars, Botulinum toxin has been investigated for potentially improving the healing of difficult wounds. Choi and coworkers injected Botox into the periorbital muscles after eyelid reconstruction of patients with risk factors for suboptimal wound healing and achieved excellent results (31). Sahinkanat et al.

used a rat model for transsection of the urethra and observed less fibrotic changes in healing urethras that had been injected with Botox as compared to saline (32).

Further work is required to fully evaluate the effect of Botox on fibrosis. The increase in fibroblast migration into the dermal wound area in Botox-treated wounds is striking and persisted throughout the experimental time frame. This could be due to the decrease in wound tension, reducing fibroblast differentiation to miofibroblasts, therefore reducing wound contraction and slowing collagen deposition. In the later stages of wound repair, perhaps the fibroblasts generated significant tension to initiate differentiation and strongly contract the wound to significantly decrease the wound area at day 28, reducing the wound size by 60%.

Modulation of wound healing to achieve the most favorable repair is currently an active research field with studies investigating factors ranging from topical treatments to gene therapy (5, 9, 10, 16).

The results reported in this study, although preliminary, suggest that Botox could possibly improve burn wound healing. These data support and further previous investigations demonstrating the positive effects of Botox on the cosmetic appearance and healing of incisions and hypertrophic scars (27, 30). Moreover, the effects of Botox inflammation may have implications in visceral wounds, especially in cases where fibrosis and adhesions are detrimental to function. Further research is required to investigate the modulation of wound healing by Botox, its full scope of action, possible detrimental effects, dose-dependence and cost effectiveness.

ACKNOWLEDGEMENTS

The study was supported by a grant from Lebanese National Council for Scientific Research and Promotion of Science.

REFERENCES

1. Meyer TN, Da Silva AL. A standard burn model using rats. Acta Cir Bras 1999; 14(4):1-7.
2. Gurfinkel R, Singer AJ, Cagnano E, Rosenberg L. Development of a novel animal burn model using radiant heat in rats and swing. Acad Emergency Med 2010; 17(5):514-20.
3. Knabl JS, Bayer GS, Bauer WA, et al. Controlled partial skin thickness burns: an animal model for studies of burnwound progression. Burns 1999; 25:229-35.
4. Santos H, Hamann C, Obispo M, Rodriguez A, Coca M. Experimental burn models. Annals of Burn and Fire Disasters 1996; 9(2):1-6.
5. Jurjus A, Atiyeh BS, Abdallah IM, et al. Pharmacological modulation of wound healing in experimental burns. Burns 2007; 33:892-907.
6. Barrientos S, Stojadinovic O, Golinko MS, Brem H, Tomic-Canic M. Growth factors and cytokines in wound healing. Wound Repair Regen 2008; 16:585-601.
1. Werner S, Grose R. Regulation of wound healing by growth factors and cytokines. Physiol Rev 2003; 83:835-70.
2. Sasaki M, Kashima M, Ito T, Watanabe A, Izumiyama N, Sano M, et al. Differential regulation of metalloproteinase production, proliferation and chemotaxis of human lung fibroblasts by PDGF, interleukin-1beta and TNF-alpha. Mediators Inflamm 2000; 9(3-4):155-60.
3. El Kahi CG, Atiyeh BS, Hajj Hussein IA, Jurjus R, Dibo SA, Jurjus A, et al. Modulation of wound contracture α-smooth muscle actin and multispecific vitronectin receptor integrin αvß3 in the rabbit's experimental model. Int Wound J 2009; 6:214-24.
4. Ling E, Robinson DS. Transforming growth factor-beta1: its anti-inflammatory and pro-fibrotic effects. Clin Exp Allergy 2002; 32:175-8.
5. Gruber BL, Marchese MJ, Kew RR. Transforming growth factor-beta 1 mediates mast cell chemotaxis. J Immunol 1994; 152:5860-67.
6. Koch RM, Roche NS, Parks WT, Ashcroft GS, Letterio JJ, Roberts AB. Incisional wound healing in transforming growth factor-beta1 null mice. Wound Repair Regen 2000; 8:179-91.
7. Edwards DR, Murphy G, Reynolds JJ, et al. Transforming growth factor beta modulates the expression of collagenase and metalloproteinase inhibitor. EMBO J 1987; 6:1899-904.
8. Weinstein DA, Kirsner RS. Refractory ulcers: the role of tumor necrosis factor-alpha. J Am Acad Dermatol 2010; 63:146-54.

9. Lee RH, Efron DT, Tantry U, et al. Inhibition of tumor necrosis factor-alpha attenuates wound breaking strength in rats. Wound Repair Regen 2000; 8:547-53.
10. Gao B, Saba TM, Tsan MF. Role of alpha(v) beta(3)-integrin in TNF-alpha-induced endothelial cell migration. Am J Physiol Cell Physiol 2002; 283:C1196-205.
11. Ten Hagen TL, Seynhaeve AL, Eggermont AM. Tumor necrosis factor-mediated interactions between inflammatory response and tumor vascular bed. Immunol Rev 2008; 222:299-315.
12. Mendez-Eastman SK. BOTOX: a review. Plast Surg Nurs 2003; 23:64-69.
13. Felber ES. Botulinum toxin in primary care medicine. J Am Osteopath Assoc 2006; 106:609-14.
14. Bansal C, Omlin KJ, Hayes CM, Rohrer TE. Novel cutaneous uses for botulinum toxin type A. J Cosmet Dermatol 2006; 5:268-72.
15. Wilson AM. Use of botulinum toxin type A to prevent widening of facial scars. Plast Reconstr Surg 2006; 117:1758-66.
16. Gassner HG, Brissett AE, Otley CC, et al. Botulinum toxin to improve facial wound healing: A prospective, blinded, placebo-controlled study. Mayo Clin Proc 2006; 81:1023-8.
17. Lee BJ, Jeong JH, Wang SG, Lee JC, Goh EK, Kim HW. Effect of botulinum toxin type a on a rat surgical wound model. Clin Exp Otorhinolaryngol 2009; 2:20-27.
18. Grove G, Grove MJ, Zerweck C, Pierce E. Computerized evaporimetry using the DermaLab TEWL probe. Skin Res Technol 1999; 5:9-13.
19. Sanders YY, Kumbla P, Hagood JS. Enhanced myofibroblastic differentiation and survival in Thy-1(-) lung fibroblasts. Am J Respir Cell Mol Biol 2007; 36:226-35.
20. Miyazaki T, Bouscarel B, Ikegami T, Honda A, Matsuzaki Y. The protective effect of taurine against hepatic damage in a model of liver disease and hepatic stellate cells. Adv Exp Med Biol 2009; 643:293-303.
21. Xiao Z, Zhang F, Lin W, Zhang M, Liu Y. Effect of botulinum toxin type A on transforming growth factor beta1 in fibroblasts derived from hypertrophic scar: a preliminary report. Aesthetic Plast Surg 2010; 34:424-7.
22. Faler BJ, Macsata RA, Plummer D, Mishra L, Sidawy AN. Transforming growth factor-beta and wound healing. Perspect Vasc Surg Endovasc Ther 2006; 18:55-62.
23. Xiao Z, Zhang F, Lin W, Zhang M, Liu Y. Effect of botulinum toxin type A on transforming growth factor beta1 in fibroblasts derived from hypertrophic scar: a preliminary report. Aesthetic Plast Surg 2010; 34:424-7.
24. Xiao Z, Zhang F, Cui Z. Treatment of hypertrophic scars with intralesional botulinum toxin type a injections: a preliminary report. Aesthetic Plast Surg 2009; 33:409-12.
25. Choi JC, Lucarelli MJ, Shore JW. Use of botulinum A toxin in patients at risk of wound complications following eyelid reconstruction. Ophthal Plast Reconstr Surg 1997; 13:259-64.
26. Sahinkanat T, Ozkan KU, Ciralik H, Ozturk S, Resim S. Botulinum toxin-A to improve urethral wound healing: an experimental study in a rat model. Urology 2009; 73:405-9.

ASSOCIATION ANALYSIS OF DOPAMINERGIC GENE VARIANTS (COMT, DRD4 AND DAT1) WITH ALZHEIMER'S DISEASE

W.Y. LIN[1,2], B.T. WU[3], C.C. LEE[2,4], J.J. SHEU[2,5], S.H. LIU[6], W.F. WANG[7], C.H. TSAI[8,9], H.P. LIU[10] and F.J. TSAI[2,5,6]

[1]Graduate Institute of Integrated Medicine, China Medical University, Taichung, Taiwan; [2]Department of Medical Research, China Medical University Hospital, Taichung, Taiwan; [3]Department of Physical Therapy, Graduate Institute of Rehabilitation Science, China Medical University, Taichung, Taiwan; [4]School of Medicine, China Medical University, Taichung, Taiwan; [5]School of Chinese Medicine, China Medical University, Taichung, Taiwan; [6]Department of Biotechnology, Asia University, Taichung, Taiwan; [7]Department of Neurology, Chang-Hua Christian Hospital, Chang-Hua, Taiwan; [8]Graduate Institute of Neural and Cognitive Sciences, China Medical University, Taichung, Taiwan; [9]Department of Neurology, China Medical University Hospital, Taichung, Taiwan; [10]Graduate Institute of Acupuncture Science, China Medical University, Taichung, Taiwan

Received March 26, 2012 – Accepted July 20, 2012

The first two authors contributed equally to this work

Defects in dopaminergic transmission play important roles in the disturbance of synaptic plasticity and even in advanced cognitive behavior. However, the relationship between genes involved in the regulation of dopamine levels and predisposition for Alzheimer's disease (AD) remains unclear. The potential association of dopamine-modulating gene polymorphisms with AD was evaluated. We performed a case-control study with 120 patients and 86 healthy controls. Two catechol-O-methyltransferase (*COMT*) single-nucleotide polymorphisms (SNPs) (rs2020917 and rs4646312), two dopamine D4 receptor (*DRD4*) SNPs (rs3758653 and rs916455), and four dopamine transporter (*DAT1*) SNPs (rs2937639, rs6347, rs12516948 and rs11133762) were investigated. The T allele at the *DRD4* SNP (rs3758653) was found to be significantly associated with AD. Our results also showed that haplotype frequencies, observed from the analyzed SNPs, were distributed significantly differently in AD patients *vs* control subjects. Moreover, a strong association was observed between the A allele at rs6347 of *DAT1* and moderate stage of dementia. These observations suggest that genetic variations in the dopamine-modulating genes, *COMT*, *DRD4* and *DAT1*, may contribute to AD pathogenesis in the Taiwanese population.

Key words: Alzheimer's disease, dopamine, polymorphism, neurotransmitter

Mailing addresses: Dr. Hsin-Ping Liu,
Graduate Institute of Acupuncture Science,
China Medical University,
No.91 Hsueh-Shih Road, Taichung 404, Taiwan
Tel.: +886 4 22053366 ext 3603 Fax: +886 4 22035191
e-mail: hpliu@mail.cmu.edu.tw

Dr. Fuu-Jen Tsai,
Department of Medical Research, China Medical University Hospital,
No. 2 Yuh Der Road, Taichung 404, Taiwan
Tel.: +886 4 22062121 ext 7076 Fax: +886 4 22033295
e-mail: d0704@www.cmuh.org.tw

0393-974X (2012)

Alzheimer's disease (AD) is the most common form of dementia worldwide. Its clinical symptoms include progressive neurodegeneration and cognitive dysfunction, and its incidence is strongly age-related. The brains of patients with AD display two neuropathological features: aggregates of senile plaques and neurofibrillary tangles, which are primarily composed of amyloid-beta (Aβ) peptides and hyperphosphorylated Tau proteins, respectively (1). Although the pathology of AD has been well characterized, most cases are sporadic and genetically complicated, which indicates that other genetic factors are responsible for the development of AD.

Certain neurotransmitters and their receptors and transporters are considered to be possible risk factors for AD. One such neurotransmitter is acetylcholine. Defects in cholinergic neuron activity may account for the cognitive decline in AD patients (2). Treating this dysfunction is a current strategy in AD treatment. Another excitatory neurotransmitter system is the glutamate. Oligomeric Aβ peptides may disturb synaptic plasticity by altering the activity, number and trafficking of α-amino-3-hydroxy-5-methyl-4-isoxazolepropionic acid receptor (AMPA) and N-methyl-d-aspartate (NMDA) glutamate receptors (3). Parameshwaran et al., provided evidence that Aβ peptides inhibit both the amplitude and frequency of postsynaptic currents through AMPA receptors (AMPARs) and decrease the probability of channel opening in hippocampal CA1 pyramidal neurons (4). Immunoprecipitation analyses have demonstrated that assembly forms of Aβ peptides can associate with NMDA receptors (NMDARs) at their NR1 and NR2A subunits (5). Ab peptides were found to induce massive calcium ion permeability in a rat study, resulting in excitotoxicity and neuronal death, and this effect was alleviated by MK-801, which is an NMDAR antagonist (6). Through selective interactions between NMDARs and Aβ peptides, changes in synaptic plasticity, such as deficits in long-term potentiation (LTP) (7) and long-term depression (LTD) induction, have been detected in rat hippocampus (8). These results seem to demonstrate that Ab-impaired synaptic plasticity may have deleterious effects on neuronal activity, leading to loss of synapses or dendrites (9), and this impairment might be responsible for the neurodegenerative process and cognitive dysfunction of AD.

Previous studies have suggested that more than just the cholinergic and glutamatergic neurotransmission systems influence synaptic failure and neuronal death in AD. Stimulation of dopamine receptors has been shown to promote AMPAR trafficking from the cytosol to the synaptic membrane, implying that newly recruited surface AMPARs may facilitate LTP induction and demonstrating the critical role of dopaminergic transmission in neuronal plasticity (10, 11). Another report indicated that activation of dopamine receptors could prevent internalization of AMPA and NMDA receptors that is caused by oligomeric Ab peptides (12). These changes in synaptic plasticity might be essential for advanced cognitive behavior and memory formation. Therefore, we explored the relationship between some genes involved in dopaminergic transmission and susceptibility to AD progression. This type of associative relationship has profound implications regarding correlations between genetic markers in the catechol-O-methyltransferase (*COMT*), dopamine D4 receptor (*DRD4*) and dopamine transporter (*DAT1*) genes and disease progression in the Taiwanese population.

MATERIALS AND METHODS

Subjects

We used the parameters in Table S1 to calculate the minimum required sample size for a case-control study. The results showed the minimum required sample sizes were 159 and 159 alleles for case and control groups, respectively. This study recruited 120 patients with late-onset of AD (mean age at onset, 74.9±6.7, 54.2% female) and 86 age-matched normal control subjects (mean age 65.9±8.7, 73% female). In this investigation, we had 234 alleles in case group and 168 alleles in control group. The sample sizes of both groups were above the minimum required sample sizes.

Participants were enrolled from the Chang-Hua Christian Hospital and China Medical University Hospital. All patients were clinically diagnosed according to guidelines from the National Institute of Neurological and Communicative Disorders and Stroke and the Alzheimer's Disease and Related Disorders Association (NINCDS–ADRDA). Dementia was diagnosed based on Diagnostic and Statistical Manual of Mental Disorders (DSM-IV) criteria. An institutional ethics committee approved this study, and informed consent was obtained

from all subjects.

Genotyping of gene variants in COMT, DRD4 and DAT1

Genomic DNA was extracted from peripheral blood samples according to a standard protocol (Genomic DNA kit, Qiagen, CA). For analysis of *COMT* gene variants, two polymorphic sites were selected for this study from the public dbSNP database: C/T (rs2020917) and T/C (rs4646312). rs2020917 was chosen because this SNP is in the upstream P2 promoter region and affects the expression of COMT by upregulating the transcription of COMT gene (13). rs4646312 was chosen because the SNPs rs4646312 and rs4680, which decreases its enzyme activity (14), are in the same haplotype block (15). When analyzing this polymorphism (rs4646312), we could test whether decreasing enzyme activity is associated with AD. To study variants in the dopamine D4 receptor (*DRD4*), two SNPs located in the 5' region near the gene T/C (rs3758653) and C/T (rs916455) were selected for this study. To genotype dopamine transporter *DAT1* (locus symbol: *SLC6A3*) variants, four SNPs located in the gene region were chosen. One is A/G SNP in intron 1 (rs2937639), one is a synonymous 1336 A/G SNP in exon 9 (rs6347), and A/G (rs12516948) and C/T (rs11133762) are two SNPs in the 3' region near the gene.

To identify the allele preference for these SNPs, PCR-Restriction Fragment Length Polymorphism (PCR-RFLP) analyses were performed. Specific primers and restriction enzymes for each PCR-RFLP reaction are shown in Table I. In brief, PCR amplification was carried out in a total volume of 25 µl with 5 ng genomic DNA and primer pairs. PCR reactions were carried out at 95°C for 5 min, followed by 40 cycles of 95°C for 30 sec, specific Tm temperatures for each primer pair for 30 sec, and 72°C for 40 sec, with a final elongation step at 72°C for 7 min. Five microliters of the PCR amplicons was digested overnight by various restriction enzymes (New England Biolabs, MA) at 37°C in a total volume of 20 µl. The sizes of the PCR products and digestion fragments were determined by agarose gel electrophoresis and visualized directly by ethidium bromide staining.

Statistical analyses

The distributions of allele and genotype frequencies for each SNP were evaluated by χ^2 test using 2 x 2 or 2 x 3 contingency tables. Statistical analysis of the

Table I. *Primers information for testing SNPs in the COMT, DRD4 and DAT1 genes by PCR-RFLP.*

SNPs	Primers	Restriction enzyme	Alleles	Allele size (bp)
COMT				
rs2020917	F: 5'-ATGAGGCTTGAACTGTCCTGA-3'	MscI	T	314
	R: 5'-TTGTCTAAGGTCCTGCTGTGCT-3'		C	(189+125)
rs4646312	F: 5'-TTCCCAAGGGTAGCAGCAGAA-3'	PflMI	T	311
	R: 5'-TGCACCTTGTGAACCACAAGA-3'		C	(215+96)
DRD4				
rs3758653	F: 5'-ACAGAGTGGTGCCCCCTTTT-3'	EcoRI	C	357
	R: 5'-CCGTTGCACAGTTGATCCTC-3'		T	(253+104)
rs916455	F: 5'-AGCTCAGGTCTTTCTGCGTCT-3'	CviQI	C	330
	R: 5'-GAGCCCAGTATTTGCTCATCT-3'		T	(233+97)
DAT1				
rs2937639	F: 5'-GAGCGAGACCTCATGTTAAA-3'	Tsp509I	G	242
	R: 5'-AAGACAGACACTCTGGTTTG-3'		A	(198+94)
rs6347	F: 5'-ACATATAGAAGGGGGCTTTT-3'	DdeI	G	425
	R: 5'-AAAGGTCTCCCAAATAATCA-3'		A	(220+205)
rs12516948	F: 5'-TACCAGATGCCATCCACAGCT-3'	BsrI	A	394
	R: 5'-CCTCATGGGCGACTGTATTAA-3'		G	(130+66+198)
rs11133762	F: 5'-CTCTGTCCACTTTTCTGATGG-3'	BstUI	T	241
	R: 5'-TGTGAGCTGTGGATGGCATCA-3'		C	(140+101)

odds ratio (OR) and 95% confidence interval (CI) were carried out using SPSS version 10.0 software (Chicago, IL) based on the presence of the reference allele and genotype frequencies. P values less than 0.05 were considered statistically significant. Adherence to Hardy-Weinberg equilibrium was tested using Pearson's χ^2 test with one degree of freedom. The haplotype approach for each individual was analyzed with Phase v2.1 software program using Bayesian statistical method (16). P values were determined by comparing a given haplotype with a combination of all other haplotypes.

RESULTS

A total of 206 subjects of Taiwan Han Chinese comprised this cohort. One hundred and twenty subjects were clinically diagnosed as having AD, and eighty-six subjects served as healthy controls. The genotype distributions within each gene variant in this study did not deviate significantly from Hardy-Weinberg equilibrium (all $p > 0.1$, Table II). After analyzing genotype and allele frequencies, neither of the *COMT* gene polymorphisms (rs2020917 and rs4646312) showed a statistically significant association with AD (Table II). Genotypic analyses indicated that only one *DAT1* gene variant (rs11133762) had a borderline significant allele frequency ($p = 0.055$). This C/T gene polymorphism located at the 3' end region of the *DAT1* gene was C:T 61.3%:38.7% in AD patients, compared with 51.8%:48.2% in controls (Table II). With genotyping two polymorphisms of *DRD4* gene (rs3758653 and rs916455), we found that gene variant, rs3758653, located at the 5' region, attained statistical difference at the 0.05 level in allele frequency. At this SNP, the T:C ratio was 73.9%:26.1% in the subjects with AD and 62.5%:37.5% in controls. The odds ratio (OR) of the T allele indicated a 1.70-fold higher risk than with the C allele (95% CI, 1.11 to 2.61) (Table II), suggesting that the T allele at rs3758653 is a risk factor that correlates with AD.

We also analyzed associations between the haplotype distributions of patients and controls. The haplotype frequencies of the *COMT* gene at two polymorphic loci are shown in Table III, and four haplotypes were observed in both AD patients and controls. The frequency of the most common haplotype (Ht1-CT) in the patients was 60.8%, compared with 55.8% in the controls. After haplotype-specific analysis, this Ht1-CT haplotype appeared to be a significant 'risk' haplotype ($p = 0.029$, OR = 1.55, 95% CI, 1.05 to 2.31) compared with the non-Ht1 haplotype in AD patients and control groups. Similar haplotype-specific analyses showed no significant differences between the two groups of subjects for the three other haplotypes, Ht2-CC, Ht3-TT and Ht4-TC. In an association analysis of *DAD4* gene haplotype distributions, subjects with the Ht1-TC haplotype at the two assayed polymorphisms may have a higher incidence of pathogenic AD ($p = 0.018$, OR = 1.62, 95% CI, 1.08 to 2.43). Conversely, subjects with the Ht2-CC haplotype may have a lower incidence of AD ($p = 0.049$, OR = 0.62, 95% CI, 0.38 to 1.00) (Table III).

Of ten observed haplotypes from four analyzed polymorphisms in the *DAT1* gene, three appeared to show significant risk effects (Ht3-AAGT, $p < 0.001$; Ht4-AAAC, $p = 0.002$; and Ht5-AGAC, $p = 0.030$) between the AD patients and control groups (Table IV). This result may be a subtle hint that individuals carrying these three haplotypes have a higher risk of developing AD. Additionally, our results indicate that two observed haplotypes were significantly different between patients and controls, suggesting that subjects carrying the Ht1-AAAT and Ht2-AAGC haplotypes ($p < 0.0001$ and $p = 0.035$, respectively) may be protected against AD progression.

We next asked whether dopamine-modulating gene variants showed associations with the clinical stages of AD. The patients were divided into three groups: a mild stage group with Mini-Mental State Examination (MMSE) scores above 20, a moderate stage group with MMSE scores between 10 and 20, and a severe stage group with MMSE scores less than 10. In the analysis of allele frequencies between the moderate and severe stage groups, strong association was observed between severe stage of AD and the A allele at rs6347 in *DAT1* gene ($p = 0.025$, OR = 2.67, 95% CI, 1.11 to 6.42) (Table V). This result suggests that the A allele could be a protective factor for patients, contributing to a lower risk of developing severe dementia. However, genotypic and allelic analyses of the other genetic variants failed to detect any significant correlations with the different clinical stages.

In order to know whether the result that *DAT1* SNP rs6347 affects stages in Alzheimer's disease

Table II. *Genotype and allele frequencies of the tested SNPs in the COMT, DAT1 and DRD4 genes in AD patients and controls.*

SNPs	Genotype/allele	Cases Number (%)	HWE[a]	Controls Number (%)	HWE	p value[b]	OR (95% CI)
COMT							
rs2020917	CC	63 (54.3)	0.713	41 (48.8)	0.545	0.740	1.32 (0.41-4.20)
	CT	46 (39.7)		37 (44.0)			1.07 (0.33-3.44)
	TT	7 (6.0)		6 (7.2)			1
	C	172 (74.1)		119 (70.8)		0.464	1.18 (0.76-1.84)
	T	60 (25.9)		49 (29.2)			1
rs4646312	TT	55 (47.0)	0.329	31 (36.0)	0.180	0.169	1.06 (0.42-2.72)
	TC	47 (40.2)		46 (53.5)			0.61 (0.24-1.54)
	CC	15 (12.8)		9 (10.5)			1
	T	157 (67.1)		108 (62.8)		0.368	1.21 (0.80-1.82)
	C	77 (32.9)		64 (37.2)			1
DAT1							
rs2937639	AA	84 (70.6)	0.219	59 (72.0)	0.140	0.702	1.06 (0.56-2.02)
	AG	34 (28.6)		23 (29.0)			1
	GG	1 (0.8)		0 (0.0)			
	A	202 (84.9)		141 (86.0)		0.759	0.92 (0.52-1.61)
	G	36 (15.1)		23 (14.0)			1
rs6347	AA	76 (71.1)	0.421	62 (75.6)	0.733	0.515	0.31 (0.03-2.81)
	AG	27 (25.2)		19 (23.2)			0.36 (0.04-3.43)
	GG	4 (3.7)		1 (1.2)			1
	A	179 (83.6)		143 (87.2)		0.336	0.75 (0.42-1.35)
	G	35 (16.4)		21 (12.8)			1
rs12516948	AA	71 (60.2)	0.231	53 (61.6)	0.615	0.879	0.74 (0.24-2.35)
	AG	38 (32.2)		28 (32.6)			0.75 (0.23-2.50)
	GG	9 (7.6)		5 (5.8)			1
	A	180 (76.3)		134 (77.9)		0.698	0.91 (0.57-1.46)
	G	56 (23.7)		38 (22.1)			1
rs11133762	CC	47 (39.5)	0.391	24 (28.6)	0.520	0.183	2.06 (0.94-4.51)
	CT	52 (43.7)		39 (46.4)			1.40 (0.67-2.93)
	TT	20 (16.8)		21 (25.0)			1
	C	146 (61.3)		87 (51.8)		0.055	1.48 (0.99-2.20)
	T	92 (38.7)		81 (48.2)			1
DRD4							
rs3758653	TT	67 (57.3)	0.152	34 (40.5)	0.580	0.057	2.33 (0.94-5.74)
	TC	39 (33.3)		37 (44.0)			1.25 (0.50-3.13)
	CC	11 (9.4)		13 (15.5)			1
	T	173 (73.9)		105 (62.5)		**0.014**	**1.70 (1.11-2.61)**
	C	61 (26.1)		63 (37.5)			1
rs916455	CC	79 (69.9)	0.281	54 (64.3)	0.705	0.698	1.17 (0.30-4.56)
	CT	29 (25.7)		26 (31.0)			0.89 (0.22-3.68)
	TT	5 (4.4)		4 (4.8)			1
	C	187 (82.7)		134 (79.8)		0.451	1.22 (0.73-2.03)
	T	39 (17.3)		34 (20.2)			1

[a] HWE, p values of deviation from Hardy-Weinberg equilibrium constant. [b] p value was compared by χ^2 test. p values less than 0.05 are highlighted in bold. OR, odds ratio; 95% CI, 95% confidence interval.

Table III. *Haplotype frequencies of COMT and DRD4 polymorphisms between AD patients and controls.*

Haplotypes		Cases (%)	Controls (%)	p value[a]	OR (95% CI)
COMT	rs2020917/ rs4646312				
Ht1	CT	146 (60.8)	96 (55.8)	**0.029**	**1.55 (1.05-2.31)**
Ht2	TC	47 (19.6)	37 (21.5)	0.632	0.89 (0.55-1.44)
Ht3	CC	33 (13.8)	27 (15.7)	0.581	0.86 (0.49-1.49)
Ht4	TT	14 (5.8)	12 (7.0)	0.638	0.83 (0.37-1.83)
DRD4	rs3758653/ rs916455				
Ht1	TC	160 (66.7)	95 (55.2)	**0.018**	**1.62 (1.08-2.43)**
Ht2	CC	41 (17.1)	43 (25.0)	**0.049**	**0.62 (0.38-1.00)**
Ht3	CT	20 (8.3)	22 (12.8)	0.140	0.62 (0.33-1.18)
Ht4	TT	19 (7.9)	12 (7.0)	0.721	1.15 (0.54-2.43)

[a] p value was compared by χ^2 test. p values less than 0.05 are highlighted in bold. OR: odds ratio; 95% CI, 95% confidence interval.

Table IV. *Haplotype frequencies of DAT1 polymorphisms in AD patients and controls.*

Haplotypes[a]		Cases (%)	Controls (%)	p value[b]	OR (95% CI)
Ht1	AAAT	49 (20.4)	73 (42.4)	**1.37×10^{-6}**	**0.35 (0.23-0.54)**
Ht2	AAGC	14 (5.8)	20 (11.6)	**0.035**	**0.47 (0.23-0.96)**
Ht3	AAGT	23 (9.6)	2 (1.2)	**4.0×10^{-4}**	**9.01 (2.09-38.75)**
Ht4	AAAC	85 (35.4)	36 (20.9)	**0.002**	**2.07 (1.32-3.26)**
Ht5	AGAC	17 (7.1)	4 (2.3)	**0.030**	**3.20 (1.06-9.69)**
Ht6	GAAC	25 (10.4)	12 (7.0)	0.229	1.55 (0.76-3.18)
Ht7	GAAT	9 (3.8)	3 (1.7)	0.233	2.19 (0.59-8.23)
Ht8	AGGC	8 (3.3)	10 (5.8)	0.225	0.56 (0.22-1.45)
Ht9	AGGT	7 (2.9)	1 (0.6)	0.090	5.14 (0.63-42.15)
Ht10	AGAT	3 (1.3)	3 (1.7)	0.680	0.71 (0.14-3.58)

[a] Haplotypes are shown in sequence: rs2937639G/A, rs6347G/A, rs12516948A/G, and rs11133762T/C. [b] p value was compared by χ^2 test. p values less than 0.05 are highlighted in bold. OR, odds ratio; 95% CI, 95% confidence interval.

is influenced by other variables [e.g. age, gender, Clinical Dementia Rating (CDR) or disease duration], we also analyzed whether there are significant differences of the variables (i.e. age, disease duration, CDR, and gender) at moderate and severe demented stages (Table S2 to S4 and Table S6). The results showed that there were significant differences of disease duration (p = 0.012, Table S4) and CDR (p = 0.012, Table S6) between moderate and severe demented stages. Next, we tested whether *DAT1* SNP (rs6347) has an interaction with disease duration (Table S5) or CDR (Table S7). Statistical analyses showed that *DAT1* SNP (rs6347) have an interaction with disease duration (p = 0.0408, Table S5). Over all, the result that *DAT1* SNP rs6347 affects stages in Alzheimer's disease is influenced

Table V. *Genotype and allele frequencies of the tested SNPs in the COMT, DRD4 and DAT1 genes in AD patients at different clinical stages[a].*

SNPs	Genotype/allele	Moderate stage[b] Number (%)	Severe stage[c] Number (%)	p value[d]
COMT				
rs2020917	CC	32 (55.2)	16 (47.1)	0.666
	CT	23 (39.7)	15 (44.1)	
	TT	3 (5.1)	3 (8.8)	
	C	87 (75.0)	47 (69.1)	0.387
	T	29 (25.0)	21 (30.9)	
rs4646312	TT	22 (38.6)	17 (48.6)	0.619
	TC	26 (45.6)	14 (40.0)	
	CC	9 (15.8)	4 (11.4)	
	T	70 (61.4)	48 (68.6)	0.325
	C	44 (38.6)	22 (31.4)	
DRD4				
rs3758653	TT	32 (54.2)	18 (54.6)	0.827
	TC	22 (37.3)	11 (23.3)	
	CC	5 (8.5)	4 (12.1)	
	T	86 (72.9)	47 (71.2)	0.808
	C	32 (27.1)	19 (28.8)	
rs916455	CC	42 (75.0)	23 (67.7)	0.522
	CT	11 (19.6)	10 (29.4)	
	TT	3 (5.4)	1 (2.9)	
	C	95 (84.8)	56 (82.4)	0.662
	T	17 (15.2)	12 (17.6)	
DAT1				
rs2937639	AA	41 (69.5)	24 (68.6)	0.926
	AG	18 (30.5)	11 (31.4)	
	GG	0 (0.0)	0 (0.0)	
	A	100 (84.7)	59 (84.3)	0.933
	G	18 (15.3)	11 (15.7)	
rs6347	AA	44 (81.5)	17 (60.8)	0.106
	AG	9 (16.7)	9 (32.1)	
	GG	1 (1.8)	2 (7.1)	
	A	97 (89.8)	43 (76.8)	**0.025**
	G	11 (10.2)	13 (23.2)	
rs12516948	AA	37 (63.8)	19 (54.3)	0.600
	AG	17 (29.3)	12 (34.3)	
	GG	4 (6.9)	4 (11.4)	
	A	91 (78.4)	50 (71.4)	0.279
	G	25 (21.6)	20 (28.6)	
rs11133762	CC	21 (36.2)	16 (44.4)	0.680
	CT	26 (44.8)	15 (41.7)	
	TT	11 (20.0)	5 (13.9)	
	C	68 (58.6)	47 (65.3)	0.363
	T	48 (41.4)	25 (34.7)	

[a] Mini-Mental State Examination (MMSE) score. [b] Moderate stage, patients with MMSE scores 10-20. [c] Severe stage, patients with MMSE scores below 10. [d] p value was compared by χ^2 test. p values less than 0.05 are highlighted in bold.

by disease duration.

DISCUSSION

Previous studies have discovered that mutations in genes encoding proteins involved in amyloidogenic processing, including amyloid precursor protein, presenilin 1 and presenilin 2, predominantly lead to amyloid plaque production in early-onset familial cases of AD (17, 18). Excessive Ab peptides demonstrably increase the risk of synaptic loss and dysfunction, which may disturb brain functions, including advanced cognitive behavior and memory formation, before neuronal death (19, 20). Most cases of AD are sporadic, and the factors important in disease development are unknown, which motivates us to identify additional genetic risk factors that are also responsible for AD progression. To evaluate whether genetic variations in dopamine-modulating genes, *COMT, DRD4* and *DAT1* are associated with AD in the Taiwanese population, we performed a case-control study and found these genetic variants and their effects on dopaminergic transmission might be the risk factors in the etiology of AD.

Previous findings indicated that dopaminergic neurotransmission regulates synaptic plasticity. Activation of the dopamine D1/D5 receptor consolidates the late-phase LTP in the CA1 of rat hippocampal slices (21), and reverses the LTD induced by NMDA or low-frequency stimulation (11). The other study also found that direct injections of dopamine receptor agonists can enhance spatial memory performance (22). These results suggest that defects in dopaminergic neurotransmission might disturb synaptic plasticity and even advanced cognitive behavior, indicating that dopamine could be a candidate risk factor for AD progression. Within the brain, the transmission efficiency of dopaminergic neurons is obviously associated with dopamine-modulating genes, which are thought to regulate dopamine levels by its production and clearance. COMT is a dopamine-modulating gene that plays an essential role in dopamine clearance by catalyzing the methylation of the hydroxyl group of dopamine (23). In our study, the allele and genotype distributions of *COMT* were found to be insignificantly associated with AD. However, one haplotype, observed involving the two assayed polymorphisms, was associated a significant increase in the risk of AD. Another gene involved in the dopamine-modulating system is the dopamine transporter (*DAT1*). Because DAT1 functions to control dopamine levels in the synaptic cleft, which limits dopamine receptor activation (24), we tried to explore the relationship between its SNPs and AD, and found that no allele or genotype frequencies of *DAT1* showed a significant correlation with AD. Among the ten haplotypes observed involving four analyzed *DAT1* gene SNPs, five haplotype distributions showed significant differences between the AD patient and control groups. Interestingly, the A allele at rs6347 in the *DAT1* gene was found to be strongly associated with clinical stage, suggesting that patients with an A allele had a lower risk of developing severe dementia. Our data also indicate that the dopamine receptor *DRD4* gene variant is a genetic risk factor for AD, and analyses of allele frequency and haplotype distributions indicate that gene variations in *DRD4* are significant risk factors for having AD.

The influence of the activities of COMT, DRD4 and DAT1 on AD remains unclear. AD patients with more severe stages of dementia frequently suffer from depression (25) and previous studies have also found that variations in the dopaminergic system may be risk factors for AD and/or depression. For example, a functional genetic variant in COMT, wherein valine to methionine substitution at codon 108/158 (rs4680) decreases its enzyme activity, which increases susceptibility to psychosis in AD (26) and schizophrenia (27). Functional genomic experiments have indicated that SNPs located at distal promoter region of the *COMT* gene alter its transcriptional efficiency, potentially changing the COMT activity (13). A study by Grunblatt et al. showed that allelic repeats in the DRD4 gene appeared to have no significant influences on the outcome of AD or depressive symptoms in their European population (28). Previous reports have found that *DAT1* gene polymorphism has no correlation with AD etiology (29), but a demonstrable association with schizophrenia phenotype was detected (30). Here, we determined that COMT, DRD4 and DAT1 gene variants have associations with AD in the Taiwanese population. In contrast with prior studies, we found significant associations between these dopamine-

modulating genes and AD development. Our data provide some guidance for understanding how dopaminergic-system gene variations lead to AD susceptibility and identification of AD-modulating genes opens a new path for understanding the pathogenesis of this disease.

ACKNOWLEDGEMENTS

This study was supported by grants from the China Medical University and Hospital (CMU98-S-21, CMU95-287, CMU98-S-03, DMR-98-081, DMR-97-054) and supported in part by Taiwan Department of Health Clinical Trial and Research Center of Excellence (DOH101-TD-B-111-004).

REFERENCES

1. Goedert M, Wischik CM, Crowther RA, Walker JE, Klug A. Cloning and sequencing of the cDNA encoding a core protein of the paired helical filament of Alzheimer disease: identification as the microtubule-associated protein tau. Proc Natl Acad Sci USA 1988; 85(11):4051-5.
2. Sivaprakasam K. Towards a unifying hypothesis of Alzheimer's disease: cholinergic system linked to plaques, tangles and neuroinflammation. Curr Med Chem 2006; 13(18):2179-88.
3. Parameshwaran K, Dhanasekaran M, Suppiramaniam V. Amyloid beta peptides and glutamatergic synaptic dysregulation. Exp Neurol 2008; 210(1):7-13.
4. Parameshwaran K, Sims C, Kanju P, Vaithianathan T, Shonesy BC, Dhanasekaran M, et al. Amyloid beta-peptide Abeta(1-42) but not Abeta(1-40) attenuates synaptic AMPA receptor function. Synapse 2007; 61(6):367-74.
5. Venkitaramani DV, Chin J, Netzer WJ, et al. Beta-amyloid modulation of synaptic transmission and plasticity. J Neurosci 2007; 27(44):11832-7.
6. Harkany T, Abraham I, Timmerman W, et al. beta-amyloid neurotoxicity is mediated by a glutamate-triggered excitotoxic cascade in rat nucleus basalis. Eur J Neurosci 2000; 12(8):2735-45.
7. Walsh DM, Klyubin I, Fadeeva JV, et al. Naturally secreted oligomers of amyloid beta protein potently inhibit hippocampal long-term potentiation in vivo. Nature 2002; 416(6880):535-9.
8. Li S, Hong S, Shepardson NE, Walsh DM, Shankar GM, Selkoe D. Soluble oligomers of amyloid Beta protein facilitate hippocampal long-term depression by disrupting neuronal glutamate uptake. Neuron 2009; 62(6):788-801.
9. Walsh DM, Klyubin I, Fadeeva JV, Rowan MJ, Selkoe DJ. Amyloid-beta oligomers: their production, toxicity and therapeutic inhibition. Biochem Soc Trans 2002; 30(4):552-7.
10. Gao C, Sun X, Wolf ME. Activation of D1 dopamine receptors increases surface expression of AMPA receptors and facilitates their synaptic incorporation in cultured hippocampal neurons. J Neurochem 2006; 98(5):1664-77.
11. Mockett BG, Guevremont D, Williams JM, Abraham WC. Dopamine D1/D5 receptor activation reverses NMDA receptor-dependent long-term depression in rat hippocampus. J Neurosci 2007; 27(11):2918-26.
12. Jurgensen S, Antonio LL, Mussi GE, et al. Activation of D1/D5 dopamine receptors protects neurons from synapse dysfunction induced by amyloid-beta oligomers. J Biol Chem 2011; 286(5):3270-6.
13. Ji Y, Olson J, Zhang J, Hildebrandt M, et al. Breast cancer risk reduction and membrane-bound catechol O-methyltransferase genetic polymorphisms. Cancer research 2008; 68(14):5997-6005.
14. Lachman HM, Papolos DF, Saito T, Yu YM, Szumlanski CL, Weinshilboum RM. Human catechol-O-methyltransferase pharmacogenetics: description of a functional polymorphism and its potential application to neuropsychiatric disorders. Pharmacogenetics 1996; 6(3):243-50.
15. Chen CY, Lu RB, Yeh YW, Shih MC, Huang SY. Association study of catechol-O-methyltransferase gene polymorphisms with schizophrenia and psychopathological symptoms in Han Chinese. Genes, brain, and behavior 2011; 10(3):316-24.
16. Stephens M, Donnelly P. A comparison of bayesian methods for haplotype reconstruction from population genotype data. Am J Hum Genet 2003; 73(5):1162-9.
17. Sherrington R, Rogaev EI, Liang Y, et al. Cloning of a gene bearing missense mutations in early-onset familial Alzheimer's disease. Nature 1995; 375(6534):754-60.
18. Steiner H, Romig H, Grim MG, et al. The biological

and pathological function of the presenilin-1 Deltaexon 9 mutation is independent of its defect to undergo proteolytic processing. J Biol Chem 1999; 274(12):7615-8.
19. Kim JH, Anwyl R, Suh YH, Djamgoz MB, Rowan MJ. Use-dependent effects of amyloidogenic fragments of (beta)-amyloid precursor protein on synaptic plasticity in rat hippocampus in vivo. J Neurosci 2001; 21(4):1327-33.
20. Yoshiyama Y, Higuchi M, Zhang B, et al. Synapse loss and microglial activation precede tangles in a P301S tauopathy mouse model. Neuron 2007; 53(3):337-51.
21. Navakkode S, Sajikumar S, Frey JU. Synergistic requirements for the induction of dopaminergic D1/D5-receptor-mediated LTP in hippocampal slices of rat CA1 in vitro. Neuropharmacology 2007; 52(7):1547-54.
22. White NM, Packard MG, Seamans J. Memory enhancement by post-training peripheral administration of low doses of dopamine agonists: possible autoreceptor effect. Behav Neural Biol 1993; 59(3):230-41.
23. Mannisto PT, Kaakkola S. Catechol-O-methyltransferase (COMT): biochemistry, molecular biology, pharmacology, and clinical efficacy of the new selective COMT inhibitors. Pharmacol Rev 1999; 51(4):593-628.
24. Vandenbergh DJ, Persico AM, Hawkins AL, et al. Human dopamine transporter gene (DAT1) maps to chromosome 5p15.3 and displays a VNTR. Genomics 1992; 14(4):1104-6.
25. Fischer P, Simanyi M, Danielczyk W. Depression in dementia of the Alzheimer type and in multi-infarct dementia. Am J Psychiatry 1990; 147(11):1484-7.
26. Sweet RA, Devlin B, Pollock BG, et al. Catechol-O-methyltransferase haplotypes are associated with psychosis in Alzheimer disease. Molecular psychiatry 2005; 10(11):1026-36.
27. Glatt SJ, Faraone SV, Tsuang MT. Association between a functional catechol O-methyltransferase gene polymorphism and schizophrenia: meta-analysis of case-control and family-based studies. Am J Psychiatry 2003; 160(3):469-76.
28. Grunblatt E, Zehetmayer S, Bartl J, et al. Genetic risk factors and markers for Alzheimer's disease and/or depression in the VITA study. J Psychiatr Res 2009; 43(3):298-308.
29. Nicholl DJ, Bennett P, Hiller L, et al. A study of five candidate genes in Parkinson's disease and related neurodegenerative disorders. European Study Group on Atypical Parkinsonism. Neurology 1999; 53(7):1415-21.
30. Cordeiro Q, Siqueira-Roberto J, Vallada H. Association between the SLC6A3 A1343G polymorphism and schizophrenia. Arq Neuropsiquiatr 2010; 68(5):716-9.

OBESE VISCERAL ADIPOSE TISSUE GRAFTED IN LEAN MICE CAN ALTER GLUCOSE HOMEOSTASIS AND ENERGY EFFICIENCY

C. BARRERA, A. GATICA and C. MORGAN

Laboratory of Nutrition and Metabolic Regulation, Institute of Nutrition and Food Technology (INTA), University of Chile, Santiago, Chile

Received April 26, 2012 – Accepted June 4, 2012

Fat transplantation experiments have previously shown regulatory properties of lean adipose tissue on glucose homeostasis in the whole animal. In the current study, we addressed whether obese visceral white adipose tissue grafted in lean mice could alter glucose homeostasis. Obese visceral fat (VF) tissue was effective in increasing body weight gain and energy efficiency but not energy intake, when transplanted into the epididymal VF depot in lean recipient mice. These changes were accompanied by impaired glucose and insulin tolerance tests, showing altered glucose homeostasis. None of these effects were observed when transplants were grafted subcutaneously. These effects show that both physiologic state of donor VF (obese *vs* lean) and graft location (epididymal *vs* subcutaneous) in the recipient animal are critical to express deleterious effects of VF on glucose homeostasis in the whole organism.

Obesity is currently a growing epidemic of public health importance in western societies (1) and it is a major risk factor for developing systemic insulin resistance, and further type-2 diabetes, atherosclerosis, cardiovascular disease, non-alcoholic fatty liver disease, polycystic ovary, some cancers and neurodegenerative diseases (2, 3). Mostly, diet-induced obesity (DIO) and its comorbidities are referred to as Metabolic Syndrome. It is thought that increasing adoption of western lifestyle, characterized by sedentary way of life, abundance of calories, daily access to energy dense foods, offer of highly palatable diets, high consumption of refined sugars and alcohol, scarcity of vegetables and fruits, disruption of dark-light and sleep-awake cycles, lack of leisure time and, commonly living in polluted environments and under stress conditions, is a historical determinant in the rise of obesity during the last three or more decades (4).

A hallmark in obesity research came from Hotamisligil and associates' works describing that obesity induces inflammatory changes in visceral adipose tissue, leading to systemic insulin resistance (5). Briefly, macrophages populate visceral adipose tissue under metabolic stress and alongside adipocytes induce expression of proinflammatory cytokines, like TNF-α and IL-6, which are able to generate insulin resistance in visceral adipose tissue by inhibiting insulin signaling transduction network. In addition, other pro-hyperglycemic adipokines are elevated in visceral obese adipose tissue, accompanied by leptin resistance that also contributes to reinforce the obese phenotype. In this way, lipogenesis is impaired in obese visceral adipose tissue and dietary lipids are diverted chronically to liver, muscle and other tissues, thus leading to fat liver condition and contributing to extend the insulin-resistant phenotype to other tissues. Finally,

Key words: fat transplantation, glucose homeostasis, insulin resistance, mouse, obesity

Mailing address: Dr Carlos Morgan,
Av. El Líbano 5524,
Macul, Santiago 138-11,
Chile RM 7830490
Tel.: +562 978 1488
Fax: +562- 221 4030
e-mail: cmorgan@inta.uchile.cl

0393-974X (2012)

chronic hyperglycemia and hyperlipidemia can exert glucotoxicity and lipotoxicity on pancreatic β-cells, losing endogenous insulin function and gathering overt type-2 diabetes mellitus (6).

Within this context, we need to recall that adipose tissue develops in two main body compartments: as subcutaneous fat (SCF) depots, with presence of white and brown fat cells, extending under the most of body surface and, as visceral fat (VF) that is white, visceral adipose tissue distributed inside peritoneal cavity, mostly associated to the visceral organs, i.e., epididymal, perirhenal, perintestinal, parametrial, retroperitoneal, omental fat. Epididymal fat is commonly taken as a study model of VF, mainly because it is easy to identify, manipulate and remove and, also because it becomes prominent in obese rodents (7). Regarding DIO, VF responds to metabolic stress inducing its characteristic inflammation (also termed, metaflammation, as proposed by Hotamisligil) and its consequences over development of Metabolic Syndrome. However, SCF is not known to develop extensive inflammation as VF does and, importantly, has a great capacity to secrete adiponectin, an anti-hyperglycemic adipokine, whose expression is compromised in obese VF. In fact, inducing adiponectin expression from SCF can help even to counteract genetic obesity (8). Removal of omental fat, the main VF depot in humans, recovered normal insulin sensitivity (9, 10) as does epydidimal fat removal in obese B6 mice (C. Morgan, unpublished results). In contrast, subcutaneous liposuction has not shown any positive effects (11).

In the current study, we proposed that endocrine function of obese VF should be enough to alter glucose homeostasis, even in lean, healthy animals fed regular diet (RD). For this purpose, fat transplantation technique was used, which is a bioassay useful to detect and characterize properties of adipose tissue, *in vivo*, as formerly used by Reitman, Klebanov, and Kahn and associates, among others (12-15). In the first case, parametrial fat from lean mice was grafted subcutaneously in lipoatrophic mice, which have no capacity to develop adipose tissue, improving glucose tolerance and insulin sensitivity and then, suggesting that certain development of adipose tissue is required to achieving a normal glucose homeostasis, likely due to replacement of adipokines (12). In the second case, a similar reasoning was followed to transplant subcutaneously epididymal fat from wild type animals in genetically leptin-deficient mice (13); as a consequence, the recipient animals did recover normal fat mass as well as lipid and glucose homeostasis and fertility. A more recent study showed that SCF but not VF transplanted from lean donor mice either into subcutaneous or intraperitoneal compartments in lean recipient animals leads to decreased body weight and total fat mass, and lower glucose and insulin levels in recipient animals subjected to high-fat feeding (14). Thus, it seems that both the anatomic compartment in which the fat depot is grafted in the recipient animal and intrinsic differences between SCF and VF tissues from the donor animal are important factors for achieving metabolic effects after fat transplantation. These findings agree in that lean adipose tissue has protective effects under insulin resistance conditions. Nevertheless, the importance of physiologic status of donor adipose tissue has not been evidenced by these means. Such approach should reveal whether endocrine function of obese adipose tissue is a condition sufficient to alter whole-organism fuel homeostasis in otherwise healthy, lean subjects. We hypothesized that transplantation of VF from obese to lean mice should replicate at least in part the obese phenotype in those lean animals, and that the metabolic effects produced could in part depend on the fat compartment receiving the graft. To address this question, we studied whether VF transplanted from diet-induced obese, insulin-resistant mice into either the subcutaneous or visceral fat compartments can alter glucose homeostasis in lean mice fed RD.

MATERIALS AND METHODS

Animals

CD1 Swiss mice (ICR) were purchased by the Animal Facility of the Faculty of Dentistry at the University of Chile. Experiments using animals were performed at INTA Animal Facility and maintained in a 12/12 h light/dark cycle and 21.5±1.5ºC room temperature. Animals fed *ad libitum* either RD, (cat Nº D1450B, 10 kcal% fat) or high fat diet (HFD, cat N° D12492, 60 kcal% fat) both provided by Research Diets (New Brunswick, NJ 08901, USA), to induce obesity during 12 weeks of feeding from one week after weaning (mice were weaned at 21 days

postpartum). Body weight (in g), energy intake (in kcal/week), and intake energy efficiency - defined as the body weight change divided per energy intake during a week (in g/kcal) - were measured weekly. The protocols for animal research were approved by the Committee of Bioethics at INTA, University of Chile, and by the Advisory Committee of Bioethics at FONDECYT (Chilean funding agency of science and technology).

Fat transplantation experiments

Sixteen-week-old male mice fed high fat diet (HFD) during 12 weeks were used as donors of epididymal fat (VF). Lean age-matched male mice fed RD were recipients of fat transplantation either by subcutaneous injection of 1.8±0.1 g VF under the flank skin (SC in Fig. 1 and Table I) or by injecting 1.6±0.1 g VF directly into the endogenous epididymal fat depots (IVF in Fig. 1 and Table 1) after opening the peritoneal cavity under sterile conditions. All animals were i.p. anesthetized with 100mg/kg ketamine/10mg/kg xylazine during surgery. Peritoneal wall and abdominal skin were stitched after IVF transplantation and IVF sham surgery. All transplanted and sham control animals were fed RD before and after transplantation. Upon sacrifice, at week 12 after fat transplantation, the grafts were inspected visually and those animals showing necrotic grafts were excluded from the study.

Tolerance tests

Glucose and insulin tolerance tests were performed after 6-h fasting. Either 1.5 mg/g glucose or 1.5 IU/Kg insulin were i.p. injected (time zero) to perform glucose tolerance test (GTT) or insulin tolerance test (ITT), respectively. Then, blood drops were collected from the tail vein at time points 0, 15, 30, 60, 90, and 120 min to determine glucose levels using a glucometer ACCU-CHEK® Sensor comfort (Roche, Basel, Switzerland).

Triglycerides and cholesterol determinations

Triglyceride and cholesterol levels were determined in plasma and liver, using the Infinity TG kit from Thermo Scientific USA and the enzymatic Colestat kit from Wiener lab (2000 Rosario, Argentina), which is based on the Allain et al. method (16). Briefly, total lipids are extracted with Bligh and Dyer standard protocol (17), and then resuspended by extensive sonication in 0.05% Triton X-100 before using the kits, according to the manufacturer's instructions.

Statistical analyses

Data are expressed as means ± S.E.M. Unpaired two-tailed Student's *t*-test was used to compare two groups at a single time point. One-way ANOVA was used to compare more than two groups at a single-time point. Time-course data were analyzed by repeated measures (RM) ANOVA. Plasma and liver determinations from SC or IVF control (sham operated) and transplanted (recipient) animals were compared by two-way ANOVA. *Post hoc* analyses of intergroup comparisons were performed with the Bonferroni multiple comparisons test whenever P ANOVA < 0.05. Statistical analyses were performed in Prism 5 (GraphPad Software, Inc., CA, USA) and significance was set at $P < 0.05$.

RESULTS

Fig. 2 indicates that mice fed HFD showed significant increases in body weight (Fig. 2A) and energy efficiency (Fig. 2C) but not in energy intake (Fig. 2B) as compared to animals fed RD. Concomitantly, mice fed HFD exhibited elevated fasting blood glucose levels and impaired GTT (Fig. 2D) and ITT (Fig. 2E) compared to animals fed RD.

SC transplantation of VF from obese animals into lean recipient mice did not result in altered glucose homeostasis as compared to sham control animals, during the 12-week observation period (Fig. 1). In contrast, transplantation of obese VF into the epididymal fat pad of lean recipient mice led to increased body weight gain, intake energy efficiency and, impaired GTT and ITT, with no change in energy intake when compared to non-transplanted, sham control mice (Fig. 1). Those results suggest that presence of obese adipose tissue in a lean animal can alter glucose homeostasis depending of the location of grafts (IVF *vs* SC), showing that location helps to explain deleterious effects of obese visceral adipose tissue on glucose homeostasis. In addition, obese VF grafted IVF but not SC in lean recipient mice showed increased body weight gain and energy intake efficiency with no change in energy intake (Fig. 1B).

At the endpoint of fat transplantation experiments, plasma and liver cholesterol and triglycerides levels were determined as well as liver weight (Table I). IVF recipient mice showed significantly increased plasma cholesterol and liver triglyceride levels compared to IVF sham operated mice ($p < 0.05$), while plasma triglyceride, liver cholesterol and liver weight did not show any difference. In contrast, SC recipient mice did not show any significant changes in the parameters.

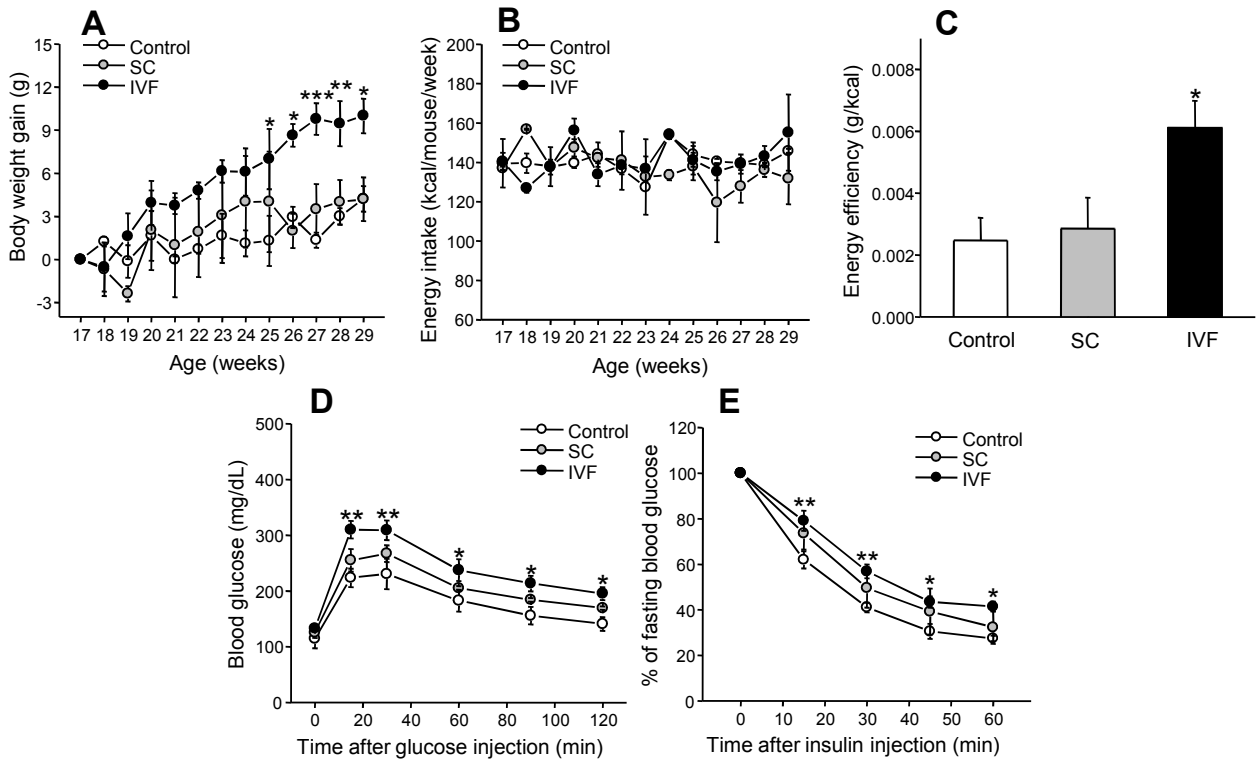

Fig. 1. *Metabolic changes induced in mice after visceral fat transplantation. Body weight gain (**A**) and energy intake (**B**) were measured during 12 weeks after obese fat grafting into the subcutaneous (SC) compartment or directly into the endogenous epididymal fat depot (IVF); sham mice were used as controls (data from SC and IVF sham control mice were undistinguishable and then pooled into one control group). Energy efficiency (**C**), glucose tolerance (**D**) and insulin tolerance were determined 12-13 weeks after obese fat transplantation or sham procedure. Data are mean values ± SEM. For A, B, D and E, time-course data were analyzed by RM ANOVA (P ANOVA were < 0.0001, = 0.3218, < 0.0001 and < 0.0001, respectively) followed by the Bonferroni multiple comparisons test (*P < 0.05, **P < 0.01, ***P < 0.001). One-way ANOVA was used to compare the three groups in C (*P ANOVA = 0.0104) followed by the Bonferroni multiple comparisons test (*P < 0.05). All differences detected were found between control group and IVF recipients group (n = 5 in each group).*

DISCUSSION

In the present study, we transplanted VF from diet-induced obese donor mice into lean recipient mice. DIO mice responded to HFD feeding as expected, showing increased body weight and energy efficiency due to expanding fat mass under HFD feeding. Thereafter, developing insulin resistance was evidenced by elevated fasting blood glucose and higher areas under GTT and ITT curves (Fig. 2). These results confirm the validity of our approach to get DIO insulin-resistant donor mice. Lean recipient animals grew up under *ad libitum* RD feeding and achieved a steady state body weight value before transplantation.

In order to assess our hypothesis that obese visceral adipose tissue may lead the whole-organism to altering glucose homeostasis, we performed a fat transplantation study. We essentially sought to alter glucose homeostasis in animals receiving epididymal VF tissue from obese donors and observe the influence of grafting location on the putative effects. SC recipient mice did not show any alterations on glucose homeostasis (fasting blood glucose levels, or glucose and insulin tolerance tests) nor in body weight gain, energy intake and efficiency (Fig. 1). Interestingly, when obese VF was grafted into the endogenous epididymal but not in the subcutaneous

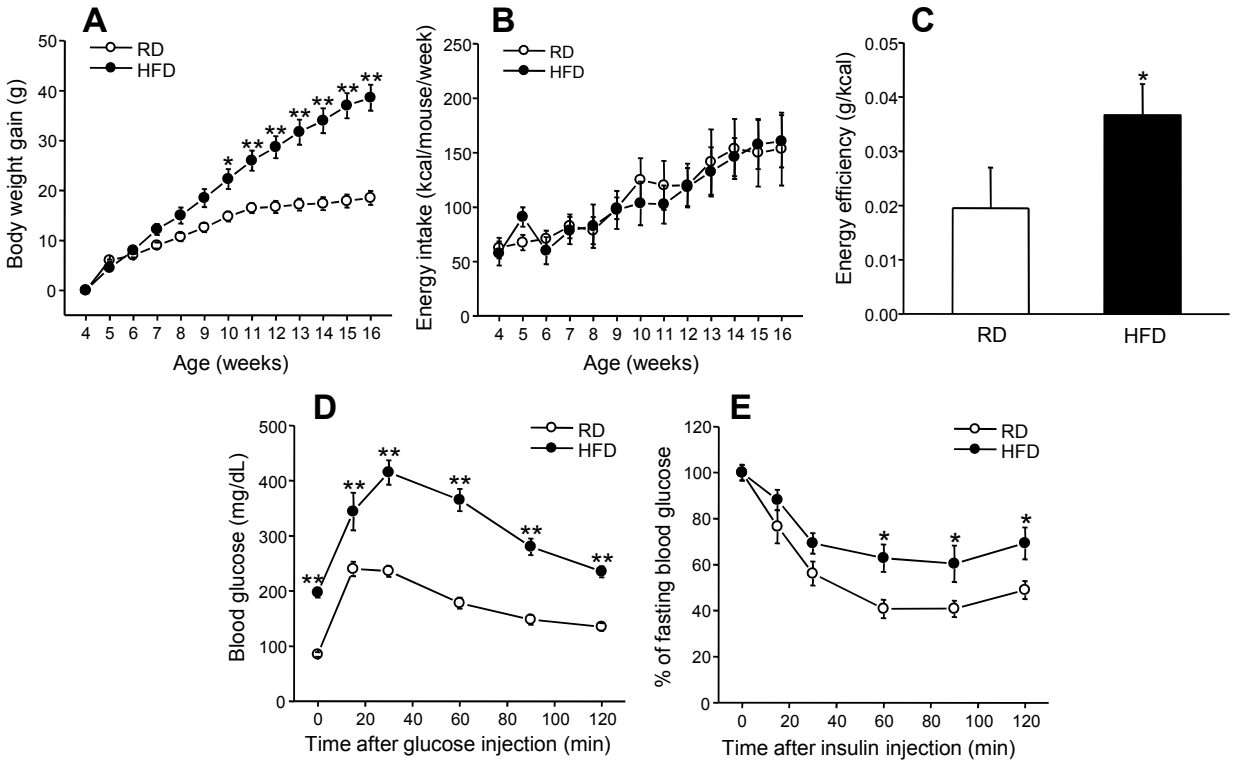

Fig. 2. *Diet-induced obesity in mice. Body weight gain (**A**) and energy intake (**B**) were measured during 12 weeks either on RD or HFD. Energy efficiency (**C**), glucose tolerance (**D**) and insulin tolerance were determined after 12 weeks either on RD or HFD. Data are expressed as mean values ± SEM (n = 5 in each group). For A, B, D and E, time-course data were analyzed by RM ANOVA (P ANOVA values were < 0.0001, = 0.7118, < 0.0001 and < 0.0001, respectively) followed by the Bonferroni multiple comparisons test (*P < 0.05, **P < 0.001). Unpaired two-tailed Student's t-test was used to compare the two groups in C (*P < 0.001).*

Table I. *Determinations of plasma and liver cholesterol and triglycerides levels three months after transplantation.*

Group	Plasma Cholesterol (mg/ml)	Plasma Triglycerides (mg/ml)	Liver Cholesterol (µg/mg)	Liver Triglycerides (µg/mg)	Liver weight (g)
SC Sham	1.04±0.03	0.50±0.16	2.07±0.31	3.70±1.08	1.85±0.15
SC Recipient	1.30±0.09	0.51±0.03	2.25±0.23	6.59±1.51	2.07±0.15
IVF Sham	1.05±0.03	0.34±0.03	2.11±0.07	3.35±0.16	1.70±0.10
IVF Recipient	1.37±0.15 *	0.45±0.12	2.45±0.15	7.13±1.01 *	1.92±0.12
P ANOVA Transplant factor	0.0053	0.5654	0.2335	0.0062	0.1143
P ANOVA Location factor	0.6627	0.2979	0.5756	0.9297	0.2716
P ANOVA Interaction	0.7432	0.6314	0.7082	0.6801	1.0000

Data are expressed as mean values ± SEM (n = 5 in each group). All SC Recipients (animals receiving VF transplantation by subcutaneous injection), IVF Recipients (VF injected directly into the endogenous epididymal fat depot), SC sham and IVF sham groups were compared by two-way ANOVA (transplantation factor distinguishes sham or recipient groups, whereas graft location factor distinguishes SC or IVF groups) P ANOVA values are shown for every factor and their interaction. (*) P < 0.05 when transplanted recipients are compared with respective sham control animals by Bonferroni post hoc test.

fat depot of lean recipient mice (Fig. 1), almost all the variables measured (body weight gain and energy intake efficiency, areas under both GTT and ITT curves) were found to increase though animals were kept feeding RD. It should be noted that to our knowledge no previous works have studied the metabolic effects of obese fat transplantation into lean subjects.

Our current observations suggest that both the physiologic status (obese *vs* lean) and the site of grafting (IVF *vs* SC) of VF determine its effect on glucose homeostasis. Whenever lean recipient animals were IVF transplanted, their glucose homeostasis was impaired, showing larger areas under both GTT and ITT curves (Figs. 1D and E), thus demonstrating that IVF transplantation of obese VF into lean recipients can alter glucose homeostasis. Nevertheless, the effect was not immediate and, reproducibly took about eight weeks after transplantation to be detected. Interestingly, body weight gain increased in IVF but not in SC recipient animals, reaching significant differences from eight weeks after transplantation, suggesting that impairment of glucose homeostasis and increased body weight gain might be related. Reasonably, the moderate but significant increase (12±1%) in body weight observed in IVF recipients likely represents an increase in fat mass because experimental animals were already adults at the time of transplantation. This overweight did not result in liver steatosis as was inferred by unchanged liver weight and liver appearance. Nevertheless, liver triglyceride and plasma cholesterol levels significantly increased in IVF recipient mice, suggesting that some alteration in lipid homeostasis could happen. However, plasma triglycerides and liver cholesterol levels did not show any differences.

Seemingly, an endocrine effect of obese VF graft pads if well irrigated should be similar irrespective of the site of transplantation. However, a potential qualitative difference between both sites of transplantation resides in the fact that while SC grafts were injected under the skin with no infiltration of endogenous fat depots, which are both separated and clearly distinguishable, IVF injection was performed inside the recipient's epididymal fat depot mixing both exogenous and endogenous fat tissues. We speculate that IVF grafting may allow paracrine mechanisms to operate between endogenous and exogenous tissues rather than in the case of our SC grafts, which can be easily separated from endogenous subcutaneous fat tissue. Alternatively, we have not yet discarded that IVF grafts could retain neuroendocrine communication between exogenous VF and sympathetic nerve activity.

Most likely, obese VF grafts do not represent a major source of triglycerides in the whole animal, since no more than 4% of body weight was transplanted (< 2 g per recipient) in the experiments reported here. In our conditions, a diet-induced obese animal usually exhibits over 30% of body weight in adipose tissue, while in a lean animal it is usually less than 15%. Then, the impairment of glucose homeostasis observed in the current work is unlikely due to the supply of triglycerides by fat transplants, but likely due to VF-derived factors involved in increasing body weight gain, involving the called fat-brain axis (18).

In summary, the present results show for the first time that transplantation of a small graft of obese VF injected in IVF but not in SC compartment of lean mice leads to impaired glucose homeostasis and increased energy efficiency in animals fed RD. These effects show that both physiologic state of VF (obese *vs* lean) and graft location (IVF *vs* SC) are critical to express deleterious effects of VF on glucose homeostasis in the whole organism. Further efforts will be required to elucidate the molecular basis underlying the effects described here on increasing body weight gain and impaired glucose homeostasis in absence of increased food intake.

ACKNOWLEDGEMENTS

This work was mainly supported by grant FONDECYT #1090230 and in part by an EMF/INF fellowship in Nutrition and Infection awarded to CM as well as by a Nevin Scrimshaw INF research grant awarded to AG.

REFERENCES

1. Rodgers A. Quantifying selected major risks to health. In World Health Report 2002: Reducing risks, promoting healthy life. World Health Organization, Geneva, 2002; p. 57-61.

2. Saltiel AR, Kahn CR. Insulin signalling and the regulation of glucose and lipid metabolism. Nature 2001; 414:799-806.
3. Biddinger SB, Kahn CR. From mice to men: insights into the insulin resistance syndromes. Annu Rev Physiol 2006; 68:123-58.
4. Hossain P, Kawar B, El Nahas M. Obesity and diabetes in the developing world: a growing challenge New Engl J Med 2007; 356:213-215.
5. Hotamisligil GS. Inflammation and metabolic disorders. Nature 2006; 444:860-67.
6. Gupta D, Krueger CB, Lastra G. Over-nutrition, obesity and insulin resistance in the development of beta-cell dysfunction. Curr Diabetes Rev 2012; 8:76-83.
7. Ibrahim MM. Subcutaneous and visceral adipose tissue: structural and functional differences. Obes Rev 2010; 11:11-18.
8. Kim JY, van de Wall E, Laplante M, et al. Obesity-associated improvements in metabolic profile through expansion of adipose tissue. J Clin Invest 2007; 117:2621-37.
9. Barzilai N, She L, Liu BQ, Vuguin P, Cohen P, Wang J, Rossetti L. Surgical removal of visceral fat reverses hepatic insulin resistance. Diabetes 1999; 48:94-98.
10. Thorne A, Lonnqvist F, Apelman J, Hellers G, Arner P. A pilot study of long-term effects of a novel obesity treatment: omentectomy in connection with adjustable gastric banding. Int J Obes Relat Metab Disord 2002; 26:193-99.
11. Klein S, Fontana L, Young VL, Coggan AR, Kilo C, Patterson BW, Mohammed BS. Absence of an effect of liposuction on insulin action and risk factors for coronary heart disease. New Engl J Med 2004; 350:2549-57.
12. Gavrilova O, Marcus-Samuels B, Graham D, Kim JK, Shulman GI, Castle AL, Vinson C, Eckhaus M, Reitman ML. Surgical implantation of adipose tissue reverses diabetes in lipoatrophic mice. J Clin Invest 2000; 105:271-78.
13. Klebanov S, Astle CM, DeSimone O, Ablamunits V, Harrison DE. Adipose tissue transplantation protects ob/ob mice from obesity, normalizes insulin sensitivity and restores fertility. J Endocrinol 2005; 186:203-11.
14. Tran TT, Yamamoto Y, Gesta S, Kahn CR. Beneficial effects of subcutaneous fat transplantation on metabolism. Cell Metab 2008; 7:410-20.
15. Konrad D, Rudich A, Schoenle EJ. Improved glucose tolerance in mice receiving intraperitoneal transplantation of normal fat tissue. Diabetologia 2007; 50:833-9.
16. Allain CC, Poon LS, Chan CSG, Richmond W, Fu PC. Enzymatic determination of total serum cholesterol. Clin Chem 1974; 20:470-5.
17. Bligh EG, Dyer WJ. A rapid method of total lipid extraction and purification. Can J Biochem Physiol 1959; 37:911-17.
18. Leibel RL. Molecular Molecular physiology of weight regulation in mice and humans. Int J Obes (Lond) 2008; 32:S98-108.

COCAINE- AND AMPHETAMINE-REGULATED TRANSCRIPT : IDENTIFICATION AND DISTRIBUTION IN HUMAN GASTROINTESTINAL TRACT

I. KASACKA[1], Ż. PIOTROWSKA[1], H. CAR[2], I. JANIUK[3] and W. ŁEBKOWSKI[4]

[1]Department of Histology and Cytophysiology, Medical University, Białystok, Poland; [2]Department of Experimental Pharmacology, Medical University, Białystok, Poland; [3]Department of Vertebrates Morphology, Siedlce University of Natural Sciences and Humanities, Siedlce, Poland; [4]Department of Neurosurgery, Medical University, Białystok, Poland

Received March 26, 2012 – Accepted May 31, 2012

Cocaine- and amphetamine-regulated transcript (CART) was identified in the central and peripheral nervous system, including the gastrointestinal tract of rodents and pig. CART was also expressed in neuroendocrine cells of the rats stomach antral mucosa. The knowledge of the presence and functional role of CART peptide in the human alimentary tract is very limited due to difficulties in obtaining human samples (especially from healthy individuals). The presence of CART peptide in the gastrointestinal tract of the human was investigated immunohistochemically. CART-immunoreactive (IR) neural structures were observed in all studied fragments of alimentary tract. CART-like immunoreactive nerve fibers were numerous within the muscle in layers of muscularis externa and in the myenteric plexus of all gastrointestinal segments (from esophagus to colon), while they were moderate or few in density in other layers of gastrointestinal tract. The presence of CART peptides in the neuroendocrine cells was demonstrated predominantly in the pyloric, duodenum and fundus, and only few in the rest parts of the small intestine. CART-IR neuroendocrine cells could not be detected in the mucosa of large intestine. The present study reports for the first time a detailed description of the CART distribution pattern within the human alimentary tract. Our findings may hopefully provide some contribution towards a more complete and comprehensive understanding of the function and role of the CART peptide in the alimentary system.

The peptide CART (cocaine- and amphetamine-regulated transcript) is a newly known neurotransmitter of both the central and the peripheral nervous system. It was, for the first time, sequenced as a peptide of unknown function (1), while only afterwards, it was found that the expression of its mRNA was significantly upregulated in the rat's ventral striatum in response to cocaine or amphetamine, administered into the brain ventricles (2). It was also demonstrated that peptide expression depends on leptin presence (peptide which is secreted as a satiety signal transmitter to the hypothalamus) (3, 4).

Strong CART expression has been indicated in the central nervous system, particularly in areas responsible for feeding (5), including: the ventromedial nucleus of the hypothalamus, the lateral hypothalamus, the arcuate nucleus, the paraventricular nucleus (PVN), the nucleus of the solitary tract and the nucleus accumbens (6, 7).

Key words: cocaine- and amphetamine-regulated transcript (CART), alimentary tract, immunohistochemistry, human

Mailing address: Prof. dr hab. Kasacka Irena,
Department of Histology and Cytophysiology,
Medical University of Białystok,
ul. Kilińskiego 1, 15-089 Białystok, Poland
Tel.: +48 85 748 54 58
Fax. +48 85 748 55 16
e-mail: kasacka@umb.edu.pl

0393-974X (2012)

The presence of CART peptides was also demonstrated in brain areas, involved in motor activity (8), and in the peripheral nervous system, including preganglionic sympathetic nerves (9), pancreatic ganglia, neurons innervating biliary tracts and the gallbladder and enteric nervous system (10-13). Beyond the nervous system, CART has been localized as well in the endocrine glands of rat, for example, in the pituitary gland, in the adrenal core (2, 14) and in the pancreatic islet cells (13, 15). CART has also been identified in certain cells, belonging to diffuse neuroendocrine system (DNES), among others, in C cells of pig thyroid gland (13), as well as in G cells of rat stomach (10).

CART may activate the hypothalamus - pituitary - adrenal axis (HPA), which plays a central role in food intake control and energy homeostasis regulation, therefore, it is a key neuropeptide, functionally associated with energy balance (16-18).

Functional studies have mainly been focused on CART participation in feeding behavior (12), since this peptide shows strong anorexigenic properties (19). After CART administration to brain ventricles, reduction of food consumption levels was observed (7, 14, 16).

CART effects on adipose tissue, providing obesity control, have been confirmed in a number of current research projects (20). Influences of CART with regards to the secretion of the gastric acids, gastric motility and gastric emptying has been demonstrated by researchers as well (21, 22). Other studies (8, 23-25), involving a thorough observation of rats behavior after CART administration into brain ventricles, confirm the influence of CART on motor activity. Moreover CART is involved in pain, anxiety or stress perception (26), and appears to contribute in psychostimulants addiction by strengthening the psychostimulant stimulation of pleasure centers (8, 27).

The results of studies, conducted by various scientific centers (6, 28, 29), confirm CART impacts on endocrine functions of the pancreas, suggesting its probable role in the survival and differentiation of pancreatic cells. Interestingly enough, CART reveals also certain properties to promote the survival of enteric neurons in mice *in vitro* (10).

CART distribution in the gastrointestinal tract of mammals has been investigated in rats (8, 11), pigs (13, 30), guinea pigs (12) and sheep (31), whereas the available knowledge about the quantity and distribution of CART in the human gastrointestinal tract is limited to the data from a short description of two pathological cases (Hirschsprung's disease and ulcerative colitis), concerning only some restricted parts of the intestine (32, 33).

Although the principal site of CART synthesis has already been identified, our to-date's knowledge of the subject is mainly based on – and thus limited to – a research, conducted on animals, due to difficulties with obtaining human samples. Therefore, the primary goal of this reported study was to identify and examine the distribution and occurrence of CART-IR structures in the alimentary tract of healthy human subjects.

MATERIALS AND METHODS

Ethical issues

The study protocol was approved by the Ethics Committee at the Medical University of Białystok (R-I-002/345/2007) and a written, informed consent had previously been obtained from each subject or from his/her family member(s).

Collecting and preparation of the samples

Nineteen donors of organs with normal alimentary tract were used in the study. There were 10 men at the mean age of 43.9 yrs; the range from 21 to 65 yrs, with mean body weight of 83.25 kg and mean BMI of 26.54, and 9 women at the mean age of 46.3 yrs; the range from 19 to 58 yrs, with mean body weight of 66.33 kg and mean BMI of 24.55. BMIs were calculated as the ratio of body weight (kg) to squared height (m) and expressed as BMI SD scores (BMISDS). We used the currently applicable and updated local growth charts for height and weight for the Polish population, aged 19–65 yrs.

Each subject had been treated at the ICU (Intensive Care Unit), due to brain damage, caused by brain injury or cerebral hemorrhage, while in a few cases only, the brain damage was secondary in origin, due to primary cardiac arrest. The patients were artificially ventilated, received circulatory support and were provided with parenteral and enteral nutrition. No one received steroids.

Each of the subjects, presenting with clinical symptoms of brain death, was considered to be an organ donor. Irreversible brain damage was confirmed by special clinical examination and angiography (no blood flow within the brain arteries).

After brain death was diagnosed and individual death

was confirmed by doctors committee, esophagus, stomach (cardia, fundus and pylorus), duodenum, jejunum, ileum and colon (the same part of the individual sections of alimentary tract) samples about 1 cm long, were collected from each body after other organs (kidneys, heart, liver) for transplantation were harvested.Samples of the alimentary tract were immediately fixed in Bouin's solution and routinely embedded in paraffin. Specimens were stained with hematoxylin and eosin for general histological examination and processed by immunohistochemistry for CART detection using an EnVision Plus-HRP Detection Kit (K 4011, Dako; Glostrup, Denmark) (34).

Immunohistochemical procedure

Paraffin blocks were cut into 4-μm sections (5 sections from individual sections of alimentary tract and from each subject) and attached to positively charged glass slides. Immunostaining was performed by the following protocol: paraffin-embedded sections were deparaffinized and hydrated in pure alcohols. For antigen retrieval, the sections were subjected to pretreatment in pressure chamber heating for 1 min at 21 psi (One pound force per square inch (1 psi) equates to 6.895 kPa, (the conversion factor has been provided by the United Kingdom National Physical Laboratory) at 125ºC, using Target Retrieval Solution with pH of 9.0 S 2367 (Dako; Glostrup, Denmark). After cooling down to room temperature, the sections were incubated with Peroxidase Blocking Reagent S 2001 (Dako; Glostrup, Denmark) for 10 min to block endogenous peroxidase activity.

The sections were incubated with the primary antibody to CART peptide (No H-003-61) (1:10 000 dilution) overnight at 4ºC in a humidified chamber. The CART antiserum, a rabbit polyclonal, purchased at the Phoenix Pharmaceuticals, Inc. (Mountain View, CA, USA) was used. The antiserum was diluted in Antibody Diluent (S 0809 DakoCytomation, Denmark). Followed by incubation with secondary antibody (conjugated to horseradish peroxidase-labeled polymer), the bound antibodies were visualized by 1-min incubation with liquid 3,3'-diaminobenzidine substrate chromogen.

The sections were finally counterstained in QS hematoxylin (Vector, H-3404), mounted and evaluated under light microscope. Appropriate washing with Wash Buffer (S 3006, Dako; Glostrup, Denmark) was performed between each step.

Specificity tests were performed for the CART antibody included: negative control, where the antibody was replaced by normal rabbit serum (Vector Laboratories; Burlingame, CA, USA) at respective dilution and a positive control was prepared with specific tissue, as recommended by the manufacturer; rat hypothalamus for CART. Histological preparations were subjected to a visual analysis, using an Olympus B×41 microscope.

As for the semi-quantitative evaluation of the density of CART-IR structures, an arbitrary scale was used, where (–) means the absence of structures studied; (+) - single element; (++) – few structures; (+++) – moderate number; (++++) – dense; (+++++) – and very dense

Morphometric analysis

The densities of CART-IR neuroendocrine cells in each part of the human gastrointestinal tract were estimated. After taking digital photographs under a light microscope with a digital camera (DP12-2; Olympus, Japan), the number of cells in each section was counted and the area of the mucosal layer in each section was measured using a computerized image analysis program, NIS Elements BR: 2240. Immunopositive cells were counted in ten (10) microscopic fields, each field of 0.785 mm^2, in magnification of 200x (20x the lens and 10x the eyepiece). Five sections of each region of the gastrointestinal tract were analysed. The average number of CART-IR cells per mm^2 was counted to quantify their distribution density.

The corresponding mean values were computed automatically; significant differences were determined by Student's *t*-test; $p<0.05$ was taken as the level of significance.

RESULTS

Staining for CART was performed on sections from esophagus, cardias, fundus and pylorus of the stomach, duodenum, jejunum and ileum of the small intestine and colon of the large intestine. It was found that CART-IR structures existed in all regions of the human gastrointestinal tract. According to the location and situation in examined parts of alimentary tract, different regional distribution and relative frequencies of CART-IR structures were observed. These differences are shown in Table I.

Immunhistochemical analyses revealed that both nerve cell bodies and nerve fibers immunoreactivity to CART is present in the human alimentary tract. In addition to neurons, CART was found in a population of endocrine cells in the stomach (fundus, pylorus) and small intestine mainly in the duodenum mucosa.

In the human esophagus, CART-IR nerve cells bodies and nerve fibers were found in myenteric plexus, on moderate level, while in the submucous ganglia no CART immunopositive structures were observed in this part of gastrointestinal tract. Immunohistochemically labelled CART containing

nerve fibers, innervating muscle fibers in layers of esophagus muscularis externa were thin and delicate (Fig. 1A).

Abundant CART-IR elements were observed in the stomach (Fig. 1B, C, D) especially in its pyloric part (Fig. 1E and F).

CART-IR fibers and nerve cell bodies were detected in all the studied regions of the human stomach. The dense number of thick and long CART-IT nerve fibers was seen in all the muscularis externa layers and in myenteric plexus, where this immunoreactivity was also present in nerve cell bodies, while in the submucous ganglia no CART immunopositive nerve cell bodies were observed in the stomach. In addition to neurons, CART immunoreactivity was demonstrated in neuroendocrine cells in both fundus and pylorus part of the stomach, but they were rare in the fundus (4.2±1.18) and numerous in pylorus (41.3±13.27).

Immunohistochemical studies showed that the most abundant concentration of CART-IR material in the small intestine was localized in the duodenum (Fig. 2A, B) and, with a gradually decreasing intensity, in the jejunum (Fig. 2C, D) and the ileum (Fig. 2E, F). That observation did not refer to muscularis externa, where CART-immunoreactive nerve fibers were equally numerous in all the three regions in question, their numbers being always either dense or very dense (Fig. 2B, D and F).

CART containing nerve cells and fibers were abundant in myenteric plexus in all the analysed sections of the small intestine. Numerous ganglia contained a very dense meshwork of such fibers and strong immune stained nerve cell bodies were seen in the myenteric plexus. Lower numbers of CART positive nerve fibers and cells were generally observed in the submucous plexus, when compared with the density of CART-IR elements within the myenteric plexus. Some of the submucosa ganglia, especially in the distal parts of the intestine, were devoid of CART containing structures.

Immunostaining for CART revealed a moderate number of CART-IR nerve fibers in the lamina propria of the duodenum and sparse number of CART containing fibers innervating muscularis mucosa of jejunum and ileum. It can be seen that this immunoreactivity was also present in the subpopulation of neuroendocrine cells distributed among the epithelium of the intestinal mucosa. Some of these immune reactive cells were detected

Table I. *Relative prevalence of individual CART-IR structures within particular parts of the human digestive tract.*

Part of the human GIT		Mucosa			Submucosa	Muscular coating			
		villi	endocrine cells	muscularis mucosa	submucosus plexus	oblique smooth muscle layer	circular smooth muscle layer	longitudinal smooth muscle layer	myenteric plexus
Esophagus				-	-		++	++	+++
Stomach	cardia		-	-	-	++	+++	+++	+++
	fundus		++	-	-	++	+++	+++	++++
	pylorus		+++++	+	-	+++	++++	+++	++++/+++++
Small intenstine	duodeum	++	+++	+++	++		++++	+++/++++	+++++
	jejunum	+	+	+	+		++++	+++	++++/+++++
	ileum	+	-/+	-	-		+++/++++	+++	++++/+++++
Large intensine			-	-	-		+++/++++	+	++++

Subjective density rating of CART-IR nerve structures:-, not found; +, single structures; ++, few structures; +++, moderate number; ++++, dense; +++++, very dense

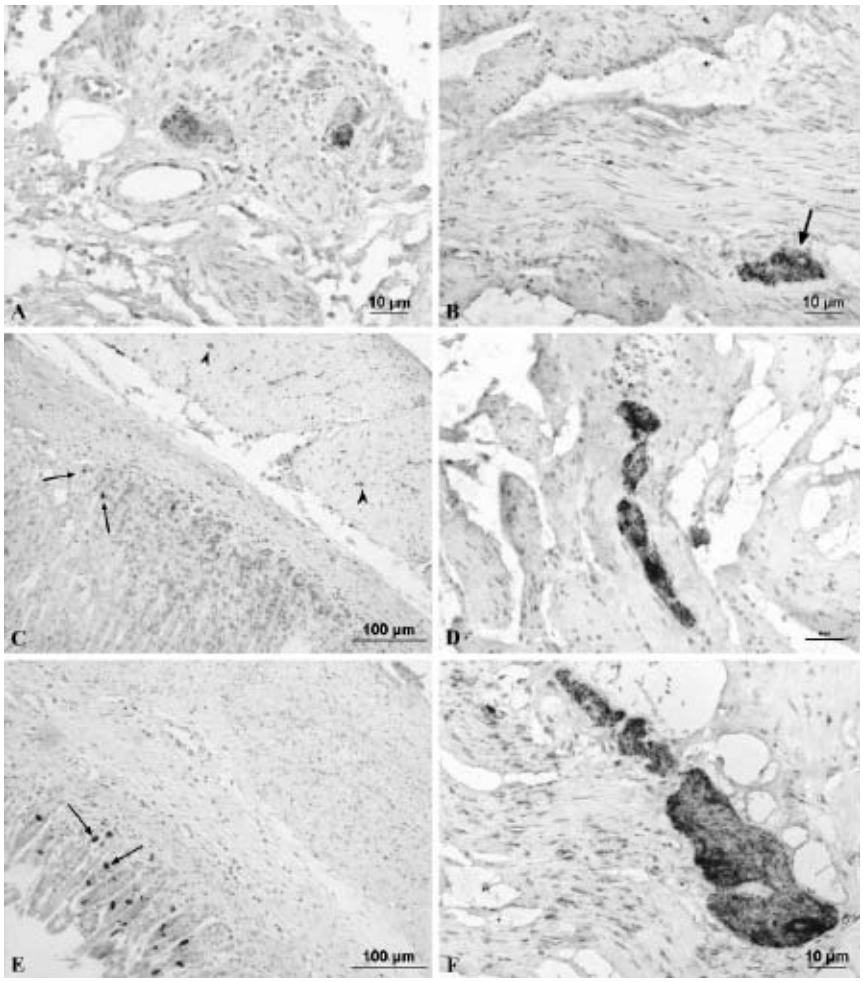

Fig. 1. *Immunohistochemical reactivity for CART (**A**) in the muscularis externa of esophagus (**B**) myenteric ganglion (arrow) and delicate fibers staining within the muscularis externa layers in cardia of the stomach (**C, D**) single CART-IR endocrine cells (arrows) in the mucosa and nerve fibers within the muscularis externa (arrowheads) and myenteric ganglia in the fundus wall of the stomach (**E, F**) numerous CART-IR cells in the glands of the mucosa (arrows), myenteric ganglion and nerve fibers innervating muscle fibers in the muscularis externa in the pylorus of the stomach.*

in the epithelial mucosa of duodenum (5.6±1.72, Fig. 2A), and only a few of them existed in the epithelium of the jejunum (0.45±0.51, Fig. 2C) and ileum (0.21±0.43, Fig. 2E).

Less CART-IR structures were demonstrated in the mucosa and submucosa of the large intestine than in those of the small intestine. In the large intestine CART positive structures were distributed mainly in the muscularis externa. CART containing nerve fibers were dense and thick in the circular layer but these innervating the longitudinal layer were thin and single. CART-IR myenteric nerve cell bodies were rather rarely observed while strongly CART-stained nerve fibers formed dense meshwork in these ganglia of large intestine (Fig. 2G). In the submucous plexus and in the mucosa/submucosa of the large intestine very rarely CART containing structures were observed. CART-IR neuroendocrine cells could not be detected in the mucosa of large intestine (Fig. 2H).

DISCUSSION

Over the last year, CART containing structures have been demonstrated in different organs, and different functions of this peptide have been

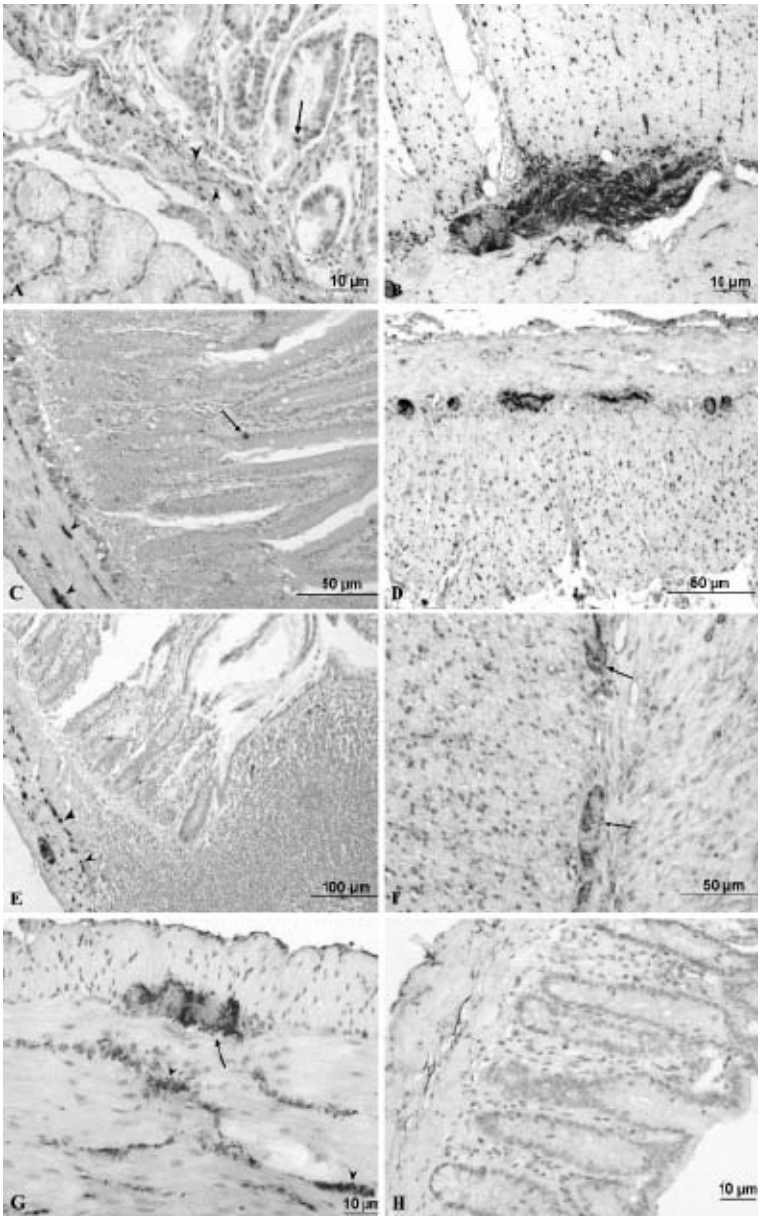

Fig. 2. *Immunoreactivity for CART in the wall of small and large intestine. (**A, B**) wall of the duodenum; neuroendocrine cells (arrow), nerve fibers in muscularis mucosa (arrowheads) and nerve fibers within the muscle layers passing parallel to the smooth muscle fibers and neuronal bodies and fibers staining in the myoenteric plexus (**C, D**) wall of the jejunum; single endocrine cells (arrow), nerve fibers innervating muscle cells (arrowheads) and numerous myoenteric plexus in the muscularis externa (**E, F**) all thickness of ileum wall, large nerve trunk (arrowheads), nerve fibers and ganglia in the muscularis externa (arrows) (**G, H**) large intestine; dense and thick nerve fibers containing CART in the myoenteric ganglia (arrow) and circular layer of muscularis externa (arrowheads), no CART immunoreactive structures in the mucosa and submucosa.*

proposed but, so far, very little is known about CART expression and functions in man. In this study we attempted to present, for the first time, CART-IR structures in all the parts of the human alimentary tract. In the presented report, the most abundant occurrence of the CART peptide was observed in neuronal elements, with regards to all the studied parts of the human alimentary tract. The majority of CART-IR fibers and nerve cell bodies were detected in myenteric ganglia and CART-containing nerve fibers

innervating the external muscle layers while in the mucosa, the submucosa and the submucosal ganglia, the CART peptide was found in the duodenum and stomach, and only rarely in the remaining parts of the small intestines.

Alimentary tract activities, such as peristalsis and secretion, are controlled and coordinated by neuronal reflexes, involving both extrinsic and intramural neurons and endocrine cells. The myenteric and submucous plexus constitute the two main collections of nerve cell bodies within the alimentary tract wall (10). It is known that the gastrointestinal neurons constitutes an adaptive and plastic system, but also vulnerable to lesions and that any disturbances of this system may be of pathogenic importance in functional diseases of the alimentary tract. Prokunina-Olsson and Hall (35) suggest that CART may play an important role, related to the brain-islet-gut regulation of metabolism. The universality of CART prevalence in numerous organs and a broad spectrum of its different functions indicate that this peptide may have a considerable position in the regulation of systemic homeostasis. Therefore, the knowledge on the distribution of CART immune positive structures in a healthy human organism may turn out necessary, both for further studies and a proper evaluation of changes, associated with various pathologies and diseases of the alimentary tract. Unfortunately, there are problems, connected with samples gaining from healthy subjects.

In the current study, CART peptide was detected particularly in the myenteric neurons and CART-IR fibers were abundant within ganglia and in the nerve fibers innervating the muscular layers. This remains analogous with the observations in the gastrointestinal tract of rats, guinea pigs and pigs, in which CART is widely expressed in the enteric nervous system with a similar distribution pattern as in the human alimentary tract (11–13, 30).

To date, very little is known about the presence and the functional role of the CART peptide in the human gastrointestinal tract. Preliminary studies of human tissues (large intestine), obtained during surgery, revealed innervation of CART-immunoreactive fibers, similar to that in our observations in the same part of the intestine. Thus, a dense nerve fiber network, particularly in smooth muscles and myenteric ganglia, and intrinsic CART-IR nerve cell bodies were confirmed (32).

Regarding the human alimentary tract, CART was for the first time demonstrated in large intestine sections from patients with Hirschprung's disease, in which, disorders of gastrointestinal motility demonstrated the presence of scarce CART immunoreactive nerve fibers in the muscular layer of intestinal wall. That picture differed from the one, obtained in parallel studies of intestine sections, unaffected by pathological changes, where the presence of numerous CART-immune positive cells and nerve fibers was demonstrated in the muscular layer of intestinal wall, especially in myenteric ganglia (32).

The quantity and layout of structures, which demonstrated CART presence in the large intestine wall, as observed in our study, were close to the values reported by Gunnarsdóttir et al. (33), regarding the pathologically unchanged intestine sections. In another study of biopsy sections from young patients with ulcerating colitis, an evident increase of CART-IR structures was demonstrated in the large intestine wall vs. patients in the control group (33). Following these observations, one may conclude with the assumption that a significant role of CART in pathological states of the human gastric tract can be assumed (33).

The topographic distribution of CART peptide-containing nerve fibers in the muscle layer and of the CART-IR nerve cell bodies in the myenteric ganglia in man was found to be similar to that, previously described in pigs (13, 30), guinea pigs (12) and rats (11).

The localization of CART peptide in the myenteric neurons and nerve fibers in the smooth muscle layers in human and animal subjects suggests CART to have a functional role in gastrointestinal motility, possibly as a modulator of neurohormonal functions (33).

In the mucosa and submucosa we detected CART-immunopositive nerve fibers in the duodenum and only rarely in the remaining parts of the small intestine or in the stomach. No CART peptide was found in those parts of the large intestine wall.

The distribution of CART in the mucosa or submucosa of the human alimentary tract differed somewhat from that in the porcine gastrointestinal tract, where CART-IR is usually more frequently

detected (13, 30). In our studies, a moderate occurrence of the CART peptide was observed in duodenal mucosa, while merely single, CART-containing fibers were observed in the other alimentary tract sections. This differed from findings by Ekblad et al. (11), who observed moderate number of CART-IR nerve fibres in rat's stomach We were able to detect some CART-containing endocrine cells in the GI-tract (gastrointestinal tract), especially numerous in the antrum. Similar distribution was observed in rats where CART was also present in great propotion of G-cells within gastric antrum. On the other hand, our findings are contradiction with results of Wierup et al., who noted lack of CART in G-cells within mice's stomach (11). Our results are in contrast to those of Ekblad, who reported no CART expressing endocrine cells in either human or porcine intestine (13, 33). CART expression in neuroendocrine cells indicate a hormonal role of the gastric CART peptide.

A number of neuropeptides, that were initially discovered in the brain, have subsequently been shown to reveal their activity also in the digestive tract. The findings of the reported study support the concept that neuropeptides found in the brain, have often significant regulatory effects upon tissues of the gastrointestinal tract. The CART peptide may be the newest brain–digestive tract neuropeptide with activity in both sites.

The role of CART peptides in the gastrointestinal tract is still somewhat enigmatic.

Abundant CART-IR neuronal elements are present particularly in smooth muscles and myenteric ganglia in all the parts of GI-tract, as demonstrated in rats, guinea-pigs, pigs and man and can suggest a certain participation of the peptide in the internal regulation of intestinal peristalsis and stomach spasms and emptying and, in this way, may imply its role in chyme flow control.

This suggestion is supported by its coexistence with many, biologically active substances, which control gastric motor activity, such as the calcitonin gene-related peptide (CGRP) (30) or the vasoactive intestinal peptide (VIP) (11-13, 30). The location of CART in VIP containing neurons suggests that CART is involved in GI-motor functions, since VIP-containing neurons are known to play some role in motor control (13). Okumura et al. (37) reported that centrally injected CART peptide reduced colonic motility, inhibited gastric emptying and gastric acid secretion. CART still remains a rather little known neuropeptide and further physiological studies are needed to reveal in detail its mechanisms of action and its physiological relevance in the alimentary tract.

Hopefully, the knowledge, acquired throughout our study, may lead to a more complete and comprehensive understanding of the function or may lead to an identification of other, still unknown, roles of CART in physiological and pathological conditions.

REFERENCES

1. Spiess J, Villarreal J, Vale W. Isolation and sequence analysis of a somatostatin-like polypeptide from ovine hypothalamus. Biochemistry 1981; 20:1982-8.
2. Douglass J, McKinzie AA, Couceyro P. PCR differential display identifies a rat brain mRNA that is transcriptionally regulated by cocaine and amphetamine. J Neurosci 1995; 15:2471-81.
3. Stachowicz M, Mazurek U, Nowakowska-Zajdel E, Niedworok E, Fatyga E, Muc-Wierzgon M. Leptin and its receptors in obese patients with colorectal cancer. J Biol Regul Homeost Agents 2010; 24:287-95.
4. Kuhar MJ, Dall Vechia SE. CART peptides: novel addiction- and feeding-related neuropeptides. Trends Neurosci 1999; 22:316-20.
5. Elmquist JK, Elias CF, Saper CB. From lesions to leptin: hypothalamic control of food intake and body weight. Neuron 1999; 22:221-32.
6. Davidowa H, Li Y, Plagemann A. The main effect of cocaine- and amphetamine-regulated transcript (CART) peptide on hypothalamic neuronal activity depends on the nutritional state of rats. Neuro Endocrinol Lett 2005; 26:29-34.
7. Vicentic A, Jones DC. The CART (cocaine- and amphetamine-regulated transcript) system in appetite and drug addiction. J Pharmacol Exp Ther 2007; 320:499-506.
8. Couceyro PR, Evans C, McKinzie A et al. Cocaine- and amphetamine-regulated transcript (CART) peptides modulate the locomotor and motivational properties of psychostimulants. J Pharmacol Exp

Ther 2005; 315:1091-100.
9. Dun NJ, Dun SL, Kwok EH, Yang J, Chang J. Cocaine- and amphetamine-regulated transcript-immunoreactivity in the rat sympatho-adrenal axis. Neurosci Lett 2000; 283:97-100.
10. Ekblad E. CART in the enteric nervous system. Peptides 2006; 27:2024-30.
11. Ekblad E, Kuhar M, Wierup N, Sundler F. Cocaine- and amphetamine-regulated transcript: distribution and function in rat gastrointestinal tract. Neurogastroenterol Motil 2003; 15:545-57.
12. Ellis LM, Mawe GM. Distribution and chemical coding of cocaine- and amphetamine-regulated transcript peptide (CART)-immunoreactive neurons in the guinea pig bowel. Cell Tissue Res 2003; 312:265-74.
13. Wierup N, Gunnarsdóttir A, Ekblad E, Sundler F. Characterisation of CART-containing neurons and cells in the porcine pancreas, gastro-intestinal tract, adrenal and thyroid glands. BMC Neurosci 2007; 8:51.
14. Koylu EO, Couceyro PR, Lambert PD, Ling NC, DeSouza EB, Kuhar MJ. Immunohistochemical localization of novel CART peptides in rat hypothalamus, pituitary and adrenal gland. J Neuroendocrinol 1997; 9:823-33.
15. Jensen PB, Kristensen P, Clausen JT et al. The hypothalamic satiety peptide CART is expressed in anorectic and non-anorectic pancreatic islet tumors and in the normal islet of Langerhans. FEBS Lett 1999; 447:139-43.
16. Bai F, Sözen MA, Lukiw WJ, Argyropoulos G. Expression of AgRP, NPY, POMC and CART in human fetal and adult hippocampus. Neuropeptides 2005; 39:439-43.
17. Schwartz MW. Brain pathways controlling food intake and body weight. Exp Biol Med (Maywood) 2001; 226:978-81.
18. Schwartz MW, Woods SC, Porte D Jr, Seeley RJ, Baskin DG. Central nervous system control of food intake. Nature 2000; 404:661-71.
19. Lambert PD, Couceyro PR, McGirr KM, Dall Vechia SE, Smith Y, Kuhar MJ. CART peptides in the central control of feeding and interactions with neuropeptide Y. Synapse 1998; 29:293-8.
20. Rohner-Jeanrenaud F, Craft LS, Bridwell J et al. Chronic central infusion of cocaine- and amphetamine-regulated transcript (CART 55-102): effects on body weight homeostasis in lean and high-fat-fed obese rats. Int J Obes Relat Metab Disord 2002; 26:143-9.
21. Asakawa A, Inui A, Yuzuriha H, Nagata T, Kaga T, Ueno N, Fujino MA, Kasuga M. Cocaine-amphetamine-regulated transcript influences energy metabolism, anxiety and gastric emptying in mice. Horm Metab Res 2001; 33:554-8.
22. Okumura T, Yamada H, Motomura W, Kohgo Y. Cocaine-amphetamine-regulated transcript (CART) acts in the central nervous system to inhibit gastric acid secretion via brain corticotropin-releasing factor system. Endocrinology 2000; 141:2854-60.
23. Bannon AW, Seda J, Carmouche M, Francis JM, Jarosinski MA, Douglass J. Multiple behavioral effects of cocaine- and amphetamine-regulated transcript (CART) peptides in mice: CART 42-89 and CART 49-89 differ in potency and activity. J Pharmacol Exp Ther 2001; 299:1021-6.
24. Kimmel HL, Thim L, Kuhar MJ. Activity of various CART peptides in changing locomotor activity in the rat. Neuropeptides 2002; 36:9-12.
25. Kimmel HL, Gong W, Vechia SD, Hunter RG, Kuhar MJ. Intra-ventral tegmental area injection of rat cocaine and amphetamine-regulated transcript peptide 55-102 induces locomotor activity and promotes conditioned place preference. J Pharmacol Exp Ther 2000; 294:784-92.
26. Kask A, Schiöth HB, Mutulis F, Wikberg JE, Rägo L. Anorexigenic cocaine- and amphetamine-regulated transcript peptide intensifies fear reactions in rats. Brain Res 2000; 857:283-5.
27. Hunter RG, Kuhar MJ. CART peptides as targets for CNS drug development. Curr Drug Targets CNS Neurol Disord 2003; 2:201-5.
28. Cowles RA, Segura BJ, Mulholland MW. Stimulation of rat pancreatic exocrine secretion by cocaine- and amphetamine-regulated transcript peptide. Regul Pept 2001; 99:61-8.
29. Wierup N, Björkqvist M, Kuhar MJ, Mulder H, Sundler F. CART regulates islet hormone secretion and is expressed in the beta-cells of type 2 diabetic rats. Diabetes 2006; 55:305-11.
30. Gonkowski S, Burliński P, Skobowiat C, Majewski

M, Arciszewski MB, Radziszewski P, Całka J. Distribution of cocaine- and amphetamine-regulated transcript-like immunoreactive (CART-LI) nerve structures in the porcine large intestine. Acta Vet Hung 2009; 57:509-20.

31. Arciszewski MB, Barabasz S, Skobowiat C, Maksymowicz W, Majewski M. Immunodetection of cocaine- and amphetamine-regulated transcript in the rumen, reticulum, omasum and abomasum of the sheep. Anat Histol Embryol 2009; 38:62-7.
32. Gunnarsdóttir A, Wierup N, Larsson LT, Kuhar MJ, Ekblad E. CART-peptide immunoreactivity in enteric nerves in patients with Hirschsprung's disease. Eur J Pediatr Surg 2007; 17:184-9.
33. Gonkowski S, Kamińska B, Burliński P, Kroll A, Całka J. The influence of drug-resistant ulcerative colitis on the number of cocaine- and amphetamine-regulated transcript peptide-like immunoreactive (CART-LI) mucosal nerve fibres of the descending colon in children. Przeglad Gastroenterologiczny 2009; 4:147-51.
34. Herman GE, Elfont EA. The taming of immunohistochemistry: the new era of quality control. Biotech Histochem 1991; 66:194-9.
35. Prokunina-Olsson L, Hall JL. Evidence for neuroendocrine function of a unique splicing form of TCF7L2 in human brain, islets and gut. Diabetologia 2010; 53:712-6.

THE EFFECT OF PGE ADMINISTRATION ON THE ACTIVITY OF OXIDATIVE SYSTEM IN ERYTHROCYTES AND PLATELETS DURING ISCHEMIA REPERFUSION INJURY AND ON POSTOPERATIVE RENAL FUNCTION IN PATIENTS UNDERGOING OPEN ABDOMINAL AORTIC ANEURYSM RECONSTRUCTION

W. BŁOGOWSKI[1,2], B. DOŁĘGOWSKA[1], E. PIKUŁA[3], P. GUTOWSKI[3] and T. STARZYŃSKA[2]

[1]Department of Medical Analytics, Pomeranian Medical University in Szczecin, Poland;
[2]Department of Gastroenterology, Pomeranian Medical University in Szczecin, Poland;
[3]Department of Vascular Surgery and Angiology, Pomeranian Medical University in Szczecin, Poland

Received January 3, 2012 – Accepted June 14, 2012

Postoperative decline of renal function remains a common and unpredictable complication after abdominal aortic aneurysm (AAA) reconstruction. The oxidative stress that occurs during perioperative ischemia/reperfusion injury (I/R) may contribute to the development of this complication. In this study, the influence of intraoperative prostaglandin E (alprostadil) administration on erythrocyte and platelet antioxidants as well as postoperative kidney function modulation were verified. AAA patients were randomly divided into control and study/alprostadil groups. Blood samples were collected directly before aortic clamping and 5 min after aortic declamping. Superoxide dismutase, catalase, glutathione, glutathione peroxidase (GPx), and glutathione transferase (GST) were measured using spectrophotometry. During I/R, the activity of catalase (57.14±30.65 *vs* 128.35±91.94 U/mg protein; P < 0.009), GPx (0.21±0.18 *vs* 0.35±0.21 mU/g protein; P = 0.028), and GST (217.49±101.39 *vs* 310.66±88.86 mU/g protein; P = 0.0006) significantly increased in the control group. GST activity before the aortic clamping was significantly lower in the study/alprostadil group (2.84±2.28 *vs* 3.48±2.30 U/g Hb; P = 0.05). The activity of the selected antioxidants proved to be of a diagnostic value for predicting postoperative decline in renal function. In conclusion, during I/R after AAA reconstruction, activation of various erythrocyte and platelet antioxidants occurs. Perioperative administration of alprostadil is associated with disruption of this activation.

The development of systemic inflammatory response syndrome (SIRS) or organ failure after abdominal aortic aneurysm (AAA) repair operation remains a quite common complication that affects operated patients' early- and long-term outcomes (1). This tendency is at least partially caused by the fact that the need for aortic clamping occurs during AAA open repair surgery, which leads to temporary ischemia of the lower half of the body that profoundly affects the function of various organs, including the kidneys, by increasing systemic oxidative stress. In earlier studies, even temporary ischemic/oxidative injury initiated dramatic deterioration of kidney function in 9% of AAA patients, which ultimately

Key words: aortic aneurysm abdominal, alprostadil, kidney, reperfusion injury, oxidative stress

Mailing address: Wojciech Błogowski, MD
Department of Medical Analytics,
ul. Powstańców Wielkopolskich 72,
70-111 Szczecin, Poland
Tel.: +48 91 466 1490
Fax: +48 91 466 1492
e-mail: drannab@wp.pl

0393-974X (2012)

DISCLOSURE: ALL AUTHORS REPORT NO CONFLICTS OF INTEREST RELEVANT TO THIS ARTICLE.

resulted in renal failure (2, 3). Unfortunately, to date, neither biochemical nor molecular markers have been identified that could be used in routine clinical practice to predict such declines in postoperative kidney function.

Renal cells are very susceptible to the oxidative stress that accompanies both phases of ischemia/reperfusion (I/R) injury (4, 5). Therefore, to survive such injury, these cells possess a wide armament of protective mechanisms that enable modulation or limitation of unfavorable conditions in a local or systemic manner. One such mechanism is the ability to synthesize active metabolites of arachidonic acid called eicosanoids, such as thromboxanes, hydroxyeicosatetraenoic acids, and prostaglandins (PGs) (6-10). Unfortunately, although several *in vitro* or experimental animal models have proven the potential beneficial influence of PG action on kidney metabolism, perioperative use of PGE or PGI analogs during AAA surgery to prevent tissue ischemia and postoperative declines in renal function yielded conflicting results (11-14).

Other researchers and we have already demonstrated that red blood cells (RBCs) and platelets possess a wide panel of antioxidative enzymes, the actions of which during renal I/R injury may significantly contribute to the limitation of "systemic" oxidative stress and be associated with postoperative clinical kidney (allograft) function (15, 16). Interestingly, the RBC and platelet antioxidative armaments may also be strongly influenced by PGE action. In particular, during various injurious stimuli associated with I/R (such as oxidative stress), this eicosanoid exerts a significant influence on cellular metabolism, as PGE action is very closely related to intracellular antioxidant levels, primarily glutathione-related compounds (17, 18).

Unfortunately, no studies to date have addressed the question of whether the activity of RBC and platelet oxidative systems during I/R injury may influence postoperative kidney function in patients undergoing AAA repair operation or whether perioperative PGE administration may modulate this molecular response. Hence, this study was designed to: (i) comprehensively analyze the changes in the activities of erythrocyte and platelet antioxidative systems during I/R injury associated with AAA repair operation, (ii) determine whether perioperative administration of a PGE analog (alprostadil) affects the antioxidative response to I/R injury after AAA operation, and iii) verify whether the perioperative activity of these enzymes is associated with postoperative kidney function in patients who undergo AAA reconstruction. Our hypotheses were that the significant changes in the perioperative activities of the RBC and platelet antioxidative armaments occuring during I/R injury are influenced by alprostadil administration, and they are associated with postoperative clinical kidney function in patients who undergo AAA repair operation.

MATERIALS AND METHODS

Patients

After providing informed consent, 68 consecutive patients (54 men and 14 women) with the American Society of Anesthesiologists II and III operative risk score were included in this randomized and prospective study. The patients were randomly divided into 2 groups: a control group of 34 patients underwent conventional AAA repair operation and a study (alprostadil) group of 34 individuals with AAA who were additionally given the PGE_1 analog alprostadil (Prostavasin, Schwarz Pharma AG, Germany) during AAA surgery. Constant intravenous administration of alprostadil (13 $ng \cdot kg^{-1} \cdot min^{-1}$) started after anesthesia was induced and was continued until the end of surgery. Individuals with a history of myocardial infarction (<6 months prior to surgery), active peptic or duodenal ulcers, or liver or renal failure as well as those who qualified for endovascular aneurysm repair operations were excluded from the study. The general characteristics of the patients and surgical setting are presented in Table I.

Methods

Blood samples (5 mL each) were collected perioperatively from the superior vena cava directly before aortic clamping (A) and 5 min after aortic declamping (B). The samples were centrifuged (10 min; 20°C; 664 g). Erythrocytes, platelet-poor plasma (PPP), and platelet-rich plasma (PRP) were prepared and separated as previously described (6, 15, 16). Isolated erythrocytes were washed 3 times with 0.9% NaCl-buffered solution. Platelet sediments were washed twice and then suspended in Tyrode buffer (1 mL; pH 7.4). The erythrocytes, PPP, and PRP were then frozen at -80°C and stored according to previously published recommendations until the assays were performed (19, 20).

Measurement of the antioxidant systems of erythrocytes and platelets

Before analyses, erythrocytes and platelets were

thawed. Washed erythrocyte/platelet lysates were diluted with distilled water and cooled to 4°C. Activities and levels of the erythrocyte antioxidants, i.e., superoxide dismutase (SOD), catalase, glutathione, glutathione peroxidase (GPx), and glutathione transferase (GST) were measured using Bioxytech kits (Oxis Research, Portland, OR, USA) and an ultraviolet/visible (UV/VIS) Lambda 40 spectrophotometer (Perkin Elmer, Wellesley, MA, USA) as previously described (15, 16, 21, 22) or as per the manufacturer's instructions. Briefly, the erythrocyte, PPP, and PRP suspensions were defrosted at room temperature (37°C). The obtained lysates were then diluted, mixed with precipitating solutions, incubated (5 min, 4°C), and centrifuged (550 g; 10 min). The supernatants were diluted with phosphoric buffer (pH 7.9), DTNB was added, and the mixture was incubated (15 min, 25°C). Detection wavelengths of λ = 412 nm for GSH, λ = 322 nm for SOD, λ = 240 nm for catalase, λ = 340 nm for GPx and GST analyses were applied. The activities of the analyzed enzymes were calculated per 1 g of Hb in erythrocytes or per 1 g of protein in platelet lysates. Hemoglobin levels were assayed using Drabkin's method, and protein concentrations were analyzed using Lowry's method. Analyses of the concentrations of examined enzymes were performed using a UV/VIS Lambda 40 spectrophotometer (Perkin-Elmer).

Estimation of kidney function

Serum creatinine levels were measured on the preoperative and fifth postoperative days, and glomerular filtration rate (GFR) values were calculated using the Cockroft-Gault formula.

Statistical analysis

To determine the distribution of variables, Shapiro–Wilk's test was used. For comparison of the mean parameter values between the examined groups, Student's *t*-test was used (for normally distributed variables). Abnormally distributed variables were log transformed. If normal distribution was achieved, variables were also compared using Student's *t*-test. However, if this transformation did not change the distribution, the Mann-Whitney test was performed. Differences between concentrations/activity of analyzed parameters in consecutive minutes of reperfusion were assessed by Wilcoxon`s paired test (not normally distributed parameters) or paired T test (normally distributed variables). To evaluate the effect(s) of continuous variables on post-operative renal function, multivariate regression analyses were performed with a stepwise selection method. Variables excluded from the initial model were re-entered individually to exclude residual confounding. Receiver operating characteristics (ROC) curves were constructed for all analyzed parameters as diagnostics for changes in post-operative kidney function, and the area under each ROC curve (AUC) was calculated. Statistical analysis was performed using SPSS statistical analysis software. Statistical significance was defined when p values were less than 0.05.

This study protocol was approved by the Bioethical Committee of the Pomeranian Medical University in Szczecin, and patients provided informed written consent for participation.

RESULTS

Antioxidative responses of RBCs and platelets to I/R injury

Our study results demonstrated that after I/R injury in AAA patients in the control group, no significant differences in perioperative activities or levels of erythrocyte SOD, GSH, GPx, or GST were observed (Table II). Interestingly, catalase was the only antioxidant that seemed to be significantly "affected" by the presence of the reperfusion phenomenon. Its activity significantly increased within the reperfusion period in both RBCs and platelets derived from the control individuals (Tables II and III). Analogically to catalase, thrombocyte GPx and GST actions were significantly increased during the fifth minute of reperfusion (Table III). No statistically significant differences in the perioperative activities and levels of platelet SOD or GSH were detected in the control individuals.

Influence of alprostadil administration on RBC and platelet antioxidative responses to perioperative I/R

In our study, perioperative administration of alprostadil was associated with selected alterations in both RBC and platelet antioxidative responses to I/R. Namely, individuals from the study/alprostadil group had significantly lower RBC GST activity before aortic clamping, and this significantly increased during the reperfusion period, reaching comparable levels to those detected in the control individuals (Table II). Moreover, while RBC and platelet catalase activities significantly increased during the reperfusion period in the control individuals, such tendencies were not observed in the patients who received perioperative administration of alprostadil. Patients in the study (alprostadil) group had significantly lower platelet catalase activity during the fifth minute of reperfusion compared to that of the

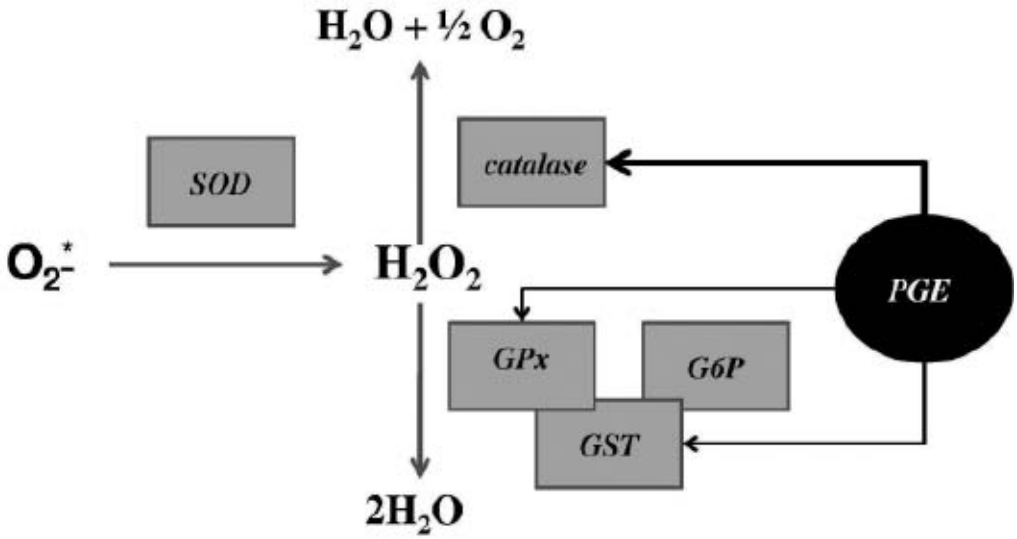

Fig. 1. *Simplified illustration of enzymatic pathways of free radicals dismutation. Superoxide radical is neutralized by superoxide dismutase, leading to hydrogen peroxide synthesis. Afterwards, two possible pathways of hydrogen peroxide neutralisation exists – either via catalase activity or via glutathione-related compounds i.e. mainly by glutathione peroxidase that cooperates with glutathione transferase and glucose-6-phosphate dehydrogenase. Glutathione, itself, is the most important "stabiliser" of intracellular oxidative balance. According to the results of our study peri-operative administration of prostaglandin E analogue results in limitation of a peri-operative increase in catalase activity in both – erythrocytes and platelets (bold black arrow), as well as, in GST and GPx activity (in platelets only – thinner black arrow). SOD: superoxide dismutase; GPx: glutathione peroxidase; GST: glutathione transferase; G6P: glucose-6-phosphate dehydrogenase; O_2^{*-}: superoxide radical ; H_2O_2: hydrogen peroxide; PGE: prostaglandin E*

control individuals (128.35±91.94 *vs* 57.75±49.47 U/mg protein; P = 0.006). Perioperative administration of the PGE analog was also associated with a lack of a significant increase in the perioperative activities of platelet GSH and GPx; however, the activities of these antioxidants were statistically comparable between the examined groups.

Perioperative changes in clinical renal function and their association with the antioxidative responses of platelets and erythrocyte

The next question we wanted to answer was whether the perioperative activities of erythrocyte and platelet antioxidants are associated with or may determine postoperative kidney function in patients subjected to open AAA reconstruction. In our analysis, we did not observe any significant differences in the GFR values measured prior to (88.36±12.15 *vs* 89.89±15.60 mL/min; P = 0.84) or 5 days after surgery (93.72±20.50 *vs* 93.46±18.46 mL/min; P = 0.60) between the groups; in addition, the GFR changes (expressed in our study by ΔGFR parameter) were comparable between the study and control individuals (Table I). However, GFR values increased slightly, although not significantly, in both groups (88.36±12.15 *vs* 93.72±20.50 mL/min, P = 0.35, and 89.89±15.60 *vs* 93.46±18.46 mL/min, P = 0.11, for the control and the study group, respectively).

The results of multivariate regression model analysis performed in the control group (on which no "outside" influence on the I/R injury scenario was exerted) demonstrated that perioperative changes in renal function in AAA patients were strongly associated with antioxidative activity of erythrocyte and platelet enzymes. Namely, RBC GST activity before aortic clamping ($\beta = 0.51$; $R^2 = 0.26$; $P < 0.03$) and after aortic declamping ($\beta = 0.61$; $R^2 = 0.37$; $P = 0.006$) as well as platelet GSH and GPx activities before ischemia ($\beta = 0.69$ and $\beta = 0.51$, respectively;

Table I. *General characteristic of surgical procedure and of individuals enrolled in the study (means ± SD).*

	Control group	Study group	P
Age (years)	68.95±4.94	66.3±8.29	0.28
Gender (M-men/W-women)	(26-M/8-W)	(28-M/6-W)	0.62
Weight (kg)	81.21±12.56	82.43±13.92	0.85
GFR 1 (mL/min)	88.36±12.15	89.89±15.60	0.84
GFR 2 (mL/min)	93.72±20.50	93.46±18.46	0.60
Δ GFR (mL/min)	5.36±12.59	3.57±13.65	0.61
Diuresis (L/24 h)	1.52±0.95	1.82±0.78	0.21
Aneurysm size (mm)	55.47±11.14	56.91±7.24	0.79
Ischemia time (min)	40.74±18.44	40.17±16.90	0.82
Duration of surgical procedure (min)	127.11±40.67	119.52±37.69	0.75
MAP during aortic clamping (mmHg)	94.21±13.26	93.13±13.38	0.76
CVP during aortic clamping (mmHg)	10.05±2.93	10.04±3.57	0.52
MAP during aortic declamping (mmHg)	71.68±11.56	73.96±10.74	0.31
CVP during aortic declamping (mmHg)	10.47±2.80	10.52±2.87	0.90
Length of hospitalization (days)	7±2	7±1	0.54

GFR 1 and 2 – Glomerular Filtration Rate measured one day prior to surgery (1) and on the fifth post-operative day (2); ΔGFR: difference between GFR values measured on the fifth post-operative day and one day prior surgery. MAP: mean arterial pressure; CVP: central venous pressure; P: level of significance.

$R^2 = 0.72$; $P < 0.0001$) were proven to be strongly associated with perioperative changes in GFR levels.

Finally, we performed a pilot analysis to determine whether perioperative measurements of the activities of RBC and platelet antioxidants may offer some clinical diagnostic values for the prediction of postoperative kidney function among AAA patients. To realize this aim, we divided our patients from the examined groups (separately) into 2 outcome subgroups. If the postoperative GFR value was not <95% of the preoperative GFR value, then the patient was assigned to the "normal/increase" outcome subgroup (23 individuals from the control group and 21 from the study group met this criterion). However, if postoperative GFR values decreased to <95% of the preoperative GFR level, the individual was assigned to the "decrease" outcome subgroup (11 patients from the control group and 13 from the study group met this criterion).

Our pilot analysis demonstrated that among all examined parameters (both clinical and molecular) erythrocyte GST activity was the strongest candidate

Table II. *Mean activity/levels of erythrocytes` anti-oxidants and statistical analysis of examined parameters (means ± standard deviation).*

Parameter	Control group			Study group		
	A	B	P A vs B	A	B	P A vs B
SOD [U/gHb]	1462.35±314.86	1373.77±321.17	0.241	1565.27±690.06	1364.30 ± 341.06	0.181
Catalase [U/gHb]	5140.36±934.05	5592.71±1048.58	**0.049**	5311.99±767.37	5541.41 ± 936.86	0.236
GSH [mmol/gHb]	0.034±0.013	0.035±0.011	0.670	0.028±0.007	0.029 ± 0.006	0.094
GPx [U/gHb]	2.13±1.01	1.97±0.94	0.245	2.27±1.31	1.99 ± 1.15	0.215
GST [U/gHb]	3.80±1.73	4.10±2.29	0.117	2.84±2.28*	3.48 ± 2.30	**0.003**

*SOD: superoxide dismutase; GSH: glutathione; GPx: glutathione peroxidase; GST: glutathione transferase; A: before aortic clamping; B – 5th minute of reperfusion; P: level of significance; *P=0.05 (study vs control group)*

Table III. Mean activity/levels of platelets` anti-oxidants and statistical analysis of examined parameters (means ± standard deviation).

Parameter	Control group			Study group		
	A	B	P A vs B	A	B	P A vs B
SOD [U/mg Protein]	1315.13±538.78	1250.63±897.88	0.316	1308.81±984.59	861.89 ± 676.57	0.784
Catalase [U/mg Protein]	57.14±30.65	128.35±91.94	**0.009**	43.85±39.20	57.75 ± 49.47*	0.842
GSH [mmol/g Protein]	24.12±17.91	21.83±16.91	0.653	25.16±22.68	25.49 ± 21.92	0.825
GPx [mU/g Protein]	0.21±0.18	0.35±0.21	**0.028**	0.36±0.34	0.37 ± 0.32	0.512
GST [mU/g Protein]	217.49±101.39	310.66±88.86	**0.0006**	269.62±133.40	266.31 ± 98.23	0.125

*SOD: superoxide dismutase; GSH: glutathione; GPx: glutathione peroxidase; GST: glutathione transferase; A: before aortic clamping; B: 5th minute of reperfusion; P: level of significance; * P=0.006 (study vs control group)*

Table IV. *Diagnostic value of glutathione transferase and clinical parameters for prediction of post-operative kidney function in control and study groups.*

Parameter	GFR(1)	Creatinine(1)	Age	Weight	**GST(A)**
Control group					
Area under curve	0.72	0.51	0.55	0.64	**0.86**
P	0.14	0.93	0.73	0.34	**0.01**
95% CI	0.47-0.97	0.20-0.82	0.26-0.85	0.33-0.95	**0.69-0.96**
Study group					
Area under curve	0.36	0.52	0.56	0.27	**0.77**
P	0.26	0.85	0.64	0.07	**0.03**
95% CI	0.13-0.60	0.28-0.77	0.32-0.80	0.05-0.50	**0.56-0.97**

GFR(1) and creatinine(1) – pre-operative glomerular filtration rate and creatinine levels (respectively); GST: glutathione transferase; AUC: area under curve; P: level of significance; CI: confidence interval

for such a marker (Table IV). Since alprostadil administration resulted in decreased GST activity in patients from the study group in the current study, we decided to estimate this enzyme`s predictive value separately in both groups. ROC analysis proved that GST activity measured directly before aortic clamping possesses a powerful potential in differentiating "normal/increase" from "decrease" outcomes. However, perioperative administration of alprostadil decreases its predictive value. Interestingly, in our study, GST activity proved to be a much better candidate marker of postoperative kidney function than previously suggested parameters used in a clinical setting, such as patient age, weight, or preoperative GFR level. The lower 95% confidence interval bound value of all of these parameters was <0.50 in our study; in addition, their area under the curve values were much lower than those of the newly introduced parameter and did not reach significant levels (Table IV).

DISCUSSION

The I/R injury that accompanies AAA repair operation contributes to postoperative morbidity and mortality of the patients. Among several factors that are known to determine I/R injury intensity, the action of free radicals is especially highlighted, since oxidative stress exerts unfavorable influence on ischemic cells, causing peroxidation of cellular membrane phospholipids. It also stimulates the synthesis of proinflammatory cytokines (such as TNFα) that accelerate ischemic cell destruction, finally leading to SIRS, thrombotic complications, or organ failure.

Several studies have already suggested that intraoperative administration of various antioxidants may significantly modulate perioperative oxidative stress intensity and translate to kidney protection. Interestingly, some authors have also demonstrated that RBC and platelet metabolism may strongly influence the outcome of AAA patients (23, 24). Hence, in this study, we decided to combine these observations and accepted the challenge to comprehensively examine the endogenous antioxidative responses of RBCs and platelets to I/R injury that occurs during AAA reconstruction and verify its potential association with postoperative kidney function in AAA patients.

In the present study, we found that several intracellular RBC and platelet antioxidants become activated during I/R injury following AAA reconstruction. Similar to our previous studies conducted in a renal transplantation setting, platelet antioxidative responses seemed to be more "active" than those of erythrocytes since the activities of most platelet antioxidants increased during reperfusion injury (15, 16). However, what we additionally observed was the fact that perioperative PGE administration inhibited this endogenous antioxidative protection, as it was associated with a lack of a perioperative increase in the activity of glutathione-related compounds of the platelet antioxidative armament as well as of catalase activity in both cell types (Figure 1). We hypothesize that this effect of PGE may be exerted via an inhibited platelet–endothelium interaction since it was demonstrated in previous studies that clinical doses of PGE analogs significantly influence platelet metabolism due to inhibition of cyclooxygenase pathways and intracellular adenosine diphosphate-dependent signaling (25-27). These observations have not been verified in terms of RBC activity. Nevertheless, although the exact mechanisms responsible for this phenomenon remain to be fully elucidated, our study demonstrated that in the actual clinical setting, RBC and platelet antioxidative responses can be modulated using biochemical compounds such PGE analogs. Our clinical observations are also in agreement with the results of a recently published experimental study concerning the influence of PGE on AAA development in which the authors demonstrated that in $LDLR^{-/-}$ mice with AAA, PGE seems to be one of the main causes of intensive oxidative stress occurring in both a systemic and local manner (28). Our study indirectly confirms these previous observations and indicates that this unfavorable influence of PGE may be also exerted by systemic disruption of erythrocyte and platelet antioxidative responses, since both free radical scavenging pathways (Figure 1) were affected by alprostadil supplementation. This may also explain the results of a clinical study performed by Gabriel and colleagues (12) in which these authors observed intensified disruption of cellular oxygen use in patients undergoing AAA reconstruction when PGE1

intravenous treatment was also administered.

From the clinical point of view, it is essential to highlight that in our study, the activities of RBC and platelet antioxidative systems were strongly associated with perioperative changes in kidney function, and according to our pilot analysis, some antioxidants possess promising potential than the currently used parameters to serve as better clinical markers of postoperative kidney function in AAA patients (29, 30). However, disruption of this antioxidative response by perioperative administration of PGE analogs did not directly translate into significantly worse postoperative kidney function in patients who underwent AAA reconstruction. This observation may be explained by the fact that we administered relatively small doses of alprostadil in our study compared to the doses used by others (12, 13).

Various experimental studies have demonstrated that PGE action seems to be strongly dose- rather than time-dependent (31, 32). We speculate that the administration of higher doses of PGE analogs will result in a much more pronounced inhibition of the antioxidative capacities of RBC and platelet and translate to a postoperative decline in renal function. This may also explain why conflicting results regarding the beneficial action of PGE supplementation on postoperative kidney function in AAA patients were reported by various studies (11-14). Nevertheless, our results are based on the analysis of a relatively small group of patients and must be verified in further experimental and clinical studies.

In summary, our study demonstrated the following: (i) perioperative upregulation of selected components of erythrocyte and platelet antioxidative systems occurs during I/R injury that is induced during AAA reconstruction; (ii) continuous perioperative PGE administration is associated with inhibition of the activity of selected erythrocyte and platelet antioxidative enzymes; and (iii) the observed molecular antioxidative responses of RBCs and platelets are associated with postoperative kidney function in patients undergoing AAA repair operation. Finally, the results of our pilot analysis suggest that RBC GST activity seems to possess promising potential for predicting the postoperative changes in kidney function associated with AAA reconstruction. Nevertheless, further studies are needed to validate its perioperative predictive potential.

REFERENCES

1. Bown MJ, Nicholson ML, Bell PR, Sayers RD. The systemic inflammatory response syndrome, organ failure, and mortality after abdominal aortic aneurysm repair. J Vasc Surg 2003; 37:600-6.
2. Vemuri C, Wainess RM, Dimick JB, Cowan JA Jr, Henke PK, Stanley JC, Upchurch GR Jr. Effect of increasing patient age on complications rates following intact abdominal aortic aneurysm repair in the United States. J Surg Res 2004; 118:26-31.
3. Powell RJ, Roddy SP, Meier GH, Gusberg RJ, Conte MS, Sumpio BE. Effect of renal insufficiency on outcome following infrarenal aortic surgery. Am J Surg 1997; 174:126-30.
4. Breggia AC, Himmelfarb J. Primary mouse renal tubular epithelial cells have variable injury tolerance to ischemic and chemical mediators of oxidative stress. Oxid Med Cell Longev 2008; 1:33-8.
5. Han HJ, Yoon BC, Park SH, Park JY, Oh YJ, Lee YJ, Park KM. Ginsenosides protect apical transporters of cultured proximal tubule cells from dysfunctions induced by H2O2. Kidney Blood Press Res 2002; 25:308-14.
6. Dołęgowska B, Błogowski W, Kędzierska K, Safranow K, Jakubowska K, Olszewska M, Rac M, Chlubek D, Ciechanowski K. Platelets arachidonic acid metabolism in patients with essential hypertension. Platelets 2009; 20:242-9.
7. Dołęgowska B, Błogowski W, Domanski L. Is it possible to predict the early post-transplant allograft function using 20-HETE measurements? A preliminary report. Transpl Int 2009; 22:546-53.
8. Jia Z, Person MD, Dong J, Shen J, Hensley SC, Stevens JL, Monks TJ, Lau SS. Grp78 is essential for 11-deoxy-16,16-dimethyl PGE2-mediated cytoprotection in renal epithelial cells. Am J Physiol Renal Physiol 2004; 287:F1113-24.
9. Dołęgowska B, Błogowski W, Safranow K, Domanski L, Jakubowska K, Olszewska M. Lipoxygenase-derived hydroxyeicosatetraenoic acids – novel

perioperative markers of early post-transplant allograft function? Nephrol Dial Transplant 2010; 25:2346-51.
10. Dołęgowska B, Błogowski W, Domanski L. Dynamics of thromboxane level changes during early phase of allograft reperfusion. Clin Transplant 2009; 23:716-22.
11. Dolegowska B, Pikula E, Safranow K, Olszewska M, Jakubowska K, Chlubek D, Gutowski P. Metabolism of eicosanoids and their action on renal function during ischaemia and reperfusion: the effect of alprostadil. Prostaglandins Leukot Essent Fatty Acids 2006; 75:403-11.
12. Gabriel A, Werba A, Mares P, et al. Influence of prostaglandin E1 on tissue ischemia during surgical repair of the abdominal aorta. J Cardiothorac Vasc Anesth 1996; 10:201-6.
13. Sako H, Hadama T, Miyamoto S, et al. Effect of prostaglandin E1 on ischemia-reperfusion injury during abdominal aortic aneurysm surgery. Surg Today 2006; 36:140-6.
14. Reiher L, Vosberg H, Sandmann W. Kidney protection in preventing post-ischemic renal failure during thoracoabdominal aortic aneurysm repair: does prostaglandin E1 together with cooling provide more protection than cooling alone? Vasa 2001; 30:21-3.
15. Domanski L, Dolegowska B, Safranow K, et al. Early phase of reperfusion of human kidney allograft does not affect an erythrocyte anti-oxidative system. Nephrology 2006; 11:467-70.
16. Dolegowska B, Blogowski W, Domanski L. Association between the perioperative antioxidative ability of platelets and early post-transplant function of kidney allografts. A pilot study. PLoS One 2012; 7:e29779.
17. Taogoshi T, Nagai J, Yumoto R, Takano M. Transport of prostaglandin E1 across rat erythrocyte membrane. Biol Pharm Bull 2008; 31:1288-91.
18. Jakobsson PJ, Thoren S, Morgenstern R, Samuelsson B. Identification of human prostaglandin E synthase: a microsomal, glutathione-dependent, inducible enzyme, constituting a potential novel drug target. Proc Natl Acad Sci 1999; 96:7220-5.
19. Reid TJ, Esteban G, Clear M, Gorogias M. Platelets membrane integrity during storage and activation. Transfusion 1999; 39:616-24.
20. Rothwell SW, Maglasang P, Reid TJ, Gorogias M, Krishnamurti C. Correlation of in vivo and in vitro functions of fresh and stored human platelets. Transfusion 2000; 40:988-93.
21. Pandey NR, Kaur G, Chandra M, Sanwal GG, Misra MK. Enzymatic oxidants and anti-oxidants of human blood platelets in unstable angina and myocardial infarction. Int J Cardiol 2000; 76:33-8.
22. Wachowicz B, Olas B, Żbikowska HM, Buczynski A. Generation of reactive oxygen species in blood platelets. Platelets 2002; 13:175-82.
23. Dołęgowska B, Błogowski W, Domanski L. Clinical evidence of the association between serum perioperative changes in xanthine metabolizing enzymes` activity and early post-transplant kidney allograft function. J Am Coll Surg 2010; 211:587-95.
24. Diehm N, Benenati JF, Becker GJ, Quesada R, Tsoukas AI, Katzen BT, Kovacs M. Anemia is associated with abdominal aortic aneurysm (AAA) size and decreased long-term survival after endovascular AAA repair. J Vasc Surg 2007; 46:676-81.
25. Koga T, Az-ma T, Yuge O. Prostaglandin E1 at clinically relevant concentrations inhibits aggregation of platelets under synergic interaction with endothelial cells. Acta Anaesthesiol Scand 2002; 46:987-93.
26. Iyu D, Glenn JR, White AE, Johnson AJ, Fox SC, Heptinstall S. The role of prostanoid receptors in mediating the effects of PGE(2) on human platelet function. Platelets 2010; 21:329-42.
27. Petrucci G, De Cristofaro R, Rutella S, Ranelletti FO, Pocaterra D, Lancellotti S, Habib A, Patrono C, Rocca B. Prostaglandin E2 differentially modulates human platelet function through the prostanoid EP2 and EP3 receptors. J Pharmacol Exp Ther 2011; 336:391-402.
28. Wang M, Lee E, Song W, Ricciotti E, Rader DJ, Lawson JA, Pure E, FitzGerald GA. Microsomal prostaglandin E synthase -1 deletion suppresses oxidative stress and angiotensin II induced abdominal aortic aneurysm formation. Circulation 2008; 117:1302-9.
29. Nakamura S, Yoshihara F, Kamide K, Nakahama H, Nishigami K, Fukuchi K, Ogino H, Kawano Y.

Microalbuminuria and deterioration of renal function after elective repair of infrarenal abdominal aortic aneurysm. Clin Nephrol 2006; 65:165-72.
30. Norwood MG, Sayers RD. Urinary albumin:creatinine ratio (ACR) and the prediction of postoperative complications after abdominal aortic aneurysm repair. Eur J Vasc Endovasc Surg 2005; 30:353-8.
31. Muller MK, Wojzek M, Runzi M, von Schonfeld J, Goebell H, Singer MV. Cytoprotective and dose-dependent inhibitory effect of prostaglandin E1 on rat pancreas treated with ciclosporin A. Digestion 1991; 50:112-9.
32. Wong F, Massie D, Hsu P, Dudley F. Dose-dependent effects of oral misoprostol on renal function in alcoholic cirrhosis. Gastroenterology 1994; 106:658-63.

PERCEPTION OF OCCUPATIONAL RISK BY RURAL WORKERS IN AN AREA OF CENTRAL ITALY

A. ANTONUCCI[1], E. SICILIANO[2], D. LADIANA[3], P. BOSCOLO[1] and M. DI SIVO[3]

[1]Operative Unit of Occupational Medicine, University "G. d'Annunzio" of Chieti-Pescara, Italy; [2]INAIL CONTARP Abruzzo, Italy; [3]Department IDEA, University "G. d'Annunzio" of Chieti-Pescara, Italy

Received May 4, 2012 – Accepted July 19, 2012

The aim of this study is to analyze the subjective perception of risks for rural workers in Abruzzo, an area of central Italy. A group of 273 workers were asked to fill in a questionnaire which included, apart from general information, questions relative to six different types of risks normally found in the field of agriculture. The types of risks considered were: falling from a height, manually moving loads, overturning/accident whilst driving an agricultural tractor, noise and vibration, use of pesticides, the risk of being cut/injured. The workers were requested to assess, on a scale of 1 to 3, both the probability of an accident taking place and the consequent damage which could result from each of the risks considered. The assessment of the risks provided by the workers was related to the objective assessment of the risks carried out by the study group, also on the basis of objective data provided by INAIL (Italian insurance company) indexes, to highlight the eventual under/over estimations of risk. Furthermore, the possible correlation was evaluated between having received specific training regarding work safety and the workers' perception of the risk. The results showed that approximately 11% of the workers do not consider their job as being dangerous; the risk perceived by the workers is higher for accidents that cause an immediate injury compared to those which cause professional illnesses, except the risk deriving from noise/vibrations. A direct correlation was found between considering one's job as being dangerous and having attended courses on accident prevention.

The perception of risk is a cognitive process involved in various daily activities which guides the behavior of people faced with decisions involving potential risks. The perception of risk in a working environment is influenced by numerous variables: individual, social, professional, organizational which involve different dimensions, such as the immediate and future consequences and their implications both on a rational and objective level as well as an emotional and subjective level. Summarizing what has been reported by authoritative scholars (1-3) on the definition of the various types and perceptions of risk, we can consider that the perception of risk is based on three main prospectives: the realistic (objective) prospective, from a scientific point of view, defines risk as the product between probability of a determined industrial accident taking place and the damage it can cause. The relativistic (subjective) prospective, on the other hand, defines the risk considering only how the individual evaluates the event and the consequent damage from an individual point of view. The combination of the preceding two

Key words: safety, injury, occupational risk

Mailing address: Dr Andrea Antonucci,
Università G. d'Annunzio,
via dei Vestini 31,
Chieti Scalo, Italy
Tel.: +39 0871 3556747
Fax: +39 0871 3556706
e-mail: andrea.antonucci@unich.it

0393-974X (2012)

DISCLOSURE: ALL AUTHORS REPORT NO CONFLICTS OF INTEREST RELEVANT TO THIS ARTICLE.

prospectives, provides the sociocultural perception of risk, according to which risk is an objective threat, but is influenced by culture, for example, the conviction to be able to control or avoid a risk. Study has underlined that in many cases a discrepancy exists between the subjective perception of the risk and the objective evaluation (4, 5). In other words, sometimes people fear certain activities which are not actually dangerous and do not fear activities which could have very dramatic consequences.

It has, however, been consolidated that a correct perception of risk in work environments can be important in reducing industrial accidents and the onset of professional illnesses as it modifies the behavior of the worker, and consequently the actions which he carries out to safeguard himself.

Different reasons exist which lead people to perceive some activities as being dangerous and others less so, and there are marked differences between different individuals (7). Nevertheless, general mechanisms can be verified which subtend the way in which people elaborate information deriving from their surroundings and also that which they remember. These processes, called heuristic, have a fundamental role in the way in which people evaluate the risks of an activity. In particular, it deals with the strategies of thought which usually act on an unconscious level (6). The following are included among these factors: how much control is it possible to exercise on the events which can develop a risk (for example, is it thought to be able to exercise great control in the cases cited in the manual and very little in cases of natural cataclysms); how willingly have people decided to face a dangerous situation; how serious are the possible consequences; etc. (4). Using this type of factorial analysis, these variables can be grouped into two principal factors: "terrifying risk" and "unknown risk". The first factor indicates the level of how catastrophic the risk is associated to a certain activity, whilst the second factor indicates how much that risk can be observed and controlled. Using these two factors, it is possible to make a cognitive map of the danger which each person associates with a determined activity. In this way it is possible to understand how people can associate different risks to an activity which has the same probability of producing negative consequences (8).

One important result obtained by the study group of the perception of risk was to highlight that people perceive the relationship between risks and benefits of an activity in a different way to which

that relationship is actually realized (9). In fact, from an objective point of view, many activities which involve a possible risk also offer some advantages (e.g. X-rays in medical practice); it is worth noting that in the environment risks and benefits are correlated in a positive way. Besides, the benefit is often found in the field of work associated to the use of machinery and tools which undoubtedly help in production and reduce the physical exertion of manual work, and it is for this reason that the workers often evaluate the use of machinery and tools associating a low level of risk compared to the benefits obtained by their use.

In other cases, however, fear prevails regarding the use of tools and the individual therefore considers it to be of little advantage to carry out actions which he unconsciously considers risky. Consequently, people who are afraid of flying associate a type of negative emotion with this action and do not recognize the possible benefits. On the contrary, people who see the benefits offered by the possibility of travelling by air associate a positive emotion to this activity which will lead to underestimate the possible risks (6).

This manner of reasoning depends in a determining way on the way in which the human cognitive system functions and is particularly due to the use of the so-called intuitive thought system which acts mainly on an unconscious level and which influences our conscious evaluations on the basis of emotional reactions which we associate with different objective stimulations, people or activities (10).

Taking into account, therefore, the different ways of perceiving and interpreting risks, this study aims to compare the objective risk, evaluated with standard analytical methods originating from statistical data of the cases of industrial injuries and professional illnesses, with the subjective risk, i.e. the sociocultural risk, in other words that perceived by the workers, using analytic research methods.

MATERIALS AND METHODS

This study was carried out on 273 workers in the field of agriculture aged between 20 and 80 years, most of

whom (77.8%) were general, mainly independent farmers, 10.9% were stockbreeders, and the remaining 11.3% were cellar men and laboratory analysts. The majority were under contract as independent workers, most of whom had had a secondary or high school education.

Check lists were compiled made up of 55 questions to ask the worker with the aim of identifying, from the typical main aspects of his own work situation, information relative to: training and information received regarding safety, the main risks to which the worker considers he is exposed, use of PPE, behavioral standards for using phytosanitary products, risks connected to the use of agricultural vehicles, previous work injuries.

The charts were distributed to the workers during meetings organized for this purpose, subject to consent of the host company, and according to the laws regarding the use of personal data.

Help was given in administering the questionnaires from the trade associations, mainly from the Confederazione Italiana Agricoltori (Italian Federation of Agricultural Workers) of the provinces of Chieti and Pescara, and from the Olive Growers Association of the CISL of Pescara. During the meetings the aim of our research was explained to the workers and where necessary they were given clear information on the meaning of the questions asked, to guarantee a good understanding of the questionnaire.

Furthermore, charts were compiled (Table I) to identify a list of possible dangers:

1. the magnitude of the damage which the worker judges can result from such danger;
2. the frequency of injury/professional illness which the worker considers to be connected to such danger.

The worker had to indicate on a scale of 1 to 3 the probability of this event (Table II, point 1) and the damage (Table II, point 2) corresponding to each danger. This allowed us to evaluate the risks which the worker associated to the dangers examined, calculated using the known formula: $R = P * D$, where R is the risk, P the probability of such event, and D is the estimated consequent damage. The same calculation was made by our work group, taking into consideration the official data on accidents in the agricultural section provided by the National Institute for Work Insurance (INAIL), as well as the analysis of the risks identified in similar studies.

Table I. *List of the analyzed dangers found in agriculture.*

1. falling from a three meter-high ladder
2. strain from repeatedly lifting and carrying 25 kg loads
3. danger of injury whilst driving an agricultural tractor
4. dangers from the use of pesticides
5. dangers derived from the use of noisy or vibrating machinery
6. dangers connected to the use of manual tools which can cause cuts and abrasions

Table II. *Questions relative to individual dangers.*

1) With what probability do you think this risk occurs in an agricultural firm?		
1	2	3
Never/Extremely unlikely	Probable	Very probable
2) What do you think would be the damage resulting from such an event? (e.g. a fall from a three meter high ladder)		
1	2	3
No injury	Injuries that could require medication and that could be disabling	There could be injuries that may even be fatal
3) How possible do you feel it is to avoid this risk? (with the safety procedures and the PPE at your disposal)		
1	2	3
I cannot avoid it	I can partially avoid it	I can always avoid it
4) How useful do you find the training received for this risk and on the procedures for reducing it?		
1	2	3
Useless /never had any training	Useful	Very useful

The two risk evaluations were compared to identify eventual under/overestimates of the analysis of the workers compared to the risk calculated by the group of experts. In this study we indicate the risk calculated by our work group as "possible real risk".

The workers were also asked to indicate on a scale of 1 to 3, for each dangerous situation, how possible it was to reduce or eliminate the risk by adopting the prescribed safety measures and the appropriate personal protection equipment. The aim of this question was to investigate the amount of confidence the worker had in the real possibility of reducing the risk in a dangerous situation by using the correct prevention methods (Table II point 3).

For the last analysis the worker was asked to indicate how useful he had found the training on individual risks, with the aim of drawing useful indications on the quality of training undergone, as perceived by the worker (Table II point 4)

RESULTS

From the analysis of the results it emerged that 11% of the workers, mainly independent ones, do not feel that their work is risky for their health/safety; about 50% consider it as equally risky as other manual work; 19% feel that their work is risky only if you have little experience, reducing the risk to mainly accidental events, above all connected to driving agricultural vehicles, rather than the risk of professional illnesses.

19.5% hold that their work is more risky than other manual jobs, this percentage is mainly composed of workers who work in the open and who feel that they are more subject to the risk of injuries which are difficult to foresee, such as insect bites, slipping and falling due to rough ground.

In Table III are reported the values in percentage of probability and damage for each type of identified danger. The opinions expressed by the workers refer to standard situations, as defined by the work group who gave out the questionnaire.

In following we calculated the risk value by multiplying the probability by the damage. The damage was identified as that most probable as chosen by the workers. The compared values of probability and consequent damage are reported in table IV, as calculated by the workers and our work group.

From the comparison of the data (Fig. 1) it emerged that the workers who participated in our research evaluate the risk connected to the possibility of an accident while driving an agricultural vehicle as the highest one, with a risk value very similar to that calculated by the work group. Similar risk values were also obtained regarding exposure to noise and vibrations and concerning the risk of cuts/injuries. We feel that the risk of a fall from a three meter-high ladder was slightly underestimated, above all in regard to the possible consequent damage. Substantial difference was found instead for the risk in the use of pesticides and in that connected to the

Table III. *Percentage of probability and damage for each type of identified danger.*

Fall from a 3m-high ladder				**Injuries/professional illnesses from repeatedly lifting and carrying a 25 kg load**				**Injury whilst driving an agricultural tractor**			
probability	**%**	**damage**	**%**	**probability**	**%**	**damage**	**%**	**probability**	**%**	**damage**	**%**
improbable	13.7	none	1.95	improbable	21.1	none	25.5	improbable	11.4	none	0.8
probable	75.7	Medical treatment/ disabling	52.35	probable	68.4	Medical treatment/ disabling	71.8	probable	72.8	Medical treatment/ disabling	11
very probable	10.6	very serious /fatal	45.7	very probable	10.5	very serious /fatal	2.7	very probable	15.8	very serious /fatal	88.2
Illnesses deriving from noise and vibrations				**Illnesses deriving from the use of pesticides**				**Injuries due to possible cuts/wounds**			
probability	**%**	**damage**	**%**	**probability**	**%**	**damage**	**%**	**probability**	**%**	**damage**	**%**
improbable	18.7	none	12.2	improbable	7.7	none	4.2	improbable	8.6	none	8.6
probable	70.5	Medical treatment/ disabling	80.7	probable	71.9	Medical treatment/ disabling	50	probable	71.7	Medical treatment/ disabling	75.8
very probable	10.8	very serious /fatal	7.1	very probable	20.4	very serious /fatal	45.8	very probable	19.7	very serious /fatal	15.6

Table IV. *Risk evaluated by workers.*

	Fall	heavy load	agric. vehicle	noise/vibr	pesticides	wounds
P	1.97	1.89	2.04	1.92	2.13	2.11
D	2.44	1.77	2.87	1.95	2.42	2.07
R	4.81	3.34	5.85	3.74	5.15	4.37
Possible real risk						
	Fall	**heavy load**	**agric. vehicle**	**noise/vibr**	**pesticides**	**wounds**
P	1.8	2.7	2	2.3	2.5	2.8
D	2.75	2	2.8	2	2.7	1.7
R	4.95	5.4	5.6	4.6	6.75	4.76

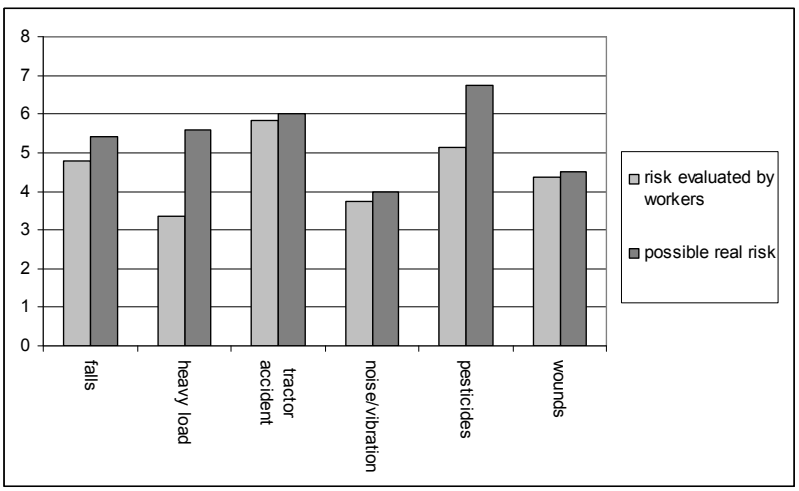

Fig. 1. *Comparison of the risk values evaluated by the workers compared to those evaluated by our work group.*

manual movement of loads. In both cases the risk value calculated by the workers was lower than that calculated by the work group, for the probability of it happening as well as for the consequent damage.

The values expressed by the workers on the possibility of avoiding injuries/illnesses following exposure to the identified dangers are reported in Fig. 2. From the results it emerges that the workers have a medium-high trust in the protection equipment and in the safety procedures with regard to the possibility of avoiding the identified risks.

Less confidence was found in the possibility of avoiding risks connected to the manual movement of loads and the possibility of cuts/injuries during work, activities for which a high percentage of workers feel that it is not possible to avoid injuries/professional illnesses.

With regard to the use of personal protection equipment, among the most salient points it emerged that, according to the workers, 25% of them did not use a mask to protect the respiratory tract during the use of phytosanitary products and 50% did not avoid eating, drinking or smoking during this treatment. Among those who do not use the PPE, 47% stated to not have any, 21% that it was not very efficacious, 15% that it was uncomfortable, about 6% forgot to use it, the rest had worn it out or did not know when to wear it. Another important point that emerged is that about 50% of the workers had not been vaccinated against tetanus in the last ten years.

Regarding training, 35% of the workers stated to not have undergone any specific form of training on the subject of prevention and safety. The opinion on the usefulness/importance of the received training was medium, the highest values obtained were relative to the importance of training on the

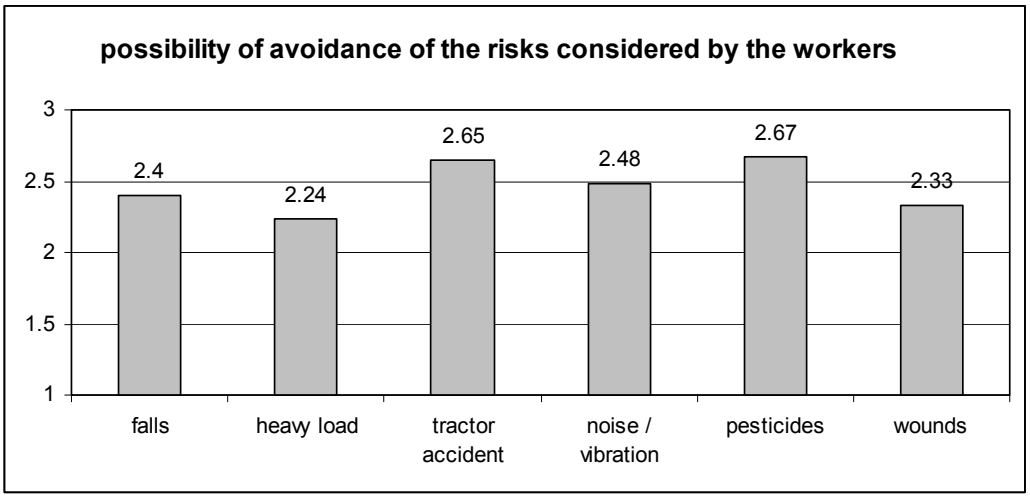

Fig. 2. *Possibility of avoidance of the risks considered by the workers.*

risks of using agricultural vehicles and the use of phytosanitary products.

In the last analysis we investigated as to whether there is correspondence between having attended training courses and consideration of the risks at work. This correspondence may indicate the impact of the training courses on how aware the workers are of the existence of risks. From the results it emerged that 88% of them who had not attended courses on safety stated that their work was not risky, while the percentage dropped to 10% among those who had attended safety training courses.

DISCUSSION

This work has brought to light some differences in terms of objective and subjective perception of the risks in agriculture. The study examines some of the main types of dangers present in agriculture and the workers were asked to quantify the possibility of them occurring and the consequent damage in order to quantize the risk they perceived. This risk was then compared to the objective one calculated by our work group, on the base of statistical data on accidents (INAIL) and on the base of the technical experience of our researchers as well as data available in literature. Although risk is a quantity that must be carefully evaluated case by case as it various in every work environment, we tried to identify in our study simple situations of generalized character for which it is possible to express an opinion in merit on the quantization of risk. From the results it emerged that the workers underestimate the risks deriving from manual movement of loads, even though the illnesses connected to the spinal column are the second cause of absenteeism from work after the common cold in the USA, and it is estimated that about 80% of adults have suffered at least once in their lives from backache (15). The possibility to put into act remedies for reducing the onset of professional illnesses connected to the manual movement of loads also resulted as not plausible according to the majority of the interviewed workers.

The other underestimated risk was the damage to health deriving from the use of pesticides, this in relation to the fact that a good percentage of them consider that there is not a very high probability of being at risk of serious illnesses due to the use of phytosanitary products without due protection. This opinion affects the use of personal protection equipment, such as a mask to protect the respiratory tract, that, according to the workers, is not used by 25% of them during treatment with phytosanitary products. A correlation did emerge however between having had training on safety and consideration of the work risks. This datum is to be considered positive in that it is to be hoped that training influences the awareness of the workers on the risks they run during

their work activities.

REFERENCES

1. Sjöberg L. (2000), Factors in Risk Perception. Risk Analysis, 20: 1–12. doi: 10.1111/0272-4332.00001
2. Dake K, Wildavsky A. Theories of risk perception: Who fears What and why? Risk by Burger E. JR Editor, Michigan 1993 p. 40-60.
3. Kurzenhäuser S, Epp A. Perception of health risks: psychological and social factors. Bundesgesundheitsblatt Gesundheitsforschung Gesundheitsschutz. 2009; 52:1141-6.
4. Slovic P. Perception of risk. Science 1987; 236:280-85.
5. Strenfert S, Taylor EA. Objective risk levels and subjective risk perception. National Technical 1971, p. 1.
6. Ruminati R, Legrenzi P, Bonini N. Percezione e valutazione del rischio. In: M. D'Alessio, N. Dazzi and P. Ricci Bitti (a cura di) Indicatori psicologici e sociali del rischio. Napoli 1995; Gnocchi.
7. Slovoc P. Psychological study of human judgment: Implications for investment decision making. J Psychology Financial Markets 2001; 2:160-72.
8. Mullet E, Lazreg C, Candela C, Neto F. The Scandinavian way of perceiving societal risks. J Risk Res 2005; 819-30.
9. Alhakami AS, Slovic P. A psychological study of the inverse relationship between perceived risk and perceived benefits. Risk Analysis 1994; 14:1085-96.
10. Slovic P, Finucane M, et al. Risk as analysis and risk as feelings : some thoughts about affect, reason, risk and rationality. Risk analysis 2004; 24:311-22.
11. Antonucci A, et al. Safety in construction yards: perception of occupational risk by Italian building workers. Eur J Inflamm 2010; 8:107-15.
12. Di Giampaolo L, Antonucci A, Stocchi M, et al. The perception of risk in construction workers. J Ital Med Lav Erg 2007; 29(S):728-30.
13. Bulter G, Mathews A. Anticipating anxiety and risk perception. Cognitive Quality Res 1987; 11:551-65.
14. Finucane ML. Alhakami A, et al. The affect heuristic in judgments of risk and benefits. J Behav Decision Making 2000; 13:11-17.
15. NIOSH Worker Health Chartbook, 2004. National Institute for Occupational Health and Safety (NIOSH) NIOSH Publication Number 2004-146.

NANOTECHNOLOGY AND VASCULAR NEUROSURGERY: AN *IN VIVO* EXPERIMENTAL STUDY ON MICROVESSELS REPAIR USING LASER PHOTOACTIVATION OF A NANOSTRUCTURED HYALURONAN SOLDER

G. ESPOSITO[1], F. ROSSI[2], P. MATTEINI[2], F. RATTO[2], G. SABATINO[1], A. PUCA[1], A. ALBANESE[1], G. ROSSI[3], E. MARCHESE[1], G. MAIRA[1] and R. PINI[2]

[1]Institute of Neurosurgery, Catholic University School of Medicine, Rome, Italy; [2]"Nello Carrara" Institute of Applied Physics, Italian National Research Council, Sesto Fiorentino (FI), Italy; [3]Faculty of Veterinary Medicine, University of Camerino, Matelica (MC), Italy

Received November 9, 2011 – Accepted July 13, 2012

Sealing tissues by laser in neurosurgical procedures may overcome problems related to the use of conventional suturing methods which can be associated with various degrees of vascular wall damage. Despite the significant experimental and clinical achievements of the past, a standardized clinical application of laser-welding technology has not yet been implemented. The main problem is related to the use of common organic chromophores. A substantial breakthrough in the laser welding of biological tissues may come from the advent of nanotechnologies. In this paper we describe an experimental study, to confirm the feasibility of an innovative laser-assisted vascular repair (LAVR) technique based on diode laser irradiation and subsequent photoactivation of a hyaluronan solder embedded with near infrared (NIR) absorbing gold nanorods (GNRs), and to analyze the induced closuring effect in a follow-up study performed in animal model. Twenty New Zealand rabbits underwent closure of a 3-mm longitudinal incision performed on the common carotid artery (CCA) by means of 810 nm diode laser irradiation, in conjunction with the topical application of an optimized GNR composite. Effective closure of the arterial wound was accomplished by using very low laser intensity (30 W/cm^2). The average CCA occlusion time was as low as 50 sec. Animals underwent different follow-up periods (2, 8, 30 days). After follow-up, they were re-anesthetized, the patency of the treated vessels was tested (Doppler analysis) and then the irradiated vessels were excised and subjected to histological evaluations. Morphological examinations of the samples documented the integrity of the vascular wall. No host reaction to nanoparticles occurred. Collagen and elastic fibers returned to their normal architecture 30 days after treatment. A Scanning Electron Microscopy (SEM) examination and immuno-histochemical analysis demonstrated a full re-endothelization of the vessel walls. We thus confirmed that a laser-based approach is technically easy to perform, and provides several advantages, such as a simplification of the surgical procedure, a reduction in the operative time, and the suppression of bleeding. The use of GNRs improves the selectivity of welding and minimizes the surgical trauma to vessels, resulting in an optimal healing process.

Arterial injuries which may occur during neurosurgical procedures are commonly repaired by

Key words: nanotechnology, neurosurgery, microsurgery, vessel repair, diode laser, gold nanoparticles, laser soldering, photothermal effect

Mailing address: G. Sabatino, MD
Institute of Neurosurgery,
Catholic University School of Medicine,
L.go A. Gemelli, 8
00168 Rome, Italy
Tel.: +39 06 30154841 Fax: +39 06 3051343
e-mail: giosaba@inwind.it

0393-974X (2012)

the use of temporary clips and microsutures. However, the use of suture material and of penetrating needles may be associated with various degrees of vascular wall damage, ultimately predisposing to vessel thrombosis and occlusion. Moreover, direct suturing can sometimes be difficult, especially when thin and fragile vascular structures have to be repaired or in the case of a deep and narrow operative corridor. Finally, a prolonged occlusion time necessary for suturing of cerebral arteries can be associated with the onset of cerebral ischemia (1-3).

To overcome these problems, laser-based techniques have raised interest in microvascular surgery (4-8). Laser welding is a technique used to seal biotissues. It relies on the interaction between laser light and an optical absorber to produce a photothermal effect, thus inducing thermal modifications within the tissue (thermally-induced cross-linking between the solder and the main tissue components) (9-10). When the welding is mediated by the topical application of a semisolid material that can be activated by the laser light, the technique is referred to as laser soldering. The use of a photosensitizer applied topically to the wound was found to induce a controllable rise in the local temperature and a selective thermal effect (5). Despite the experimental and clinical advances in laser technology (5-11), a standardized clinical application, to date, is still lacking. The main limitations are ascribed to the use of organic dyes as exogenous optical absorbers: these suffer, due to poor stability in aqueous and physiological solutions and under laser irradiation, and present excessive diffusiveness in the biological environment once they have been applied to the wound (12-16).

Recent progression in nanotechnology has led to the development of a new generation of nanochromophores, such as gold nanoparticles, whose physiochemical characteristics are potentially well-suited for biomedical applications. A special type of gold nanoparticle is represented by GNRs. These consist of cylindrical nanoparticles with high photothermal efficiency, suitable stability under high laser fluences and lower diffusivity in respect to that of organic photosensitizers. This provides for a more precise localization of the heat generated by the photothermal conversion. Additional favorable features of these nanoparticles are their biocompatibility, easy synthesis and high chemical versatility, which depict them as being highly promising for targeted and safe applications in humans (17-20). Preliminary results have recently been obtained by combining GNRs and NIR diode lasers in the laser soldering of vascular tissue (21-22).

The purpose of the present work is to assess the applicability and feasibility of a very innovative LAVR technique that is characterized by the use of diode laser irradiation in association with GNRs.

MATERIALS AND METHODS

Laser and materials

The laser used in the tests was an AlGaAs laser diode (EL.EN. Mod. WELD 800, Italy), with the following emission parameters: wavelength 810 nm, maximum output power: 10W, emission modality: pulsed or continuous wave. The device is enclosed in a compact cabinet (24 x 18 x 36 cm) and is equipped with a fiber optic transmission system that can be sterilized. The fiber tip is mounted on a handpiece that enables easy handling under the operating microscope. A 300-µm core optical fiber was used.

All chemicals were purchased from Sigma-Aldrich (Saint Louis, Missouri), unless otherwise noted, and used without further purification. Methoxypoly-(ethylene glycol) (mPEG-SH) with a 5000-Da mass was supplied by Laysan Bio Incorporated (Arab, Alabama). We used hyaluronan obtained from a bacterial source to minimize any possible protein-mediated aggregation of polymer chains when being stored for a long time in aqueous solutions. In particular, hyaluronan sodium salt from *Streptococcus equi* (Esperis S.p.A., Milan, Italy) with a molecular mass of approximately 1000 kDa and a protein content of less than 0.025%, as previously measured (23), was used in the experiment.

Fabrication of the nanostructured hyaluronan solder

GNRs of 59±9 nm in length x 15±2 nm in diameter with an average aspect ratio (i.e. the ratio of the nanoparticle length to its diameter) of about 4 were obtained in accordance with a variant of the surfactant-directed Nikoobakht reaction (22). After concentrating the 0.1 nM nanoparticle solution thus obtained to 1.6 nM, the particles were functionalized with methoxypoly(ethylene glycol thiol), which stabilized them against aggregation by strongly binding the gold surface and imparting biocompatible properties (24). Once PEGylated, the GNRs were transferred in phosphate-buffered saline

(PBS, pH 7.4) and powdered hyaluronic acid (Esperis S.p.A., Milan, Italy) was added to the suspension until a final 10% (w/v) homogeneous dark-red gel was obtained. The formulation was left to equilibrate at room temperature for at least 2 days, resulting in a stable hydrogel network, which was stored at 4°C until the moment of surgery. The exogenous chromophore consisted of a gel-like paste of functionalized GNRs.

Animal model

The experiments were performed on 20 New Zealand rabbits that weighed from 3500 g to 5500 g at the Experimental Centre of the Catholic University in Rome. The animals were anesthetized with ketamine hydrochloride (50 mg/kg) and medetomidine (0.3 mg/kg) intramuscularly, local anesthesia was performed with 2% Xylocaine. During the first 2 weeks of the follow-up period, the animals were treated with antibiotics (10 mg/kg of enrofloxacin per day). Different follow-up periods were established, as reported here as follows, in order to evaluate the vascular healing process and histological modifications over time. At the end of every follow-up period, the animals were re-anesthetized, the patency of the laser irradiated vessels was evaluated, and the vascular segment of interest was harvested for purposes of histological analyses. The animals were then sacrificed. The protocols used for animal tests were in accordance with the recommendations and regulations of the Italian Ministry of Health.

Surgical procedure

After anesthesia, a 4-cm longitudinal incision was performed in the anterior cervical midline of the animals. Thereafter, the procedure was performed with the aid of a surgical microscope. The right CCA was dissected for a tract of 2.5 cm. After proximal and distal temporary clipping of the exposed arterial segment, a 3-mm longitudinal cut was performed on the arterial wall by means of a sharp-point knife and micro-scissors. The arterial lumen was first flushed with heparinized solution, and then with sterile water. Then, 10 mg of the nanosolder paste was applied to the cut using a syringe, and the excess material was immediately removed with a spatula, in order to avoid the possible entrance of solder material into the lumen and also to confine the photothermal effect to the vascular surface. Afterwards, the incision was treated with the diode laser. The proposed new technique is schematized in Fig. 1.

The laser treatment consisted of a slow and continuous motion of the fiber-tip, which was held at a constant distance of 2-3 mm from the external artery surface. A continuous laser power of 0.2 W, corresponding to a power density of 30 W/cm^2 on the surface of the artery, proved effective for optimal vessel closuring (Fig. 2 A). The overall treatment time was 20 sec. At the end of the procedure, the clips were removed, the closed segment was checked.

Intraoperative microdoppler (IMD) analysis was performed both before temporary clipping and after lasering and removal of the clips, in order to assess the patency and to detect any blood flow reduction in the treated vessel. The blood flow velocities were recorded. As described by Stendel et al. (25, 26), a laser-soldered vessel was considered as stenotic when the two following findings were detected: 1) increase of the blood flow velocity more than 10%, when compared to the baseline (pre-laser treatment) values, in the arterial segment proximally to the repaired lesion, 2) decrease of the systolic velocity distally to the stenosed arterial segment. The treated carotid segment, as well as the proximal and distal part of carotid artery, were insonated using a 20-MHz microprobe of 1 mm diameter (Compumedics DWL Multidop x digital). This flexible microprobe was inserted in a number 3 suction cannula and secured to the distal extremity by bone, in order to give stiffness and improve its handling.

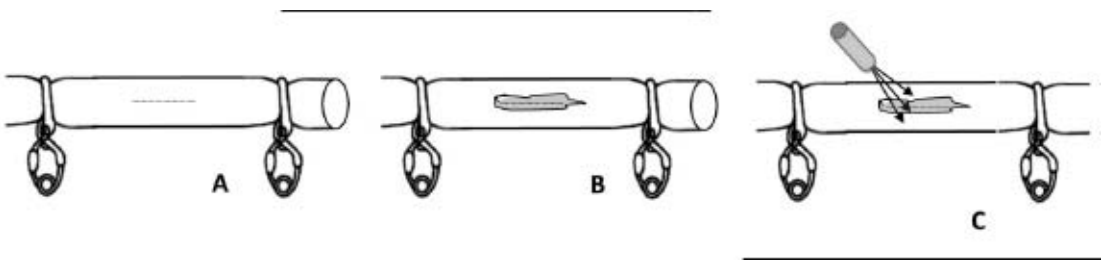

Fig. 1. *Sketch of LAVR procedure with hyaluronan-GNRs formulation. **A)** A longitudinal arterial lesion is performed on the clamped artery, (**B**) hyaluronan-GNRs is applied to the arterial lesion (**C**). Diode laser irradiation is delivered to the external surface.*

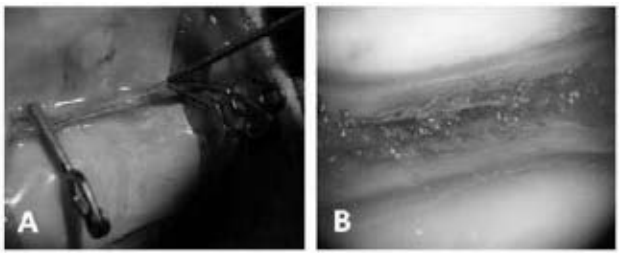

Fig. 2. *In vivo repair of a 3-mm longitudinal cut by using diode laser irradiation and hyaluronan-GNRs formulation (**A**). The result is an immediate closure of the wound, with no bleeding when the clamp is released (**B**).*

Lastly, the wound was closed in layers, and the animals were left to recover from the anesthesia.

Follow-up

The animals were directed to different follow-up periods: 2 days (n = 6), 8 days (n = 6), 30 days (n=8). At the end of every follow-up period, the animals were re-anesthetized. A new IMD analysis was executed to assess carotid artery patency as well as the evidence of any blood flow reduction or turbulence in the treated vessel. Then, the vascular segments of interest were sampled and examined by means of histochemical, immunohistochemical and ultrastructural analyses.

Morphological analysis

In brief, the samples were fixed in 10% buffered formalin, embedded in paraffin, and sectioned. Coronal sections of each treated and untreated vessel were performed, and the final geometry of the sections included a total view of the area of vascular wall synthesis, from the two hemilines of the endothelium welded to media and adventitial portions of the soldered vessel wall. The sections were then deparaffinized, rehydrated, and stained with haematoxylin and eosin (H&E), Unna-Tanzer-Livini (UTL) stain specific for elastic fibres, and Masson's trichrome (MT) stain for connective tissue. The histological evaluation included an assessment of the inflammation, myointimal hyperplasia, thrombosis and elastic-fiber damage. Evaluations were performed by attributing scores from 0 to 3 according to the following criteria.

Inflammation (neutrophils and mononuclear cell infiltration) was classified as: absent (score of 0) when there was none or only single sporadic cells per high-power field (HPF, using 400X magnification) (<5cells); mild (score of 1) for a few cells (5 to 19 cells) per HPF; moderate (score of 2) for several cells (20 to 49 cells) per HPF; and marked (score of 3) (50 to 99 cells) per HPF.

Myointimal hyperplasia was evaluated by a calibrate ocular apparatus and the value, expressed in μm, was the mean value obtained from four values in different areas of the vascular wall. Scores varied from: 0 = absence; 1 = 10–20 μm-thick; 2=20–50 μm-thick; 3 = greater than 50 μm-thick.

Thrombosis was scored as follows: 0 = absence; 1 = initial thrombus; 2 = semi-occlusive thrombus; and 3 = occlusive thrombus.

Elastic fibers damage was evaluated by using the Unna-Tanzer-Livini (UTL) method and the results were scored as follows: 0= absence of damage 1= presence of some areas of lamina elastica disorganization, 2 = fragmentation of internal and external lamina elastica, 3 = total disorganization and areas of disappearance/absence of the two laminae.

The immunohistochemical examination was performed in order to check the presence of CD31 and of the von Willebrand factor (VWF). For this purpose, monoclonal mouse anti-human CD31 and mouse anti-human factor VIII antibodies (DAKO, Glostrup, Denmark) were employed. Primary antibodies were used, both diluted 1:50 in TBS and also maintained on the sections in a moist chamber. The secondary antibody was a goat-anti mouse biotinilated (DAKO) diluted 1:200 in the same buffer. The reaction was evidenced by an avidine-biotine complex (ABC *elite*, Vector, Burlingame, UK) and developed using Diaminobenzidine hydrochloride (DAB- Vector) as the chromogen substrate, which was then counterstained with Meyer's haematoxylin. The positivity score ranged from 0 to 3 on the basis of the mean number of positively stained cells (i.e.: endothelial cells) calculated per 10 HPF randomly selected from a sample of the laser-treated vessels. The score were as follows: 0 = no stain; 1 = almost 15% of cells stained by the chromogen; 2 = almost 50% of stained cells; 3 = over 80% of stained cells.

Other samples underwent SEM and TEM examinations, using standard laboratory procedures. For the SEM analysis of the vessel's endothelial surface, samples were immediately fixed in 4% glutaraldehyde in a 0.2 M sodium cacodylate buffer solution at 4°C, dehydrated in graded concentration alcohol, dried with a critical point drier (E 3000, Polaron, West Sussex, UK), and then gold sputtered (Sputter Coater, SPI, Toronto, Canada) and observed with SEM (JEOL 5200, JEOL, Tokyo, Japan). SEM analysis allowed the evaluation of the endoluminal surface integrity. The attributed scores ranged from 0 to 3 on the basis of the percentage of uncovered altered areas of endoluminal endothelial surface of the vessel calculated per 10 HPF randomly selected per sample. The score were as follows: 0 = absence of disendothelized areas; 1 = almost 15% of the surface was disendothelized; 2 = almost 50% of disendothelization; 3 = over 80% of disendothelization.

For the TEM examination, the samples, fixed in the same medium, were post-fixed in 1% osmium tetroxide in 0.1 M sodium cacodylate buffer for 1 h at room temperature, dehydrated in ascending grades of ethanol (50%, 75%, 95%, and 100%) for 10 min each, with 2 changes, followed by immersion in 1:1 absolute ethanol-epoxy embedding resin (Poly/Bed 812, Polysciences, Warrington, PA) for 2 h, resin-infiltration in 100% epoxy embedding resin for another 2 h, and, lastly, embedding of the resin-infiltrated samples in molds with 100% epoxy resin. Before being embedded, the specimens were oriented in the molds to the point that ultra-thin sections through the resin-vessel interface were cut from the adventitial to the intimal (vessel) area of the original vessel. After the epoxy blocks were placed in a vacuum oven for 15 min to extract air bubbles, they were polymerized in an oven at 60°C for a minimum of 48 h. Ultra-thin sections of about 90 nm were cut, using a diamond knife, in an ultramicrotome (Sorvall Ultra Microtome MT5000, RMC, Tucson, AR). For the TEM examination (JEOL 1200 EX, Peabody, MA), they were positively stained with saturated uranyl acetate (UA) for 8 min and lead citrate (LC) for 3 min. TEM analysis permitted the evaluation of the collagen fibers organization. The assigned score ranged from 0 to 3 on the basis of the percentage of collagen fibers showing a persistent cross-link or storiform-fingerprint pattern, calculated per 3 fields randomly selected from a sample of the laser-treated vessel. The score were the following: 0 = over 80% of the examined area showed a parallel pattern; 1 = almost 50% of examined area showed a parallel pattern; 2 = only a 15% of examined area showed a parallel pattern; 3 = only cross-link or storiform-fingerprint pattern of the fibres observed.

RESULTS

Observations at the time of surgery

An effective closure of the cut edges was obtained by using laser intensity of 30W/cm^2. The average occlusion time of the CCA was 50 sec for the laser-treated samples. After removal of the clamps, all carotid arteries submitted to IMD analysis were found to be patent. Neither turbulence nor blood flow alterations were detected, when comparing the records performed before and after the laser-soldering. No bleeding was documented (Fig. 2 B).

Observations at follow-up times

IMD analysis showed all the soldered vessels were patent at the time of the follow-up examination, with no evidence of turbulence phemomena. No blood flow modifications were observed, when compared to pre-operative IMD-based blood flow velocity records. Neither occlusions nor signs of perivascular hemorrhage were found. No formation of a pseudoaneurysm or eversion of the vessels edges was documented at the welded sites.

Morphological analysis:
Histochemical, TEM and SEM evaluations

Morphological examinations of welded samples documented an optimal reorganization and preservation of all vascular wall structures after long-term (30 days) follow-up periods. At this point in time, no damage to the internal *lamina elastica* was observed (Fig. 3 C). No host reaction to nanoparticles, interspersed throughout the treated vascular tissue, occurred at different points in time in the histological analysis: in fact, no formation of microgranulomas or dystrophic calcification of the vessel *lamina media* and/or *intima* was evidenced, especially 8 or 30 days after treatment. Oddly enough, no inflammation observed even in "acute" phases of reparation, 2 days after welding. At that time, the only alteration observed was a strong disorganization

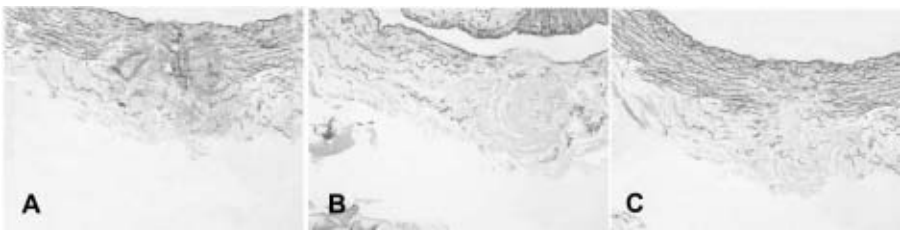

Fig. 3. *Repaired artery stained using the UTL method. The method, which is specifically employed for staining elastic fibers, indicates (**A**) the fusion among the two portions of discontinued vessel, with a partial disappearance of the collagen and elastic fibers organization pattern at the same point in time (2nd post-operative day). The fiber-disorganization process lasts for a maximum of 8 days post treatment (**B**), when UTL shows a fibers pattern "random" with storifom or in any case an intersecting arrangement. This effect of disorganization of the collagen appears, instead, to reenter 30 days after welding (**C**). UTL stain, 10X.*

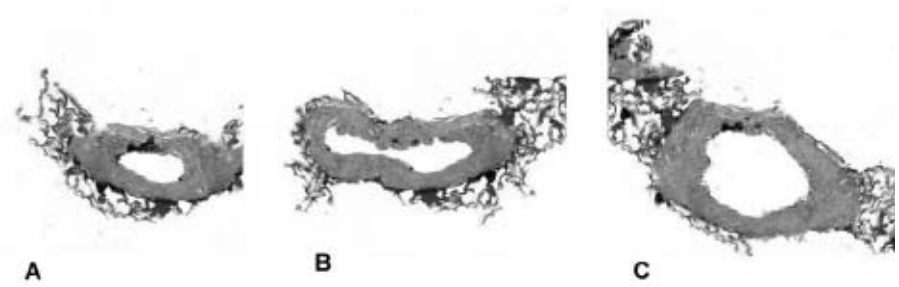

Fig. 4. *Masson's trichrome (MT) method. A panoramic view of the coronal sections of vessels, in the absence of thrombotic processes inside the vessel's lumen at all the time points. Note the presence of an altered area in the vessel's wall (**A**) 2 days after the surgery, which disappeared at the second (**B**: 8th day) and third (**C**: 30th day) time points. MT stain, 2X.*

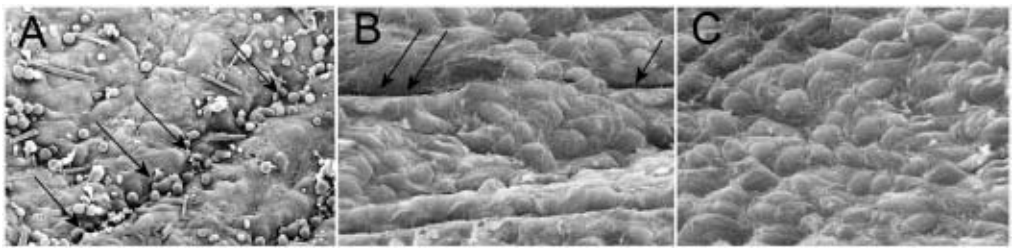

Fig. 5. ***A**) SEM appearance of endothelium covering the GNRs – laser-soldered area. Note the appearance of the endothelial surface, 2 days after treatment. An evident area corresponding to the line of surgical dissection is uncovered by endothelial cells (arrows) and some red blood cells admixed with leucocytes and fibrin fragments adhere to the uncovered area. **B**) Endothelium aspect 8 days after treatment with micro areas not totally covered by cells, the line of the surgery is still evident (line and arrows).**C**) Another endothelial view 90 days after treatment, with complete re-covering of the endothelial surface. At this follow up time, no residual traces of surgery and welding are observed (10 KV, 2000 enlargements).*

of the collagen and elastic fibers in the vascular walls, as shown in Fig. 3 A. At the same time, a light basophilic aspect of the treated area, evidenced by UTL stain, and a hyaline-homogeneous aspect of the collagen of the welded portion of vascular wall were observed after 8 and 30 post-operative days (Fig. 3 B and C). It is interesting to note that the collagen and elastic fibers returned to their normal appearance 30 days after treatment (Fig. 3 C), while 8 days after treatment a notable subversion of the structure of the vessel wall was evident (Fig. 3 B).

Another important observation concerns the absence of endoluminal alterations. In Fig. 4 a panoramic view is shown of the coronal sections of vessels, in the absence of thrombotic processes inside the vessel's lumen at all the time points. Two days after surgery it was possible to note the presence of an altered area in the vessel's wall (Fig. 4A), which disappeared at the second (Fig. 4B- 8th day) and third (Fig. 4 C - 30th day) time points.

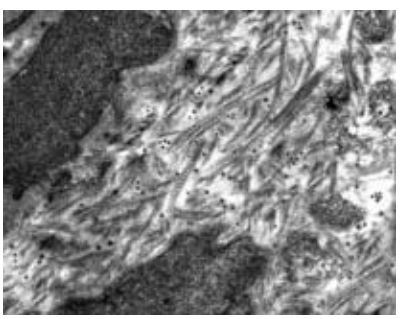

Fig. 6. *Eight days follow-up, transmission electron microphotograph evidences a still persistence of cross-linking or storiform-fingerprint arrangement of the collagen fibers, admixed with gold nanorods. This arrangement is considered atypical, differing to a parallel and well-oriented arrangement of the collagen fibers observed at 30 days follow-up. (15000 enlargements)*

After a moderate alteration in endoluminal surface of treated vessel, consisting in a linear

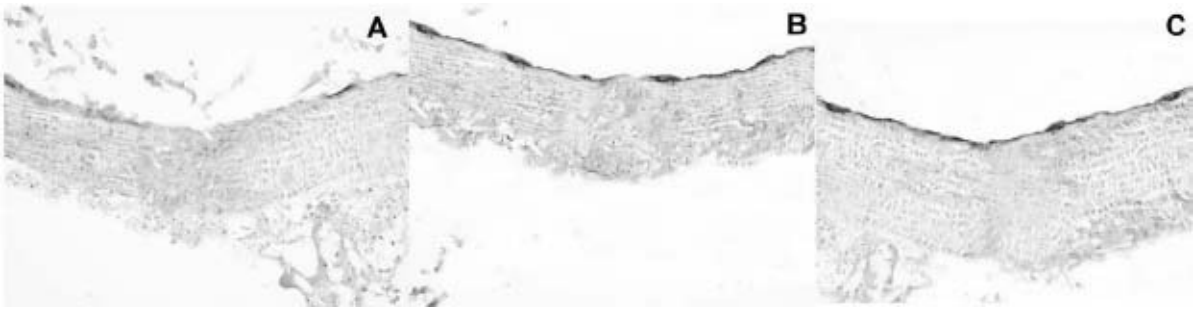

Fig. 7. *CD31 expression by endotheliocites 2 (**A**), 8 (**B**), and 30 (**C**) days after laser-assisted vessel repair, with GNRs dispersed in hyaluronan as solder. Note the weak expression of the chromogen 2 days after welding. A strong expression of CD31 in endotheliocites is evidenced, starting from the second follow-up time, 8 days after surgery, and is maintained in the third group, 30 days after surgery. IHC, 10X.*

Fig. 8. *vWF expression by endotheliocites 30 days after laser-assisted vessel repair. IHC, 10X.*

disendotelialization and adherence of few groups of cells, observed by SEM 2 days after treatment (Fig. 5A), further evidence of the total endothelial integrity restoration was observed in the impending areas of the treatment 8 and 30 days after surgery (Fig. 5 B and 5 C, respectively).

In Fig. 6 a TEM image of the treated area shows that, at 8 days follow-up, the reorganization process of the collagen fibers pattern is still incomplete. Morpfhological results are summarized in Table I.

Immunohistochemical evaluation

Immunohistochemical analysis supported the observation of endothelial integrity documented by the SEM examination. Furthermore, this exam was indicative of a good viability of the endothelium, which appeared to have been preserved in an optimal metabolic state by means of a constant and intense expression of CD31 and vWF. Immunohistochemical results demonstrated a full re-endothelialization at the application site of GNRs, starting 8 days after treatment (Fig. 7 B and C). There was a weak expression of the chromogen 2 days after welding (Fig. 7 A). A strong expression of CD31 in endotheliocites was evidenced, starting from the second follow-up time, 8 days after surgery (Fig. 7B) and was maintained in the third control, 30 days after surgery (Fig. 7 C). Comparable findings can be observed in the samples with expression of vWF (Fig. 8). Immunohistochemical results are summarized in Table I.

DISCUSSION

Laser soldering for the repair of microvessels can permit an immediate closure of the wound with minimal side effects (29). The replacement of traditional organic dyes with nanostructured chromophores is a very intriguing possibility. In an earlier report, we demonstrated for the first time that GNRs can mediate an effective photothermal effect in a model connective tissue (21). More recently, we provided a preliminary demonstration of the possibility of using GNRs for the *in-vivo* laser closure of a rabbit carotid artery by means of a manageable formulation consisting of a mixture of GNRs embedded in a hyaluronan viscous solution (22). In that case, GNRs with an average length of 102 nm and an average diameter of 25 nm were

Table I. *Microscopical findings at the 2nd, 8th, and 30th post-operative days.*

Follow-up group	Morphological analysis			Histochemical	Immuno-histochemical		TEM	SEM
	H&E			UTL	Factor VIII	CD-31		
	Inflammation	*Myointimal hyperplasia*	*Trombosis*	*Elastic Fiber Damage*	*Re-endothelization*	*Healthy endothelial cells*	*Collagen pattern*	*Endothelial aspect*
2 days	2.33±0.81	1.83±0.75	0.16±0.48	2.83±0.40	0.33±0.51	0.16±0.40	3	1.16±0.75
8 days	1.16±1.32	0.33±0.51	0	0.5±0.83	3	2.16±1.16	1±0.89	0.5±0.54
30 days	0.25±0.46	0.25±0.46	0	0.125±0.35	3	3	0	0

The table summarizes morphological and immunohistochemical results. The score criteria are described in the materials and methods section.

irradiated with a laser intensity of 40 W/cm^2 to obtain a closure of the vessel. Despite research having highlighted the feasibility of *in-vivo* laser-soldering operations by means of NIR-absorbing GNRs, very few experimental procedures have been performed and reported, and only one follow-up period (30 days) has been considered.

In the present study, the technique of laser soldering with GNRs used to repair a 3-mm incision on rabbit CCA was optimized. Furthermore, a consistent number of experimental procedures were performed in order to track both the morphological reorganization of vascular architecture and the fate of the GNRs within an irradiated site at different follow-up (2-8-30 days) periods.

GNRs were functionalized with a biopolymeric shell and then embedded in a viscous solution of hyaluronan to achieve a highly stabilized and handy material. The choice of hyaluronan offers the advantage of having well-known physiochemical and biological properties (23), which makes it a unique solution for the preparation of new biocompatible and biodegradable composites for wound repair purposes (27). To enhance the efficiency of the nanoparticles, their dimensions were reduced (28) so that lower laser intensity was necessary (as compared to previous tests). This is important in order to avoid lesions of irradiated tissues due to overheating and to eliminate the risk of undesired damage to surrounding structures, mostly for the application in fields such as neurosurgery and microvascular surgery. During a preliminary learning phase, the results of which are not reported in this work, the laser welding approach was further improved by optimization of the distribution of the gel on the artery walls and delivery of the laser light, so that it was possible to obtain a repeatable and standardized welding effect. In the optimized procedure, effective closure of the cut edges was obtained by using a 30 W/cm^2 laser intensity, which is lower as compared to previous results (22). The power reduction expressed the possibility of obtaining a good approximation of the margins without any deformation or overheating signs. The occlusion time of the treated vessels was 50 sec.

The GNR-mediated laser soldering approach was shown to induce effective local tissue fusion while preserving the endothelial viability and preventing thermally-induced thrombogenesis, which resulted technically easy to perform and has been found to minimize the surgical trauma to vessels.

At follow-up examinations, all the treated vessels were patent (100% patency) and no eversion of vessel edges or pseudoaneurysm formation was observed.

Morphological evaluation at different follow-up times showed the process of vessel repair starts in the immediate (2 days) post-operative period, through a strong action of depolimerization and re-polimerization of the collagen matrix, with a partial disappearance of the collagen and elastic fibers at the same point in time. The impending endothelium, however, maintains a metabolic activity, as demonstrated by the expression of factors such as

CD31 (Fig. 7) and vWF (Fig. 8). A vascular wall reconstitution is observed 8 days after treatment, even if the pattern of the collagen and elastic fibers shows a *random* course, as is deduced from a UTL specific stain (Fig. 3), and confirmed by means of a TEM examination (Fig. 6). Instead, the organization of the collagen appears to be regained after the 30th post-operative day, when a normal three-dimensional pattern of collagen and elastic fibers in the vessels seems to be almost restored (Fig. 3).

These results definitively confirm the previously-reported advantages of the combination of laser soldering and nanotechnologies, as compared to both conventional suturing methods and to other welding/soldering techniques based on the application of exogenous chromophores. However, there is a concern that still remains as an open question: the pathways for gold nanoparticles to leave the body after welding. A specific study on the biodistribution of the GNRS during the follow-up, as well as an investigation of their potential toxicity should be set up, in order to correctly estimate the benefits of nanotechnology over standard procedures (30).

In conclusion, this technique was shown to be effective and provides several advantages over conventional suturing methods. An optimal reorganization of vascular-wall structures was documented, together with a regaining of the physiological endothelial morphology (similar to a *restitutio ad integrum*) in the absence of thrombogenetic effects. This work further improves the existing knowledge on laser welding and nanotechnology applications in medical fields, in particular in microvascular repair surgery.

REFERENCES

1. Sanai N, Zador Z, Lawton MT. Bypass surgery for complex brain aneurysms: an assessment of intracranial-intracranial bypass. Neurosurgery 2009; 65:670-83.
2. Hanel RA, Spetzler RF. Surgical treatment of complex intracranial aneurysms. Neurosurgery 2008; 62(S):1289-97.
3. Lawton MT, Quinones-Hinojosa A, Sanai N, Malek JY, Dowd CF. Combined microsurgical and endovascular management of complex intracranial aneurysms. Neurosurgery 2008; 62(S):1503-15.
4. Gelli R, Pini R, Toncelli F, Chiarugi C, Reali UM. Vessel wall recovery after diode laser assisted microvascular anastomosis: Clinical and histological analysis on long term follow-up. J Reconstr Microsurg 1997; 13:199-205.
5. Puca A, Albanese A, Esposito G, Maira G, Tirpakova B, Rossi G, Mannocci A, Pini R. Diode laser-assisted carotid bypass surgery: an experimental study with morphological and immunohistochemical evaluations. Neurosurgery 2006; 59(6):1286-94.
6. Pini R, Rossi F, Matteini P, Ratto F. Laser tissue welding in minimally invasive surgery and microsurgery. In: Pavesi L, Fauchet PM, eds. Biophotonics, Berlin: Springer, 2008, p. 275-99.
7. Puca A, Esposito G, Albanese A, Maira G, Rossi F, Pini R. Minimally occlusive laser vascular anastomosis (MOLVA): experimental study. Acta Neurochir 2009 151:363-8.
8. Esposito G, Rossi F, Puca A, et al. An experimental study on minimally occlusive laser-assisted vascular anastomosis in bypass surgery: the importance of temperature monitoring during laser welding procedures. J Biol Regul Homeost Agents 2010; 24(3):307-15.
9. Bass LS, Treat MR. Laser tissue welding: a comprehensive review of current and future clinical applications. Lasers Surg Med 1995; 17:315-49.
10. Esposito G, Rossi F, Matteini P, Puca A, Albanese A, Sabatino G, Maira G, Pini R. Present status and new perspectives in laser welding of vascular tissues. J Biol Regul Homeost Agents 2011; 25(2):145-52.
11. Wolf-de Jonge IC, Beek JF, Balm R. 25 years of laser assisted vascular anastomosis (LAVA): what have we learned? Eur J Vasc Endovasc Surg 2004; 27(5):466-76.
12. Gathje, J, Steuer, RR, Nicholes, KR. Stability studies on indocyanine green dye J Appl Physiol 1970; 29(2):181-5.
13. Landsman MLJ, Kwant G, Mook GA, Zijlstra WG. Light-absorbing properties, stability, and spectral stabilization of indocyanine green. J Appl Physiol 1976; 40:575-83.
14. Saxena V, Sadoqi M, Shao J. Degradation kinetics of indocyanine green in aqueous solution. J Pharm Sci-Us 2003; 92(10):2090-97.
15. Holzer W, Mauerer M, Penzkofer A, Szeimies RM,

Abels C, Landthaler M, Baumler W. Photostability and thermal stability of indocyanine green. J Photochem Photobiol B 1998; 47(2-3):155-64.
16. Sutterer WF, Hardin SE, Benson RW, Krovetz LJ, Schiebler GL. Optical behavior of indocyanine green dye in blood and in aqueous solution. Am Heart J 1966; 72(3):345-50.
17. Gobin AM, O'Neal DP, Watkins DM, Halas NJ, Drezek RA, West JL. Near infrared laser-tissue welding using nanoshells as an exogenous absorber. Lasers Surg Med 2005; 37(2):123-9.
18. Hu M, Chen J, Li ZY, Au L, Hartland GV, Li X, Marqueze M, Xia Y. Gold nanostructures: engineering their plasmonic properties for biomedical applications, Chem Soc Rev 2006; 35:1084-94.
19. Jain PK, Lee KS, El-Sayed IH, El-Sayed MA. Calculated absorption and scattering properties of gold nanoparticles of different size, shape, and composition: applications in biological imaging and biomedicine. J Phys Chem B 2006; 110(14):7238-48.
20. Ratto F, Matteini P, Rossi F, Pini R. Size and shape control in the overgrowth of gold nanorods. J Nanopart 2009; 12(6):2029-36.
21. Ratto F, Matteini P, Rossi F, Menabuoni L, Tiwari N, Kulkarni SK, Pini R. Photothermal effects in connective tissues mediated by laser-activated gold nanorods. Nanomedicine 2009; 5:143-51.
22. Matteini P, Ratto F, Rossi F, Rossi G, Esposito G, Puca A, Albanese A, Maira G, Pini R. In vivo carotid artery closure by laser activation of hyaluronan-embedded gold nanorods. J Biomed Opt 2010; 15(4):041508.
23. Matteini P, Dei L, Carretti E, Volpi N, Goti A, Pini R. Structural behavior of hyaluronan under high concentration conditions. Biomacromolecules 2009; 10:1516-22.
24. Niidome T, Yamagata M, Okamoto Y, Akiyama Y, Takahashi H, Kawano T, Katayama Y, Niidome Y. PEG-modified gold nanorods with a stealth character for in vivo applications. J Control Release 2006; 114(3):343-7.
25. Stendel R, Pietilä T, Al Hassan AA, Schilling A, Brock M. Intraoperative microvascular Doppler ultrasonography in cerebral aneurysm surgery. J Neurol Neurosurg Psychiatry 2000; 68(1):29-35.
26. Marchese E, Albanese A, Denaro L, Vignati A, Fernandez E, Maira G. Intraoperative microvascular Doppler in intracranial aneurysm surgery. Surg Neurol 2005; 63(4):336-42.
27. Chen WYJ, Abatangelo G. Function of hyaluronan in wound repair. Wound Repair Regen 1999; 7:79-89.
28. Baffou G, Quidant R, Girard C. Heat generation in plasmonic nanostructures: Influence of morphology. Appl Phys Lett 2009; 94:153109.
29. Alander J, Kaartinen I, Laakso A, et al. A review of indocyanine green fluorescent imaging in surgery. Int J Biomed Imag. In press (2012).
30. Terentyuk GS, Maslyakova GN, Suleymanova LV, et al. Circulation and distribution of gold nanoparticles and induced alterations of tissue morphology at intravenous particle delivery. J Biophotonics 2009; 2(5):292-302.

VIRAL SEQUENCE ANALYSIS OF OCCULT HBV INFECTION AND ITS REACTIVATION IN IMMUNOSUPPRESSED PATIENTS

D. FERRARO[1], P. PIZZILLO[1], N. URONE[1], E. IANNITTO[2], A. CRAXÌ[3] and R. DI STEFANO[1]

[1]Sezione di Microbiologia, Dipartimento di Scienze per la Promozione della Salute "G. D'Alessandro", University of Palermo, Palermo, Italy; [2]Unità Operativa Complessa di Ematologia con Trapianto, University of Palermo, Palermo, Italy; [3]Sezione di Gastroenterologia, Dipartimento Biomedico di Medicina Interna e Specialistica (Di.Bi.M.I.S.), University of Palermo, Palermo, Italy

Received December 21, 2011 – Accepted May 22, 2012

The first two authors contributed equally to this study

Mechanisms associated with reactivation of hepatitis B virus (HBV) in patients with occult HBV infection (OBI) remain unclear. In some cases immunosuppression is an enhancer of viral replication. However, not all patients with OBI who undergo immunosuppression experience reactivation. This study explores the role of viral heterogeneity as a determinant of occult HBV reactivation. HBV genotype, mutation patterns and quasispecies were assessed by sequencing the PreS/S region of 16 patients with OBI undergoing chemotherapy, 3 of whom experienced a OBI reactivation. The latter were also assessed at the time of reactivation. Phylogenetic analysis identified low nucleotide and amino acid diversity rates. There were no differences in the viral quasispecies, or common mutation patterns, detected between patients who underwent reactivation of OBI, and those who did not. Furthermore, upon reactivation, the quasispecies evolved towards a loss of most of the variants present during the initial OBI stage, probably representing the fittest version of the virus. The genetic variability of HBV alone did not account for the transition from occult to overt infection, which appears to be governed principally by the host's immune response.

Hepatitis B virus (HBV) can persist in a host as an occult infection (OBI), where HBV DNA can be detected in the liver, and sometimes in the serum, of patients who are seronegative for HBV surface antigen (HBsAg) (1).

In patients undergoing strong immunosuppression, OBI has been shown to reactivate overt HBV replication (2-5), resulting in an ensuing, and often severe, hepatitic flare.

When HBV infection persists, the viral genome is maintained in the nucleus of hepatocytes as a covalently closed, circular DNA (cccDNA) bound to histones and non-histone proteins and regulated by their acetylation status (6). It is estimated only a few molecules are typically detected in the liver of OBI patients (7). This condition may also explain the inability of HBsAg to be detected in serum by available diagnostic assays (8).

A number of studies have investigated the role of viral heterogeneity as a primary determinant of OBI.

Key words: occult HBV, HBV reactivation, phylogenetic analysis, molecular epidemiology

Mailing address: Dr Donatella Ferraro,
Dipartimento di Scienze
per la Promozione della Salute "G. D'Alessandro"
Via del Vespro, 133
90138 Palermo, Sicily, Italy
Tel.: +39 091 6553680 Fax: +39 091 655 3676
e-mail: dferraro@unipa.it

0393-974X (2012)

DISCLOSURE: ALL AUTHORS REPORT NO CONFLICTS OF INTEREST RELEVANT TO THIS ARTICLE.

For example, well-characterized epitope mutations have been detected in the preS/S region, especially in the major hydrophilic region (MHR) of the S gene (e.g., amino acids 100-160), which contains an "a" determinant. With this region being a main target for monoclonal antibodies used in diagnostic tests, these mutations can affect the recognition of conformational epitopes (9,10,11,12,13). Point mutations and deletions within the preS and S genes can also influence HBsAg secretion and expression, leading to low levels of HBsAg (14,15). However, the degree of variability associated with HBV quasispecies is not as well characterized (16,17). It is also not known how immune modulation and reconstitution affect the suppression and re-expansion of individual HBV clades within the HBV quasispecies at different stages of OBI. Therefore, the mechanisms underlying HBV reactivation in OBI patients remain unclear. In a previous study, we reported that 27.7% of patients with OBI that experienced an oncohematological disease requiring immunosuppression developed viral reactivation and a hepatitic flare (18). In the present study, we investigate the HBV genomic variability of a cohort of patients with OBI that undergo chemotherapy, with the goal of investigating possible differences between viral variants present in patients with OBI reactivation, versus those without reactivation. Correspondingly, HBV isolates from these patients were analyzed during the occult infection stage for genotype, subtype, and mutation patterns and then cloned to study the genetic variability of viral quasispecies. For patients in whom OBI reactivation occurred, the same studies were performed again at the time of reactivation.

MATERIALS AND METHODS

Patients

Sixteen OBI (e.g., p1 - p16) patients with onco-hematological diseases were selected retrospectively from a cohort of 75 HBsAg negative patients previously studied for OBI (18). The selected subjects were positive in serum for the four different HBV genomic regions (e.g., preS/S, preC/C, Pol, and X) by nested PCR assays (limits of sensitivity between 0.1 and 0.05 IU/ml), while HBV DNA was undetectable using a bDNA assay (bDNA, Siemens, detection limit = 357 IU/ml) and a *home made* nested-PCR (sensitivity 60 UI/ml). All patients were treated with cytotoxic chemotherapy without Rituximab, and 6 patients also received corticosteroids. Virological analyses were performed for all patients prior to initiation of chemotherapy (baseline), and during the reactivation stage for patients positive for HBsAg (Table I). During chemotherapy, 3/16 patients (p1, p2, p3) experienced a virological and clinical HBV reactivation after a mean of 8 months. These patients were found to be HBsAg- and HBeAg-positive, with HBV DNA loads of 1.6×10^6, 7.6×10^6, and 1×10^4 IU/ml for p1, p2, and p3, respectively. These patients were subsequently treated with lamivudine (100 mg/day) and remained positive for HBsAg.

HBV DNA amplification and sequencing

Sequencing was performed for a fragment of 1059 bp that spanned the entire preS1 and preS2 regions and 537 nucleotides of the S gene. Viral DNA was at first amplified using O_1 (5'-GGGTCACCATATTCTTGGGAA-3') and O_2 primers (5'-CTCAGTTTACTAGTGCCATT-3'). An aliquot of PCR product was then reamplified in three separate reactions to obtain partially overlapping genome fragments of 479, 710, and 537 bases, respectively using the following primers: O_1 and N_2 (5'-CTGTTCTGACTACTGCCTCTC-3'), N_3 (5'-AATCCGGATTGGGACTTCAA-3') and N_4 (5'-GTTCTTCTGGACTATCAAGG-3'), N_5 (5'-CATGGAGAACATCACATCAGG-3') and O_2. The amplifications were performed with 35 cycles of: 94°C for 1 min, 50°C for 1 min, and 72°C for 2 min, followed by a final incubation at 72°C for 10 min. Amplicons were sequenced with the same primers used for DNA amplification and a Big Dye Terminator v 1.1 Cycle Sequencing Kit (Applied Biosystem, Foster City, CA, USA) in an automatic DNA sequencer (ABI Prism 310 Genetic Analyzer, Applied Biosystem).

Determination of genotype, subgenotype, and mutation patterns

The three overlapping sequences, obtained by nested PCR, were assembled, edited, and aligned using BioEdit version 4.0, using the Clustal W multi-alignment system. Genotypes and subgenotypes were inferred by aligning each sequence with reference

sequences of HBV/D1 – HBV/D5 subgenotypes. Phylogenetic trees were subsequently constructed using Mega 4.1 software (19). Mutational patterns of the sequences analyzed was determined by comparison with consensus wild-type sequences specific for subtype D1 and D3, generated using sequences available in Gen-Bank database (e.g., D1: AF280817, Y07587, AF151735, L27106, X80924, M32138, AF121242, EU594396, EU594397, FJ386590, FJ904432, FJ904443, FJ904445, FJ904446, GQ167302, AB104709, AB104710, AB104711, AB104712, AB126581, AF121239, AF121240, AF121241, AY721605, AY721606, AY721607, AJ721612, AY741798, AY796030, AY796032, X02496; D3: X85254, AJ233291, AJ233292, AJ233293, AJ233294, AJ233295, AJ233296, U95551).

Cloning and quasispecies analysis

Viral quasispecies was investigated using clonal analysis, with the pGEM-T easy vector system according to the manufacturer's protocol (Promega, Madison, WI). For the occult HBV stage, where amplification was positive only after a second PCR step, the major amplicon of 710 bp (which spanned the preS1 region from nts 77-306 of the S region) was selected for cloning and quasispecies analysis. At the time of reactivation the entire 1059-bp sequence obtained at the first amplification step was cloned, because it was present in all patients. For each patient, DNA extracted from 4-10 recombinant colonies was directly sequenced. Neighbour-joining trees were then generated using MEGA 4.1 software (using 1000 bootstrap replicates) by applying

Table I. *Demographic and HBV Serological profiles of 16 patients prior to receiving immunosuppressive therapy.*

Patients	***Anti-HBc*** [a]	***Anti-HBs*** [b]	***M/F***	***Mean age (range)***	***Treatment (steroid/no steroid)*** [c]
PATIENTS WITH REACTIVATION					
p1	Neg [d]	Neg	3/0	78 (73-81)	1/2
p2	Neg	Neg			
p3	**Pos** [e]	**Pos**			
PATIENTS WITHOUT REACTIVATION					
p4	**Pos**	**Pos**	6/7	63.4 (41-81)	5/8
p5	**Pos**	Neg			
p6	Neg	Neg			
p7	**Pos**	**Pos**			
p8	Neg	Neg			
p9	Neg	neg			
p10	Neg	Neg			
p11	Neg	Neg			
p12	Neg	Neg			
p13	Neg	**Pos**			
p14	Neg	Neg			
p15	Neg	**Pos**			
p16	**Pos**	**Pos**			

[b] *HBs: surface antigen*
[c] *None of these patients were treated with Rituximab*
[d] *Neg: negative*
[e] *Pos: positive*

pairwise deletion and the Kimura-2 parameter model. This model was also used to calculate nucleotide and amino acid substitution rates.

Statistical analysis

Statistical analyses were performed using Student's t-test and the χ^2 test, with Fisher's exact test used to compare categorical data. *P* values less than 0.05 were considered statistically significant. Calculations were performed using GRAPHPAD PRISM version 5.00 (GraphPad Software Inc., San Diego, CA, USA).

RESULTS

HBV genotype and subtype

All 16 patients included in this retrospective study were infected with a genotype D HBV strain (HBV/D), with 6/16 (37.5%) having the subtype HBV/D1, and 10/16 (62.5%) having subtype HBV/D3. There were no gender- and mean age-related differences in the incidence of subtype (p = 0.15, p = 0.43). One reactivation event was reported in the HBV/D1 group and 2 were reported in the HBV/D3 group (p = 0.87).

S-gene sequences at baseline

When isolates from 16 OBI patients (p1–p16) were compared with consensus wild-type sequences specific for HBV subtypes, D1 and D3, between 3 and 37 nucleotide substitutions in the 1059 bp region of the preS/S gene were detected. The nucleotide substitutions were evenly distributed throughout the region analyzed, with only a few substitutions occurring at identical positions in all patients. Furthermore, the number of non-synonymous substitutions ranged from 2 to 20. Overall, the highest number of mutations detected in the preS1

Table II. *Complete list of amino acid changes detected in HBV isolates obtained from a patients (n=16).*

	PreS1	**PreS2**	**S**
p1[a]	A28E, A84V	P41H, P52H	S167L
p2[a]		G30E	E164G
p3[a]	W66R, Q89K	S5Y, H9L, Q10K, deletion of amino acid 22, P23H, P41H ,L54R	E2G, G10E, S31N, T115N, T123P,Q129R,T131N, P135L, C147Y, I150T,E164V
p4	A79V	T31A	P120S
p5		P36L	L89P
p6	G48R	R18K, A39V,P41H,L42I	T126S
p7	S90P, G91R, G92R, frame shift from position 96	I42L, S43L	P120S, P127L, G145A, S154P
p8	L77V		P120S, Y134H, W165S
p9	L77V,N103T		
p10	A79V		P120S
p11	L77V		P120S, Y134H, E164G, W165S
p12	L77V		Stop codon at position 30
p13	A79V		P120S
p14	L77V	G50A	L109R, P120S, Y134H, E164G, W165S
p15	L77V		Stop codon at position 30
p16	D16G,S90P, G91R	P52H	Wild-type/Stop codon at position 30, P127L, T140I, E164G

[a] *Patients with OBI reactivation under immunosuppression*

region was associated with one isolate from p7, who did not experience a reactivation of OBI. In this case, insertion of a thymidine base between nucleotides G289 and C290 caused a shift from amino acid 96 in the reading frame. L77V mutation in preS1 region was identified in six viral isolates and A79V mutation

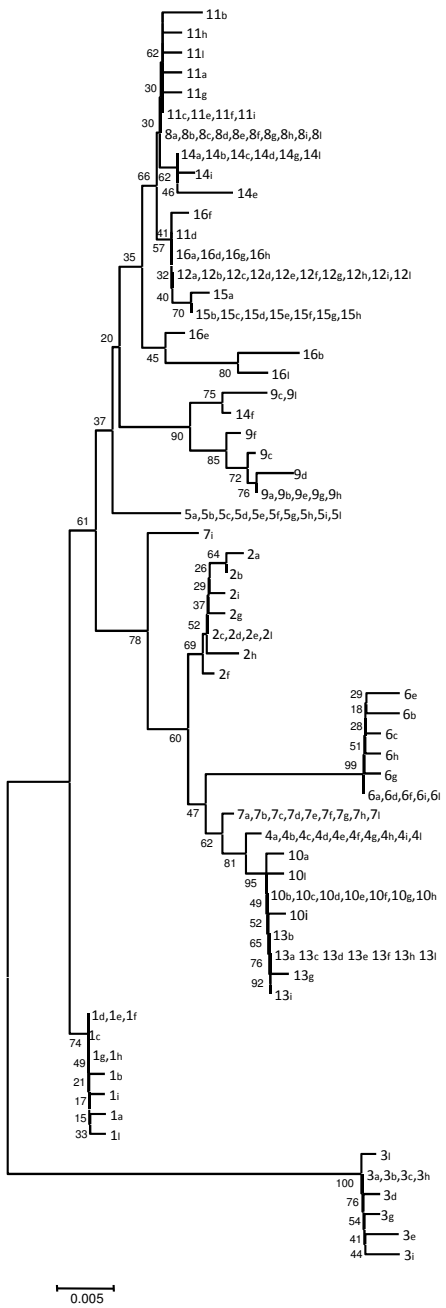

Fig. 1. *Neighbour-joining tree of the HBV preS/S region (710 bp) sequenced from 16 OBI patients prior to the start of chemotherapy. Bootstrap values from 1000 replicates were used.*

in three other viral strains isolated from the thirteen patients that did not undergo OBI reactivation

An analysis of the preS2 region identified an in-frame deletion present in a strain isolated from p3, who later experienced a reactivation of OBI with administration of chemotherapy. In the S gene of the same isolate was found an amino acid change in the putative human leukocyte antigen class I-restricted cytotoxic T lymphocyte epitope (aa 28–51) of HBsAg. For three other patients (p12, p15, p16) that did that not experience a reactivation of OBI, the same region contained a point mutation, C87T, that formed a stop codon (CAG → TAG) at position 30. Between 1 and 4 substitutions were detected within the MHR of the S gene (amino acids 100–160) in 11/13 patients without OBI reactivation. Moreover, eight viral isolates had at least one amino acid change in the "a" determinant region (aa 124–147). Of these substitutions, only the P120S mutation has previously been described in studies of vaccine escape mutants (20,21). Furthermore, of three patients who later had experienced a reactivation of OBI, only an isolate from p3 showed a peculiar mutation pattern in S region, which included 11 amino acid changes, 7 of which were present in the MHR. Furthermore, of these mutations, only the Q129R (22) and C147Y (12) mutations have been shown to correlate with a possible immune escape phenomenon. The complete list of amino acid changes in HBV isolates from all patients is listed in Table II.

The substitutions detected in the preS/S region resulted in up to 17 amino acid changes in the overlapping polymerase region, and between 1 and 4 changes in the RT domain. Furthermore, any of these mutations could potentially result in replication-defective HBV mutants, except for an isolate from p7 which was associated with a stop codon at amino acid position 281.

Phylogenetic analysis of HBV at baseline and during OBI reactivation

The genomic variability prior to chemotherapy (baseline) was studied by cloning 710 bp of HBV preS/S gene. The phylogenetic analysis of 8-10 clones for each isolate found a low nucleotide (0–1.6%) and amino acid (0–3.4%) diversity rates for all patients, with only a few mutations in individual clones not detected previously by direct sequencing.

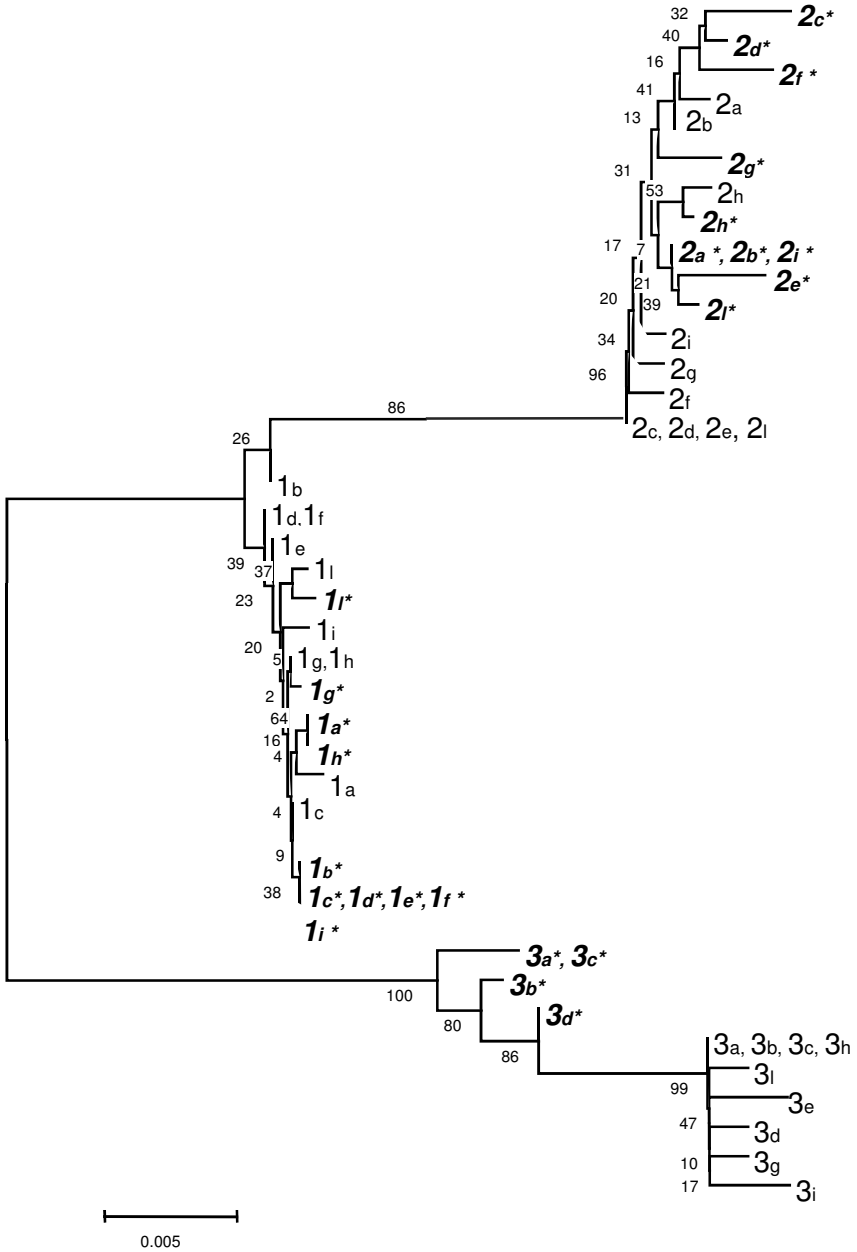

Fig. 2. *Neighbour-joining tree of the HBV preS/S region (710 bp) from 3 OBI patients prior to the start of chemotherapy and following of reactivation. Bootstrap values from 1000 replicates were used. Asterisks indicate the clones that were detected during the reactivation stage.*

The phylogenetic tree also showed that most clones for each patient were clustered, with between 4 and 10 clones being identical (Fig. 1).

For the three patients with OBI reactivation (p1, p2, p3), phylogenetic analysis was performed on isolates obtained at baseline (9-10 clones) and at the time of viral reactivation. At this time, 10 clones were obtained from p1 and p2, while only four clones were obtained from p3 due to reduced cloning efficiency attributed to insufficient DNA. Phylogenetic analysis was performed for each isolate and rates of nucleotide and amino acid diversity was found to

range from 0–2.6%, and 0–4.8%, respectively (Fig. 2). The HBV quasispecies, which was initially found to be relatively diverse, evolved during the stage of reactivation towards a loss of most of the variants present during the initial OBI stage.

DISCUSSION

It has previously been shown that the full-length HBV genome persists in an OBI patient despite suppression of its replicative activity and gene expression (1). When the immune system is induced to be unresponsive, HBV can undergo reactivation and overcome the control systems of the host. However, it remains unclear why this occurs in only some OBI patients.

The heterogeneity of HBV in 16 patients experiencing an occult infection prior to the start of strongly immunosuppressive chemotherapeutic regimens was assessed in the present study. In 3/16 patients, despite comparable degrees of immunosuppression, reactivation of OBI occurred. However, only one case involved the administration of corticosteroids.

At baseline in the OBI state, most HBV isolates did not display significant variants, although there were a few exceptions. For example, the isolate from p7, that did not undergo OBI reactivation, showed a frame shift from the amino acid 96 in the preS1 region, within the PreS2/S promoter. This mutation determines the change of a significant proportion of the *Large* protein, potentially altering its folding and function. The preS1 region has previously been shown to harbor the preS2/S promoter, the binding sites for the recognition of hepatocytes (23) and some epitopes recognized by neutralizing antibodies (11), and is involved in the incorporation of the capsid into the envelope (24). Correspondingly, a frameshift would induce the defective assembly of virions, inhibit the recognition of hepatocyte receptors, and alter antigenicity. However, an *in vitro* study of HBV variants, in which the preS2 start codon was abolished by an in-frame deletion or a point mutation, have shown that normal viral replication occurred. However, lower levels of HBsAg were associated with these variants compared with wild-type strains (16,17).

The mutations at positions 77 and 79 of pre-S1 region falls in the major cytosolic loop (residues 29-80) that interacts with core particles. These mutations could affect the formation and secretion of empty envelopes and the nucleocapsid envelopment.

A stop codon at amino acid position 30 of the S region in three other viral isolates from patients that did that not experience a reactivation of OBI, resulted in the production of a truncated protein devoid of the main antigenic HBV determinant, and of the second determinant (aa 119-128, coreceptor) required for infectivity, as described in an HBV/HDV model by Jaoudè G.A. and Sureau C.(25). Both these characteristics might help maintain the OBI state, and prevent the transition to overt infection.

In seven patients who did not undergo OBI reactivation, a P120S mutation was detected. This mutation was originally described in infants born to HBV-carrying mothers who underwent anti–HBV immunization at birth. However, more recently, an *in vitro* study found that P120S variants from isolates of OBI patients synthesize a fully functional S protein (Pollicino T., unpublished data).

Regarding the baseline status of the three patients who experienced an OBI reactivation following the administration of chemotherapy, only p3 harbored a HBV with a specific mutational pattern characterized by 20 substitutions in the *Large* protein. Moreover, a subset of these mutations have previously been reported (26) and associated with the production of a predicted novel HBsAg variant. This hypothesis is also supported by the presence of the relevant C147Y mutation. Indeed, cysteine substitutions within the "a" determinant have been shown in *in vitro* studies to alter tertiary structure (12), resulting in loss of antigenicity, consistent with a lack of detectable HBsAg reactivity. Remarkably, p3 was also found to be anti-HBs positive, suggesting that this variant may be an immune escape mutant.

Although it has been suggested that the selection of immune escape mutants is characteristic of OBI with HBV/D (27), both the findings of the present study and others (16, 7), show that are present in only a small proportion of OBI cases. In addition, taking into account the partial overlap of the open reading frames for the preS/S and P regions, none of the mutations identified in the present study have the potential to affect viral fitness by altering polymerase status, except for an isolate from p7 which bears a

stop codon within the spacer domain. However, the identification of this single isolate is not sufficient to assert that the virus infecting this patient is unable to replicate, since the variant may only represent a subset of the viral population present.

The phylogenetic analysis at baseline showed a low quasispecies diversity in all patients, with no differences found between patients with or without OBI reactivation. However, since the MHR was not analyzed, the observation of low rates of diversity must be recognized in this context.

For the three patients who underwent reactivation of OBI, the HBV quasispecies observed at the time of viral reactivation was found to contain less variants than those detected at baseline. However, the genetic diversity observed may also reflect the natural evolution of the HBV genome during an occult infection that is related to maintenance of viral replication, even if it is at low levels, prior to reactivation.

The pattern of quasispecies evolution observed in the present study may represent a "funnel effect". In the resting stage at baseline, the HBV population is hypothesized to be selected by mechanisms of immune pressure and viral senescence. This could potentially result in the generation of strains with low replicative fitness and reduced HBsAg expression. During a strong immunosuppression, a more fit virus could emerge and expand, ultimately maintaining its selective advantage over weaker competitors in the quasispecies present. Although it was not possible to investigate cellular compartments of HBV replication in this study, such as hepatocytes and peripheral blood mononuclear cells, the viruses present in serum samples would be expected to reflect the viral population maintained in liver cells.

These data, although obtained from a small number of cases, confirm that OBI is a complex phenomenon of virus-host interactions. Moreover, mutations altering the expression of preS/S and the production of new viruses have been observed in some cases, but there was not a pattern of mutations that characterizes the probability of reactivation. These considerations are in according to studies that examined HBV isolates from liver tissue occult HBV carriers (28,29) Therefore, the genetic variability of HBV alone does not explain the transition from an occult infection to an overt infection, which is principally governed by the host's immune response, and which subsequently influences the further evolution of HBV quasispecies.

REFERENCES

1. Raimondo G, Allain JP, Brunetto MR et al. Statements from the Taormina expert meeting on occult hepatitis B virus infection. J Hepatol 2008; 49:652-7.
2. Brechot C, Thiers V, Kremsdorf D, Nalpas B, Pol S, Paterlini-Brechot P. Persistent hepatitis B virus infection in subjects without hepatitis B surface antigen: clinically significant or purely "occult"?. Hepatology 2001; 34:194-203.
3. Chemin I, Trepo C. Clinical impact of occult HBV infections. J Clin Virol 2005; 34:S15-S21.
4. Hu KQ. Occult hepatitis B virus infection and its clinical implications. J Viral Hepat 2002; 9:243-57.
5. Iannitto E, Minardi V, Calvaruso G, et al.Hepatitis B reactivation and alemtuzumab therapy. Eur J Haematol 2005; 74:254-8.
6. Pollicino T, Belloni L, Raffa G, Pediconi N, Squadrito G, Raimondo G, Levrero M. Hepatitis B virus replication is regulated by the acetylation status of hepatitis B virus cccDNA-bound H3 and H4 histones. Gastroenterology 2006; 130:823-37.
7. Levrero M, Pollicino T, Petersen J, Belloni L, Raimondo G, Dandri M. Control of cccDNA function in hepatitis B virus infection. J Hepatol 2009; 51:581-92.
8. Nguyen T, Desmond P, Locarnini S. The role of quantitative hepatitis B serology in the natural history and management of chronic hepatitis B. Hepatol Int 2009; 3:S5-S15.
9. Hollinger F.B. Hepatitis B virus genetic diversity and its impact on diagnostic assays. J Viral Hepat 2007; 14:S11-S15.
10. Osiowy C. Detection of HBsAg Mutants. J Med Virol 2006; 78: S48-S51.
11. Kreuts C. Molecular, immunological and clinical properties of mutated hepatitis B viruses. J Cell Mol Med 2002; 6:113-43.
12. Katsoulidou A, Paraskevis D, Magiorkinis E, et al. Molecular characterization of occult hepatitis B cases in Greek blood donors. J Med Virol 2009; 81:815-25.

13. Weber B. Genetic variability of the S gene of hepatitis B virus. Clinical and diagnostic impact. J Clin Virol 2005; 32:102-12.
14. Khan N, Guarnieri M, Ahn SH, et al. Modulation of hepatitis B virus secretion by naturally occurring mutations in the S gene. J Virol 2004; 78:3262-70.
15. Warner N, Locarnini S. The antiviral drug selected hepatitis B virus rtA181T/sW172* mutant has a dominant negative secretion defect and alters the typical profile of viral rebound. Hepatology 2008; 48:88-98.
16. Pollicino T, Raffa G, Costantino L, Lisa A, Campello C, Squadrito G, Levrero M, Raimondo G. Molecular and functional analysis of occult hepatitis B virus isolates from patients with hepatocellular carcinoma. Hepatology 2007; 45:277-85.
17. Hass M, Hannoun C, Kalinina T, Sommer G, Manegold C, Gunther S. Functional analysis of hepatitis B virus reactivating in hepatitis B surface antigen-negative individuals. Hepatology 2005; 42:93-103.
18. Ferraro D, Pizzillo P, Di Marco V, Vultaggio A, Iannitto E, Venezia G, Craxì A, Di Stefano R. Evaluating the risk of hepatitis B reactivation in patients with haematological malignancies: is the serum hepatitis B virus profile reliable? Liver Int 2009; 29:1171-77.
19. Kumar, S., Tamura K, Nei M. MEGA3: integrated software for molecular evolutionary genetics analysis and sequence alignment. Brief Bioinform 2004; 5:150-63.
20. Wallace LA, Echevarria JE, Echevarria JM, Carman WF. Molecular characterization of envelope antigenic variants of hepatitis B virus from Spain. J Infect Dis 1994; 170:1300-303.
21. Chong-Jin O, Wei Ning C, Shiuan K, Gek Keow L. Identification of hepatitis B surface antigen variants with alterations outside the "a" determinant in immunized Singapore infants. J Infect Dis 1999; 1:259-63.
22. Hsu HY, Chang MH, Ni YH, Lin HH, Wang SM, Chen DS. Surface gene mutants of hepatitis B virus in infants who develop acute or chronic infections despite immunoprophylaxis. Hepatology 1997; 3:786-91.
23. Chouteau P, Le Seyec J, Cannie I, Nassal M, Guguen-Guillouzo C, Gripon P. A short N-proximal region in the large envelope protein harbours a determinant that contributes to the species specificity of human B hepatitis. J Virol 2001; 75:11565- 11572.
24. Seeger C, Zoulim F, Mason WS. Hepadnaviruses. In: Knipe DH, Howley PM, Griffin DE, Lamb RA, Martin MA, Roizman B, et al, editors. Fields Virology 5th ed. Philadelphia: Lippincott Williams and Wilkins; 2007.
25. Jenna S, Sureau C Role of the Antigenic Loop of the Hepatitis B Virus Envelope Proteins in Infectivity of Hepatitis Delta Virus. J Virol 2005; 79:10460-66.
26. Candotti D, Grabarczyk P, Ghiazza P, et al. Characterization of occult hepatitis B virus from blood donors carrying genotype A2 or genotype D strains. J Hepatol 2008; 49:537-47.
27. Schaefer S. Hepatitis B virus. Significance of genotypes. J Viral Hepat 2005; 12:111-24.
28. Cacciola I, Pollicino T, Squadrito G, Cerenzia G, Orlando ME, Raimondo G. Occult hepatitis B virus infection in patients with chronic hepatitis C liver disease N Engl J Med 1999; 341:22-26.
29. Pollicino T, Squadrito G, Cerenzia G, et al. Hepatitis B virus maintains its pro-oncogenic properties in the case of occult HBV infection. Gastroenterology 2004; 126:102-10.

TREATMENT OF RADICULOPATHIES: A STUDY OF EFFICACY AND TOLLERABILITY OF PARAVERTEBRAL OXYGEN-OZONE INJECTIONS COMPARED WITH PHARMACOLOGICAL ANTI-INFLAMMATORY TREATMENT

D. MELCHIONDA[1], P. MILILLO[2], G. MANENTE[3], L. STOPPINO[2] and L. MACARINI[2]

[1]Department of Neurology, Azienda Ospedaliero-Universitaria di Foggia, Italy; [2]Department of Radiology, University of Foggia, Italy; [3]Neurology Operative Unit, Ospedale Civile di Teramo, Italy

Received December 13, 2011 – Accepted June 22, 2012

The study was performed to evaluate the effectiveness of lumbar paravertebral injections of a gas mixture of Oxygen and Ozone in patients with lumbar radiculopathies caused by L4-L5 or L5-S1 disk herniations compared to a pharmacological therapy based on non-steroidal anti-inflammatory drugs. Lumbar radiculopathy caused by disc herniation is widely spread. Many therapeutic options are available before steering patients to the surgery. Low back pain and sciatica represent some of the most frequent causes of antinflammatory-analgesic drugs overuse. Recent findings have shown that medical Ozone can be used in the treatment of radicular syndrome caused by herniated intervertebral discs. Although widely spread, there are insufficient published data supporting the effectiveness of this approach in clinical practice. We studied 38 affected patients with acute L5 or S1 radicolopathy. The patients were randomly divided in two groups: A) 20 patients treated with lumbar paravertebral injections of Oxygen and Ozone; B) 18 patients treated pharmacologically with antinflammatory-analgesic drugs. All patients underwent a clinical and neurological examination at baseline (T1) and after 1 (T2), 2 (T3), 4 weeks (T4) and after 3 (T5) and 6 months (T6). An MRI and EMG examination were performed at baseline and after 6 months. The intensity of pain and the outcome of treatments were evaluated in all patients with the Visual Analogue Scale and with the Oswestry Disability Index. We found a reduction of pain and discomfort soon after one week with oxygen-ozone injections compared with pharmacological treatment, but this difference of response became statistically significant after two weeks (50% *vs* 16.6%) and is confirmed after 3 and 6 months, when 80% of patients treated with injections turned out pain free compared with half of the patients treated pharmacologically. No statistical difference were found in MRI and EMG examinations. No adverse effects were found in any patient of group A. We hypothesize that oxygen-ozone injections in paravertebral regions can induce a direct reduction of root inflammation with a corresponding reduction of pain. The paravertebral injections of oxygen-ozone represent a rapidly effective therapy, easily practicable and secure, in patients with lumbar radicolopathies secondary to disc herniation.

Low back pain (LBP) and sciatica caused by lumbar disc herniation are considered some of the most common diseases and the most frequent cause of absence from work. It has been reported

Key words: roots impingement, disk herniation, NSAIDs, VAS, sciatica, lumbar radiculopathy

Mailing address: Dr Donato Melchionda,
S.C. di Neurologia Universitaria,
Azienda Ospedaliero-Universitaria di Foggia,
Viale Pinto 1,
71011 Foggia, Italy
Tel.: +39 3383308485 Fax: +39 0881732473
e-mail: dmelchiond@ospedaliriunitifoggia.it

0393-974X (2012)

DISCLOSURE: ALL AUTHORS REPORT NO CONFLICTS OF INTEREST RELEVANT TO THIS ARTICLE.

that protruded discs can be found in 20-30% of the normal population (1). The incidence of symptomatic lumbar disc herniation in the American population is estimated to be 1% to 2% (1, 2). There is substantial controversy regarding its treatment. Many reports recently clearly demonstrated that most patients with lumbar radiculopathy caused by disk herniation will get better spontaneously and the herniation can disappear in a few months without any treatment (2). Prithvi Raj et al. (3) considers 90% of all patients suffering with radicular pain caused by disc herniation will obtain satisfactory pain relief by conservative measures. These conservative treatments take the form of oral analgesics, corticosteroids, antiepileptic and antidepressive drugs, no dynamic stabilization, gentle tractions. In fact, LBP and sciatica represent some of the most frequent causes of antinflammatory-analgesic drugs overuse (4). All recent guidelines recommend the prescription of nonsteroidal anti-inflammatory drugs (NSAIDs) as first option for symptomatic relief in the management of LBP, even if it may take many days to be effective (5).

Patients failing to respond to conservative treatment are steered to an invasive approach. Surgery is less invasive than it was in the past thanks to new microsurgical techniques. However, its success rate is not optimal: pain resolution is present in no more than 80%–85% of patients (6), and a failed back surgery syndrome develops in 10%–40% of patients (7).

Recent findings have shown that medical ozone can be used in the treatment of radicular syndrome caused by herniated intervertebral discs (8-12). The technique was developed by C. Verga et al. in 1983 and consist of some injections of a mixture of oxygen-ozone (O_2-O_3) in the paravertebral region near the herniated disc repeated many times. The ozone is the oxygen triatomic molecule, an instable, colourless, irritant gas with a strong antiossidant and stimulating capabilities (13). Althought this method is largely spread and used in Europe, especially in outpatient, there is insufficient published data supporting the effectiveness in clinical practice.

The aim of this study is to show: a) the effectiveness of the injection of paravertebral O_2-O_3 mixture to reduce symptoms in radicular lumbar mononeuropathy caused by disc herniation compared with a pharmacological treatment; b) the effects on clinical, neurophysiological and neuroradiological examinations; and c) an analysis of tolerability and feasibility of this technique.

MATERIALS AND METHODS

We studied 38 patient (22 men, age range 24-75 years) with L5 or S1 mono-radiculopathy caused by monolateral L4-L5 or L5-S1 disc herniation. All clinical data are reported in Table I. Preliminary clinical evaluation was performed in all patients by three experienced neurologists (mean 10 years experience), working in different consulting rooms, who performed a detailed neurological examination including sensibility examination in dermatome regions (L5-S1), muscular strenght in miomeric regions (L5-S1) using the MRC (Medical Research Council) scale, osteotendon reflexes, straight leg raising test. The mean duration of radicular pain at the time of treatment was 1 month, so intensive as to cause a total inability to work. On admission, every patient underwent to a complete physical examination, general blood biochemical and haematological examination, EKG, Magnetic Resonance (MR) imaging of lumbar region, neurophysiological examinations (Electromyography – EMG) to study the morphological and functional involvement of L5-S1 roots. The intensity of pain and the outcome of treatments were evaluated in all patients with the Visual Analogue Scale (VAS) and with the Oswestry Disability Index (ODI).

Inclusion criteria comprised: 1) acute radicular pain in the L5-S1 region (sciatica) lasting 1 month; 2) paresthesia/numbness or weakness (>4 MRC scale), alteration of osteo-tendon reflexes with proper radicular distribution; 3) positivity to straight leg raising test; 4) neurophysiological examination with radicular signs (spontaneous activity, reduction of maximal voluntary muscles activation); 5) MRI evidence of disc herniation corresponding to the level of symptoms and neurological signs (the entity of herniation was classified in three types: protrusion, extrusion and free fragments, according to the Modic classification) (14).

Exclusion criteria were: pregnancy, allergy to proposed drugs, major neurological deficits, previous spine surgery, bone lesions, stenosis of spinal canal, intense miotomal weakness causing leg paralysis, calcification of the disc.

We obtained a written informed consent from all the patients before therapy. Participants were free to interrupt or continue the assigned treatment depending on their impressions of improvement and satisfaction. The procedures followed were approved by the Committee on Human Experimentation of the institutions involved.

All the 38 patients were assigned randomly to 2 groups (A and B). Group A included 20 patients (12 men; mean

age 53.2 years) treated with injections of O_2-O_3 mixture prepared and injected quickly (about 10 seconds), under sterile conditions, at a concentration of 40 µg/ml using a Multiossigen PM95 generator (Multiossigen s.r.l., Gorle, Bergamo, Italy). The mixture of injected gas was 20 ml, 10 ml per side of the paravertebral region, 1.5 cm lateral to the spinosus process of L4 (for L5 radiculopathy) or L5 (for S1 radiculopathy), using 22 G needle injected perpendiculary to the major body axis. The gas injection were applied 3 timed per week for a total of 12 injections. No premedication or anesthesia was given, and the procedure was performed in an outpatient clinic. Group B included 18 patients (10 men; mean age 52.7 years) treated with pharmacological therapy, consisting in Ketoprofen 100 mg i.m.injection/die for 15 day, followed by ketoprofen 200 mg x os/die for other 15 days. All patients of group B were treated with lansoprazole 30 mg/die per 45 days.

All patients were clinically evaluated at baseline (T1) and after 7 days (T2), 14 days (T3), 30 days (T4), 3 months (T5) and 6 months (T6) with physical examination and with VAS and ODI scales. For all the patients the assessors were different from the investigators who enrolled the participants and blind to the assigned treatments.

After 6 months all patients underwent an MRI examination of the lumbar region and repeated an EMG examination. In all patients, MRI or EMG examinations were performed by the same doctor and results were compared to the same examinations obtained 6 months before.

The primary outcome measures were the number of patients who showed a reduction of VAS score under 4 and a reduction of ODI score under 40% at T3 and T6. Secondary outcome measures included changes in MRI and EMG examinations at T6 and tolerability and feasibility of the technique.

Neuroradiologic and neurophysiologic examinations

MRI was performed using a 1.5-T system (ACHIEVA®, Philips Medical System, Eindhoven, The Netherlands) with a maximum gradient strength of 30 mT/m and a spine coil. The details of the sequences used for lumbar MRI are described in Table II. Neurophysiological examinations were performed using a Synergy instrument (Medelec Synergy N-EP, Oxford Instruments Medical, Inc., UK) and consisted in a needle-examination in the muscles of miomeric region L5 and S1.

Statistical analysis

An evaluation of the success rate was performed for both groups on the basis of VAS and ODI. The success rates at 7-days, 14-days, 1-month, 3-months and 6 months follow-up for groups A and B were compared by means of the Fisher exact test. $P<.05$ was considered to indicate a statistically significant difference. Data were processed using Epi Info 3.3 software (CDC, Atlanta, GA, USA).

RESULTS

Table III shows the results of all the parameters we studied. Although in Group A the treatment led to a reduction of pain and discomfort in 3 (15%) of

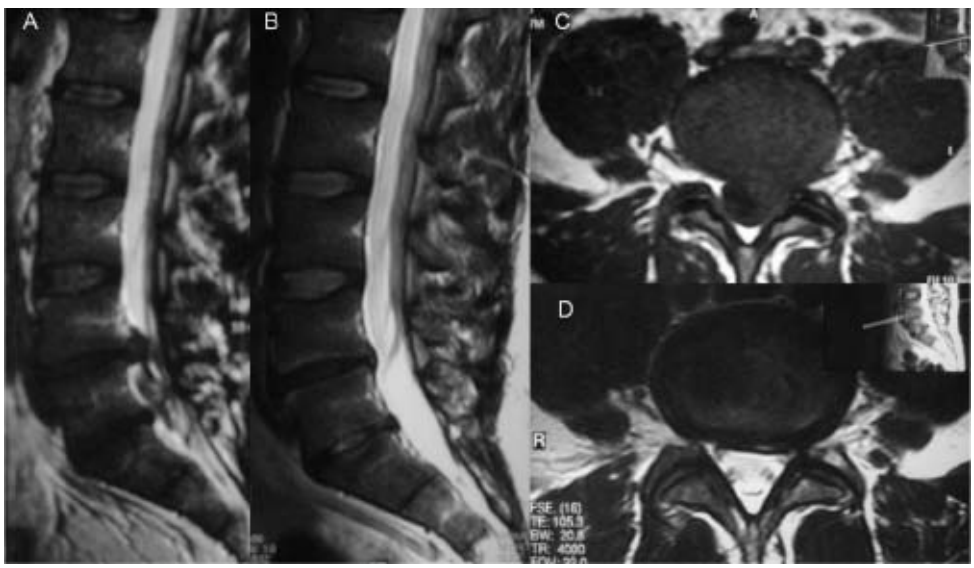

Fig. 1. *A 32-year-old man with L5 left radiculopathy caused by a great disc herniation (**A** and **C**). Both in axial and sagittal MR images (T2-weighted) disc is "extruded" in spinal canal and the material press left L5 root. After 6 months in the same patient, treated with O2-O3 injections, MR shows strong reduction of herniated disc clear both in axial and sagittal images (**B** and **D**).*

Table I. *Clinical features of the patients involved in thVAS:Visual Analogue Scale ; ODI (Oswestry Disability Index).*

	Group A	Group B
Patients	20	18
Sex (male)	12 (60%)	10 (65.5%)
Radiculopathy S1	9 (45%)	10 (55.5%)
Radiculopathy L5	11 (55%)	8 (45%)
Age	53.2 (12.5 SD)	52.7 (10.3 SD)
VAS (T1)	8.4	8.1
ODI (T1)	74%	72%

VAS:Visual Analogue Scale ; ODI (Oswestry Disability Index).

Table II. *MR protocol of the lumbar spine.*

Parameter	T2-TSE	T1-TSE	T2-STIR	T2-TSE
Plane	sagittal	sagittal	sagittal	axial
FOV (mm)	320-340	320-340	320-340	160-220
TR (ms)	2550	380	2800	2880
TE (ms)	105	8.0	120	120
Matrix	173x256	228x512	210x512	110x256
Slice thickness (mm)	4	4	4	4
Gap (%)	10	10	10	10
Time (s)	180	120	240	100

20 patients after 7-days with return to normal daily activities, the most significant finding is a strong improvement of VAS and ODI scores after only another week (i.e. total 6 injections – T3 -) in patients of Group A, with 10 patients (45%) with VAS <4 and ODI <40% while only in one and in three patient respectively of Group B the pharmacological treatment was a success. Until the end of the follow-up we found a larger response in patients of group A compared with the ones of Group B, with a total of

Table III. *Outcomes of group A and group B patients based on their responses to the VAS and ODI and on MRI and EMG examinations at different times of follow-up.*

VAS <4 **ODI <40%**	Group A *(number of patients and %)*	Group B *(number of patients and %)*	p^*
T2 (7 days)	3 (15%)	1 (5.5%)	n.s.
T3 (14 days)	10 (50%)	3 (16.6%)	p= 0.043
T4 (1 month)	12 (60%)	5 (27.5%)	n.s.
T5 (3 months)	15 (75%)	7 (38.9%)	p=0.047
T6 (6 months)	16 (80%)	8 (44.4%)	p=0.042
MRI			
T6 (6 months)	13 (65%)	8 (44.4%)	n.s.
EMG			
T6 (6 months)	11 (55%)	9 (50%)	n.s.

Differences are considered statistically significant if p<.05.*
VAS: visual analogue scale; ODI: Oswestry Disability Index; n.s. not significant

16 patient (80%) of Group A compared to 9 patients (50%) of Group B.

Only 1 patient of Group A interrupted the treatment before the end of the study period because of unsatisfactory result. Three patients in group B interrupted the treatment before the end of the study period because of unsatisfactory result and 2 patients because of complications related to the drugs.

MRI examinations after 6 months showed a reduction of disc herniation in 13 patients (65%) in Group A, especially in subjects with disc extrusions and free-fragments (Fig. 1), with 8 patients (44.4%) in Group B. In Group A 11 patients (55%) showed a reduction of spontaneous activity with and increase of pattern of maximal strength activation (EMG) while 9 (50%) in Group B.

The statistical analysis with Fisher exact test showed that the different outcome at 7-days and one month were not significant. After 14 days the differences became statistically significant (P<.05) and remain significant at T3 and T6. Differences in MRI and EMG results (pattern of strength activation) obtained after 6-months were not statistically significant.

Complications

For all the patients treated with O_2-O_3 injections we did not observed adverse reactions and side

effects, exception made for 1 patient who had a fainting phenomenon soon after gas injection. In group B we recorded 2 drop-out related to the onset of gastro-intestinal symptoms, while in two cases we found hypertension in two different patients.

DISCUSSION

The appropriate treatment of sciatica caused by lumbar disc herniation is a challenge. The large majority of these patients receive as a first line treatment NSAIDs or steroids in different formulations, with inconstant responses (15-16). In many cases for positive responses many days elapse during which the patients are unable to work. Furthermore, frequently they are addressed to mini-invasive procedures or surgical treatment (17-19). Epidural injections with local anesthetics and steroids are one of the most commonly used interventions in managing chronic low back pain and lower extremity pain of various causes (20-21).

In our series, the injections of oxygen-ozone in the paravertebral regions showed a better and faster response compared with NSAIDs. In our opinion, the reduction of pain and discomfort is remarkable just after one week compared with pharmacological treatment. This difference of response became statistically significant after two weeks and again after three months and until the end (six months) of the study, when 80% of patients treated with injections turned out pain free. Half of the patients with pharmacological treatment at the end of the study turned out pain free with a poor response until 6 months. MRI was performed after 6 months according to previous studies and the clinical condition of most of the patients effectively stabilized after six months (22-23).

To explain this quick effect we hypothesize that O_2-O_3 injections in the paravertebral regions can induce a direct reduction of root inflammation with a corresponding reduction of pain. This effect can be explained by the rapid diffusion of gas mixture in the lumbar radicular zone and its reaction with organic molecules containing double and triple bonds. The properties of the oxygen-ozone mixture to reduce pain and to decrease inflammation is well known: the inhibition of the synthesis of proinflammatory prostaglandins, the release of bradykinin, the release of anti-algogenic compounds, the increased release of antagonists or soluble receptors that neutralize proinflammatory and immunosoppressor cytokines, interferon-α and tumor necrosis factor-α (8, 13, 24, 25). In our work we did not evaluate objective inflammation indeces in all patients because our aim was to study the effect of O_2-O_3 injections on pain and functional items (the Visual Analogue Scale and the Oswestry Disability Index). More studies investigating these aspects are needed. Furthermore, hyperoxygenation carried out by O_2-O_3 injections can improve the hypoxiemia of the root district induced by a chronic "stasis" in venous and arterial flow. All these effects, due to to the local contribution of oxygen-ozone injected near the involved root, can explain the favorable action produced from the injections of oxygen-ozone on pain compared with the pharmacological treatment. The effects of NSAIDs on radicular pain is slow and less effective, probably due to the systemic distribution of the drugs with antiinflammatory and pain-relief effects and the difficulty to reach the site of action, unlike O_2-O_3 injections acting directly on the intervertebral space near the site of the root compression (16). Another possible effect of oxygen-ozone injections could be related to the pain relieving effect on the muscle and fascial structures of the lumbar region near the affected radicular region. In fact, many sensitive branches of the spinal nerve soon after its origin go to paravertebral muscles and fascial structures of the lumbar region. Antiinflammatory-anaesthetic effect of oxygen-ozone can act on these small branches of the spinal nerves with an anaesthetic effect, reducing the lumbar pain.

A recent work by Paoloni et al. (11) marked the usefulness of paravertebral oxygen-ozone injections in strongly reducing symptoms of acute low back pain compared with a simulated lumbar paravertebral injections. Our reports are in agreement with this study, showing the effectiveness of these injections to reduce the pain, although the patients pain free at the end of follow-up are higher in our study (80% *vs* 61.1%). These Authors found the higher response between 3 and 6 months, while the best response was between the first and the second week and no changes in disc alterations on MRI.

These differences could be explained with the clinical features of the former sample (patients with

acute low back pain) compared with the latter (acute radiculopaties). Regarding the MRI results, we found a reduction of disc herniation in patients treated with oxygen-ozone injections but this report, compared with the same obtained in pharmacological patients, is not statistically significant. This is consistent with the scientific data reported in previous works that clearly showed that the natural evolution of disc herniation is towards a spontaneous regression, expecially the largest lumbar disc herniations are most likely to show the greatest regression in size over time (4, 17, 18). The exact mechanism remains unknown. The hypotesis states that the herniated disc regression is due to gradual dehydratation and shrinkage, or an enzymatic degradation and phagocytosis by an inflammatory reaction and neovascularization of disc herniation (19). Therefore how can we explain the mismatch in clinical response and imaging pictures? Our work is in agreement with the reports that recently have given much attention to the biochemical and microcirculation effects of root impingement caused by disc herniation, that also independently can induce a radicular pain by mechanical means. In fact, often it is possible to see a morphologically evident disproportion of disc herniation and pain and other symptoms (26). Therefore, the effect of the gas mixture is essentially biochemical and vascular, without any mechanical effect. Indirectly, the stimulation of fibroblastic activities induced by O_2-O_3 injections can induce the start of the reparative processes, with activation of the natural mechanism of destruction of disc materials and a destruction of proteoglycans molecules with consequent loss of water and reduction of disc volume and root compression.

The discrepancy between the direct action of ozone confirmed by an early, rapid initial reduction of pain in our patients and the final effect after 6 months of treatment are due to the action of ozone, expressed not only on the mediators of inflammation, but also on other factors such as mechanical and immune systems; moreover, in chronic radicular pain the complexities of anatomy, physiology, and psychology of pain is also significant (8, 13, 24, 25).

Neurophysiological examinations show an inconsistent pattern of responses. Although the long latency responses are used in neurophysiological examinations to study the proximal share of the spinal nerves (roots included) we did not use these tests because considered extremely variable. The data obtained with needle-EMG examinations did not correlate well with improvement of the clinical pictures in patients with sciatica, both in patients treated with O_2-O_3 and patients treated pharmacologically. The subjectivity of the EMG examination and the difficulty to give a standard reproducible in the different sessions could be a possible explanation of these results.

We are aware of several limitations of the study. They are mainly due to the small size of the samples and the absence of a true control arm. Further studies with a large population are needed to confirm our hypothesis. The absence of a control group without treatment to quantify the placebo-effect on patients of both groups is another big limitation.

For all patients treated with O_2-O_3 we did not observe adverse reactions or side effects, excepted for one patient who showed a lipotimic reaction a few minutes after the gas injection. Only some patients felt a sensation of "pressure" near the lumbar region, or pain in the injection site, but all these symptoms disappear after a few minutes. This technique is quick and easy, also in an outpatient setting. Although we did not carry out a cost benefit analysis, it is important to point-out that oxygen-ozone injections are a very cheap technique: the only costs are the ozone-machine, periodical use of oxygen, upkeep, with substantial absence of risks or side effects and with good tolerability. Pharmacological treatments instead are accompanied by many potential adverse effects.

We can finally say that O_2-O_3 is a technique with a good and rapid result and feasibility without adverse effects that can be applied largely in hospital and outpatient settings for low back pain of radicular type, before addressing the patients to minimally-invasive techniques or surgical treatments.

REFERENCES

1. Long MD. Decision making in lumbar disc disease. Clinical Neurosurg 1991; 39:36-51.
2. Saal JA. Natural history and nonoperative treatment of lumbar disc herniation. Spine 1996; 21(suppl 24):2S–9S.
3. Raj PP. Intervertebral disc: anatomy-physiology-

pathophysiology-treatment. Pain Pract 2008; 8(1):18–44.
4. Komori H, Shinomiya K, Nakai O, Yamaura I, Takeda S, Furuya K. The natural history of herniated nucleus pulposus with radiculopathy. Spine 1996; 21:225–229.
5. Bach SM, Holten KB. Guideline update: what's the best approach to acute low back pain? J Fam Pract 2009; 58(12):E1.
6. Bruggeman AJ, Decker RC. Surgical treatment and outcomes of lumbar radiculopathy. Phys Med Rehabil Clin N Am 2011; 22(1):161-77.
7. Osborn AG. Non-neoplastic disorders of the spine and spinal cord. In: Diagnostic neuroradiology. St Louis, Mo: Mosby 1994; 820–875.
8. Steppan J, Meaders T, Muto M, Murphy KJ. A metaanalysis of the effectiveness and safety of ozone treatments for herniated lumbar discs. J Vasc Interv Radiol 2010; 21(4):534-48.
9. Buric J, Molino Lova R. Ozone chemonucleolysis in non-contained lumbar disc herniations: a pilot study with 12 months follow-up. Acta Neurochir Suppl 2005; 92:93–97.
10. Staal JB, de Bie RA, de Vet HC, Hildebrandt J, Nelemans P. Injection therapy for subacute and chronic low back pain: an updated Cochrane review. Spine (Phila Pa 1976) 2009; 34(1):49-59.
11. Paoloni M, Di Sante L, Cacchio A, Apuzzo D, Marotta S, Razzano M, Franzini M, Santilli V. Intramuscular oxygen-ozone therapy in the treatment of acute back pain with lumbar disc herniation: a multicenter, randomized, double-blind, clinical trial of active and simulated lumbar paravertebral injection. Spine 2009; 34(13):1337–1344.
12. Bonetti M, Fontana A, Cotticelli B, Voltaa GD, Guindani M, Leonardi M. Intraforaminal O2-O3 versus periradicular steroidal infiltrations in lower back pain: randomized controlled study. Am J Neuroradiol 2005; 26:996–1000.
13. Bocci V, Luzzi E, Corradeschi F, Paulesu L, Di Stefano A. Studies on the biological effects of ozone. III. An attempt to define conditions for optimal induction of cytokines. Lymphokine Cytokine Res 1993; 12:121–126.
14. Modic MT. Degenerative disc disease and back pain. Magn Reson Imaging Clin N Am 1999; 7(3):481-91.
15. Johnson M, Neher JO, St Anna L. Clinical inquiries. How effective--and safe--are systemic steroids for acute low back pain? J Fam Pract 2011; 60(5):297-8.
16. Chou R. Pharmacological management of low back pain. Drugs 2010; 70(4):387-402.
17. Weber H. The natural history of disc herniation and the influence of intervention. Spine 1994;19:2234–2238.
18. Valat JP, Genevay S, Marty M, Rozenberg S, Koes B. Sciatica. Best Pract Res Clin Rheumatol 2010; 24(2):241-52.
19. Pengel LH, Herbert RD, Maher CG, Refshauge KM. Acute low back pain: systematic review of its prognosis. BMJ 2003; 327:3.
20. Parr AT, Manchikanti L, Hameed H, Conn A, Manchikanti KN, Benyamin RM, Diwan S, Singh V, Abdi S. Caudal epidural injections in the management of chronic low back pain: a systematic appraisal of the literature. Pain Physician 2012; 15(3):59-98.
21. Manchikanti L, Buenaventura RM, Manchikanti KN, Ruan X, Gupta S, Smith HS, Christo PJ, Ward SP. Effectiveness of therapeutic lumbar transforaminal epidural steroid injections in managing lumbar spinal pain. Pain Physician 2012; 15(3):199-245.
22. Andreula CF, Simonetti L, De Santis F, Agati R, Ricci R, Leonardi M. Minimally Invasive Oxygen-Ozone Therapy for Lumbar Disk Herniation. AJNR 2003; 24:996-1000.
23. Andreula C. Ozone therapy. Neuroradiology 2011; 53 Suppl 1:S207-9.
24. Bocci V. Autohaemotherapy after treatment of blood with ozone: a reappraisal. J Int Med Res 1994; 22:131-44.
25. Larini A, Bocci V. Effects of ozone on isolated peripheral blood mononuclear cells. Toxicol In Vitro 2005; 19:55-61.
26. van Tulder M, Koes B, Bombardier C. Low back pain. Best Pract Res Clin Rheumatol 2002;16:761–775.

PLATELET RICH FIBRIN MATRIX EFFECTS ON SKELETAL MUSCLE LESIONS: AN EXPERIMENTAL STUDY

A. GIGANTE[1], M. DEL TORTO[1], S. MANZOTTI[1], M. CIANFORLINI[1], A. BUSILACCHI[1], P.A. DAVIDSON[2], F. GRECO[1] and M. MATTIOLI-BELMONTE[1]

[1]Department of Clinical and Molecular Sciences, School of Medicine, Università Politecnica delle Marche, Ancona, Italy; [2]Heiden Orthopaedics, Park City, Utah, USA

Received March 21, 2012 – Accepted June 7, 2012

Even though muscle injuries are very common, few scientific data on their effective treatment exist. Growth Factors (GFs) may have a role in accelerating muscle repair processes and a currently available strategy for their delivery into the lesion site is the use of autologous platelet-rich plasma (PRP). The present study is focused on the use of Platelet Rich Fibrin Matrix (PRFM), as a source of GFs. Bilateral muscular lesions were created on the longissimus dorsi muscle of Wistar rats. One side of the lesion was filled with a PRFM while the contralateral was left untreated (controls). Animals were sacrificed at 5, 10, 40 and 60 days from surgery. Histological, immunohistochemical and histomorphometric analyses were performed to evaluate muscle regeneration, neovascularization, fibrosis and inflammation. The presence of metaplasia zones, calcifications and heterotopic ossification were also assessed. PRFM treated muscles exhibited an improved muscular regeneration, an increase in neovascularization, and a slight reduction of fibrosis compared with controls. No differences were detected for inflammation. Metaplasia, ossification and heterotopic calcification were not detected. This preliminary morphological experimental study shows that PRFM use can improve muscle regeneration and long-term vascularization. Since autologous blood products are safe, PRFM may be a useful and handy product in clinical treatment of muscle injuries.

Muscle injuries are very common with an incidence that varies from 10% to 55% of all injuries sustained in sport (1). Despite this frequent occurrence and the presence of several data on muscular injuries pathophysiology, none of the treatment strategies performed have proven to be really effective in strictly controlled trials (1, 2). One possible explanation for this apparent paradox is the broad heterogeneity and wide variety of severity in this type of injury (3, 4).

Most current muscle injury treatments are based upon limited experimental data and/or they were only empirically tested (3). For muscle injuries of lesser severity, usually non-surgical treatment results in good functional outcomes (4). As a rule, the treatment is limited to RICE (i.e. Rest, Ice, Compression and Elevation), Non-Steroidal Anti-Inflammatory Drugs (NSAID) and physical therapy (active and passive modalities) (5). An alternative to non-surgical treatment of muscle injury is surgical re-approximation of muscle tears (3). Unfortunately, in extensive muscle lesions these therapeutic approaches are often unsatisfactory, especially in athletes with a high functional demand (4, 6).

Key words: platelet rich plasma, skeletal muscle injuries, growth factors

Mailing address: Dr. Antonio Gigante
Department of Clinical and Molecular Sciences,
Università Politecnica delle Marche,
Via Tronto 10
60126, Ancona, Italy
Tel.: +39 071 220 6069 Fax: +39 071 220 6069
e-mail: a.gigante@univpm.it

0393-974X (2012)

DISCLOSURE: ALL AUTHORS REPORT NO CONFLICTS OF INTEREST RELEVANT TO THIS ARTICLE.

Healing is a complex and dynamic process characterized by a cascade of events triggered by the tissue injury itself, which results in the restoration of anatomic continuity and function (7). Several Growth Factors (GFs), including, Fibroblast Growth Factor (FGF-2), Insulin-Like Growth Factor I (IGF-1), Vascular Endothelial Growth Factor, (VEGF) and Platelet-Derived Growth Factor (PDGF), have been tested in vivo and in vitro to potentiate tissue healing, angiogenesis, arteriogenesis.(5, 7-10). Specific GFs have also a fundamental role in accelerating the repair processes and in facilitating a faster and more complete muscle repair (3, 11-13). Although the peculiar role of all GFs involved in the healing process is only partially known, the efficacy of many of them has been extensively demonstrated and recently reviewed by Borrione and co-workers (7).

A currently available strategy to deliver GFs into the lesion site is the use of autologous platelet-rich plasma (PRP). This is an autologous blood derivative with a platelet concentration five times greater (approximately 12±2 x10^5/microliter) than physiological levels (13). PRP has already been extensively studied in bone, cartilage, and tendon and ligament regeneration and in wound treatment (14-17). Reduced rates of infection and enhanced analgesia after PRP administration, possibly associated with PRP enhancement of the immune response (18), have also been reported.

The present study is focused on the use of Platelet Rich Fibrin Matrix (PRFM) as a source of GFs. For its preparation, plasma taken from venous blood is centrifuged in order to separate cellular components and yielding the PRP as a supernatant. The PRP is then placed in a tube with calcium chloride ($CaCl_2$) and centrifuged to create the PRFM (19), in which non-degranulated platelets are embedded into a fibrin matrix. This preparation could be tailored on the basis of the clinical needs, being a liquid (i.e. that can be injected) or a dense matrix (i.e. that can be sutured). The novelty of PRFM in comparison with traditional PRP preparations is related to the presence of non-degranulated platelets within the fibrin matrix. These embedded platelets will subsequently release a pool of known GFs (i.e. IGF-1, EGF, FGF-2, PDGF-A, B, Transforming growth factor-beta1, TGF-β_1 and VEGF) able to accelerate muscle repair (19-23). This release of GFs by the PRFM is extended, with measurable levels of continued GF synthesis and release over several weeks (10, 24, 25)._

No histological studies analysing muscle regeneration with PRP or PRFM are available. Therefore, the principal aim of the present experimental *in vivo* study is a morphological and morphometrical evaluation of the PRFM effect on full thickness muscle lesions in an animal model.

MATERIALS AND METHODS

Twenty male Wistar rats (340±60 g/BW) were used (Experimental Animal Models for Aging Units Research Department, I.N.R.C.A. / I.R.R.C.S., Ancona, Italy). The rats were inbred, therefore they could be considered genetically identical. The policies and procedures of their use and maintenance were in accordance with those detailed by the directive n° 86/609/CEE regarding animal care and experimental usage.

PRFM preparation

PRFM was prepared using Cascade Medical Enterprises 2 tube kit (Cascade Medical Enterprises, Wayne, NJ) according to the manufacturer instruction. Briefly, blood necessary for PRFM preparation was obtained by intracardiac puncture from three rats using a 10 mL syringe containing citrate phosphonate dextrose (CPD) in ratio 5:1. The sample was initially centrifuged at 1100 x g for 6 minutes to separate PRP from white and red blood cells. The supernatant was then transferred to a second tube containing $CaCl_2$ in excess and spun at 1450 x g for 15 min. The obtained PRFM is a dense matrix (25). The syngeneic nature of the inbred rats allowed us to consider the blood of one animal autologous to blood from another animal.

Surgical procedure and sample preparation

Animals were anesthetized with ketamine (40 mg/Kg) and xylazine (5 mg/kg) intramuscular puncture and placed prone on a warm pad (38.5ºC). A sterile airway was maintained throughout the procedure. Bilateral cutaneous incisions (2 per animal) 3 cm in length were performed in the paravertebral region. Bilateral muscular tear lesions (0.7 x 0.3 cm) were then performed on the longissimus dorsi muscle using a standard pincer technique. This muscle was chosen because the presence of the supraspinatus ligament and fascia allow bilateral lesions. Moreover, the longissimus dorsi position prevents rats from interfering (i.e. biting or scratching) with the surgical treatment.

Each muscular diastasis site was marked by placing a sterile semi-cylindrical (hollow) polyvinyl chloride

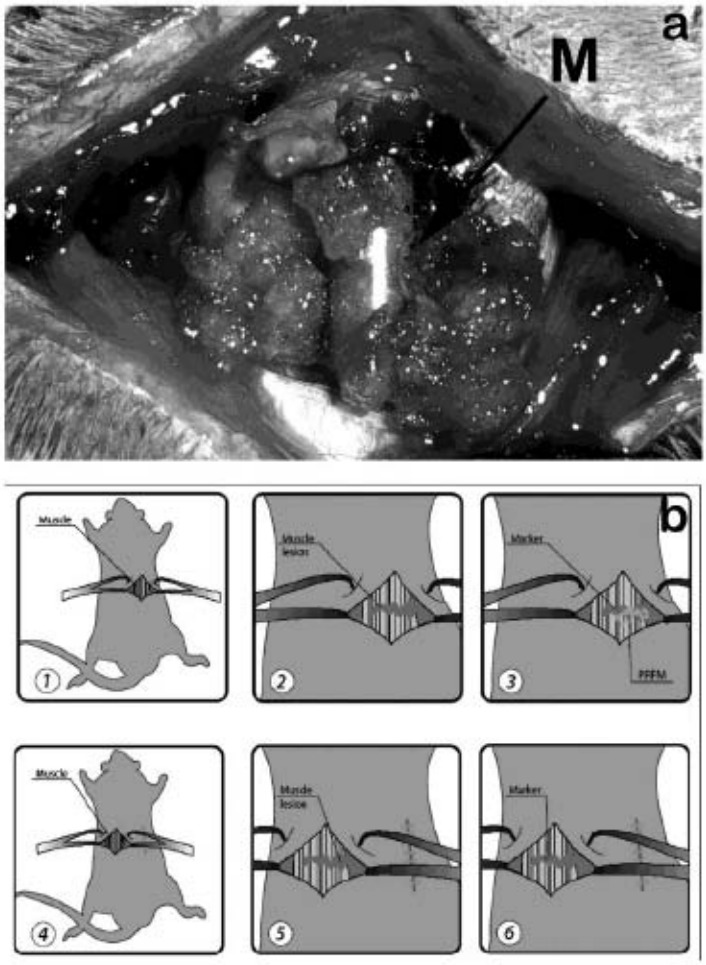

Fig 1. ***a)*** *Male Wister rat: dorsal incision and muscle lesion identified by PVC marker (M);* ***b)*** *Scheme of the experimental surgical procedure in male Wistar rats: (1) cutaneous incision (3 cm in length) in the paravertebral region; (2) muscular tear lesion on the longissimus dorsi; (3) placement of the PVC marker filled with PRFM; (4-6) cutaneous incision, muscular tear lesion on the longissimus dorsi and placement of the PVC marker on the contralateral control side.*

(PVC) tube (0.5 cm x 0.3 mm) at the bottom or ventral side of the defects (Fig. 1a) in order to identify the repair site at the time of necropsy.

One lesion was filled with PRFM while the contralateral injury was left untreated (CTRL) (Fig. 1b). PVC marker was placed also in the contralateral lesion. The side choice of treated and control lesions was randomized. In all cases muscle was left unsutured, the fascia and skin were closed in standard way, preserving separation between the two sites. Animals were maintained with a normal diet and no forced exercise was induced. Five animals were sacrificed at each time interval of 5, 10, 40 and 60 days from surgery. The experimental sites were dissected and collected samples were fixed in formaldehyde 4%, embedded in paraffin, sectioned (5 μm). For light microscopy sections were stained with haematoxylin-eosin and Van Gieson's trichrome stains.

Histological evaluation

Each sample was evaluated in a blinded manner from two different observers. The blinded examiner considered three fields for each section (5 sections for lesion). Both longitudinal and transverse sections were made. All sections were evaluated at 10X magnification using a qualitative score considering the following parameters: muscle regeneration, neovascularization, fibrosis and inflammation. The following score (26) was assigned:

Vascularization and *muscle regeneration*:

- score 0: no evidence of neovascularization and no new muscular tissue;
- score 1: repair site with less than 25% of the

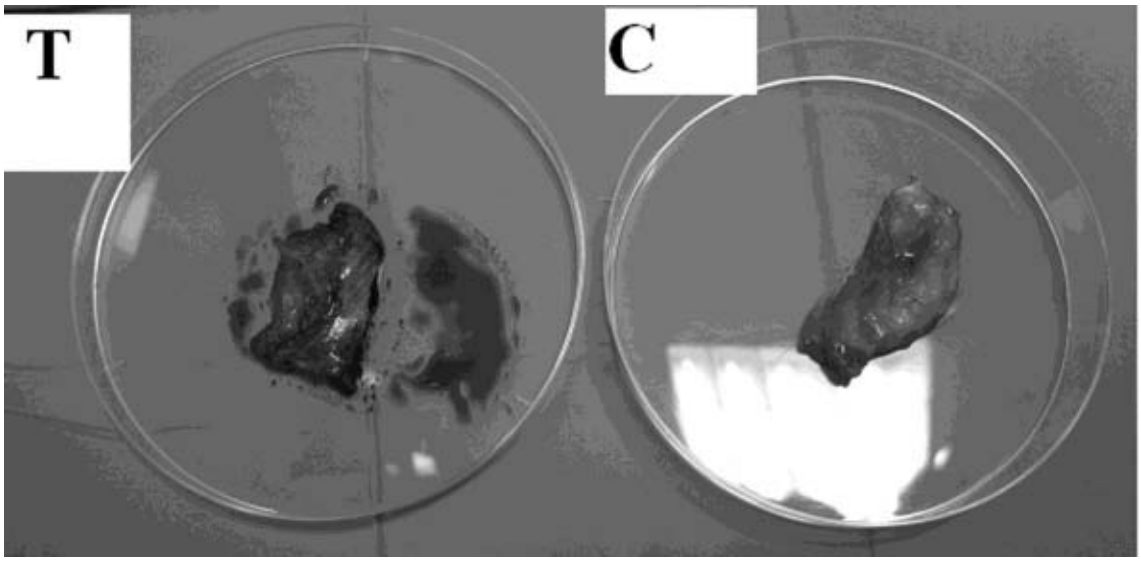

Fig. 2. *Macroscopic aspect of a PRFM treated muscle (T) and of the control lesion (C) 40 days after surgery showing the presence of an intense bleeding in the treated samples.*

Table I. *Histological score analysis.*

	5 days		10 days		40 days		60days	
	PRFM	CTRL	PRFM	CTRL	PRFM	CTRL	PRFM	CTRL
Neovascularization	2.0±0.3	2.1±0.7	1.9±0.8	2.1±1.0	2.0±0.9	1.6±0,7	1.7±0.9	1.1±0.6
Muscle regeneration	2.0±0.7	1.1±0.5	3.1±0.6	2.2±0.7	1.4±0.9	1.4±0.4	1.4±0.9	1.1±0.6
Fibrosis	1.5±0.3	1.7±0.4	1.0±0.6	1.7±0.5	0.8±0.3	1.1±0.5	1.4±0.5	1.6±0.5
Inflammation	2.1±0.7	1.9±0.8	1.1±0.7	1.3±0.3	1.3±0.5	1.3±1.0	1.6±0.7	1.7±0.9

PRFM: platelet-rich fibrin matrix treated lesion; CTRL: Contralateral untreated lesion. Score analysis is explained in Material and Methods

microscopic field covered with new vessels and new muscular tissue;

- score 2: lesion with 25% - 50 % of the field covered with new vessels and new muscular tissue;
- Score 3: repair site with more than 50% of the field covered with new vessels and new muscular tissue.

Inflammation and *fibrosi*s:

- Score 0: more than 50 % of the field covered with inflammation and fibrosis.
- Score 1: 25% - 50 % of the field covered with inflammation and fibrosis.
- score 2:less than 25 % of the microscopic field covered with inflammation and fibrosis;
- score 3: no evidence of inflammation and fibrosis

The presence of metaplasic zones, calcifications and heterotopic ossifications was further evaluated by histological analysis

Histomorphometric evaluation

Computerized morphometric analysis was performed with the use of the Leica Q5OOMC Image Analysis System (Leica Leitz DMRBE, Cambridge, England). The software used for image analysis was the Leica Q500MC Image Analysis System for Windows 3.11. The analysed field was selected and acquired on the screen under the control of the image server. The camera images were digitized and modified in a binary way to make them suitable for measurement. Likewise to histological analysis considered parameters were: muscle regeneration, neovascularization, fibrosis and inflammation.

All morphometric steps, except for the selection of the first microscopic field, were automated. After standard filtration procedures for background smoothing, the system identified all the regenerating muscle fibres and the others parameters according to a threshold value set by the operator displaying them on the screen in colour.

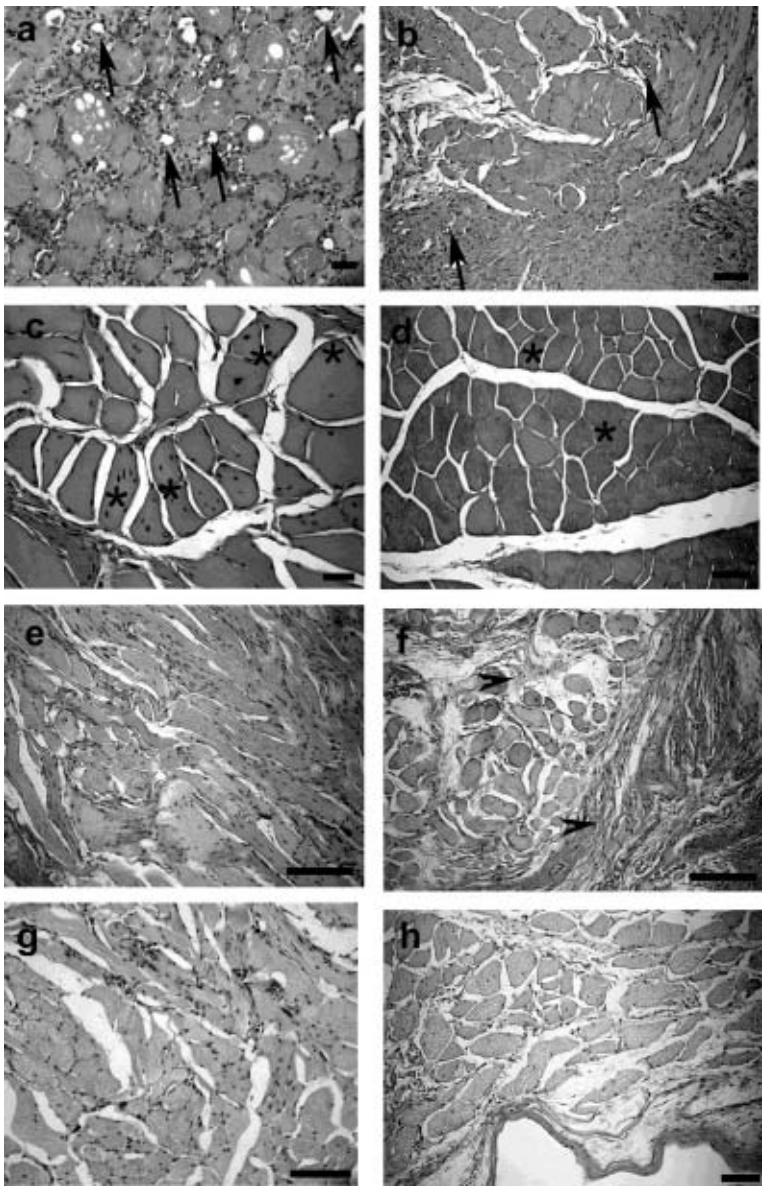

Fig. 3. *Histological sections of longissimus dorsi muscle treated with PRFM (a,c,e,g) and of untreated lesion (b,d,f,h) at the different time points. 5 days after surgery an abundant neovascularization (→) and muscle regeneration is present in muscle treated with PRFM (**a**), while in control group (**b**) muscle regeneration with a low number of vessels (→) are evident. (H/E); at 10 days the presence of fibres with central nuclei (*) are suggestive for muscle regeneration in lesion treated with PRFM (**c**); these feature are less evident in control lesion (**d**) (H/E); Van Gieson's trichrome stain performed on sections at 40 days after surgery showed muscle regeneration in PRFM treated lesion (**e**) and slight signs of fibrosis (➤)in control groups (**g**); at 60 days from surgery differences between lesions treated with PRFM (**g**) and untreated ones (**h**) were also evident (Van Gieson's trichrome stain). Scale bars 100 µm.*

Editing facilities allowed for the correction of automatic identification. Closer inspection of the sample was allowed by a zoom.

On the basis of a calibration factor determined by a suitable procedure in the setup menu, the system calculates the fraction area (Aa %) occupied by the selected parameters (muscle regeneration, neovascularization, fibrosis and inflammatory cells) on the whole field. Five fields were studied for each section. Data are expressed as mean ± Standard deviation (SD).

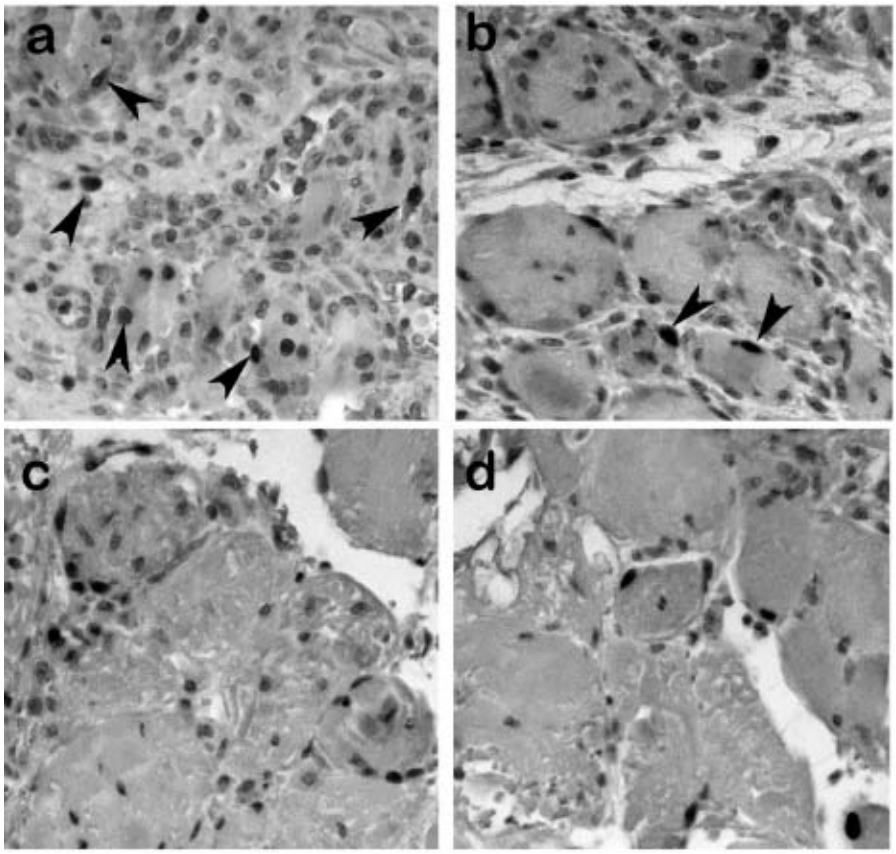

Fig. 4. *Immunoistochemical detection of myogenin (**a**,**b**) and MyoD (**c**,**d**) in 5 day animals. The number of myogenin positive cells (→) was higher in PRFM treated lesion (a) in comparison with control ones; in the same animals, no differences were detected for MyoD immuno-staining between treated (c) and untreated (d) lesions. MyoD- and myogenin-positive cells were located both inside the basal lamina of fiber and in the interstitial spaces in muscle.*

Immunohistochemical analysis

For immunohistochemistry Polysine® slides (Menzel-Gläser, Braunschweig, Germany) were used. Dewaxing, rehydration and antigen unmasking were performed with EnVision™ FLEX Target retrieval Solution High pH (Dako, Carpinteria, CA, USA) by PT Module (Lab Vision Corporation, CA, USA). Endogenous peroxidase activity was quenched by incubating the sections in 3% H_2O_2 for 10' at Room Temperature (RT). Sections were then incubated with the monoclonal antibodies anti-MyoD (5.8A) and anti-Myogenin (5FD) (both Santa Cruz Biotechnology, CA, USA) diluted 1.150 in Antibody Diluent with Background Reducing Components (Dako) for 1h at RT in a humidified atmosphere. Reaction was visualized with LSAB®Plus System-HRP DAB+ kit (Dako) according to the manufacturer's instructions. Sections were counterstained with Mayer haematoxylin (Bio-Optica SpA, Milano, Italy) and then dehydrated, clarified and mounted. Negative control was represented by primary antibody untreated sections. Reaction was examined with a light microscope (Nikon Eclipse 600).

Statistical analysis

Statistical analysis of histomorphometric data was performed with Wilcoxon non parametric test. The level of statistical significance was established at $p<0.05$.

RESULTS

Macroscopically muscle treated with PRP showed more intense bleeding in comparison with untreated contralateral lesion (Fig. 2).

Histological score analysis is summarized in

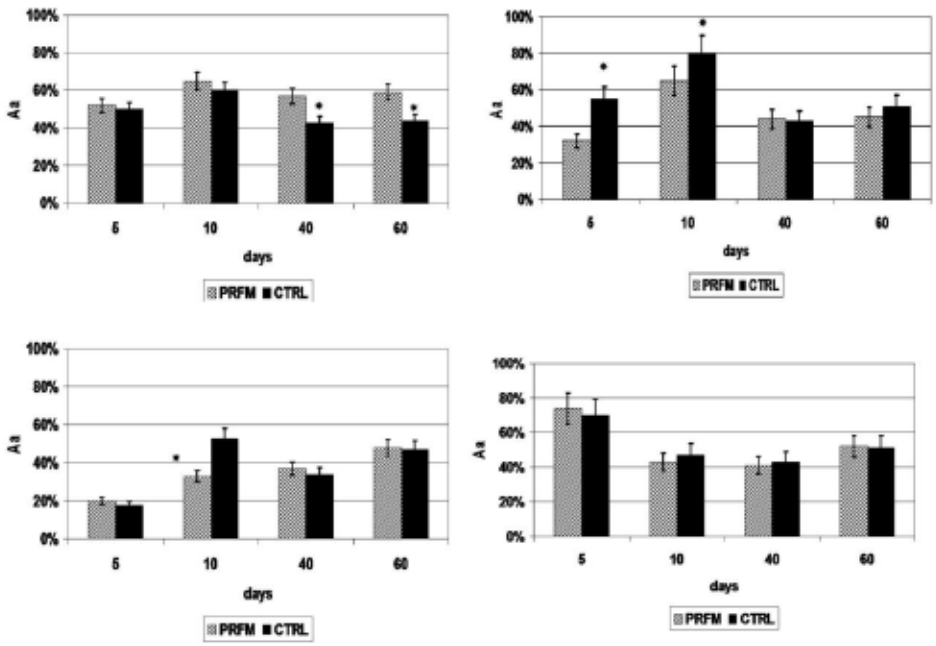

Fig. 5. *Histograms of the histomorphometric analysis performed at 5, 10, 40 and 60 days after surgery evaluating neovascularization (**a**), muscle regeneration (**b**), fibrosis (**c**) and inflammation (**d**). Data are expressed as the fraction area (Aa%) occupied by the selected parameters; *p<0.05*

Table I.

Muscular regeneration was greater in treated samples in comparison with controls at the earlier time points of 5 and 10 days, and was comparable at 40 and 60 days (Fig. 3). Immunohistochemistry, performed in 5 days treated animals, evidenced a higher Myogenin positivity in PRFM treated lesion. No differences were detected for MyoD immune-staining (Figure 4). Neovascularization was comparable between treated and control samples at 5 and 10 days but was greater in PRFM treated samples at 40 and 60 days after surgery (Fig. 3).

A reduced fibrosis was observed 10 days after surgery, while no differences were detected at both 40 and 60 days from surgery. As far as inflammation is concerned, no differences were detected between the groups throughout follow-up. A good correspondence between histological and histomorphometric data was observed. Muscular regeneration was significantly greater in PRFM treated lesions in comparison with controls at 5 (54±8% *vs* 30±6%; $p<0.05$) and 10 (80±9% *vs* 63±4%; $p<0.05$) days after surgery, while it was comparable at 40 and 60 days (Fig. 5).

Differences in neovascularization between PRFM treated lesions and control ones were observed 40 and 60 days after surgery with a significant ($p<0.05$) increase of vascularization in treated lesion (Fig. 5). Histomorphometric data confirmed the reduction of fibrosis in PRFM treated lesions and the absence of differences in inflammation between the two groups throughout follow-up (Fig. 5).

DISCUSSION

The phases of the healing process after direct or indirect muscle injury are well defined. The initial degeneration/necrosis phase is principally characterized by the formation of a haematoma. The subsequent inflammatory/cell response phase and the repair-fibrosis phase are interrelated and time-dependent (11, 25). Local swelling and haematoma formation occur rapidly after injury (degeneration/necrosis phase) with clot formation and associated platelet degranulation. The latter leads to a local

release of GFs and cytokines that, in turn, determines the chemotactic migration of neutrophils and macrophages (11, 18, 26). Subsequently, myogenic precursor cells (also known as satellite cells) undergo activation and proliferation, also facilitated by GFs (5, 7, 27).

These satellite cells, which are located between the basal lamina and the plasma membrane of each individual myofibers (28), are quiescent in the uninjured state and following activation they proliferate and differentiate into multinucleated myotubes and, eventually, into myofibers. Many of these cells are able to fuse with existing necrotic myofibers and may prevent the muscle fibres from complete degeneration. Regenerating cells are centrally nucleated and are easily histologically identifiable (24). In the majority of cases this healing process leads to the formation of regenerated muscles with an area of fibrotic scar tissue, differing in size on the basis of the primary lesion (1), and with an incomplete restoration of their functional capacity. In fact, in extensive muscle injury, fibroblasts proliferation can quickly lead to an excessive scar formation, which hampers muscle regeneration and results in an incomplete or poor functional recovery (1). Therefore, the reparative capacity of muscle lesions varies widely and depends on the trauma severity. Recently, use of PRP has been proposed as a potential method for the local of delivery of increased concentrations of a variety of bioactive autologous GFs, in an effort to optimize tissue healing (14-17).

This study evaluates by means of histological parameters the effects of PRFM, a novel processed form of PRP, on muscle regeneration. The healing potential of PRP and PRFM has been attributed to the release of multiple GFs from the platelet concentrate (13). The enhancement of tissue healing related to the use of supraphysiologic concentrations of autologous platelets in tissue injury or surgery sites is supported by basic science and clinical studies (24, 29, 30). Several studies (31, 32) have underlined the presence of differences in platelet and GF concentrations in PRP produced by different platelet separation systems, including the ones tested here. More recently, Tiffany and co-workers (32) have strengthened the validity of the system used in the present study using a single-donor model also quantizing platelet, white blood cell (WBC), fibrinogen, and growth factor concentrations.

Indeed, few studies concerning PRP use in muscle injures have been performed: in 1986 Jodczyk (33) studied its effect on muscle regeneration in a sheep model, reporting only preliminary results; more recently, Hammond and co-workers (34) studied PRP effects in rats muscle strain injuries showing a shortening in recovery time.

In the present study, in order to evaluate the efficacy of PRFM in muscle regeneration the following parameters were considered: muscle regeneration, neovascularization, inflammation and fibrosis. The latter parameters were selected for the assessment of potential side effects and to our knowledge this is the first study that attempts to investigate the possible local adverse outcomes of the use of platelet derivate (PRP and/or PRFM) in muscular tissue.

In this respect, Visser and co-workers (25) demonstrated that *in vitro* PRFM elute high concentrations of TGF- β, able to significantly increase connective cell proliferation over time when compared with a whole blood concentrate of similar volume. On the contrary in our *in vivo* study, we did not observe an increase of fibrotic tissue formation during PRFM treatment in comparison with controls; therefore we can hypothesize that *in vivo* PRFM releases an amount of TGF-β not sufficient for this occurrence.

Our morphological study indicates that PRFM use in experimental muscle lesions can speed up muscle regeneration. Immunohistochemical data further strengthens this hypothesis: both MyoD and myogenin play a key role during embryonic and neonatal myogenesis and they have a crucial regulatory function in the processes of plasticity, adaptation, and regeneration in adult muscle. MyoD- and myogenin-positive cells are located both inside the basal lamina of the fiber and in the interstitial spaces in the muscle sacrificed at 5 days. No staining was detected in 10 days-sacrificed animals, nor in 40 and 60 days animals.

These findings are therefore consistent with a significant enhancement of early formation of new muscle and subsequent neovascularization in the presence of PRFM compared to untreated control lesions. The recoded level of fibrosis and inflammation in comparison with controls, as well

as the absence of metaplasia, ectopic calcification and heterotopic ossification observed both in PRFM treated lesions and in control groups, point out the lack of side effects related to PRFM use in the treatment of muscle injury.

Our data, confirmed the results obtained by Hammond (34) in a different experimental muscle injury and PRP preparation (i.e. liquid). Overall these studies suggest that the beneficial effects of PRFM or PRP in the healing of muscular injury must be considered in the treatment of a very common pathology associated with traumatic and/or sport injuries. In fact, on the basis of our experience, its use resulted an effective, economical, handily and safe procedure to enhance healing of muscle injury.

Finally, it must be underlined that the potential limitation of using blood derivatives in the clinical setting, related to the concern expressed by the World Anti-Doping Association (WADA) on the use of GFs in sports, is overcome. In fact, while the 2010 WADA Prohibited List demanded a declaration of use for the peritendinous, intratendinous and intrarticular routes of PRP administration and prohibited its intramuscular use, requiring a Therapeutic Use Exemption (TUE) for PRP local use at the site of injury (34), no limitation on this matter are present in the 2011 WADA Prohibited List (35).

Our preliminary morphological experimental study on muscle healing after PRFM administration is however an incomplete representation of the clinical situation and lacks data on functional recovery. Further experimental studies that include the quantification of specific GFs released by PRFM, additional details on angiogenesis and myogenesis, as well as functional recovery, are required to ultimately validate our hypothesis and before PRFM use in a wide clinical application.

ACKNOWLEDGEMENTS

The authors are grateful to Dr. F. Orlando for clinical assistance and to Mr. M. Venneri for his contribution of the graphics.

REFERENCES

1. Brentano MA, Martins Kruel LF. A review on strength exercise-induced muscle damage: applications, adaptation mechanisms and limitations. J Sports Med Phys Fitness 2011; 51:1-10.
2. Woolf AD, Pfleyer B. Burden of major musculoskeletal conditions. Bull World Health Organ 2003; 81:646-56.
3. Järvinen TA, Järvinen TL, Kääriäinen M, Kalimo H, Järvinen M. Muscle injuries: biology and treatment. Am J Sports Med 2005; 33:745-64.
4. Järvinen TA, Järvinen TL, Kääriäinen M, Aärimaa V, Vaittinen S, Kalimo H, Järvinen M. Muscle injuries: optimising recovery. Best Pract Res Clin Rheumatol 2007; 21:317-31.
5. Kasemkijwattana C, Menetrey J, Bosch P, Somogyi G, Moreland MS, Fu FH, Buranapanitkit B, Watkins SS, Huard J. Use of growth factors to improve muscle healing after strain injury. Clin Orthop Relat Res 2000; 370:272-85.
6. Hurme T, Kalimo H, Lehto M, Järvinen M. Healing of skeletal muscle injury: an ultrastructural and immunohistochemical study. Med Sci Sports Exerc 1991; 23:801-10.
7. Borrione P, Di Gianfrancesco A, Pereira MT, Pigozzi F. Platelet-rich plasma in muscle healing. Am J Phys Med Rehabil 2010; 89:854-61.
8. Bir SC, Esaki J, Yamahara K, Tsubota H, Ikeda T, Sakata R. Angiogenic properties of sustained release platelet-rich plasma: characterization in-vitro and in the ischemic hind limb of the mouse. J Vasc Surg 2009; 50(4):870-879.e2.
9. Pintucci G, Froum S, Pinnell J, Mignatti P, Rafii S, Green D. Trophic effects of platelets on cultured endothelial cells are mediated by platelet-associated fibroblast growth factor-2 (FGF-2) and vascular endothelial growth factor (VEGF). Thromb Haemost 2002; 88(5):834-42.
10. Molloy T, Wang Y, Murrel GA. The roles of growth factors in tendon and ligament healing. Sport Med 2003; 33:381-94.
11. Huard J, Li Y, Fu F H. Muscle Injuries and Repair: Current Trends in Research. J Bone Joint Surg Am 2002; 84:822-32.
12. Campion DR. The muscle satellite cell: A review. Int Rev Cytol 1984; 87:225-51.
13. Foster TE, Puskas BL, Mandelbaum BR, Gerhardt MB, Rodeo SA. Platelet-rich plasma: From basic science to clinical applications. Am J Sports Med 2009; 37:2259-72.

14. Aspenberg P, Virchenko O. Platelet concentrate injection improves Achilles tendon repair in rats. Acta Orthop Scand 2004; 75:93-9.
15. Eppley BL, Woodell JE, Higgins J. Platelet quantification and growth factor analysis from platelet-rich plasma: implications for wound healing. Plast Reconstr Surg 2004; 114:1502-8.
16. Gigante A, Cappella M, Manzotti S, Cecconi S, Greco F, Di Primio R, Mattioli-Belmonte M. Osteoinduction properties of different growth factors on cells from non-union patients: in vitro study for clinical application. J Biol Regul Homeost Agents 2010; 24:51-62.
17. Sánchez M, Anitua E, Orive G, Mujika I, Andia I. Platelet-rich therapies in the treatment of orthopaedic sport injuries. Sports Med 2009; 39:345-54.
18. Cieslik-Bielecka A, Bielecki T, Gadzik TS, Cieslik T. Why the platelet-rich Gel has antimicrobical activity? Oral Surg Oral Med Oral Pathol Oral Radiol Endod 2007; 103:303-5.
19. O'Connel SM, Impeduglia T, Hessler K, Wang XJ, Carroll RJ, Dardik H. Autologus platelet-rich fibrin matrix as cell therapy in the healing of chronic lower-extremity ulcers. Wound Repair Regen 2008; 16:749-56.
20. Sporn MB, Roberts AB, Wakefield LM, Assoian RK. Transforming growth factor beta: Biological function and chemical structure. Science 1986; 233:532-4.
21. Li Y, Foster W, Deasy BM, Chan Y, Prisk V, Tang Y, Cummins J, Huard J. Transforming growth factor beta-1 induces the differentiation of myogenic cells into fibrotic cells in injured skeletalmuscle: Key event in muscle fibrogenesis. Am J Path 2004; 164:1007-19.
22. Deasy BM, Qu-Peterson Z, Greenberger JS, Huard J. Mechanisms of muscle stem cell expansion with cytokines. Stem Cells 2002; 20:50-60.
23. Germani A, Di Carlo A, Mangoni A, Straino S, Giacinti C, Turrini P, Biglioli P, Capogrossi MC. Vascular endothelial growth factor modulates skeletal myoblast function. Am J Pathol 2003; 163:1417-28.
24. Carroll RJ, Arnoczky SP, Graham S. Characterization of autologus growth factors in Cascade platelet rich fibrin matrix (PRFM). Edison, NJ: Musculoskeletal Transplant Foundation 2005.
25. Visser LC, Arnoczky SP, Caballero O, Egerbacher M. Platelet-rich fibrin constructs elute higher concentrations of transforming growth factor-β1 and increase tendon cell proliferation over time when compared to blood clots: a comparative in vitro analysis. Vet Surg 2010; 39:811-17.
26. Ranly DM, Lohmann CH, Andreacchio D, Boyan B.D., Schwartz Z. Platelet-rich plasma inhibits demineralized bone matrix-induced bone formation in nude mice. J Bone Joint Surg 2007; 89:139-47.
27. Chargé SBP, Rudnicki MA. Cellular and molecular regulation of muscle regeneration. Physiol Rev 2004; 84:209-38.
28. Collins CA. Satellite cell self-renewal. Curr Opin Pharmacol 2006; 6:301-6.
29. Anitua E, Andia I, Ardanza B, Nurden P, Nurden AT. Autologous platelets as a source of proteins for healing and tissue regeneration. Thromb Haemost 2004; 91:4-15.
30. Arnoczky SP, Warren RF, Spivak JM. Meniscal repair using an exogenous fibrin clot: An experimental study in dogs. J Bone Joint Surg Am 1998; 70:1209-17.
31. Tamimi FM, Montalvo S, Tresguerres I, Blanco Jerez L. A comparative study of 2 methods for obtaining platelet-rich plasma. J Oral Maxillofac Surg 2007; 65(6):1084-93.
32. Castillo TN, Pouliot MA, Kim HJ, Dragoo JL. Comparison of growth factor and platelet concentration from commercial platelet-rich plasma separation systems. Am J Sports Med 2011; 39:266.
33. Jodczyk KJ, Bańkowski E, Borys A. Stimulatory effect of platelet-breakdown products on muscle regeneration. Zentralbl Allg Pathol 1986; 131:357-61.
34. Hammond JW, Hinton RY, Curl LA, Muriel JM, Lovering RM. Use of autologous platelet-rich plasma to treat muscle strain injuries. Am J Sports Med 2009; 37:1135-42.
35. http://www.wada-ama.org/Documents/World_Anti-Doping_Program/WADP-Prohibited-list/WADA_Prohibited_List_2011_EN.pdf

ASSESSMENT OF NGAL AS AN EARLY BIOMARKER OF ACUTE KIDNEY INJURY IN ADULT CARDIAC SURGERY PATIENTS

V. SARGENTINI[1], P. MARIANI[2], M. D'ALESSANDRO[2], V. PISTOLESI[3], M.P. LAURETTA[4], F. PACINI[4], L. TRITAPEPE[4], S. MORABITO[3] and A. BACHETONI[1]

[1]Dipartimento di Medicina Sperimentale, Sapienza Università di Roma, Rome, Italy; [2]Dipartimento di Chirurgia Generale-Specialistica "P. Stefanini", Sapienza Università di Roma, Rome, Italy; [3]Dipartimento di Nefrologia e Urologia, UOS Emodialisi, Sapienza Università di Roma, Rome, Italy; [4]Dipartimento di Scienze Cardiovascolari, Respiratorie, Nefrologiche, Geriatriche, Sapienza Università di Roma, Policlinico Umberto I, Rome, Italy

Received April 6, 2012 – Accepted June 1, 2012

Early and predictive acute kidney injury (AKI) markers may be decisive for the clinical outcome of heart surgery. Hence, this study set out to evaluate the biological variability of urinary neutrophil gelatinase-associated lipocalin (uNGAL) levels in adult cardiac surgery patients, to test their feasibility as a biomarker of early AKI in a routine laboratory setting. uNGAL levels were measured with an automated immunoassay in urine samples from patients undergoing cardiac surgery using cardiopulmonary bypass, at the time of admission (T0) and 4 hours (T1) and 24 hours (T2) after surgery. Patients without post-operative AKI did not show significant differences in urine NGAL levels after surgery. In contrast, patients developing AKI displayed a significant increase (*P*=0.011) in uNGAL levels compared to T0. This increase was detectable at an earlier time point (T1, 4 hours) with respect to serum creatinine (T2, 24 hours). Confirming its utility as a biomarker, at T1 the uNGAL levels were significantly higher in AKI patients than in non-AKI patients (*P*=0.021). A receiver operating characteristic curve analysis of the uNGAL assay gave a sensitivity of 55.3 (95% confidence interval [CI], 26.59-78.73), a specificity of 72.9 (95% CI, 55.88-86.21), and a cut-off value for AKI prediction of 55.2. These results support the notion that urinary NGAL is an earlier marker of AKI than serum creatinine. However, the cut-off value of the assay was too low to consider it as a positive or negative diagnostic marker in AKI patients with moderate degree of severity. Likewise, its sensitivity and specificity were not high enough for it to be considered better than the others currently in use.

Acute kidney injury (AKI) is a frequent and serious complication encountered in 30% to 50% of patients after cardiac surgery (1, 2). As renal damage increases morbidity and mortality, the identification of reliable biomarkers that allow earlier diagnosis of AKI in the postoperative period may potentially increase the success of therapeutic interventions and secondary prevention strategies.

In current clinical practice, urea, creatinine, estimated creatinine clearance and urine output are used as biomarkers of renal function. However, as they tend to provide poor estimates of underlying

Key words: cardiac surgery, acute kidney injury, early biomarker, urinary neutrophil gelatinase-associated lipocalin

Mailing address: Valeria Sargentini, PhD
Sapienza Università di Roma
Dipartimento di Medicina Sperimentale,
Policlinico Umberto I, V.le del Policlinico 155,
00161 Rome, Italy
Tel.: +39 06 49970480 Fax: +39 06 49970443
e-mail: valeria.sargentini@uniroma1.it

0393-974X (2012)

changes in glomerular filtration rate, their accuracy in predicting the likelihood of postoperative AKI is limited, as is their usefulness as an early marker. Moreover, although serum creatinine level is routinely used as a marker of renal function, it has limited sensitivity and performs poorly in immediate postoperative AKI, due to its slow rate of change. In fact, serum creatinine usually rises only 24-36 hours after renal tubular damage, therefore limiting its usefulness in the early detection of AKI (3-5). Hence, there is still a need to find a rapidly available, sensitive and specific biomarker to predict AKI early on, in order to optimize intensive care.

Initially discovered in neutrophils, the 25-kDa secretory protein neutrophil gelatinase associated lipocalin (NGAL) was later shown to accumulate in the kidneys after ischemic renal injury (6, 7). The first studies on NGAL were mainly conducted in children, considered an ideal group for studying biomarkers due to comorbidities occurring only rarely; in particular, Mishra et al (8) found that acute renal failure could be detected with high diagnostic sensitivity and specificity in children two hours after cardiopulmonary bypass through substantial increases in urinary and serum NGAL. Moreover, they reported that these changes were appreciable 34 hours before serum creatinine could detect acute renal failure.

However, as acute renal failure is mainly multifactorial in origin and occurs more commonly in adults with pre-existing diabetes or chronic kidney disease, it was necessary for this line of research to be extended to the adult population. Among other things, these studies demonstrated that increased urinary NGAL (uNGAL) concentrations are associated with an increased occurrence of postoperative acute renal dysfunction in adult cardiac surgical patients (9), making it a potentially useful biomarker in these patients. Indeed, among the number of novel and more specific alternatives to serum creatinine proposed in recent years, i.e. kidney injury molecule-1, interleukin-18, hepatocyte growth factor, cystatin C, N-acetyl-β-D-glucosaminidase, vascular endothelial growth factor and chemokine interferon-inducible protein 10 (10-12), uNGAL is certainly the most promising emerging biomarker for the early diagnosis of AKI (5, 13, 14).

Nonetheless, it should be mentioned that although many authors initially considered NGAL as one of the best candidates for the early diagnosis of AKI, some recently discovered limitations have dampened their enthusiasm. Indeed, great variability in baseline concentrations of NGAL has been described in patients who did not go on to develop AKI (15, 16). Furthermore, meta-analyses have suggested that the sensitivity and specificity of this test vary at very different cut-off values, depending on the population considered (17, 18).

In order to evaluate the usefulness of this potential biomarker in a homogeneous group of adult cardiac surgery patients, we set out to measure uNGAL concentration, normalized to urine creatinine rather than absolute, using an automated method (Abbott Diagnostics, Italy), as a fully automated assay should improve performance as well as reduce the turn around time of the result — a vital factor in such a dangerous condition (19). Our aim was to determine whether there is a discernable association between uNGAL level and AKI in these patients, whether the former could be considered an effective earlier biomarker of the latter with respect to serum creatinine, and finally to evaluate the sensitivity and specificity of this test to determine the clinical course of AKI; in particular we focused on a cohort of patients that developed AKI with a moderate degree of severity in order to apply this test to the routine clinical laboratory setting.

MATERIALS AND METHODS

Patients

All adult patients undergoing cardiac surgery at Policlinico Umberto I Hospital (Rome, Italy) were eligible for enrolment. A total of 52 patients at the Cardiovascular, Respiratory, Nephrology and Geriatric Sciences Department were prospectively studied between September 2010 and June 2011. They all gave informed consent prior to participation, and the study was approved by the Policlinico Umberto I Hospital Ethics Committee.

The diagnostic criteria used to characterize postoperative AKI were an abrupt (within 48 hours) reduction in kidney function, currently defined as an absolute increase in serum creatinine of more than or equal to 0.3 mg/dl (≥ 26.4 μmol/l), a percentage increase in serum creatinine of more than or equal to 50% (1.5-fold from baseline), or a reduction in urine output (documented oliguria of less than 0.5 ml/kg per hour for more than six hours). Patients were then classified according to the

severity of their kidney failure according to AKIN (Acute Kidney Injury Network) guidelines, a modified set of criteria based on the RIFLE approach, as follows: stage 1 (Risk), stage 2 (Injury) and stage 3 (Failure) (20, 21).

Sample collection and procedure

Random urine specimens were collected upon patients' admission (T0), and again at 4 hours (T1) and 24 hours (T2) after cardiopulmonary bypass. Serum samples were collected at T0, T1, T2, and 48 hours after cardiopulmonary bypass (T3). Urine samples were immediately centrifuged at 4000 rpm for 10 minutes at 4°C, and supernatants were stored at -70°C until use. uNGAL levels were measured by means of an ARCHITECT i1000 analyzer Urine NGAL assay (Abbott Diagnostics, Italy), based on two-step chemiluminescent microparticle immunoassay.

To compensate for possible urinary dilution or concentration, commonly expected in patients who undergo cardiopulmonary bypass, urine creatinine was measured in the same samples using Cobas E 601 (Roche Diagnostics, Italy) and the results were expressed as uNGAL/urinary creatinine ratio. Serum creatinine and protein levels were also determined using Cobas E 601. In addition, urinary sediments were analysed to exclude microbial contamination and fungal growth (Iris Diagnostic iQ^{TM}200 Automated Urine Microscopy Analyzer, USA).

Statistical analysis

uNGAL and creatinine data were non-normally distributed (Kolmogorov-Smirnov test), and non-parametric tests were therefore used. The Mann-Whitney (Wilcoxon rank) and Wilcoxon matched pair tests were performed to compare uNGAL and creatinine data between un-paired and paired groups. $p < 0.05$ was considered statistically significant. Results are presented as median with interquartile range (IQR). A receiver operating characteristic (ROC) curve was constructed to evaluate the effect of different cut-off values of NGAL concentrations at T1 in AKI patients versus the non-AKI group. The area under the curve (AUC), the corresponding 95% confident interval (CI) and the *p*-value were calculated. The optimum cut-point value with the best combination of sensitivity and specificity was evaluated. All analyses were performed using GraphPad Prism Software 4 (San Diego, CA).

RESULTS

Patient characteristics

Fifty-two patients were enrolled, and all underwent cardiac surgery under cardiopulmonary bypass. Of these, fifteen patients (29%) developed post-operative AKI and 37 (71%) did not. This latter group therefore served as control (non-AKI patients). According to the AKIN criteria, 73% of the AKI group were classed as having Stage 1 AKI, 14% had Stage 2 AKI and 13% Stage 3 AKI.

uNGAL was successfully analysed in all. Table I shows the clinical characteristics and main perioperative parameters of the AKI and control groups.

Serum creatinine as biomarker in patients developing AKI

Before surgery, all 52 patients enrolled in the study were shown to have normal kidney function by normal serum creatinine values (ranging from 0.7 and 1.2 mg/dL) and urine protein/urine creatinine ratios (less than or equal to 200 mg/g). Measurements of serum creatinine showed that there were no significant differences in baseline level (T0) between non-AKI and AKI patients (p=0.2634). In non-AKI patients, there were no significant changes in serum creatinine values within the first 48 hours after cardiac surgery (Fig. 1A). As expected, in AKI patients, while there was no change in this parameter 4 hours after surgery (T1), a significant increase was detected at 24 hours (T2), and again at 48 hours (T3) (Fig. 1B).

uNGAL/creatinine as biomarker in patients developing AKI

Urine samples obtained from AKI and non-AKI patients were analysed for uNGAL and creatinine levels. No significant difference (p=0.6104) in baseline (T0) uNGAL levels per g creatinine in patients was found between patients who developed AKI in the post-operative period and those who did not. In the 37 patients of the non-AKI group, the uNGAL levels per g creatinine at T0 were 9.7 (5.2–25.5) mg/g creatinine (median and IQR). A moderate, but not significant, increase was detected at T1 [20.1 (6.3–58.7) mg/g creatinine] and another at T2 [18.6 (12.9–36.7) mg/g creatinine] (Fig. 2A). In contrast, in the 15 patients with AKI, the uNGAL levels per g creatinine at T1 were significantly higher than at T0 [55.4 (32.5-117.3) mg/g creatinine *vs* 17.8 (4.3–23.8) mg/g creatinine, *p=0.011*], while at T2 the values returned to baseline levels [29.6 (1393.1)

Table I. *Clinical data of patients who did not develop AKI and those who did.*

	NON AKI (control) group (N=37)	**AKI group (N=15)**
Age (mean±SD)	66.7±11	74±6
Females (%)	29.7	27
Weight (Kg) (mean±SD)	71±12	72±12
Mitral valve replacement surgery (%)	14.2	25
Coronary artery bypass grafting surgery (%)	39.3	50
Simultaneous mitral valve and bypass surgery (%)	7.1	12.5
Simultaneous mitral and aortic valve replacement surgery (%)	10.7	-
Simultaneous bypass grafting and aortic valve replacement surgery (%)	3.6	12.5
Simultaneous aortic valve and ascending aorta replacement surgery (%)	24.9	-
Diabetes (%)	0.1	0.2
Pre-operative SAH (%)	42.8	53.3
Pre-operative EF >50% (%)	57.5	69.2
ECC >120 min (%)	54.2	64.2
Post-operative AF (%)	2.8	13.3
Post-operative IABP (%)	2.7	6.7
Days in ICU (mean±DS)	2±1.5	3±2.5
N° erythrocyte units transfused (mean±SD)	2.5±2.2	4.8±5
N° plasma units transfused (mean±SD)	3.1±3.9	5±4.7
N° platelet units transfused (mean±SD)	0.4±1.5	2.5±5

SAH: systemic arterial hypertension; EF: ejection fraction; ECC: extra-corporeal circulation; AF: atrial fibrillation; IABP: intra-aortic balloon pump; ICU: intensive care unit.

mg/g creatinine] that did not differ significantly from those at T0 (Fig. 2B).

The intergroup analysis showed that four hours after cardiopulmonary bypass (T1), the uNGAL levels per g creatinine were significantly higher in patients who developed AKI than in non-AKI patients [55.4 (32.5-117.3) mg/g creatinine *vs* 20.1 (6.3-58.7) mg/g creatinine, p=0.021]. In contrast, at

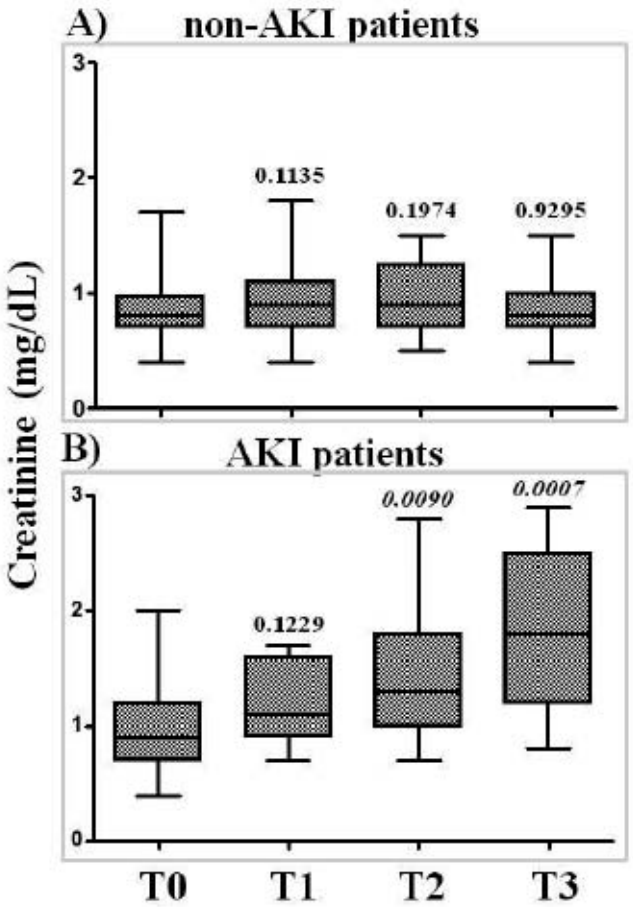

Fig. 1. *Serum creatinine levels before and after cardiac surgery in non-AKI and AKI patients. Box and Whisker plots showing serum creatinine levels before (T0) and at different time points (T1-T3) after surgery in patients without post-operative AKI (A) and with post-operative AKI (B). Results are shown as the median (horizontal line) creatinine with range and IQR (Inter Quartile Range). Differences were considered significant at p-values of < 0.05.*

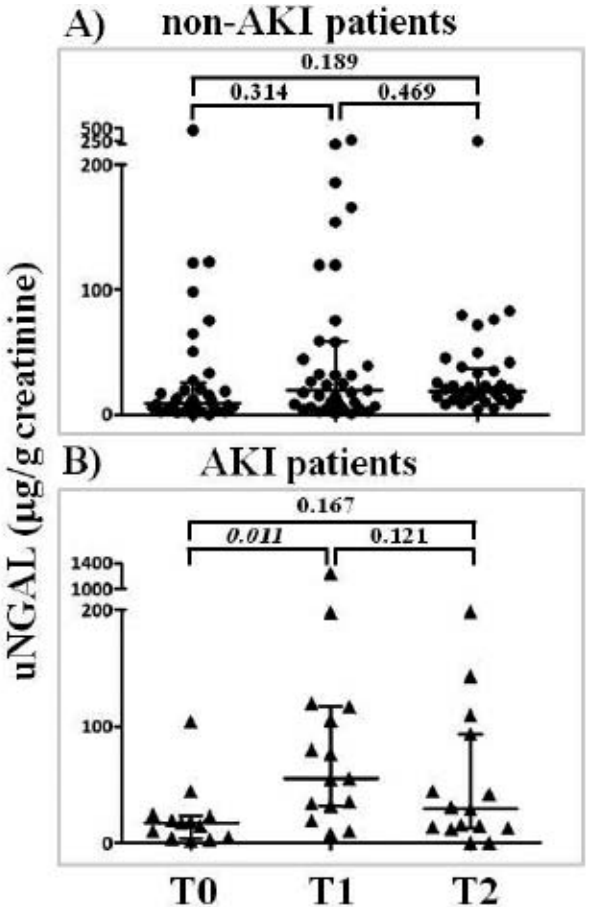

Fig. 2. *uNGAL levels before and after cardiac surgery in non-AKI and AKI patients. Scatter plots shows uNGAL levels in patients without post-operative AKI (A) and with post-operative AKI (B). uNGAL levels were normalized to urine creatinine and were plotted on a linear Y-axis. Results are shown as the median (horizontal line) with IQR uNGAL levels (mg/g creatinine). Differences between the indicated populations were considered significant at p-values of < 0.05.*

T0 and at T2 there were no differences in the values between the AKI group and the non-AKI group (p= 0.641 and p=0.316, respectively) (Fig. 3).

A comparative analysis between men and women showed that there was no significant difference in the two groups at any time (p=0.246, p=0.384, p=0.437 at T0, T1, and T2, respectively). A ROC curve analysis was performed using the uNGAL/creatinine values obtained at T1 (4 hours after cardiopulmonary bypass, Fig. 4). The AUC was 0.7054 (95% CI 0.56-0.85), and the corresponding statistical significance was 0.02134. Moreover, using a cut- off value of 55.2 mg NGAL/g creatinine for discrimination of AKI patients, the sensitivity was 55.33 (95% CI 26.59-78.63), and the specificity was 72.97 (95% CI 55.88-86.21). The modest 4-hour uNGAL levels presumably correlated with the moderate degree of AKI severity observed in the patients enrolled in the study.

DISCUSSION

Rapid clinical intervention for AKI is hampered by the limitations of current diagnostic assays and

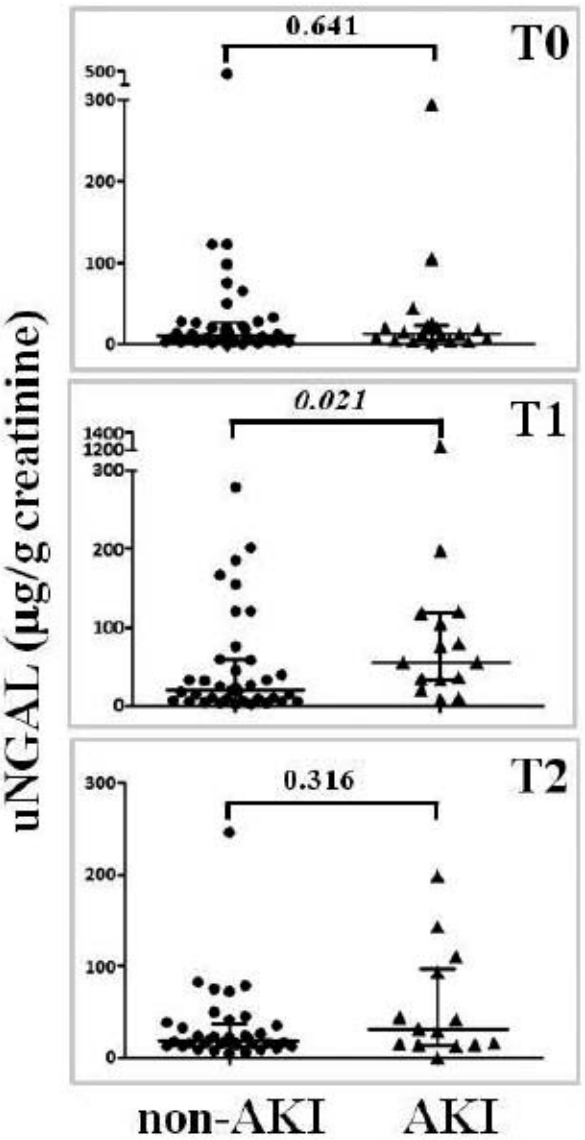

Fig. 3. *Comparative analysis of uNGAL levels in AKI and non-AKI patients at different time points. uNGAL concentration in patients at admission (T0) and 4 and 24 hours after cardiac surgery (T1 and T2, respectively). uNGAL measurements were normalized to urine creatinine and plotted on a linear Y-axis. Results are shown as the individual (circles and triangles) and median (horizontal line) with IQR uNGAL levels (mg/g creatinine) in patients without and with AKI. Differences between the indicated populations were considered significant when the p-values were < 0.05.*

standards (22). NGAL has been proposed as an earlier, more sensitive and more specific biomarker for AKI than other potential candidates (23). In particular, a recent multicentre cohort study of biomarkers, in children undergoing surgery for congenital cardiac lesions, demonstrated that urine NGAL and IL-18 are early biomarkers that can predict the onset of severe AKI and provide additional prognostic information with regard to dialysis, length of stay and mechanical ventilation after cardiac surgery (24).

The results of our study lend weight to the notion that uNGAL could be used as an early marker of AKI onset. Unlike similar studies, which have used *absolute* NGAL values (5, 25, 26), we normalized the uNGAL values to the levels of urine creatinine, considering that alterations in hydration status may influence uNGAL as well as other urinary biomarker concentrations. Indeed, taking account that random urine samples are potentially more influenced by varying osmolality, the use of uNGAL/urinary creatinine ratio allowed us to compensate for possible urinary dilution or concentration, commonly expected in patients who underwent cardiopulmonary bypass. This approach, together with the use of an automated system, no doubt contributed to the excellent performance of the test, and could reduce the intra-individual variation observed in NGAL measurements in other studies (27, 28).

However, in accordance with the recent literature, our results also reveal some limitations of uNGAL as an AKI biomarker, which could affect its value as a diagnostic aid and clinical treatment guide. In fact, previous studies have reported that the sensitivity and specificity of uNGAL assays vary at widely different cut-offs, and that pathological NGAL values vary between patients (3, 14, 17, 29). Moreover, a wide variability in baseline concentrations of NGAL has been reported for patients not developing AKI (15, 16). However, this by no means exclude the utility of NGAL, merely suggesting that serial measurements may be more useful than single-point measurements, a feasible procedure when exploiting a fully automated assay.

In this context, our study shows that, despite the comparable baseline uNGAL values seen in AKI and non-AKI patients, the median values detected in AKI patients were 2-fold higher than in non-AKI patients at T1, suggesting that this increase could be an accurate indicator of tissue damage. Nevertheless, the cut-off values and the sensitivity and specificity

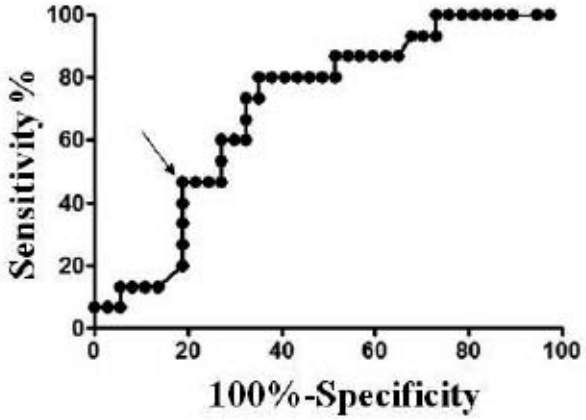

	Cut-off 55.20 µg NGAL/g Cr
AUC (95% CI)	0.7054 (0.5604-0.8505)
P-value	0.02134
Sensitivity (95% CI)	53.33 (26.59%-78.63%)
Specificity (95% CI)	72.97 (55.88%-86.21%)

Fig. 4. *Specificity and sensitivity of the uNGAL assay. ROC curve was generated plotting sensitivity (%) versus 100%-specificity to examine the effect of different cut-points of NGAL concentration at T1 in AKI patients versus non-AKI patients. Circles indicate the various cut-off values used to calculate the corresponding sensitivity and specificity. Arrow indicates the optimum cut-off (55.2) with the best combination of sensitivity and specificity. On the right the AUC (area under the curve) and the statistical significance of the ROC curve and the sensitivity and specificity corresponding to the optimum cut-off are indicated.*

are among the main factors in determining whether a laboratory test could be used in routine laboratory practice as a better biomarker than the existing standard. Unfortunately, the sensitivity and specificity of the assay performed in this study were not high enough for it to be considered superior to the others currently used; indeed the cut-off established (55.2 mg NGAL/g creatinine) is probably too low to permit the use of NGAL as a positive or negative diagnostic marker. Furthermore, the cardiac surgery adult population we considered presented uNGAL values lower than those described in literature (5, 13, 15, 29, 30).

In order to partially explain the low sensitivity of the test in our patient population, it should be considered that a proportion of AKI, observed in the cardiac surgery ICU, could be related to pre-renal causes, such as hypovolaemia and/or transient renal hypoperfusion, known conditions in which uNGAL levels are expected to remain unchanged (29). In this regard, in order to discriminate functional forms of AKI, we would need to rely on the traditionally urinary index (i.e., fractional excretion of sodium and urea), commonly used for the differential diagnosis of acute renal failure, along with an assay of NGAL.

The moderate, albeit significant, nature of the increase in uNGAL we observed could be explained by the low degree of severity of the AKI in most of the patients enrolled. Indeed, Parikh et al. have already postulated that this biomarker is significantly less robust for predicting less severe degrees of AKI (24). It would therefore be interesting to analyse urine samples of adult cardiac surgery patients with very severe AKI (i.e. AKIN-3), in order to determine if the measurement of uNGAL could be applied to the routine laboratory setting with a view to detecting at least more severe clinical states.

Although uNGAL has recently been described as the most prominent commercially available marker for AKI, it is difficult to directly compare its diagnostic performance among these studies because the pathological thresholds have been too variable. Hence, before consensus dictates that uNGAL is suitable as an early and available marker for AKI of any severity, the issues outlined above, particularly in view of the high current costs associated with this test, still remain to be resolved.

ACKNOWLEDGEMENTS

We thank Alessandra Pari and Irene Morfea for their technical contributions to performing

assays, Sabrina Mariotti for her help with statistical analysis of data and Federica Sallusto for reviewing the manuscript. We are also grateful to Abbott Diagnostics (Italy), in particular Chiara Spadaro, for their technical services and to Anna Forster for linguistic assistance.

REFERENCES

1. Haase M, Haase-Fielitz A, Bagshaw SM, Ronco C, Bellomo R. Cardiopulmonary bypass-associated acute kidney injury: a pigment nephropathy? Contrib Nephrol 2007; 156:340-53.
2. Rosner MH, Okusa MD. Acute kidney injury associated with cardiac surgery. Clin J Am Soc Nephrol 2006; 1:19-32.
3. Devarajan P. Neutrophil gelatinase-associated lipocalin: A promising biomarker for human acute kidney injury. Biomark Med 2010; 4:265-80.
4. Star RA. Treatment of acute renal failure. Kidney Int 1998; 54:1817-31.
5. Tuladar S.M., Puntmann V.O., Soni M., Punjabi P.P., Bogle R.G. Rapid detection of acute kidney injury by plasma and neutrophil gelatinase-associated lipocalin after cardiopulmonary bypass. J Cardiovasc Pharmacol 2009; 53(3):261-6.
6. Kjeldsen L, Jhonsen AH, Sengelov H, Borregaard N. Isolation and primary structure of NGAL, a novel protein associated with human neutrophil gelatinase. J Biol Chem 1993; 268:10425-32.
7. Mishra J, Ma Q, Prada A, et al. Identification of neutrophil gelatinase-associated lipocalin as a novel early urinary biomarker for ischemic renal injury. J Am Soc Nephrol 2003; 14:2534-43.
8. Mishra J, Dent C, Tarabishi R, et al. Neutrophil gelatinase associated lipocalin as a biomarker for acute renal injury following cardiac surgery. Lancet 2005; 365:1231-8.
9. Wagener G, Jan M, Kim M, et al. Association between increases in urinary neutrophil gelatinase-associated lipocalin and acute renal dysfunction after adult cardiac surgery. Anesthesiology 2006; 105(3):485-91.
10. McIlroy DR, Wagener G, Lee HT. Biomarkers of acute kidney injury: an evolving domain. Anesthesiology 2010; 112(4):998-1004.
11. Han WK, Wagener G, Zhu Y, Wang S, Lee HT. Urinary biomarkers in the early detection of acute kidney injury after cardiac surgery. Clin J Am Soc Nephrol 2009; 4(5):873-82.
12. Vaidya VS, Waikar SS, Ferguson MA, et al. Urinary biomarkers for sensitive and specific detection of acute kidney injury in humans. Clin Transl Sci 2008; 1(3):200-8.
13. Wagener G, Gubitosa G, Wang S, Borregaard N, Kim M, Lee HT. Urinary neutrophil gelatinase-associated lipocalin and acute kidney injury after cardiac surgery. Am J Kidney Dis 2008; 52:425-33.
14. Cai L, Borowiec J, Xu S, Han W, Venge P. Assays of urine levels of NHL/NGAL in patients undergoing cardiac surgery and impact of antibody configuration on their clinical performances. Clin Chim Acta 2009; 403(1-2):121-5.
15. Zappitelli M, Washburn KK, Arikan AA, et al. Urine neutrophil gelatinase-associated lipocalin is an early marker of acute kidney injury in critically ill children: A prospective cohort study. Crit Care 2007; 11:R84.
16. Siew ED, Ware LB, Gebretsadik T, et al. Urine neutrophil gelatinase-associated lipocalin moderately predicts acute kidney injury in critically ill adults. J Am Soc Nephrol 2009; 20:1823-32.
17. Haase M, Bellomo R, Devarajan P, et al. Accuracy of neutrophil gelatinase-associated lipocalin in diagnosis and prognosis in acute kidney injury: A systemic review and meta-analysis. Am J Kidney Dis 2009; 54:1012-24.
18. Smertka M, Chudek J. Using NGAL as an early diagnostic test of acute kidney injury. Ren Fail 2012; 34(1):130-3.
19. Bachetoni A, Mariani P, D'Alessandro M, et al. Preliminary evaluation of the new TACR flex method versus MEIA method in the therapeutic monitoring of tacrolimus in organ transplantation. Transplant Proc 2007; 39(6):2008-9.
20. Levin A, Warnock DG, Mehta RL, et al. Improving outcomes from acute kidney injury: report of an initiative. Am J Kidney Dis 2007; 50:1-4.
21. Bellomo R, Ronco C, Kellum JA, Mehta RL, Palevsky P. Acute Dialysis Quality Initiative Workgroup. Acute renal failure—definition, outcome measures, animal models, fluid therapy and information technology needs: the Second

International Consensus Conference of the Acute Dialysis Quality Initiative (ADQI) Group. Crit Care 2004; 8:R204-12.

22. Ronco C. N-GAL: Diagnosing AKI as soon as possible. Crit Care 2007; 11:173.
23. Soni SS, Ronco C, Katz N, Cruz DN. Early diagnosis of acute kidney injury: The promise of novel biomarkers. Blood Purif 2009; 28:165-74.
24. Parikh CR, Devarajan P, Zappitelli M, Sint K, Thiessen-Philbrook H, Li S, et al. Postoperative biomarkers predict acute kidney injury and poor outcomes after pediatric cardiac surgery. J Am Soc Nephrol 2011; 22(9):1737-47.
25. Bennet M, Dent CL, Ma Q, et al. Urine NGAL predicts severity of acute kidney injury after cardiac surgery: a prospective study. Clin J Am Soc Nephrol 2008; 3(3):665-73.
26. Krawczeski CD, Woo JG, Wang Y, Bennet MR, Ma Q, Devarajan P. Neutrophil gelatinase-associated lipocalin concentrations predict development of acute kidney injury in neonates and children after cardiopulmonary bypass. J Pediatr 2011; 158(6):1009-15.
27. Delanaye P, Rozet E, Krzesinsky JR, Cavalier E. Urinary NGAL measurement: Biological variation and ratio to creatinine. Clin Chim Acta 2011; 412(3-4):390.
28. Tomonaga Y, Szucs T, Ambühl P, Nock S, Risch M, Risch L. Insights on urinary NGAL obtained in a primary care setting. Clin Chim Acta 2012; 413(7-8):733-9.
29. Nickolas TL, O'Rourke MJ, Yang J, et al. Sensitivity and specificity of a single emergency department measurement of urinary neutrophil gelatinase-associated lipocalin for diagnosing acute kidney injury. Ann Intern Med 2008; 148(11):810-9.
30. Koyner JL, Bennett MR, Worcester EM, et al. Urinary cystatin C as an early biomarker of acute kidney injury following adult cardiothoracic surgery. Kidney Int 2008; 74:1059-69.

INHIBITION OF P-GLYCOPROTEIN-MEDIATED TRANSPORT BY S-ADENOSYLMETHIONINE AND CYNARIN IN MULTIDRUG-RESISTANT HUMAN UTERINE SARCOMA MES-SA/Dx5 CELLS

A. ANGELINI[1,2], R. DI PIETRO[1], L. CENTURIONE[1], M.L. CASTELLANI[1], P. CONTI[3], E. PORRECA[1,2], F. CUCCURULLO[1,2] and C. DI ILIO[4]

[1]Department of Medicine and Aging Sciences, School of Medicine "G. d'Annunzio" University Chieti-Pescara; [2]Aging Research Center, Ce.S.I. "G. d'Annunzio" University Foundation, Chieti-Pescara; [3]Department of Biomedical Sciences and [4]Department of Biochemical Sciences, "G. d'Annunzio" University Chieti-Pescara, Italy

Received April 18, 2012 – Accepted July 26, 2012

Multidrug resistance (MDR) to anticancer chemotherapy is often mediated by the overexpression of the plasma membrane drug transporter P-glycoprotein (Pgp) encoded by multidrug resistance gene (MDR1). Various chemosensitizing agents are able to inhibit Pgp activity but their clinical application is limited by their toxicity. Furthermore, hepatotoxicity related to chemotherapy causes delays of treatment in cancer patients and often requires supplementation of anti-tumour therapy with hepatoprotective agents. In this *in vitro* study, we investigated the effectiveness of an endogenous hepatoprotective agent, S-adenosylmethionine (SAMe), and a natural hepatoprotective compound, Cynarin (Cyn), to inhibit Pgp activity in order to evaluate their potential use as chemosensitizing agents. Human doxorubicin (doxo) resistant uterine sarcoma cells (MES-SA/Dx5) expressing high levels of Pgp were treated with two hepatoprotectors at various concentrations (1, 5 and 10 μM) that are clinically achievable, in the presence or absence of three different concentrations of doxo (2, 4 and 8 μM). In order to evaluate the effects of both hepatoprotectors, we measured the intracellular accumulation and cytotoxicity of doxo, the cellular GSH level, ROS production and catalase (CAT) activity. We found that treatment with 2, 4 and 8 μM doxo in the presence of SAMe or Cyn significantly increased the doxo accumulation and cytotoxicity on MES-SA/Dx5 cells, when compared to control cells receiving doxo alone. Moreover, treatment with SAMe or Cyn significantly increased GSH content (> 80% and >60%, respectively) and CAT activity (>60% and 150%, respectively) in resistant cancer cells, while ROS production was below the values of corresponding untreated control cells. Our *in vitro* findings provide a rationale for the potential clinical use of these hepatoprotectors both as chemosensitizing agents, to reverse Pgp-mediated MDR, and as antioxidants to protect normal cells from chemotherapy-induced cytotoxixity.

Multidrug resistance (MDR) is a major cause of failure of conventional chemotherapy in numerous human cancers (1-8). In a majority of human tumours this phenomenon is related to overexpression of a 170 kDa permeability glycoprotein (Pgp). This transmembrane protein, encoded by the MDR-

Key words: P-glycoprotein, MES-SA/Dx5, Cynarin, S-adenosylmethionine, doxo

Mailing address: Dr. Antonio Angelini,
Università "G. d'Annunzio",
Centro di Scienze dell'Invecchiamento (Ce.S.I.),
Campus Universitario, Via Colle dell'Ara,
66013 Chieti Scalo, Italy
Tel./Fax: 0871 541420
e-mail: aangelini@unich.it

0393-974X (2012)

1 gene, is an energy-dependent efflux pump that actively extrudes a wide range of structurally and pharmacologically unrelated lipophilic drugs (vinca alkaloids, colchicines, anthracyclines etc.) often used for anticancer therapy, thereby reducing their intracellular concentration and cytotoxicity (9-13). Hepatic injury caused by administration of several drugs is a serious chemotherapy-related effect in cancer patients that can determine a dose reduction of anticancer agents and chemotherapy delays or discontinuation with decrease of the therapeutic effects. Therefore, administration of hepatoprotective compounds concomitantly with chemotherapy is frequently used in the management of oncologic patients to promote the regeneration of hepatocytes exposed to damage caused by cytostatic drugs. In recent years, three generations of chemosensitizing agents have been tested both *in vivo* and *in vitro* in combination with conventional anticancer chemotherapy in several MDR tumours to reverse Pgp-mediated resistance (14-21). However, their toxicity and adverse side effects at reversing concentrations limit their clinical use and stimulate the search for novel highly effective non-toxic inhibitors of Pgp-mediated anticancer drug transport. In our previous *in vitro* study we have shown the effectiveness of two side effect-free natural sedatives, flavonoids and honokiol, as modulators of Pgp-mediated MDR (22). In this study, we investigated whether an endogenous hepatoprotective agent, S-adenosylmethionine (SAMe), biosynthesized from methionine (23-27) and one natural hepatoprotective product such as Cynarin (Cyn), the active principle of globe artichoke extracts (cynara cardunculus) (28-29), could interfere with Pgp-mediated drug transport activity in a human sarcoma MES-SA/Dx5 cell line expressing this protein at a high level and exhibiting high resistance (100-fold) to doxo (30). If so, these compounds could be used as both hepatoprotectors and chemosensitizers to increase sensitivity of MDR cells toward anti-neoplastic agents, thus improving cancer chemotherapy. For this purpose, resistant sarcoma cells were treated with different concentrations of doxo (2, 4 and 8 μM), in the absence or presence of various concentrations of exogenous SAMe and Cyn, and intracellular accumulation of doxo and growth inhibition were measured. In addition, because several cytostatic drugs such as doxo induce oxidative stress damage interacting with the respiratory chain, we evaluated whether SAMe and Cyn are effective in the protection against oxidation in this type of cancer cells. Therefore, we measured the levels of total intracellular glutathione (GSH), the catalase activity (CAT) and the production of ROS after treatment of MES-SA/Dx5 cells with various concentrations of hepatoprotectors. The results were then compared to those obtained with Verapamil (Ver), a well-known Pgp inhibitor, used as a positive control (31). The molar concentrations of doxo and hepatoprotective agents used in this study can be achieved in the blood of patients who undergo anti-cancer chemotherapy.

MATERIALS AND METHODS

Chemicals

Doxorubicin (doxorubicin hydrochloride), Verapamil and 3-(4,5 dimethylthiazol-2-yl)-2,5-diphenyltetrazolium bromide (MTT), S-adenosyl-l-methionine chloride (SAMe), and 1,3-dicaffeoylquinic acid (Cyn), dichlorofluorescein diacetate (DCF-DA), and dimethyl sulfoxide (DMSO) were purchased from Sigma-Aldrich Co. (St Louis, MO, USA). All chemicals and drugs were freshly dissolved before use, except for doxorubicin, which was stored in a stock solution of 1 mM in 1X Phosphate Buffered Saline (PBS) at -20° C in the dark.

Cell lines and cell cultures

Doxo-resistant human uterus sarcoma cell line MES-SA/Dx5 was obtained from the European Collection of Cell Cultures (Salisbury, UK). The cells were grown in 25 cm^2 plastic culture flasks (Iwaki Company, Japan) containing 15 ml McCoy's 5a medium (Euroclone, Wetherby West Yorkshire, UK) supplemented with 10% heat-inactivated foetal bovine serum (Euroclone), 2 mM L-glutamine, penicillin (1000 U/ml) and streptomycin (100 μg/ml) in a humidified atmosphere of 95% air and 5% CO_2 at 37°C. Cells were sub-cultured every 3-4 days after treatment with 0.05% trypsin and 0.02% EDTA in Ca^{++} and Mg^{++} free 1X PBS. Cells were periodically checked for mycoplasma contamination.

Intracellular accumulation of doxorubicin

MES-SA-Dx5 cells were seeded on 24-well culture dishes at a density of $1x10^5$ cells/well (Corning-Costar Corp., Corning New York) and incubated for 72 h in growth medium alone at 37°C in an atmosphere containing 5% CO_2 - 95% air to allow cell attachment. At confluence, cells were washed three times with 1X PBS

at 37°C and treated with three different concentrations of SAMe (1, 5 and 10 μM) or Cyn (1, 5 and 10 μM) at 37°C. After culturing for 24 h, all pre-treated cells were exposed to 3 different doxo concentrations (2, 4 and 8 μM) and the monolayer cultures were then incubated for 3 h at 37°C. In these experiments, Ver (10 μM) was used as a positive control drug. All values were averaged from at least three wells for each experiment. After incubation, wells were washed three times with ice-cold PBS (pH 7.4) to stop doxo accumulation and cells were solubilized with 250 μl of 4 M NaOH for 2 h and neutralized with 500 μl of 2 M HCl. The concentration of doxo was determined fluorimetrically (excitation 475 nm; emission 580 nm) with a fluorescence spectrophotometer (Perkin Elmer LS 45). The amount of doxo accumulated inside cancer cells pre-treated with the hepatoprotective compounds or Ver was expressed as the percentage of doxo retention in control cells (doxo alone) at the selected concentrations (2, 4 and 8 μM) and was measured using the following formula: doxo accumulation (%): 100 x (F treated – F control) / F treated, where F treated = mean fluorescence of wells treated with SAMe, Cyn or Ver prior treatment with doxo; F control = mean fluorescence of wells treated with doxo alone.

Cytotoxicity assay

MES-SA/Dx-5 cells were plated at $2.5x10^4$ cells/well in a volume of 100 μl medium in 96-well microtiter plates (Iwaki Company, Japan) at 37°C. At confluence, the culture medium was changed and the cells were treated with 2 μM, 4 μM or 8 μM doxo in the presence or absence of 1, 5 and 10 μM SAMe or 1, 5 and 10 μM Cyn for 72 h. MES-SA/Dx5 cells containing medium alone were used as a negative control. Cells treated with 10 μM Ver were used as a positive control. The *in vitro* cytotoxicity assay was performed using a standard MTT method (32). Briefly, after incubation, wells were rinsed with PBS before adding to each well 100 μl of MTT (0.5 mg/ml) in drug-free medium. After incubation for additional 4 h, the soluble formazan dye produced by metabolically active cells was solubilized in 100 μl of 0.04 N HCl-isopropyl alcohol and quantified at 37°C on a Spectra max 190 Microplate Spectrophotometer reader (Molecular Devices) at the wavelength of 550 nm. The cytotoxicity of each single compound was also measured. Each experiment was performed in triplicate. The percent of cell growth inhibition was calculated as: (1-OD treated well/OD control well) x 100, where OD treated well corresponded to the mean absorbance values of cells treated with hepatoprotective compounds or Ver, whereas OD control well corresponded to the mean absorbance values of unpretreated malignant cells.

The percentage of cancer cells survival (Fig. 3) was calculated by subtracting the corresponding cytotoxicity values of each drug alone from the respective values obtained in combination with the different doxo concentrations according to the formula: 100 x (OD treated well/OD control well).

Measurement of intracellular glutathione

The total intracellular GSH levels of MES-SA/Dx5 cells were measured according to Ellman's method (33). Briefly, MES-SA-Dx5 cells were seeded on 24-well culture dishes at a density of $1x10^6$ cells /well (Corning-Costar Corp., Corning New York) and incubated for 72 h in growth medium alone at 37°C in an atmosphere containing 5% CO_2 - 95% air. The monolayers were then exposed for 3 h to SAMe (1, 5 and 10 μM), Cyn (1, 5 and 10 μM) or Ver (10 μM) at 37° C. For total GSH determinations, the cells were washed with PBS and solubilized with 250 μl of 4 M NaOH for 2 h and neutralized with 500 μl of 2 M HCl. Then, for deproteinization 1 ml of 5% 5-sulphosalycilic acid was added to 3.75 ml of cell lysate for 10 min at room temperature. After centrifugation, 0.1 ml aliquot of supernatants was added to 0.9 ml of phosphate/EDTA buffer (0.2 M potassium phosphate, 0.01 M EDTA, pH 7.4) containing dithionitrobenzoic acid (DNTB, 0.2 mg/ml) and the increase in absorbance at 412 nm (TNB formation) was monitored with a Cary 3C UV-visible Spectrophotometer for 15 min against an appropriate blank and quantified using molar adsorption coefficient ε=13600 M^{-1} cm^{-1}. Control MES-SA/Dx5 wells containing medium only were used as control. The assay was carried out in triplicate. Cellular GSH concentrations (nmoles for $1x10^6$ cells) were expressed as percent of control.

Quantification of intracellular ROS

Cellular ROS were measured using the fluorogenic reagent DFC-DA. Briefly, MES-SA/Dx5 cells were seeded on 24-well culture dishes and incubated at 37°C in 5% CO_2 as above. After this period, the cells were treated with SAMe (1, 5 and 10 μM), Cyn (1, 5 and 10 μM), or Ver (10 μM) for 24 h at 37°C. Thereafter cells were washed three times with PBS and resuspended with PBS containing 20 μM DCF-DA and incubated for 45 min at 37°C. The DCF-DA is a non-polar molecule that diffuses into the cells and within the cytosol the acetate group is cleaved by intracellular esterase to produce a hydrophobic non-fluorescent molecule that is retained by the cells. This non-fluorescent molecule can be oxidized by ROS to a highly fluorescent compound 2,7-dichlorofluorescein and fluorescence intensity is proportional to the amount of oxidant species produced by the cells (34). Measurements of the change in fluorescence signals were detected using a spectrofluorimeter (Perkin Elmer LS 45; excitation at 485 nm and emission at 530). Cells containing medium alone

were used as control. Intracellular ROS levels (DCF) were expressed as percent of control.

Catalase activity

We determined catalase activities in MES-SA/Dx5 cells by measuring the decrease in absorption of hydrogen peroxide at 240 nm at 25°C (35). Briefly, attached cancer cells were collected after trypsinization and washed three times with PBS. Aliquots of 1 ml of cell suspension containing $2x10^6$ cells were incubated for 24 h in growth medium in polystyrene round-bottom tubes (Iwaki Company, Japan) at 37°C in 5% CO_2. Thereafter, the cell media were removed before 1 ml of fresh medium containing SAMe (1, 5 and 10 μM) or Cyn (1, 5 and 10 μM) or Ver (10 μM) were added to each tubes and incubated for 24 h at 37°C. Cells containing medium alone were used as control. After incubation, growth media were removed and 1 ml sonication solution (200 ml KH_2PO_4 0.05 M; 300 ml Na_2HPO_4 x 12 H_2O 0.05 M; 9.7 μl Triton X-114) was added to each tube and then cells were lysed on ice with ultrasound treatment (10 cycles, 0.5 sec. 70 amplitude). Thereafter, a volume of 40 μl/well of lysates were dispensed in a 96-well UV microplate (Corning-Costar Corp.. Corning. NY) and a volume of 140 μl of a buffer solution (200 ml KH_2PO_4 0.05 M; 300 ml Na_2HPO_4 x 12 H_2O 0.05 M) and 20 μl of H_2O_2 (100 mM) were added using a multichannel pipette. Absorption was measured every min for 10 min on a microplate spectrophotometer (Molecular Devices, Spectra Max 190) against a blank containing the reaction solution without H_2O_2. The CAT activity was calculated as: Δ Absorbance/43.7 x 1/mg/ml prot, where 43.7 is the dilution coefficient. CAT activities (nmoles for $2x10^6$ cells) were expressed as percent of control.

Statistical analysis

The results are expressed as mean ±SD and analysed for statistical significance with the Student's *t* test between the control and compounds. p-values of <0.05 were considered significant.

RESULTS

Effects of hepatoprotectors on doxo accumulation in MES-SA/Dx5 cells

As can be seen in Fig. 1, pre-incubation of MES-SA/Dx-5 cells with various concentrations of SAMe or Cyn significantly increased the intracellular concentration of doxo at all doxo concentrations when compared to cells treated with doxo alone ($p<0.05$). The mean percentages of doxo accumulation capacity at 2, 4 and 8 μM concentrations of doxo in combination with SAMe 1, 5 and 10 μM were 12±5.5; 7.1±4.8; 5.2±1.2 and 16.5±3.5; 9.3±1.5; 7±2.3 and 25.3±2.1; 17.5±2.7; 14.2±1.9, respectively, while in combination with 1, 5 and 10 μM Cyn were 16.5±3.5; 14.2±1.7; 7±2.3 and 22.5±3; 16.7±2.8; 14.4±2.3 and 28.7±3.7; 25.2±1.7; 16.5±1.3, respectively. The values of Ver (10 μM) used in combination with 2, 4 and 8 μM doxo were 36.7±2; 36.5±2.2 and 18.4±1.5, respectively (Fig. 2). All values were significant compared to control cells ($p<0.05$).

Effects of hepatoprotectors on doxo cytotoxicity and cell survival in MES-SA/Dx5 cells

The data reported in Table I show that both Ver and hepatoprotectors significantly enhanced the sensitivity of MES-SA/Dx5 cells to doxo after incubation of 72 h at 37°C, when compared to control cells treated with doxo alone ($p<0.05$). In fact, growth inhibition using 2, 4 and 8 μM doxo concentrations in the presence of SAMe (1, 5 and 10 μM) increased 1.05; 1.17; 1.41 (SAMe 1 μM) and 1.04; 1.15; 1.4 (SAMe 5 μM) and 1.02; 1.13; 1.19 fold (SAMe 10 μM) respectively, whereas in combination with Cyn (1, 5 and 10 μM) increased 1.4; 1.7; 2.1 (Cyn 1 μM) and 1.16; 1.32; 1.9 (Cyn 5 μM) and 1.15; 1.2; and 1.34 fold (Cyn 10 μM) respectively, when compared to the corresponding cells treated with doxo alone. In addition, results normalized for toxicity of both hepatoprotectors reported in Fig. 3 show that SAMe was able to reduce significantly ($p<0.05$) the percentage of survival at 10 μM concentration in combination with 4 μM and 8 μM doxo concentrations, while Cyn was able to reduce significantly ($p<0.05$) cell survival at 5 μM and 10 μM concentrations in combination with all doxo concentrations, when compared to cancer cells treated with doxo alone, such as Ver.

Effects of hepatoprotectors on cellular GSH concentrations, CAT activity and ROS production in MES-SA/Dx5 cells

As shown in Fig. 4, the cellular GSH levels and CAT activities were significantly more elevated in cells pre-treated with SAMe and Cyn when compared to untreated control ($p<0.05$). In particular, the intracellular concentrations of GSH

Table I. *Cytotoxic effects of doxo alone and in combination with hepatoprotectors or Ver in MES-SA/Dx5 cells.*

treatment	A_{550nm}	Growth inhibition (%)*
Control	1.4±0.02	----
Doxo2	1.28±0.02	8.6±1.6
Doxo4	1.16±0.03	16.6±2.1
Doxo8	1.05±0.03	26±5.1
Ver10	1.3±0.01	7.5±1.2
SAMe1	1.39±0.01	0.6±1.1
SAMe5	1.38±0.01	1.6±1.5
SAMe10	1.37±0.01	2.3±0.6
Cyn1	1.37±0.02	2.5±0.5
Cyn5	1.35±0.02	3.6±1.4
Cyn10	1.34±0.01	4.4±0.6
Doxo2		
Ver10	1±0.04	28±2.6
SAMe1	1.27±0.02	9.5±3
SAMe5	1.26±0.04	10.6±2.5
SAMe10	1.2±0.06	12.6±4.1
Cyn1	1.22±0.02	13±2
Cyn5	1.18±0.05	16±5.5
Cyn10	1.14±0.08	19.6±4.1
Doxo4		
Ver10	0.9±0.02	36±1
SAMe1	1.15±0.04	17.3±2.5
SAMe5	1.13±0.06	19.2±3.7
SAMe10	1.08±0.03	23.3±1.5
Cyn1	1.12±0.08	19.3±5.1
Cyn5	1.11±0.05	22±7
Cyn10	0.97±0.01	31.6±1.6
Doxo8		
Ver10	0.85±0.03	39.4±2.2
SAMe1	1±0.06	27.3±4.7
SAMe5	0.98±0.02	30.3±2.3
SAMe10	0.95±0.05	32±3.1
Cyn1	0.98±0.02	30±1.5
Cyn5	0.95±0.02	32.3±2.1
Cyn10	0.91±0.03	35±1.8

** Each value represents the mean ± SD of three separate experiments*

were higher in cells pre-treated with SAMe than Cyn at all concentrations (153±14; 171±9; 184±11 and 130±7; 154±13; 163±7, respectively), compared to control cells, while the catalytic activities were significantly more elevated in cells pre-treated with Cyn than SAMe at all concentrations (148±2;

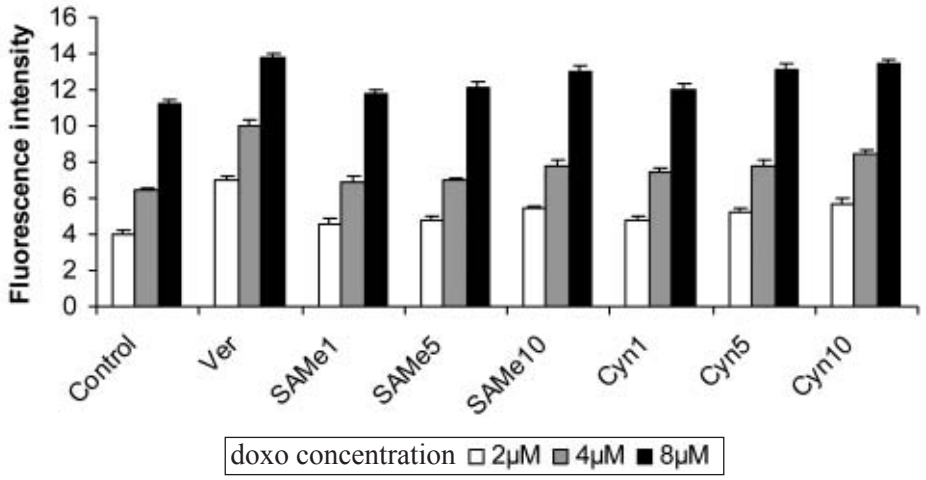

Fig. 1. *Mean intracellular doxo fluorescence intensities retained in MES-SA/DX5 cells pre-treated for 24 h at 37°C with Ver (10 μM), SAMe (1, 5, 10 μM) and Cyn (1, 5, 10 μM) after incubation for 3 h at 37°C with three different doxo concentrations (2, 4 and 8 μM). Cells treated with doxo alone were used as control. All values (Ver, SAMe1, SAMe5, SAMe5, SAMe10, Cyn1, Cyn5, Cyn10) were significant (p<0.05) when compared with Control. Data are the mean ± S.D. of three separate experiments.*

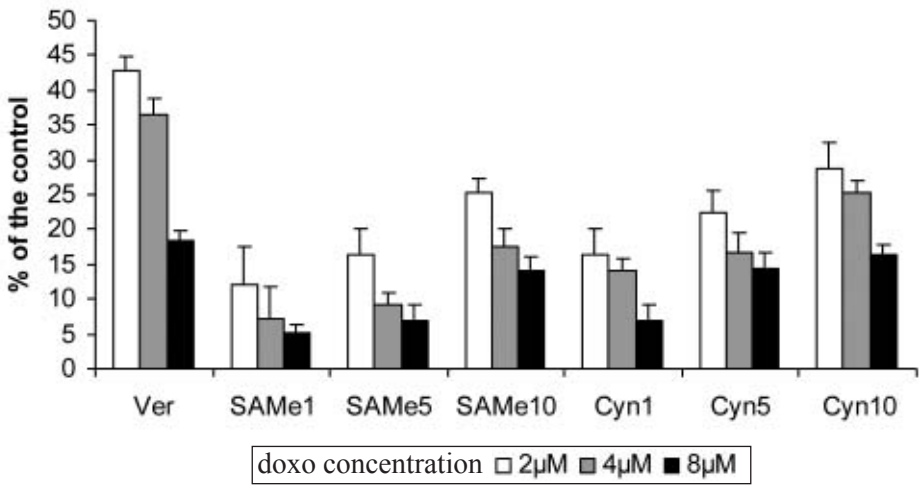

Fig. 2. *Mean percentage of increase in intracellular doxo accumulation in cells pre-treated with Ver (10 μM), SAMe (1, 5, 10 μM) and Cyn (1, 5, 10 μM) in combination with three different doxo concentrations (2, 4 and 8 μM), relative to corresponding control cultures (doxo alone) calculated as described in "Materials and Methods". All values (Ver, SAMe1, SAMe5, SAMe5, SAMe10, Cyn1, Cyn5, Cyn10) were significant (p<0.05) when compared with Control. Data are the mean ± S.D. of three separate experiments.*

150±2.6; 250±2 and 135±3; 140±2.5; 160±3.7, respectively), compared to corresponding untreated control cells ($p<0.05$). In addition, after pre-treatment of MES-SA/Dx5 cells with hepatoprotectors ROS production remained below the control values at all concentrations, when compared to corresponding control cultures.

DISCUSSION

The Pgp-mediated multidrug resistance has been shown to be a major impediment to the success of

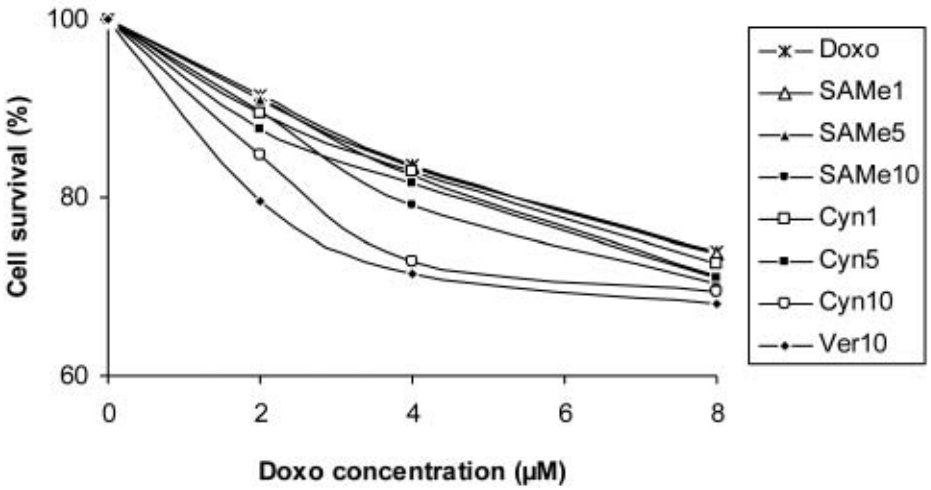

Fig. 3. *Mean percentage of cell survival measured in resistant sarcoma cells after incubation for 72 h at 37°C with doxo alone as control (asterisk), and in combination with SAMe 1 μM (open triangle), SAMe 5μM (solid triangle), SAMe 10 μM (solid circle), and Cyn 1 μM (open square), Cyn 5 μM (solid square), Cyn 10 μM (open circle) and Ver 10 μM (solid rumble). The results are normalized for the toxicity of SAMe, Cyn or Ver in MES-SA/Dx5 cells at the indicated concentrations and calculated as described in "Materials and Methods". Values obtained with SAMe 10 μM in combination with 4 and 8 μM doxo and Cyn 5 and 10 μM in combination with all doxo concentrations were significant ($p<0.05$) vs control cells (doxo alone). Each data point is the mean ± S.D. of three separate experiments.*

anticancer chemotherapy in many human tumours. One strategy to reverse MDR in cells expressing Pgp is the combined use of anticancer drugs with effective and non-toxic chemo-sensitizers. In our present study, we found that intracellular doxo concentrations in Pgp-over-expressing cancer cells pre-treated with SAMe or Cyn were significantly higher in comparison with cells treated with doxo alone at all doxo concentrations (2, 4 and 8 μM), in comparison to the corresponding untreated control cells ($p<0.05$). In particular, as shown in Fig. 1 the percentage of the intracellular doxo levels achieved by cells pre-treated with Cyn (1, 5 or 10 μM) resulted higher than that observed in the presence of SAMe at all doxo concentrations, when compared to control cultures ($p<0.05$). Furthermore, the highest increase in doxo retention was achieved using higher concentrations of hepatoprotectors in combination with a low molar concentration of doxo (2 μM) (Fig. 2). The exact molecular mechanism, however, to explain this last effect remains to be established. We suggest that at lower concentrations of doxo, both SAMe and Cyn might function as common substrates for Pgp binding sites of doxo to Pgp, inhibiting the Pgp-mediated doxo transport out of the cells with a competitive way and increasing intracellular doxo concentration. Conversely, more elevated extracellular doxo concentrations could induce conformational changes of Pgp structure reducing the binding of hepatoprotectors on Pgp sites and increasing efficiency of doxo efflux. These data are consistent with an increased sensitivity of resistant sarcoma cells toward doxo treatment measured with MTT assay. In fact, as shown in Table I, both SAMe and Cyn enhanced the cytotoxic effects of doxo in MES-SA/Dx5 cells at all doxo concentrations (2, 4 and 8 μM) ($p<0.05$) and the increase was more elevated in the presence of the lowest molar concentration (2 μM or 1.1 μg/ml) of doxo (1.1; 1.23; 1.46 and 1.51; 1.86; 2.27 fold, respectively), that is less than maximal serum concentrations achieved when the standard dose is used in clinical protocols (8 μg/ml). Therefore, these findings have a clinical importance because, through a combined chemotherapy of SAMe or Cyn with doxo, it could be possible to reduce doxo concentration and its cumulative myelotoxicity and cardiotoxicity when administered systemically, without reducing its

antineoplastic activity. In addition, exposure of cells to hepatoprotectors induced a significant increase in GSH production and catalytic activity in resistant sarcoma cells ($p<0.05$), while no increase in ROS generation was observed at all concentrations (Fig. 3), when compared to corresponding un-pre-treated control cells. In particular, we found that SAMe induced the highest increases in cellular GSH levels at all concentrations (with increase up to 85% at 10 μM), compared to control values, likely due to their tightly interrelated metabolic pathway (36). Instead, Cyn was able to induce more elevated CAT activities at all concentrations and increases up to 100% (at 10 μM) in comparison to control values ($p<0.05$). These strong increases in intracellular GSH levels and CAT activity reduced the ROS production in resistant cells below the levels measured in corresponding untreated control cells (without SAMe and Cyn). These results suggest that SAMe and Cyn could induce opposite effects in this type of cells: on one hand they could increase the doxo sensitivity of MES-SA/Dx5 cells via the modulation of Pgp activity (Fig. 2); on the other hand, they could have an anti-oxidative capacity by decreasing cellular ROS production, induced by doxo treatment, and reducing its cytotoxicity. These anti-oxidative effects of SAMe and Cyn, however, could be useful to selectively protect MDR-negative normal cells, that do not overexpress Pgp, against the damage caused by generation of free oxygen radicals during anti-tumour chemotherapy, while the extrusion of these antioxidants from resistant malignant cells via Pgp could reduce the protective effects of cancer cells, increasing doxo cytotoxicity. In synthesis, our results demonstrate that both hepatoprotectors tested increase the sensitivity to doxo in MES-SA/Dx5 cells at clinically achievable concentrations (0.1-1 μM) and result much less toxic than Ver at the same molar concentration (10 μM) (2.3 and 1.7 fold, respectively). In addition, the combination of 8 μM doxo and 10 μM SAMe or Cyn significantly ($p<0.05$) reduced cell survival (70.3 and 69.4%, respectively), compared to control cells, at values similar to that obtained with conventional and more toxic Ver (68.1%) shown in Fig. 3. In conclusion, our findings offer a rationale for a potential clinical application of these hepatoprotectors or their derivatives as chemosensitizing agents in order to (1) reverse Pgp-mediated drug resistance in cancer patients, (2) prevent drug-induced normal cell damage and (3) shorten the anticancer chemotherapy duration.

REFERENCES

1. Ling V. Multidrug resistance: molecular mechanism and clinical relevance. Cancer Chemother Pharmacol 1997; 40:3-8.
2. Juliano RL, Ling V. A surface glycoprotein modulating drug permeability in Chinese hamster ovary cell mutants.Biochim Biophys Acta 1976; 455:152-62.
3. Pastan I, Gottesman MM. Multiple-drug resistance in human cancer. N Engl J Med 1987; 316:1388-93.
4. Gottesman MM, Pastan I. Biochemistry of multidrug resistance mediated by the multidrug transporter. Annu Rev Biochem 1993; 62:385-427.
5. Ambudkar SV, Dey S, Hrycyna CA, Ramachandra M, Pastan I, Gottesman MM. Biochemical, cellular and pharmacological aspects of the multidrug transporter. Annu Rev Pharmacol Toxicol 1991; 39:361-98.
6. Nooter K, Stoter G: Molecular mechanism of multidrug resistance in cancer chemotherapy. Pathol Res Pract 1996; 192:768-80.
7. Seeber S, Asieka R, Schmidt CG, Achterrath W, Crooke GT. In vivo resistance towards anthracycline, etoposide and cisdiaminedichloroplatinum. Cancer Res 1982; 42:4719-25.
8. Gottesman MM. Mechanisms of cancer drug resistance. Annu Rev Med 2002; 53:615-27.
9. Gottesman MM, Fojo T, Bates SE. Multidrug resistance in cancer: role of ATP-dependent transporters. Nat Rev Cancer 2002; 2:48-58.
10. Chaudhary PM, Mechetner EB, Roninson IB. Expression and activity of the multidrug resistance P-glycoprotein in human peripheral blood lymphocytes. Blood 1992; 80:2735-9.
11. Endicott JA, and Ling VZ. The biochemistry of P-glycoprotein mediated multidrug resistance. Annu Rev Biochem 1989; 58:137-71.
12. Higgins CF. ABC transporters: from microorganism to man. Annu Rev Cell Biol 1992; 8:67-113.
13. Sauna ZE, Smith MM, Muller M, Kerr KM and Ambudkar SV: The mechanism of action of

multidrug-resistance-linked P-glycoprotein. J Bioenerg Biomembr 2001; 33:481-91.
14. Krishna R, Mayer LD. Multidrug resistance (MDR) in cancer. Mechanisms, reversal using modulators of MDR and role of MDR modulators in influencing the pharmacokinetics of anticancer drugs. Eur J Pharm Sci 2000; 11:265-83.
15. Borowski E, Bontemps-Gracz MM, Piwkowska A. Strategies for overcoming ABC-transporters-mediated multidrug resistance (MDR) of tumor cells. Acta Biochim Pol 2005; 52:609-27.
16. Thomas H, Coley HM. Overcoming multidrug resistance in cancer: An update on the clinical strategy of inhibiting P-glycoprotein. Cancer Control 2003; 10:159-65.
17. Sarkadi B, Müller M. Search for specific inhibitors of multidrug resistance in cancer. Semin Cancer Biol 1997; 8:171-82.
18. Twentymann PR, Bleehen NM. Resistance modification by PSC 833, a novel non-immunosuppressive cyclosporine. Eur J Cancer 1991; 7:1639-42.
19. Green LJ, Marder P, Slapack CA. Modulation by LY335979 of P-glycoprotein function in multidrug-resistant cell lines and human natural killer cells. Biochem Pharmacol 2001; 61:1393-9.
20. Bardelmeijer HA, Beijnen JH, Brouwer KR, Rosing H, Nooijen WJ, Shellens JH, van Tellingen O. Increased oral bioavailability of paclitaxel by GF120918 in mice through selective modulation of P-glycoprotein. Clin Cancer Res 2000; 6:4416-21.
21. Sikic BI, Fisher GA, Lum BL, Halsey J, Beketic-Oreskovic L, Chen G. Modulation and prevention of multidrug resistance by inhibitors of P-glycoprotein. Cancer Chemother Pharmacol 1997; 40:13-19.
22. Angelini A, Di Ilio C, Castellani ML, Conti P, Cuccurullo F. Modulation of multidrug resistance P-glycoprotein activity by flavonoids and honokiol in human doxorubicin-resistant sarcoma cells (MES-SA/Dx5): implications for natural sedatives as chemosensitizing agents in cancer therapy. J Biol Regul Homeost Agents 2010; 24:197-205.
23. Mato JM, Lu SC. Role of S-Adenosyl-L-Metionine in liver health and injury. Hepatology 2007; 45:1306-12.
24. Martinez-Chantar ML, Garcia-Trevijano ER, Latasa MU, Mato IP, Del Pino MS, Corrales FJ, Avila MA, Mato JM. Importance of a deficiency in S-adenosyl-L-methionine synthesis in the pathogenesis of liver injury. Am J Clin Nutr 2002; 76:1177-82.
25. Vincenzi B, Daniele S, Frezza AM, Berti P, Vespasiani, Picardi A, Tonini G. The role of S-adenosilymethionine in preventing oxaliplatin-induced liver toxicity: a retrospective analysis in metastatic colorectalcancer patients treated with bevacizumab plus oxaliplatin-based regimen. Support Care Cancer 2012; 20:135-9.
26. Santini D, Vincenzi B, Massacesi C, et al. S-adenosylmethionine (AdoMet) supplementation for treatment of chemotherapy-induced liver injury. Anticancer Res 2003; 23:5173-9.
27. Vincenzi B, Santini D, Frezza AM, Berti P, Vespasiani U, Picardi A, Tonini G. The role of S-adenosyl methionine in preventing FOLFOX-induced liver toxicity: a retrospective analysis in patients affected by resected colorectal cancer treated with adjuvant FOLFOX regimen. Exp Opin Drug Saf 2011; 10:345-49.
28. Gebhardt R, Fausel M. Antioxidant and hepatoprotective effects of artichoke extracts and constituents in cultured rat hepatocytes. Toxicology in Vitro 1997; 11:669-72.
29. Mehmetcik G, Ozdemirler G, Kocak-Toker N, Cevikbas U, Uysal M. Effect of pre-treatment with artichoke extract on carbon tetrachloride-induced liver injury and oxidative stress. Exp Toxicol Pathol 2008; 60:475-80.
30. Wesolowska O, Paprocka M, Koziak J, Motohashi N, Dus D, Michalak K. Human sarcoma cell lines MES-SA and MES-SA/Dx5 as a model for multidrug resistance modulators screening. Anticancer Res 2005; 25:383-9.
31. Tsuruo T, Iida H, Tsukagoshi S, Sakurai Y. Overcoming of vincristine resistance in P388 leukemia in vivo and in vitro through enhanced cytotoxicity of vincristine and vinblastine by verapamil. Cancer Res 2005; 41(5):1967-72.
32. Mosmann TJ. rapid colorimetric assay for cellular growth and survival: application to proliferation and cytotoxicity assay. J Immunol Methods 1983; 65:55-63.
33. Ellman GC. Tissue sulfhydrylic groups. Arch Biochem Biophys 1959, 82:70-77.
34. Jakubowski W, Bartosz G: 2,7-dichlorofluorescein

oxidation and reactive oxygen species: what does it measure. Cell Biol Int 2000; 24:757-60.
35. Beers RF, Sizer IW. A spectrophotometric method for measuring the breakdown of hydrogen peroxide by catalase. Bio Chem 1952; 195:133-40.
36. Mato JM, Corrales FJ, Lu SC, Avila MA. S-Adenosylmethionine: a control switch that regulates liver function. FASEB 2002; 16:15-26.

INFLUENCE OF TITANIUM LASER SURFACE GEOMETRY ON PROLIFERATION AND ON MORPHOLOGICAL FEATURES OF HUMAN MANDIBULAR PRIMARY OSTEOBLASTS

B. SINJARI[1], S. GUARNIERI[2], F. DIOMEDE[1], I. MERCIARO[1], M.A. MARIGGIO[2], S. CAPUTI[1] and O. TRUBIANI[1]

[1]Department of Medical, Oral and Biotechnological Sciences, Department of Neuroscience and Imaging, University "G. d'Annunzio" of Chieti-Pescara, Italy; [2]Center for Ageing Sciences Foundation, University "G. d'Annunzio" of Chieti-Pescara, Italy

Received May 28, 2012 – Accepted July 24, 2012

The aim of this study is to assess *in vitro* the proliferation and the morphological changes of primary osteoblast-like cells (HOst) seeded on titanium dish grade 4 and 5 with different roughness and different titanium grade: machined (M), sandblasted (SBT), laser-treated with pitches of 20-µm diameter and 30-µm interpore distance. The titanium disks were divided into two groups: group A (titanium grade 4) and Group B (titanium Grade 5), respectively. Proliferation rate of attached cells was evaluated at different time (24, 48, 72 h and 1 week) by the quantitative colorimetric MTT assay. Our results showed a cell growth decrease evident in M titanium surfaces in both Groups A and B, while the cells seeded on the STB and laser disks displayed an increase of cells growth, more evident in laser titanium surfaces in groups A and B. Morphological changes of the biocomplex cells/titanium was assessed by light, scanning and confocal microscopy. In fact, the microscopic analysis helped to clarify the behavior of the cells in contact with the titanium surfaces, in particular the M surface induced significant morphological changes, which were less evident in the SBT surfaces. Laser-engineered porous titanium surfaces promoted viability and proliferation of the osteoblasts. In particular, hemispherical porosity of 20 µm could be responsible for the higher HOst activation, in terms of cells proliferation, adhesion and morphological features.

The use of Titanium (Ti) implants in dentistry to restore mastication, phonation, esthetics and its long-term predictability is well documented. However, the biological phenomenon at bone/implant interface leading to dental implant osseointegration depends on different factors such as: implant macrostructure, surface microstructure and ultrastructure properties. The superficial layer of titanium-oxide and the implant surface microstructure seem to deeply affect bone/fixture interactions (1-2).

From a surface chemistry perspective, many processes and methods have been attempted to increase bone early healing around implants. These include titanium or hydroxyapatite coating by plasma spraying, acid etching or anodization on implant surfaces (3), introduction and/or addition of chemical elements in the surface atomic composition profile (4-5), surface impregnation with different kinds of crystals of various thickness (6-7). Although the positive results *in vitro* (8) of chemical modifications in bone reactions, and lack of properly designed prospective and retrospective

Key words: dental implant, titanium surfaces, primary human osteoblasts

Mailing address: Trubiani Oriana, MD
Department of Medical,
Oral and Biotechnological Sciences,
University of Chieti-Pescara,
Via Vestini 31 I-66100 Chieti, Italy
Tel.: +39 0871 3554097 Fax: +39 0871 3554070
email: trubiani@unich.it

0393-974X (2012)

clinical studies have limited a better understanding of surface modifications of dental implants (9-2-4) .

However, it is general consensus that moderate surface texturing is desirable regardless of surface chemistry processed on dental implant surfaces (9-2).

Recently, the modification of implant roughness at the nanoscale level to simulate the topography of normal bone becomes one of the major research interests.

Moderately rough surfaces have been shown to improve early fixation of implants compared with as-machined surfaces (9-2). A recent study has shown increased biomechanical fixation results for low impregnation with Ca and P on a moderately rough surface compared with alumina-blasting/dual acid etching surfaces (10).

Webster (1999) and Webster and Ejiofor (2004) reported that the osteoblast adhesion on nanophase metals was significantly greater than the conventional ceramics and conventional metals, respectively (11-12). It has been shown that the regular rough surface increases cellular proliferation and differentiation more than sandblasted or etched surfaces (13-14). One technique for obtaining regular and predetermined hemispherical porosities on titanium surfaces is laser engineering. Laser micromachining obtains a highly clean surface structure, without contamination by foreign elements (15).

The laser system is a Q-switched diode-pumped solid Nd-YAG laser (DPSS) used for surface micromachining. This technique generates a pulse laser beam able to obtain controlled and regular size pores. Although the influence of this technique on the osteoblast cell line is demonstrated there is lack of information on cellular viability and responsiveness on primary osteoblasts (16).

The objective of this study is to evaluate *in vitro* the biological behavior of HOst cells, cultured on three different titanium surfaces, smooth, sandblasted and laser treated, by investigating cell morphology, adhesion, and proliferation at light, scanning and laser confocal microscopy.

MATERIALS AND METHODS

Titanium discs

Disks were 6 mm diameter and 2.5 mm height and were prepared from grade 4 and 5 unalloyed ISO 5832/2 titanium rods (Geass s.r.l., Udine, Italy). Disks were made of three different surfaces: 1) machined; 2) sandblasted and 3) laser-treated with hemispherical cavities of 20 μm diameter and 30 μm of interpore distance. Sandblasted titanium (SBT) disks were prepared by sandblasting with 100 mesh ultrapure Al_2O_3. Laser micromachining was performed by means of a Q-switched DPSS Nd:YAG laser. After surface treatment, samples were washed in 3% surfactant solution, rinsed with ultrapure water, and finally disks were sterilized by electron beam irradiation before cell culturing.

Cell culture

Human mandibular periosteum biopsies were carried out after informed consent on five volunteers aged 20–35 years. No subject showed systemic or oral diseases. Explants were obtained from maxilla periosteum by scraping the roots of non-carious third molars with a Gracey's curette. The osteoblasts were obtained and cultured in OGM basal medium (Lonza Walkersville Inc, Walkersville, MD, USA) at 37°C, in a humidified atmosphere of 5% CO_2. Cells migrated from the explants and on day 14 they were 80–90% confluent as determined by phase contrast microscopy. Cell population obtained was immunochemically characterized by a specific alkaline phosphatase and CD 44 antigen (Becton Dickinson, San Jose, CA, USA) (17).

Adherent cells were isolated using 0.1% trypsin solution, seeded on Titanium disks provided by the Geass Company. Cells were periodically checked under a phase contrast light microscope and at 70-80% of confluence were detached and used for the morphological and biochemical experiments. All tests were carried out using cells at the second passage and repeated with two different cell lines with similar results. Controls consisted of HOst grown without titanium disks.

MTT assay

The viability of HOst cells seeded with or without machined, sandblasted and laser-treated disks was measured by the quantitative colorimetric MTT (3- [4,5-dimethyl-2-thiazolyl]-2,5-diphenyl-2H- tetrazoliumbromide test) (Promega, Milan, Italy). 5,000 cells/well were seeded into a 96-well culture plate with OBM medium, after 24, 48, 72 h and 1 week of incubation at 37°C, 15 μl/ well of MTT was added to culture medium, and cells were incubated for 3 h at 37°C. The supernatants were read at 650 nm wavelength using an ND-1000 NanoDrop Spectrophotometer (NanoDrop Technologies, Rockland, DE, USA). The MTT assay was performed in four independent experiments, six replicate wells for each experimental point.

Immunofluorescence staining and confocal laser scanning microscope analysis

Cells grown on titanium surfaces were fixed for 10 min

at room temperature (RT) with 4% paraformaldehyde in 0.1M sodium phosphate buffer (PBS), pH 7.4. After washing in PBS, cultures were processed for immunofluorescence labeling. The samples were incubated with Alexa Fluor 594 phalloidin (dil.1:200, red fluorescence) (Molecular Probes, Invitrogen, Eugene, OR, USA), as a marker of the actin cytoskeleton. Before mounting for microscope observation, samples were briefly washed with dH_2O and cell nuclei were stained with TOPRO (dil. 1:200, far red fluorescence) (Molecular Probes) for 5 min. The titanium disks were placed face down on glass slides and mounted with Prolong antifade (Molecular Probes).

Staining of samples was visualized using a Zeiss LSM510 META confocal system (Jena, Germany), connected to an inverted Zeiss Axiovert 200 microscope equipped with a Plan Neo-fluar oil-immersion objective (40×/1.3 NA) (22, 23). Images were sampled using an Argon laser beam with excitation line at 488 nm to register the reflected light from titanium surface alone (detected using a band pass filter set (BP) a 500-530 nm, pseudocolored in green), or simultaneously with a Helium-Neon 543 nm and 633 nm lines in triple labeling acquisition together with phalloidin (detected using a BP at 560-615 nm, pseudocolored in red) and TOPRO (detected using a BP at 648-800 nm, pseudocolored in blue).

Scanning electron microscopy analysis

The samples were fixed for 4 h at 4°C in 4% Glutaraldehyde in 0.05 M phosphate buffer (pH 7.4), dehydrated in increasing ethanol concentrations and then critical point dried. They were then mounted on aluminum stubs and gold-coated in an Emitech K550 (Emitech Ltd. Ashford, UK) sputter-coater before imaging by means of a SEM (ZEISS, EVO 50).

Statistical analysis

The cell growth was analyzed by Sigma Plo 9.0 (Systat Software, Inc., Point Richmond, CA, USA).

Statistical analysis was performed using two-way Anova tests and the Holm–Sidak method for multiple comparisons, to evaluate the main effect and the interaction of the two factors under investigation.

RESULTS

In the present study, normal human primary osteoblasts were used. The primary culture of the cells displayed fibroblastic and cubic morphological features with roundish or elliptical nucleus containing one or more nucleoli (Fig. 1B, inset).

In vitro cell culture provides an ideal tool to

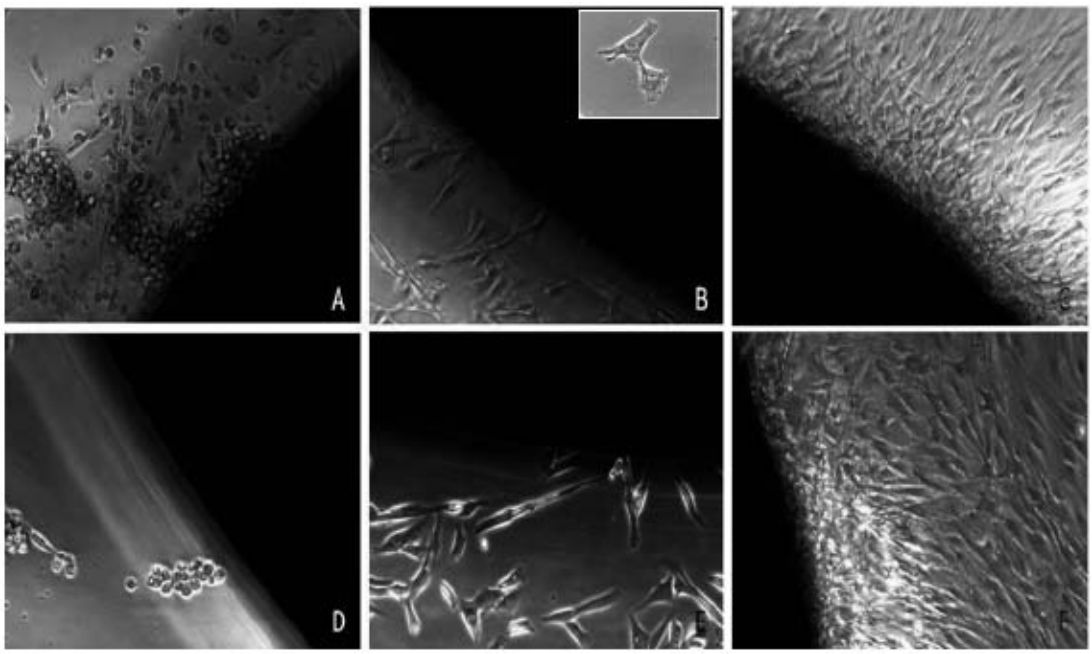

Fig. 1. *Light Microscopy: Human primary osteoblast culture placed with six different implant surfaces: (**A**) Machined surface grade 4; (**B**) Sandblasted surface grade 4 ; (**C**) Laser surface grade 4; (**D**) Machined surface grade 5; (**E**) Sandblasted surface grade 5; (**F**) Laser surface grade 5.*
Inset, section B: Typical morphology of normal human periosteum osteoblasts, could be observed in the control group. Original magnification:10x.

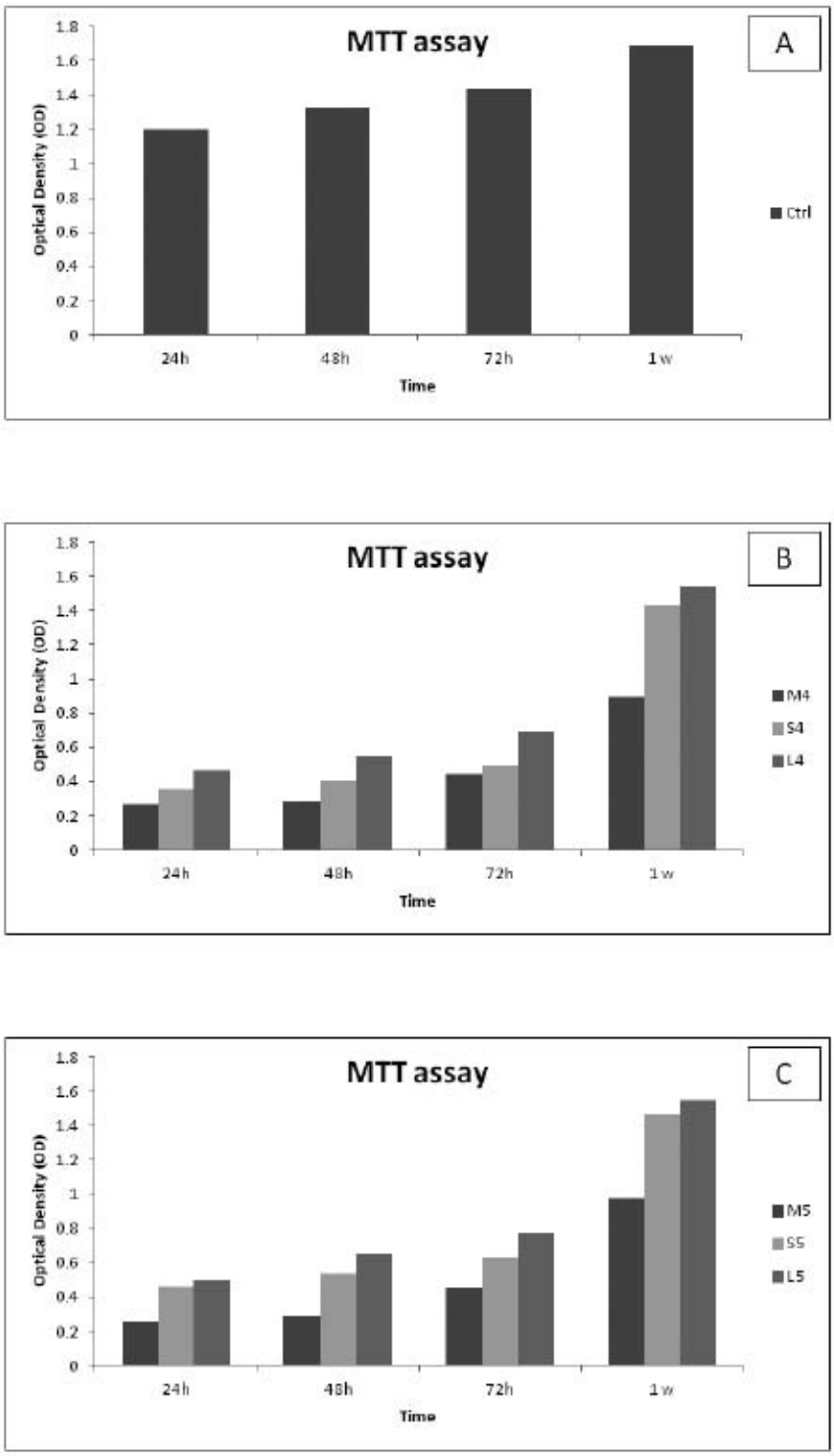

Fig. 2. *MTT Assay: Cellular response of HOsts placed in contact with different implant surfaces. Cytotoxicity was evaluated at different time points: 24, 48, 72 h and after 1 week.*
A) *cell growth at different time of culture.* ***B*** *and* ***C)*** *evaluation of the cell growth of osteoblasts seeded on machined, sandblast and laser group 4 and 5 disks. A cell growth was evident during all time of incubation. Error bars indicate ±SD (ANOVA, Tukey, α=0.05).*

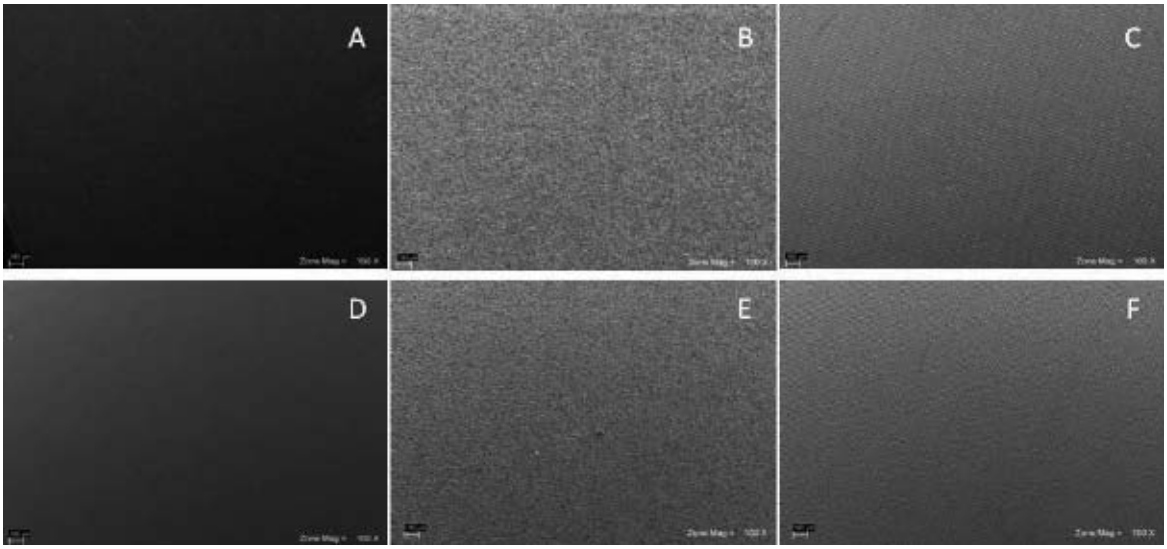

Fig. 3. *SEM images of **A** and **D**: machined surfaces grade 4 and 5; **B** and **E**: sandblasted surfaces grade 4 and 5; **C** and **F**: Laser treated surfaces group 4 and 5.*

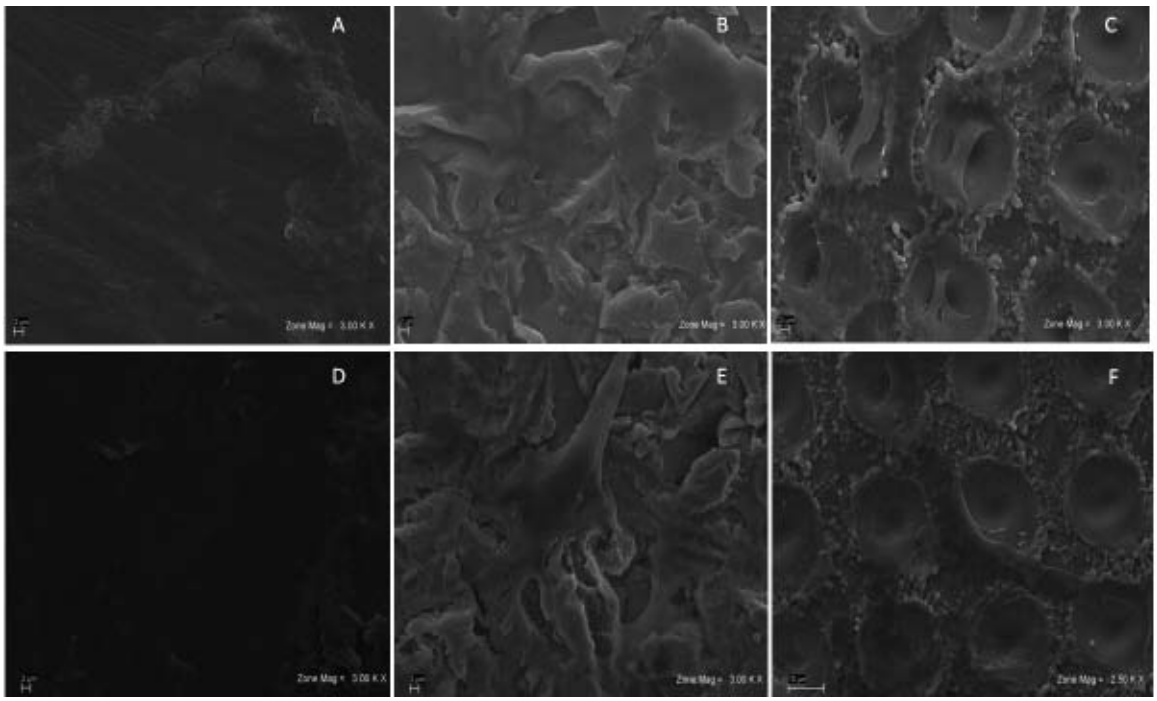

Fig. 4. *SEM analysis: Human osteoblast cultures placed with six different implant surfaces: (**A**) Machined surface grade 4; (**B**) Sandblasted surface grade 4; (**C**) Laser surface grade 4; (**D**) Machined surface grade 5; (**E**) Sandblasted surface grade 5; (**F**) Laser surface grade 5.it is possible to note the characteristic cell morphology.*

investigate the biocompatibility of many different surfaces, and in the current study we assessed the cellular response to the following titanium disks: 1) machined 4 and 5; 2) sandblasted 4 and 5, and 3) laser-treated disks 4 and 5 with hemispherical cavities of 20 μm diameter and 30 μm of interpore distance.

By MTT assay, we evaluated the proliferation rate and viability of HOst incubated for 24, 48, 72 h and 1 week with the above-mentioned surfaces.

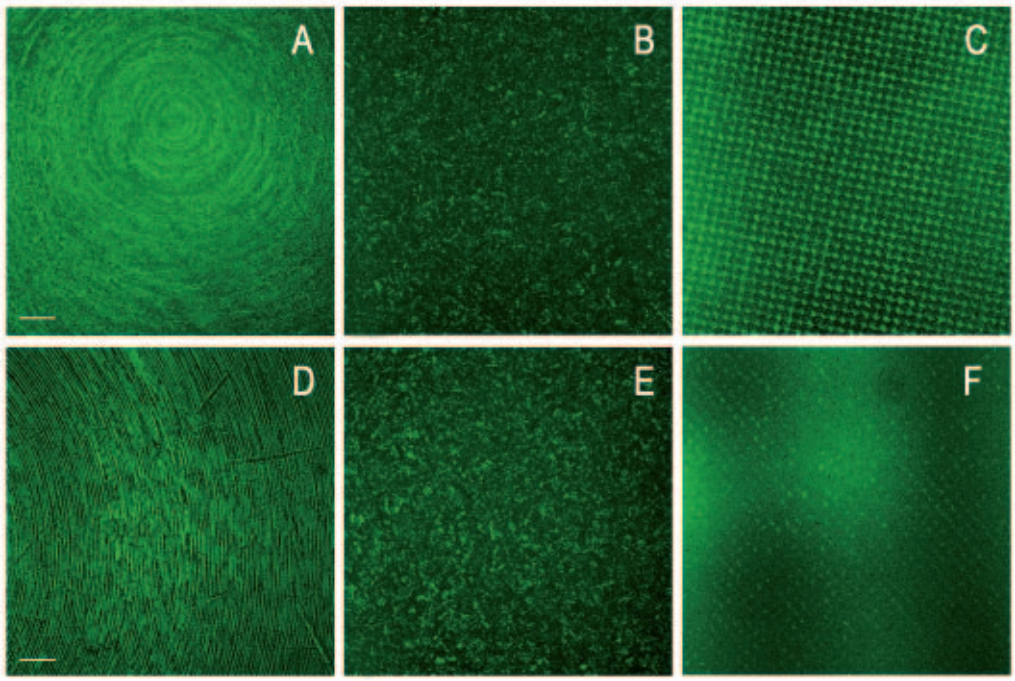

Fig. 5. *CLSM acquisition: Geometrical features of different titanium implant surfaces.* ***A)*** *Sandblasted surface grade 4;* ***(B)*** *Machined surface grade 4;* ***(C)*** *Laser surface grade 4;* ***(D)*** *Sandblasted surface grade 5;* ***(E)*** *Machined surface grade 5;* ***(F)*** *Laser surface grade 5. Scale bar 100 µm.*

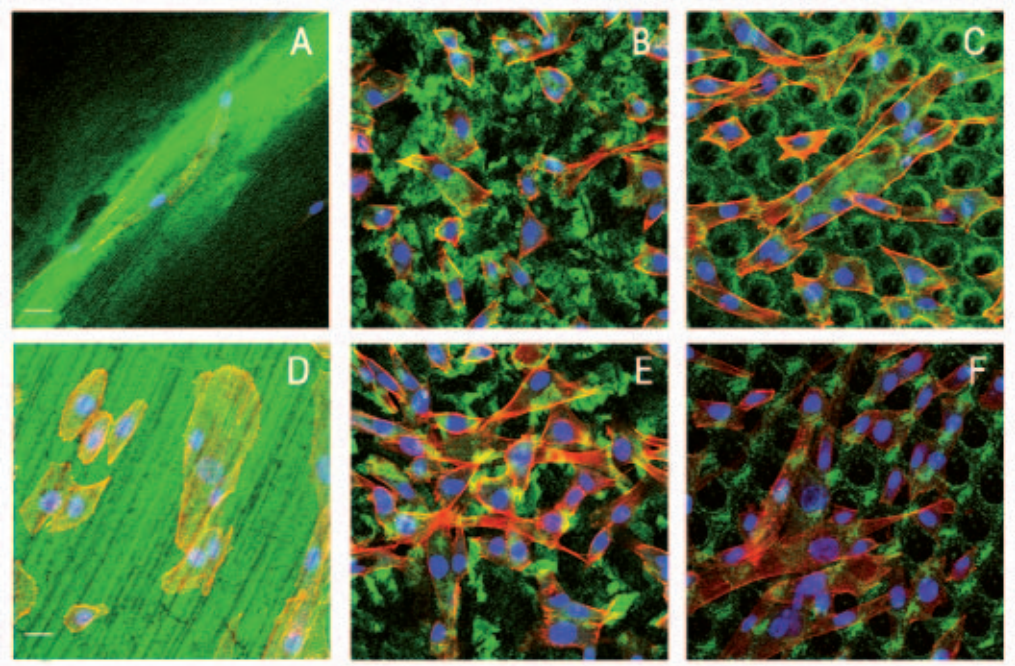

Fig. 6. *CLSM investigation: Human osteoblasts staining with phalloidin (red) for cytoskeleton actin and TOPRO (blue) for nucleus.* ***A)*** *Sandblasted surface grade 4;* ***(B)*** *Machined surface grade 4;* ***(C)*** *Laser surface grade 4;* ***(D)*** *Sandblasted surface grade 5;* ***(E)*** *Machined surface grade 5;* ***(F)*** *Laser surface grade 5. Scale bar 20 µm. Changes to morphological organization are present only in machined surface, the resting samples show the morphological features of the primary osteoblasts.*

Fig. 2, section A shows the cell proliferation of human mandibular osteoblasts at different time points. Section B reports the cell growth in samples seeded on machined, sandblast and laser treated disks, group 4. A higher cell growth was evident in HOst incubated on sandblasted surfaces and in particular on laser-treated surfaces during all culture times. The better results, in terms of cell proliferation, were obtained for titanium disks, group 5. In particular, during all phases of culture, the HOst cells exhibited a high proliferative ability when seeded on laser-treated group 5 disks.

The studies carried out by light microscopy and scanning electron microscopy confirmed the results obtained by MTT assay.

After 24 h of incubation, during the first contact between cells and the titanium disks, the adhesive process was observed, in particular in sandblasted and laser-treated disks group A and B confirming the good biocompatibility of the three-dimensional materials examined.

With light and scanning microscopy, proliferating spindle-shaped cells with extended cellular processes as filopodia and lamellipodia on sandblasted titanium grade 4 and 5 surfaces and laser-treated titanium grade disks 4 and 5 were detectable (Fig. 1 and Fig. 4, section B, C, E, F). On the contrary on the machined surfaces group A and B dramatic morphological changes were present; the cells were smaller, retracted and the greater part of them was roundish, and uneven changes of the cytoskeleton structure were evident; the presence of cells detached from the bottom well was suggestive of cell death (Fig. 1, section A and D; Fig.4, section A and D).

Scanning electron microscopy and CLSM observations helped to clarify the geometry of the analyzed disks (Fig. 3 and Fig. 4, Section A and D, Machined surfaces grade 4 and 5, Section B and E: Sandblast surface grade 4 and 5 respectively; Section C and F: Laser surfaces grade 4 and 5.

Figs. 4 and 6 showed the performance of the cells in contact with the titanium disks; the usual morphological organization of the cells in intimate contact with the Sandblasted 4 (section B) and Sandblast 5 (section E) and laser–treated disks 4 (section C) and 5 (section F) was evident.

Instead, in primary osteoblasts culture seeded on machined surface grade 4 (section A) and 5 (section D) many changes were detectable in cell morphology: the cells were smaller, a few roundish, with the cytoskeleton actin filament not well defined, indicative of cell suffering.

DISCUSSION

Biocompatibility is a major concern in the manufacture of novel implant materials. Direct apposition of bone matrix to the implant surface without intervening soft or fibrous tissue is mandatory for the development and maintenance of the bone-implant surface. Even if numerous studies have investigated the osteoblast response to metal implants, little is known about the initial intracellular events occurring at the osteoblast/implant interface, loading to endosseous integration. The composition and the geometry of the metal have been shown to influence osteoblast adhesion, growth and phenotypic expression, including the integrin pattern (24-26).

An excellent load-bearing orthopedic and dental implant for clinical application should meet four elements: (i) good biocompatibility, which is the primary requirement for the implant; (ii) high bioactivity. After being implanted in the body, the implant can guide the biological behaviors of cells, including cellular adhesion, proliferation, differentiation, and migration. In other words, the implants should have good osteoconductivity even osteoinductivity; (iii) good integration with surrounding bone to prevent movement and migration; and (iv) proper mechanical properties that can not only carry load, but also avoid the stress shielding to peripheral bone (27).

Various techniques have been developed to obtain biocompatible titanium dental surfaces including: plasma spraying, hydroxyapatite coating, anodization, grit blasting, acid etching, laser treatment and a combination of these techniques (28).

Some important advantages have been attributed to surface roughness in increasing the cell attachment to implant surface and to enhance the bone implant biomechanical interaction (29).

A key theory of bone tissue engineering is that the development of bioactive surface can stimulate cell behaviors in the absence of chemical treatment,

regulating the over-expression of bone-related genes.

Evidence has been presented showing that the micro topography of titanium surfaces is able to influence not only the cell shape and orientation but the deposition of extracellular matrix, collagen synthesis, and alkaline phosphatase activity (30).

In this study we investigated the primary human osteoblasts, from human mandibular periostium, in contact with different surfaces, prepared from grade 4 and 5, as: 1) machined; 2) sandblasted and 3) laser-treated disks with hemispherical cavities of 20 μm diameter and 30 μm of interpore distance.

The viability MTT test carried out at 24, 48, 72 h until 1 week showed a more evident cell growth increase in cells in contact with sandblasted and laser-treated surfaces in respect to cells seeded on machined titanium disks.

At morphological level, the construct cells/ titanium analyzed offered the opportunity to observe flattened osteoblasts establishing a strong focal adhesion on the bottom pores on the titanium disks platform and in particular on the hemispherical cavities of the laser 4 and 5 surfaces.

We retain that the microstructure surfaces can be considered of perceptible importance for implant performance and its topography may induce changes in cell shape and structure which in turn may lead to the modification of cellular growth and differentiation acting also on the mechano-transductive pathways.

In conclusion, our *in vitro* experiments using human mandibular osteoblast indicate that a fine laser surface structure promote optimal cell adhesion and proliferation suggesting that this surface geometry could plays a crucial roles in regenerative medicine.

A future goal will be to clarify whether laser titanium surfaces can induce a cascade of osteogenic-related molecules in primary osteoblasts.

REFERENCES

1. Albrektsson T, Johansson C. In: Davies JE, editor. Quantified bone tissue reactions to various mateallic materials with reference to the socalled osseointegration concept. The bone-biomaterial interface. Toronto: University of Toronto press, 1991; p. 357-63.
2. Albrektsson T, Wennenberg A. Oral implant surfaces: Part 2-review focusing on clinical knowledge of different surfaces. Int J Prosthodont 2004; 17:544-64.
3. Le Guéhennec L, Soueidan A, Layrolle P, Amouriq Y. Surface treatments of titanium dental implants for rapid osseointegration. Dent Mater 2007; 23:844-54.
4. Coelho PG, Granjeiro JM, Romanos Ge, Suzuki M, Silva NR, Cardaropoli G, Thompson VP, Lemons JE. Basic research methods and current trends of dental implants surfaces. J Biomed Mater Res B Appl Biomater 2009; 88:579-96.
5. Kang BS, Sul YT, Oh SJ, Lee HJ, Albrektsson T. XPS, AES and SEM analysis of recent dental implants. Acta Biomater 2009; 5:2222-9.
6. Yang Y, Kim KH, Ong JL. A review on calcium phosphate coating produced using a sputtering process-an alternative to plasma spraying. Biomaterials 2005; 26:327-37.
7. Garanto R, Marin C, Suzuki M, Gil JN, Janal MN, Coelho PG. Biomechanical and histomorphometric evaluation of a thin ion beam bioceramic deposition on plateau root form implants: an experimental study in dogs. J Biomed Mater Res B Appl Biomater 2009; 90:396-403.
8. Lamolle SF, Monjo M, Rubert M, Haugen HJ, Lyngstadaas SP, Ellingsen JE. The effect of hydrofluoric acid treatment of titanium surface on nanostructural and chemical changes and the growth of MC3T3-E1 cells. Biomaterials 2009; 30:736-742.
9. Albrektsson T, Wennenberg A. Oral implant surfaces: Part 1-review focusing on topographic and chemical properties of different surfaces and in vivo response to them. Int J Prosthodont 2004; 17:536-43.
10. Trubiani O, Isgro A, Zini N, et al. Functional interleukin-7/interleukin-7Ralpha, and SDF-1alpha/ CXCR4 are expressed by human periodontal ligament derived mesenchymal stem cells. J Cell Physiol 2008; 214:706-713.
11. Marin C, Granato R, Suzuki M, Gil JN, Piattelli A, Coelho PG. Removal torque and histomorphometric evaluation of bioceramic grit-blasted/acid–etched and dual acid-etched implant surfaces: an experimental study in dogs. J Periodontol 2008; 79:1942-9.
12. Webster TJ, Siegel RW, Bizios R. Osteoblasts adhesion on nanophase ceramics. Biomaterials 1999; 20:1222-7.
13. Webster TJ, Ejifor JU. Increased osteoblasts adhesion

on nanophase metals: Ti, Ti6Al4V, and CoCrMo. Biomaterials 2004; 25:4731-9.
14. Zinger O, Anselme K, Denzer A, Habersetzer P, Wieland M, Jeanfils J, Hardouin P, Landolt D. Time dependent morphology and adhesion of osteoblastic cells on titanium model surfaces featuring scale-resorved topography. Biomaterials 2004; 25:2695-711.
15. Zinger O, Zhao G, Schwartz Z, Simpson J, Wieland M, Landolt D, Boyan B. Differential regulation of osteoblasts by substrate microstructural features. Biomaterials 2005; 26:1837-47.
16. Gaggl A, Schultes G, Müller WD, Kärcher H. Scanning electron microscopical analysis of laser-reated titanium implant surfaces - A comparative study. Biomaterials 2000; 21:1067-73.
17. Berardi D, De Benedittis S, Polimeni A, Malagola C, Cassinelli C, Perfetti G. In vitro evaluation of the efficacy of a new laser surface implant: cellular adhesion and alkaline phosphatase production test. Int J Immunopathol Pharmacol 2009; 22:125-31.
18. Trubiani O, Fulle S, Traini T, Paludi M, la Rovere R, Orciani M, Caputi S, Piattelli A. Functional assay, expression of growth factors and proteins modulating bone-arrangement in human osteoblasts seeded on an anorganic bovine bone biomaterial. Eur Cells Materials 2010; 20:72-83.
19. Orciani M, Trubiani O, Vignini A, Mattioli-Belmonte M, Di Primio R, Salvolini E. Nitric oxide production during the osteogenic differentiation of human periodontal ligament mesenchymal stem cells. Acta Histochem 2009; 111:15-24.
20. Trubiani O, Cataldi A, De Angelis F, D'Arcangelo C, Caputi S. Overexpression of interleukin-6 and -8, cell growth inhibition and morphological changes in 2-hydroxyethyl methacrylate-treated human dental pulp mesenchymal stem cells. Int Endod J 2012; 45:19-25.
21. Trubiani O, Zalzal SF, Paganelli R, et al. Expression profile of the embryonic markers nanog, OCT-4, SSEA-1, SSEA-4, and frizzled-9 receptor in human periodontal ligament mesenchymal stem cells. J Cell Physiol 2010; 225:123-31.
22. Di Stefano A, D'Aurizio E, Trubiani O, et al. Viscoelastic properties of Staphylococcus aureus and Staphylococcus epidermidis mono-microbial biofilms. Microb Biotechnol 2009; 2:634-41.
23. Cellini L, Grande R, Di Campli E, Di Bartolomeo S, Di Giulio M, Traini T, Trubiani O. Characterization of an Helicobacter pylori environmental strain. J Appl Microbiol 2008; 105:761-769.
24. Vrouwenvelder WC, Groot CG, de Groot K. Histological and biochemical evaluation of osteoblasts cultured on bioactive glass, hydroxylapatite, titanium alloy, and stainless steel. J Biomed Mater Res 1993; 27:465-75.
25. Mustafa K, Wennerberg A, Wroblewski J, Hultenby K, Lopez BS, Arvidson K. Determining optimal surface roughness of TiO(2) blasted titanium implant material for attachment, proliferation and differentiation of cells derived from human mandibular alveolar bone. Clin Oral Implants Res 2001; 12:515-25.
26. Chrzanowski W, Szade J, Hart AD, Knowles JC, Dalby MJ. Biocompatible, smooth, plasma-treated nickel-titanium surface--an adequate platform for cell growth. J Biomater Appl 2012; 26:707-31.
27. Coelho PG, Cardaropoli G, Suzuki M, Lemons JE. Early healing f nanothickness boceramic coatings on dental implants. An experimental study in dogs. J Biomed Mater Res B Appl Biomater 2009; 88:387-93.
28. Ellingsen JE, Surface configurations of dental implants. Periodont 2000 1998; 17:36-46.
29. Cei S, Legitimi A, Barachini S, Consolini R, Sammartino G, Mattii L, Gabriele M, Graziani F. Effect of laser micromachining of titanium on viability and responsiveness of osteoblast-like cells. Implant Dentistry 2011; 20:285-91.
30. Kononen M, Hormia M, Kivilahti J, Hautaniemi J, Thesleff I. Effects of surface processing on the attachment, orientation, and proliferation of human gingival fibroblasts on titanium. J Biomed Mater Res 1992; 26:1325-41.

ENTEROPATHOGENIC *E.COLI* SUSTAINS IODOACETAMIDE-INDUCED ULCERATIVE COLITIS-LIKE COLITIS IN RATS: MODULATION OF IL-1β , IL-6, TNF-α, COX-2, AND APOPTOSIS

I. ABDALLAH HAJJ HUSSEIN[1], J.N. FREUND[2], J.M. REIMUND[3,4], A. SHAMS[1], M. YAMINE[1], A. LEONE[5] and A.R. JURJUS[1]

[1]Department of Anatomy, Cell Biology and Physiology, Faculty of Medicine, American University Beirut, Beirut, Lebanon; [2]INSERM U682, Strasbourg, France; [3]Université de Caen Basse-Normandie, SFR ICORE, UFR de Médecine, Caen Sedex, France; [4]CHU de Caen, Service d'Hépato-Gastro-Entérologie et Nutrition, Caen Cedex , France; [5]BioNec, Section of Histology and Embryology, University of Palermo, Faculty of Medicine, Palermo, Italy

Received December 5, 2011 – Accepted February 23, 2012

Pathogenic or non-pathogenic bacteria from flora may play a key role in inflammatory bowel disease (IBD) pathogenesis. However, a specific infectious agent causing IBD has not been identified. This study assessed the impact of enteropathogenic *E. coli* (EPEC) on the modulation of IL-1β, IL-6, TNF-α, COX-2, BAX and Bcl-2 expression, in sustaining inflammation of a rat colitis model. Two hundred male Sprague-Dawley rats (4 groups) were inoculated weekly or bi-weekly for 70 days, with 1% methylcellulose (MC), (b) 6% iodoacetamide (IA) in 1% MC, (c) $4x10^8$ CFU of EPEC, and (d) IA+EPEC. After a month, treatment was stopped in half of the animals in each group. IL-1β, IL-6, TNF-α, COX-2, BAX and Bcl-2 expression were measured in colonic mucosa scrapings. IL-1β, IL-6, TNF-α, and COX-2 were significantly increased in colonic mucosa of the IA+EPEC group and to a lesser but significant level in the IA group compared to controls, or EPEC alone, both in continued and discontinued treatment groups. Additionally, the BAX/Bcl-2 ratio decreased, indicating less apoptosis in the IA+EPEC group which exhibited more necrosis. These effects increased with experiment duration. This work provides new arguments favouring the role of bacteria in IBD pathogenesis.

Over the past decade inflammatory bowel disease research (IBD: Crohn's disease (CD) and ulcerative colitis (UC)) induced the generation of a series of experimental animal models as well as numerous data concerning, etiology, pathways analysis, and therapeutic targeting (1, 2). The wide variety of triggering agents included chemicals and rarely bacteria in addition to transgenic manipulations (3-5). The hypothesis addressed by the study was that bacteria, either pathogenic or part of flora, in particular, enteropathogenic *Escherichia Coli* (EPEC), play an active role in the induction of IBD. Such bacteria could also sustain a chronic colitis based on an earlier report describing the development of a chronic UC-like colitis model, by combining iodoacetamide (IA), a sulfhydryl group blocker, and enteropathogenic *Escherichia coli* (EPEC), a strain with adhesion and effacing properties, instilled repetitively into the descending colon of Sprague Dawley rats (4). Further characterization of the

Key words: ulcerative colitis, animal model, enteropathogenic Escherichia coli, inflammation

Mailing Address: Dr. Angelo Leone,
Section of Histology and Embryology,
University of Palermo,
Faculty of Medicine,
Via del Vespro, 127 90129 Palermo, Italy
Tel: ++39 0916553582 Fax: ++39 0916553586
e-mail: angelo.leone@unipa.it

0393-974X (2012)

chronic model and the interplay of various cytokines was needed in an in depth investigation.

Although a precise infectious agent has not been identified as specifically causing IBD, bacteria are suggested to participate in its pathogenesis (6). This has been reported in CD with data showing a high prevalence of adherent-invasive *Escherichia coli* (*E. coli*) (AIEC) in ileal CD (7), a bacteria adhering to and invading epithelial cells through interaction with a specific adhesion molecule (CEACAM6) (8). High prevalence of this microorganism in CD ileum is supposed to result from genetic predisposition leading to loss of bacterial clearance. Other hypotheses suggested that IBD results from an excessive immune response to gut-residing intestinal flora (break of tolerance and disruption of immune regulatory mechanisms) or as a consequence of a breakdown in the balance between "protective" and "harmful" bacteria from the intestinal flora ("dysbiosis") (9). Finally, clinical studies indicated that the disease affects mostly gut areas with the highest bacterial concentrations coming from various species including *E. coli* (9).

The primary consequence of the interaction between genetic susceptibility (10) and luminal pathogenic or commensal bacteria in IBD is the sustained activation of mucosal immunity, and the release of various pro-inflammatory mediators exacerbating and maintaining mucosal inflammation. Therefore, many pro-inflammatory and immune-regulating cytokines are deregulated in IBD patients' intestinal mucosa (11).

Finally, several studies have reported a 3-5-fold increased risk for colorectal cancer (CRC) (12, 13). Why chronic or recurrent mucosal inflammation during IBD could lead to CRC development in colonic CD or in UC is not fully understood (14). Nevertheless, there is clinical evidence that chronic inflammation plays a central role in colitis-associated cancer (CAC). Recently, several pro-inflammatory mediators have been considered of particular interest by driving inflamed non-dysplastic mucosa to CAC. For example, a recent work by Popivanova et al. established the role of TNF-α as a key mediator in inflammation-driven CAC development (15, 16).

A role for prostaglandins (PGs) in IBD pathogenesis has also been suggested. Cyclooxygenase-2 is normally expressed at a very low level in the intestinal epithelium, but is increased in inflamed IBD colon and highly expressed in human CRC (17). Cyclooxygenase-2 over-expression was also associated with resistance to apoptosis in human cancer cells (18).

Finally, Bcl-2/BAX ratio has been shown to significantly influence cellular transformation to malignant phenotype. Bcl-2, the anti-apoptotic protein, is over-expressed and could be neutralized by BAX activity, one of the pro-apoptotic proteins, by forming heterodimers. It was also proven that there were both host and pathogen encoded inhibitors of apoptosis (18, 19).

Herein, we report further characterization of this novel chronic model by assessment of the inflammatory response in colonic mucosa by analysing the long term expression of TNF-α, IL-1β, IL-6 and COX-2 mRNA. The behavior of such parameters was well documented in respect to IBD, in particular, when coupled with histopathological changes inflicted in IBD. It would be pertinent to compare our data to relevant existing data. Furthermore, preliminary data regarding apoptotic signalling as assessed by evaluating the BAX/Bcl-2 ratio, was in support of chronicity.

MATERIALS AND METHODS

Chronic UC-like colitis model

The chronic colitis model used has been fully described previously (6). In the present study male Sprague-Dawley rats were divided into 4 groups: (a) controls inoculated with 1% methylcellulose (MC); (b) a group treated by 100 μL of 6% iodoacetamide (IA) in 1% MC; (c) a group inoculated by EPEC (200 μL containing 4 x 10^8 colony factor unit of EPEC) (B); and (d) a group treated with IA followed by EPEC inoculation after 2 days (IA+B). Twenty-eight days post-treatment, each group was divided into 2 subgroups: the inoculation was stopped for one subgroup ("discontinued" injection subgroup) and the other subgroup continued with bi-weekly inoculation until day 70 ("continued" injection subgroup).

Clinical parameters

Animals were observed daily and clinical parameters (diarrhoea, tenderness, megacolon, body weight) were recorded (4).

Histopathology

The severity of colitis was evaluated by the colonic

histopathology according to previously described criteria (4). Colon biopsies were taken at day 3, 7, 14, 28, 42 and 70, fixed in 4% paraformaldehyde and processed for optical microscopy, or frozen at -80°C.

TNF-α, IL-1β, IL-6, COX-2, BAX and Bcl-2 mRNA by Real Time Polymerase Chain Reaction (RT-PCR)

Total RNA was extracted from scrapings of colonic mucosa by TRIR reagent (Invitrogen, Grand Island, NY 14072, USA) at 4°C as described previously (4). RNA was resuspended in RNase free water and purity verified by the optical density (OD) absorption ratio OD 260 nm/OD 280 nm. The integrity was electrophoretically assessed by formaldehyde agarose gel stained with ethidium bromide.

Two µg of RNA were reverse transcribed to cDNA using the Thermoscript RT-PCR system (Invitrogen) following the manufacturer's instructions. Quantitative real-time PCR was performed for each template using the corresponding primer enlisted in Table I. The cDNA was amplified (duplicate) using iQ SYBR Green supermix (Bio-Rad Laboratories, Hercules, CA, USA). PCR efficiencies were calculated by performing a dilution over a 100-fold range in a five point standard curve including the concentration of the tested samples.

The real-time PCR program using the i-cycler machine (BioRad Laboratories), programmed for 95°C for 10 minutes, consisted of 40 cycles of denaturation (95°C for 20 seconds) with annealing temperature (59°C for 15 seconds) and extension (72°C for 8 seconds). Amplification specificity was checked using the melting curve following the manufacturer's instructions. All genes were normalized by comparison to *β-actin* (housekeeping gene), and results expressed as the ratio to *β-actin* in which the standard curve and comparative threshold cycle (delta CT method) was used. To use *β-actin* as housekeeping genes, both the gene and the method were standardized using controls and accurate procedures. It has also been reported that *β-actin* could be used as housekeeping gene to study the impact of enteropathogenic *E. coli*; its expression remains stable with the treatment (20).

Statistical analysis

Data were expressed as means ± SEM. Variation in each gene level and its corresponding mRNA were determined by averaging the values obtained for each group at the indicated time interval. Statistical analysis used two-way ANOVA and Student's *t*-test. A p value < 0.05 was considered statistically significant.

RESULTS

Clinical observations and histopathology

Our results were in accordance with previous data demonstrating that our experimental UC-like colitis

Table I. *Characteristics of primers used for quantitative real-time PCR.*

Gene	***Forward Primer***	***Reverse Primer***
β-actin (Thermo Scientific,Germany)	5'-AAATCCCTCACCCTCCC AAAAG-3'	5'-AAGCAATGCTGTCA CCTTCCC-3'
TNF-α (Thermo Scientific, Germany)	5'-AAATGGGCTCCCTCTCA TCAGTTC-3'	5'- TCTGCTTGGTGGTTT GCTACGAC-3'
IL-1β (Thermo Scientific, Germany)	5'- AAATGGGCTCCCTCTC ATCAGTTC-3'	5'- GGGTTCCATGGTGA AGTCAAC-3'
IL-6 (Thermo Scientific, Germany)	5'- TCCTACCCCAACTTCC AATGCTC-3'	5'- TTGGATGGTCTTGG TCCTTAGCC-3'
BAX (Thermo Scientific, Germany)	5'- CTGTATCCCGCCCTG GTG-3'	5'- GGCAGAGCTAGGA CCTACTTGG-3'
Bcl_2 (Thermo Scientific, Germany)	5'- CTCAGTCATCCACAGG GCGA-3'	5'- TAGGGTGAGCATC GGGGAG-3'
COX-2 (TIB MOLBIOL)	5'- TGGGATGACGAGCGA CTGT-3'	5'- CAGAGGCAATGCGG TTCGG-3'

(a)

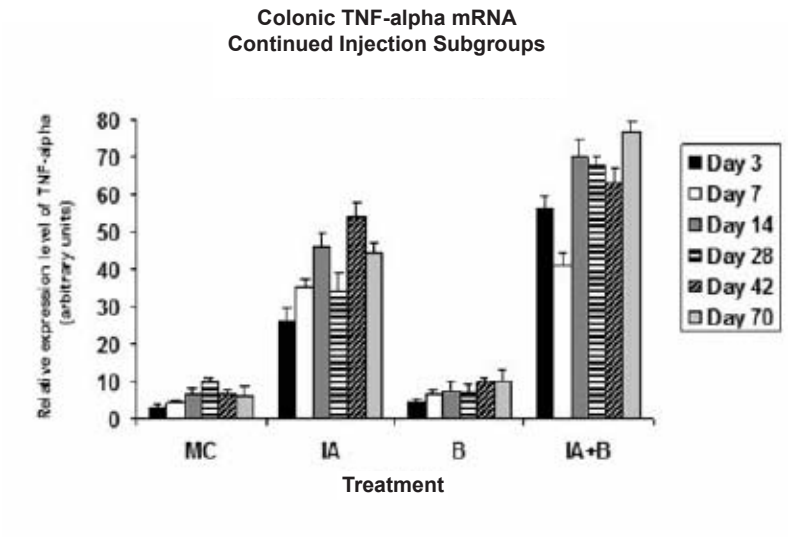

(b)

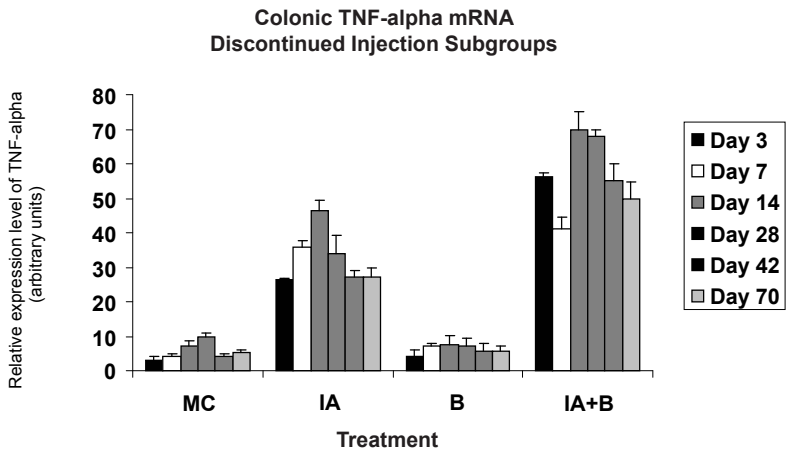

Fig. 1. *Real-time PCR fold increase of TNF-α mRNA in mucosal scrapings of rat colon in various experimental groups, both in the continued (**a**) and discontinued (**b**) injection subgroups. The target mRNA was normalized to that of the 'house-keeping' gene β-actin. Statistical significance was detected with reference to control levels (MC and B-treated groups).*

model resembled human UC. The clinical course for more than 2 months and the major symptoms - decreased body weight, diarrhoea, rectal bleeding - in addition to the clinical profile, which was further supported by macroscopic pathology and histological tissue alterations typical of human UC, were all in favor of resembling, supporting the resemblance of this model to human UC. It was reproducible with characteristics of chronicity.

TNF-α gene expression

Colonic TNF-α gene expression was compared using real-time PCR. Results were comparable with previously reported data (4). TNF-α expression levels in "continued" and "discontinued" treatment for the various groups and time points were illustrated in Fig. 1. As expected, we observed that TNF-α mRNA expression levels were well above the control levels (MC and B-treated groups) in the

(a)

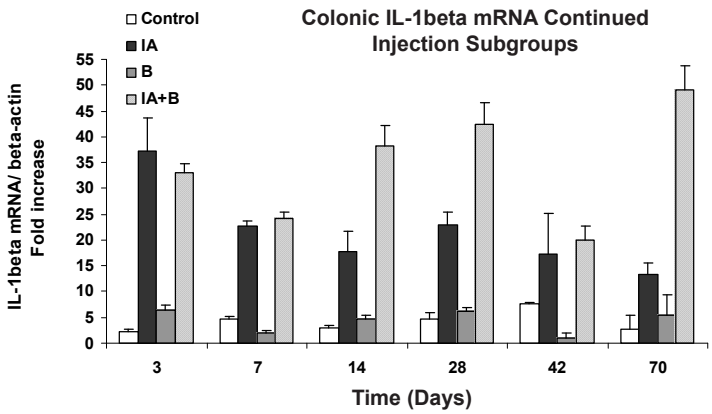

(b)

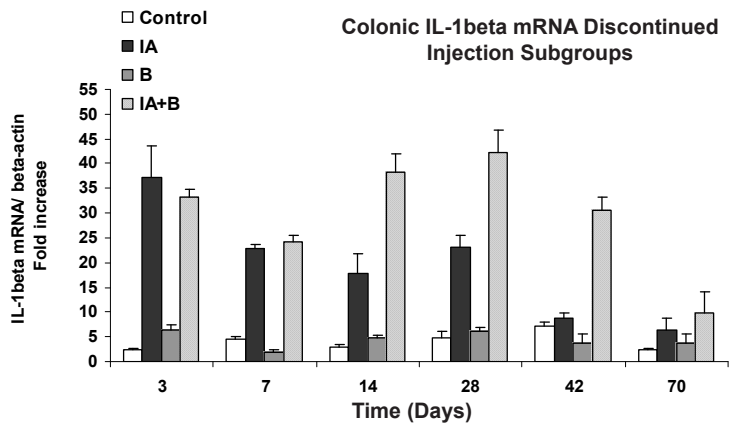

Fig. 2. *Real-time PCR fold increase of IL-1β mRNA in mucosal scrapings of rat colon in various experimental groups both in the continued (**a**) and discontinued (**b**) injection subgroups. The target mRNA was normalized to that of the 'house-keeping' gene β-actin. Statistical significance was detected with reference to control levels (MC and B-treated groups).*

experimental categories (IA and IA+B groups), both in the "continued" and "discontinued" subgroups ($p < 0.01$). The results show a 23- to 39-fold increase in TNF-α mRNA levels in IA-treated rats when compared to MC and B groups ($p < 0.05$; Fig. 1). The results of the subgroup of rats continuing to receive IA treatment maintained a relatively high level of TNF-α mRNA expression (peak expression of a 44-fold increase on day 42). In contrast, there was a time-dependent decrease in the IA "discontinued" group following day 28 to day 70 (Fig. 1b).

IL-1β mRNA expression

Interleukin-1β mRNA expression in the IA+B group was consistently increased all through the experimental duration to very significant levels compared to control group(s) (Fig. 2). A particular pattern was noted in the undulating activity of IL-1β

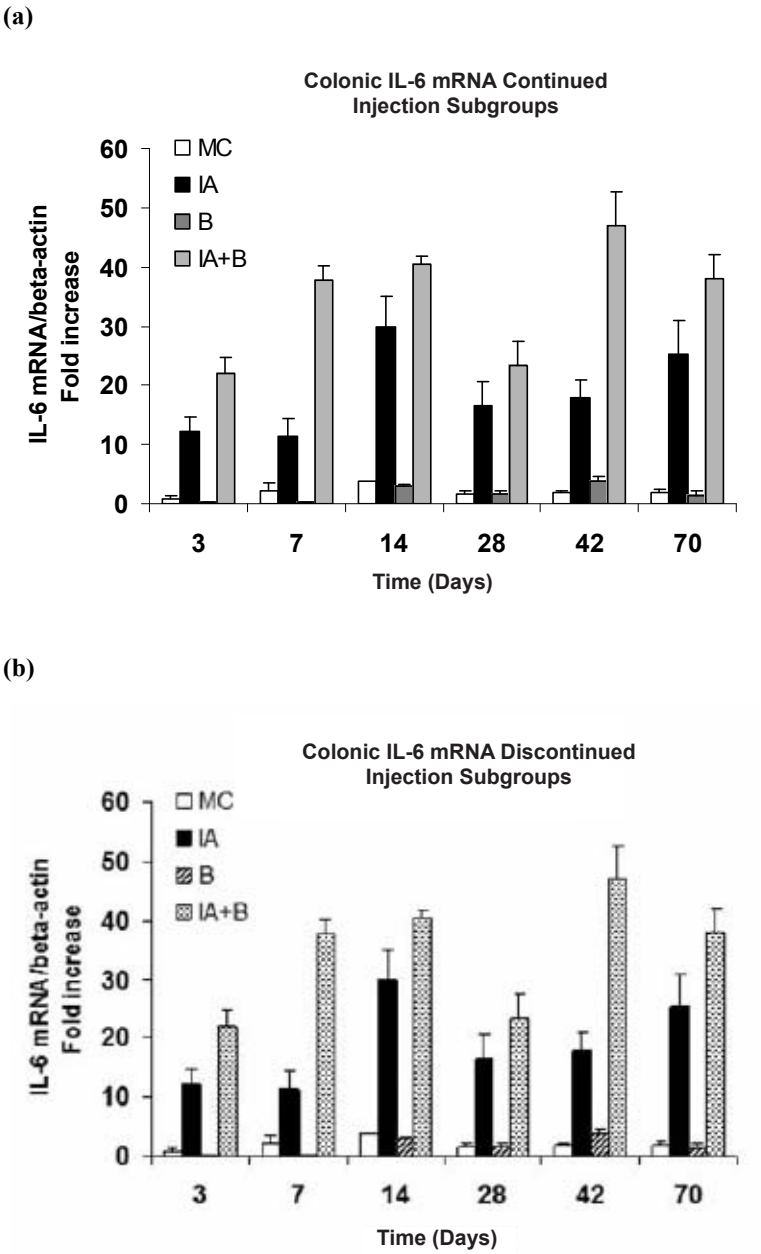

Fig. 3. *Real-time PCR fold increase of IL-6 mRNA in mucosal scrapings of rat colon in various experimental groups both in the continued (**a**) and discontinued (**b**) injection subgroups. The target mRNA was normalized to that of the 'house-keeping' gene β-actin. Statistical significance was detected with reference to control levels (MC and B-treated groups).*

expression in both "continued" and "discontinued" IA+B subgroups. This trend of undulation corresponded probably to periods of remission and exacerbation of inflammatory activity.

A close look at the data of the IA-treated "continuous" injection subgroup showed again a significantly increased mRNA expression during all the duration of the experiment compared to other groups. There was a significant transient rise of IL-1β mRNA expression in the IA group slightly higher than in the IA+B group at day 3 of the experiment. However, in the "discontinued" IA-treated subgroup, there was a time-dependent decrease in the IL-β mRNA expression following day 28 to day 70 post-treatment. However, it remained more expressed than in controls at all time points (Fig. 2b).

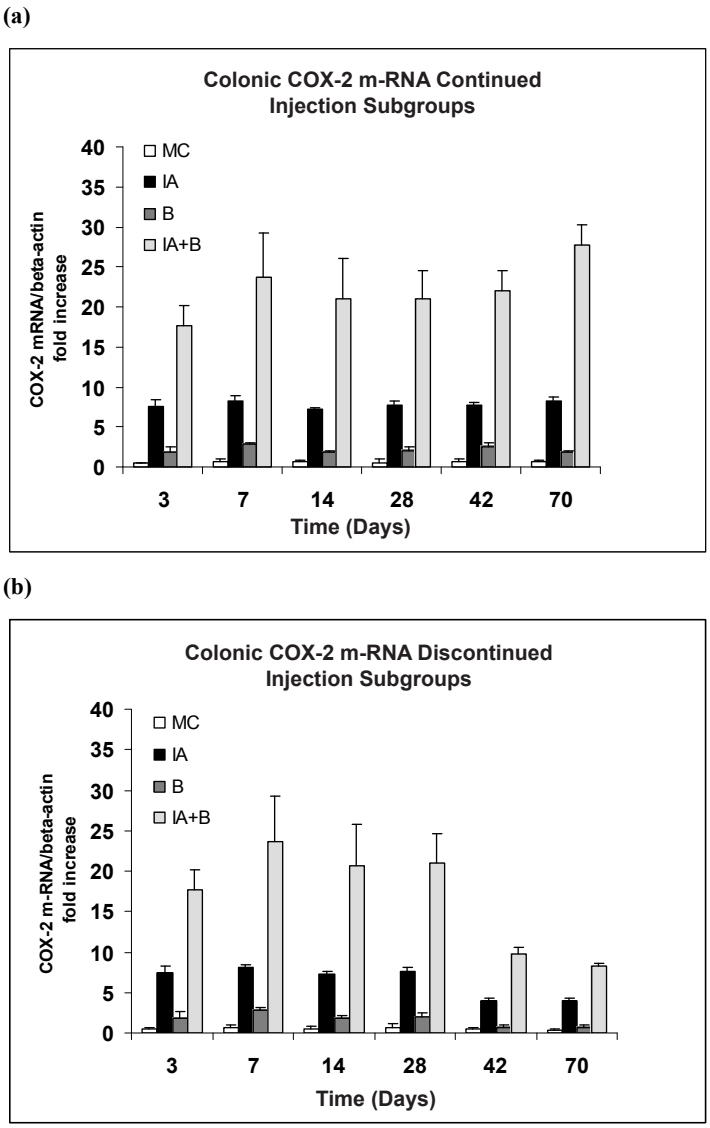

Fig. 4. *Real-time PCR fold increase of COX-2 mRNA in mucosal scrapings of rat colon in various experimental groups both in the continued (**a**) and discontinued (**b**) injection subgroups. The target mRNA was normalized to that of the 'house-keeping' gene β-actin. Statistical significance was detected with reference to control levels (MC and B-treated groups).*

IL-6 mRNA expression

This pro-inflammatory cytokine was consistently increased in colonic tissues in IA and IA+B groups. The IL-6 mRNA expression showed, all through the experiment, very significantly higher levels between control and experimental groups at all time points tested (Fig. 3). The difference ranged from 10-fold on day 3 to 40-fold on day 70. This IL-6 mRNA increased expression correlated with the exacerbation of the chronic inflammation at various points. Additionally, the presence of the bacteria with IA seemed to have increased further such expression in colonic mucosa. In almost all points the increase in IL-6 mRNA expression in the combined IA+B group was significantly higher than in the IA group. The same pattern was expressed in both "continued"

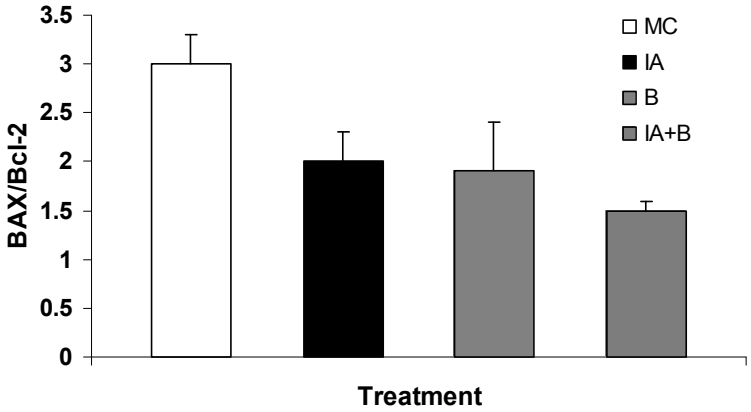

Fig. 5. *BAX/Bcl-2 ratio in the various experimental groups across the experimental duration (Readings represent average of days 7, 28, and 70 in each group). Statistical significance was detected with reference control levels (MC and B-treated groups).*

and "discontinued" subgroups (Fig. 3).

COX-2 mRNA expression

Colonic mucosal COX-2 mRNA expression was the lowest in the MC and B-treated groups, significantly higher in the IA group, and the highest in the IA+B group, from day 3 to 70 (Fig. 4). In the "discontinued" subgroup (Fig. 4a), after day 28, COX-2 mRNA expression maintained its increase, although to a lesser extent than in the "continuous" subgroup. In rats injected by IA alone, COX-2 mRNA expression increased all through the experiment compared to the MC and B-treated groups. This increase was consistently lower than in the IA+B group at almost all time points. After day 28, when all inoculations stopped in the "discontinued" group, COX-2 mRNA expression values remained higher than in controls; they were lower, almost half, than those in the "combined" continued IA+B subgroup (Fig. 4).

Apoptotic signalling: Bcl-2 and BAX mRNA expression

The Bcl-2 mRNA expression levels during the experimental course in all four groups were relatively close to each other and not significantly different between groups. This observation may be due to the baseline low level of Bcl-2 mRNA in the colon and to the fact that the major factor influencing the intrinsic apoptotic pathway in the colon is the BAX expression. The BAX mRNA expression declined steadily from control to the combined IA+B group (results not shown). The BAX/Bcl-2 ratio is commonly used as an estimate of the net apoptotic rate. A high ratio signs apoptosis promotion. The BAX/Bcl-2 ratio in the combined IA+B group was the lowest among all four groups (Fig. 5).

DISCUSSION

Our results, showing the up-regulation of the pro-inflammatory cytokines TNF-α, IL-1β, IL-6 in addition to COX-2, consolidate previous data from our group, indicating that the experimental colitis model we developed using an SH blocker and EPEC resembles to human UC and was reproducible with characteristics indicative of chronicity. As demonstrated earlier, the clinical course of the induced disease for almost a hundred days or even six months (unpublished personal data), together with the histological alterations typical of human UC, and the consistent increase of tissue myeloperoxidase activity in the IA+B group, indicate a severe inflammatory process in the descending colonic mucosa (4). Now, the presence of a significant increase in TNF-α, IL-1β, and IL-6 mRNA expression, especially in the IA+B group, reinforced the validity and the usefulness of this UC-like colitis model. In addition to the increased pro-inflammatory cytokines expression, we reported a

COX-2 up-regulation specifically in the IA+B group - an increase which paralleled TNF-α up-regulation - and finally, a down-regulation of apoptosis.

Such elevated levels of pro-inflammatory cytokines and COX-2 have been reported in human UC and CD (15, 19) and have been demonstrated to play an important role in IBD pathogenesis by driving the chronic inflammatory process leading to tissue injury, and finally to the clinical symptoms. These high levels of pro-inflammatory cytokines in the lamina propria have been associated with the severity of tissue injury, but have also been found in normal-appearing mucosa in CD (19) where they may be predictive of early recurrence (21). Interestingly, the fact that the additional bacterial challenge by EPEC increased the magnitude of the colonic inflammatory/ immune response *vs* chemical IA induction alone, is in accordance with the current main hypothesis of IBD pathogenesis of the involvement of bacteria [pathogen(s) or from the normal flora] inducing intestinal inflammation in genetically predisposed subjects (19). TNF- α is also one of the most important mediators of the response to Gram negative bacteria and plays a role in the immune response to other micro-organisms (21). For example, endotoxins or lipopolysaccharides (LPS), derived from the outer membrane of Gram negative enteropathogenic *E. coli* interact with CD14 of mononuclear cell surface membrane, triggering a signalling cascade leading to the production and release of IL-1β, IL-6, TNF-α (10, 19). In this respect, these cytokines and LPS (or their receptors on the involved inflammatory and immune cells) may represent putative therapeutic targets for UC and in fact, anti-TNF antibodies infliximab and adalimumab are efficient in UC induction and maintenance treatment (22).

The results of the present study demonstrate that the mucosal scrapings of the colon contained significantly elevated TNF-α mRNA levels in IA+B group, in both subgroups and at all time points compared to control. It is worth noting that increased local expression of IL-1β, IL-6, and in particular TNF-α is of prime importance in inducing COX-2 production which might lead to blocking apoptosis, resulting in driving chronic inflammation and mediating tissue injury. By contrast to normal rat or human colonic tissue where COX-2 is not or very low expressed, COX-2 expression is usually high in the affected intestinal segments of IBD patients with mRNA levels of up to 5-fold compared to normal mucosa (23). This effect is thought to result from increased pro-inflammatory cytokine expression as stated earlier, but also to mitogens, and endotoxins from invasive bacteria. Additionally, it has been shown that infection of intestinal epithelial cells with invasive bacteria induces COX-2 in the affected part of the gastrointestinal tract (24). In some studies, COX-2 expression is induced within a few hours of exposure to invasive organisms and then is lost over a period of approximately 24 hours. However, within 24 hours of colitis induction, there was a marked up-regulation of colonic COX-2 mRNA, remaining elevated for at least 2 weeks after induction (24). Our data on COX-2 expression depicted a profile similar to what was previously reported in UC (25). Cyclooxygenase-2 was found to be highly expressed in the IA+B group compared to the MC group throughout the duration of the experiment until day 70. During the entire experiment duration, the combined treatment group exhibited the highest COX-2 levels in the "continued" injection subgroup, as compared to other groups. Cyclooxygenase-2 was probably induced by the pro-inflammatory cytokine TNF-α which was also increased in response to IA and IA+B treatments. This concordance between TNF-α and COX-2 over-expression may be also the result of the bacterial endotoxin originating from the EPEC instilled in the colon (25). A similar increase in COX-2 mRNA expression has also been reported in the trinitrobenzene sulfonic acid (TNBS)-induced rat colitis model, with a six-fold increase 72 hours after the TNBS administration (25 Theoretically, these results may suggest that inhibition of COX-2 expression represented a valuable therapeutic target. However, as non-steroidal anti-inflammatory drugs (including selective COX-2 inhibitors) have been considered to potentially induce or worsen IBD attacks, (despite some controversy on their deleterious effects), COX-2 targeting was until now not considered as promising in IBD treatment (23, 24, 26, 27).

Finally, we report a marked decrease in the BAX/ Bcl-2 ratio more pronounced in the IA+B group, than in the IA or the B groups. Cells in the colon scrapings of the IA+B group expressed lower levels of BAX whereas Bcl-2 expression was unchanged,

with a net BAX/Bcl-2 ratio indicating resistance to apoptosis. This resistance to apoptosis in the "combined" treatment group may probably be related, at least in part, to COX-2 over-expression, known to effectively inhibit apoptosis (28). Cyclooxygenase-2 can directly promote cell survival through activating the active protein kinase (Akt)-dependent pathway by increasing Akt expression either directly or via protein kinase C (PKC) (29). Inhibition of Akt is known to activate the pro-apoptotic BAX (or BAD) and inhibits the anti-apoptotic Bcl-2 and Bcl_{XL}, effects that can either directly induce apoptosis and/or trigger subsequent activation of caspase-9, an initiator of pro-apoptotic signal. Activated caspase-9 cleaves and activates down-stream effector caspases (e.g. caspase-3) to induce apoptosis. Induction of COX-2, has also been reported to inhibit caspase-3, probably due to its ability to inhibit BAX and to activate Bcl-2 and Bcl_{XL} (29). Like in our experimental colitis model, resistance to apoptosis has been reported in some clinical studies in both CD and UC (28) and infliximab (but not etanercept, an anti-p75 TNF-α receptor antibody used in chronic inflammatory rheumatologic diseases) have been shown to be able to induce apoptosis, which might be one of their mechanisms of action (30).

In conclusion, the present study added interesting new data to those previously reported (4), supporting the possible role of EPEC, the validity and the potential interest of our experimental UC-like rat colitis model (32). It mimicked many aspects of human UC. Interestingly, and despite numerous IBD animal models having been developed to increase our understanding of CD and UC pathogenesis (1, 3), this model is one of the rare models combining an inflammatory and immune activation (chemically or genetically-induced) and a bacterial challenge, which is close to the current view of IBD pathogenesis. To our knowledge, only three other animal models used bacterial challenge to induce colitis in two cases (31, 32) and CAC in the third one (33). The two models described by Carvalho et al. (31, 32) used AIEC inoculated in wild type BALB/c/J mice with dextran sulphate sodium-induced colitis for the first one, and to transgenic mice expressing CEACAM6 (CEABAC10 transgenic mice) for the second one. Surprisingly, and contrasting with the fact that AIEC have only been found to be associated with human ileal but not colonic CD, these mice exhibited colitis with increased IL-1β, IL-17 and decreased IL-10 mRNA expression in the colonic mucosa in the second model (32). The third experimental model combined inoculation of *Helicobacter* species to a genetically-induced inflammation (Smad 3/Rag2 double null mice with transforming growth factor-β dysregulation) characterized by an increased expression of interferon-γ, IL-1α and β, IL-6, TNF-α, an increased Bcl_{XL} and Bcl-2 expression, as well as an increase in c-*Myc* expression, finally leading to a greater incidence of CAC (33). Therefore, we anticipate that it would be interesting to study colon aberrant crypt foci, adenomas and CAC formation in our model (for example by adding to IA and EPEC, a colonic instillation of a chemical carcinogen such as azoxymethane or 1,2-dimethylhydrazine) (15, 34), as it induces for over 70 days over-expression of some of the major inflammatory factors currently considered to lead to CAC (e.g. TNF-α, COX-2), despite the controversy concerning COX-2 role in CAC pathogenesis (35, 36).

ACKNOWLEDGEMENTS

This work was supported by a grant from the Lebanese National Council for Scientific Research, and the Medical Practice Plan of the Faculty of Medicine, AUB.

REFERENCES

1. Dotan I, Mayer L. Immunopathogenesis of inflammatory bowel disease. Curr Opin Gastroenterol 2002; 18:421-7.
2. Strober W, Fuss I, Mannon P. The fundamental basis of inflammatory bowel disease. J Clin Invest 2007; 117:514-21.
3. Jurjus AR, Khoury NN, Reimund JM. Animal models of inflammatory bowel disease. J Pharmacol Toxicol Methods 2004; 50:81-92.
4. Hajj Hussein IA, Rania T, Barada K, et al. Inflammatory bowel disease in rats: bacterial and chemical interaction. World J Gastroenterol 2008; 14:4028-39.
5. Barada KA, Mourad FH, Sawah SI, et al. Localized colonic inflammation increases cytokine levels in

distant small intestinal segments in the rat. Life Sci 2006; 79:2032-42.
6. Sartor RB. Microbial influences in inflammatory bowel diseases. Gastrenterology 2008; 134:577-94.
7. Darfeuille-Michaud A, Boudeau J, Bulois P, et al. High prevalence of adherent-invasive *Escherichia coli* associated with ileal mucosa in Crohn's disease. Gastroenterology 2004; 127:412-21.
8. Barnich N, Carvalho FA, Glasser AL, et al. CEACAM6 acts as a receptor for adherent-invasive *E. coli*, supporting ileal mucosa colonization in Crohn's disease. J Clin Invest 2007; 117:1566-74.
9. Sokol H, Pigneur BH, Watterlot LB, et al. *Faecalibacterium prausnitzii* is an anti-inflammatory commensal bacterium identified by gut microbiota analysis of Crohn disease patients, Proc Natl Acad Sci USA 2008; 105:16731-6.
10. Reimund JM, Wittersheim C, Dumont S, et al. Mucosal inflammatory cytokine production by intestinal biopsies in patients with ulcerative colitis and Crohn's disease. J Clin Immunol 1996; 16:44-50.
11. Papadakis KA, Targan SR. Role of cytokines in the pathogenesis of inflammatory bowel disease. Annu Rev Med 2000; 51:289-98.
12. Eaden JA, Abrams KR, Mayberry JF. The risk of colorectal cancer in ulcerative colitis: a meta-analysis. Gut 2001; 48:526-35.
13. Jess T, Gamborg M, Matzen P, et al. Increased risk of intestinal cancer in Crohn's disease. Am J Gastroenterol 2005; 100:2724-9.
14. Rutter M, Saunders B, Wilkinson K, et al. Severity of inflammation is a risk factor for colorectal neoplasia in ulcerative colitis. Gastroenterology 2004; 126:451-9.
15. Popivanova BK, Kitamura K, Wu Y, et al. Blocking TNF-α in mice reduces colorectal carcinogenesis associated with chronic colitis. J Clin Invest 2008; 118:560-70.
16. Burstein E, Fearon ER. Colitis and cancer: a tale of inflammatory cells and their cytokines. J Clin Invest 2008; 118:464-7.
17. Danese S, Mantovani A. Inflammatory bowel disease and intestinal cancer: a paradigm of the Yin-Yan interplay between inflammation and cancer. Oncogene 2010; 29:3313-23.
18. Sun X, Tang XM, Half E, et al. Cyclooxygenase-2 overexpression reduces apoptotic susceptibility by inhibiting the cytochrome c-dependent apoptotic pathway in human colon cancer cells. Cancer Res 2002; 62:6323-8.
19. Reimund JM, Wittersheim C, Dumont S, et al. Increased production of tumor necrosis factor –alpha, IL-1β and IL-6 by morphologically normal intestinal biopsies in Crohn's disease. Gut 1996; 39:144-50.
20. Jandu N, HO NKL, Donato KA, Karmali MA, Mascarenhas M, Duffy SP, Tailor C, Sherman PM. Enterochemorrhagic Escherichia Coli O 157:H7 gene expression profiling in response to the growth in the presence of host epithelia. PLoS One 2009; 4(3):e4889. Epub 2009.
21. Ishigura Y. Mucosal proinflammatory cytokine production correlates with endoscopic activity of ulcerative colitis. J Gastroenterol 1999; 34:66-74.
22. Reinisch W, Sandborn WJ, Hommes DW, et al. Adalimumab for induction of clinical remission in moderately to severely active ulcerative colitis: results of a randomised controlled trial. Gut 2011; 60:780-7.
23. McCartney S, Mitchell J, Fairclough P, et al. Selective COX-2 inhibitors and human inflammatory bowel disease. Aliment Pharmacol Ther 1999; 8:1115-17.
24. Matuk R, Crawford J, Abreu MT, et al. The spectrum of gastrointestinal toxicity and effect on disease activity of selective cyclooxygenase-2 inhibitors in patients with inflammatory bowel disease. Inflamm Bowel Dis 2004; 10:352-6.
25. Singer I, Kawka D, Schloemann S, et al. Cyclooxygenase 2 is induced in colonic epithelial cells. Gastroenterology 1998; 115:297-306.
26. El Miedany Y, Youssef S, Ahmed I, et al. The gastrointestinal safety and effect on disease activity of etoricoxib, a selective Cox-2 inhibitor in inflammatory bowel disease. Am J Gastroenterol 2006; 101:311-7.
27. Tanaka KI, Suemasu S, Ishihara T, et al. Inhibition of both COX-1 and COX-2 and decrease in the level of prostaglandins E_2 is responsible for non-steroidal anti-inflammatory drug (NSAID)-dependent exacerbation of colitis. Eur J Pharmacol 2009; 603:120-32.
28. Limura M, Nakamura T, Shinozaski S, et al. Bax

is downregulated in inflamed colonic mucosa of ulcerative colitis. Gut 2000; 47:228-35.
29. Badawi AF. The role of prostaglandin synthesis in prostate cancer. B J Urol Intern 2000; 85:451-62.
30. ten Hove T, van Montfrans C, Peppelenbosch MP, et al. Infliximab treatment induces apoptosis of lamina propria T lymphocytes in Crohn's disease. Gut 2002; 50:206-11.
31. Carvalho FA, Barnich N, Sauvanet P, et al. Crohn's disease-asociated *Escherichia coli* LF82 aggravates colitis in injured mice colon via signaling by flagellin. Inflamm Bowel Dis 2008; 14:1051-60.
32. Carvalho FA, Barnich N, Sivignon A, et al. Crohn's disease adherent-invasive *Escherichia coli* colonize and induce strong gut inflammation in transgenic mice expressing human CEACAM. J Exp Med 2009; 206:2179-89.
33. Maggio-Price L, Treuting P, Bielefeldt-Ohmann H, et al. Bacterial infection of Smad3/Rag 2 double-null mice with transforming growth factor-β dysregulation as a model for studying inflammation-associated colon cancer. Am J Pathol 2009; 174:317-29.
34. Gali-Muhtasib H, Ocker M, Kuester D, et al. Thymoquinone reduces mouse colon tumor cell invasion and inhibits tumor growth in murine colon cancer models. J Cell Mod Med 2008; 12:330-42.
35. Wang D, DuBois RN. The role of COX-2 in intestinal inflammation and colorectal cancer. Oncogene 2010; 29:781-8.
36. Ishikawa T, Herschman HR. Tumor formation of a mouse model of colitis-associated colon cancer does not require COX-1 or COX-2 expression Carcinogenesis 2010; 31:729-36.

CORRELATION BETWEEN VIRAL LOAD, PLASMA LEVELS OF CD4 - CD8 T LYMPHOCYTES AND AIDS-RELATED ORAL DISEASES: A MULTICENTRE STUDY ON 30 HIV+ CHILDREN IN THE HAART ERA

M. NESTI[1], E. CARLI[1], C. GIAQUINTO[2], O. RAMPON[2], S. NASTASIO[3] and M.R. GIUCA[4]

[1]Dipartimento di Chirurgia Sezione di Odontostomatologia, Università di Pisa; [2]Dipartimento di Infettivologia Pediatrica "Salus Pueri", Università di Padova; [3]Dipartimento di Pediatria, Università di Pisa; [4]Malattie Odontostomatologiche, Dipartimento di Chirurgia Odontostomatologica, Università di Pisa

Received August 1, 2011 – Accepted June 22, 2012

This experimental retrospective multicenter study carried out on 30 seropositive children treated with Highly Active Antiretroviral Therapy (HAART), between the ages of 18 months and 14 years, in the clinical categories Centers for Disease Control (CDC) classification 1993 A (mildly symptomatic), B (moderately symptomatic) and C (severely symptomatic) aims to: 1) clinically and immunologically demonstrate the therapeutic benefits of HAART; 2) monitor the frequency of AIDS-related oral diseases in seropositive children with HAART therapy; 3) monitor the plasma levels of total CD4, CD4%, CD8%, CD4-CD8 lymphocytes and viral load from 1997 to 30 April, 2011. The statistic methods used are the analysis of covariance and the Bonferroni Test. More than 100 AIDS-related oral diseases were found in the study samples, the most frequent being: oral candidiasis, oropharyngeal candidiasis, HSV-1 herpetic esophagyitis, herpetic gingivolstomatitis (RHOG), recurrent aphthous stomatitis (RAS), parotid swelling, oral hairy leukoplakia (OHL), Herpes simplex 1 (HSV-1), linear gingival erythema (LGE), necrotizing gingivitis (NUG), facial lipodistrophy, facial-cervical lymphadenopathy (FCL), xerostomia, dysgeusia, hyposmia, oral mucosa hyperpigmentation (OMP). The Bonferroni test showed a significant difference between the mean plasma values (mpVTL) of total CD4, CD4 percentage, CD4-CD8 T lymphocytes and Viral Load (VL) of the various oral diseases found in the study samples. The therapeutic benefits of HAART are: immune reconstitution; reduction of the HIV/AIDS-related stomatology diseases; prevention and cure of the AIDS correlated neoplasias; reduction in maternal-fetal transmission of the HIV virus. The negative effects of HAART in relation to odontostomatolgy are: increase in oral lesions from HPV; xerostomia; dysgeusia/ageusia, hyposmia, perioral paresthesia; hyperpigmentation of oral mucosa; facial lipodystrophy, recurrent aphthous stomatitis (RAS). No case of immune reconstitution inflammatory syndrome or human papillomavirus (HPV)-related oral diseases were found in this study.

In the pre-HAART era, the renowned German epidemiologist, Jonathan Mann stated: "AIDS has taken to the world and the world must equip itself to fight the HIV virus" (1). Highly Active Antiretroviral

Key words: HIV positive children, HIV/AIDS, HAART, viral load, T lymphocytes, lymphocytic depletion, immune reconstitution, AIDS-related oral diseases

Mailing address: Dr. Marco Nesti,
Dipartimento di Chirurgia Odontostomatologica,
Edificio 17,
via Roma 67,
56100 Pisa, Italy
Tel.: +39 347 3502087 Fax: +39 050/555232
e-mail: nestimarco@alice.it

0393-974X (2012)

Therapy (HAART), introduced in the two-year period 1996-97, has greatly changed the viral conditions - immunological and clinical – regarding odontostomatology in pediatric and adult HIV+ patients in industrialized countries, transforming a fatal disease into a syndrome that is continually acquiring a chronic character.

HAART, which consists in the administration of multiple antiviral drugs, has the following aims:

1) to guarantee the HIV-positive pediatric patient a high and good quality of life, impeding the loss of the "hereditary immunity" through the suppression of viral replication; 2) to prevent the maternal-fetal transmission of the HIV virus in pregnant women (2-5).

HAART was usually defined as the association of a non-nucleoside reverse transcriptase inhibitor (NNRTI), with a nucleoside reverse transcriptase inhibitor (NRTI) and a PI or the association of two NNRTI and PI (6-7).

Perinatal HIV infection is noticeably different from that of adults in that it develops in an immature organism whose immune system is still developing, and this influences the clinical characteristics.

In our study, as in the study of Patton LL and Ivan Dieb Miziara, the progression of pediatric HIV infection is monitored by two laboratory markers: 1) serum CD4+ cell count (used to asses immune competence); 2) HIV – RNA levels (used to asses HIV replication or viral load). Both are also used as markers of immune and virologic failure/success induced by Highly Active Antiretroviral Therapy (6-7).

This retrospective multicenter study, carried out in collaboration with the "Salus Pueri" Pediatric AIDS Centre of the University of Padua aims to: evaluate the effect of HAART on the progress of the immune response and on the suppression of viral replication (through monitoring of the plasma levels of the T lymphocyte total CD4, CD4%, CD8%, CD4-CD8 and of the viral load) and consequently of the quality of life of the 30 HIV+ pediatric patients; monitor the frequency of AIDS-related oral diseases of pediatric patients in the study sample; document the stomatological side-effects induced by HAART in the study sample; verify the efficacy of HAART in the prevention of maternal-fetal transmission of the HIV virus in the study sample.

MATERIALS AND METHODS

The study sample consisted of 30 HIV+ pediatric patients between the ages of 18 months and 14 years, born to HIV-infected mothers, in the immunoclinical categories A (mildly symptomatic), B (moderately symptomatic), C (severely symptomatic) Centers for Disease Control (CDC) classification 1993 (8-9), regularly visited at the centre in Padua and treated with HAART from birth. The data relative to the patients was collected from medical records, with particular attention to the hematic and viral parameters, to the clinical notes and the therapies adopted, from 1997 to 30th April, 2011 (Fig. 1, 2, 3) (Tables I, II).

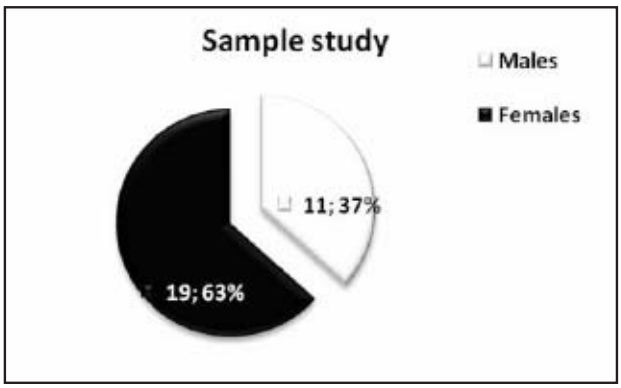

Fig. 1. *Sample study: HIV-positive males and females.*

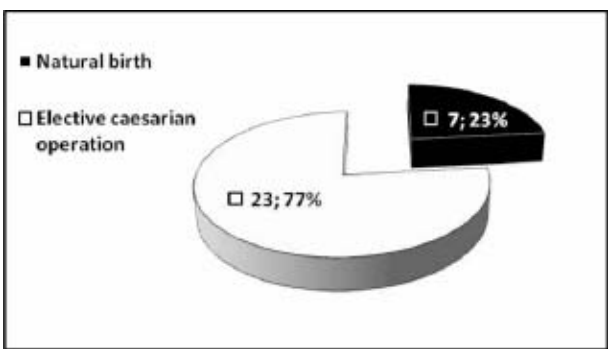

Fig. 2. *Sample study: type of delivery.*

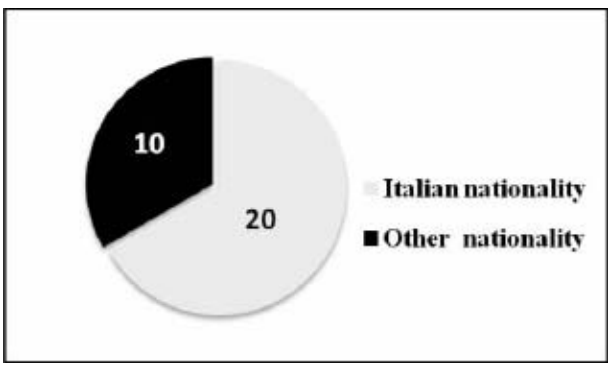

Fig. 3. *Sample study: nationality of HIV-positive children.*

Table I. *Pediatric classification (CDC 1993) of human immunodeficiency virus infection.*

	Clinical categories			
Immunologic categories	**N***	**A***	**B***	**C***
1: No evidence of immunosuppression	**N1**	**A1**	**B1**	**C1**
2: Moderate immunosuppression	**N2**	**A2**	**B2**	**C2**
3: Severe immunosuppression	**N3**	**A3**	**B3**	**C3**

***N**: no signs/symptoms; **A**: signs/slight symptoms; **B**: signs/moderate symptoms; **C**: signs/serious symptoms*

Table II. *Immunologic categories based on the percentage and absolute values, according to age, of CD4+ T lymphocytes.*

Immunologic categories	Age of the children					
	< 12 months		1-5 years		6-12 years	
	µL	%	µL	%	µL	%
1: No evidence of immunosuppression	**≥ 1500**	**≥ 25**	**≥ 1000**	**≥ 25**	**≥ 500**	**≥ 25**
2: Moderate immunosuppression	**750-1499**	**15-24**	**500-999**	**15-24**	**200-500**	**15-24**
3: Severe immunosuppression	**< 750**	**< 15**	**< 500**	**< 15**	**< 200**	**< 15**

Study sample: 11 males, 19 females; 20 patients of Italian nationality, 10 of other nationalities; 23 patients born by elective caesarian operation, 7 by natural birth. All the patients had undergone post-exposure prophylaxis after birth (Protocol ACG076), had been bottle-fed with artificial milk and were currently undergoing HAART regimen.

Three non-Italian newborn, of one-and-a-half, 2 months and 3 months, were excluded from the study as their seropositivity is still to be ascertained. These newborn, on 30/04/2011, did not present any stomatological symptons. Each pediatric patient underwent an accurate intra- and extra-oral clinical examination and palpation of the lymph nodes in the head-neck area. A specific odontostomatological case history (Table III) was compiled for each pediatric patient as follows:

1. a section for history data, dedicated to physiologic, family, past medical, past odontostomatologic, recent medical and recent odontostomatologic histories;
2. a section dedicated to the diagnosis of the pediatric patient with HIV infection;
3. a section totally pertaining to odontostomatologic interest including a relevant table: on odontostomatologic lesions and their relative plasma levels; on the therapy used for such lesions; on the radiodiagnostics of odontostomatologic interest;
4. a section dedicated to HAART which indicates the type of therapy carried out.

Statistical analyses

Covariance analysis was used to calculate the mean plasma values of the CD4 Tot, CD4%, CD8%, CD4-CD8 lymphocytes and the viral load of the oral diseases using the onset date as covariant.

The Bonferroni Test was used to calculate and compare the differences between the mean lymphocyte plasma values and viral load of the multiple lesions found in the study sample using ALFA value equal to 0.05.

Multiple comparisons were carried out for multiple diseases. For the viral load, the calculations were carried out on the transformed log values (Logvir). The calculations were made using SAS System software.

RESULTS

Our experimental study is a multicenter retrospective of the few present in the scientific literature that asses the correlation between viral load, CD4 lymphocytes and the multiple oral diseases manifested in HIV^+ children in the HAART era.

More than 100 oral diseases were found in

Table III. *Odontostomatologic medical record.*

Medical Record

1) HISTORY

Physiological history

Name_____Surname_____Date of birth_____
Place of birth _____ Sex _____
Childbirth: natural/ cesarian
Feeding: breast/ bottle
*Apgar score index*_____
First physiological actions:
- talking_____
- walking _____

Parent

Name _____ Surname _____ Age____ Tel_____

Name _____ Surname _____Age _____ Tel_____
Schooling / profession _____

Family history

List eventual hereditary pathologies:_____

HIV positive: YES NO father mode of contagion
YES NO mother mode of contagion
YES NO child mode of contagion

Past medical pathological history

List all medical precedents

_____
_____

Past medical history

List all odontostomatologic past history

_____
_____

Recent medical history

_____
_____

Recent odontostomatologic history

_____
_____

Objective exam

_____
_____
_____

2) DIAGNOSTIC FRAMEWORK OF THE CHILD WITH HIV INFECTION. HIV VIRUS IDENTIFICATION TEST

	Within 15 days from birth	After 6 months
PCR	Positive/ Negative	Positive / Negative
- o viral isolation	Positive / Negative	Positive/ Negative
- o Ag p 24 isolation	Positive / Negative	Positive / Negative

	3 mnth	6 mnth	9 mnth	12 mnth	15 mnth	18 mnth
WESTERN BLOT	Positive / Negative	Positive/ Negative	Positive/ Negative	Positive / Negative	Positive / Negative	Positive/ Negative

2. ODONTOSTOMATOLOGIC ONSET AND PLASMA LEVELS

Date	Dental lesion	CD4 Tot	CD4 %	CD8 %	CD4/ CD8	VIREMIA

Odontostomatologic therapy

Dental lesion	Drug	Dosage

Odontostomatology Radiodiagnostic tests

Typology Test	Radiodiagnosed Pathology

4) HAART THERAPY

□ Single name of drug _____
□ Double name of drug _____
□ Triple name of drug _____

Date of therapy	Type	Dosage

the study sample, the most frequent being: oral candidiasis, oropharyngeal candidiasis, HSV-1 herpetic esophagyitis, herpetic gingivolstomatitis (RHOG), recurrent aphthous stomatitis (RAS), parotid swelling, oral hairy leukoplakia (OHL), Herpes simplex 1 (HSV-1), linear gingival erythema (LGE), necrotizing gingivitis (NUG), facial lipodistrophy, facial-cervical lymphadenopathy (FCL), xerostomia, dysgeusia, hyposmia, oral mucosa hyperpigmentation (OMP) (Fig. 4).

The following are some of the numerous mean plasma values of T lymphocytes (mpVTL) and the Viral Load (VL) during HIV/AIDS-related Oral Diseases (Fig. 5, 6, 7, 8).

- In the 7 cases of recurrent oral mucosa hyperpigmentation (OMP) associated with recurrent aphthous stomatitis (RAS), mpVTL: CD4 Tot was 390 μL; CD4% was 13.01; CD8% was 0.3; CD4-

CD8 was 0.175; VL (logVir) was 11.082.

- In the 8 cases of parotid tumefaction associated with linear gingival erythema (LGE), mpVTL: CD4 Tot was 1753 µL; CD4% was 45.9; CD8% was 28.2; CD4-CD8 was 0.87; VL (logVir) was 3.951.
- In the 10 cases of recurrent aphthous stomatitis (RAS) associated with linear gingival erythema (LGE), the mpVTL: CD4 Tot was 552.00 µL; CD4% was 26.3; CD8% 57.9; CD4-CD8 was 0.5; VL (logVir) was 3.688.
- In the 4 cases of recurrent necrotizing gingivitis (NUG) associated with recurrent herpetic gingivolstomatitis (RHOG) and facial-cervical lymphadenopathy (FCL), the mpVTL: CD4 Tot was 48.50 µL; CD4% was 2.06; CD8% was 61.6; CD4-CD8 was 0.009. VL (logVir) was 9.01.
- In the 7 cases of recurrent oral hairy leukoplakia (OHL) associated with recurrent aphthous stomatitis (RAS), the mpVTL was CD4 Tot 395.00 µL; CD4% was 13.925; CD8% was 41.225; CD4-CD8 was 0.325; VL (logVir) was 9.109.
- In the 7 cases of recurrent oropharyngeal candidiasis associated with HSV-1 herpetic esophagyitis (Esoph. HSV-1) and facial-cervical lymphadenopathy (FCL), the mpVTL: CD4 Tot was 2.15 µL; CD4% was 2.3; CD8% was 36.6; CD4-CD8 was 0.009; VL (logVir) was 12.33.

The results of our study show that AIDS-related oral disease are important indicators for evaluating immune (immune competence/immune reconstitution) and/or virological success or failure induced by HAART in HIV^+ children.

In fact, in 8 cases of recurrent parotid swelling associated with linear erythema (EL), the mpVTL: CD4 Tot was 1753 µL, CD4% was 45.9. These average lymphocyte values found in the sample study in the course of AIDS-related oral diseases allowed us, by using the immunoclinical classification of the CDC (1993) based on age, to classify these children in the 'no evidence of immunosuppression' category: Lymphocytes TCD4 +> 1500 µL; CD4 ≥ 25% (Table II).

In the 10 cases of recurrent aphthous stomatitis (RAS) associated with linear gingival erythema (EL), the mpVTL: CD4 Tot was 552.00 µL; CD4% was 26.3. These average lymphocyte values found in the sample study in the course of AIDS-related oral diseases allowed us, by using the immunoclinical classification of the CDC (1993) based on

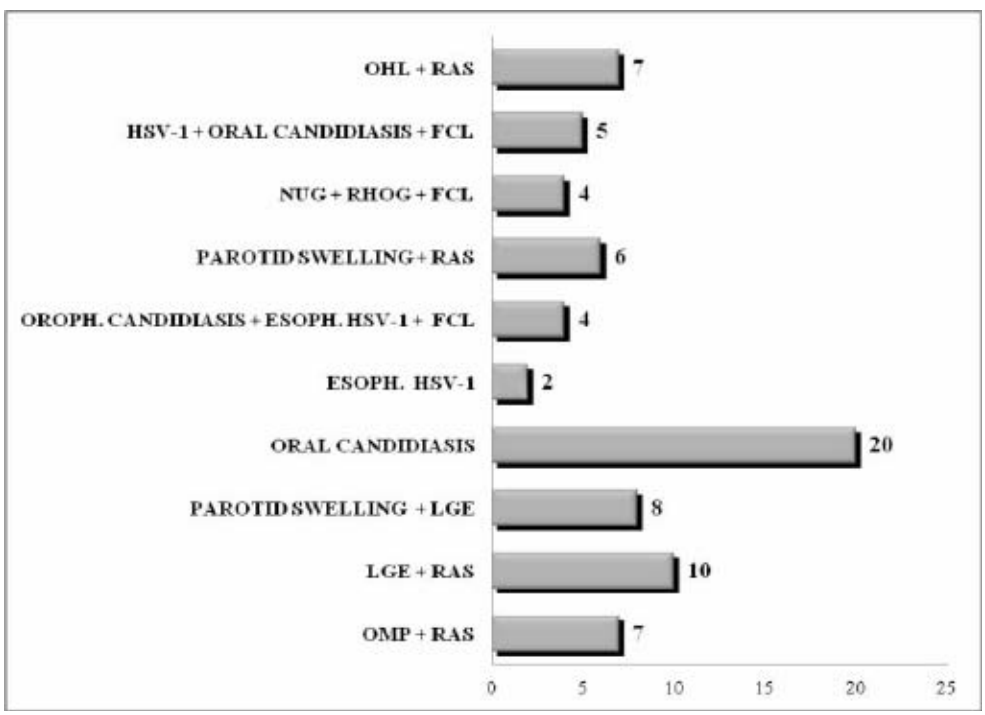

Fig. 4. *Frequency of AIDS-related oral diseases revealed in the study sample.*

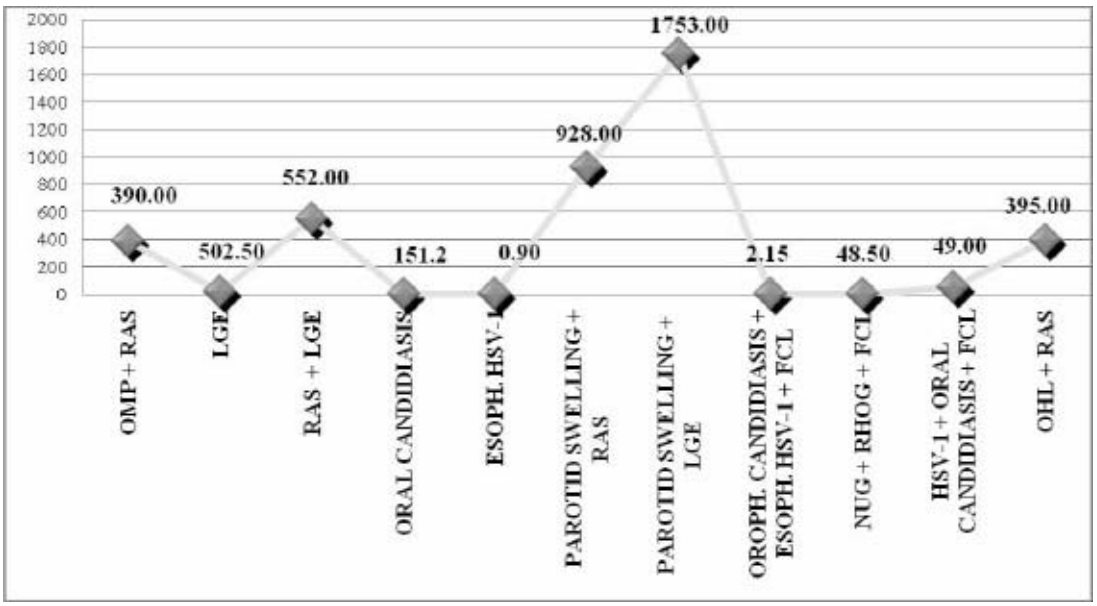

Fig. 5. *Mean values of CD4 T lymphocyte plasma totals revealed in AIDS-related oral diseases. OMP: Oral mucosa hyperpigmentation; RAS: Recurrent Aphthous Stomatitis; LGE: Linear Gingival Erythema; Oral candidiasis; Oroph. Candidiasis; HSV-1: Herpes simplex 1; Esoph. HSV-1: HSV-1 herpetic esophagitis; NUG: Necrotizing gingivitis; RHOG: Recurring herpetic gingivostomatitis (HSV-1); OHL: Oral Leukoplakia; FCL: Facial cervical lymphadenopathy.*

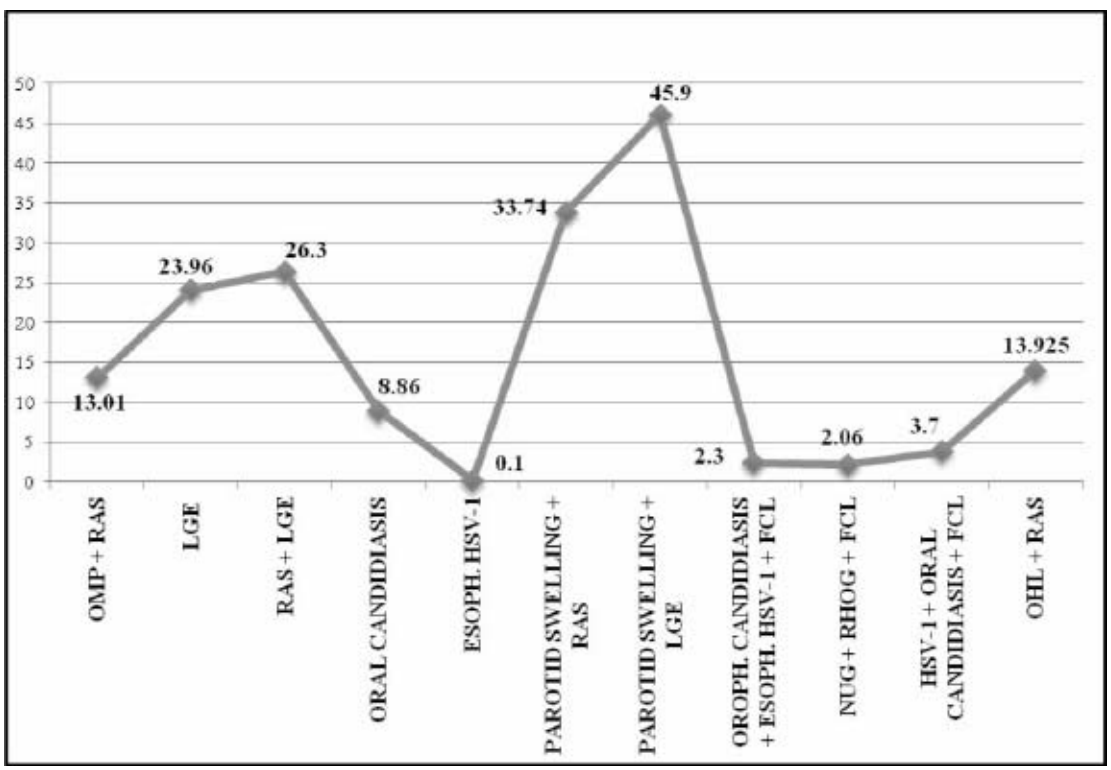

Fig. 6. *Mean values of CD4 % T lymphocyte plasma revealed in AIDS-related oral diseases.OMP: Oral mucosa hyperpigmentation; RAS: Recurrent Aphthous Stomatitis; LGE: Linear Gingival Erythema; Oral candidiasis; Oroph. Candidiasis; HSV-1: Herpes simplex 1; Esoph. HSV-1: HSV-1 herpetic esophagitis; NUG: Necrotizing gingivitis; RHOG: Recurring herpetic gingivostomatitis (HSV-1); OHL: Oral Leukoplakia; FCL: Facial cervical lymphadenopathy.*

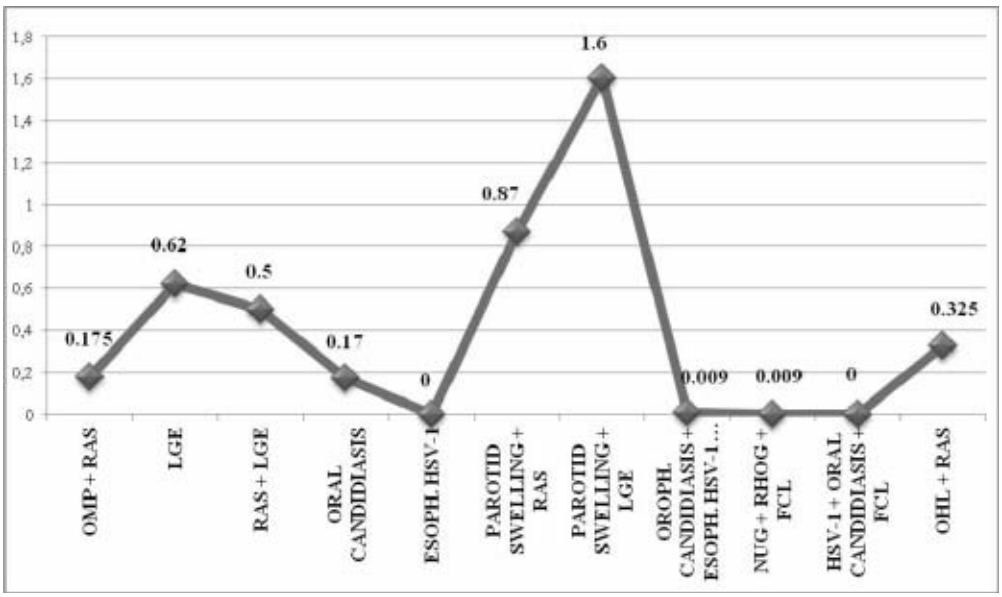

Fig. 7. *Mean values of plasma of CD4 – CD8 T lymphocytes revealed in AIDS-related oral diseases. OMP: Oral mucosa hyperpigmentation; RAS: Recurrent Aphthous Stomatitis; LGE: Linear Gingival Erythema; Oral candidiasis; Oroph. Candidiasis; HSV-1: Herpes simplex 1; Esoph. HSV-1: HSV-1 herpetic esophagitis; NUG: Necrotizing gingivitis; RHOG: Recurring herpetic gingivostomatitis (HSV-1); OHL: Oral Leukoplakia; FCL: Facial cervical lymphadenopathy.*

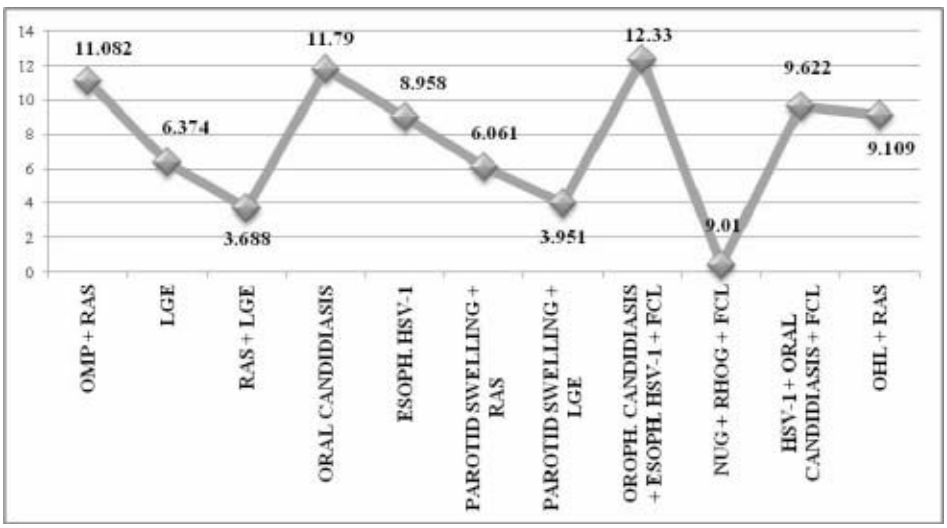

Fig. 8. *Mean viral load (logVir) in AIDS-related oral diseases. OMP: Oral mucosa hyperpigmentation; RAS: Recurrent Aphthous Stomatitis; LGE: Linear Gingival Erythema; Oral candidiasis; Oroph. Candidiasis; HSV-1: Herpes simplex 1; Esoph. HSV-1: HSV-1 herpetic esophagitis; NUG: Necrotizing gingivitis; RHOG: Recurring herpetic gingivostomatitis (HSV-1); OHL: Oral Leukoplakia; FCL: Facial cervical lymphadenopathy.*

age, to classify these children in the 'moderate immunosuppression' category: Lymphocytes TCD4+ 500-999 μL; CD4% 15-24% (Table II).

In the 4 cases of recurrent oropharyngeal candidiasis associated with herpetic esophagitis and facial-cervico lymphadenopathy (FCL), the mpVTL: CD4 Tot was 2.15 Ml; CD4% was 2.3. These average values measured in lymphocyte samples of oral diseases during AIDS-related studies allowed us, by using the immunoclinical classification of the CDC

(1993) based on age, to classify these children in the 'severe immunosuppression' category: Lymphocytes TCD4+ <200μL; Lymphocytes CD4% <15 (Table II).

In our study we found a strong correlation between OMP (which is both a side effect of HAART and a pseudo pathology) and RAS.

DISCUSSION

Our study is in agreement with the Patton study, carried out between 1995 and 1999 on 606 patients (159 patients <12 years, 209 patients = 12 years, 238 patients > 12 years) which concluded that AIDS-related oral diseases are strongly suggestive, and associated with immune suppression and modestly associated with high viral load (10).

Our study is in agreement with a recent study by Gaita'n-Cepeda et al. which concluded that oral candidiasis should be considered a predictor of clinical failure in immuno patients adult and pediatric patients with HIV / AIDS undergoing HAART(11).

The correlation between viral load, plasma values of CD4 Tot, CD4 %, CD8 %, CD4-CD8 T lymphocytes and AIDS-related oral diseases, found in this retrospective multicenter study, shows that lymphocytic depletion is the basic element in the onset of such diseases.

From this retrospective study, carried out on a population of seropositive children, it emerges that:

1) The CD4 lymphocyte, for which the HIV virus has a high tropism, is the principle base of the entire immune system, being able to regulate like "the conductor of an orchestra" the activity of all the other cells responsible for immune defence and the viral load has a low predictive value on the progression of the illness and on death rate.

With regard to the difference between the mean plasma values of the CD4 T lymphocytes detected in our sample study, the Bonferroni Test showed a significant difference between the values revealed (Table IV):

In parotid swelling associated with linear gingival erythema and oropharyngeal candidiasis associated with herpetic esophagitis equal to 1750.85 μL;

- In parotid swelling associated with recurrent aphthous stomatitis and Herpes Simplex 1 (HSV-1) associated with oral candidiasis and facial cervical lymphadenopathy equal to 879 μL;
- In recurrent aphthous stomatitis associated with linear gingival erythema and necrotizing gingivitis associated with recurring herpetic gingivostomatitis and with facial cervical lymphadenopathy equal to 503.5 μL.

Regarding the difference between the mean plasma values of the percentages (%) of the CD4 T lymphocytes, the Bonferroni test showed a significant difference between the values revealed (Table V):

- in the parotid swelling associated with linear gingival erythema and oropharyngeal candidiasis associated with herpetic esophagitis equal to 43.7;
- in the parotid swelling associated with recurrent aphthous stomatitis and necrotizing gingivitis associated with recurring herpetic gingivostomatitis and with facial cervical lymphadenopathy equal to 31.68;
- in recurrent aphthous stomatitis associated with linear gingival erythema and Herpes Simplex 1 associated with oral candidiasis and facial cervical lymphadenopathy equal to 22.6.

Regarding the difference between the mean plasma values of the CD4 – CD8 T lymphocytes, the Bonferroni test showed a significant difference between the values revealed (Table VI):

- in the parotid swelling associated with linear gingival erythema and herpes Simplex 1 (HSV-1) associated with oral candidiasis e facial cervical lymphadenopathy equal to 1.6;
- in the parotid swelling associated with recurrent aphthous stomatitis and necrotizing gingivitis associated with recurring herpetic gingivostomatitis and with facial cervical lymphadenopathy equal to 0.8607;
- In recurrent aphthous stomatitis associated with linear gingival erythema and oropharyngeal candidiasis associated with herpetic esophagitis equal to 0.491.

With regard to the difference between the mean values of the viral load (expressed in logVir), the Bonferroni test showed a significant difference between the values revealed (Table VII) :

- In the oropharyngeal candidiasis associated with herpetic esophagitis and parotid swelling associated with linear gingival erythema equal to 8.379;

Table IV. *Difference between the mean plasma values of the CD4 Tot lymphocytes: the Bonferroni test.*

Oral Diseases AIDS-related	mpVTL CD4 µL		mpVTL CD4 µL	Difference mean plasma values of the CD4 Tot lymphocytes
Parotid Swelling + LGE	*1753.00*	*Oroph. Candisiasis + Esoph. HSV-1 + FCL*	*2.15*	*1750.85 µL*
Parotid Swelling + RAS	*928.00*	*HSV-1 + Oral Candidiasis + FCL*	*49*	*879.00 µL*
RAS + LGE	*552*	*NUG + RHOG + FCL*	*48.50*	*503.50 µL*

Table V. *Difference between the mean plasma values of the CD4 % lymphocytes: the Bonferroni test.*

Oral Diseases AIDS-related	mpVTL CD4 %		mpVTL CD4 %	Difference mean plasma values of the CD4 % lymphocytes
Parotid Swelling + LGE	*46.00*	*Oroph. Candisiasis + Esoph. HSV-1 + FCL*	*2.03*	*43.7 %*
Parotid Swelling + RAS	*33.74*	*NUG + RHOG + FCL*	*2.06*	*31.68 %*
RAS + LGE	*26.3*	*HSV-1 + Oral Candidiasis + FCL*	*3.7*	*22.6%*

Table VI. *Difference between the mean plasma values of the CD4 – CD8 lymphocytes: the Bonferroni test.*

Oral Diseases AIDS-related	mpVTL CD4-CD8		mpVTL CD4-CD8	Difference mean plasma values of the CD4- CD8 lymphocytes
Parotid Swelling + LGE	*1.6*	*HSV-1 + Oral Candidiasis + FCL*	*0*	*1.6*
Parotid Swelling + RAS	*0.8697*	*NUG + RHOG + FCL*	*0.009*	*0.8607*
RAS + LGE	*0.5*	*Oroph. Candisiasis + Esoph. HSV-1 + FCL*	*0.009*	*0.491*

Table VII. *Difference between the mean Viral Load (Logvir): the Bonferroni test.*

Oral Diseases AIDS-related	Viral load (Logvir)		Viral load (Logvir)	Difference mean Viral Load (Logvir)
Oroph. Candisiasis + Esoph. HSV-1 + FCL	*12.33*	*Parotid Swelling + LGE*	*3.951*	*8.379 Logvir*
HSV-1 + Oral Candidiasis + FCL	*9.622*		*3.688*	*5.934 Logvir*

• In Herpes Simplex 1 (HSV-1) associated with oral candidiasis and facial cervical lymphadenopathy and recurrent aphthous stomatitis associated with linear gingival erythema equal to 5.934.

From these mean plasma values (mpVTL) detected by statistical analysis (Bonferroni test and analysis of covariance) it is clear that the progressive depletion of the CD4+ T cells in the peripheral blood represents the fundamental immunologic event which characterizes HIV infection in all its stages. Such depletion, inevitably, exposes the pediatric patient to a series of oral manifestations of various nature. Today, thanks to Highly Active Antiretroviral Therapy, HAART-induced immunologic reconstitution has drastically reduced the frequency of AIDS-related opportunistic infections (12-16), with the exception of oro-pharyngeal-esophageal/ pulmonary candidiasis which in 2010 was 33.6% *vs*

11.2% of the pre-HAART era (14).

The variability of mean plasma values and viral load detected in the sample study, in the course of AIDS-related oral diseases in HIV-positive children depend:

- on the immunological clinical category to which the pediatric patients belongs (CDC A, B, C);
- on the pediatric patient adhering to the HAART regimen;
- on the drug resistance.

2) Our study, in agreement with the studies of Ranganathan K, King MD, Dollfus C support that HAART is accompanied also by odontostomatologic side effects such as: an increase of HPV oral lesions, xerostomia, ageusia, disgeusia, hyposmia, perioral paresthesia, hyperpigmentation of the oral mucosa, facial lipodistrophy with atrophy of the perinasal adipose tissue and of the Bichat's fat pad (17 - 21).

In the pre-HAART era, the slow but inexorable decline of immune competence followed by progressive CD4 lymphocyte depletion was behind the development and/or recurrence of serious opportunistic AIDS-related oral diseases (Kaposi's sarcoma, pharyngeal and esophageal candidiasis, herpetic esophagitis, CMV infection, lymphoma).

Our experimental retrospective multicenter document that:

1. Highly Active Antiretroviral Therapy, introduced in the two year period of 1996-1997, has greatly changed the viral conditions - immunological and clinical - regarding odontostomatology in pediatric HIV-positive in industrialized countries, transforming a fatal disease into a syndrome that is continually acquiring a chronic character;

2. The intra and extra-oral clinical examination and palpation of the lymph nodes in the head-neck area for AIDS related oral diseases among HIV-positive children, performed by a specialist in Medicine and Oral Oncology is an invaluable screening test for diagnosis and clinical monitoring of pediatric HIV infection from the initial to the advanced stage, and to assess whether the presence/absence of oral opportunistic diseases or success/failure of immune and viral diseases is induced by HAART;

3. The plasma values of T lymphocyte and viral load are two irreplaceable laboratory markers to assess the immune competence, and replication or viral load;

4. The plasma values of T lymphocytes $CD4^+$ in children HIV-positive, compared to adults, are higher and show a considerable variability in the first 4 years of life, and then decreased with age until it reaches values of adult HIV / AIDS to the 6-7 years of life;

5. The viral load, however, has a low predictive value on disease progression and mortality.

This multicentric retrospective study is in contrast with the strong current correlation in the scientific view between HAART and an increase in HPV-related lesions in HIV-positive children. In our study sample of 30 HIV-positive children from different immuno clinical categories, no cases of HPV-related oral diseases were noted, nor any cases of immune reconstitution inflammatory syndrome, which is characterized by a "paradoxical" reactivation and reproliferation of neoplasias and latent opportunistic infections triggered by delayed hypersensitive immune reactions.

Concluding with a citation by A. BLOCH: "A drug is not only a molecule which, when inoculated into an experimental animal, produces a scientific article".

REFERENCES

1. AIDS in the World II. Ed. Jonathan Mann and Daniel J. M. Tarantola. ISBN13: 9780195090970. ISBN10: 0195090977 Paperback, 1996; p 648.
2. Thorne C, Newell M-L, Botet FA, et al., for the European Collaborative Study. Older children and adolescents surviving with vertically acquired HIV Infection. J Acquir Immune Defic Syndr 2002; 29 (4):396-401.
3. French Perinatal Study And European Collaborative Study. Morbility and mortility in European children vertically infected by HIV-1. J Acquir Immune Defic Syndr 1997; 14 (5):442-50.
4. Andiman W, Boucher M, et al.: The International Perinatal HIV group. The mode of delivery and the risk of vertical transmission of human immunodeficiency virus type 1. N Engl J Med 1999; 340 (13):977-87.
5. De Martino M, Tovo PA, Tozzi AE. HIV-1 transmission through breast-milk: appraisal of risk according to duration of feeding. AIDS 1992; 6

(9):991-7.

6. Patton LL. Sensitivity, specificity, and positive predictive value of oral opportunistic infections in adults with HIV/AIDS as markers of immune suppression and viral burden. Oral Surg Oral Med Oral Pathol Oral Radiol Endod 2000; 90:182-8.
7. Ivan Dieb Miziara, Raimar Weber**.** Oral lesions as predictors of highly active antiretroviral therapy failure in Brazilian HIV-infected children. J Oral Pathol Med (2008) 37: 9-106.
8. CDC. 1993 revised classification system for HIV infection and expanded surveillance case definition for AIDS among adolescents and adults. MMWR 1992; 41(RR-17):1-19.
9. CDC: Revision 1994 of Classification system for HIV infection in children under 13 years of age MMWR 1994; 43 RR-12.
10. Patton LL. Sensitivity, specificity, and positive predictive value of oral opportunistic infections in adults with HIV/AIDS as markers of immune suppression and viral burden. Oral Surg Oral Med Oral Pathol Oral Radiol Endod 2000; 90:182-8.
11. Gaitán-Cepeda LA, Martınez-González MM, Ceballos-Salobreña A. Oral candidosis as a clinical marker of immune failure in patients with HIV/AIDS on HAART. AIDS Patient Care STDS 2005; 19:70-7.
12. Siliciano R. Viral Reservoirs and Ongoing Virus Replication in Patients on HAART: Implications for Clinical Management. 8th Conference on Retrovirus and Opportunistic Infections 2001; Chicago. Abs. n. L5.
13. Stevenson M. HIV-1 pathogenesis. Nature Medicine 2003; 9 (7):853-60.
14. Suligoi B, Boros S, Camoni L et al. Aggiornamento delle nuove diagnosi da HIV e dei casi di AIDS in Italia al 31 dicembre 2009. Notiziario dell'Istituto Superiore di Sanità 2010, Vol 23 -Nr 4 - S1:13-14. ISSN 0394-930.
15. Pienaar ED, Young T, Holmes H. Interventions for the prevention and management of oropharyngeal candidiasis associated with HIV infection in adults and children. Cochrane Database Syst Rev.2010; (11):CD003940.
16. Ogunbosi BO, Oladokun RE, Brown BJ, Osinusi KI. Prevalence and clinical pattern of paediatric HIV infection at the University College Hospital, Ibadan, Nigeria: a prospective cross-sectional study. Ital J Pediatr 2011;3 7:29.
17. Carr A, Cooper DA. Adverse effects of antiretroviral therapy. Lancet 2000; 356:1423-30.
18. King MD, Reznik D, O'Daniels CM, Larsen NM, Osterholt D, Blumberg HM. Human papillomavirus-associated oral warts among human immunodeficiency virus-seropositive patients in the era of highly active antiretroviral therapy: an emerging infection. Clin Infect Dis 2002; 34(5):641-8.
19. Ficarra G, Shillitoe EJ, Adler-Storthz K, Gaglioti D, Di Pietro M, Riccardi R, Forti G. Oral melanotic macules in patients infected with human immunodeficiency virus. Oral Surg Oral Med Oral Pathol 1990; 70(6):748-50.
20. Duggal MS, Abudiak H, Dunn C, Tong HJ, Munyombwe T. Effect of CD4+ lymphocyte count, viral load, and duration of taking anti-retroviral treatment on presence of oral lesions in a sample of South African children with HIV+/AIDS. Eur Arch Pediatr Dent 2010; 11(5):242-6.
21. Dollfus C, Blanche S, Trocme N, Funck-Brentano I, Bonnet F, Levan P. Correction of facial lipoatrophy using autologous fat transplants in HIV-infected adolescents. HIV Med 2009; 10(5):263-8.

POSTOPERATIVE PAIN MANAGEMENT AT TIRANA UNIVERSITY HOSPITAL CENTER "MOTHER TERESA", TIRANA, ALBANIA

A. DIBRA[1], S. KELLICI[2] and I. AKSHIJA[3]

[1]First Surgical Clinic, Tirana University Hospital Center "Mother Teresa", Tirana, Albania;
[2]Pharmaceutical Department, Faculty of Medicine, Tirana University, Tirana, Albania;
[3]Department of Statistics, Tirana University Hospital Center "Mother Teresa", Tirana, Albania

Received November 23, 2011 – Accepted June 21, 2012

There is no or little evidence on postoperative pain assessment and treatment in Albanian hospitals. This study is based on our every day work and aims to highlight our experience. We conducted a descriptive drug utilization study which implied data collection over 6 months. Evidence of the enrolled patients was kept by maintaining records and the completed structured questionnaires. Postoperative pain was assessed through a five-category verbal rating scale (VRS). Metamizole was the most prescribed and administered analgesic drug as single therapy and in combination therapy, and acetaminophen was the least prescribed drug. The compliance between the prescribed dosages and those administered was higher in patients treated with a single analgesic compared to multiple therapies. A few patients reported adverse events (4.2%). There is much variability in postoperative pain management methods used by medical staff within the Tirana University Hospital. In Albania to date there is no standard protocol for postoperative pain treatment. This study shows that there are no essential differences in patients' outcomes in terms of efficacy of analgesic treatment. This leads to the conclusion that a postoperative protocol/guideline for pain management should be prepared, based on our local study findings and also on international experience. Moreover, the guidelines should consider use of balanced analgesia.

Pain is a personal, subjective experience that involves sensory, emotional and behavioral factors associated with actual or potential tissue injury (1). An appropriate pain management aims to improve the quality of the patient's life, to facilitate the recovery, to reduce the morbidity and to allow rapid discharge from hospital (2).

There is much evidence of individual variations in reacting to pain and this is influenced by genetics, age, sex and cultural background. Pediatric patients, geriatric patients and patients suffering from critical illness as well as other groups of patients, with inadequate pain control therefore require special attention (3, 4).

When discussing pain associated to surgery, we may observe two types: acute and chronic pain. Both can arise from skin, deep somatic or visceral structures. The first is experienced immediately after surgery (up to 5-7 days) the chronic instead can last more than 3 months (5). Continuous and periodic pain assessment is of relevant importance in postoperative pain management. Pain must be quantified through appropriate assessment scales (6, 7).

There is no or little evidence on postoperative pain assessment and treatment in Albanian hospitals. This

Key words: surgery, pain management, pain assessment, anti-inflammatory drugs

Mailing address: Dr. Arvin Dibra,
Universiteti Zoja e Keshillit te Mire,
Rruga Dritan Hoxha,
Tirana, Albania
Tel: +355 672031602
Fax: +35542273291
e-mail: a.dibra@unizkm.edu.al

0393-974X (2012)

study, based on every day work, aims to highlight our experience. The objective is to describe and improve knowledge on the prevalence, severity and treatment outcomes of pain syndromes after three main abdominal surgery types: 1) inguinal hernia (recurrent and/or bilateral); 2) open cholecystectomy; and 3) gastric surgery, (either elective or emergency surgeries) performed at the University Hospital Center in Albania. In Albania surgery-associated pain has traditionally been managed by using classic treatments, a combination of two or more analgesics, or by combining an analgesic and an antispasmodic drug. We must mention that there are no available guidelines on pain treatment in Albanian hospitals.

MATERIALS AND METHODS

We evaluated a sample of 545 consecutive patients undergoing surgical treatment in the First Surgical Clinic of Tirana University Hospital Center. This cross-sectional study describes drug utilization and implies data collection over a 6 months period (from 1/1/2011 to 30/6/2011). We kept evidence of the enrolled patients by maintaining their records and the completed questionnaire prepared by our group (each patient included in the study provided their consent to use the information gathered).

We considered only cases of the three following types of operative procedure: 1) inguinal hernia (including recurrent and/or bilateral); 2) open cholecystectomy and 3) gastric surgery (including malignant tumor, gastric ulcer, duodenal ulcer) considering these examples of simple, middle and aggressive surgery, respectively.

Clinical data collected regarded age, sex, presence of other diseases, current medicinal treatments, analgesics used to treat postoperative pain (specifying the name of drug, dose and route of administration, dosing schedule, the dose prescribed and that administered, adverse events experienced during treatment etc). (8)

Data showed that postoperative pain of enrolled patients was managed through several treatment schemes:

1. Metamizole 50%-2 ml
2. Metamizole 50%/2 ml associated to Diazepam 10mg/2 ml
3. Metamizole 50%/2 ml associated to Papaverine 4%-1ml
4. Metamizole 50%/2 ml associated to Butylscopolamine bromide 20mg/1ml
5. Tramadol hydrochloride 100mg/2ml
6. Ketoprofen 160mg/2ml
7. Meloxicam 15mg/1.5ml
8. Diclofenac sodium 75mg/3ml
9. Acetaminophen 150 mg/ml – 6.7 ml
10. Pethidine hydrochloride 5%- 2 ml
11. Morphine hydrochloride 10 mg- 1 ml

Postoperative pain was assessed using a five category verbal rating scale (VRS). Patients were asked to rate their pain on a five-point scale: none, mild, moderate, severe or very severe. Evaluation was made on the first day post surgery (9-11).

RESULTS

A total number of 545 patients were enrolled in the study (258 Male and 287 Female patients) 219 (40.2%) of whom had undergone inguinal hernia and 65 (11.9%) gastric surgery. Cholecystectomy was performed by traditional dexter subcostal laparotomie and was carried out on 261 patients (or 47.90%). The patients' average age was 57.04; the median age was 59.6, SD 15.96. The age of enrolled patients was in a 72.7 years range (the youngest being 14.0 and the oldest 86.7).

Of the enrolled patients, 298 (54.67%) did not suffer from other pathologies, 124 (22.75%) reported HTA (arterial hypertension) and/or cardiac dysfunctions; 58 (10.64%) suffered from chronic respiratory diseases and 78 (14.31%) had had gastric abnormalities treated at least once in their life.

Analgesic treatments at post surgery were administered as perfusion or injection, a usual procedure in our clinic. Of the 1056 analgesic doses administered in the first 24 h, 667 were intravenous, 339 intramuscular and none oral or rectal. Thirteen patients (2.38%) did not receive any postoperative pain treatment.

The most prescribed drug for postoperative pain management (administered as single therapy) is Metamizole with 12.7% of the prescriptions. When classifying prescriptions in opioid and non-opioid ones, we found that 31.3% of prescribed drugs are opioid and 66.3% non-opioid ones. One hundred and seventy (32%) patients were treated with a combination of opioid and non-opioid drugs; 75 (14.1%) patients were treated with either one opioid or a combination of two opioid drugs (pethidine/tramadol or morphine/tramadol). Eighty-five (5.6%) patients were treated combining non-opioid metamizole with diazepam, 44 (8.07%) patients were treated with a combination of metamizole with papaverine and 40 (7.33%) were treated with

Table I. *Quantity and number of dosages applied accompanied with the compliance expressed as administered dosages (ADD) on the prescribed dosages (PDD) (based on drugs used to manage postoperative pain).*

	Analgine	Valium	Papverine	Butylsc.	Tramadol	Ketoprofen	meloxicam	Diclofenac	Acetaminofen	Petidine	Morfine
Mean Dose PDD (mg)	2440.3	24.1	113.6	92.0	261.8	232.0	16.4	130.7	2928.6	148.9	11.9
Mean Number of Doses	2.44	1.21	2.84	4.60	2.62	1.45	1.09	1.74	2.93	1.49	1.19
Mean Dose ADD (mg)	2162.1	20.1	123.6	89.5	213.5	208.0	15.9	117.9	2714.3	117.0	11.6
Mean Number of Doses	2.16	1.01	3.09	4.48	2.14	1.30	1.06	1.57	2.71	1.17	1.16
Compliance with prescription ADD/PDD*100	89	83	109	97	82	90	97	90	93	79	97

Table II. *Proportions of dosages prescribed and those administered (compliance add/pdd), the relative number of dosages, based on different treatment schemes.*

	Analgine	Analgine	Valium	Analgine	Papverine	Analgine	Buskopan	Tramadol	Ketoprofen	meloxicam	Diclofenac	Acetaminofen	Petidine	Analgine	Tramadol	Morfine	Analgine	Tramadol
Mean Dose PDD (mg)	**2913.0**	**2411.8**	**24.1**	**2840.9**	**113.6**	**2375.0**	**92.0**	**280.7**	**232.0**	**16.4**	**130.7**	**2928.6**	**148.9**	**872.3**	**12.8**	**11.9**	**1000.0**	**12.5**
Mean Number of Doses	**2.91**	**2.41**	**2.41**	**2.84**	**2.84**	**2.38**	**4.60**	**2.81**	**1.45**	**1.09**	**1.74**	**2.93**	**1.49**	**0.87**	**0.13**	**1.19**	**1.00**	**0.13**
Mean Dose ADD (mg)	**2500**	**2011.8**	**20.12**	**2522.7**	**123.6**	**2275**	**89.5**	**226**	**208**	**15.91**	**117.9**	**2714**	**117.02**	**851.06**	**12.766**	**11.563**	**1000**	**12.5**
Mean Number of Doses	**2.5**	**2.0118**	**2.012**	**2.5227**	**3.091**	**2.275**	**4.475**	**2.26**	**1.3**	**1.061**	**1.571**	**2.714**	**1.1702**	**0.8511**	**0.1277**	**1.1563**	**1**	**0.125**
Compliance with prescription ADD/PDD*100	**85.8**	**83.4**	**83.4**	**88.8**	**108.8**	**95.8**	**97.3**	**80.5**	**89.7**	**97.2**	**90.2**	**92.7**	**78.6**	**97.6**	**100.0**	**97.4**	**100.0**	**100.0**

a combination of metamizole with butylscopolamine bromide. Metamizole was the most prescribed and administered drug, not only as analgesic single therapy but also in combination therapy (283 patients with metamizole). The less prescribed and administered drug was acetaminophen (used only on 14 patients, 2.56% of the total patients). 2.38 % patients needed no treatment.

Table I shows differences in administered dosages of analgesics based on drug type.

Collected clinical data showed that there were clear instructions on dose and dosage regimen for the analgesic, opioid and non-opioid drugs being used. Table II shows the proportions of dosages prescribed and those administered related to the number of dosages. Data refers to different treatment schemes.

The compliance between dosages prescribed and those administered was higher in patients treated with only one analgesic (especially for opioid therapy) as compared to co-prescriptions of analgesic drugs. Data analysis shows that compliance reduces especially when prescribed NSAID-s were recommended “as

Table III. *Results of pain assessment (VRS) as reported by patients at 24 hours.*

Categorical rating scale	Worst pain at any time first 24 h	Pain at 24 h
No pain	49 (9%)	122 (22%)
Mild	104 (19%)	181 (33%)
Moderate	147 (27%)	196 (36%)
Severe	158 (29%)	27 (5%)
Very severe	76 (14%)	8 (1,5%)
Patients non assessed	11 (2%)	11 (2%)
Total number of patients	545	545

needed".

Twenty-three (4.2%) patients reported adverse events after NSAID administration, 17 (3.1%) after administration of combined opioid with non-opioid and 7 (1.2%) after opioid administration. The most reported adverse events after analgesic treatment were: nausea, sedation and respiratory discomfort. It is difficult to establish a clear connection between analgesic treatment and the mentioned adverse events and the underlying pathology, although a consideration can be made. The type of adverse events are the same as those reported in classical analgesic treatment (12-14).

Pain assessment was evaluated through a five category verbal rating scale (VRS). Table III shows results of pain assessment as reported by patients.

In the total pool of subjects enrolled, only for 534 (98%) patients could we assess pain severity through a five category verbal rating scale (VRS). Patients were asked to rate their pain on a five point scale as "none, mild, moderate, severe or very severe". Evaluation was made on day one after surgery. Patients were asked to assess into 5 categories the worst pain perceived in the first 24 hours and to assess the pain at 24 hours. It was not possible to apply this assessment for 11 patients (2%). Of the total 545 patients considered, 43% reported severe to very severe pain as worst pain perceived in the first 24 hours and 28% reported no or mild pain for the same period. No significant correlation was found between the applied therapy and this assessment. Assessment at 24 hours showed an increased number of patients reporting no pain to moderate pain and a considerable reduction in patients reporting severe to very severe pain. No significant differences in pain perception was related to either age or gender.

DISCUSSION

Postoperative pain treatment and management is of great relevance in hospital settings. It impacts directly the wellbeing of patients, recovery and the number of hospitalization days. The techniques employed during surgery as well as analgesic medication delivered pre-, intra- and post-operatively can have an impact on patient outcomes (15-18).

There are at least 11 various treatment schemes in postoperative pain management, as seen in this study, just among medical staff at Tirana University Hospital (14 surgeons). Such variability in prescription is particularly observed on drug regimen dosage and on physician preferences to opioid or non-opioid analgesics. It would be helpful to compare our results with those from previous similar studies, unfortunately a literature review did not reveal any past experiences in this field in Albania.

In Albania to date there is no standard protocol in place for postoperative pain treatment. The present study shows that there are no essential differences in patients' outcomes in terms of efficacy of analgesic treatment. This leads to conclude that a postoperative protocol/guideline for pain management should be prepared, based on our local study findings and also on international experience.

Such a protocol would also have an impact on the analgesic drug availability in our hospitals which, as noted in a few cases may condition the use of treatments schemes. Protocols must consider the possibility of balanced analgesia (analgesia that

uses two or more analgesic agents that act through different mechanisms to achieve a superior analgesic effect without increasing adverse events compared with increased doses of single agents) (19, 20).

Patient's compliance is a broadly discussed concept nowadays. It is important to treat patients and to minimize their discomfort, but it is also important to support them, to prescribe the most effective treatment with as fewer side effects as possible and with the most suitable dosage regimen for each of them. Therefore we suggest to prescribe as few drugs as possible considering that multiple therapy resulted to provide lower compliance (21-24).

REFERENCES

1. Raj PP. Taxonomy and classification of pain. The handbook of chronic pain, Nocva Biomedical Books, 2007; p.9.
2. Cullen L, Greiner J, Titler MG. Pain management in the culture of critical care. Crit Care Nurs Clin North Am 2001; 13:151-66.
3. AGS panel on persistent pain in older persons. J Am Geriatr Soc 2002; 24.
4. Bonham VL. Race, ethnicity and pain treatment striving to understand the causes and solutions to the disparities in pain treatment. J Law Med Ethics 2001; 29:52-68.
5. Brown AK, Christo PJ, Wu CL. Strategies for postoperative pain management. Best Pract Res Clin Anaesth 2004; 18:703-17.
6. Breivik H, Borchgreivink PC, Allen SM, Rosseland LA, Romundstad L, Hals EK, Kvarstein G, Stubhaug A. Assessment of pain. Br J Anaesth 2008; 17-24.
7. Bader P, Echtle D, Fonteyne V, Livadas K, De Meerleer G, Paez Borda A, Papaioannou EG, Vranken JH. Post-operative pain management. In Guidelines on pain management. Arnhem, The Netherlands: European Association of Urology (EAU) 2010; 61-82.
8. Manias E, Botti M, Bucknall T. Observation of pain assessment and management - the complexities of clinical practice**.** J Clin Nurs 2002; 11:726-33.
9. Klopper H, Andersson H, Minkkinen M, et al. Strategies in assessing post operative pain - a South African study. Intensive Crit Care Nurs 2006; 22:12-21.
10. Aubrun F, Langeron O, Quesnel C, et al. Relationships between measurement of pain using visual analog score and morphine requirements during postoperative intravenous morphine titration. Anesthesiology 2003; 98:1415-21.
11. Persson K, Östman M**.** The Swedish version of the PACU-Behavioural Pain Rating Scale: A reliable method of assessing postoperative pain? Scan J Caring Sci 2004; 18:304-9.
12. Cashman NJ, Dolin SJ. Respiratory and haemodynamic effects of acute post operative pain management: Evidence from published data. Br J Anaesth 2004; 93:212-23.
13. Dolin SJ, Cashman JN. Tolerability of acute postoperative pain management: nausea, vomiting, sedation, pruritus and urinary retention. Br J Anaesth 2005; 95:584-91.
14. Institute for safe medication Practices; Safety issues with patient-controlled analgesia. ISMP Medication Safety Alert, 2003; 1-3.
15. American Pain Society. Principles of analgesic use in the treatment of acute pain and cancer pain. American Pain Society; 2003.
16. Hutchinson RW. Challenges in acute postoperative pain management. Am J Health Syst Pharm 2007; S2-S5.
17. MacLellan K. Postoperative pain: strategy for improving patient experiences. J Adv Nurs 2004; 46:179-85.
18. Svensson I, Sjöström B, Haljamäe H. Assessment of pain experiences after elective surgery. J Pain Symptom Manag 2000; 20:193-201.
19. Gordon DB, Pellino T, Miaskowski C, et al. A 10-year review of quality improvement monitoring in pain management: Recommendations for standardized outcomes measures. Pain Manage Nurs 2002; 116-30.
20. Manias E. Medication trends and documentation of pain management following surgery. Nurs Health Sci 2003; 5:85-94.
21. Apfelbaum JL, Chen C, Mehta S, et al. Postoperative pain experience: results from a national survey suggesting postoperative pain continues to be undermanaged. Anesth Analg 2003; 97:534-40.
22. Dolin SJ, Cashman JN, Bland JM. Effectiveness of acute postoperative pain management. Br J Anaesth

2002; 409-23.

23. Chung JWY, Lui JCZ. Postoperative pain management: Study of patients' level of pain and satisfaction with health care providers' responsiveness to their reports of pain. Nurs Health Sci 2003; 5:13-42.
24. Goldstein DH, Ellis J, Brown R, et al. Meeting proceedings: recommendations for improved acute pain services: Canadian Collaborative Acute Pain Initiative. Pain Res Manage 2004; 123-30.

ENTEROCOCCUS FAECALIS LEAKAGE OF ROOT CANAL SEALERS: AN *EX VIVO* STUDY

S. D'ERCOLE[1,2], A. FILIPPAKOS[1], R. de TOLEDO LEONARDO[3], C.H. PAMEIJER[4] and D. TRIPODI[1]

[1]Department of Medical, Oral and Biotechnological Sciences, Dental School, University "G. D'Annunzio" of Chieti-Pescara, Chieti, Italy; [2]Department of Biomedical Science, Dental School, University "G. D'Annunzio" of Chieti-Pescara, Chieti, Italy; [3]Department of Restorative Dentistry, Araraquara Dental School, UNESP, Araraquara São Paulo, Brazil; [4]University of Connecticut, Farmington, Connecticut, USA

Received January 18, 2012 – Accepted August 6, 2012

The aim of this *ex vivo* study was to evaluate bacterial penetration after filling root canals using 3 different techniques. Three experimental groups of 25 teeth each, obturated with lateral-warm-vertical condensation of gutta-percha, Microseal technique and EndoREZ® system, respectively, were tested in a split chamber model system using *Enterococcus faecalis* and monitored for 180 days to determine bacterial penetration. A statistical analysis was performed using the Kaplan-Meier method. Median survival time was 25 days for Microseal system, 41 for lateral-warm-vertical condensation and 81 for EndoREZ®. Significant differences were demonstrated between Microseal and EndoREZ® ($p<0.001$) and between Microseal and lateral-warm-vertical condensation technique ($p<0.05$). No statistically significant differences were observed between EndoREZ® and lateral-warm-vertical condensation. After 180 days of assessment, 20% of the EndoREZ® samples resisted bacterial penetration and furthermore, the EndoREZ® system has the potential to be a filler system compatible with other currently used systems.

Root canal therapy consists of filling three-dimensionally the endodontic space after thorough cleaning and shaping. Numerous studies have demonstrated the necessity to seal the three-dimensional space previously occupied by the pulp in order to prevent bacteria from entering the interface between filling material and the walls of the root canal (1, 2-4).

Gutta-percha is the most used endodontic filling material; it needs to be combined with a sealer and may be used with various condensation techniques. Cold or lateral condensation of gutta-percha are the most widely used methods, and are generally considered the gold standard in root canal filling (1, 5, 6). Warm vertical condensation establishes excellent sealing since, as opposed to lateral condensation, it takes advantage of the physical properties of gutta-percha to deform, as at low fusion temperatures gutta-percha is more pliable (1).

De Fazio et al. (7) proposed to use a practical approach, in which all advantages and positive aspects of lateral and vertical condensation were combined and introduced a lateral-warm vertical technique. This method of thermoplasticized gutta-

Key words: resin sealer, gutta-percha, filling method, leakage, bacteria, biocompatibility

Mailing address: Prof. Domenico Tripodi,
Department of Medical, Oral and Biotechnological Sciences,
Dental School,
University "G. Via dei Vestini, 31
66100 Chieti, Italy
Tel.: +3908713554063
e-mail: tripodi@unich.it

0393-974X (2012)

DISCLOSURE: ALL AUTHORS REPORT NO CONFLICTS OF INTEREST RELEVANT TO THIS ARTICLE.

percha produces a more homogeneous filling and better adaptation to the canal walls, which, as a result, resist bacterial infiltration better than lateral condensation (1, 7).

Different types of endodontic sealers are used in combination with gutta-percha and several studies have indicated that resin-based cements are characterized by an apical seal and parietal root canal adhesion that are superior to other dental cements (8, 9). EndoREZ® (ER) (Ultradent Products Inc) is a relatively new UDMA (urethane-dimethylacrylate)-based root canal sealer, which is dual-cure, and which, according to the manufacturer, possesses ideal properties of a root canal sealer. In combination with resin-coated gutta-percha (RCGP), a chemical bond of sealer to the RCGP is established, while the hydrophilic property of ER promotes deep penetration into the dentinal tubules, thus establishing a "monoblock". Polymerization of ER can also be accelerated with the use of a catalyst. To date, there are only a few studies in the literature that have analyzed these characteristics but none have reported the penetration of bacteria with the use of this system (10-14). Bacterial leakage tests have been used to test the sealing properties of endodontic sealers and are the preferred tests in endodontic research. Some recent articles using a methodology on which the design of this study was based have been reported (5, 10, 15-19).

The aim of this study was to evaluate *ex vivo* the efficacy of the apical seal using ER, RCGP cones and the accelerator, and subject it to bacterial penetration of *Enterococcus faecalis*. A comparison was made with other root canal condensation methods using gutta-percha and zinc-oxide-eugenol sealers, used with lateral-warm vertical condensation and the Microseal system, thermoplasticized gutta-percha cemented with Pulp Canal Sealer.

MATERIALS AND METHODS

Tooth preparation

Ninety-five extracted intact single-rooted teeth were selected from a pool of teeth after examination for defects with transillumination. They were stored in a physiological saline solution until use. The teeth were decoronated using a diamond wheel at a distance of 16 mm from the root apex. Subsequently, the pulp chambers were accessed with a course round diamond bur (FO 112, Dentsply Maillefer, Ballaigues, Switzerland) under copious water cooling. A #10 stainless steel file was used to establish patency and the working length was determined at 1 mm short of the measured length. After the use of each file 5.25% sodium hypochlorite was used with a final irrigation with 17% ethylenediaminetetraacetic acid (EDTA). The teeth were assigned at random to five groups: three experimental groups consisting of 25 teeth each, and two control groups of 10. All materials were used according to the manufacturer's instructions.

Group 1. The teeth were prepared with manual stainless steel files (Dentsply Maillefer) and filled with gutta-percha and zinc-oxide-eugenol (ZOE) cement (G. OGNA & FIGLI, Muggiò, Italy) using the lateral-warm vertical condensation technique. The teeth were filled in the apical 1/3rd and middle 1/3rd using warm lateral condensation technique. For coronal 1/3rd of canal length, the warm and plasticized gutta-percha was vertically compacted with root canal pluggers.

Group 2. The teeth were prepared with nickel-titanium M-Two files (Sweden & Martina, Due Carrare, Padova, Italy) and filled with the Microseal technique (Sybron Endo Corporation, West Collins Orange, USA) and Pulp Canal Sealer (Sybron Endo Corporation). In the Microseal system a master gutta-percha cone was first compacted laterally with a spreader and then thermoplasticized gutta-percha was delivered and compacted with an electric compactor in order to unite with the master cone and fill the rest of the root.

Group 3. The teeth were prepared with the Endo-Eze stainless system (Ultradent Products Inc., South Jordan, UTAH, USA) and filled with the EndoREZ® system using resin coated gutta-percha points (RCGP), EndoREZ® sealer, EndoREZ® accelerator (Ultradent Products Inc.). After insertion of EndoREZ® the RCGP points were dipped into the accelerator and placed in the EndoREZ®. The accelerator polymerized the sealer in approximately 6 minutes;

Group 4. Positive control teeth were prepared with a manual stainless steel files (Dentsply Maillefer) and not filled;

Group 5. Negative control teeth were prepared with a manual stainless steel file (Dentsply Maillefer).

With the exception of Group 3 in which EndoREZ® was used and the canal was left moist, all other root canals were thoroughly dried with paper points prior to insertion of the sealer.

Following completion of obturation radiographs were made of each tooth in a bucco-lingual and mesiodistal direction to evaluate the quality of the root canal fillings relative to the homogeneity and apical extension. Inadequate root fills and fillings <1 mm from the apex were discarded and replaced. All teeth were then incubated at

37°C, 100% humidity for one week to allow for complete setting of the sealers.

Subsequently, all teeth of groups 1-3 were entirely coated with nail varnish except for the apical 3 mm. The negative control teeth were entirely varnished, while the positive controls had no varnish.

Bacterial leakage preparation

This system was essentially similar to that reported by numerous authors (5, 10, 15-19). The tapered ends of 1.5 mL Eppendorf tubes (Eppendorf, Milan, Italy) were cut and the teeth were inserted through the opening, exposing 10 mm of the root. The interface tube and root were sealed with an epoxy resin. This was then attached to a 15-ml test tube bottle-top and the junctions sealed with epoxy resin. The samples were then stored in an incubator at a temperature of 60°C for 24 h to ensure complete hardening of the epoxy resin. All samples were then sterilized with ethylene oxide (Bioster SpA, Seriate Laboratories of Popoli, Pescara, Italy). This assembly when placed in the 15 ml test tube, which served as the upper chamber of the apparatus (Fig. 1). After sterilization the upper chambers were attached to the lower chamber, which was filled with 12 ml of brain-heart infusion (BHI) broth (Oxoid LTD, Basingstoke, Hampshire, England) in such a way that 2 mm of the tooth roots were immersed in BHI (Fig. 1). This assembly was then incubated at 37°C for 7 days to verify absolute sterility of the samples. Any sample showing turbidity of the BHI would be discarded and replaced with a new one.

Inoculation

Enterococcus faecalis ATCC 29212 was cultured at 37°C for 24 h in BHI broth. The bacterial suspension was evaluated using a spectrophotometer (Agilent Technologies 8453 UV, Santa Clara, USA) to assure an optical density of 0.5 McFarland corresponding to 10^8 Colony Forming Units (CFU)/mL. Using a micropipette, 100 mL of *E. faecalis* bacterial suspension was inoculated into the upper chambers of the apparatus. All samples were then incubated aerobically at 37°C for 180 days. The culture broth in the lower chamber and the *E. faecalis* inoculum in the upper chamber were replaced every 3 days. The bacterial penetration along the root canal obturation was determined by the observation of turbidity of the broth in the lower chamber. The samples were checked daily and presence or absence of turbidity recorded. In case of the turbidity of the lower chamber being noted, the broth was analyzed with a Gram stain and by colony morphology in MacConkey plates without crystal violet (Difco™, Becton, Dickinson and Company; Sparks USA), incubated at 37°C for 24 h to confirm the purity of the microorganism which had been inoculated into the upper chamber.

Statistical evaluation

The Kaplan-Meier method was used to evaluate the estimates of the probability of infiltration survival separately for three materials and techniques. Statistical significance between curves was evaluated using the log-rank test. All statistical analyses were performed using SPSS® Advanced Statistical™ 11 (2004, Chicago, IL, USA) software package. For all analyses a p-value of less than 0.05 was considered significant.

RESULTS

The Kaplan-Meier survival probability for the three test groups is shown in Fig. 2. No growth was seen when the sterilization of the entire system was verified. None of the negative controls samples showed turbidity, indicating an absence of bacterial infiltration. On the other hand, all positive control samples were positive for turbidity, which occurred within 24-48 h. Gram staining and culture on the MacConkey agar plate without crystal violet showed that in cases of turbidity of the inferior chamber, there was no contamination and the infiltration was only due to the bacterial inoculum of the superior chamber. The median survival time was 25 days for the Microseal system, 41 days for the lateral-warm vertical condensation and 81 days for the EndoREZ® system (Fig. 2).

Samples belonging to all three condensation groups showed a bacterial penetration within the first 30 days of observation (Table I). The 50-day infiltration survival was 28.0±9.0% for the Microseal system and Pulp Canal Sealer; 44.0±9.9% for the lateral-warm vertical condensation and ZOE cement, and 88.0±6.5% for the EndoREZ® system. Pair wise comparison of curves showed no statistically significant difference between the EndoREZ® system and the lateral-warm vertical condensation system (p=0.118) Significant differences were demonstrated between the Microseal and EndoREZ® system (p<0.001) and between the Microseal and lateral-warm vertical condensation system (p<0.05).

DISCUSSION

This study evaluated coronal microbial penetration in teeth with different root canal fillings over a period of 180 days. The model used followed the guidelines proposed by numerous authors except

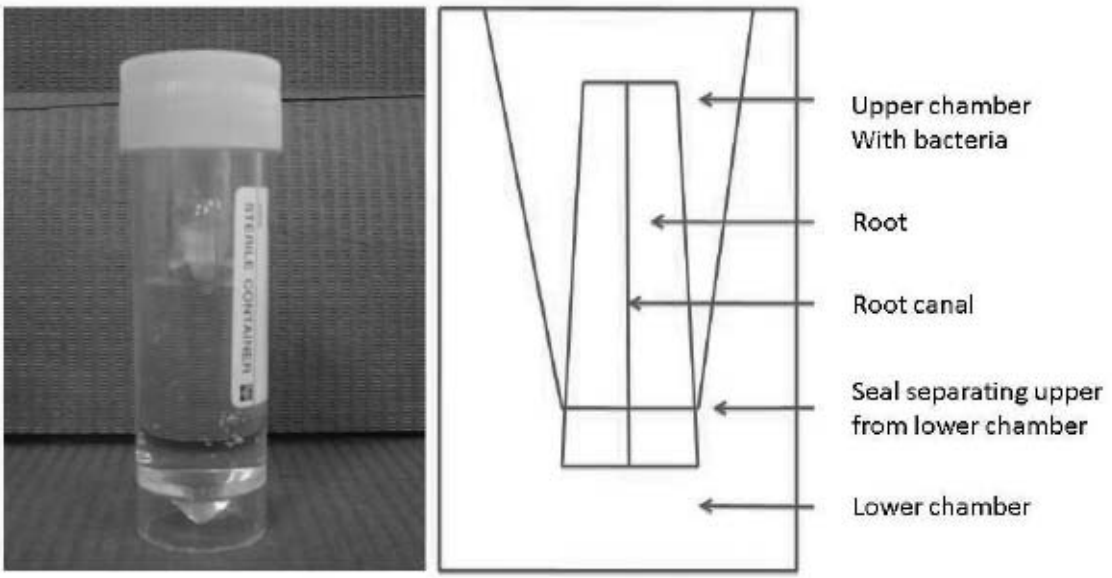

Fig. 1. *The bacterial leakage model used in this study. The upper chamber contains the tooth in an Eppendorf test-tube. The junctions were sealed with epoxy resin. The lower chamber consisted of a 15 mL test tube. The upper chamber was placed on top of the lower chamber, filled with 12 mL of BHI broth and the apical 2 mm of the root immersed in the broth.*

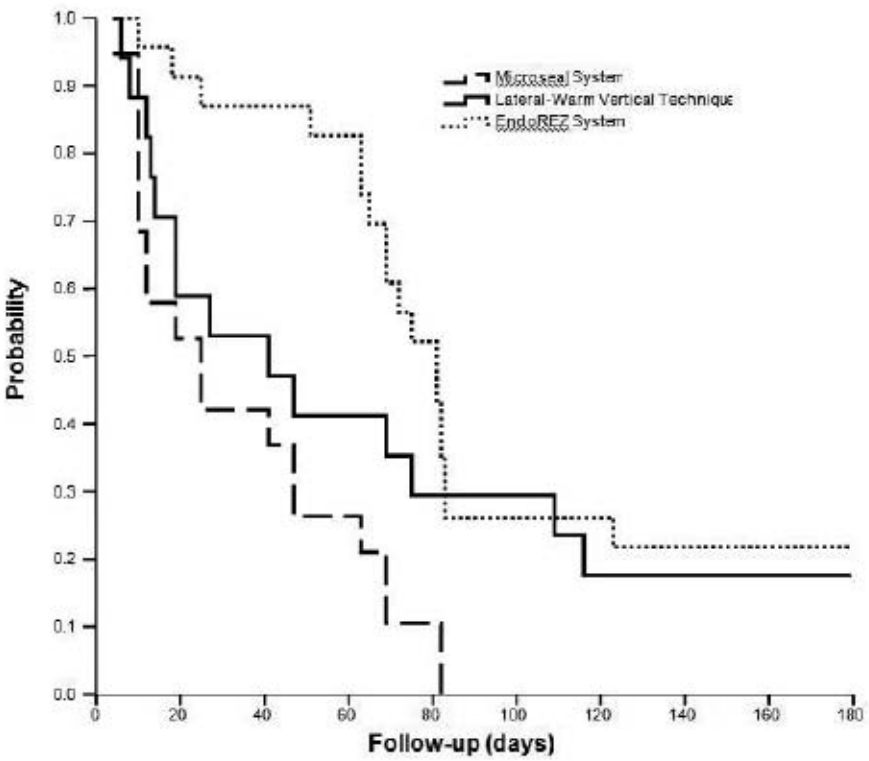

Fig. 2. *Kaplan-Meier probabilities of infiltration-free survival for three different groups. The difference between the Microseal method and the EndoREZ® system and between the Microseal and lateral-warm vertical condensation system were statistically significant (log rank test $p < 0.001$, $p < 0.05$ respectively).*

Table I. *Samples showing turbidity per 30-day interval.*

		Period (Days)						
Group	N	1-30	31-60	61-90	91-120	121-150	151-180	No Leakage
Microseal technique	25	14	4	7	0	0	0	0
Lateral-warm vertical technique	25	11	3	3	3	0	0	5
EndoREZ® technique	25	3	1	13	0	1	0	7

for minor changes in the selection of the sealants that were tested (5, 10, 11, 15-19).

Enterococcus faecalis was used as it is a Gram-positive, facultative anaerobic microorganism frequently isolated from root canals that were filled but have shown signs of a chronic periapical lesion (2, 20-22). *E. faecalis* is common in the oral cavity and can survive extreme environmental conditions such as acid or alkaline pH, high concentration of salts of heavy metals and aerobic/anaerobic conditions. It is known to invade dentinal tubules, can bind to collagen and owes its virulence to the ability to resist the action of intra-canal drugs. It has the ability to survive in root canals as a single body without the support of other bacteria (22-25).

It has been reported that the length of the root filling can affect the coronal seal as it has been demonstrated that root canals with a shorter fillings, allowed for penetration of bacteria faster than longer root canals fills. Based on these findings the length of the canals in this experiment was standardized and measured 16 mm.

Regardless of the condensation method, all three techniques demonstrated bacterial penetration in the early days (Table I). This is in agreement with Brosco et al. (17). The quality of the root fillings was assessed with radiographs and all samples were considered satisfactory, showing well-condensed fillings without voids. However, according to Siqueira et al. (6) there is little correlation between the radiographic image interpretation and quality of a filling. Voids and small defects that are not observed in radiographs may lead to rapid contamination of the endodontic system. Studies have shown that gutta-percha seals better when used in combination with a sealer (5). Consequently, the quality of the seal provided by root filling is very much dependent on the capabilities of sealants that are used. Many endodontic sealers have antibacterial and cytotoxic effects and these properties may limit the entry of bacteria (26, 27-30). Furthermore, the physical properties of a sealer may influence the penetration of bacteria. With this system of infiltration, antimicrobial activity of the sealer itself can affect the results in addition to its sealing properties. EndoREZ® does not possess antibacterial properties but nevertheless it showed less bacterial invasion, which can be attributed to other factors such as adhesion to the root canal system and low solubility. According to Ahlberg et al. (13), EndoREZ®'s hydrophilic properties are responsible for the ability to penetrate the dentinal tubules, thus establishing a superior seal. Conflicting data has been reported about the sealing ability of Pulp Canal Sealer. A high incidence of infiltration, 100% after 3 weeks, was demonstrated by DeDeus et al. (5), while less infiltration was seen by McDougall et al. (31-33). These differences may be attributed to the technical aspects of root fillings as it is widely reported that the filling technique may influence the coronal seal. It has also been reported that infiltration can occur between

the surfaces of gutta-percha/gutta-percha when, in addition to the master cone, accessories are used (17). Alternative techniques to traditional methods have been proposed using thermoplasticized gutta-percha, which is more homogeneous and provides better adaptation to the canal walls, which results in less bacterial infiltration (34-37). In this study Pulp Canal Sealer, an antimicrobial sealer, was used with thermoplasticized gutta-percha (Microseal). After 90 days 100% of the samples had infiltrated. Brosco et al. (17), however, reported an infiltration rate of only 16.7% of Microseal, even after a longer period of 120 days.

Our results suggest that a better quality of gutta-percha fillings with the use of thermoplasticized gutta-percha combined with an antimicrobial sealer does not necessarily ensure a coronal seal that prevents infiltration of bacteria. One explanation for this failure may be because the gutta-percha used in the thermoplasticized condensation method tends to shrink, which causes spaces through which bacteria can penetrate. Our results are in agreement with other studies in which lateral condensation techniques demonstrated less infiltration than the thermoplasticized technique (16, 17, 19).

Methacrylate resin-based endodontic sealers that establish a chemical bond with polycaprolactone points or with resin coated gutta-percha points have been commercially available for 8-12 years and have gained in popularity (38-40). The resin coated gutta-percha cones are recommended for use as a single master cone with EndoREZ® sealer. This system showed a median survival time of 81 days, and after 180 days of assessment 20% of the samples resisted bacterial penetration. The results of our study contradict Eldeniz et al. (10) who reported a rapid bacterial infiltration of root canals filled with EndoREZ® (within 13 days) and De-Deus et al. (5), who reported 88.9% of samples infiltrated after 9 weeks. These authors have stated that among other causes, the shrinkage caused gap formation between resin and dentin thus causing early bacterial infiltration. Both authors also reported that they completely dried the root canals with paper points. In doing so they created a hydrophobic environment, yet they used a hydrophilic sealer (EndoREZ®), which requires a moist root canal. As a result, optimum resin tag penetration did not take place, leading to leakage. The use of the accelerator with EndoREZ® produced rapid setting thus reducing polymerization shrinkage. A moist root canal together with reduced polymerization shrinkage promotes the formation of resin tags and a hybrid layer with dentin thus establishing a monoblock, which is more resistant to bacterial penetration.

In conclusion, at present there is no material or technique that completely seals the entire root canal system. Therefore, the search for endodontic filling materials that establish a complete seal that prevents bacterial penetration over long periods of time must continue. Based on the results of this study the EndoREZ® system with resin coated gutta-percha cones and an accelerator have demonstrated to be an obturation system that compares well with other currently used systems.

ACKNOWLEDGEMENTS

The authors wish to thank Mrs. Marta Di Nicola for assisting with the statistical analysis of the data.

REFERENCES

1. Marciano J, Michailesco PM. Dental gutta-percha: chemical composition, X-ray identification, enthalpic studies, and clinical implications. J Endod 1989; 15:149-53.
2. Siqueira JF Jr, Rocas IN. Exploiting molecular methods to explore endodontic infections: part 2 – Redefining the endodontic microbiota. J Endod 2005; 31:488-98.
3. Figdor D, Sundqvist G. A big role for the very small--understanding the endodontic microbial flora. Aust Dent J 2007; 52:S38-51.
4. Siqueira JF Jr, Rôças IN. Clinical implications and microbiology of bacterial persistence after treatment procedures. J Endod 2008; 34:1291-1301
5. De Deus G, Coutinho-Filho T, Reis CM, Murad C, Paciornik S. Polymicrobial leakage of four root canal sealer at two different thickness. J Endod 2006; 32:998-1001.
6. Siqueira JF, Rocas IN, Favieri A, Abad EC, Castro AJR, Gahyva SM. Bacterial leakage in coronally unsealed canals obturated with 3 different techniques. Oral Surg Oral Med Oral Phatol Oral Radiol Endod

2000; 90:647-50.
7. De Fazio P. Endodonzia Clinica. Edizione Masson 1997.
8. Lee KW, Williams MC, Camps JJ, Pashley DH. Adhesion of endodontic sealers to dentin and gutta-percha. J Endod 2002; 28:684-8.
9. Pommel L, About I, Pashley DH, Camps JJ. Apical leakage of four endodontic sealers. J Endod 2003; 29:208-10.
10. Eldeniz AU, Ørstavik D. A laboratory assessment of coronal bacterial leakage in root canals filled with new and conventional sealers. Int Endod J 2009; 42:303-12.
11. De Deus G, Murad C, Paciornik S, Reis CM, Coutinho-Filho T. The effect of the canal filled area on bacterial leakage of oval-shaped canals. Int Endod J 2008; 41:183-90.
12. Zmener O. Tissue response to a new methacrylate-based root canal sealer: preliminary observations in the subcutaneous connective tissue of rats. J Endod 2004; 30:348-51.
13. Ahlberg KM, Tay WM. A methacrylate-based cement used as root canal sealer. Int Endo J 1998; 31:15-21.
14. Zmener O, Pameijer CH. Clinical and radiographic evaluation of a resin-based root canal sealer. Am J Dent 2004; 17:19-22.
15. Fransen JN, He J, Glickman GN, Rios A, Shulman JD, Honeyman A. Comparative assessment of ActiV GP/Glass Ionomer Sealer, Resilon/Epiphany, and Guttapercha/AH Plus Obturation: a bacterial leakage study. J Endod 2008; 34:725-7.
16. Yücel AC, Çifçi A. Effects of different canal obturation techniques on bacterial penetration. Oral Surg Oral Med Oral Phatol Oral Radiol Endod 2006; 102:88-92.
17. Brosco VH, Berardinelli N, Torres SA, et al. Bacterial leakage in root canals obturated by different techniques. Part 1: Microbiologic evaluation. Oral Surg Oral Med Oral Phatol Oral Radiol Endod 2008; 105:48-53.
18. Siqueira JF Jr, Rôças IN, Alves FR, Campos LC. Periradicular status related to the quality of coronal restorations and root canal fillings in a Brazilian population. Oral Surg Oral Med Oral Phatol Oral Radiol Endod 2005; 100:369-74.
19. Brosco VH, Bernardineli N, Torres SA, et al. Bacterial leakage in obturated root canals-part 2: a comparative histologic and microbiologic analyses. Oral Surg Oral Med Oral Pathol Oral Radiol Endod 2010; 109:788-94.
20. Zoletti GO, Pereira EM, Schuenck RP, Teixeira LM, Siqueira JF Jr, Dos Santos KR. Characterization of virulence factors and clonal diversity of *Enterococcus faecalis* isolates from treated dental root canals. Res Microbiol 2010; 162(2):151-8.
21. Peters LB, Wesselink PR, van Winkelhoff AJ. Combinations of bacterial species in endodontic infections. Int Endod J 2002; 35:698-702.
22. Sedgley CM, Lennan SL, Appelbe OK. Survival of *Enterococcus faecalis* in root canals *ex vivo*. Int Endod J 2005; 38:735-42.
23. Marsh PD. Are dental diseases examples of ecological catastrophes? Microbiology 2003; 149:279-94.
24. Cheung GS, Ho MW. Microbial flora of root canal-treated teeth associated with asymptomatic periapical radiolucent lesions. Oral Microbiol Immunol 2001; 16:332-7.
25. Er K, Tasdemir T, Bayramoglu G, Siso HS. Comparison of the sealing of different dentin bonding adhesives in root-end cavities: a bacterial leakage study. Oral Surg Oral Med Oral Phatol Oral Radiol Endod 2008; 106:152-8.
26. Leonardo MR, da Silva LA, Tanomaru Filho M, Bonifácio KC, Ito IY. In vitro evaluation of antimicrobial activity of sealers and pastes used in endodontics. J Endod 2000; 26:391-4.
27. Thom DC, Davies JE, Santerre JP, Friedman S. The hemolytic and cytotoxic properties of a zeolite-containing root filling material in vitro. Oral Surg Oral Med Oral Phatol Oral Radiol Endod 2003; 95:101-8.
28. Colombo C, Faelli N, Tirelli AS, et al. Analysis of inflammatory and immune response biomarkers in sputum and exhaled breath condensate by a multi-parametric biochip array in cystic fibrosis. Int J Immunopathol Pharmacol 2011; 24:423-32.
29. Bassi A, D'Erme AM, Gola M. Erythema multiforme-like irritant contact dermatitis after application of an antiscabies treatment. Int J Immunopathol Pharmacol 2011; 24:545-7.
30. Pierangeli A, Degener AM, Ferreri ML, et al.

Interferon-induced gene expression in cervical mucosa during human papillomavirus infection. Int J Immunopathol Pharmacol. 2011;24(1):217-23.

31. McDougall IG, Patel V, Santerre P, Friedman S. Resistance of experimental glass ionomer cement sealers to bacterial penetration *in vitro*. J Endod 1999; 25:739-42.
32. Tremolada S, Delbue S, Ferraresso M, Carloni C, Elia F, Larocca S, Bortolani E, Ferrante P. Search for genomic sequences of microbial agents in atherosclerotic plaques. Int J Immunopathol Pharmacol. 2011;24(1):243-6.
33. Symeonidou I, Hatzistilianou M, Papadopoulos E, Dovas CI, Karagouni E, Pappa S, Pantzartzi CN, Kourelis A, Frydas S. Susceptibility and resistance to canine leishmaniosis is associated to polymorphisms of the canine TNF-α gene. Eur J Inflamm 2011;9:23-29.
34. Zmener O, Pameijer CH, Serrano SA, Vidueira M, Macchi RI. The significance of moist root canal dentin with the use of methacrylate-based endodontic sealers: an *in vitro* coronal dye leakage study. J Endod 2008; 34:76-9.
35. Silambarasan G, Ramanathan T, Nabeel MA, Kalaichelvan VK, Kathiresan K, Balasubramanian T. Anti-inflammatory activity of the marine *cyanobacterium trichodesmium erythraeum* against carrageenan-induced paw oedema in wistar albino rats. Eur J Inflamm 2011;9:53-56.
36. Marzano AV, Cugno M, Trevisan V, Lazzari R, Fanoni D, Berti E, Crosti C. Inflammatory cells, cytokines and matrix metalloproteinases in amicrobial pustulosis of the folds and other neutrophilic dermatoses. Int J Immunopathol Pharmacol 2011; 24:451-60.
37. Zhang C-Y, Shao S-H, Chen X, Shi Y-L. Anti-frostbite effects of *prunus tomentosa thunb* total flavone Eur J Inflamm 2011;9:65-71.
38. Zmener O, Pameijer CH. "Adhesive" endodontics – Development and introduction of methacrylate based resin sealers. In Pameijer CH et al – Methacrylate Based Resin Sealers: A Paradigm Shift in Endodontics. Page 6, 7. Ultradent Press 2009 South Jordan UT.
39. Saggini A, Anogeianaki A, Maccauro G, Teté S, Salini V, Caraffa A, Conti P, Shaik-Dasthagirisaheb YB. What you should know about *Escherichia coli* infection. Eur J Inflamm 2011;9:103-106.
40. Tripodi D, D'Ercole S, Pasini M, Nastasio S, Bonini S, Giuca MR. Inflammatory and immunitary modifications in saliva of subjects with labial and tongue piercing. Eur J Inflamm 2011; 9:185-191.

DENTAL AND PERIODONTAL COMPLICATIONS OF LABIAL AND TONGUE PIERCING

M.R. GIUCA[1], M. PASINI[1], S. NASTASIO[2], S. D'ERCOLE[3] and D. TRIPODI[3]

[1]Department of Surgery, University of Pisa, Pisa, Italy; [2]Department of Pediatrics, University of Pisa, Pisa, Italy; [1]Departments of Medical, Oral, and Biotechnological Sciences, Dental School, University "G. D'Annunzio" of Chieti-Pescara, Chieti, Italy

Received January 28, 2012 – Accepted August 7, 2012

Piercing is the practice of puncturing some parts of the body to apply ornamental objects. The presence of oral and perioral piercings are a risk factor for many acute and chronic complications, such as chipping of the dental enamel, periodontal lesions and infection. The aim of this study is to assess the prevalence of lip and tongue piercing complications in the dental and periodontal tissues in a sample of young adults. Twenty-five adult patients were examined (test group: 11 males and 14 females with an average age of 23.4±3.6 years) who had had a minimum of one labial or tongue piercing for at least 1 year and were compared with 25 subjects (control group: 11 males - 44%, and 14 females - 56%) without any lingual or labial piercing. A questionnaire was compiled for each patient and a clinical examination was performed. The following parameters were examined by the same operator: abnormal toothwear, tooth chipping or cracking, clinical attachment loss (CAL), probing pocket depth (PD) and gingival recession (GR, classified by using Miller's classification). The data were analyzed using χ^2 or Fisher's exact test for small numbers and non-parametric Mann–Whitney or Kruskal–Wallis tests to examine for differences in continuity; the level of significance was $p< 0.05$. According to the results found in the present study the prevalence of abnormal tooth wear and tooth chipping was higher in the subjects with labial or lingual piercing. Moreover, patients with tongue or labial piercing exhibited a higher GR in comparison to control subjects without any oral piercing. No differences were observed between the two groups as regards CAL and PD. A significant association between the duration of piercing and dental defects was found in the group of patients with piercings with greater prevalence of tooth and periodontal defects in the group of 13 subjects who had had the piercings for a period $\geq$ 4 years.

Oral and facial piercings have seen a rapid increase in popularity. Body art, that is the art of permanently decorating, personalizing and adorning one's body, is an old practice and examples have been found going back to ancient times (1). Men have, transformed, marked or painted their bodies for an instinctive need to differ from animals. Piercings and tattoos are ways of communicating emotions, the need for personal identity and relationship with society through the body (2). Body piercing involves the insertion of a needle to create an opening through which decorative ornaments such as jewellery may be worn (3).

Recently piercing has become more popular, not only with the young but also among adults, for numerous reasons such as belonging to a group,

Key words: piercing, dental complications, periodontal status

Mailing address: Prof. Domenico Tripodi,
Departments of Medical, Oral,
and Biotechnologies Sciences Dental School,
University "G. d'Annunzio" Chieti-Pescara
Via dei Vestini, 31 66100 Chieti, Italy
Tel.: +39 08713554063 Fax: +39 08713554392
e-mail: tripodi@unich.it

0393-974X (2012)

rebellion or as a reminder of particularly important events, and it now represents a mass phenomena that interests a population of heterogeneous individuals of all ages, cultures and social standing (4).

Jewels or objects that are used in piercings are of different materials such as titanium, Teflon, plexiglass and polyacrilic resins or natural materials such as wood, bone, amber and ivory. The site of the piercing may regard numerous areas of the body, including oral and perioral ones: tongue, lips, cheek, labial fraenum, tongue fraenum and uvula (5).

The presence of oral and perioral piercings, above all on the tongue, involve a higher risk of damage, directly and indirectly, to the soft and hard oral tissue, as well as systemic risks (6-7). Many complications, mainly oral and perioral, can occur following the placing of a piercing (Table I).

In particular, among dental-periodontal complications, the most frequent are dehiscence, gum recession, loss of localized attachment with consequent bone defect (generally following labial or tongue piercing that compresses or abrades the periodontal tissue) and above all trauma to the hard dental tissue (8-9).

As piercings invade the subcutaneous area, there is also a high potential for infection; in fact, piercings may act as vehicles for transmitting illnesses such as hepatitis B,C,D and G, AIDS, Herpes simplex, tetanus, papilloma, syphilis and tuberculosis (10-11). In general, any infectious disease, transmittable through continuous lesions of the mucosa, is a risk for subjects who undergo piercing. The prevention of these diseases is based on the principle of disinfecting and sterilizing the operational area, the instruments and the material to be inserted (12-13). A transitory bacteremia is normal following a piercing with a simple rise in temperature that falls in a few days; however, if it does not decrease septicemia may set in and, in the most serious cases, septic shock (14-15).

The aim of this study is to assess the prevalence of lip and tongue piercing complications in the dental and periodontal tissues in a sample of young adults.

MATERIALS AND METHODS

In this study 50 subjects were enrolled at the Department of Dental Sciences of the University of Pisa: 25 adult patients (11 males - 44%, and 14 females - 56%) who had had a minimum of one labial or tongue piercing for at least 1 year formed the test group. The control group consisted of 25 subjects (11 males - 44%, and 14 females - 56%) without any lingual or labial piercing.

The average age ± standard deviation (SD) was 23.4±3.6 years in the test group and 24.6±3.9 years in the control group (Table II). All the patients gave written informed consent to participate in the study and all procedures were conducted according to the principles expressed in the Declaration of Helsinki.

Each patient compiled a questionnaire regarding sex, age, and the presence of local or systemic pathologies. Moreover, in the test group the questionnaire also regards the type of piercing, length of time since insertion, who performed the piercing, the type of jewel used, if they had had any post-operative complications, any increase in saliva flow or other adverse effects after the application, with what frequency they removed the piercing for cleaning and which products they used.

Of the test subjects examined, 64% (16) had only one piercing; in particular, among the patients with only one piercing, 36% (9) had a small bar with a small ball and a flat surface in labial position, while 28% (7) had a bar with 2 small balls, one dorsal and one ventral on the tongue. 36% (9) of the subjects had more than one piercing of whom 12% (3) had a bar with 2 small balls on the lower lip and a bar with one small ball and a flat surface on the upper lip. Another 12% (3) of the patients had a bar with 2 small balls on the tongue and a bar with 2 small balls on the lower lip. Only one patient (4%) had a bar with a small ball and a flat surface on the upper lip and a bar with 2 small balls on the tongue. One patient (4%) had two bars with 2 small balls on the lower lip and a bar with 2 small balls on the tongue, while another patient (4%) had a ring with a small ball on the lower lip and a bar with 2 small balls on the tongue and a bar with one small ball and a flat surface on the upper lip.

The test group patients had the piercings for at least 1 year; mean ± SD of the duration of the piercings was 4±2.6 years. Almost all the subjects, 92% (23), had been to a specialized center for the application of the piercings. One patient, however, had had the piercing applied by a friend and one had done it himself.

Regarding the frequency of removal of the piercings for hygiene, only 8% (2) of the subjects took them out daily, 64% (16) removed them every other day, while 28% (7) of the patients stated that they never took them out.

The products used for cleaning the piercings were 48% (12) ethyl alcohol while 24% (6) of the subjects used a mouthwash.

Each patient was subjected to a clinical examination at the dental clinic of the University of Pisa and the following parameters were examined by the same operator: abnormal toothwear, tooth chipping or cracking, clinical attachment loss (CAL), probing pocket depth (PD) and gingival recession (GR, classified by using Miller's classification) (16, 17).

CAL, PD and GR were assessed at 6 sites for each tooth by using a 15-mm North-Carolina probe.

Data were analyzed using the statistics programme SPSS 15.0 for Windows. X^2 or Fisher's exact test for small numbers were used and non-parametric Mann–Whitney or Kruskal–Wallis tests were used to examine for differences in continuity; the level of significance was $p< 0.05$.

RESULTS

All the subjects of the test group had experienced swelling and pain in the days following the application of the piercing with phonatory, swallowing and chewing difficulties; all the symptoms, however, disappeared within about two weeks. The subjects with piercings on the tongue referred an increase in the flow of saliva, above all during phonation. In 3 subjects with labial piercings there had been a localized infection with the formation of an abscess, and antibiotic treatment had been necessary to complete the on-site healing.

Other self- reported oral piercing complications were as follows: inflammation (19 patients), GR (14 patients), increased salivary flow (15 subjects).

Fig. I shows the dental defects found in the test and in the control group. At the clinical examination, all subjects of the test group showed slight molar toothwear. Furthermore, lower incisal tooth chipping (10 subjects), upper incisal tooth chipping (4 subjects) and lower molar cracking (1 subject) were observed in the sample. In the control group 8 subjects exhibited a slight molar toothwear. Moreover, 2 subjects showed a mandibular incisor chipping and 1 patient showed an upper incisor cracking as a result of a previous dental trauma.

After comparison between the groups, a significant difference was found according to tooth chipping and dental toothwear ($p< 0.05$). Instead, no significant difference ($p> 0.05$) was observed according to tooth cracking.

As regards the periodontal status (Table III), 15 patients (5 with tongue piercings, 2 with labial piercings and 8 with both tongue and labial piercings) presented a gingival recession at the the adjacent teeth. The mean GR depth for affected teeth adjacent to ornaments was 1.9±1 mm. Three patients showed a Miller Class II defect, the other 12 patients exhibited a Miller Class I defect.

In the control group a GR was found in 4 subjects and the mean GR value was 0.5±0.4 mm. Comparing the two groups a statistically significant difference was found ($p< 0.05$). In the test group, a PD >3 mm was found in 3 teeth (2 lower incisors and 1 lower molar) adjacent to pierced sites (2 lip, 1 tongue) of

Table I. *Acute and chronic complications due to the presence of piercings in the tongue and labial areas.*

ACUTE COMPLICATIONS	CHRONIC COMPLICATIONS
• Swelling • Pain • Infections • Prolonged hemorrhaging • Phonatory alterations • Allergy to the metal in the piercing • Galvanic currents between the jewel and metal used in dental restoration • Hypersaliosis • Ludwig's Angina	• Accumulation of plaque and tartar on the jewel • Nerve damage • Halitosis • Dental and gum trauma • Persistent phonatory and chewing difficulties • Malignant hyperplasia and neoplasia • Bifid tongue • Transmission of systemic infections • Cerebral abscess • Endocarditis

Table II. *Description for each patient of the test group of the number, localization and length of time since insertion of the piercings, sex, age.*

Pz	SEX	AGE	DURATION OF THE PIERCING	TONGUE PIERCING	LOW MEDIAN LABIAL PIERCING	LOW LABIAL SIDE PIERCING	UPPER LABIAL PIERCING
1	M	25	4	1	0	0	0
2	M	18	3	0	0	1	0
3	F	22	4	1	0	0	0
4	M	22	1	0	0	1	0
5	M	19	4	0	0	1	0
6	M	34	13	1	0	1	1
7	M	28	7	1	0	0	0
8	F	21	7	1	0	0	0
9	M	22	6	1	0	0	0
10	M	20	3	0	1	0	1
11	F	23	4	1	0	0	1
12	F	22	4	0	1	0	0
13	F	24	2	0	1	0	0
14	F	21	2	1	0	0	0
15	F	23	1	0	1	0	0
16	M	22	2	1	0	0	0
17	F	24	8	0	1	0	1
18	F	28	1	0	0	0	1
19	M	24	4	1	1	0	0
20	F	27	3	1	1	0	0
21	F	28	2	0	0	1	0
22	M	18	3	0	1	0	0
23	F	22	4	0	1	0	1
24	F	24	5	1	1	0	0
25	F	25	3	1	0	1	0

three different patients. Also in the control group a PD >3 mm was found in 3 teeth (1 lower premolar and 2 mandibular molars) of three different patients. No significant difference was observed between the two groups ($p > 0.05$)

In the test group, a CAL > 3 mm at the level of the lower incisors was found only in 1 patient with both labial and lingual piercing. Instead, none of the patients of the control group exhibited a CAL > 3 mm. Comparing the two groups, no significant differences were noticed ($p > 0.05$). The time period of ornament wear affected the prevalence of dental defects and GR values.

There was a statistically significant association between the duration of piercing and dental defects with greater prevalence of dental and periodontal defects in the group of 13 subjects who had had the piercings for a period ≥ 4 years. Dental defects and soft tissue defects did not differ significantly between the tongue and lip piercing groups.

DISCUSSION

Oral piercings have become popular among young adults during recent years, however piercing is not without risks, and both immediate and delayed

Table III. *Periodontal parameters measured in the two groups: clinical attachment loss (CAL), probing pocket depth (PD) and gingival recession (GR).*

	TEST	*CONTROL*	*p- value*
GR	*15 (*1.9±1 mm)	*4 (*0.5±0.4 mm)	*P< 0.05*
PD	*3*	*3*	*N.S.*
CAL	*1*	*0*	*N.S.*

N.S: not significant

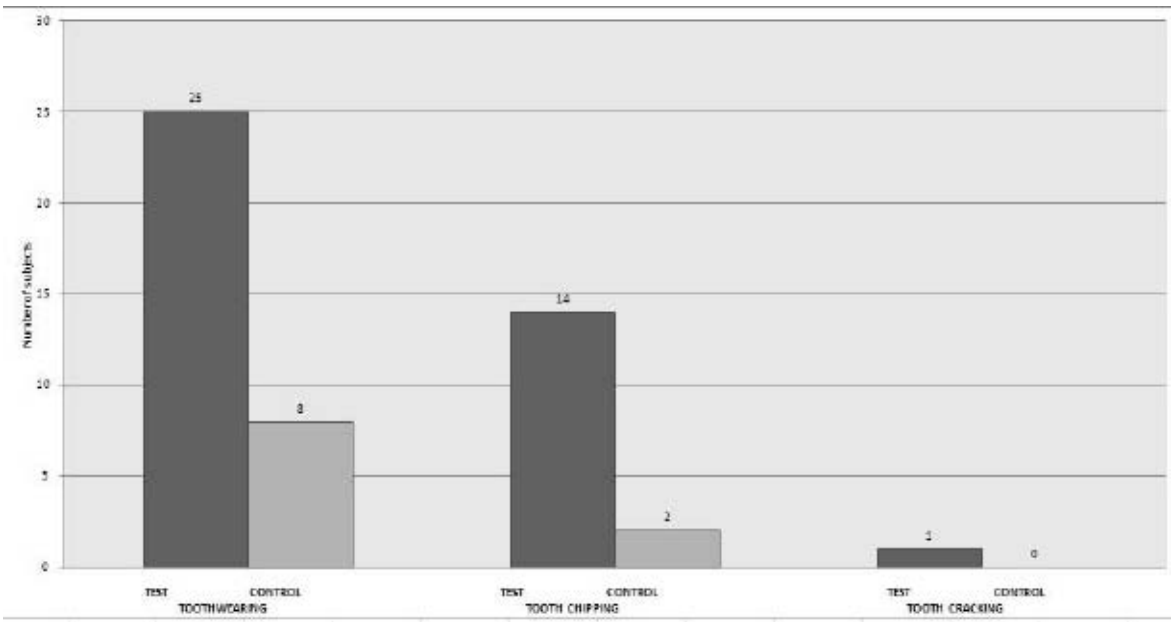

Fig. I. *Number of subjects with dental defects (toothwear, chipping and cracking) in the test group (with piercing) and in the control group (without piercing).*

complications have been described in literature (13).

In the present study slight dental defects were found in all the patients of the test group, in particular at the level of the lower molars and incisors. Often, in fact, subjects with tooth fractures reported a habit of biting the piercings or knocking or clacking them against the teeth (18-21). In particular, fractured teeth are associated with tongue piercings; however, only in rare cases the fracture was so severe that the tooth had to be extracted (22-25). In the present study, a tooth cracking was found only in one lower molar of the test group, while most of the dental defects were tooth chipping.

Subjects with oral and perioral piercing have to learn how to chew differently and to be careful when eating to avoid biting on the piercing (26-32). Playing with the ornament can also damage the parodontal status and lead to GR and periodontal pockets: often the jewellery-associated recession develops as a narrow, cleft-like defect on the lingual aspect of the lower incisors, with recession depths of 2–3 mm or greater, often extending to or beyond the level of the mucogingival junction. Thinner gingival tissues may be at greater risk of breakdown and recession than thicker gingival tissues (22).

In this study GR were observed at the level of

the lower incisors in the patients with lingual or both lingual and labial piercings; moreover, in the test group the mean GR value was higher than that found in the controls. The GR observed in the control group was probably due to an abnormal dental brushing.

Previous case reports showed a correlation between periodontitis and oral and perioral piercing the periodontal attachment loss generally occurred at the frontal lower teeth and the mean probing depth and⁄or clinical attachment loss varied from 3 to 9 mm (22, 26). According to the results of the present study, no statistical association was found between periodontitis and piercings. In fact, no statistically significant alterations were observed with regard to CAL and PD.

For the affected sites, the mean GR depth found in the present study (1.9 mm) was slightly lower than the GR observed in previous studies: Plessas et al. found a mean value of 2.65 mm (17), while Campbell et al. observed a mean value of 2.53 mm (33-35).

With the increased number of patients with piercings at intraoral and perioral sites, dental operators should consider the potential risks to the teeth and the periodontium as well as the risk of oral inflammation due to the presence of oral and perioral piercings (36-39). Dentists should give information to their patients of oral and perioral piercing consequences for both teeth and gingiva. Moreover, the patients should be informed that the longer the wear time, the greater the chance to present with oral complications and that piercing habits increase the possibility of developing dental defects and GR (15-18).

According to the results found in the present study the prevalence of abnormal tooth wear and tooth chipping was higher in the subjects with labial or lingual piercing. Moreover, patients with tongue or labial piercing exhibited a higher GR in comparison to control subjects without any oral piercing.

No differences were observed between the two groups with regard to CAL and PD.

A significant association between the duration of piercing and dental defects was found in the group of patients with piercings with greater prevalence of tooth and periodontal defects in the group of 13 subjects who had had the piercings for a period ≥ 4 years.

REFERENCES

1. Biber JT. Oral piercing: the hole story. Northwest Dent 2003; 82:13-17.
2. Choe J, Almas K, Schoor R. Tongue piercing as risk factor to periodontal health. NY State Dent J 2005; 71:40-3.
3. Ventä I, Lakoma A, Haahtela S, Peltola J, Ylipaavalniemi P, Turtola L. Oral piercings among first-year university students. Oral Surg Oral Med Oral Pathol Oral Radiol Endod 2005; 99:546-9.
4. Chen M, Scully C. Tongue piercing: a new fad in body art. Br Dental J 1992; 172:87.
5. Peticolas T, Tilliss TS, Cross-Poline GN. Oral and perioral piercing: a unique form of self-expression. J Contemp Dent Pract 2000; 1:30-46.
6. Dunn WJ, Reeves TE. Tongue piercing: case report and ethical overview. Gen Dent 2004; 52:244-7.
7. Fleming PS, Flood TR. Bifid tongue – a complication of tongue piercing. Br Dent J 2005; 198:265-66.
8. Kopp WK. Piercing. J Am Dent Assoc 1998; 129:16.
9. De Moor RJ, De Witte AM, De Bruyne MA. Tongue piercing and associated oral and dental complications. Endod Dent Traumatol 2001; 16:232-7.
10. Olsen JC. Lingual Abscess secondary to body piercing J Emerg Med 2001; 20:409.
11. Braithwaite R, Robillard A, Woodring T, Stephens T, Arriola KJ. Tattooing and body piercing among adolescent detainees: relationship to alcohol and other drug use. J Subst Abuse 2001; 13:5-16.
12. Friedel JM, Stehlik J, Desai M, Granato JE. Infective endocarditis after oral body piercing. Cardiol Rev 2003; 11:252-5.
13. Keog IJ, O'Leary G. Serious complication of tongue piercing. J Laryngol Otol 2001; 115:233-4.
14. Martinello RA, Cooney EI. Cerebellar brain abscess associated with tongue piercing. Clin Infect Dis 2003; 36:E32-4.
15. Khanna R, Kumar SS, Raju BS, Kumar AV. Body piercing in the accident and emergency department J Accident Emerg Med 1999; 16:418-21.
16. Miller PD. A classification of marginal tissue recession. Int J Periodontics Restorative Dent 1985; 5:9-13.
17. D'Ercole S, Catamo G, Tripodi D, Piccolomini R. Comparison of culture methods and multiplex PCR

for the detection of periodontopathogenic bacteria in biofilm associated with severe forms of periodontitis. New Microbiol 2008; 31(3):383-91.
18. Plessas A, Pepelassi E. Dental and periodontal complications of lip and tongue piercing: prevalence and influencing factors. Aust Dent J 2012; 57(1):71-8.
19. Berardi D, De Benedittis S, Scoccia A, Perfetti G. Evaluation of neridronate on the osseointegration process of endeous titanium implants in animal models. Eur J Inflamm 2011; 9:141-9.
20. Zizzi A, Aspriello SD, Rubini C, Goteri G. Peri-implant diseases and host inflammatory response involving mast cells: a review. Int J Immunopathol Pharmacol 2011; 24:557-66.
21. Carlesimo M, Narcisi A, Orsini D, Cortesi G, Abruzzese C, Giovagnoli S, Giubettini M, Camplone G. A rare case of sarcoidosis and morphea. Eur J Inflamm 2011; 9:297-9.
22. Hennequin-Hoenderdos NL, Slot DE, Van der Weijden GA. Complications of oral and peri-oral piercings: a summary of case reports. Int J Dent Hyg 2011 May; 9(2):101-9.
23. Varvara G, Caputi S, D'Arcangelo C, Murmura G. Soft-tissue healing and impression technique in implant dentistry: a case report. Eur J Inflamm 2012; 10:153-57.
24. Artini M, Scoarughi GL, Papa R, et al. A new anti-infective strategy to reduce adhesion-mediated virulence in Staphylococcus aureus affecting surface proteins. Int J Immunopathol Pharmacol 2011; 24:661-72.
25. Betto P, Cerimele S, Rassu M, Fornasa CV, Di Pietro M, Sessa R. Cutaneous infection of *Nocardia altamirensis*: the first case report. Eur J Inflamm 2011; 9:301-303.
26. Rawal SY, Claman LJ, Kalmar JR, Tatakis DN. Traumatic lesions of the gingiva: a case series. J Periodontol 2004; 75:762-9.
27. Boyaci H, Pala A, Argun Bariş S, Başyigit I, Yildiz F, Ilgazli A. The effects of inhaled steroid and theophylline on systemic inflammation in COPD. Eur J Inflamm 2011;9:241-8.
28. Ciprandi G, De Amici M, Marseglia GL. Serum IL-9 levels and sublingual immunotherapy: preliminary report. J Biol Regul Homeost Agents 2011; 25:295-7.
29. Meglio P, Giampietro PG, Gabriele I, Carello R, Avitabile S, Galli E. Oral desensitisation with food is food-specific and protein-specific. Int J Immunopathol Pharmacol 2011; 24:803-11.
30. Isik M, **Çalgüneri** M, Doğan **İ,** Yeşilkaya Y, Shourbagi A. Aseptic abscess: a report of two cases. Eur J Inflamm 2012; 10:143-47.
31. Bernacchioni C, Cencetti F, Kwon MJ, Gwak HS, Jeong SK, Bruni P, Donati C. The sphingosine kinase activator K6PC-5 stimulates C2C12 myoblast differentiation. Int J Immunopathol Pharmacol 2011; 24(1):55-62.
32. D'Alimonte I, Nargi E, Mastrangelo F, et al. Vascular endothelial growth factor enhances *in vitro* proliferation and osteogenic differentiation of human dental pulp stem cells. J Biol Regul Homeost Agents 2011; 25:57-69.
33. Campbell A, Moore A, Williams E, Stephens J, Tatakis DN. Tongue piercing: impact of time and barbell stem length on lingual gingival recession and tooth chipping. J Periodontol 2002; 73:289-97.
34. Colombo C, Faelli N, Tirelli AS, et al. Analysis of inflammatory and immune response biomarkers in sputum and exhaled breath condensate by a multi-parametric biochip array in cystic fibrosis. Int J Immunopathol Pharmacol 2011; 24:423-32.
35. Pietropaoli D, Monaco A, Del Pinto R, Cifone MG, Marzo G, Giannoni M. Advanced glycation end products: possible link between metabolic syndrome and periodontal diseases. Int J Immunopathol Pharmacol 2012; 25(1):9-17.
36. Tripodi D, D'Ercole S, Pasini M, Nastasio S, Bonini S, Giuca MR. Inflammatory and immunitary modifications in saliva of subjects with labial and tongue piercing. Eur J Inflamm 2011; 9:175-83.
37. Torretta S, Marchisio P, Esposito S, Garavello W, Cappadona M, Clemente IA, Pignataro L. Exhaled nitric oxide levels in children with chronic adenotonsillar disease. Int J Immunopathol Pharmacol 2011; 24:471-80.
38. Benucci M, Saviola G, Baiardi P, Manfredi M, Sarzi-Puttini P, Atzeni F. Efficacy and safety of leflunomide or methotrexate plus subcutaneous tumour necrosis factor-alpha blocking agents in rheumatoid arthritis. Int J Immunopathol Pharmacol 2011; 24(1):269-74.
39. Giuca MR, Giuggioli E, Metelli MR, Pasini M, Iezzi

G, D Ercole S, Tripodi D. Effects of cigarette smoke on salivary superoxide dismutase and glutathione peroxidase activity. J Biol Regul Homeost Agents 2010; 24(3):359-66.

ADMA, SDMA, L-ARGININE AND NITRIC OXIDE IN ALLERGIC PEDIATRIC BRONCHIAL ASTHMA

G. RICCIONI[1], V. BUCCIARELLI[2], M. VERINI[3], N.P. CONSILVIO[3], S. GALLINA[4], F. MARTINI[2], A. ACETO[2], L. SCOTTI[2] and T. BUCCIARELLI[2]

[1]Cardiology Care Unit, San Camillo de Lellis Hospital, Manfredonia, Foggia, Italy; [2]Clinical Biochemistry, Department of Biomedical Science, "G. D'Annunzio", University of Chieti, Italy; [3]Allergologic and Pneumological Service, Department of Pediatrics, University "G. D'Annunzio", University of Chieti, Italy; [4]Cardiology, Department of Neuroscience and Imaging, University G. D'Annunzio, Chieti, Italy

Received March 20, 2012 – Accepted July 3, 2012

Published data regarding asymmetric dimethylarginine (ADMA), symmetric dimethylarginine (SDMA), L-arginine (L-ARG) and nitric oxide fraction in exhaled air (FeNO) in pediatric bronchial asthma are limited. Many question remain open about plasma concentration of these substances. The aim of this study is to evaluate ADMA, SDMA, L-ARG and FeNO concentration in allergic pediatric mild asthmatic patients in respect to healthy subjects. In this case-control study 60 children (50 asthmatics and 10 healthy) underwent a complete clinical visit, baseline respiratory function, allergy tests and biochemical analyses. The statistical significance of the different concentrations between the two groups were studied using one-way analysis of variance (ANOVA). A p value < 0.05 was considered statistically significant. The mean plasma ADMA (0.58 *vs* 0.68 µmol/L), SDMA (0.40 *vs* 0.45 µmol/L) and L-ARG (52.2 *vs* 74.13 µmol/L) concentration were significantly lower (p<0.001) in the asthmatic patients in respect to healthy subjects (control group). The concentration of FeNO was significantly higher in the asthmatic subjects in respect to the control group (9.18 *vs* 4.2 µmol/L; p<0.001). Low plasma concentrations of ADMA, SDMA, L-ARG and high concentration of FeNO are associated with bronchial asthma and indicate an important role in airway disease through NO metabolism.

Nitric oxide (NO) is one of the most important mediators synthesized from L-arginine (L-ARG) by a family of NO syntheses (NOS), involved in the regulation of vascular tone, neurotransmission and mitochondrial respiration (1). The availability of NO in a given cell depends on many factors including expression and activity of several NOS (neuronal, inducible, and endothelial), abundance of NOS substrate, L-ARG, and its cofactor, tetrahydrobiopterin (THB) (2). NO production may also be regulated by endogenous NOS inhibitors, in particular asymmetric dimethylarginine (ADMA), synthesized during the methylation of protein arginine residues by protein arginine methyltransferases.

ADMA is a competitive inhibitor of NOS, decreases NO availability and is eliminated by renal excretion or metabolized by dimethylarginine dimethylaminohydrolases (DDAH) to citrulline and dimethylamine (3). Two other endogenous methylarginines are also synthesized by

Key words: asymmetric dimethylarginine, bronchial asthma, L-arginine, nitric oxide, symmetric dimethylarginine

Mailing address: Prof. Luca Scotti,
Clinical Biochemistry,
Dept. of Biomedical Science,
"G. D'Annunzio" University,
Via Dei Vestini, 13 66100 Chieti, Italy
Tel.: +3908713554721 Fax: +3908713554736
e-mail: l.scotti@unich.it

0393-974X (2012)

protein-arginine methyltransferases (PRMT): N-monomethyl-L-arginine (L-NMMA) and symmetric dimethylarginine (SDMA) (4). ADMA regulate NOS activity under physiological and pathological conditions, is metabolized by the endothelium and represent an important index of endothelial dysfunction (5). Published data regarding ADMA, SDMA, L-ARG and nitric oxide fraction in exhaled air (FeNO) in pediatric bronchial asthma are limited. The aim of this study is to evaluate ADMA, SDMA, L-ARG and FeNO concentration in mild asthmatic stable patients in respect to healthy subjects.

MATERIALS AND METHODS

Study population

Between March and July 2010 we enrolled 60 Caucasian subjects (50 asthmatics, 10 healthy; aged between 6 and 15 years), with at least a 2-year history of mild-persistent allergic bronchial asthma at Allergologic and Pneumological Service, (Department of Pediatric, University "G. D'Annunzio", Chieti, Italy). Medical and surgical history, physical condition, and medication were recorded. After inclusion, an EDTA or heparin blood sample was drawn from an indwelling arterial line for determination of ADMA, SDMA, L-ARG, and NO. Simultaneously, laboratory parameters indicating renal (creatinine, urea) and hepatic function [aspartate aminotransferase (AST), alanine aminotransferase (ALT)], complete haematocytometer exam, and baseline respiratory function test were determined. The diagnosis of allergic asthma was made by a pediatric respiratory physician and based on typical symptoms and laboratory tests, and according to ATS/ERS criteria (6). Allergic sensitization was evaluated by Skin Prick Test (SPT) and serum-specific IgE measurements for the most common respiratory allergens: Dust Mite (Dermatophagoides *Pteronyssinus*, and *Farinae*), Grass, *Parietaria*, *Artemisia Vulgaris*, Olive, Cypress, Lime, Stone, Elm, Plane, Cat and Dog dander, *Alternaria Alternata*, and *Aspergillus Fumigatus* (moulds).

Exclusion criteria for the study were: emergency treatment for an asthma exacerbation within the previous month; upper airway infections in the previous three weeks; hospitalization for asthma in the three months previous to enrolment; presence of autoimmune, hepatic or renal disorders, malabsorption, drug or alcohol-addiction. The study was approved by the Ethics Committee of the University of Chieti. Written informed consent was obtained from all parents and oral consent from all children.

Sample collection, storage and preparation

Blood samples were collected in polypropylene tubes containing 1 mM EDTA. Samples were stored in an ice box prior to centrifugation at 3000 g for 10 min at 4°C. 200 µl aliquots of plasma were transferred into Eppendorf tubes. Plasma samples were either used for extraction immediately or stored in the dark at -80°C until analysis was performed.

Biochemical analysis

The concentration of ADMA, SDMA and L-ARG were determined by high-performance liquid chromatography (HPLC) (7). In brief, solid-phase extraction on polymeric cation-exchange columns was performed after addition of monomethylarginine as the internal standard (IS). After derivatization with ortho-phtaldialdehyde reagent containing 3-mercaptopropionic acid, analytes were separated by isocratic reversed-phase HPLC with fluorescence detection (Figs. I and II).

Baseline functional respiratory test

Asthma was classified according to GINA guidelines at the beginning of the study (8). Subjects had to complete at least three forced vital capacity (FVC) to reach the ERS/ATS Guidelines (9).

Exhaled NO measurement

In all subjects FeNO value was determined with an on-line method using a single breath exhalation and a sensitive chemiluminescence assay (Ecomedics CLD 88), according to ATS-ERS procedures (10). Subjects made an inspiration of eNO-free air via a mouthpiece immediately followed by full exhalation at a constant rate (50mL/sec) for at least 5 seconds. The mean of three readings at the end of the expiration (plateau phase) was taken as the representative value for each measurements. Twelve ppb or more were considered elevated values, according to ATS-ERS criteria (11).

Statistical analysis

All values are expressed as means ± standard deviation (SD). Student's *t* test for paired data was used. Comparison between two groups was assessed using one-way analysis of variance (ANOVA) with Tukey-Kramer multiple comparison post-test. A p value <0.05 was required for statistical significance. Data were computed using the SPSS 7.0 statistical package.

RESULTS

Characteristics of subjects and lung function

Personal data and clinical details of subjects are summarized in Table I. We studied 60 subjects, 50

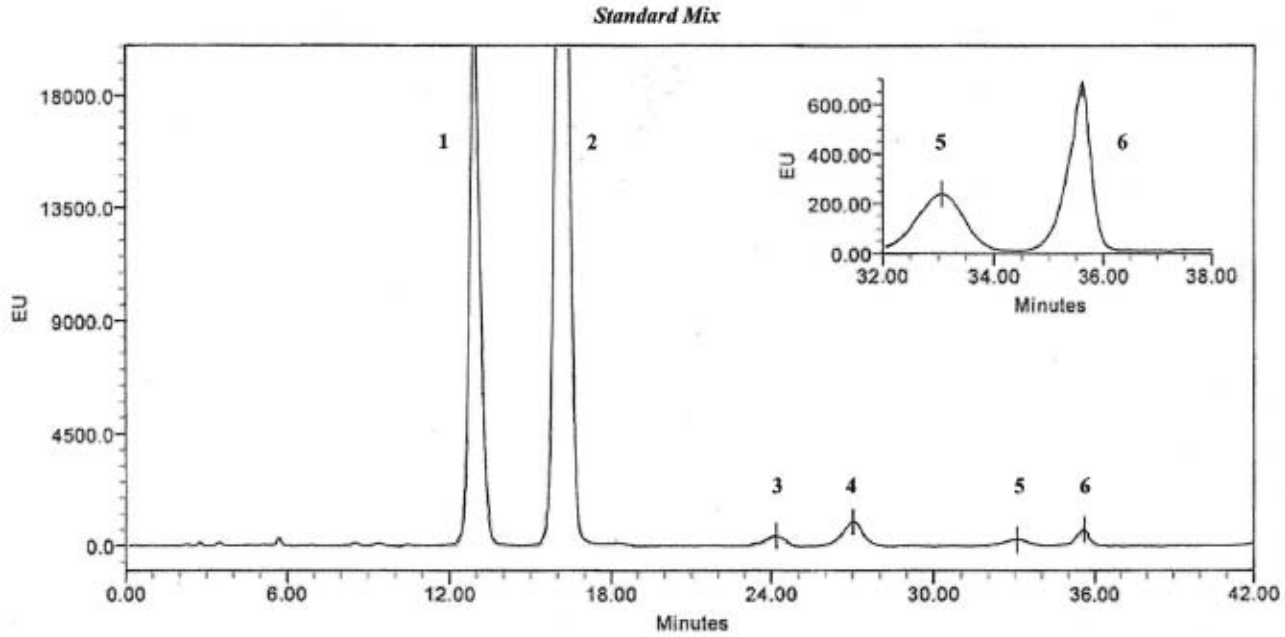

Fig. 1. *Chromatogram of combined standard containing: 50 µM citrulline, 120 µM arginine, 1.5 µM MMA (IS), 4 µM homoarginine, 1.2 µM ADMA, 1.7 µM SDMA. Peak identification: 1 citrulline; 2, arginine; 3, MMA (IS); 4, homoarginine; 5, ADMA; 6, SDMA.*

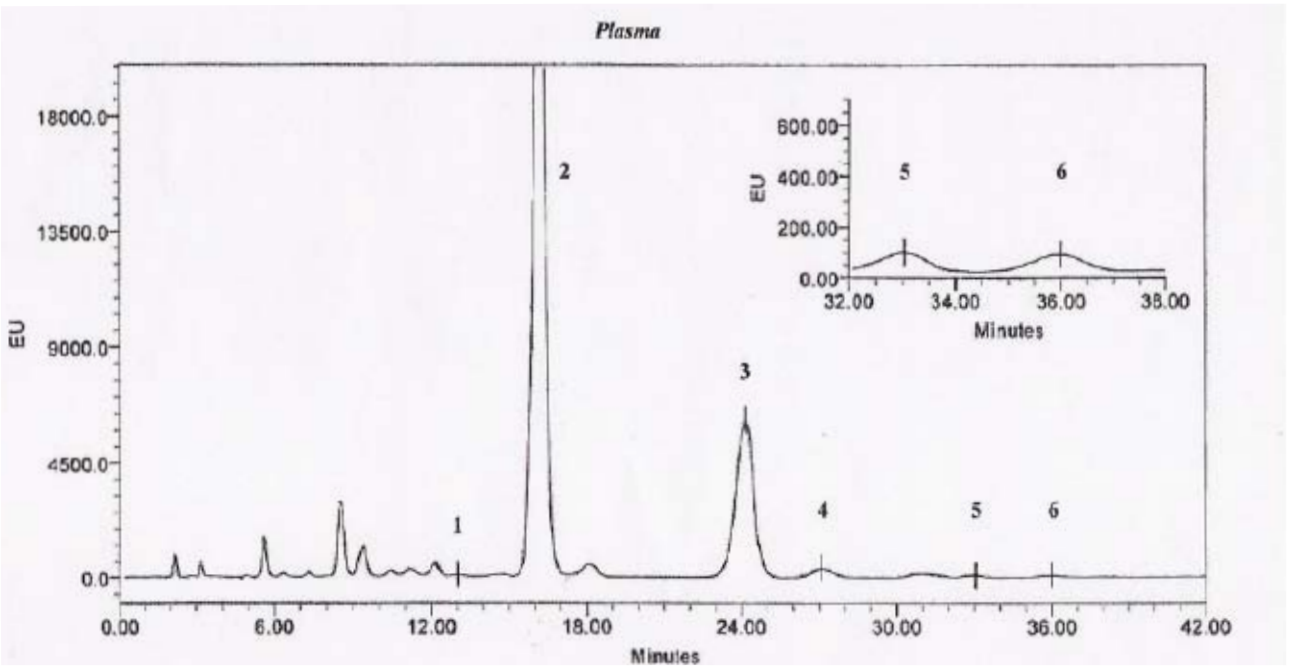

Fig. 2. *Plasma sample containing: citrulline (not quantified), 85 µM arginine, 25 µM MMA (IS), 1.6 µM homoarginine, 0,3 µM ADMA, 0,3 µM SDMA. Peak identification: 1 citrulline; 2, arginine; 3, MMA (IS); 4, homoarginine; 5, ADMA; 6, SDMA.*

asthmatics (mean age 11±2.5 yrs) and 10 healthy (mean age 11±2.1 yrs), 31 males (26 asthmatics) and 29 females (24 asthmatics). The two groups were similar for age, sex, weight, and height without significant differences. Regarding pulmonary parameters function (FEV1, PEF, and FVC) there

Table I. *Characteristic of subjects and spirometric values.*

	Asthmatics	Controls	p
No subjects	50 (26/24)	10 (5/5)	-
Sex (male/female)	26/24	5/5	ns
Age (years)	11 ± 2.5	11 ± 2.1	ns
Weight (kg)	40.7 ± 3.78	41.1 ± 4.14	ns
Height (cm)	142 ± 7.5	141 ± 6.5	ns
Spirometric values			
FEV1 (% predicted)	85 ± 12	100 ± 10.2	< 0.01
FVC (% predicted)	86 ± 11	99 ± 11.7	< 0.01
PEF (% predicted)	88 ± 10	101 ± 10.5	< 0.01

Table II. *Biochemical analyses.*

	Asthmatics	Controls	p
ADMA (μmol/L)	0.58 ± 0.05	0.68 ± 0.06	< 0.001
SDMA (μmol/L)	0.40 ± 0.03	0.45 ± 0.03	< 0.001
L-ARG (μmol/L)	52.2 ± 10.5	74.13 ± 11.2	< 0.001
FeNO (ppb)	9.18 ± 2.12	4.2 ± 1.12	< 0.001

were significant differences among the two groups (asthmatic *vs* control groups). Lung function testing values of FEV1, PEF, and FVC were > 100% of predicted vales in control group, while in the asthmatic group these values were between 80-100% of the predicted value.

Biochemical analyses

The mean plasma ADMA (0.58 *vs* 0.68 μmol/L), SDMA (0.40 *vs* 0.45 μmol/L) and L-ARG (52.2 *vs* 74.13 μmol/L) concentration were significantly lower in the asthmatic respect to control group ($p<0.001$). The concentration of FeNO was significantly higher in the asthmatic subjects in respect to the control group (9.18 *vs* 4.2 ppb; $p<0.001$) (see Table II). There was no difference in laboratory parameters indicating renal (creatinine, urea) and hepatic (AST, ALT) functions, and complete hematologic examination (hemoglobin, red and white cells, hematocrit) between the two groups.

DISCUSSION

The aim of this study is to assess ADMA, SDMA and L-ARG plasma levels in asthmatic children. A recent study reports that in lung epithelium of murine model, in human adult lung specimens, and sputum samples from pediatric patients with bronchial asthma ADMA and SDMA levels are increased 1.7- and 1.8-fold, respectively. However, these differences did not reach statistical significance for ADMA because of the relatively small sample size. The authors concluded that ADMA levels are increased in asthma and contribute to NOS-related pathophysiology (12). In our study ADMA, SDMA and L-ARG plasma levels of asthmatic children significantly decreased in respect to the control group, and FeNO level increases. ADMA and SDMA plasma values were decreased to improve NOS activity and increase NO level in systemic pathways of L-ARG. Little is known about ADMA metabolism

in the pathogenesis of bronchial asthma. ADMA and SDMA are synthesized during the methylation of protein arginine residues by S-adenosylmethionine: protein arginine methyltransferases (protein methylases, PMRT), which exist in multiple isoforms encoded by separate genes (13). We suggest that the difference of ADMA and SDMA found in sputum samples and lung epithelium derives from compensatory mechanism to eliminate local ADMA and SDMA resulting from epithelial injury and as another physiological bronchial excretion way (14).

Arginine (ARG) is one of the 20 amino acids (AA) found in proteins and synthesized by human cells. However, ARG is also the substrate for a series of reactions leading to the synthesis of other AA and is an obligatory substrate for two enzymes with diverging actions, arginases and NOS, giving origin to urea and NO, respectively. Intracellular L-ARG levels are regulated by at least three distinct mechanisms: (a) cellular uptake by cationic amino acid (CAT) transporters, (b) metabolism NOS and arginases, and (c) recycling from L-citrulline. Changes in L-ARG homeostasis may contribute to asthma disease by increased production of NO, a potent vasodilator when produced by eNOS. Airway inflammation is associated with an enhanced expression of iNOS (15, 16).

Measurement of FeNO is a very useful non-invasive method in the treatment monitoring of asthma (11, 16). A large body of scientific literature suggests that high NO plasma levels correlate to some pulmonary diseases, such as asthma, and corticosteroid treatment decreases NO levels in exacerbation asthma cases (11, 17). Published studies have shown a significant correlation between FeNO and respiratory symptoms, bronchial hyperresponsiveness (BHR), and airways inflammation (18-21).

Recent studies revealed that FeNO is a potentially useful measure to evaluate the role of airways inflammation in asthma, as it represents the forerunner of an important event in asthma: the remodeling of bronchial airways (22). Increased FeNO value and decreased L-ARG plasma level, indeed confirm that L-ARG is metabolized by NOS to form NO and produce Ng-hydroxy-L-ARG, which inhibits the arginase pathway (23-25).

Our findings reveal that L-ARG, ADMA, SDMA and NO in exhaled air are correlated with airway inflammatory diseases. Thus, further studies are desirable to examine the role of L-ARG, ADMA, SDMA plasma levels and exhaled NO.

REFERENCES

1. Christopherson KS, Bredt DS. Nitric oxide in excitable tissues: physiological roles and disease. J Clin Invest 1997; 100:2424-9.
2. Moncada S, Higgs EA. The discovery of nitric oxide and its role in vascular biology. Br J Pharmacol 2006; 147:193-201.
3. Blackwell S. The biochemistry, measurement and current clinical significance of asymmetric dimethylarginine. Ann Clin Biochem 2010; 47:17-28.
4. Pope AJ, Karuppiah K, Cardounel AJ. Role of the PRMT-DDAH-ADMA axis in the regulation of endothelial nitric oxide production. Pharmacol Res 2009; 60:461-5.
5. Pope AJ, Karrupiah K, Kearns PN, Xia Y, Cardounel AJ. Role of dimethylarginine dimethylaminohydrolases in the regulation of endothelial nitric oxide production. J Biol Chem 2009; 284:35338-47.
6. National Asthma Education and Prevention Program, "NAEPP expert panel report guidelines for the diagnosis and management of asthma-update on selected topics 2002"; National Institute of Health, 2006.
7. Teerlink T, Nijveldt RJ, de Jong S, van Leeuwen PA. Determination of arginine, asymmetric dimethylarginine, and symmetric dimethylarginine in human plasma and other biological samples by high-performance liquid chromatography. Anal Biochem 2002; 303:131-7.
8. GINA World Report 2006, "Global Strategy for Asthma Management and Prevention. Available at http://www.ginasma.it/ or http://www.ginasthma.com.
9. Laszlo G. Standardization of lung function testing: helpful guidance from the ATS/ERS Task Force. Thorax 2006; 61:744-6.
10. American Thoracic Society; European Respiratory Society. ATS/ERS recommendations for standardized procedures for the online and offline measurement of exhaled lower respiratory nitric oxide and nasal

nitric oxide, 2005. Am J Respir Crit Care Med 2005; 171:912-30.
11. Baraldi E, de Jongste JC, Gaston B, et al. Measurement of exhaled nitric oxide in children, 2001. Eur Respir J 2002; 20:223-37
12. Sott JA, North ML, Rafii M, Huang H, Pencharz P, Subbarao P, Belik J, Grasemann H. Asymmetric dimethylarginine is increased in asthma. Am J Respir Crit Care Med 2011; 184:779-85.
13. Vallance P, Leiper J. Cardiovascular biology of the symmetric dymethyarginine: dimethylarginine dimethyaminohydrolase pathway. Arterioscl Thromb Vasc Biol 2004; 24:1023-30.
14. Zakrzewicz D, Eickelberg O. From arghinine methylation to ADMA: a novel mechanism with therapeutic potential in chronic lung disease. BMC Pulmonary Medicine 2009; 9:5.
15. Kharitonov SA, Yates D, Robbins RA, Logan-Sinclair R, Shinebourne EA, Barnes PJ. Increased nitric oxide in exhaled air of asthmatic patients. Lancet 1994; 343:133-5.
16. Lane C, Knight D, Burgess S, Franklin P, Horak F, Legg J, Moeller A, Stick S. Epithelial inducible nitric oxide synthase activity is the major determinant of nitric oxide concentration in exhaled breath. Thorax 2004; 59:757-60.
17. Baraldi E, Azzolin NM, Zanconato S, Dario C, Zacchello F. Corticosteroids decrease exhaled nitric oxide in children with acute asthma. J Pediatr 1997; 131:381-5.
18. Steerenberg PA, Janssen NAH, de Meer G, et al. Relationship between exhaled NO, respiratory symptoms, lung function, bronchial hyperresponsiveness, and blood eosinophilia in school children. Thorax 2003; 58:242-5.
19. Miraglia Del Giudice M, Pedullà M, et al. Neutrophilic cells in sputum of allergic asthma children. Eur J Inflamm 2010; 8:151-6.
20. Franklin PJ, Turner SW, Le Sou¨ef PN, Stick SM. Exhaled nitric oxide and asthma: complex interactions between atopy, airway responsiveness, and symptoms in a community population of children. Thorax 2003; 58:1048-52.
21. Riccioni G, Prencipe GA, Bucciarelli V, et al. Left ventricular noncompaction cardiomyopathy. J Biol Regul Homeost Agents 2011; 25(4):679-81.
22. Rosato E, Carello R, Gabriele I, et al. Recurrent infections in children with nickel allergic contact dermatitis. J Biol Regul Homeost Agents 2011; 25(4):661-5.
23. Barberi S, Villa MP, Pajno GB, et al. Immune response to sublingual immunotherapy in children allergic to mites. J Biol Regul Homeost Agents 2011; 25(4):627-34.
24. Angelini A, Centurione L, Sancilio S, et al. The effect of the plasticizer diethylhexyl phthalate on transport activity and expression of P-glycoprotein in parental and doxo-resistant human sarcoma cell lines. J Biol Regul Homeost Agents 2011; 25(2):203-11.
25. Aslani S, Hossein-Nezhad A, Mirzaei K, et al. Tandem repeats of the CATT element of macrophage migration inhibitory factor gene may predict gestational diabetes mellitus severity. Eur J Inflamm 2011; 9:193-7.

LETTER TO THE EDITOR

PRION SEARCH AND CELLULAR PRION PROTEIN EXPRESSION IN STRANDED DOLPHINS

G. DI GUARDO[1], C. COCUMELLI[2], R. MEOLI[2], K. BARBARO[2], G. TERRACCIANO[3], C.E. DI FRANCESCO[1], S. MAZZARIOL[4] and C. ELENI[2]

[1]Department of Comparative Biomedical Sciences, University of Teramo, Teramo, Italy; [2]Istituto Zooprofilattico Sperimentale (IZS) delle Regioni Lazio e Toscana, Rome, Italy; [3]IZS delle Regioni Lazio e Toscana, Pisa, Italy; [4]Department of Comparative Biomedicine and Food Science, University of Padova, AGRIPOLIS, Legnaro, Padua, Italy

Received May 18, 2012 – Accepted July 18, 2012

The recent description of a prion disease (PD) case in a free-ranging bottlenose dolphin (*Tursiops truncatus*) prompted us to carry out an extensive search for the "disease-associated" isoform (PrP^{Sc}) of the cellular prion protein (PrP^{C}) in the brain and in a range of lymphoid tissues from 23 striped dolphins (*Stenella coeruleoalba*), 5 bottlenose dolphins and 2 Risso's dolphins (*Grampus griseus*) found stranded between 2007 and 2012 along the Italian coastline. Three striped dolphins and one bottlenose dolphin showed microscopic lesions of encephalitis, with no evidence of spongiform brain lesions being detected in any of the 30 free-ranging cetaceans investigated herein. Nevertheless, we could still observe a prominent PrP^{C} immunoreactivity in the brain as well as in lymphoid tissues from these dolphins. Although immunohistochemical and Western blot investigations yielded negative results for PrP^{Sc} deposition in all tissues from the dolphins under study, the reported occurrence of a spontaneous PD case in a wild dolphin is an intriguing issue and a matter of concern for both prion biology and intra/inter-species transmissibility, as well as for cetacean conservation medicine.

The recent description of a naturally occurring prion disease (PD), or transmissible spongiform encephalopathy (TSE), in a free-ranging bottlenose dolphin (*Tursiops truncatus*) (1) is an intriguing

finding and a matter of concern for a number of reasons. First of all, apart from this being the first report of a spontaneous PD condition in any cetacean and, more in general, in any aquatic mammal, it should be also emphasized that the prion protein (PrP) gene (*PRNP*) sequence from eight cetacean species has previously been shown to be very close to that of cattle, sheep and goat (2), thus providing additional support to the existence of a common ancestor for ruminants and cetaceans (3).

Secondly, on the basis of the high sequence homology between cetacean *PRNP* gene and that of the aforementioned ungulate species, which may naturally develop bovine spongiform encephalopathy (BSE) and scrapie (4), susceptibility to and occurrence of TSEs in cetaceans have been deemed plausible (2). Additionally, one of the most, if not even the most intriguing feature of a TSE-like condition in a free-living cetacean refers to the route(s) through which such prion infection may have been acquired by the animal under study (1).

Following the description of this really

Key words: *prions, prion diseases, transmissible spongiform encephalopathies, dolphins, cetaceans*

Mailing address: Prof. Giovanni Di Guardo, *DVM, Dipl. ECVP*,
Department of Comparative Biomedical Sciences,
University of Teramo,
Piazza Aldo Moro, 45 64100 Teramo, Italy
Tel.: +39 0861 266933 Fax: +39 0861 266865
e-mail: gdiguardo@unite.it

0393-974X (2012)

impressive PD case in a wild dolphin (1), we decided to extensively investigate our collection of tissue specimens from stranded cetaceans, in order to properly assess whether any evidence of PrP^{Sc} deposition occurred within these tissues.

To accomplish this, we selected a total of 30 free-ranging odontocete cetaceans found stranded between 2007 and 2012 along the Italian coastline, 23 of which were striped dolphins (*Stenella coeruleoalba*), 5 of them being bottlenose dolphins and the remaining 2 being Risso's dolphins (*Grampus griseus*).

Three striped dolphins and one bottlenose dolphin showed microscopic lesions of encephalitis, with no evidence of spongiform brain lesions being detected in any of the 30 wild cetaceans investigated herein. More in detail, these three striped dolphins exhibited a multifocal, subacute to chronic, non-suppurative morbilliviral encephalitis, while the bottlenose dolphin showed a multifocal, non-suppurative encephalitis (secondary to concurrent *Morbillivirus* and *Toxoplasma gondii* infection), associated with a severe, *Staphylococcus aureus*-induced purulent encephalitis.

Paraffin-embedded sections, along with homogenates of the brain and a range of lymphoid tissues (spleen, mesenteric, pulmonary and prescapular lymph nodes) from the above cetaceans, were submitted to an in-depth search for the "disease-associated" isoform (PrP^{Sc}) of the cellular prion protein (PrP^{C}) by means of *ad hoc* immunohistochemistry (IHC) and Western blot (WB) investigations. More in detail, F89 (F89/160.1.5) and F99 (F99/97.6.1), two commercially available (*VMRD,* Inc., Pullman, WA, USA) anti-PrP mouse monoclonal antibodies (mAbs), were utilized in parallel for both IHC and WB analyses, with the 6H4 murine mAb (Prionics AG, Switzerland) being additionally employed for WB investigations.

Furthermore, on paraffin-embedded sections obtained from well-preserved tissue samples (brain, spleen, mesenteric, pulmonary and prescapular lymph nodes) of 10 striped dolphins and 3 bottlenose dolphins, we also tried to evaluate, by means of IHC, the expression pattern(s) of PrP^{C} within such tissues. Indeed, the preservation status represents a matter of crucial concern in stranded cetaceans, the corpses of which are frequently found in advanced *post-mortem* autolysis, a condition which may dramatically

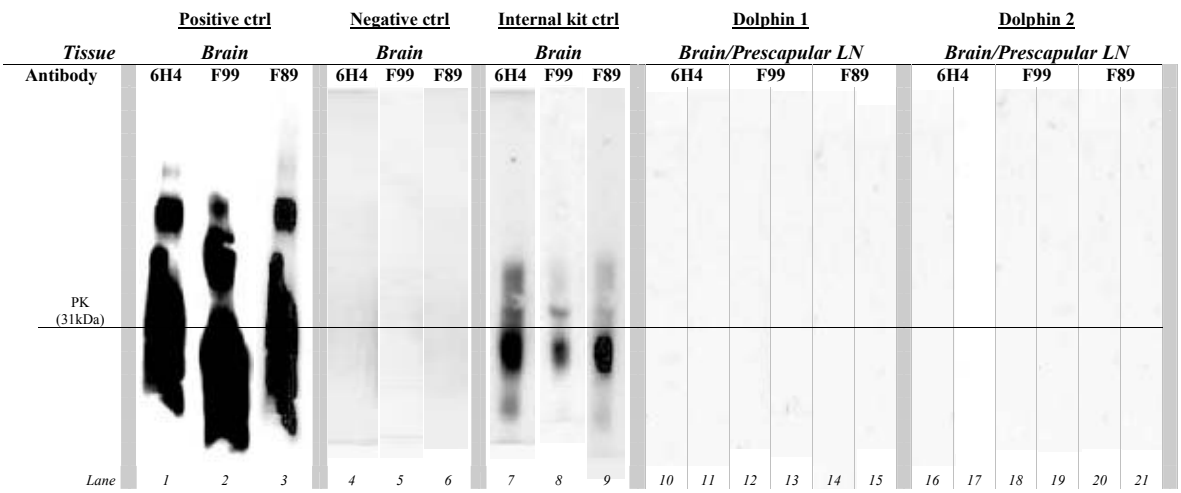

Fig. 1. *Results of Western blot (WB) investigations for PrP^{Sc} deposition in tissues (brain and lymphoid tissues) from stranded cetaceans, with WB analyses having been carried out by means of 6H4, F99 (F99/97.6.1) and F89 (F89/160.1.5) anti-PrP mouse monoclonal antibodies (mAbs). Molecular weight (MW) marker: Proteinase K (PK).* ***Lanes 1-3****: Positive control (ctrl) brain from a scrapie-affected sheep.* ***Lanes 4-6****: Negative ctrl brain from a scrapie-uninfected sheep.* ***Lanes 7-9****: Internal kit positive ctrl brain sample (Prionics AG, Switzerland).* ***Lanes 10, 12, 14****: Striped dolphin (Stenella coeruleoalba). Brain tissue samples with no evidence of PrP^{Sc} deposition.* ***Lanes 11, 13, 15****: Striped dolphin (S. coeruleoalba); same animal as in lanes 10, 12, 14. Prescapular lymph node (LN) tissue samples with no evidence of PrP^{Sc} deposition.* ***Lanes 16, 18, 20****: Striped dolphin (S. coeruleoalba). Brain tissue samples from another animal showing no evidence of PrP^{Sc} deposition.* ***Lanes 17, 19, 21****: Striped dolphin (S. coeruleoalba); same animal as in lanes 16, 18, 20. Prescapular LN tissue samples with no evidence of PrP^{Sc} deposition.*

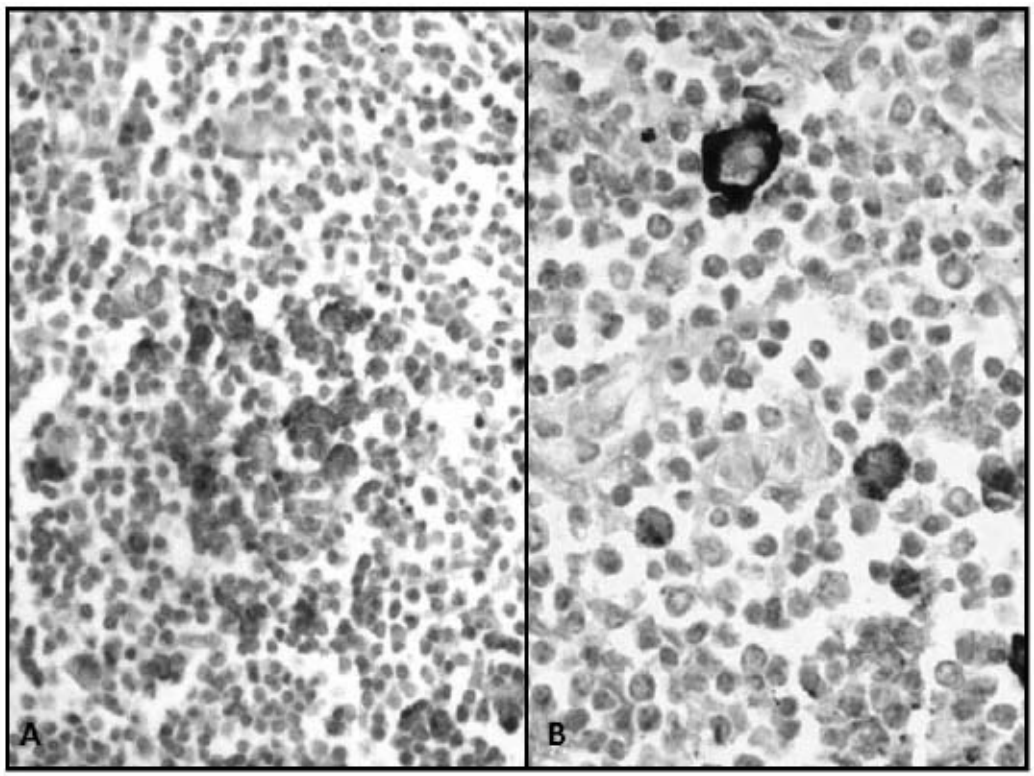

Fig. 2. *Mesenteric LN from a striped dolphin (S. coeruleoalba). A prominent PrP^C immunoreactivity (IR) is apparent in cellular elements which are topographically and morphologically consistent with follicular dendritic cells (FDCs) residing in secondary lymphoid organs and tissues (panel **A**). Prescapular LN from another striped dolphin (S. coeruleoalba). A strong PrP^C IR pattern is shown on the membrane and, to a lesser extent, within the cytoplasmic compartment of FDC-like cells (panel **B**). Final magnification: x250 (x20 objective, panel A); x500 (x40 objective, panel B). PrP immunohistochemistry (IHC) with the F99 mAb. Mayer's haematoxylin counterstain.*

affect, in its turn, the results of the evaluation of PrP^C expression within their tissues, provided that PrP^C - differently from PrP^{Sc} - is very sensitive to proteolytic digestion (4).

All IHC and WB analyses which were performed, albeit extensive, showed no evidence of PrP^{Sc} deposition in all tissues from the dolphins under study (Fig. 1). Interestingly enough, however, we were able to document a prominent PrP^C immunoreactivity (IR) at the level of the cerebral parenchyma and of the lymphoid tissues investigated herein, with such PrP^C IR pattern being particularly evident along neuronal axons and dendrites from many brain regions, as well as on the membrane and - to a lesser degree - inside the cytoplasm of cells which appeared to be topographically and morphologically consistent with follicular dendritic cells (FDCs) residing in secondary lymphoid tissues (Fig. 2, panels A and B).

On the basis of the results obtained herein, no evidence of PrP^{Sc} deposition was found in any of the stranded cetaceans under study. Differently from the PD case reported in a wild dolphin (1), however, none of the 30 animals included in our survey showed any evidence of spongiform degeneration inside their brain. In this respect, while we feel it would be important to add prions and TSE-like diseases to the list of neurotropic pathogens and neurological conditions affecting free-ranging cetaceans, we also believe that the prominent PrP^C IR detected within the brain and in

lymphoid tissues from the dolphins investigated herein provides a solid ground of biological plausibility for prion colonization of the above cetacean tissues. This is additionally underscored by

the finding of a PrP^C expression pattern which was topographically and morphologically consistent with that of FDCs. As a matter of fact, new insights have been recently gained into FDC role and biological significance (5), with FDCs residing inside host's lymphoid tissues being also of crucial relevance for prion replication and for the early pathogenesis of natural and experimental scrapie (6-8), which is unanimously considered to be the PD, or TSE "prototype" (9).

As previously mentioned, one of the most, if not even the most challenging feature of a PD condition in free-living cetaceans refers to the route(s) through which infection may be acquired. In this respect, whenever a "sporadic" form of PD developed in a dolphin, similarly to what has been known for over 90 years in humans (4), this would probably lead to a different "scenario" from that which we would face in the case of wild dolphins being found to be susceptible to an "infectious" PD condition, as in the well-documented example of sheep scrapie (4). In fact, this would represent an additional threat to cetaceans, the health and conservation status of which are dramatically impacted nowadays by many other biological and anthropogenic *noxae* (10). With reference to the above, further issues of concern regard the animal source(s) of infection and its putative "land-to-sea" flow, as already hypothesized for *Toxoplasma gondii* infection in sea otters (*Enhydra lutris*) and bottlenose dolphins (10), or the alternative existence of an "exclusively marine" cycle of infection. Finally, a particularly relevant issue is that addressing the "strategies" adopted by dolphin prions for their persistence within the marine environment, considering their progressive dilution and dispersal in sea water.

In conclusion, despite the negative results of our study, we still believe that the documented occurrence of a spontaneous TSE-like condition in a wild dolphin (1) is an intriguing issue and a matter of concern for both prion biology and intra/inter-species transmissibility, as well as for cetacean conservation medicine.

ACKNOWLEDGEMENTS

The authors wish to thank Prof. Adriano Aguzzi for critical reading and for his highly valuable comments and suggestions on this manuscript.

REFERENCES

1. Camacho M, Morales-Schehing D, Fernandez-Borges N, Castilla J, Cowan D, Soto C. Prions in the ocean: A natural case of prion disease in dolphins. In Proceedings of PRION 2011 International Conference, Montreal, Canada, 16-19 May 2011; p. 33.
2. Acutis PL, Peletto S, Greco E, et al. Comparative analysis of the prion protein (PrP) gene in cetacean species. Gene 2007; 392:230-38.
3. Milinkovitch MC. Even-toed fingerprints on whale ancestry. Nature 1997; 388:622-23.
4. Aguzzi A, Calella AM. Prions: Protein aggregation and infectious diseases. Physiol Rev 2009; 89:1105-52.
5. Aguzzi A, Krautler NJ. Characterizing follicular dendritic cells: A progress report. Eur J Immunol 2010; 40:2134-38.
6. Aguzzi A, Heikenwalder M. Pathogenesis of prion diseases: Current status and future outlook. Nat Rev Microbiol 2006; 4:765-75.
7. Mabbott NA, MacPherson GG. Prions and their lethal journey to the brain. Nat Rev Microbiol 2006; 4:201-11.
8. McCulloch L, Brown KL, Bradford BM, et al. Follicular dendritic cell-specific prion protein (PrP) expression alone is sufficient to sustain prion infection in the spleen. Plos Pathog 2011; 7(12):e1002402.
9. Prusiner SB. Prions. Proc Natl Acad Sci USA 1998; 95:13363-83.
10. Van Bressem MF, Raga JA, Di Guardo G, et al. Emerging infectious diseases in cetaceans worldwide and the possible role of environmental stressors. Dis Aquat Organ 2009; 86:143-57.

LETTER TO THE EDITOR

SOLITARY PLASMACYTOMA OF THE TONSILLAR SITE ASSOCIATED WITH ACTINOMYCES INFECTION: THE POSSIBLE ROLE OF IL-6

R. ZAPPACOSTA[1], S. ROSINI[1], F.B. AIELLO[2], A. RULLO[2], A. CROCE[3], G. LATTANZIO[2] and P. VIOLA[2]

[1]Cytopathology Unit, Biomedical Sciences Department of "G. d'Annunzio" University of Chieti-Pescara, Italy; [2]Surgical Pathology Unit, "G. d'Annunzio" University of Chieti-Pescara, Chieti, Italy; [3]Otorhinolaryngology Unit, "SS Annunziata" Hospital, Chieti, Italy

ExtraMedullary Plasmacytoma (EMP) is a rare plasma cell tumor. It can occur in the upper aerodigestive tract and presents as a large nodule causing local compressive symptoms. A 79-year old woman presented to Otorhinolaryngology Department with progressive hearing loss and no other symptoms. Following PET/TC examination due to the suspicion of a lymphoproliferative disease, the patient underwent tonsillectomy and the diagnosis of solitary EMP was formulated. In addition to that, the histological examination of the tonsillar tissue revealed large colonies of filamentous bacteria, showing abundant sulphur granules and Splendore-Hoeppli phenomenon; these evidences indicating the presence of a chronic Actinomyces infection. Immunohistochemical analysis demonstrated a marked IL-6 immunoreactivity of the neoplastic plasma cells. Interestingly, a marked IL-6 immunoreactivity was also found in the tissue surrounding the Actinomyces colonies. In the present study we report for the first time a solitary EMP associated with Actinomycosis. It is tempting to speculate that the unsuspected and untreated Actinomyces infection, through chronic IL-6 production, could contribute to the neoplastic transformation of plasma cells.

A 79-year old woman was referred to the Otorhinonolaryngology outpatient department with progressive hearing loss. The patient reported no other symptoms. The neck did not display asymmetry and there were no palpable lymphadenopathy. Oropharyngeal examination showed a large, brownish, irregular mass of approximately 1 cm in the largest dimension. The mass appeared to be arising from the left palatine tonsil and displaced the tonsil medially, but it seem to be contained within the organ. The nodule was mobile during respiration or deglutition. On palpation the mass was soft and not tender. [^{18}F] Fluorodeoxyglucose Positron Emission Tomography scanners with fused Computed Tomographic (^{18}F-FDG PET/TC) examination showed an increased left subcarinal uptake of the radio nucleoside. This picture supported the clinical diagnosis of primary tonsillar neoplasia, likely of a lymphoprolferative nature. The patient, underwent left-side tonsillectomy.

Grossly, the left tonsil consisted of an oval mass of lymphoid tissue measuring 2.6 x 1.6 x 0.9 cm. Cut section revealed a focal dark area measuring 0.8 cm in its maximum diameter. Histopathological analysis of the tonsillar tissue showed sub-epithelial lymphoid aggregates composed of sheets of plasma cells, with varying grades of maturity, in a context of a sparse and fine reticular stroma. In the dark area a high number of atypical plasma cells were observed. The plasma cells that infiltrated the tonsillar tissue, were

Key words: tonsillar neoplasia, extramedullary plasmacytoma, actinomycosis, inflammation, IL-6

Mailing address: Roberta Zappacosta, MD
Cytopathology Unit,
Biomedical Sciences Department,
"G. d'Annunzio" University of Chieti-Pescara,
Via dei Vestini, 66100 Chieti, Italy
Tel.: +39 0871 357403/04 Fax: +39 0871 357975
e-mail: zappacosta2@hotmail.com

0393-974X (2012)

DISCLOSURE: ALL AUTHORS REPORT NO CONFLICTS OF INTEREST RELEVANT TO THIS ARTICLE.

characterized by prominent and eccentric nucleoli with "spoke wheel" chromatin, and by abundant basophilic cytoplasm. Bi-tri-nucleated plasma cells and mitotic figures were also observed (Fig. 1A).

In addition to that, large colonies of filamentous bacteria were noted; they were located within tonsillar crypts (Fig. 1B), very close to the plasmacytoma (Fig. 1C). Colonies showed abundant sulphur granules, and were surrounded by a peripheral darkly staining eosinophilic rim, consisting of polymorphonuclear cells, cell debris and fibrosis (Splendore-Hoeppli phenomenon) (Fig. 1D). These evidences indicate a chronic infection by Actinomyces.

Tumor cells showed positive immunostaining for CD138 (plasma cell marker) (Fig. 1E), CD56 (Fig. 1F) and Lambda light chain (Fig. 1G). They were negative for CD20, CD3, CD15, CD30, CD68, and Kappa light chain immunostaining. The proliferation index, assessed by MIB-1 antibody, was less than 1%. The neoplastic plasma cells were also IL-6 immunoreactive (Fig. 1H). An intense IL-6 immunoreactivity was also present around the Actinomyces colonies (Fig. 1I). On the contrary, normal and non inflamed tonsil didn't show IL-6 positivity (negative control**,** data not shown**)**. To investigate whether the Actinomyces infection was immunoreactive for IL-6 in the absence of neoplastic plasma cells, IL-6 immunostaining was performed on true vocal cord tissue affected by Actinomycosis. We found a marked IL-6 immunoreactivity in the tissue surrounding the bacterial colonies (Splendore-Hoeppli phenomenon) (Figure, L). Some mononuclear cells within the inflammatory infiltrate in the close proximity of the colonies were also IL-6 positive (data not shown).

The patient was subsequently referred to the Haematological Department for further workup**,** in order to rule out multiple myeloma (MM) or disseminated disease entirely. Full blood count, urea, calcium, creatine, and β-2-microglobulin were all within normal ranges. No histological evidence of bone marrow involvement on biopsy, or distant bone lesions on radiological skeletal survey were detected. In serum protein electrophoresis, a monoclonal IgG Lambda light chain peak was detected. Urine analysis showed a high level of lambda light chain, but there was no evidence of Bence-Jones protein. After ruling out MM, the patient was diagnosed as having solitary tonsillar EMP.

Our patients did not require adjuvant radiotherapy, since excision of the entire neoplastic lesion was made. Three months after surgery the patient remained well. Repeated immunoglobulin assay showed renormalization of monoclonal IgG and light chain levels. There was no evidence of multiple myeloma on bone marrow biopsy and no lytic lesions on skeletal survey.

DISCUSSION

Plasma cell tumor (PTC) or Plasmacytoma can occur either in bone (medullary plasmacytoma) or in the soft tissue (extra medullary plasmacytoma (EMP). EMP may present with solitary or multiple lesions. The systemic disease characterized by osseous multiple lesions (multiple myeloma) represents the commonest lesion, and accounts for about 90% of all plasma cell malignancies. In contrast, EMPs are rare; they constitute approximately 4% of all plasma cell neoplasms (1, 2). Solitary EMP typically presents as a well-localized submucosal mass, sometimes with polypoidal configuration (3). Approximately 80% of EMP develop in the upper aerodigestive tract, with the most common sites being in the nasal cavity, paranasal sinus and nasopharinx (4). Tonsillar EMP is rare (about 1% of EMPs), and few cases had been reported in the literature (5, 6). The diagnosis of solitary EMP is based on the detection of a plasma cell tumor in an extramedullary site, on the absence of multiple myeloma on bone marrow examination, radiography, and on the appropriate studies of blood and urine. Solitary EMP is efficiently managed with radiotherapy, due to its radiosensitivity. The role of surgery is usually confined to the excision of small and resectable tumors, or to local-regional recurrences. If a complete surgical resection is obtained, no adjuvant radiotherapy is required. On the other hand, regular monitoring must be warranted, in order to exclude local recurrence and the development of multiple myeloma, which had been observed in about 20% of the cases (4).

PTC development presents special conceptual problems in oncology, since it represents neoplastic derivatives of a terminally differentiated cell in the B-lymphocyte lineage, the plasma cell. It's generally thought that plasma cells have only a limited number

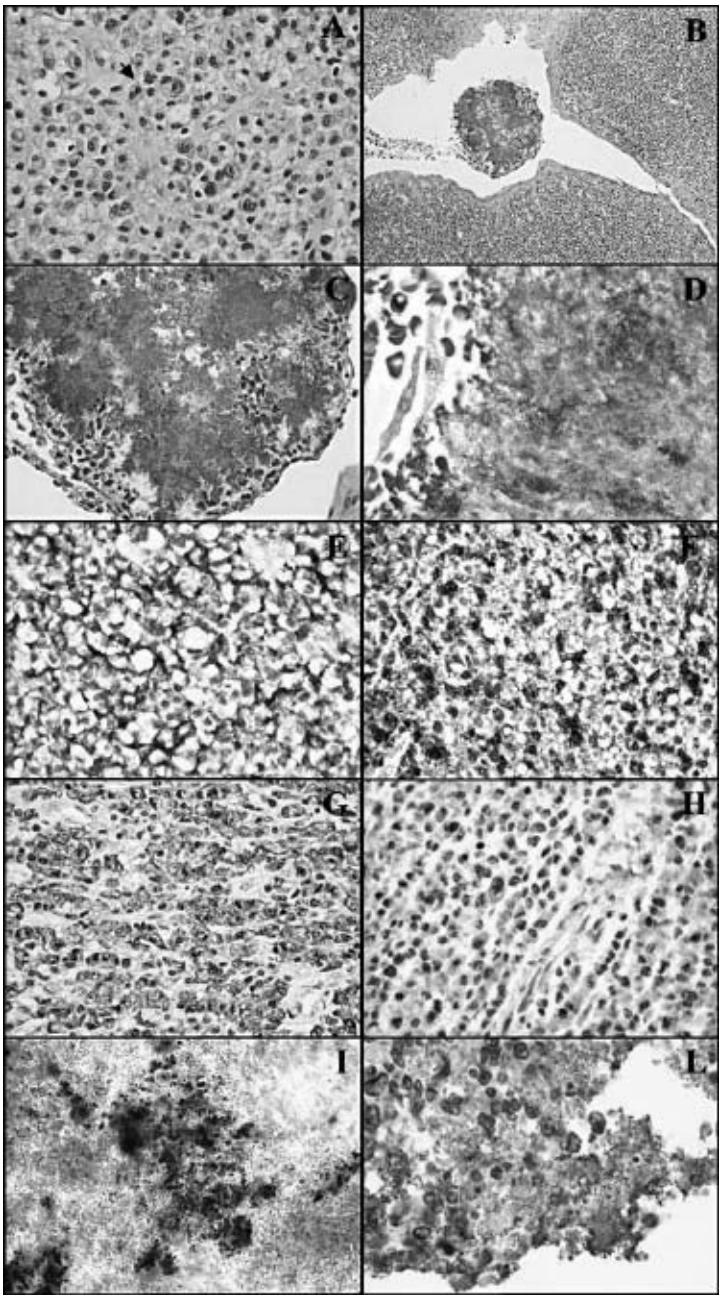

Fig. 1. *Tonsillar extramedullary plasmacytoma. **A**) diffuse atypical plasma cells with eccentric nuclei, prominent nucleoli with "spoke wheel" chromatin, and abundant basophilic cytoplasm. Black arrow: atypical binucleated cells (original magnification x63). Actinomyces colonies within tonsillar crypts (**B**, original magnifications x250) and in proximity of plasmacytoma [(**C**) original magnifications x100] showed typical sulfur granuli, and were surrounded by an eosinophilic peripheral rim, consisting of inflammatory cells, cell debris and fibrosis (**D**, original magnification x630). Immunohistochemical analysis of tonsillar tissue (streptavidine-biotin-peroxidase) showed diffuse CD138 positivity (**E**, original magnification x40), CD56 positivity (**F**, original magnifications x40) and lambda light chain immunoreactivity (**G**, original magnifications x20). Tonsillar EMP cells revealed IL-6 immunoreactivity too (**H**, original magnifications x20). In addition, IL-6 immunoreactivity was seen in the tissue surrounding the Actinomyces colonies (**I**, original magnifications x100). True vocal cord demonstrated Actinomyces colonies and marked IL-6 immunoreactivity in the tissue surrounding the bacterial colonies (Splendore-Hoeppli phenomenon) (L, original magnifications x100).*

of cell divisions before they permanently exit the cell cycle. Thus, plasma cells could be a poor target for neoplastic development. However, PTC occurs in different mammalian species, including humans. A critical point in physiological plasma cell formation is the B lymphocyte-plasma cell (B:PC) transition or differentiation. B:PC transition is associated with multiple changes in gene activity and cell-surface phenotype, such as the down regulation of the antigen binding receptor (BCR) and the major histocompatibility complex class II receptor.

A large number of models for PTC development have been generated. Among these, the most important models are those depending upon naturally arising mutagenic changes (such as pristane-induced PTC), those in which PTC is associated with oncogene activation, those of resistance to apoptosis and those of release growth factors such as interleukin-6 (IL-6) (7). PTC development could start with the extension of the longevity of a B-cell clone through the interaction with antigens (7). Kishimoto et al., for the first time in the '70 isolated and characterized B-cell stimulating factor-2 (BSF-2), also named IL-6 (8). Subsequently, many studies demonstrated a primary role of IL-6 in the development of B-cell neoplasia (9-11). IL-6 is able to regulate the final differentiation of B cells into antibody secreting plasma cells (8). *In vitro* IL-6 stimulates normal B-cells, induces plasma cell differentiation and survival/proliferation of PTCs (8).

The frequent localization of EMP in the upper aerodigestive tract has led to the hypothesis that chronic stimulation (by bacteria, viruses or chemical irritants), may promote tumorigenesis. Lattanzio et al. provided evidence for a role of IL-6 in PTC development, along with a status of chronic inflammation (12). IL-6 deficient mice did not develop B-cell tumors when infected with myc/raf-expressing retrovirus (12).

In early studies it was shown that sonic lysates of *Actinomyces viscosus* displayed mitogenic and adjuvant activities on polyclonal B cells *in vitro* (13).

Actinomyces are filamentous, Gram-positive, anaerobic bacteria, which are part of the normal oral flora. They can be found in calculus, periodontal pockets, carious lesions and oral mucosal surfaces and do not cause any pathology as long as they stay on the surface of the mucosa. If the integrity of the mucosal barrier is compromised, they can initiate a prolonged chronic inflammatory process. It is difficult to obtain Actinomyces cultures, due to the need to rely on a rapid transportation to a specialized laboratory, and to the necessity of immediate incubation in anaerobic environment. Thus, the diagnosis is more often obtained by detecting the typical colonies and "sulphur granules" in histological specimens (14-16). IL-6 mRNA level was increased when human immortalized oral epithelial cells were cultured with exudates from periradicular granuloma of *Actinomyces Viscosus* and *Israelii*, compared with untreated epithelial cells (17, 18). In addition to that, using a multiplexed beadlyte kit, Peyyala and collaborators demonstrated that biofilms of Actinomyces Naeslundii induced high levels of IL-6 in a human oral epithelial cell line (19). In supporting these evidences, we found a clear IL-6 positivity in Actinomyces granuloma arising from other side than tonsil (true vocal cord).

In this context, the adjuvant and mitogenic activity of Actinomyces on B-cells may be partly mediated by their capability to induce IL-6 (20). In other terms, Actinomyces colonies in the tonsillar site may influence B cell proliferation and differentiation through IL-6 production. For this reason the simultaneous presence of Actinomycosis and of a solitary EMP of the tonsillar site is interesting. There is no doubt that specific bacteria and parasites can promote cancer development through different and complex mechanisms. However, clinical evidences regarding the association of each pathogen with malignant diseases vary significantly. For some bacterial species this relationship is well established (21-22), whereas for other pathogens it is still lacking. Unsuspected and untreated Actinomyces infection, through IL-6 production, could promote the transformation process which leads to PTC.

REFERENCES

1. Sakai Y, Ikeya J, Morita I, Sato K. Extramedullary plasmacytoma of the tonsil diagnosed by fine-needle aspiration cytology. Ann Diagn Pathol 2008; 12:41-43.
2. Dores MG, Landgren O, McGlynnK A, Curtis RE, Linet MS, Devesa SS. Plasmacytoma of bone, extramedullary plamocytoma, and multiple myelom. Incidence and survival in the United States 1992-

2004. Br J Haematol 2009; 144:86-94.
3. Strojan P, Soba E, Lamovec J, Munda A Extramedullary plasmacytoma: clinical and histopathologic study. Int J Radiat Oncol Biol Phys 2002; 53:692-701.
4. Alexiou C, Kau RJ, Dietzfelbinger H, Kremer M. Extramedullary plasmacytoma: tumor occurrence and therapeutic concepts. Cancer 1999; 85:2305-14.
5. Bartl R, Frisch B, Fatec-Moghadam A, Kettner G, Jaeger K, Sommerfeld W. Histologic classification and staging of multiple myeloma. A retrospective and prospective study of 674 cases. Am J Clin Pathol 1987; 87:342-55.
6. Tokatli F, Puyan FO, Alas RC, Tuncbilek N, Uzal C. Extramedullary plasmacytoma: clinicopathology, immunohistochemistry and therapeutic approach to a case with a tonsillar site. Hematol Oncol Stem Cell Ther 2008; 1:241-45.
7. Potter M. Neoplastic development in plasma cells. Immunol Rev 2003; 194:177-95.
8. Kishimoto T. The biology of interleukin-6. Blood 1989; 74:1-10.
9. Reynaud D, Pietras E, Barry-Holson K, Mir A, Binnewies M, Jeanne M, Sala-Torra O, Radich JP, Passegué E. IL-6 controls leukemic multipotent progenitor cell fate and contributes to chronic myelogenous leukemia development. Cancer Cell 2011; 20:661-73.
10. Purdue MP, Lan Q, Bagni R, Hocking WG, Baris D, Reding DJ, Rothman N.
1. Prediagnostic serum levels of cytokines and other immune markers and risk of non-hodgkin lymphoma. Cancer Res 2011; 71:4898-907.
11. Breen EC, Hussain SK, Magpantay L, et al. B-cell stimulatory cytokines and markers of immune activation are elevated several years prior to the diagnosis of systemic AIDS-associated non-Hodgkin B-cell lymphoma. Cancer Epidemiol Biomarkers Prev 2011; 20:1303-14.
12. Lattanzio G, Libert C, Aquilina M, et al. Defective development of pristane-oil-induced plasmacytomas in interleukin-6-deficient BALB/c mice. Am J Pathol 1997; 151:689-96.
13. Takada H, Kimura S, Hamada S. Induction of inflammatory cytokines by a soluble moiety prepared from an enzyme lysate of Actinomyces viscosus cell walls. J Med Microbiol 1993; 38:395-400.
14. Ketata S, Ben Mabrouk M, Derbel F, et al. Tumoral form of abdominal actinomycosis: a retrospective case series of seven patients]. Rev Med Interne 2010; 31:735-41.
15. Salmasi A, Asgari M, Khodadadi N, Rezaee A. Primary Actinomycosis of the Breast Presenting as a Breast Mass. Breast Care (Basel) 2010; 5:105-7.
16. Kaplan I, Anavi K, Anavi Y, Calderon S, et al. The clinical spectrum of Actinomyces-associated lesions of the oral mucosa and jawbones: correlations with histomorphometric analysis. Oral Surg Oral Med Oral Pathol Oral Radiol Endod 2009; 108:738-46.
17. Saramas V, Rafailidis PI, Mourtzoukou EG, Peppas G and Falagas ME. Chronic bacteria and parasitic infections and cancer: a review. J Infect Dev Ctries 2010; 4:267-81.
18. Han DC, Huang GT, Lin LM, Warner NA, Gim JS, Jewett A Expression of MHC Class II, CD70, CD80, CD86 and pro-inflammatory cytokines is differentially regulated in oral epithelial cells following bacterial challenge. Oral Microbiol Immunol 2003; 18:350-8.
19. Peyyala R, Kirakodu SS, Novak KF, Ebersole JL Oral microbial biofilm stimulation of epithelial cell responses. Cytokine 2012; 58:65-72.
20. Kurz K, Garimorth K, Joannidis M, Fuchs D, Petzer A, Weiss G. Altered immune responses during septicaemia in patients suffering from haematological malignancies. Int J Immunopathol Pharmacol 2012; 25:147-56.
21. Trinchieri G. Cancer and Inflammation: An Old Intuition with Rapidly Evolving New Concepts. Annu Rev Immunol 2012; 30:677-706.
22. Hong DS, Angelo LS, Kurzrock R Interleukin-6 and its receptor in cancer: implications for translational therapeutics. Cancer 2007; 110:1911-28.